

**Department of medicine  
University of Fribourg (Switzerland)**



**Functional and structural neuroimaging in  
Parkinson's disease and assessment of the  
therapeutic potential of autologous neural cells  
ecosystem (ANCE) transplantation in a MPTP non-  
human primate model:  
a multidisciplinary study.**

THESIS

presented to the Faculty of Science of the University of Fribourg  
(Switzerland) in consideration for the award of the academic grade  
of  
**Doctor Rerum Naturalium**

By

**Simon Badoud**

From Fribourg (CH)

Thesis No: XXX

2015



Accepted by the Faculty of Science of the University of Fribourg (Switzerland) upon the recommendation of Professor Eric Rouiller, Professor Pierre Burkhard, Professor Jean-Marie Annoni, Professor Alain Kaelin and Professor François Karch.

**Fribourg,**

**Thesis supervisors:**

**Dean :**

Prof. Eric Rouiller

Prof. Fritz Müller

Prof. Pierre Burkhard





*“The health of the eye seems to demand a horizon. We are never tired, so long as we can see far enough.”*

***R. W. Emerson***

## ***Acknowledgments***

First of all, I would like to express all my gratitude to Professor Eric Rouiller and Professor Pierre Burkhard to have offered me the opportunity to conduct my thesis in their research units. By their precious advices and availability, they provided me the appropriate support to pass over the difficulties of such project and allowed be to build myself on good basis. Thank you very much.

On the same way, I would like to thank Professor Sven Haller, who co-supervised my work at the University hospitals of Geneva. By his great expertise and patience, he allowed me to get better on a scientific point of view.

I also would like to thank Jérôme Cottet and Simon Borgognon for their contributions on this project. By their enthusiasm to pickup this ambitious challenge they were of always of great support in the good and bad moments. But over their scientific contributions, I would like to thank them for their invaluable friendship and kindness. I wish them all the best for their future career that, I am sure, will be full of success.

I address a special thank to Véronique Moret who was of a precious help during all phases of my PhD thesis, the best as the worse, and actually since my bachelor work in the lab. Thank you for all.

Without the help of Dr. Jean-François Brunet, Dr. Jocelyn Bloch and all their staff, who provided us the ANCE and their priceless expertise, this project would have been stopped prematurely. Thank you very much for the fabulous opportunity you offered us.

Professor Nathalie Ginovard provided me a great support regarding the PET acquisition and post-processing of the data of the NHP part of this thesis. I would like to express to her my gratitude for her availability and her advices.

I also would like to emphasize that this project would not have been possible without the closed collaboration of several institutes and persons:

- Dr. Cristian Antonescu, Bernard Gex, Didier Maillard and all the staff of the nuclear medicine unit at the Hôpital cantonal de Fribourg (HFr).
- Prof. Henri-Marcel Hoogewoud and Eric Dafflon at the unit of radiology at the Hôpital cantonal de Fribourg (HFr).
- André Gaillard and Bernard Aebischer at the University of Fribourg who provided us the technical support necessary to conduct such a project.
- Laurent Bossy and Jacques Maillard, the animal housekeepers of the department of medicine at the University of fribourg who have done an amazing job.
- Dr. Emmanuel Procyk and Dr. Charly Wilson from the Inserm in Lyon who shared with us their great experience and expertise.
- Christiane Marti and Christine Roulin have provided their great expertise regarding the histological part of this study.

Thank you all for your help on this project and your availability.

Along this scientific journey, several colleagues and friends were of particular help. Among them, Nicolas Fasel, Florian Lanz and Adjia Hamadjida have enriched me by their humanity and scientific skill.

I also wanted to thank Dr. Eric Schmidlin, Dr. Gérard Loquet, Dr. Mélanie Kaeser, Laura Carrara, Pauline Chatagny, Michela Fregosi Anne-Dominique Gindra and Julie Savidan for their greeting, their advices and their kindness.

Professor Jean-Marie Annoni, Professor Alain Kaelin and Professor François Karch, who were member of the jury on this thesis. Thank you for your corrections and advices.

I would like to express all my gratitude to my family, especially my father, François and my mother, Marinette for their indefectible support along all these years. They offered the best education possible and transmitted me their priceless culture and knowledge. There is no word to express thankfulness.

Finally, I would like to address a particular thank to Olivia, who was always there for me when I needed, in the good and more difficult moments.

## ***Abstract***

Parkinson's disease (PD) is the second most common neurodegenerative disorder after Alzheimer's disease. It affects 1 to 2% of the population above the age of 65 and generates very important burdens for the society with dramatic consequences for families. Indeed, the costs have been evaluated to not less than 25 billions dollars per year, just for the USA.

Firstly described by the famous English physician Dr. James Parkinson in his "essay on the shacking palsy" in 1817, this pathology that progressively affects the motor system has been extensively studied, both in clinical and preclinical frames. However, despite of the important resources engaged, there are still important lacunas in the understanding of its pathophysiology. Consequently, even if some symptomatic treatments are available, none of them are able to stop its progression.

The present thesis is based on a multidisciplinary approach that aims at tackling this important challenge from two different angles: clinical and pre-clinical.

On one hand, we took advantage of an impressive neuroimaging database including almost 1000 patients scanned at the University hospitals of Geneva to performed advanced imaging analyses. Yet, in contrary to most of the published studies that compares PD patients to healthy controls, we attempt to investigate the potential differences between PD and atypical Parkinsonian syndromes. Additionally, we conducted single patients classifications in order to assess the potential of computer-aided diagnosis for future clinical applications.

Globally, our results reveal that specific patterns of degeneration are associated to different forms of parkinsonisms. Moreover, the classifier was able to discriminate at individual level PD cases from the atypical syndromes above chance level. The accuracy reached up to 97% using diffusion tensor imaging (DTI) data.

On the other hand, we decided to assess the therapeutic potential of autologous neural cells ecosystem (ANCE) transplantation in a MPTP non-human primate model of PD. After extensive behavioral training, four macaque monkeys (*Macaca fascicularis*) were subjected to a systemic MPTP lesion that especially impacted the integrity of the dopaminergic system. During this phase, a small cortical biopsy of the dorsolateral prefrontal cortex was performed. The tissues were directly sent to the University hospital of Lausanne to be put into specific culture conditions before being re-implanted in the host's striatum about eight weeks after the lesion. Out of the four animals, two exhibited mild parkinsonian symptoms while the two others much severely affected. About six months after cells implantations, all animals were exhibited a significant improvement of the motor functions at different levels. Moreover, this functional recovery came along with an increase of the  $^{18}\text{F}$ -DOPA striatal uptake according to positron emission tomography (PET) analyses.

Taken together, the present thesis brings new information regarding PD's pathophysiology and opens new perspectives in terms of alternative therapeutic and diagnostic strategies, even if there is still a long way ahead of us in order to achieve the clinical translation necessary to improve patients' quality of life.

## **Résumé**

La maladie de Parkinson représente la maladie neuro-dégénérative la plus fréquente après celle d'Alzheimer. Elle touche 1 à 2% des personnes au-delà de 65 ans, avec des conséquences dramatiques pour leur famille aussi. Les coûts pour la société sont également extrêmement lourds ; ils atteignent près de 25 milliards de dollars rien que pour les Etats-Unis d'Amérique.

Après la première description faite par le célèbre médecin anglais, le Dr James Parkinson dans son «*assay on the shaking pals* », cette pathologie qui affecte progressivement le système moteur, a été largement étudiée tant sur le plan clinique qu'au travers de modèles animaux. Cependant, malgré l'abondance des moyens engagés, d'importantes lacunes demeurent quant à la compréhension de cette pathophysiologie. Par conséquent, même si un certain nombre de traitements est aujourd'hui disponible, ceux-ci ne sont que symptomatiques et n'arrêtent en aucun cas la progression de la maladie.

Fondée sur une approche multidisciplinaire, la présente thèse a pour but de saisir cette problématique sous deux angles différents, à savoir, d'un point de vue clinique et d'un point de vue préclinique.

D'une part, en nous appuyant sur une importante base de données de neuro-imagerie de près de mille patients scannés aux Hôpitaux universitaires de Genève (HUG), nous avons procédé à des analyses poussées. Nous distançant de la plupart des études publiées à ce jour, qui avaient pour paradigme de comparer des patients parkinsoniens à des personnes saines, nous avons fait le choix d'investiguer les possibles différences entre la maladie de Parkinson, d'un côté, et, de l'autre, des syndromes parkinsoniens dits atypiques. Après quoi, nous avons évalué le potentiel de la classification automatique de patients individuels en utilisant diverses sources de données. Les résultats obtenus ont révélé que les différentes formes de syndromes parkinsoniens sont liées à des patrons de dégénération spécifiques. Par ailleurs, la classification assistée par ordinateur a permis de discriminer des

patients de manière individuelle, au-dessus du seuil de hasard, avec une précision atteignant 97%, en faisant appel notamment à des données DTI (diffusion tensor imaging).

D'autre part, nous avons conduit une étude visant à évaluer le potentiel thérapeutique de la transplantation de ANCE (autologous neural cells ecosystem) dans un modèle parkinsonien de primate non-humain, le singe macaque (*Macaca fascicularis*). Après un entraînement comportemental intensif, quatre singes ont subi une lésion de leur système dopaminergique par injection systémique de MPTP. Durant cette phase, une petite biopsie de leur cortex préfrontal dorsolatéral a été effectuée. Le tissu cortical ainsi obtenu a aussitôt été envoyé au Centre hospitalier universitaire vaudois (CHUV) pour être placé dans des conditions de culture spécifique avant d'être réimplanté, environ huit mois après la lésion, dans les striatums de l'animal. Des quatre sujets ayant subi l'intervention, deux ont présenté des symptômes parkinsoniens légers, tandis que deux autres ont été plus sévèrement affectés. Six mois environ après la transplantation cellulaire, les quatre singes ont, en revanche, manifesté une amélioration significative de leurs performances motrices mais à des degrés variables. Toutes étaient cependant accompagnées d'une augmentation de l'activité dopaminergique au niveau du striatum, comme mesuré par la  $^{18}\text{F}$ -DOAP PET.

D'une manière générale, la présente thèse apporte des informations nouvelles sur la maladie de Parkinson. Elle ouvre ainsi de réelles perspectives en termes de stratégie thérapeutique alternative et de diagnostic, même si le chemin vers une application clinique tendant à améliorer la qualité de vie des patients reste encore long.



## ***Table of content***

<b>1 - GENERAL INTRODUCTION</b>	<b>17</b>
<b>1.1 - MOTOR SYSTEM</b>	<b>21</b>
1.1.1 - MOTOR CORTICES	22
1.1.2 - CORTICOSPINAL SYSTEM	26
1.1.3 - CORTICO-MOTONEURONAL PATHWAY	28
<b>1.2 - THE BASAL GANGLIA</b>	<b>29</b>
1.2.1 - BASAL GANGLIA–THALAMOCORTICAL CIRCUITS	30
1.2.2 - ANATOMY AND FUNCTIONAL CONNECTIVITY OF THE BASAL GANGLIA	32
<b>1.3 - PARKINSON’S DISEASE</b>	<b>37</b>
1.3.1 - EPIDEMIOLOGY	38
1.3.2 - ETIOLOGY	39
1.3.3 - PATHOGENESIS AND PATHOPHYSIOLOGY	40
1.3.4 - BASAL GANGLIA AND PARKINSON’S DISEASE	45
1.3.5 - TREATMENTS	47
<b>1.4 - NON-HUMAN PRIMATE MPTP MODEL</b>	<b>58</b>
<b>1.5 - NEUROIMAGING AND PD</b>	<b>60</b>
<b>1.6 - CONTEXT AND OBJECTIVES</b>	<b>63</b>
<b>2 - MATERIALS AND METHODS</b>	<b>69</b>
<b>2.1 - CLINICAL NEUROIMAGING</b>	<b>71</b>
2.1.1 - PATIENTS AND DIAGNOSIS	71
2.1.2 - IMAGES ACQUISITIONS	72
2.1.3 - IMAGE POST-PROCESSING	72
2.1.4 - STATISTICAL ANALYSIS	72
<b>2.2 - PRECLINICAL ASSESSMENT OF ANCE TRANSPLANTATION IN NHP (NON-HUMAN PRIMATE) MPTP MODEL</b>	<b>73</b>
2.2.1 - EXPERIMENTAL PROTOCOL	73
2.2.2 - ANIMALS	75
2.2.3 - BEHAVIOURAL ASSESSMENTS	75
2.2.4 - MRI ACQUISITIONS	77
2.2.5 - PET ACQUISITION	77
2.2.6 - MPTP LESIONS	78

2.2.7 - CORTICAL BIOPSIES	79
2.2.8 - CELL CULTURES	80
2.2.9 - CELLS TRANSPLANTATION	81
2.2.10 - EUTHANASIA AND HISTOLOGY	82
<b>3 - RESULTS</b>	<b>83</b>
<b>3.1 – CLINICAL NEUROIMAGING</b>	<b>85</b>
CHAPTER 3.1.1	87
INDIVIDUAL DETECTION OF PATIENTS WITH PARKINSON DISEASE USING SUPPORT VECTOR MACHINE ANALYSIS OF DIFFUSION TENSOR IMAGING DATA: INITIAL RESULTS	87
CHAPTER 3.1.2	95
DIFFERENTIATION BETWEEN PARKINSON DISEASE AND OTHER FORMS OF PARKINSONISM USING SUPPORT VECTOR MACHINE ANALYSIS OF SUSCEPTIBILITY-WEIGHTED IMAGING (SWI): INITIAL RESULTS.	95
CHAPTER 3.1.3	105
DISTINCT SPATIOTEMPORAL PATTERNS FOR DISEASE DURATION AND STAGE IN PARKINSON’S DISEASE.	105
CHAPTER 3.1.4	115
INDIVIDUAL DIFFERENTIATION BETWEEN PARKINSON’S DISEASE AND ATYPICAL PARKINSONIAN SYNDROMES USING <sup>123</sup> I-IOFLUPANE SPECT.	115
<b>3.2 – PRE-CLINICAL ASPECTS</b>	<b>141</b>
CHAPTER 3.2.1	143
EFFECTS OF DORSOLATERAL PREFRONTAL CORTEX LESION ON MOTOR HABIT AND PERFORMANCE ASSESSED WITH MANUAL GRASPING AND CONTROL OF FORCE BEHAVIORAL TASKS IN MACAQUE MONKEYS.	143
CHAPTER 3.2.2	175
ADULT NEURAL PROGENITOR CELLS AUTOTRANSPLANTATION IN A NON-HUMAN PRIMATE MODEL OF PARKINSON’S DISEASE: A PRE-CLINICAL STUDY.	175
<b>4 – GENERAL CONSIDERATIONS AND CONCLUSION.</b>	<b>243</b>
<b>4.1 - CLINICAL ASPECTS</b>	<b>245</b>
4.1.1 -PATHOPHYSIOLOGICAL DATA	245
4.1.2 - CLINICAL RELEVANCE	247
<b>4.2 - PRE-CLINICAL EVALUATION OF ANCE TRANSPLANTATION IN A MPTP NHP MODEL OF PD</b>	<b>250</b>
<b>4.3 - INTER-SPECIES TRANSLATION</b>	<b>252</b>
<b>4.4 - CONCLUSION AND PERSPECTIVES</b>	<b>253</b>

<b>5- BIBLIOGRAPHY</b>	<b>255</b>
<b>6 - ANNEXES</b>	<b>275</b>
<b>ANNEX 1</b>	<b>277</b>
<b>(DRAWER'S DATA POST-PROCESSING)</b>	<b>277</b>
<b>ANNEX 2</b>	<b>301</b>
<b>(HISTOLOGICAL PROCEDURES)</b>	<b>301</b>
<b>ANNEX 3</b>	<b>307</b>
<b>BEHAVIORAL ASSESSMENT OF MANUAL DEXTERITY IN NON-HUMAN PRIMATES.</b>	<b>307</b>
<b>ANNEX 4</b>	<b>321</b>
<b>VARIABILITY OF MANUAL DEXTERITY PERFORMANCE IN NON-HUMAN PRIMATES (MACACA FASCICULARIS).</b>	<b>321</b>
<b>ANNEX 5</b>	<b>355</b>
<b>DISTINCTION BETWEEN HAND DOMINANCE AND HAND PREFERENCE IN PRIMATES: A BEHAVIORAL INVESTIGATION OF MANUAL DEXTERITY IN NONHUMAN PRIMATES (MACAQUES) AND HUMAN SUBJECTS.</b>	<b>355</b>
<b>6 – CURRICULUM VITAE</b>	<b>379</b>



# ***1 - General introduction***



Since its characterization in 1817 by Dr. James Parkinson in his “essay of the shaking palsy”, Parkinson’s disease (PD) has generated an enormous amount of questions and has tackled the intellect of thousands of clinicians and researchers around the world. Since 1940, the number of publications mentioning the term “Parkinson’s disease” almost reached 60’000 according to PubMed and this number increases following an exponential manner. However, and despite the large number of laboratories working on this pathology, there are still important lacunas regarding the comprehension of its ethology and pathophysiology that need to be filled in. Consequently, even if consequent improvements have been made, over the last two decades, in terms of PD patient’s management, the treatments currently available remain symptomatic and no actual cure has been proposed so far.

According to the literature, an important factor that directly impacts the prevalence in PD is the age. It is estimated that 1-2% of the population over the age of 65 years old are affected by this pathology and that this number goes up to 5% in people older than 85 (Alves et al., 2008a). For our aging societies it is so of primary interest to invest in research, in order to find concrete solutions to this public health issue. According to “The Parkinson’s disease foundation©, the annual costs generated by PD, including direct and indirect burdens, are reaching 25 billions dollars just for the United States.

Over the last decades, the increasing role of neuroimaging in the clinical routine has offered new possibilities for researchers to tackle some specific problematic from a new angle. This also highlighted new perspectives for PD patient’s management.

In parallel to that, researchers from all around the world have extensively dug the therapeutic potential of cellular transplantation for neurodegenerative disorders. In this ways, investigations on fetal tissues and human embryonic stem cells have provided a proof of feasibility for future clinical applications. A step from those two popular approaches, some scientists have put in light, with animal experimentation, the potential of autologous cells transplantation to correct parkinsonian symptoms (Arias-Carrión and Yuan, 2009; Bloch et al.,

2014; Madhavan and T. J. Collier, 2010). Yet, several important issues still need to be fixed in order to move from the lab to the patients' bed.

By tackling different aspects of PD's research, from clinical neuroimaging to preclinical assessment of an autologous cell based therapy, this thesis will, hopefully, contribute to a better understanding of this highly detrimental pathology that affects thousand of peoples worldwide with dramatic consequences for their families, and for the society.



## 1.1 - Motor system

In a general manner, the motor system refers to the different structures involved in the preparation and generation of a movement (voluntary or involuntary). It includes several cortical structures such as the primary motor area (M1), the premotor area (PM), the supplementary motor area (SMA) and the cingulate motor area (CMA). Behind those structures more involved in the planning and execution of the motor action, we can find subcortical structures that play crucial roles in the modulation of the motor information. Among them, the basal ganglia are playing key roles in the adjustment of the action through a number of cortico-basal loops. The organization of the motor system is both parallel and hierarchic with structures like the cerebral cortex and the brainstem that have direct access to the spinal cord and others, like the basal ganglia, that play more an indirect role in the generation of the motor behavior (figure 1).

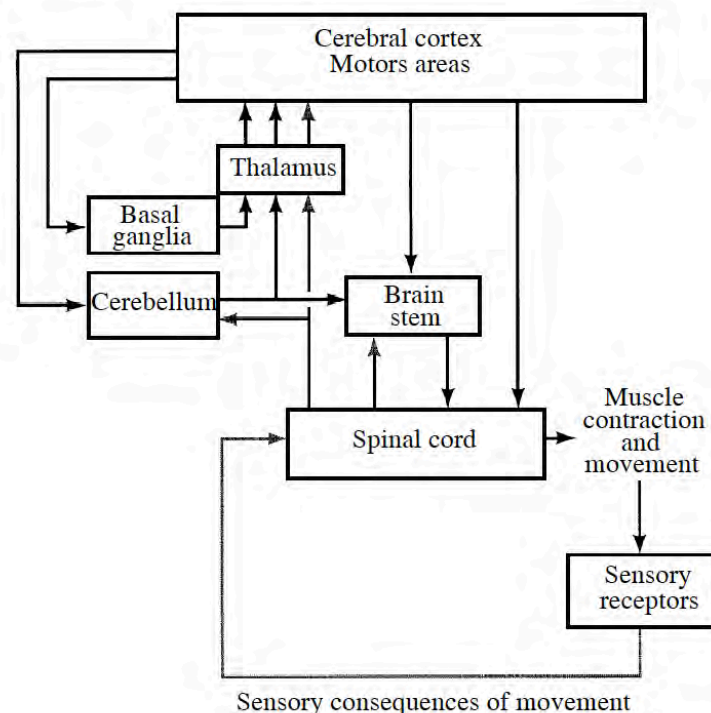


Figure 1. Schematic representation of the motor system's general organization and its main structures. (E.M. Rouiller's lecture)

### **1.1.1 - Motor cortices**

During many years, the motor cortex was anatomically described as a quite simple and homogeneous entity located on the caudal part of prefrontal cortex referring to Brodmann's area 4 and more laterally to area 6. Since then, numerous studies have pointed out a much more complex subdivision scheme based on both cytoarchitectonic and functional criteria. Those important gains of knowledge are largely due to the investigations conducted on nonhuman primates. They have built new basis for the understanding of the human motor system.

#### ***Primary motor cortex (M1 or F1)***

In the generation of a behavior, the primary motor cortex (M1) plays certainly a central role and more particularly in the execution of the motor commands (Penfield and Boldrey, 1937). Classically defined as Brodmann's area 4 (F1 in macaque monkey (Luppino and Rizzolatti, 2000)), it receives inputs from the other motor areas such as PM, SMA and CMA, but also from the thalamus and some parietal areas. It is histologically characterized by the absence of cortical layer IV and by the presence of large pyramidal neuron in layer V called Betz cells (Geyer et al., 1996). During the 50's, Penfield performed a number of experiments on humans and macaque monkeys using electrical stimulation. He was able to generate a functional map of the brain in which, each location on M1 was corresponding to a functionally related part of the body (figure 2) (Penfield and Boldrey, 1937; Penfield and Rasmussen, 1950). Those data gave birth to the famous Homunculus. This somatotopic representation has evolved with much variable representations of the body including overlaps of functional territories (Sanes et al., 1995; Schieber, 2001).

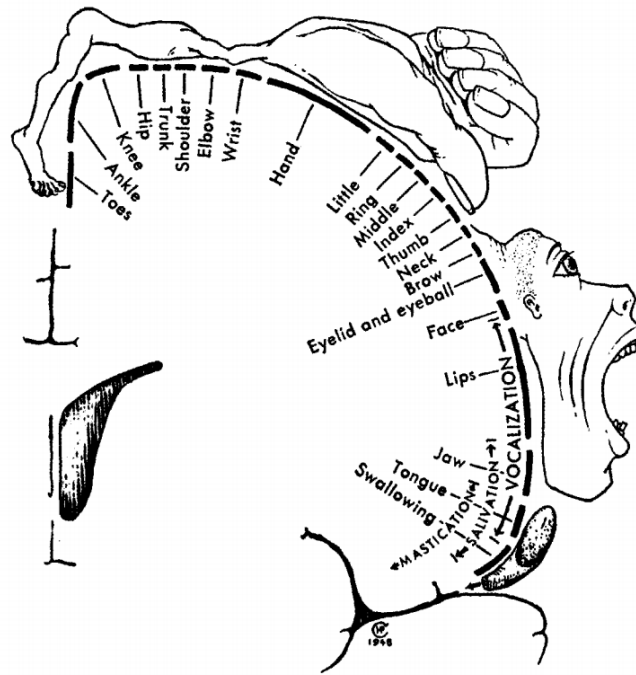


Figure 2. Representation of the motor homunculus on a frontal slice of the primary motor cortex according to Penfield and Rasmussen 1950. 11

Functionally, the primary motor cortex has a direct access to the spinal cord. It actually encompasses about 30% to 50% of the corticospinal neurons (Murray and Coulter, 1981) and so, is largely implicated in the control of the fine motor actions. Several studies have clearly shown that permanent or transient lesions of M1 led to massive motor deficit both in humans and nonhuman primates (Hoogewoud et al., 2013; Kaeser et al., 2011; Lemon, 1999; Liu and Rouiller, 1999; Rouiller et al., 1998; Wyss et al., 2013).

## ***Secondary motor areas***

If M1, as mentioned above, is playing an important role in the execution of the motor action, the secondary motor cortices are more involved in the planning and the preparation of the voluntary movements.

PM is located on the frontal lobe, anteriorly to M1 (Brodmann's area 6; F2, F4, F5, F7 in monkeys) (Luppino and Rizzolatti, 2000). It receives and processes inputs from several cortical structures including sensory areas and the prefrontal cortex. It is tightly interconnected to M1 and plays an important role

in the preparation of complex movements. PM can be separated into two main parts: the dorsal one (PMd) and the ventral one (PMv). Clinical reports including patients with lesions segregated to the dorsal area have pointed out the role of PMd in the temporal coordination of the movements and in the control of proximal muscles controlling the limbs (Fink et al., 1997; H. J. Freund, 1985; H. J. Freund and Hummelsheim, 1985). In contrary, some experiments based on functional neuroimaging acquisitions have pointed out an implication of PMv in the generation of sequences of digit movements. Similarly to M1, PM contains a number of corticospinal neurons (mostly localized in PMd) and is also organized in a somatotopic manner, but less strict than M1.

Similarly to PM, SMA works like a computer processor that receives inputs from different brain regions, integrates them and generates outputs that are then sent to different areas and in particular to M1. SMA is lying dorsally to PM and anteriorly to M1 (figure 3) (Brodmann's area 6; F6, F3 in monkeys) (Luppino and Rizzolatti, 2000). It could be subdivided into two regions: "SMA proper" and "pre-SMA" (Roland and Zilles, 1996). Functional imaging experiments conducted on professional piano players have shown that the first one is specially activated when a motor sequence is performed and that the second one is more activated when a new motor sequence has to be learned. The implication of SMA in the coordination of bimanual tasks has also been underlined in several papers both in humans and monkeys (C. Brinkman, 1981; Kazennikov et al., 1999; 1998; Kermadi et al., 2000; 1998; 1997; Sadato et al., 1997; Serrien et al., 2002; Viallet et al., 1992). Moreover, Luppino and Rizzolatti have described a role of SMA in the execution of the motor functions through corticospinal projections (Luppino and Rizzolatti, 2000; Maier et al., 2002; Rouiller et al., 1996).

Finally, the cingulate motor area (Brodmann's areas, mainly 23, 24), which is tightly interconnected with SMA, PM and M1 seems to play an important role in the selection of the motor sequence or its annulation in case of conflicting orders. According to Picard and colleagues, the activation of the different parts of the cingulate motor cortex will depend on the complexity of the task that will be executed (Picard and STRICK, 1996). The cingulate motor area also receives strong limbic information and so, plays a role in the integration of emotional inputs. To terminate, the presence of corticospinal neurons in the cingulate motor area provides it a direct access to the spinal cord.

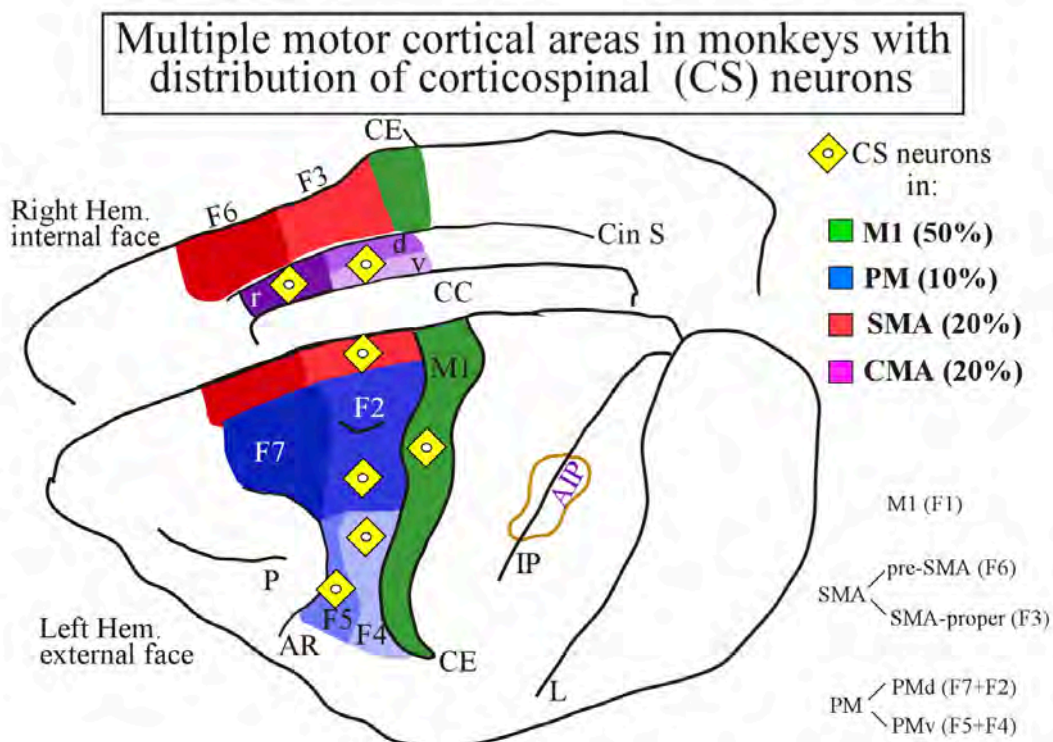


Figure 3. Anatomical representation of the motor cortical areas and distribution of the corticospinal (CS) neurons in the macaque monkey (E.M. Rouiller's lecture).

### **1.1.2 - Corticospinal system**

If the cortical structures described in the previous sections are extensively involved in the generation of behaviors in different species by their implication in the integration of multimodal information, in the planning and in the execution of the motor action, they still need to relay those commands to the effectors (muscles) through descending pathways. One of the most important of them is the corticospinal tract (CST) that provides a direct access to the spinal motoneurons, either directly or indirectly via interneurons.

At the beginning of the 20<sup>th</sup> century, Sir Charles Sherrington put ahead the concept of “the final common pathway of the motor system” which was referring to the alpha-motoneurons and its effectors (muscles).

The CST originates from the different cortical areas implicated in the generation of voluntary movements. About 30 to 50% of the CS neurons are located in M1 whereas the rest are distributed among SMA, PM, CMA and the somatosensory area (figure 3) (Murray and Coulter, 1981; Toyoshima and Sakai, 1982). On their way to reach the spinal cord, the axons of the CST will pass through the internal capsule, through the cerebral peduncle in the midbrain and the pyramid. At the level of the medulla, 90% of the fibers will decussate (pyramidal decussation) to end on the dorsolateral part of the spinal cord. Those projections are called “the lateral corticospinal tract” and are innervating interneurons or motoneurons that are responsible for the contraction of distal muscles (figure 4). The remaining 10% will not cross the midline at this level and will project on the ipsilateral side of the body or will innervate the contralateral side at a lower level (Kuypers, 1981). This last group of axons is named “the medial corticospinal tract” and plays a role in the control of proximal and axial muscles.

Even if the contribution of the CST to the motor control is now clearly established, the multiplicity of its origins has also raised the idea of its implication in multiple functions, like in the proprioceptive control of the movement.

## Descending lateral corticospinal pathway

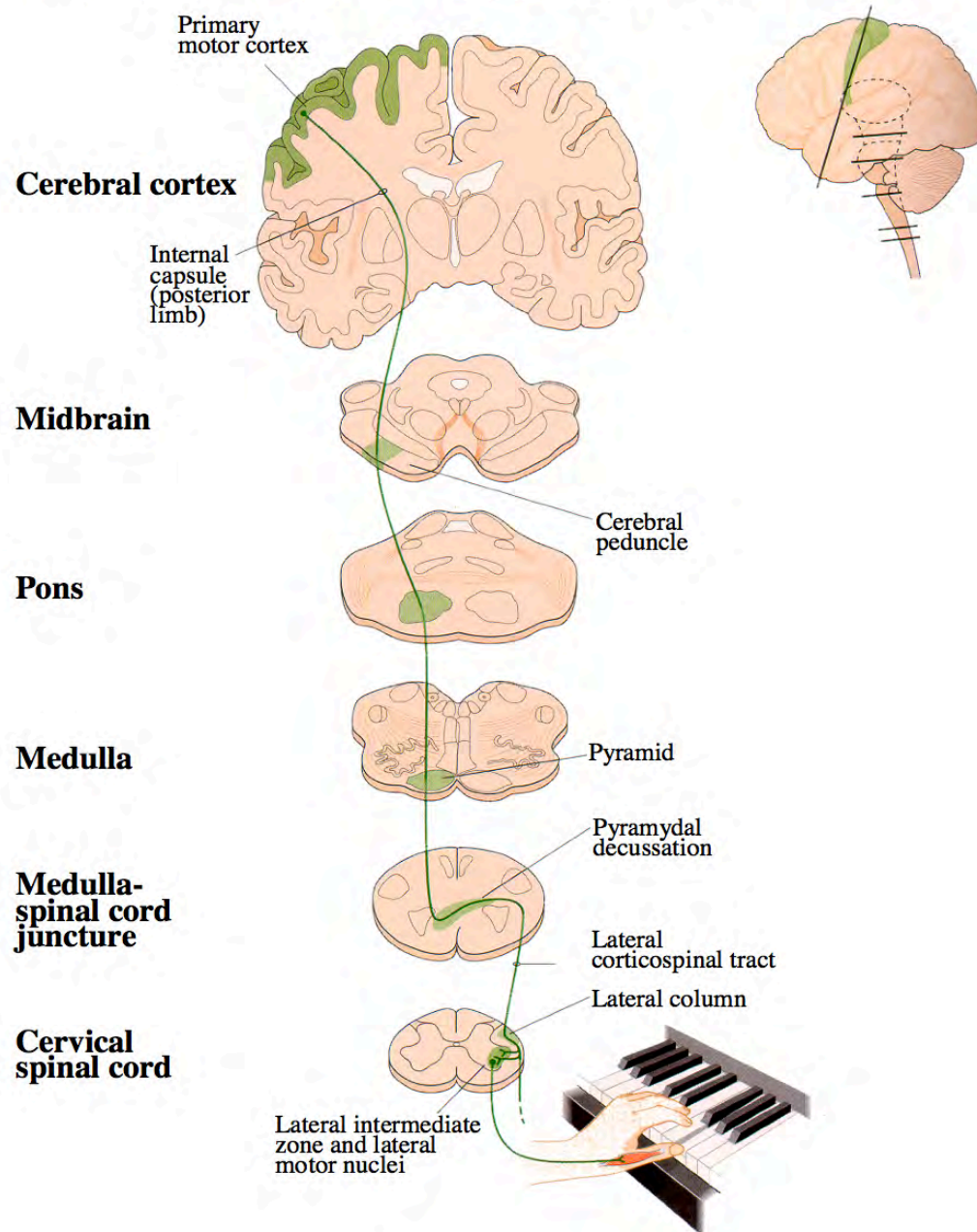


Figure 4. Representation of the descending lateral corticospinal track (in green) (Bear et al.2007).

### 1.1.3 - Cortico-motoneuronal pathway

The cortico-motoneuronal pathway (CM) is composed by a subpopulation of the CST that is ending directly on the  $\alpha$ -motoneurons and so, is forming a direct (mono-synaptic) connection with the motor cortex (J. Brinkman and Kuypers, 1973; Kuypers, 1962; Lemon, 2004; Muir and Lemon, 1983). Kuypers et al. investigated the relationship between the CM and the capacity to generate “relatively independent finger movements” (RIFM) (Kuypers, 1962). Several data coming from inter-species investigations have shown a good correlation between the index of dexterity of each species and the number of CM projections (figure 5). In fact, the opposition of the thumb and the index finger, also referred to as the precision grip, which is a particularity of primates (including human), is anatomically supported by the CM projections (Muir and Lemon, 1983). Numerous lesion studies conducted on non-human primates have brought strong evidences of this particular link between CM and fine manual dexterity (P. Freund et al., 2009; Hepp-Reymond et al., 1974; Lawrence and Kuypers, 1968; Lemon, 1999; Lemon et al., 1995; Wannier et al., 2005)

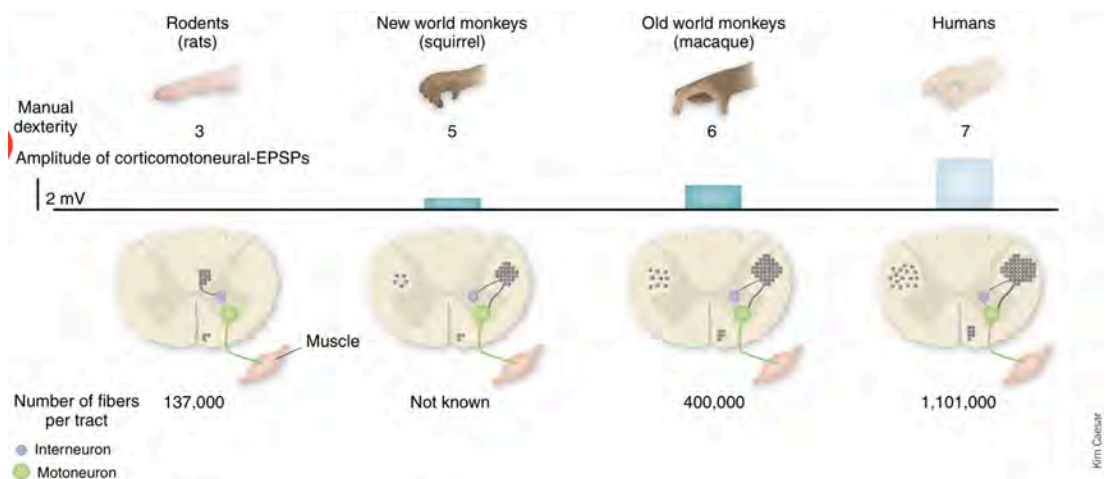


Figure 5. Relationship between the level of manual dexterity and the development of the corticospinal track in different species (Courtine et al., 2007).



## 1.2 - The basal ganglia

The first anatomical description of the basal ganglia was given by the famous anatomist of the 16<sup>th</sup> century, Andreas Vesalius. However, it is only one century later that the English physician Tomas Willis gave the name “*corpus striatum*” to one of its major components (Parent, 2012). Since then, numerous anatomists and researchers have given their contributions to improve the understanding of this complex group of subcortical structures (figure 6). Nowadays, it is clearly established that the basal ganglia are key players in the modulation of sensorimotor information and of cognitivo-emotional processes (DeLong et al., 1984; DeLong and Wichmann, 2007). In a very general manner, the role of the basal ganglia is to integrate information coming from multiple sources, to integrate them and, *in fine*, to generate an appropriate context dependent behavior. They could be considered as a computer that will receive inputs, process them, and send the outputs to other systems. In this sense, the striatum is considered as the major input structure of the basal ganglia even if other nuclei, like the *globus pallidus externus* (GPe) and the *subthalamic nucleus* (STN) are also receiving projections from cortical and thalamic structures. The output structures of the basal ganglia are mainly constituted by the *globus pallidus internus* (GPi) and by the *pars reticulata* of the *substantia nigra*. Those outputs could be segregated into two categories. On one hand, the ascending outputs that project on the frontal lobe, particularly to the premotor area and on the ventral thalamic nucleus will be implicated in the processes previously mentioned. On the other hand the descending outputs sends projections to the mesencephalon and will play a key role in the control of the posture and balance.

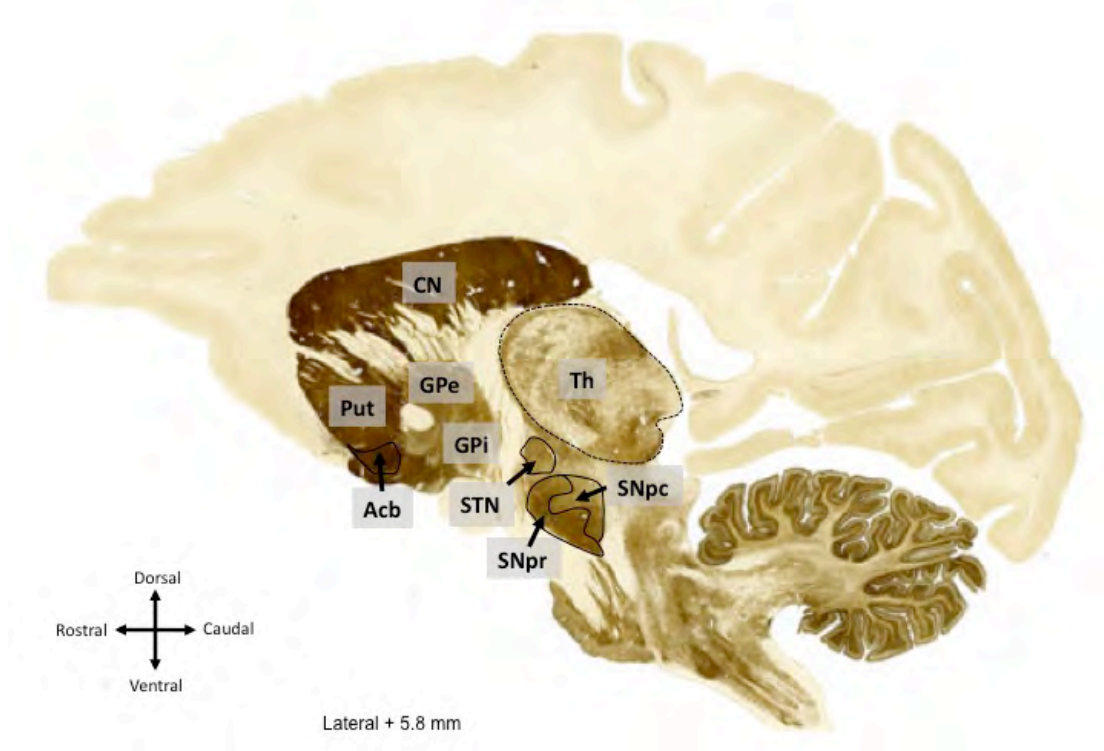


Figure 6. Histological preparation revealing the acetylcholinesterase enzyme, presenting the different structures of the basal ganglia. N.b. the thalamus has been indicated for informative purpose. Figure adapted from Lanciego 2012.

### **1.2.1 - Basal ganglia–thalamocortical circuits**

Functionally, the basal ganglia work through a number of parallel loops that are regrouped according to their functional and structural characteristics. During the 60's and 70's, several papers came out showing that interactions between cortical structures, basal ganglia and the thalamus play a role in the modulation of different brain functions including the sensorimotor system, cognitive processes or the limbic system. Heimer and Wilson were the first to postulate that those loops were organized in a parallel manner (Heimer and Wilson, 1975). However, the current theory, that is including a total of five loops, was published only ten years later (figure 7) (Alexander et al., 1986).

The five loops proposed by Alexander and colleagues are the following:

- **The motor loop**, which is dealing with the control of voluntary motor behavior.
- **The oculomotor loop**, dealing with the eyes' saccades.
- **The dorsolateral prefrontal loop**, also called cognitive loop.
- **The lateral orbitofrontal loop**, which is implicated in social behavior.
- **The anterior cingulate loop**, also known as limbic or emotional loop.

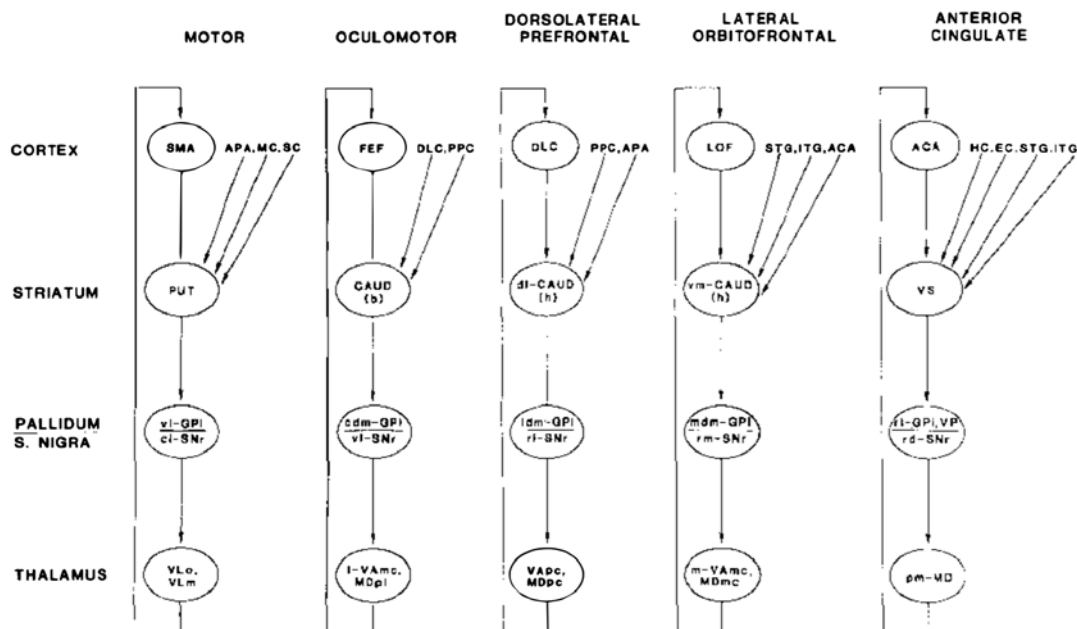


Figure 7. Schematic representation of the five cortico-baso-thalamo-cortical loops and the different structures implicated. For the nomenclature see Alexander et al. 1986.

The different circuits described above are organized in a topographic and somatotopic manner where, for instance, the sensorimotor projection are always projecting the dorsolateral part of the basal ganglia whereas the projections coming from the cognitive associated cortical areas are always targeting the medial part of the basal ganglia. Similarly, the outputs of the processed information coming out from the SNpr and the GPi are sent to different sub-nucleus of the thalamus according to their groups.

## **1.2.2 - Anatomy and functional connectivity of the basal ganglia**

### ***The striatum***

The striatum is composed by the putamen, the caudate nucleus and the nucleus accumbens. The putamen and the caudate nucleus are two very close structures separated by the internal capsule and are located on both sides of the lateral ventricles, whereas the nucleus accumbens is localized just below the junction between the putamen and caudate nucleus.

The cytoarchitecture of the striatum is mainly composed by medium-sized spiny neurons (MSN). They form not less than 95% of the striatal cells and use GABA as neurotransmitter. MSN are principally projection neurons that can be separated into two main strains regarding the neuropeptides expressed. The enkephalin producing neurons are expressing dopaminergic receptors D2 while D1 receptors can be found in neurons containing substance P or dymorphin (Gerfen, 1992a; 1992b; SMITH and BOLAM, 1990; Wichmann and DeLong, 2007). The remaining 5% are constituted by groups of interneurons (Wichmann and DeLong, 2007).

As previously mentioned, the striatum is considered as the main entrance structure of the basal ganglia and receives afferent inputs from almost all brain regions. This information is organized in a topographic manner (figure 8). The dorsolateral part of the putamen as well as, in a limited way, the lateral part of the caudate nucleus are receiving projections form the motor cortical areas and form the somatosensory cortex (Flaherty and Graybiel, 1993; Jones et al., 1977; Malach and Graybiel, 1986; Nakano et al., 2000; Nambu, 2011). It is moreover innervated by the centromedian nucleus of the thalamus. This part of the striatum is commonly referred as the “sensorimotor striatal area”.

The so-called “associative striatal area” is composed by the largest part the head of the caudate nucleus and by the ventromedial part of the putamen. This region is largely innervated by the prefrontal cortex, the parietal lobe as well as by the parafascicular nucleus of the thalamus.

Finally, the third region is formed principally by the accumbens nucleus but also by the most ventral part of the head of the caudate nucleus. It receives important inputs from the parahippocampal formation and from the CA1 region of the hippocampus. Those connections are completed by strong amygdaloidal and thalamic inputs (midline thalamic nuclei). This structure is also known as the “limbic striatal area”.

Similarly to striatal inputs, the outputs are organized according to a topographic pattern. In this way, the sensorimotor area projects to the dorsolateral part of the globus *pallidus externus* and *internus*, as well as to the ventrolateral area of the SNpr. The associative striatum projections target the medial part of GPi / GPe and the intermediate portion of the SNpr. To terminate, the limbic striatum sends its outputs to the ventral part of the *pallidum* and to the dorsomedial SNpr.

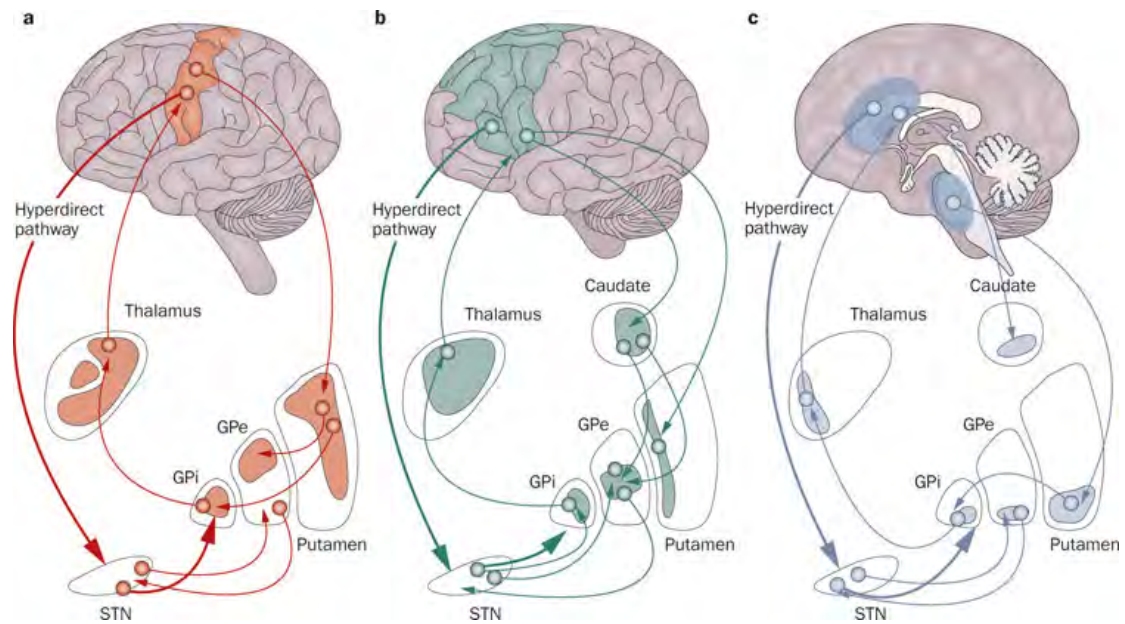


Figure 8. Representation of the topographic organization of the basal ganglia. A) The sensorimotor striatal area. B) The associative striatal area. C) The limbic striatal area. (Krack et al. 2010)

Regarding the striatofugal projections, they can be split into two distinct entities. On one hand, the direct pathway is composed by MSN expressing D1 receptors, building a monosynaptic bridge between the striatum and the GPi and the SNpr. On another hand, the so-called indirect pathway is firstly sending projections to the GPe and then to the STN, before reaching the GPi and the SNpr. The neurons constituting the indirect pathway express D2 receptors and contain enkephalin as neuropeptide.

## ***Dopaminergic & Nigrostriatal system***

The contribution of the dopaminergic projections coming mainly from the SNpc and from the ventral tegmental area (VTA) is of high importance in the

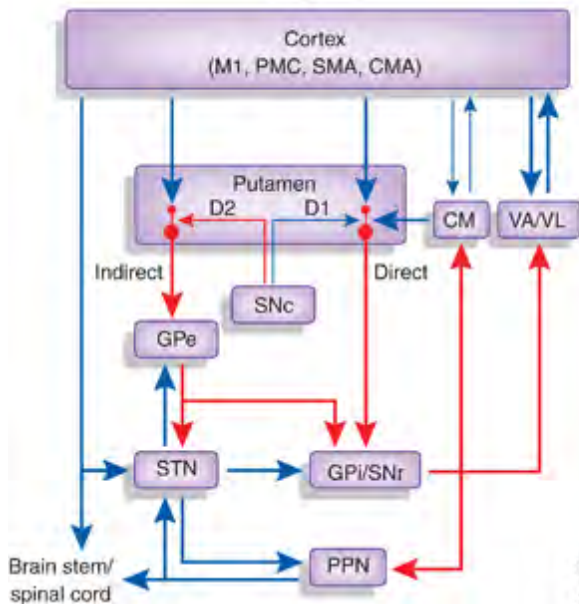


Figure 9. Schematic representation of the direct and indirect pathways. In red, the inhibitory projections. In blue, the excitatory projections (Smith 2012).

modulation of the striatal outputs.

The SNpc neurons (A9) principally project to the dorsal portion of the striatum while the VTA dopaminergic cells (A10) innervate the limbic striatum, as well as the prefrontal cortex (Haber, 2014). At synaptic level, Freund et al. have shown that the dopaminergic projections make contacts with the

MSN at the neck of their dendritic spines. The strategic position occupied by those synapses confers them an optimal role in the modulation of the output signals

and so in the regulation of the information. The previously mentioned direct and indirect pathways are directly modulated by the dopaminergic projections coming from the SNpc. The dopamine release at striatal level will have two opposite effects depending on the nature of the receptors. On one side, the direct projections (receptor D1) activity will be stimulated by the dopaminergic inputs whereas, on the other side, the dopamine release will inhibit the indirect pathway (receptor D2). In a general way, the SNpc precisely balances those two antagonist pathways and, ultimately, modulate the global outputs of the GPi and SNpr.

Regarding its inputs, the SNpc is innervated by the orbitofrontal cortex, the prefrontal cortex and the SNpr (Celada et al., 1999; Comoli et al., 2003).

## ***Globus pallidus***

As previously mentioned, the globus pallidus can be subdivided into two segments: the GPe and the GPi. The cytoarchitecture of those two parts is very similar with the presence of large neurons that are forming the vast majority of their cellular composition. The dendrites of those neurons are forming disk-like structures that are oriented perpendicularly to the striatal projections (Percheron et al., 1984). Those projections are organized in a topographic manner in which the neurons expressing D2 receptors project on the GPe while the striatopallidal projections expressing D1 receptors project on the GPi. The outputs of the GPe are mainly directed to the STN and, to a lesser extent, to the GPi. The GPi outputs project towards the thalamus and the mesencephalon (DeLong et al., 1985).

## ***Subthalamic nucleus***

Located just beside the *pedunculus*, the STN has the shape and the size of the rice bean. This tiny structure plays, however, a major role in the control of the basal ganglia's outputs. By its central implication on the indirect pathway, it modulates to a large extent the outputs of the GPi and of the SNpr through glutamatergic projections (Temel et al., 2005). Since the last three decades, and the discovery, by Benabid and colleagues, of the therapeutic potential of the deep brain stimulation (DBS), the organization of this small nucleus has become of high interest (Limousin et al., 1995). The appearance in some parkinsonian patients treated by DBS of psychiatric side effects raised the question of a topographic organization in the STN. Several animal studies, and more particularly on nonhuman primates, have put in light the hypothesis of a tripartite subdivision. According to this theory, the dorsal area would be involved in motor aspect, the medial portion in more cognitive function and the most ventral part would deal with limbic inputs (DeLong and Coyle, 1979; Haynes and Haber, 2013). However, even if this anatomical segregation seems to be relevant, some controversies remain regarding potential functional overlaps.



### **1.3 - Parkinson's disease**

According to a paper, published in 2006 by Zhang and colleagues, based on old Chinese medical archives, the features of PD were already reported in texts dating back to the 5<sup>th</sup> century BC (Zhang et al., 2006). However it is only at the beginning of the 19<sup>th</sup> century that the English physician Dr. James Parkinson gave the first formal characterization of the disease. In his "essay on the shaking palsy" published in 1817, he gave a rough description of six patients, including three persons he actually saw in the streets of London (Parkinson, 1817). The general loss of muscular power, involuntary tremors and a propensity to bend the trunk forwards were some of the major characteristics reported in this publication. James Parkinson was actually talking about "paralysis agitans", referring the akinetic state of his patients, which was contrasting with the tremulous movements of their hands.

This first description of the pathology was then largely refined by the famous French neurologist, Jean-Martin Charcot, almost 50 years later. Charcot proposed the name "Parkinson's disease" instead of the wrongly used terms of "paralysis agitans" or "shaking palsy" as all patients did not suffer from resting tremors. Since then, many researchers and clinicians gave their contribution to the understanding of this complex pathology and tried to elaborate a cure.

PD is nowadays considered as a multisystemic synucleinopathy, characterized by an abnormal protein aggregation and a progressive depletion of the dopaminergic neurons in the SNpc (Davie, 2008). The clinical presentation of the pathology is pretty complex. It includes the cardinal symptoms of PD that are bradykinesia, tremors and muscular rigidity but, also, a large panel of non-motor symptoms: cognitive impairments (attention deficits, dementia, etc.), psychiatric disorders (anxiety, depression, etc...) and many others, including sleep problems and sexual dysfunctions.

Even if science has made important advances during the last 30 years on the understanding of its pathogenesis and pathophysiology, thanks to animal experimentation, PD remains, so far, an incurable disease affecting thousands of patients worldwide with dramatic consequences for their families.

### 1.3.1 - Epidemiology

PD is known to be the second most common neurodegenerative disorder after Alzheimer's disease (AD) and the most common movement disorder together with essential tremors (ET). A study has reported a worldwide incidence of 13.4 cases in a population of 100'000 (Van Den Eeden et al., 2003). However, this incidence rate varies greatly depending on the geographical distribution of the population, on its ethnicity and on



Figure 10. Illustration of a PD patient by William Richard Gowers, 1886.

the sex of the populations (Alves et al., 2008a; Odekerken et al., 2013). Some epidemiological studies have, for example, reported an incidence rate of 9 to 19 cases in a population of 100'000 people in Western Europe while the rate reaches only 1.9/100'000 in China (1 year, age corrected). Van den Eeden and colleagues (2003) have also underlined the importance of the ethnic parameter on PD incidence rate. According to their work, black people would have twice less chance to develop the disease (9.9/100'000) as compared to Hispanic people (16.6/100'000) (Van Den Eeden et al., 2003). In the same paper, they also described the sexual asymmetry of PD with an incidence rate of 19/100'000 in males, compared to 9.9/100'000 in females.

In a general manner, PD prevalence is strongly correlated to the age of the population. In people older than 65 years of age, its prevalence is about 1-2% while in people older than 85 it can reach up to 5% (Alves et al., 2008b).

### **1.3.2 - Etiology**

The large majority of the PD cases are defined as idiopathic, due to their largely unknown etiology, while only about 10% of the cases are familial forms consequent to genetic mutations. During the last four decades, several chemical compounds and genetic factors have been put in light as being potentially implicated in the development of PD. Even if an interaction between environmental and genetic factors in the pathogenesis of idiopathic PD is nowadays largely accepted, no direct causality has been formally identified (A. H. V. Schapira, 2009).

The environmental theory arguing that external factors are implicated in the onset of PD is based on several observations in which the exposure to some chemicals led to the development of parkinsonian symptoms. In this sense, one of the most important reports was published during the 80's by Langston and colleagues. This paper was reporting the case of four young drug abusers that have suddenly developed severe parkinsonian symptoms following MPTP (1-methyl-4-phenyl-1,2,3,6-tetrahydropyridine) intake (Langston et al., 1983). This discovery was a breakthrough in the understanding of PD pathophysiology. The analogy between MPTP and some chemicals, generally used in agriculture, like Paraquat or Rotenone, taken together with a higher incidence of PD in rural areas, was pushing in the direction of an environmental influence (Richardson et al., 2009; Semchuk et al., 1992; Shastry, 2001; Tanner et al., 1990; Tanner, 1992). This was later confirmed by animal experimentations (Betarbet et al., 2000; Corrigan et al., 1998). In contrary, some behaviors like smoking tobacco or drinking coffee significantly reduce the risk of developing the disease (Ascherio et al., 2001; Baron, 1986; Palacios et al., 2012).

In 1997, the publication by Polymeropoulos and colleagues of a paper reporting the cases of some Greek families affected by PD opened the window to a whole new area of research regarding the understanding of PD pathogenesis (Polymeropoulos et al., 1997). They were actually able to identify an autosomal dominant mutation on the SNCA gene coding for the alpha-synuclein protein which is largely present in Lewy bodies (Polymeropoulos et

al., 1997; Polymeropoulos, 1998; Spillantini et al., 1997). The importance of this gene in the devolvement of the inherited forms of PD was confirmed one year later by Krüger and colleagues (Krüger et al., 1998). Since then, a dozen of genes have been shown to be implicated in the development of PD (A. H. V. Schapira, 2009).

In order to discriminate the implication of the genetic versus the environmental factors, studies on monozygotic twins have been conducted. However, even if a good concordance have been put in light for early onset of the disease (before 50 years old), the lack of correlation for later onset, as it is the case in sporadic PD, goes against a strong implication of genetic factors in the development of the idiopathic form of PD. Nevertheless, genetic polymorphism on some loci are, nowadays, considered as risk factors (Farrer et al., 2001; Tanner et al., 1999).

### ***1.3.3 - Pathogenesis and pathophysiology***

The progressive depletion of the dopaminergic neurons in the SNpc and the neuronal inclusions of proteins aggregates called Lewy bodies are the two hallmarks of PD (Dauer, 2003). During the last decades, two main approaches have tried to provide an explanation to this neurodegenerative process. On one hand, the misfolding and aggregation of alpha-synuclein proteins, together with their deficient degradation by proteasomes may explain the formation of the alpha-synuclein inclusions. On the other hand, mitochondrial dysfunctions and formation of reactive oxygen species (ROS) are also pointed out as important players in PD pathogenesis (figure 11).

The role of mitochondrial dysfunction in the neurodegenerative processes implicated in PD was emphasized following the discovery of the MPTP during the 80's (Langston et al., 1983; A. Schapira et al., 1990; 1989). The 1-methyl-4-phenylpyridinium (MPP+), which is the MPTP metabolite, is known to interfere with the complex I of the mitochondria, which plays a key role in the electrons transport chain (KINDT et al., 1987; NICKLAS et al., 1987). The inhibition of the complex I leads to two phenomena: 1) the augmentation of

the ROS production 2) the decrease of ATP production. The ROS would then play a role in the proteins misfolding and the decrease of energy production would ultimately lead to cell death. More recently, genetic approaches have stressed out the implication of several genes, including *parkin* and *PINK1* in mitochondrial dysfunction (Kamp et al., 2010). In this way, *parkin* and *PINK1* mutations have been shown to be present in some patients affected by the familial form of PD (Kitada et al., 1998; Valente et al., 2004). The fact that dopaminergic neurons in the SNpc are particularly vulnerable to ROS, due to neuromelanin, has also to be taken into account in the depletion process (Hirsch et al., 1988).

The Lewy bodies were already described in 1912 as one of the major characteristic of PD (Forster and Lewy, 1912). They are resulting of the aggregation of a wide range of different proteins including alpha-synuclein, neuro-filaments and ubiquitin (Spillantini et al., 1997). In a general manner, one talks about Lewy pathology in references to the diverse neuronal inclusions that are alpha-synuclein immunoreactive. Even if the reasons why those protein aggregates in such a pathological manner remain largely unknown, several hypotheses have been brought in front of the scene.

The discovery of the previously mentioned *parkin* gene has highlighted its implication in the ubiquitin-proteasomal system (UPS) and so, in the Lewy body formation (Kitada et al., 1998; Wakabayashi et al., 2007). The UPS plays a central role in the elimination of the misfolded or damaged proteins ( Ciehanover et al., 1978). Consequently, a diminished UPS activity could lead to protein aggregation and, *in fine*, to Lewy body formation as it has been shown in PD patient (McNaught et al., 2001). In MPTP monkeys, a decrease of the proteasomal activity of the UPS has also been described.

Beside those processes, inflammatory reactions have also been described as a possible important piece of the puzzle. It has been shown that there is a correlation between microglia activation and the progression of the disease (Halliday and Stevens, 2011). A possible role of microglia in the degradation of extracellular alpha-synuclein has also been emphasized (Halliday and Stevens, 2011). In this way, post-mortem studies have shown an over activation of microglia around the substantia nigra in PD patients and that the cytokines were particularly elevated (Hirsch and Hunot, 2000; P. L. McGeer and E. G. McGeer, 2008). This up-regulation of inflammatory processes can trigger cell apoptosis (Hirsch and Hunot, 2000).

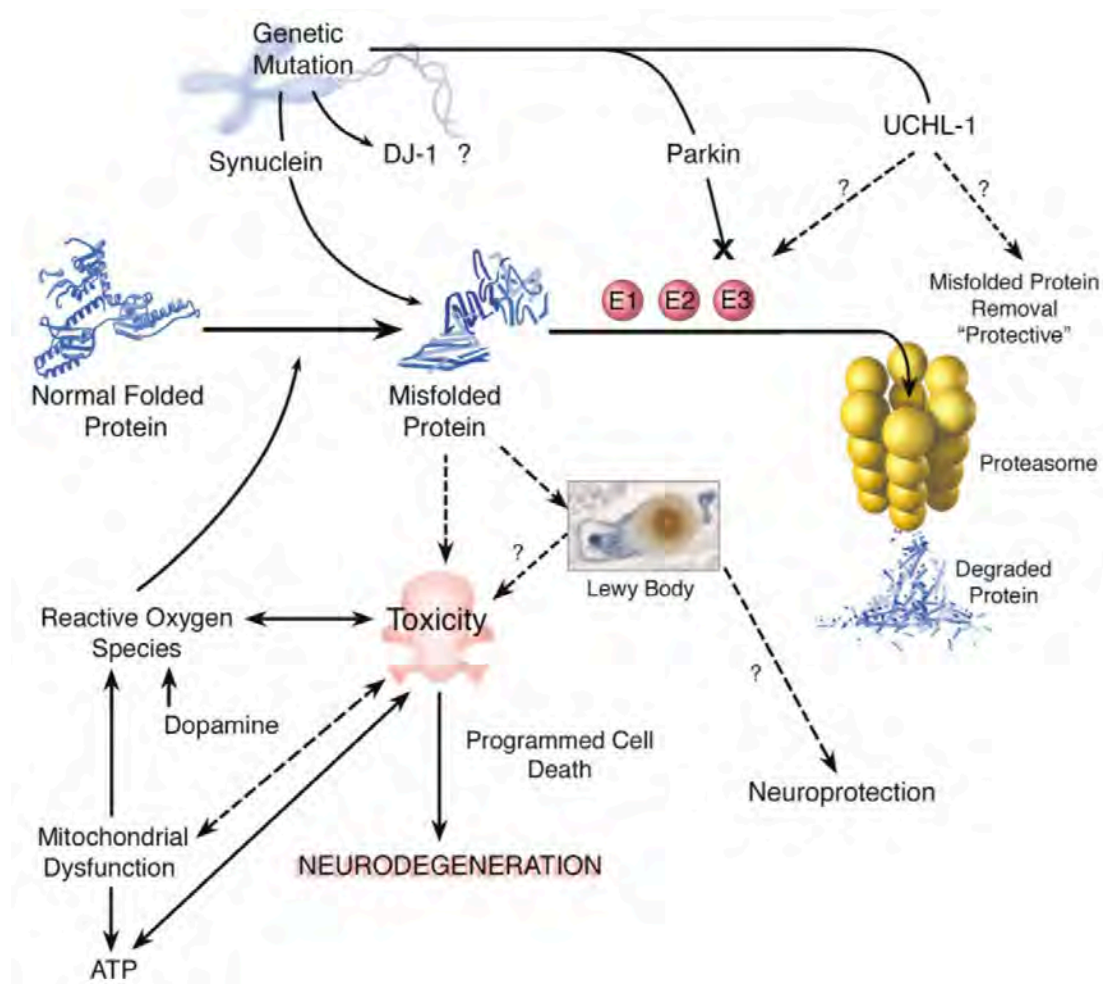


Figure 11 Illustration of the different mechanisms that may be implicated in neurodegeneration according to Dauer 2003.

The processes described above are thought to be at the origin of the slow degeneration seen in PD. According to Braak and colleagues the progression of the pathology is fairly predictable and follows a defined pattern (H. Braak et al., 2003b). In their work published in *Neurobiology of aging* in 2003, they performed autopsies and immunological analysis on the brains of 168 patients, looking for alpha-synuclein inclusions, like LB or Lewy neuritis. They were able to differentiate six stages in the pathology progression (figure 12) (H. Braak et al., 2003a). In the early stages of the disease development, alpha-synuclein inclusions are principally restricted to the autonomous parts of the brain (medulla oblongata) but it then extends to almost all regions, finishing by the neocortex. It is important to keep in mind that the Lewy pathology starts long before the onset of the clinical signs and that there is important inter-individual variability regarding the time course of its progression. This has been confirmed by positron emission tomography (PET) studies and it is commonly admitted that when motor symptoms appear almost 50 to 60% of the striatal dopaminergic projections are already depleted (Blesa et al., 2012; Morrish et al., 1995). Braak stage one and two are, in this way, considered as pre-symptomatic even if some modifications of the autonomous and sensory functions could be seen as early signs of PD (Wolters and H. Braak, 2006). Stages three and four correspond to the spread out of the pathology to the dopaminergic system (SN and VTA) and so, to the motor onset. While at stage five and six, it will reach higher brain areas resulting in cognitive deficits. Yet, PD pathology does not only affect the dopaminergic system but equally impacts on cholinergic, noradrenergic and serotonergic systems (figure 12) (H. Braak and E. Braak, 2000).

Nevertheless, the correlation between the presence of LBs in the SNpc described by Braak and the motor symptoms is not remarkable. Indeed, the depletion of the dopaminergic neurons in the SNpc shows a much better correlation with the unified Parkinson's disease rating scale (UPDRS) which reflects the motor and non-motor impairments in PD patients (Greffard et al., 2006).

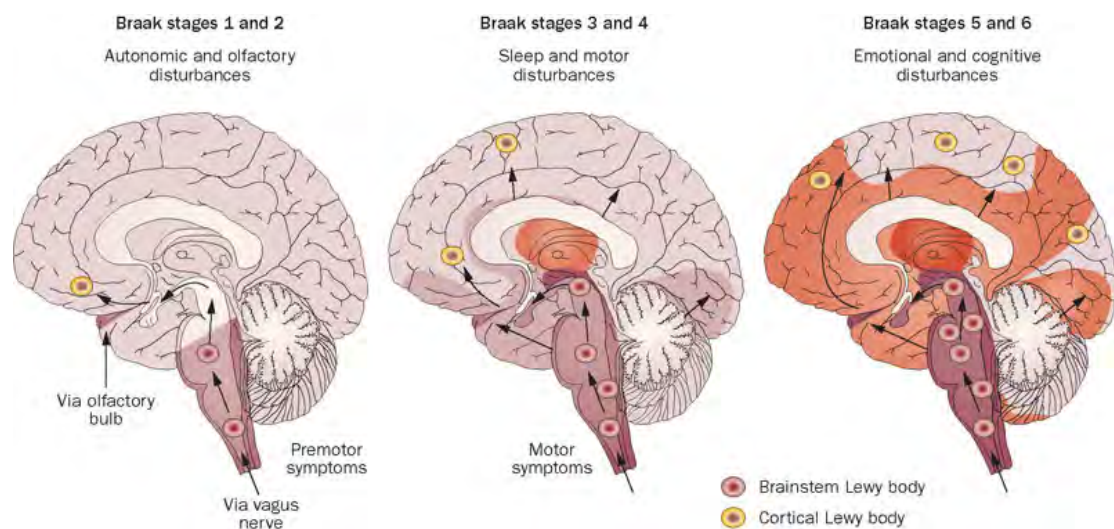


Figure 12. Description of the Braak's stages. (Doty, 2012)



### 1.3.4 - Basal ganglia and Parkinson's disease

As exposed in a preceding chapter, the basal ganglia are playing a critical role in the modulation of the motor behaviors. In PD, the slow degeneration of nigro-striatal projections will have a dual impact on the direct and indirect striatofugal projections. In normal conditions, the direct pathway, which expresses D1 receptors on its surface, will send GABAergic projections to the SNpr and to the GPi. Those inhibitory afferences on the GPi and SNpr will reduce the inhibition of those nuclei on the thalamus and so, ultimately, facilitate the movements. In contrary, the indirect projections that are expressing D2 receptors and will have an inhibitory effect on the generation of the movement through their GABAergic projections to the STN and the GPe. The STN, which sends glutamatergic efferences to the SNpr/GPi, will so be inhibited, and so, the global outputs reduced (DeLong and Wichmann, 2007; Wichmann and DeLong, 1996).

In PD, the diminution of the dopamine will, on one side, reduce its excitatory effect on the direct pathway by its action on D1 receptors and, on another side, reduce its inhibitory action on the indirect pathway through D2 receptors (Gerfen, 1995; 1992a; Obeso et al., 2009). This process will finally leads to a hypokinetic behavior. Metaphorically, the dopaminergic depletion will press on the break and release the accelerator pedal (figure 13).

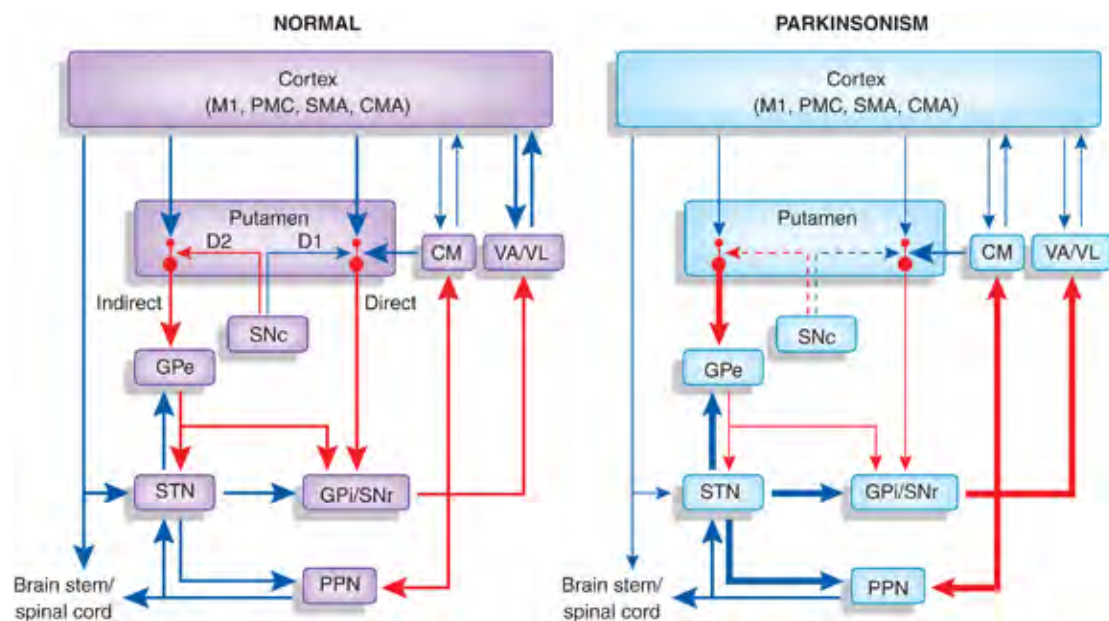


Figure 13. Schematic representation of the impact of dopaminergic depletion on the basal ganglia (Smith et al. 2012).

This phenomenon is associated with an abnormal synchronization of the different structures. It was hypothesized that this oscillatory activity was implicated, among other things, in the tremulous component of PD (Hammond et al., 2007; Rodriguez et al., 1998). This theory is supported by the fact that high frequency deep brain stimulation (DBS) of the STN will reduce both, the tremors and the rate of synchronization of the basal ganglia (A.-L. Benabid et al., 2009; Hammond et al., 2007).

As exposed in the previous chapters, the basal ganglia are not only implicated in the regulation of motor behaviors but also in cognitive and emotional processes through parallel loops. Such a dramatic change as the degeneration of the dopaminergic inputs will have important consequences on almost all associated functions. However, the mechanisms implicated are still largely unknown (Bartels and Leenders, 2009).

### **1.3.5 - Treatments**

#### ***Pharmacological***

Nowadays, several drugs are available for the treatment of PD patients. As the major symptoms in PD are resulting of a lack of dopaminergic inputs on the striatum, the main approach was to apply dopamine replacement strategies in order to restore normal motor functions.

Those treatments could be split into two main categories:

- The dopaminergic agents, which encompass the L-DOPA and the dopaminergic agonist.
- The non-dopaminergic agents.

Due to the different modes of action of those treatments, they are offering large possibilities of combinations and the possibility to adapt the therapeutic strategies in order to fit at best to each patient's characteristics. However, it is important to keep in mind that none of the mentioned treatments are stopping the progression of the pathology but that they are rather palliating the symptoms.

Levodopa remains certainly the gold standard for the early treatment of PD. This dopamine replacement treatment was discovered already in the middle of the 20<sup>th</sup> century by Alvin Carlsson following animal experiments for which he was awarded by the Nobel price (Carlsson et al., 1957). The idea was quite simple: to replace the lack of dopamine by administrating a pharmacological substitute. As dopamine itself is not able to cross the blood-brain barrier, a precursor is administered. After entering the brain, the levodopa penetrates the dopaminergic neurons and is then converted into dopamine by the dopa-decarboxylase (DDC) enzyme. It is in general co-administrated with carbidopa, a decarboxylase inhibitor that will prevent systemic degradation of the L-DOPA and increase its bioavailability and concentration into the brain. Unfortunately, following a long period of efficiency called "honeymoon phase", the therapeutic window becomes

narrower and the patients have to face the so called On/Off periods that correspond to good response to the treatment (On) and to an ineffective period (Off) (Davie, 2008). In addition, the “On” periods are frequently accompanied by disabling side effects called dyskinesia (Schrag and Quinn, 2000).

Contrary to the levodopa, the dopa-agonists will act directly on the dopamine receptors. Different classes of dopa-agonists will bind on different types of dopamine receptors. Compared to levodopa, the dopa-agonists have a longer half-life and are less potent to induce dyskinesia. Yet, dopa-agonists are less effective to correct the motor impairments of PD and have been shown to induce behavioral side effects like compulsive shopping or hypersexuality (Rascol et al., 2000).

Several other pharmacological agents are also used for their indirect impact on the dopaminergic function. For example, catechol-o-methyl transferase (COMT) inhibitors and the monoamine oxidase type B (MAO-B) inhibitors are down regulating the degradation of the dopamine in order to provide it a longer half-life whereas amantadine plays role in the control of the dyskinesia through its interactions with glutamatergic neurons.

## ***Surgical approaches***

Already during the 50's patients with severe parkinsonism were subjected to undergo surgical interventions. At the time, they consisted mainly in the ablation of the contralateral thalamus. Later on, and with the advances of the knowledge concerning the basal ganglia, the surgeons focused their intervention on the ablation of the pallidus (pallidotomy). This technic led to an improvement of the motor symptoms but had as inconvenient to be irreversible with possible dramatic consequences.

The discovery of the DBS and its applications by Benabid and colleagues in 1987 was a game changer in the therapeutic scope of PD. This technic consists in introducing thin electrodes into the basal ganglia and to stimulate at high frequency specific nuclei in order to inhibit them (figure 14). A generator is remotely placed on the clavicle and will allow fine-tuning of the electric stimulation. During the last 30 years, extensive clinical trials have been conducted and different possible targets tested including the *thalamic nucleus ventralis intermedius* (VIM), the GPi and the STN (A. Benabid, 2003; A.-L. Benabid et al., 2009; BENABID et al., 1987). Nowadays, the two most common targets for PD treatment are the STN and the GPi. Both are showing comparable improvement of the motor symptoms but with slightly different side-effects and indications (Follett et al., 2010; Odekerken et al., 2013; Stern et al., 2013; Williams and Okun, 2013). Up-to-date, more than 100'000 PD patients have been implanted with important improvement of their quality of life.

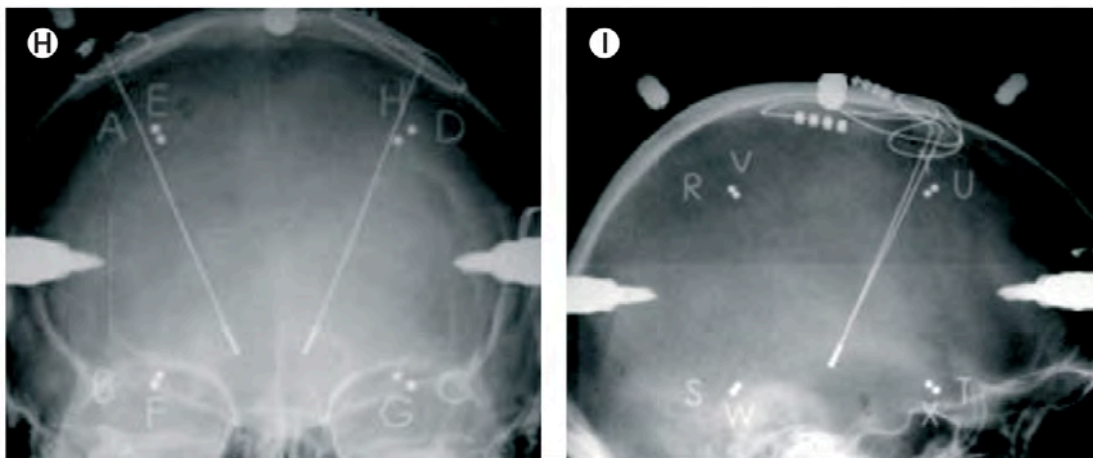


Figure 14. Radiographies of a PD patients implanted with DBS electrodes. (A.-L. Benabid et al., 2009)

On a physiological point of view, the stimulation at high frequency ( $\approx 100\text{Hz}$ ) of the STN/GPi inhibits their outputs and so re-equilibrate the balance between the direct and the indirect pathways of the basal ganglia. This will, ultimately, reduce the activity of the GABAergic outputs of the basal ganglia on the thalamus and, consequently, corrects the motor impairments (akinesia, rigidity, tremors) (Wichmann and DeLong, 2011). However, other mechanisms such as the evoked stimulation of the spared dopaminergic neurons have been recently pointed out as being potentially implicated in the motor recovery (Da Cunha et al., 2015; Molinuevo et al., 2000).

Despite the obvious positive impact of this technique on the management of PD patients, the DBS has some limitations. Firstly, the conditions for a patient to be elective for surgery are quite restrictive in order to maximize the benefice/risk ratio. Secondly, possible psychiatric side effects can arise following the implantation, such as compulsive disorder, increased risk of suicide, etc (A.-L. Benabid et al., 2009). Finally, it is important to remember that DBS is a symptomatic treatment that will not stop the progression of the pathology.

## ***Future perspectives for PD treatments***

Beside the classical treatments briefly described in the previous paragraphs, important researches were conducted during the last 30 years on the development of cell therapies for PD. This elegant concept consists in replacing the loss of dopaminergic neurons by selected cells in order to restore the motor functions.

Since the 80's, scientists have been focused on three main and distinct approaches based on different cell sources: 1) fetal mid brain tissues, 2) embryonic stem cells, 3) autologous cells (figure 15).

However, even if important progresses have been made regarding the understanding of cell engraftment mechanisms, several issues are still to be solved before considering large-scale therapeutic applications.

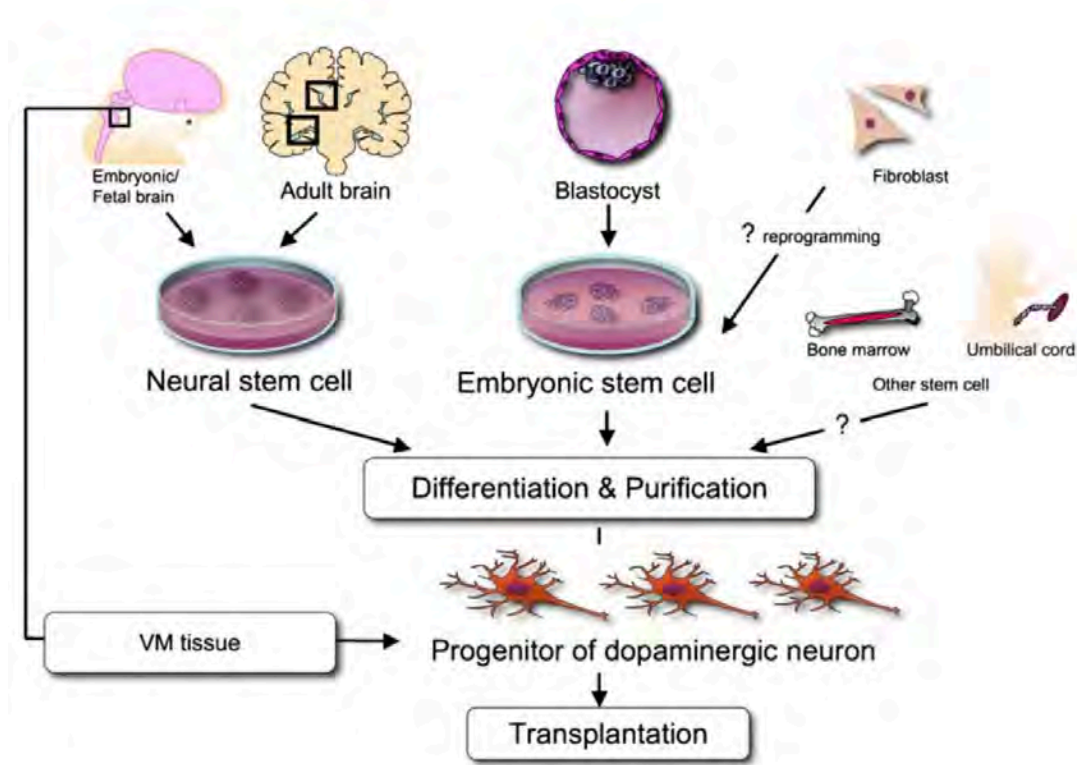


Figure 15. Different cell sources with therapeutic potential for PD treatment. (Morizane et al., 2008)

## ***Fetal tissues***

The fetal ventral mesencephalic tissues were the first cell source to catch scientific interest for PD treatment. After extensive animal testing on different models, the Swedish ethical committee gave an authorization for the first clinical trial (Bjorklund et al., 1988; Brundin and Bjorklund, 1987; Isacson et al., 1987). The same year, Brundin and colleagues achieved the first fetal tissues transplantation in PD patients (Brundin et al., 1987). Since then, more than 400 patients have been transplanted. However, the different clinical trials conducted gave contrasted results. On one hand, several studies were reporting consequent improvement of the motor symptoms including rigidity and resting tremors. Those results were supported by PET studies in which authors were able to show a significant increase in F-DOPA capitation following tissues transplantations (Brundin et al., 2000; Freed et al., 1992; Hauser et al., 1999; Kefalopoulou et al., 2014). On the other hand, two double-blind placebo controlled studies published by Freed et al. and Olanow and colleagues, were much more contrasted regarding the corrective effect of the grafted cells on the motor symptoms (Freed et al., 2001; Olanow et al., 2003).

Freed and colleagues were able to demonstrate a significant improvement of the motor score in patients younger than 60 years old. Yet, this was not the case in older patients (as it is in general the case in idiopathic PD) (Freed et al., 2001). Similarly, Olanow and colleagues failed to show any significant improvement of the motor score despite a significant augmentation of the <sup>18</sup>F-DOPA PET signal (Freed et al., 2001; Olanow et al., 2003). Those observations revealed the importance of the placebo effect in cell therapies (Freeman et al., 1999; Goetz et al., 2008). This phenomenon, which plays certainly a role in the motor improvement, was already described by Charcot at the end of the 19<sup>th</sup> century (Charcot, 1897). Moreover, some engrafted patients developed graft induced dyskinesia that were persistent even after withdraw of L-DOPA medication (off-medication dyskinesia) (Olanow et al., 2003).



In a general manner the above-mentioned studies have provided important information regarding cellular transplantation and more specially regarding a number of limitations raised by such approaches. Firstly, the important amount of fetal tissues needed for each patient (1 to 8 donors for one striatum engraftment) led to important ethical controversies. Secondly, the permanent needs of immunosuppressive drugs in order to maintain a minimal survival rate, which is directly linked to the efficacy of the grafts (Freed et al., 2001; Olanow et al., 2003). Thirdly, the possible appearance of permanent graft induced side effects. Finally, the patients selection seems to be the key to hope a positive graft outcome (Freed et al., 2001; 2004; Morizane et al., 2008).

### ***Embryonic stem cells & induced pluripotent stem cells***

The limitations coming together with the use of fetal tissues opened the doors to alternative cell sources that were extensively investigated since then. In this way, the embryonic pluripotent stem cells (ESC) were very early seen as having a great potential for the treatment of neurodegenerative disorders like PD (Lindvall, 1999). Under good conditions, ESCs exhibit two major phenotypes: 1) they are able of unlimited self-renewal; 2) they have the capacity to differentiate into almost all kind of tissues (Keller, 1995). This self-renewal capacity provides to ESCs a large advantage compared to fetal cells by solving the problematic of tissue availability and the pluripotent characteristic of those cells makes them the perfect candidate to undergo dopaminergic differentiation.

In 2000, Lee et al. and Kawasaki and colleagues published two seminal papers exposing the results of the first mouse ESC derived dopaminergic neurons transplantations. Two different techniques were used to achieve dopaminergic inductions. On one hand, Lee and colleagues decided to differentiate the ESC by exposing them to different molecules including growth factors and, on another hand, Kawasaki's team stimulated the differentiation through contact with selected mouse stromal feeder cells (Kawasaki et al., 2000; S. Lee et al., 2000). Those studies paved the way for

many other studies that showed variable behavioral results (for review (Hall et al., 2007)). In 2005, an important step was achieved with the first transplantation in a symptomatic monkey MPTP model. The results showed a significant improvement of the motor signs supported by functional neuroimaging data (Takagi et al., 2005). However, the switch from animal ESC to human ESC necessary to consider future clinical translation raised new questions and problems. In fact, the first studies using human ESC for dopaminergic induction were quite contrasted in terms of efficacy and rose the problematic of uncontrolled cellular proliferation potentially leading to tumor formation. This major safety issue was consequent to the fact that some ESC escaped the differentiation process and kept their primary characteristics including high proliferation rate (Brederlau et al., 2006; A. S. Lee et al., 2009). Another important limitation of the methods used was linked to the differentiation protocols themselves. The in-vitro differentiation processes were actually very dependent of animal products such as the use of feeder cells to support the development of neural progenitors (Ben-Hur et al., 2004; Roy et al., 2006). Such protocols were, in the state, not compatible with potential clinical use.

More recently, some researchers were able to replicate more accurately the natural development of human ESC into midbrain dopaminergic neurons (Doi et al., 2014; Kriks et al., 2011; Nakagawa et al., 2014). The cells obtained were exhibiting large similarities with “natural” dopaminergic cells and were successfully implanted in rats and monkey models with efficient behavioral corrective effects. Moreover, histological analysis revealed tumor-free grafts (Kriks et al., 2011). In 2014, Grealish et al. published a comparative study between human ESC and fetal tissues transplantation (Grealish et al., 2014). This study reported similar results between both treatments in rats and brings arguments in front of the stage for clinical translation. Nevertheless, the ethical issues remain present.

With the discovery by Yamanaka and colleagues of the possible direct conversion of fibroblasts into pluripotent stem cells, a new range of possibility was offered to researchers (Takahashi and Yamanaka, 2006). Induced pluripotent stem cells (iPSC) are generated by overexpression of four genes

in somatic cells (*Oct3/4*, *Sox2*, *Klf4*, *c-Myc*). iPSC exhibit similar characteristics as ESC including self-renewal capacity and pluripotency. A recent paper published in *Cell Stem Cell* has reported efficient and safe iPSC transplantation in MPTP treated monkeys (Hallett et al., 2015). Yet those positive results concerned only one animal out of three and have so to be considered carefully. One of the advantages of iPSC, versus ESC, is that they could be generated from the patient cells and thus avoids complicated immunotherapies. Moreover, and for the same reason, the ethical issues around ESC become obsolete.

### ***Autologous neural cell ecosystem (ANCE)***

Beside of the main research streams described in the previous chapter, several groups have been tackling the adult neural precursor cells approach (Brunet et al., 2005; Johansson et al., 1999; Uchida et al., 2000). Several papers have put in light the presence of neural stem cells in particular parts of the brain, including the dentate gyrus and the subventricular zone (Astradsson et al., 2008; Johansson et al., 1999; Morizane et al., 2008). It has been emphasized that the subventricular zone plays a role in brain repair and that the number of progenitor cells increased following brain injuries such as stroke or during Huntington's disease (Curtis et al., 2007).

In 2002, Brunet and colleagues published a new method allowing generating long-term primocultures from human cortical tissues. Following a period of incubation in preselected fetal calf serum (pFCS) the cells started to express progenitor and neuroectodermal makers like nestin, neurofilament, vimentin or glial fibril associated protein (GFAP). Similar results were then obtained from non-human primate (*Macaca fascicularis*) cortical biopsies (Brunet et al., 2005). This last experiment on monkeys additionally allowed assessing the *in vivo* behavior and survival of those cells. Following an excitotoxic cortical lesion of M1, cells obtained from previous cortical biopsies were implanted into the lesion's sties and at its periphery. One month post-implantation, the monkeys were sacrificed and histological analyses were conducted. The

implanted cells expressed nestin, the neuronal marker MAP2 and presented neuron-like morphologies (Brunet et al., 2005). Moreover, very little gliosis was observed suggesting poor immunological and inflammatory reaction.

Further investigation revealed the presence of doublecortin-positive cells (DCX+) in *in vitro* cell cultures (Bloch et al., 2011). DCX is a microtubule-associated protein that is present in migrating neuroblast and that has been pointed out to play a role in neurogenesis (Brown et al., 2003; Francis et al., 1999; Matsuo et al., 1998). In adult, DCX+ cells have been shown to be particularly present in the areas of neurogenesis including the hippocampus and the subventricular zone (Brown et al. 2003). Bloch and colleagues were able to reveal the presence of DCX+ cells in the cortex of two monkey species and human in contrast to rodent brain that were DCX-. It has been emphasized that those cells cannot be considered as stem cells but that they could encompass a neural progenitor potential (Bloch et al., 2011). *In vitro* cultures have stressed out the fact that DCX+ cells were undergoing asymmetrical divisions generating one dividing cell expressing DCX and GFAP, and one quiescent progenitor expressing only DCX. This way of division confers them a low proliferation rate and so those cells are less prone to generate tumors (Bloch et al., 2011). However, DCX+ cells alone are not able to survive. They need the close support of astrocytes, which are building a kind of niche necessary to sustain DCX+ cells development. This association is referred as adult neural cell ecosystems (ANCE).

In a therapeutic perspective, ANCE have been implanted in asymptomatic MPTP St. Kitts green monkeys. In this study ANCE were unilaterally implanted in four monkeys systemically intoxicated with MPTP. Four months post-implantation, the histological analysis revealed a surprisingly high survival with only 50% of cellular death and important migratory potential (Brunet et al., 2009). Compared to control MPTP monkeys, the reimplanted ANCE had a significantly higher rate of TH+ cell both in the striatum and in the SNpc. It was postulated that ANCE are producing neurotrophic and neuroprotective factors. This was supported by the detection of GDNF and BDNF in the culture medium and by immunodetection of a significantly higher level of GDNF around the implantation sites (Brunet et al., 2009).

More recently, a study on a symptomatic MPTP monkey model was published (Bloch et al., 2014). In this study, that was including seven St. Kitts green monkeys, the monkey's behaviors were assessed by blind experimenters over all the experimental process. Following the MPTP lesions, all animals were exhibiting marked to severe parkinsonian symptoms. Five out of the seven monkeys were then implanted with the cells obtained from previous cortical biopsies cultured in vitro for seven weeks according to previously published protocols (Brunet et al., 2003; 2002), one received killed cells and the last one did not received any engraftment. Six months post-implantation, the monkeys were sacrificed for histological purposes. All the ANCE implanted animals, except one, exhibited a statistically significant reduction of the symptoms while the two others (shame and killed graft) did not show any improvement. The monkey that received the treatment but did not respond was engrafted with twice more cells than the others, which may indicate a therapeutic limit in terms of cell quantity. Histological readout revealed a survival rate of about 30% and a significantly higher TH+ cells in all transplanted animals as compared to the non-implanted or shame implanted animals (Bloch et al., 2014).

Taken together, the studies reported above gave promising support for future clinical applications. The ANCE exhibits clear advantages in comparison with fetal tissues and ESCs: 1) Their high survival rate, 2) the poor inflammatory reaction and the absence of immunorejection 3) their high migration capacity 4) the low risk of tumor formation (Bloch et al., 2014; 2011; Brunet et al., 2009; 2005).

Moreover, the implantation of ANCE has been shown to be followed by behavioral recovery in non-human primate model of PD (Bloch et al., 2014). One major limitation remains, however, the lack of information regarding the fate of those cells and the mode of action underling functional recovery.

## ***1.4 - Non-human primate MPTP model***

The accidental discovery during the 80's of the 1-methyl-4-phenyl-1,2,3,6-tetrahydropyridine (MPTP) provoked a little revolution in the field of PD research by providing a whole new insight on its pathophysiology (Kopin and Markey, 1988; Langston et al., 1983). By its proximity to the human pathology, non-human primate (NHP) MPTP models are still considered as the gold standard for physiological investigation or for preclinical evaluation of new treatments (Emborg, 2007; Forno et al., 1993; Imbert et al., 2000). Systemic injections of MPTP gradually destroy the dopaminergic neurons and consequently provoke the appearance of parkinsonian motor symptoms, including bradykinesia, rigidity, akinesia, postural instability and tremors. Parkinsonian monkeys also exhibit a number of non-motor symptoms such as cognitive impairments and sleep disturbances (Blesa et al., 2010; Schneider and Kovelowski, 1990).

Similarly to PD, the dopaminergic depletion in NHP MPTP model follows the same global pattern with more prominent cell loss in ventral and lateral segments of the SNpc, as compared to VTA (Varastet et al., 1994). This seems to be due to a particular susceptibility of the neuromelanin containing neurons (Herrero et al., 1993).

Concretely, electrophysiological experiments allowed to underline the role of the STN hyper activation in the appearance of motor symptoms and to build strong basis for therapeutic strategies, like high frequency DBS that is now validated for clinical use (Bergman et al., 1990; Limousin et al., 1995). Moreover, MPTP treated monkeys are Levodopa responsive and develop, on the long term, dyskinesia, offering a suitable model for researchers and clinicians.

The model has, despite of that, some limitations. Firstly, unlike in PD, histological readouts did not reveal the presence of Lewy body-like structures, although some neuronal inclusion can be found (Forno et al., 1993). Secondly, the impact of the toxin on other monoaminergic systems seems to differ from the human pathology (Forno et al., 1993; Pifl et al., 1991). Finally, the large inter-individual variability of responses to the treatment remains an important limitation in terms of reproducibility (T. Collier et al., 2003).

On a molecular point of view, the MPTP, which is a highly lipophilic molecule, easily and quickly passes the blood brain barrier (Markey et al., 1984). As

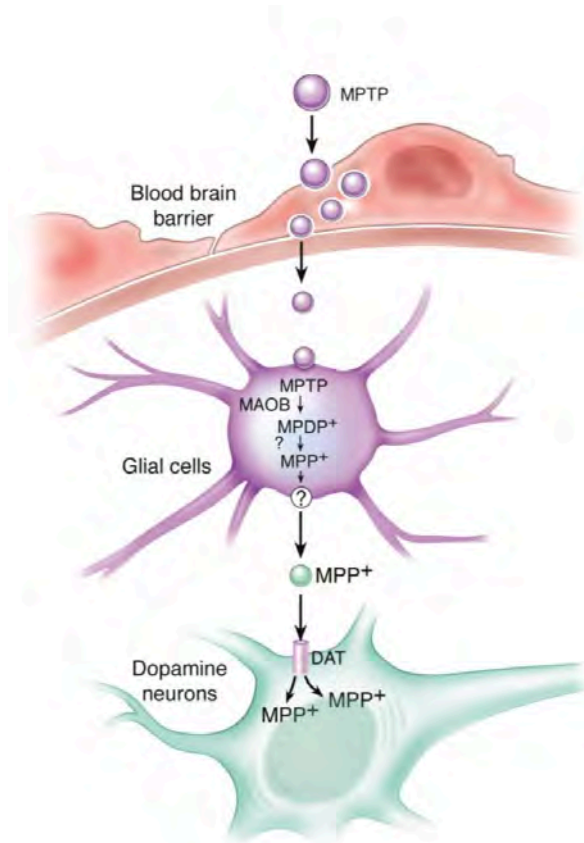


Figure 16. Illustration of the conversion of MPTP into MPP+ at cellular level. (Dauer, 2003)

MPTP itself is not toxic, it needs to be converted into 1-methyl-4-phenylpyridinium (MPP+) by monoamine oxidase B (MAOB) (figure 16). This enzyme is present only in glial cells and serotonergic neurons. MPP+ is then transported inside the dopaminergic neurons by dopamine transporters (DAT) (Mayer et al., 1986). Once inside the neuron, the MPP+ enters the mitochondria and interferes with the complex 1 that plays an important role in the respiratory chain (A. Schapira et al., 1989). Although the exact mechanisms inducing

cellular death remain unclear, the decrease of ATP production and the augmentation of the ROS production by the intoxicated mitochondria are both placed in the dock.

In summary, the MPTP NHP model remains, so far, a crucial source of information and an important step towards clinical trials for new treatments (Barraud et al., 2009; T. Collier et al., 2003; Porrás et al., 2012; Wichmann and DeLong, 2003). Moreover, the proximity of NHP neuroanatomy and especially of its motor system to the human one allows fine monitoring of the animal behavior as well as to assess the potential side-effects of treatments (Courtine et al., 2007).

## 1.5 - Neuroimaging and PD

Although over the last 30 years neuroimaging techniques have undergone extensive improvements, their roles in the clinical management of PD patients remain secondary. The important costs of those techniques and the difficulties to interpret their results certainly represent important limitations to the generalization of their use in clinical routine (Brooks, 2010; Politis, 2014). However, when analyzed by trained specialists, those imaging techniques can represent a major asset in terms of differential diagnosis and can avoid extra burdens for patients and extra costs to the health system (Bajaj et al., 2013; Politis, 2014). In terms of research, the information provided by structural and functional imaging techniques are worthwhile for clinical and basic investigations by offering an insight into pathophysiological processes as well as a follow-up possibility for the development of new therapeutic strategies. Historically, the *in vivo* investigation of the dopaminergic system was the first to tackle scientists' interest in regards with PD.

$^{18}\text{F}$ -DOPA is a radiotracer resulting of the fluorination of L-DOPA. Once injected into the vascular system,  $^{18}\text{F}$ -DOPA will rapidly cross the blood-brain barrier where it will be converted into  $^{18}\text{F}$ -fluorodopamine by the dopa-decarboxylase at dopaminergic neurons' terminals. The  $^{18}\text{F}$ -DOPA tracer was already used during the 80's for research purposes. The images obtained with PET scan setup allowed the first *in vivo* observations of the striatal dopaminergic activity in human (Garnett et al., 1983). Those observations were followed by a large number of investigations on human and animal models of PD (Blesa et al., 2010; Guttman et al., 1988; Morrish et al., 1996; Thobois et al., 2001). Moreover,  $^{18}\text{F}$ -DOPA PET was very early seen as an important tool for the assessment of the functional impact of cell transplantation therapeutic strategies (Brundin et al., 2000; Doudet et al., 2004; Lindvall et al., 1990; 1989; Olanow et al., 1996; Politis, 2010).

On a clinical point of view,  $^{18}\text{F}$ -DOPA PET data offers an objective way to assess the state of the dopaminergic system (Brooks and Pavese, 2011). Those measures can be useful to discriminate patients with neurodegenerative disorders from those without and as well as a follow-up tool of the disease progression. However, the differential diagnosis between



idiopathic PD and atypical forms of parkinsonism remains very limited due to visually similar patterns of degenerations, although some subtle differences have been underlined (Darcourt et al., 2014).

More recently,  $^{123}\text{I}$ -ioflupane SPECT has been introduced and validated for clinical use in PD (Booij et al., 1997b).  $^{123}\text{I}$ -ioflupane is a radiotracer composed by a cocaine analog molecule labeled by iodine isotope 123 ( $^{123}\text{I}$ ). This radiotracer has a high affinity with the presynaptic dopamine transporters (DAT). As the striatal DAT density has been highlighted to be inversely correlated with parkinsonian symptoms,  $^{123}\text{I}$ -ioflupane SPECT has been seen as a potent tool for monitoring PD progression (Baldwin et al., 1995; Booij et al., 1997b; 1997a; Kaufman and Madras, 1991). Similarly to  $^{18}\text{F}$ -DOPA PET,  $^{123}\text{I}$ -ioflupane SPECT is useful in clinic for differentiating degenerative cases of PD from pathologies that did not affect the dopaminergic system. Despite of that, the distinction between the atypical forms of parkinsonism is still not reliable (Bajaj et al., 2013; Brooks, 2012; Djang et al., 2012; Gaig et al., 2006; Kägi et al., 2009; Marek et al., 2000; Marshall and Grosset, 2003; Pirker et al., 2000a).

In a general manner, literature did not underline any differences between PET and SPECT techniques in terms of diagnosis accuracy (Burn et al., 1994; Politis, 2014). Nevertheless, compared to  $^{18}\text{F}$ -DOPA PET,  $^{123}\text{I}$ -ioflupane SPECT is more advantageous in terms of costs and more convenient to use because of the longer half-life of its isotope. Moreover, in contrary to  $^{18}\text{F}$ -DOPA PET,  $^{123}\text{I}$ -ioflupane SPECT acquisitions are much less prone to be influenced by dopaminergic substitutive drugs (Ahlskog et al., 1999; Innis et al., 1999).

If the functional imaging techniques described above play an important role in research and in the clinical management of PD patient, structural imaging data are also of primary interest. Magnetic resonance imaging (MRI) allows the acquisition of structural data that provide a direct insight into the patient's neuroanatomy. In PD, MRI is in general used to exclude secondary causes of parkinsonism like the presence of tumor, of micro-bleeding (vascular

parkinsonism), of abnormal pressure hydrocephalus, etc. (Brooks, 2010). It is conventionally accepted that classical MRI sequences (T1, T2) performed on 3 Tesla scanners are not able to reveal significant modification in PD that would be appropriate for clinical use (Brooks, 2010). Despite of that, many researchers investigated the potential of newly introduced MRI sequences. For instance, the use diffusion tensor imaging (DTI) which assesses diffusion of water into the brain, has revealed some interesting modifications within the SNpc related to PD (Prodoehl et al., 2013). Susceptibility weighted imaging (SWI), which is able to reveal iron deposition, has recently been used by Schwartz and colleagues who have pointed out the disappearance of a “swallow tail” pattern in the midbrain in PD patients (Haacke et al., 2004; Schwarz et al., 2014).

Besides of diagnostic purposes, MRI techniques play a crucial role in the preparation of surgical interventions. For example, the DBS requires an extreme precision in the selection of the targets that will be stimulated in order to optimize the benefice-risk ratio (A.-L. Benabid et al., 2009).

In summary, there are many different radiotracers and MRI sequences that are used for particular purposes in specific pathologies. However, none of them are currently able to discriminate accurately the different forms of parkinsonism. In the future, the combination of different neuroimaging modalities will certainly be a key feature to sustain more accuracy in differential diagnosis (Haller et al., 2014).

## **1.6 - Context and objectives**

This Ph.D. thesis was originally part of a large consortium composed by seven research teams each highly specialized in a particular and complementary domain. The project, called “Prometheus” (Sinergia project of Swiss National Science Foundation), aimed at developing a new therapeutic strategy based on human embryonic stem cells, from cellular basis towards clinical application. The close interactions between the partners, coming from cell biology, animal experimentation, neurology, neurosurgery, ethics, safety and immunology, was supposed to result in a synergic effect leading to human application within an extremely short timeframe of four years. However, despite keen interest, the consortium failed at providing human stem cells fulfilling the safety and efficacy criteria required for preclinical testing on monkeys and, *de facto*, for clinical trial purposes.

Along general lines, different batches of stem cells were produced according to different differentiation protocols. Those cells were then implanted into the striatum of NOD/SCID mice that are deprived of immune system. The first batches of cells, after implantation, generated massive teratoma, certainly due to the poor level of differentiation of the ESC. With a better selection of the cells, the group of Prof. Krause at Geneva University was able to produce cells with lower proliferation rate and that were better characterized. Nonetheless, neuroepithelial tumors and strong astrocytic reactions were observed in subsequent histological analyses. Under those conditions, the transfer to the non-human primate model was totally excluded for ethical reasons. Additionally, the implantation of human cells into the brain of non-human primates also raised the problematic of the immune response. Although the immunosuppression of the monkeys was theoretically possible using cyclosporine or tacrolimus, however at massive doses, the impact of those heavy treatments on the fates of the implanted cells remained uncertain, without mentioning possible secondary effects on the monkeys.

Meanwhile, at the University of Fribourg, four monkeys (*Macaca fascicularis*) were trained to perform motor tasks in order to evaluate their motor ability in the context of this Sinergia project. After three years of daily training, the monkeys that reached a so-called “plateau of performance” were ready for

MPTP lesions and cell engraftments. Despite the lack of results concerning the stem cells production, they were maintained during several months in case of a significant improvement regarding the safety and efficacy standards. Unfortunately, for different reasons, the results of cell implantations conducted at University of Geneva on rodents were not convincing enough to go for a translation on the non-human primates in Fribourg.

In this particular context, in order to reallocate the tremendous preparatory work that was conducted on the four macaque monkeys, it was decided to reorient the project by considering an alternative source of cells to re-implant after MPTP treatment. Taking advantage of a former collaboration between Prof. Rouiller's group and the University Hospital of Lausanne (CHUV), with Dr. Jean-François Brunet and Dr. Jocelyn Bloch, on autologous adult progenitor cells transplantation as therapeutic strategy tested on a primate model of stroke (Bloch et al., 2011; Brunet et al., 2005; Kaeser et al., 2011), we decided to adopt the same therapeutic strategy, but on MPTP monkeys in the present case.

As mentioned in the chapter regarding cellular treatment of PD, Dr. Jean-François Brunet and Dr. Jocelyn Bloch published several articles providing promising results regarding ANCE transplantation in a MPTP non-human primate model of PD (Bloch et al., 2014; Brunet et al., 2009). They were able to show a significant improvement of the motor function in transplanted monkeys as compared to control animals; in addition, there was an impressive survival rate of the engrafted cell. However, in the perspective of future clinical trials, several questions still needed to be answered and this was the goal of the present Ph.D. thesis work.

To summarize, at some point Prof. Rouiller's team had four monkeys ready for MPTP lesion and for an experimental cell transplantation protocol whereas the team at the CHUV aimed at testing new hypotheses regarding their ANCE approach on a similar model of PD. Moreover, due to the autologous nature of the cells to be transplanted, this new protocol would solve two major issues raised by hESC based therapies: 1) the safety obstacle linked to the high risk

of uncontrolled cell proliferation. 2) The problematic of the immune rejection and the impact of immunosuppressive drugs on the cell development.

In the context of these mutual interests between the colleagues at the CHUV and our team in Fribourg, mid 2013, the decision was taken to go for the autologous cells transplantation strategy and to adapt our protocol to the new steps required. As specified above, Bloch and colleagues (2014) already provided some evidences of the efficacy of ANCE transplantation by comparing treated animals with controls. As the present study included only a limited number of animals (four monkeys), the strategy was rather to assess them on an individual basis and to monitor them with quantitative and qualitative follow-up tools. In other words, each monkey was his own control. A major and original emphasis of the present thesis lies in a specific bias to evaluate quantitatively distal motor function (manual dexterity), a motor attribute which was relatively poorly covered in previous MPTP monkey studies. This thesis was fully integrated in all aspects of this project from behavioral assessment of the animals to neuroimaging and histological readouts. The specific goals of the present Ph.D. thesis were as follows:

- 1) To generate quantitative behavioral data regarding the impact of the cortical biopsies on the motor function, with emphasis on manual dexterity.**
- 2) To provide a refined assessment of the motor control in a MPTP non-human primate model engrafted with ANCE.**
- 3) To provide quantitative data regarding the impact of the ANCE on the dopaminergic system, *in vivo*, using <sup>18</sup>F-DOPA PET technology.**
- 4) To provide data regarding the fate of the transplanted cells and their impacts on the host's striatum through histological analysis.**

Beside of this preclinical study, a former collaboration with Prof. Pierre Burkhard, from the department of neurology at the University Hospital of Geneva (HUG) and Prof. Sven Haller from the service of neuro-diagnostic and neuro-interventional DISIM, HUG, awaken in me a great interest for clinical neurosciences and neuroimaging. Several chapters of the present thesis derive from these collaborations.

Between 2003 and 2013, almost 1000 patients have undergone  $^{123}\text{I}$ -ioflupane SPECT scans for clinical purposes at the HUG. Individually, those scans provided important information for patients' differential diagnosis but their value for research purposes remained very limited. Nevertheless, taken together those data represent a goldmine for the clinical researchers.

Regarding the neuroimaging part of this thesis conducted at the HUG, the main objectives are listed below.

- 1) To generate a neuroimaging database for clinical research purposes based on a pool of almost 1000 patients that have undergone  $^{123}\text{I}$ -ioflupane SPECT scans.**
- 2) To take advantage of this database in order to produce new information regarding the pathophysiology of different parkinsonian pathologies.**
- 3) To investigate the potential of computer assisted differential diagnostic tools for future clinical applications.**

In a general manner, the opportunity was given to me to conduct both projects in parallel (human and NHP) that are representing, in my view, the two faces of the same coin. On one hand, the clinical investigation would provide me a direct and concrete insight on PD related issues and, on the other hand, the preclinical part of this thesis on NHP would allow me to tackle those issues

form a different perspective. Ultimately, the idea was to generate a synergic effect and to potentially build new bridges between basic and clinical research in order to take a step forwards towards an improvement of PD patient's quality of life.





## ***2 - Materials and Methods***



This chapter aims at providing a broad overview of the different techniques used to generate the results of the present thesis. Some specific procedures will nevertheless be described in full details in the corresponding chapter/article of the results part.

## **2.1 - Clinical neuroimaging**

### **2.1.1 - Patients and diagnosis**

All the procedures performed in the frame of this study were approved by the local ethical committee. A total of 970 patients were consecutively scanned following a  $^{123}\text{I}$ -ioflupane SPECT protocol, over a period extending from October 2003 to September 2013. The diagnoses were set by an experienced movement disorders specialist following extensive neurological assessments and confirmed by follow-up (at least one year). The PD diagnosis was settled according to the UK Parkinson's disease society brain bank criteria that encompass mandatorily the presence of bradykinesia combined with, at least, one of the following signs: postural instability, 4-6 Hz tremor at rest or rigidity. A clear and sustained response to levodopa was, among others, considered as a supportive feature.

Atypical forms of parkinsonism that encompass multiple system atrophy (MSA), corticobasal degeneration (CBD) and parasupranuclear palsy (PSP), were diagnosed according to established criteria.

$^{123}\text{I}$ -ioflupane SPECT neuroimaging data were mostly used to exclude pathologies that do not affect the dopaminergic system as, for example, essential tremors, psychogenic parkinsonism or drug-induced parkinsonism. MRI based structural imaging data were used by a trained neuroradiologist to exclude patients with brain micro bleeding or with anatomical abnormalities such as hydrocephalus.

## **2.1.2 - Images acquisitions**

### **2.1.2.1 - $^{123}\text{I}$ -ioflupane SPECT**

Patients were all scanned with the same triple-head gamma camera (Toshiba Medical Systems, Tokyo, Japan) with fan-beam, low-energy, high-resolution collimator. The scans were performed four hours after intravenous injection of about 185 MBq of  $^{123}\text{I}$ -ioflupane, following sodium perchlorate or Lugol solution intake for thyroid's protection purposes. The acquisition was done with a 128x128 matrix, by frames of 6° over 360°. Images were corrected for photon attenuation and scatter.

### **2.1.2.2 - MRI**

MRI acquisitions were conducted as part of the clinical routine over a period of ten years. For this reason variable MRI sequences were collected depending on patients' specific characteristics. However, all patients had a minimum of a T2, fluid attenuation inversion recovery (FLAIR) and diffusion tensor imaging (DTI) or diffusion weighted imaging (DWI) to assess anatomical brain integrity. MR system (Magnetom Trio, Siemens, Erlangen Germany) 3.0 Tesla was used to obtain the data.

### **2.1.3 - Image post-processing**

All DICOM (Digital Imaging and Communications in Medicine) images were firstly converted into nifty format using dcm2nii software (NITRC© 2010) to be subsequently analyzed with FSL (FMRIB Software Library version 5.0 <http://fsl.fmrib.ox.ac.uk/fsl/fslwiki>). The procedures specific to each investigation are described in details the corresponding chapters (3.1.1– 4).

### **2.1.4 - Statistical analysis**

Statistical analyses were performed with GraphPad Prism (version 6.0, [www.graphpad.com](http://www.graphpad.com)), Matlab and FSL.

## **2.2 - Preclinical assessment of ANCE transplantation in NHP (non-human primate) MPTP model**

All experimental procedures performed during this study were covered by the veterinary authorisation n° FR 22010, issued by the veterinary office of the canton of Fribourg.

### **2.2.1 - Experimental protocol**

In a global manner, the present study could be split into three main phases: the pre-lesion phase, the post-lesion phase and the post-implantation phase. The pre-lesion phase ranged from spring 2010 to summer 2014 and encompasses the training of the animals to the different motor tasks. The post-lesion phase consisted in the behavioural follow-up of the monkeys, during a period of eight weeks, to assess the impact of the MPTP lesion on their motor performances. Finally the post-implantation phase, that covered a period of six months, was dedicated to the monitoring of the monkeys in order to assess any potential effect of the treatment. As the treatment tested is based on *in vitro* culture of cortical tissues, two biopsies were obtained for each animal (one during the pre-lesion phase and one during the MPTP protocol).

Within each period the state of the dopaminergic system was assessed by <sup>18</sup>F-DOPA PET scans. Moreover, structural MRI images were acquired to determine the location of the biopsies and to identify the stereotaxic coordinates needed for the transplantation surgeries. At the end of the protocol, the monkeys were sacrificed for histological purposes. The time course of the experiment can be found in figure 17.

# Experimental schedule

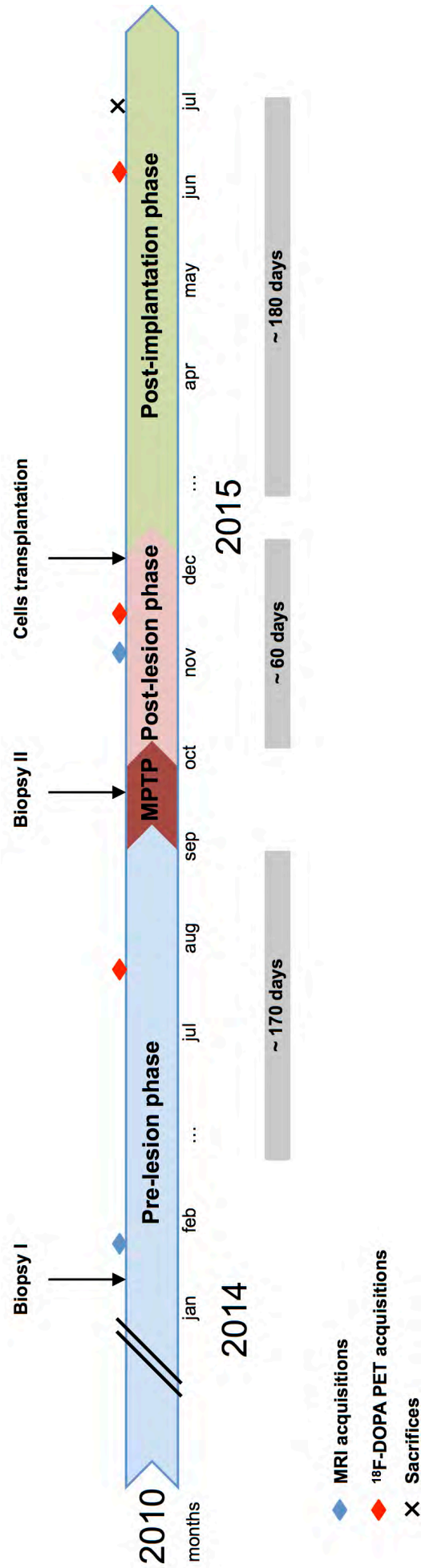


Figure 17. Timeline representing the major steps of the project. The periods in light grey are indicating the data presented in this thesis.

### **2.2.2 - Animals**

Four young adult female macaque monkeys (*Macaca fascicularis*) weighing between 3 and 5 kg and aged from 6 to 10 years old were included in the present investigation. They were kept in captivity in an animal house facility at the University of Fribourg fulfilling all guidelines enforced by the Swiss legislation. The 45m<sup>3</sup> room that had a direct access to an outdoor aviary, was enriched for the wellbeing of the monkeys. Moreover the animals had free access to water. They were fed on a daily basis, at once at the end of each experimental session. The food rations were composed by pellets specially adapted to their needs and by fresh vegetables and fruits. Additionally, the health statute of each monkey was closely monitored by different measures including weight follow-up, global state and social behaviour assessments.

### **2.2.3 - Behavioural assessments**

As mentioned above, the monkeys' behaviors were continuously monitored during all phases of this study on a daily basis. The data were collected with the help of the VigiePrimate software and of two specific motor tasks: the modified Brinkmann board task and the reach and grasp drawer task. Following several years of training, the monkeys reached a so-called "plateau of performance". This plateau corresponds to a stable level of performance that can then be used as a reference to assess the impact of the MPTP lesion and to monitor a possible effect consecutive to cells transplantation. This particular method allowed performing intra-individual comparisons. In other word, each monkey was her own control (comparisons across the three phases mentioned above).

#### **2.2.3.1 - Spontaneous activity**

The spontaneous motor activity of each monkey was recorded individually with the help of the VigiePrimate® system developed by ViewPoint® behavior

technology (Lyon, France). The animal's activity was measured daily, during a period of 30 minutes at the beginning of each experimental session. The detailed protocol is described in chapter 3.2.2.

### **2.2.3.2 - Motor tasks**

As mentioned above, the four monkeys were extensively trained to perform two motor tasks. The modified Brinkmann board task was scheduled daily while the reach and grasp drawer task was performed two to three times a week (working days).

The full procedure regarding animals' handling is detailed in annex 3.

#### **2.2.3.2.1 - Modified Brinkman board task**

Composed by 50 slots (25 horizontal and 25 vertical), the modified Brinkman board allows to quantify the fine manual dexterity by forcing the animal to use the precision grip (opposition of the thumb and index finger) in order to retrieve food rewards consisting of banana pellets. The modified Brinkman board task has been described in detail in previous reports from our laboratory (e.g. Rouiller et al., 1998; Liu and Rouiller, 1999; Schmidlin et al., 2011; Kaeser et al., 2013). Video analyses of the daily sessions allowed then to generate behavioral scores reflecting manual dexterity, as well as identifying behavioral strategies' patterns. The full procedure is described in chapter 3

#### **2.2.3.2.2 - Reach and grasp drawer task**

The reach and grasp drawer task consists in a setup composed by a drawer and multiple sensors. In this task, the monkey has to grasp the knob of the drawer and to pull it against variable resistances (from 0N to 2.75N) and to retrieve a banana pellet inside a circular hole. This method allowed, for



example, determining the temporal sequence of a movement that involved proximal and distal muscles. The detailed protocol is presented in chapter 1.

#### **2.2.4 - MRI acquisitions**

Structural MRI images were acquired at the service of radiology of the Fribourg's state hospital (HFr) on 3.0 Tesla GE Medical system (Discovery MR750). The monkeys were placed into the setup in pronation position with the head in a knee antenna (C-GE-HDx TR Knee PA, G-CoilType=8). The acquisition's parameters of the 3DT1 sequence were the following: 0.7mm isotropic voxel; TE=3.0/TR=7.2; 256x256 acquisition matrix. For the wellbeing of the animals and to avoid any movements' artifacts, they were fully anesthetized according to a specific protocol specially adapted to their physiology. The anesthesia induction was performed at the animal facility by intramuscular injection (i.m) of a mixture of midazolam (0.1mg/kg) and ketamine (10mg/kg). A continuous intravenous (i.v.) perfusion (3.75 mg/kg/h) of a mixed solution of propofol 1%, ringer-lactate and ketamine (ringer-lactate 20ml, ketamine 1.25ml, propofol 20ml) was used to maintain the anesthesia during the whole procedure. Additionally, the animal's heart rate was closely monitored by electrocardiogram (ECG) and the anesthetics perfusion adapted to individual reactions. They also received oxygen supply to optimized blood saturation (3.0l/min).

At the end of each MRI session, the animals were surveyed during a period of about 4 hours to track anesthesia related complications.

#### **2.2.5 - PET acquisition**

The PET data acquisitions were performed at the Hfr on the four animals at during main phase of the project (figure 17). The protocol consisted in a 1.5 hours dynamic acquisition (28 frames) following the i.v. injection of  $^{18}\text{F}$ -DOPA ( $\approx 125$  MBq). The detailed PET acquisition procedure can be found in chapter 3.2.2.

### 2.2.6 - MPTP lesions

Due to the highly toxic nature of MPTP, the protocol of lesion was conducted in accordance with the American national institutes of health (NIH) recommendations and based on a technical review (Przedborski et al., 2001). The present protocol was adapted after Mounayar and colleagues' publication (Mounayar et al., 2007). It consisted in series of daily i.m. MPTP (0.5mg/kg; MPTP-HCl; Sigma-Aldrich Co., dissolved in saline solution) injections, separated by break periods (table 1). To avoid extra burdens for the animals and to ensure experimenters' safety, the monkeys were mechanically restrained in a specially adapted cage to perform the injections. The total amount of MPTP injected varied from 6.25mg/kg to 7.75mg/kg. During the whole procedure, the animal were closely monitored by trained experimenters and the level of the lesions were assessed using the Schneider MPTP rating scale (Schneider et al., 1995). During the last week, and according to the symptoms exhibited by each individual monkey, the decision was taken to adapt or not the amount of MPTP injected (table 1).

Days	Dosage mg/kg			
	Mk-MI	Mk-MY	Mk-LY	Mk-LL
1	0.5	0.5	0.5	0.5
2	0.5	0.5	0.5	0.5
3	0.5	0.5	0.5	0.5
4	0.5	0.5	0.5	0.5
Break	0	0	0	0
10	0.5	0.5	0.5	0.5
11	0.5	0.5	0.5	0.5
12	0.5	0.5	0.5	0.5
13	0.5	0.5	0.5	0.5
Break	0	0	0	0
17	0.5	0.5	0.5	0.5
18	0.5	0.5	0.5	0.5
Break	0	0	0	0
30	0.5	0.5	0.25	0.25
32	0.5	0.25	0.25	0.25
34	0.5	0.25	0.25	0.25
36	0.75	0.25	0.25	0.25
37	0.5	0	0.25	0.25
<b>Total</b>	<b>7.75</b>	<b>6.25</b>	<b>6.25</b>	<b>6.25</b>

Table 1. MPTP injections' schedule and dosage per animal.

### **2.2.7 - Cortical biopsies**

Two cortical biopsies were obtained from each monkey's dorsolateral prefrontal cortex (dlPFC). The aim of the first biopsy, which was performed nine months prior to the MPTP lesion, was to assess their impact on the motor tasks of interest (modified Brinkman board and drawer task) and to refine the cell culture procedure conducted at the CHUV. The second (relevant one) biopsy was performed during the MPTP phase to be closer to the clinical reality and to provide the material needed for the cell cultures and generate the ANCE which will be subsequently re-implanted in the MPTP monkeys.

The surgeries were performed under deep anesthesia and sterile conditions. The monkeys were firstly sedated by i.v. injection of a cocktail of Dormicum and Ketamine, (Ketasol 0.1mg/kg; 10mg/kg), completed with methadone (0.2mg/kg). The premedication was composed by dexamethasone (0.3ml/kg; Dexadreson, diluted in NaCl solution 1:1; intramuscular (i.m.)) to avoid cerebral edema, antibiotics (8.75mg/kg, Synulox, subcutaneous (s.c.)), Caprofen (4mg/kg; Rymadyl, s.c.) for analgesic purposes and atropine (0.05mg/kg, i.m.). During all the surgical procedure the anesthesia was maintained by continuous i.v. perfusion (3.75 mg/kg/h) of a mixed solution of propofol 1%, ringer-lactate and ketamine (ringer-lactate 40ml, ketamine 1.25ml, propofol 20ml), similarly to the MRI protocol described previously. The head of the monkey was placed in a surgical stereotaxic frame to keep it stable during the surgical intervention. Before opening the skin, lidocaine (10mg/ml, Rapidocain) was injected subcutaneously as local anesthetic. The next step consisted in performing a little craniotomy (about 1cm<sup>2</sup>) and, subsequently, in creating an opening in the *dura mater*. During this step the monkey received an additional opioid analgesic through the perfusion (6.0µg/kg/h diluted in NaCl solution 1:1; Fentanyl). A small piece of cortex was then withdrawn from the dlPFC of each animal (about 7 to 16mm<sup>3</sup>) and immediately placed in a sterile medium and sent to the CHUV to be put in culture conditions. The piece of skull was put back in place and fixed with histological glue. Finally, the wound was sutured and disinfected.

During the procedure, the monkeys were monitored by ECG, blood saturation device and internal temperature probe. Moreover an electric blanket was used to avoid hypothermia and the animals received oxygen supply.

Postop. medication consisted in antibiotic and anti-inflammatory drugs administered twice a day for ten days *per os* (12.5mg/kg, Clavubactin; 10mg, Rimadyl).

### **2.2.8 - Cell cultures**

Once the biopsies performed, the cortical samples were immediately sent to the CHUV (centre de production cellulaire, CHUV, Epalinges) to put into culture conditions. The detailed culture procedure can be seen in (Bloch et al., 2014; Brunet et al., 2003; 2005). In contrary to the mentioned studies the present culture protocol was conducted according to the GMP (good manufacture practice) standards in a Swissmedic accredited facility. Prior to implantations, the cells were labeled with PKH67 (MINI67; Sigma-Aldrich), a fluorescent dye that irreversibly by to the cells' membrane. This step would allow to track the cells at histological analyses.

### **2.2.9 - Cells transplantation**

The first step was to determine the precise sites for the cells implantation and to extract the exact stereotaxic coordinates. This was achieved using the individual MRI structural images (3DT1 sequence) previously obtained and with the support of the Osirix<sup>®</sup> software. Each coordinate was then cross-checked with the Paxinos anatomical brain atlas of the macaque (Paxinos et al., 1999). The surgical and anesthesia protocols were the same as presented in the preceding chapter except that two windows were made on the skull instead of one, as the implantations of the ANCE were conducted bilaterally. The implantation of the cells was made with a Hamilton syringe (100µl, 22g) placed on a nano-injector (Stoelting<sup>®</sup>) fixed on the stereotaxic frame. Two sites in the putamen (one rostral and one caudal) and one site in the caudate nucleus were implanted bilaterally with 10µl of cell suspension at a flow rate of 2µl/min. After each injection, the needle was slowly withdrawn in order to avoid a suction effect that would have impacted on the position of the grafts. The number of cells transplanted per site varied from 250'000 to 400'000 (table 2).

Postoperative care was the same as described in the chapter concerning the biopsy protocol.

<b>Animal</b>	<b>Cells per spot</b>	<b>Total cells (6 spots)</b>
<b>Mk-LL</b>	401'000	2'406'000
<b>Mk-MI</b>	276'000	1'656'000
<b>Mk-LY</b>	258'000	1'548'000
<b>Mk-MY</b>	351'000	2'106'000

Table 2. Approximation of the number of cells implanted per spot for the different animals.

### **2.2.10 - Euthanasia and histology**

In order to get histological data, the animals were sacrificed about six months after the ANCE engraftments. For this purpose, the animals were firstly sedated by i.m. injection of ketamine (10mg/kg) before being gradually ECG injected with a deadly dose of sodium pento-barbital (60mg/kg, i.v.). When the monkeys were deeply anesthetized (as indicated by a significant drop of heart rate monitored with ECG) and did not respond anymore to external stimuli, the thoracic cage was opened and the transcardiac perfusion was initiated with 400ml, 0.9% NaCl. In order to block blood coagulation, 1ml of heparin was preventively injected into the left ventricle. The following solutions were successively perfused in order to fix and preserve brain tissues: 3L of 4% paraformaldehyde in 0.1M phosphate buffer (pH 7.6) and 3 times 2L of sucrose solutions of increasing concentrations (10%, 20%, 30%). The brains were then extracted and dissected before being placed for about ten days in a 30% sucrose solution. Two brains were firstly frozen with dry ice and the two other brains were directly cut into ten series of 50µm thick sections using a cryostat (HM560, MICROM, Volketswil, Switzerland). The series were then placed in a cryoprotective buffer (50mM phosphate buffer, 25% glycerol, 35% ethylene glycol) at -20°C. The detailed histological procedures are presented in chapter 3.2.2 and in annex 2.

## ***3 - Results***





## ***3.1 – Clinical neuroimaging***



## ***Chapter 3.1.1***

### ***Individual Detection of Patients with Parkinson Disease using Support Vector Machine Analysis of Diffusion Tensor Imaging Data: Initial Results***

S. Haller S. Badoud D. Nguyen V. Garibotto K.O. Lovblad P.R Burkhard

Published in American Journal of Neuroradiology (2012)



ORIGINAL  
RESEARCHS. Haller  
S. Badoud  
D. Nguyen  
V. Garibotto  
K.O. Lovblad  
P.R. Burkhard

# Individual Detection of Patients with Parkinson Disease using Support Vector Machine Analysis of Diffusion Tensor Imaging Data: Initial Results

**BACKGROUND AND PURPOSE:** Brain MR imaging is routinely performed in the work-up of suspected PD, yet its role is essentially limited to the exclusion of other pathologies. We performed a pattern-recognition analysis based on DTI data to detect subjects with PD at the individual level.

**MATERIALS AND METHODS:** We included 40 consecutive patients with Parkinsonism suggestive of PD who had DTI at 3T, brain  $^{123}\text{I}$  ioflupane SPECT (DaTSCAN), and extensive neurologic testing including follow-up (17 PD: age range,  $67.8 \pm 6.7$  years; 9 women; 23 Other: consisting of atypical forms of Parkinsonism; age range,  $67.2 \pm 9.7$  years; 7 women). Data analysis included group-level TBSS and individual-level SVM classification.

**RESULTS:** At the group level, patients with PD versus Other had spatially consistent increase in FA and decrease in RD and MD in a bilateral network, predominantly in the right frontal white matter. At the individual level, SVM correctly classified patients with PD at the individual level with accuracies up to 97%.

**CONCLUSIONS:** Support vector machine–based pattern recognition of DTI data provides highly accurate detection of patients with PD among those with suspected PD at an individual level, which is potentially clinically applicable. Because most suspected subjects with PD undergo brain MR imaging, already existing MR imaging data may be reused; this practice is very cost-efficient.

**ABBREVIATIONS:** FA = fractional anisotropy;  $^{123}\text{I}$  = iodine 123; LD = longitudinal diffusivity; MD = mean diffusivity; MSA = multisystem atrophy; PD = Parkinson disease; PSP = progressive supranuclear palsy; RD = radial diffusivity; SVM = support vector machine; TBSS = tract-based spatial statistics; VBM = voxel-based morphometry

PD is the most common degenerative movement disorder in the general population, named after the English doctor James Parkinson, who published its first detailed description in 1817. Brain MR imaging is routinely performed in the diagnostic work-up, yet its role is essentially limited to the exclusion of other pathologies such as normal-pressure hydrocephalus or chronic subdural hematoma, among others. One of the rare reported alterations visible on conventional MR imaging is narrowing or disappearance of the pars compacta of the substantia nigra on T2-weighted imaging,<sup>1</sup> yet this sign has low sensitivity and specificity and does not contribute to the diagnosis of PD, in particular at an early stage.

On the basis of the assumption that PD is associated with systematic changes in brain MR imaging, which are too subtle to be detected by visual analysis, we analyzed brain MR imaging of subjects with suspected PD by using an advanced computer-based method aiming to contribute to the diagnosis of

PD at an individual level. There are 2 fundamental approaches of advanced MR imaging data analysis. The first and more frequently implemented type of group-level studies typically compares  $\geq 1$  group of patients with healthy controls with the aim of detecting disease-related structural alterations, for example.<sup>2-6</sup> Although fascinating from a research perspective, the disadvantage of these group-level studies is that the results cannot be applied to the diagnosis of individual patients in clinical neuroradiology. The second type of analysis aims to detect or classify individual patients. Because the composition of the included subjects may bias the classification accuracy, the study groups should ideally consist of unselected and consecutive patients with suspicion of a given disease (see “Discussion”). The individual classification is potentially clinically applicable. The disadvantage is the difficulty or even impossibility of interpreting the results from a neuropathologic perspective.

To achieve a potentially clinically applicable individual diagnosis, we performed a study of the second type, implementing a pattern-recognition approach. This pattern recognition can be illustrated in short in the example of face recognition. Individual faces are not detected on the basis of single features such as the tip of the nose, ears, eyes, and so forth, but by the combination of multiple features—even though each individual feature may be not significantly different between groups. In the present study, the entire brain is included in the pattern-recognition analysis to obtain 1 individual predictive value per subject. More technically, classification analyses can be explained best for a simple example of only 2 features, which can be represented by an x-y plot. If one assumes that all subjects of group A are in the upper left part and all subjects of group B are

Received January 29, 2012; accepted after revision February 26.

From the Service Neuro-Diagnostique et Neuro-Interventionnel (S.H., K.O.L.), Département de l’Imagerie et Science de l’Information Médical, University Hospitals of Geneva, Geneva, Switzerland; Department of Neurology (S.B., P.R.B.), Geneva University Hospitals and Faculty of Medicine, University of Geneva, Geneva, Switzerland; Centre Diagnostic Radiologique Carouge (D.N.), Carouge, Switzerland; and Nuclear Medicine and Molecular Imaging Unit (V.G.), Département de l’Imagerie et Science de l’Information Médical, Geneva University Hospitals and Faculty of Medicine, University of Geneva, Switzerland.

Please address correspondence to Sven Haller, MD, MSc, Service Neuro-Diagnostique et Neuro-Interventionnel, Département de l’Imagerie et Science de l’Information Médical, Hôpitaux Universitaires de Genève, Rue Gabrielle Perret-Gentil 4, 1211 Genève 14; e-mail: sven.haller@hcuge.ch

Indicates article with supplemental on-line table.

<http://dx.doi.org/10.3174/ajnr.A3126>

in the lower right part of the plot, the 2 groups can be discriminated by an oblique ascending line. Of all possible lines to discriminate between groups, the SVM<sup>7</sup> identifies the line that best discriminates between groups. For a more detailed discussion, see a recent review of SVM classification in neurodegenerative diseases by Haller et al.<sup>8</sup>

Because the most relevant clinical question is not the discrimination of PD versus healthy controls but the detection of idiopathic PD versus other atypical forms of Parkinsonism including MSA and PSP, we included 40 consecutive subjects with suspected PD rather than healthy control subjects. Inclusion criteria were brain <sup>123</sup>I ioflupane SPECT (DaTSCAN; GE Healthcare, Buckinghamshire, United Kingdom) as a reference and extensive neurologic testing, including long-term follow-up. We analyzed DTI data because a number of recent investigations in various neurodegenerative disorders<sup>6,9-12</sup> demonstrated that white matter DTI TBSS<sup>13</sup> analysis is more sensitive than gray matter VBM.<sup>14</sup> A recent study implementing an equivalent approach successfully discriminated between stable versus progressive mild cognitive impairment in the domain of dementia.<sup>15</sup>

We show that the data analysis chain of TBSS preprocessing of DTI data followed by SVM classification provides a highly accurate individual detection of PD in consecutive subjects with Parkinsonism, despite the absence of visually detectable brain MR imaging differences.

## Materials and Methods

### Subjects

This retrospective study was approved by the local ethics committee. We included all consecutive patients in our institution between 2006 and 2011 with suspected PD who met the following criteria: 1) DTI at 3T without motion artifacts, 2) brain <sup>123</sup>I ioflupane SPECT (DaTSCAN) as a reference, 3) extensive neurologic testing including follow-up, and 4) the absence of morphologic findings on brain MR imaging. All patients were evaluated by an experienced movement disorders specialist.

### MR Imaging

MR imaging was performed on a 3T clinical routine whole-body scanner (Magnetom Trio; Siemens, Erlangen, Germany). We used a standard DTI sequence: 30 diffusion directions,  $b=1000$  s/mm<sup>2</sup> isotropically distributed on a sphere, 1 reference  $b=0$  s/mm<sup>2</sup> image with no diffusion-weighting,  $128 \times 128 \times 64$  matrix,  $2 \times 2 \times 2$  mm voxel size, TE = 92 ms, TR = 9000 ms, 1 average. Additional sequences (axial spin-echo T1-weighted or gradient-echo 3D T1-weighted, axial spin-echo T2-weighted, coronal FLAIR, axial gradient-echo T2\*) were acquired and analyzed to exclude brain pathology, such as ischemic stroke, subdural hematomas, or space-occupying lesions by an experienced radiologist during clinical work-up. In particular, white matter lesions were analyzed according to the score of Fazekas et al.<sup>16</sup>

### Image Processing

Preprocessing of the DTI data was performed by using the standard procedure of TBSS, as described in detail before,<sup>13,17</sup> in the FSL software package (<http://www.fmrib.ox.ac.uk/fsl/>).<sup>18</sup> In principle, TBSS projects all subjects' FA data onto a mean FA tract skeleton by using nonlinear registration. The tract skeleton is the basis for voxelwise cross-subject statistics and reduces potential misregistrations as the

source for false-positive or -negative analysis results. The other DTI-derived parameters, LD (also known as axial diffusivity, the first eigenvalue), RD (the average of second and third eigenvalues), and MD (the average of all 3 eigenvalues), were analyzed in the same way by using spatial transformation parameters that were estimated in the initial FA analysis.

### Statistical Analysis

**Analysis of Demographic and Clinical Data.** The statistical analyses of the demographic and clinical data were performed in GraphPad Prism, Version 5 (GraphPad software, [www.graphpad.com](http://www.graphpad.com)). Age was analyzed by using parametric 2-sample 2-tailed *t* tests, while sex and Fazekas score were analyzed by using the nonparametric 2-sample 2-tailed Mann-Whitney *U* tests.

**Group-Level TBSS Analysis.** Voxelwise statistical analyses were corrected for multiple comparisons implementing threshold-free cluster enhancement, considering fully corrected *P* values < .05 as significant.<sup>19</sup> Age and sex were used as nonexplanatory coregressors. We used Johns Hopkins University DTI-based white matter atlases, which are distributed in the FSL package, for anatomic labeling of the suprathreshold voxels.

**Individual-Level SVM Analysis.** The individual SVM classification analysis is identical to that in a previous study.<sup>15</sup> The TBSS preprocessed DTI FA data were converted into a Waikato Environment for Knowledge Analysis-compatible data format. The individual classification was analyzed in the freely available Waikato Environment for Knowledge Analysis software package (<http://www.cs.waikato.ac.nz/ml/weka>, Version 3.6.1). The analysis included 2 steps. In a first step, we performed a RELIEFF<sup>20</sup> feature selection (<http://rss.acs.unt.edu/Rdoc/library/dprep/html/relief.html>). The rationale behind this step is that not all voxels discriminate between groups. Both the inclusion of nondiscriminative voxels and the exclusion of discriminative voxels reduce the classification accuracy. We selected the top 100, 250, 500, 750, and 1000 features implementing 10-fold cross-validation. The second step consisted of the "actual" classification analyses by using the SVM algorithm sequential minimal optimization<sup>21</sup> (distributed in the Waikato Environment for Knowledge Analysis package) with a radial basis function kernel.<sup>22</sup> There are 2 parameters while using radial basis function kernels: *C* and  $\gamma$ .  $\gamma$  represents the width of the radial basis function, and *C* represents the error/trade-off parameter that adjusts the importance of the separation error in the creation of the separation surface. On the basis of our previous experience,  $\gamma$  was iteratively explored from 0.01 to 0.09 with an increment of 0.01, while *C* was fixed to 1.00. We performed 10 repetitions of a 10-fold cross-validation technique.

## Results

### Clinical Data

The final sample included 17 PD subjects (age range,  $67.8 \pm 6.7$  years; 9 women) and 23 Other subjects (age range,  $67.2 \pm 9.7$  years; 7 women). Age, sex, and Fazekas score did not differ significantly between the 2 groups (Table 1). For the PD group, a diagnosis of PD was made in the presence of typical, asymmetric, and levodopa-responsive Parkinsonism meeting the UK Parkinson's Disease Society Brain Bank criteria, including at least 2 supportive criteria such as slow progression or peak-dose dyskinesia. PD was moderately advanced (mean Hoehn and Yahr stage<sup>23</sup>:  $2.4 \pm 0.6$ ), and none of these patients had atypical features, even after at least 2.5 years of follow-up

**Table 1: Demographic and clinical characteristics<sup>a</sup>**

Variables	PD	Other	Statistics
Age (yr)	67.8 ± 6.7	67.2 ± 9.7	NS
Sex (f/m)	9/8	7/16	NS
Fazekas score	1.0 ± 0.1	1.2 ± 0.5	NS
Hoehn and Yahr stage	2.4 ± 0.6		
Disease duration (yr)	6.3 ± 3.1	2.8 ± 1.9	

**Note:**—NS indicates nonsignificant ( $P > .05$ ).

<sup>a</sup> Essential demographic and clinical characteristics of the 2 study groups, PD and Other. Data are presented as mean ± SD.

(mean follow-up duration, 6.3 ± 3.1 years). In addition, all had an asymmetrical decrease of <sup>123</sup>I ioflupane uptake in the posterior aspect of 1 or both putamina on the DaTSCAN. The Other group was more heterogeneous, reflecting the prevalence of common PD-mimicking conditions in the daily activity of a movement disorders clinic. All of these patients exhibited Parkinsonism, defined as the presence of bradykinesia associated with resting tremor or rigidity. It included pathologies as varied as MSA ( $n = 5$ ), PSP ( $n = 1$ ), dementia with Lewy bodies ( $n = 2$ ), vascular Parkinsonism ( $n = 3$ ), frontotemporal dementia with Parkinsonism ( $n = 1$ ), drug-induced Parkinsonism ( $n = 2$ ), atypical tremor ( $n = 2$ ), traumatic brain injury ( $n = 1$ ), and psychogenic Parkinsonism ( $n = 1$ ). Diagnoses were established according to widely accepted clinical criteria, whenever available, including those by Gilman et al for MSA,<sup>24</sup> by Litvan et al for PSP,<sup>25</sup> by McKeith et al for dementia with Lewy bodies,<sup>26</sup> and by Roman et al for vascular dementia.<sup>27</sup> In 5 cases, a firm clinical diagnosis could not be established at last assessment and these patients were labeled as having unspecified Parkinsonism.

### TBSS Group Differences

The PD group compared with the Other group had a significant increase in FA and a corresponding significant decrease in RD and MD, in particular in the right frontal white matter (Fig 1 and On-line Table). The level of significance of FA was slightly lower compared with RD and MD. LD had spatially overlapping changes, which were just below threshold (not illustrated).

The inverse comparisons yielded no suprathreshold clusters.

### SVM Individual Classification Analysis

SVM analysis of FA provided a correct classification between PD versus Other with accuracies of up to 97.50 ± 7.54%. The spatial distribution of the most discriminative voxels (features) overlapped substantially with the results of the group-level TBSS analysis as illustrated in Fig 1 and Table 2.

### Discussion

Despite the absence of visually evident alterations in brain MR imaging, computer-based SVM analysis of DTI data provides highly accurate individual detection of patients with PD and is potentially applicable in clinical neuroradiology. Brain MR imaging is routinely performed in the work-up of Parkinsonism, notably to exclude concomitant diseases. Available MR imaging data are reused by using advanced data analysis, making this a very cost-effective method, which is not intended to replace but to complement existing methods to obtain an early and specific diagnosis of PD.

### Group-Level TBSS Analysis

The first part of the analysis was a group-level analysis of white matter changes in subjects with suspected PD.

Most previous advanced MR neuroimaging studies in the domain of PD compared subjects with PD with healthy controls, with the objective of identifying disease-related alterations in brain morphometry. For example, one of the rare DTI studies in PD demonstrated a lower FA in the substantia nigra in PD compared with healthy controls, which inversely correlated with the clinical severity of PD.<sup>2</sup> Two studies used manually defined ROIs in the substantia nigra showing diminished FA in PD versus healthy controls.<sup>2,28</sup> Another study used multiple ROIs in 10 patients with PD without dementia and 10 healthy controls, showing decrease in FA and increase in MD in the genu of the corpus callosum and in the superior longitudinal fasciculus.<sup>5</sup> Yet other studies found differences in DTI FA in patients with PD with olfactory impairment,<sup>29</sup> patients with PD and depression,<sup>30</sup> or between patients with PD and familial essential tremor<sup>4</sup> or corticobasal syndrome.<sup>31</sup> Another recent study assessed different MR imaging parameters including R2\*, R2-, and R1-mapping, magnetization transfer, and DTI in 31 patients with various forms of Parkinsonism and found that manually defined ROIs of DTI are most useful for identifying PSP, yet less useful for PD.<sup>32</sup> Most interesting, a recent study assessed white matter in 36 subjects with PD and 23 controls on the basis of another technique, notably magnetization transfer imaging.<sup>33</sup> PD-related changes in WM were more sensitive than gray matter volume or attenuation derived from T1-weighted images.

All of these studies have in common that they included very selected control groups.

In contrast to these studies, the aim of the present investigation was to use DTI as a marker to detect individual patients with PD in a group of subjects with suspected PD. We, therefore, deliberately included consecutive nonselected patients with various forms of Parkinsonism. We observed, in our sample, alterations in FA, a measure of axonal integrity,<sup>34</sup> as well as RD and MD in a bilateral right-dominant frontal network. The observed increase in FA in our study is in agreement in principle with the observed increase in FA in de novo patients with PD versus healthy controls in a recent combined T1-weighted and DTI study,<sup>3</sup> while another study in 12 subjects with nondemented PD and 13 controls demonstrated a decrease in FA bilaterally in the frontal lobes.<sup>6</sup> Differences in disease duration, severity, and characteristics might explain this discrepancy. Moreover, the increase in FA in PD versus Other subjects in our study is probably due to a decrease in FA in the Other group, rather than due to an increase in FA in the PD group. Due to the heterogeneous constitution of our control group, the results of our group-level comparison should be interpreted with caution and are presented mainly to visualize the presence of detectable DTI changes between subjects with PD versus Other, as a basis for the later individual-level pattern-recognition analysis.

### Individual-Level SVM Classification Analysis

To obtain individual discrimination of subjects with PD, we adopted a complex methodology including a chain of TBSS preprocessing of DTI FA data, feature selection of the most discriminative voxels, and subsequent SVM classification.<sup>15,35</sup>



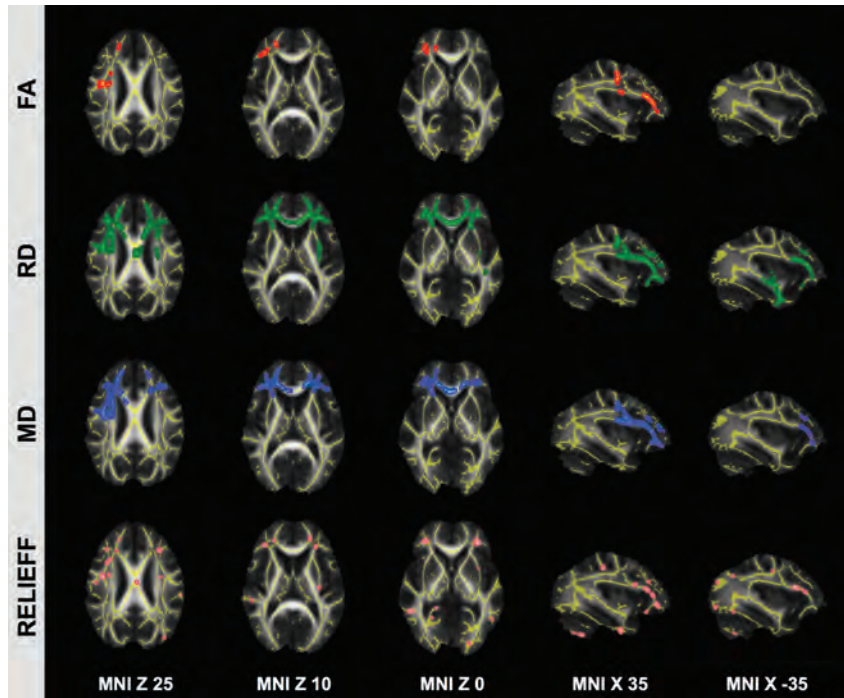


**Fig 1.** TBSS analysis in PD. Patients with idiopathic PD versus Other had a spatially consistent increase in FA (red) and a decrease in RD (green) and MD (blue) in a bilateral network predominantly in the right frontal white matter. The spatially consistent difference in LD was just below threshold (not illustrated). The inverse comparison yielded no suprathreshold clusters. The most discriminative voxels (features) identified by using the RELIEFF feature-selection algorithm, which are the basis for the individual level SVM analysis, are illustrated for comparison in pink. Note the good overlap despite the fundamentally different methodology. Axial and sagittal sections are at the indicated position in Montreal Neurological Institute standard space coordinates (radiologic convention with the right hemisphere on the left-hand side). Gray indicates mean FA value; yellow, average skeleton. FA, RD, and MD clusters are TFCE corrected for multiple comparisons at  $P < .05$ . Suprathreshold voxels are enlarged by using TBSS fill (part of FSL) for illustrative purposes.

**Table 2: Individual SVM classification of PD based on DTI FA TBSS**

17 PD, 23 Other: Chance Rate of Classification Accuracy, 57.5% (23/40)<sup>a</sup>

No. of Features	Accuracy	TP Rate	FP Rate	TN Rate	FN Rate
100	97.50 (7.54)	0.94 (0.19)	0.00 (0.00)	1.00 (0.00)	0.06 (0.19)
250	95.50 (10.29)	0.90 (0.25)	0.00 (0.00)	1.00 (0.00)	0.11 (0.25)
500	96.25 (9.65)	0.91 (0.24)	0.00 (0.00)	1.00 (0.00)	0.09 (0.24)
750	97.25 (7.86)	0.94 (0.20)	0.00 (0.00)	1.00 (0.00)	0.07 (0.20)
1000	96.25 (9.65)	0.92 (0.23)	0.00 (0.00)	1.00 (0.00)	0.09 (0.23)

**Note:**—TP indicates true-positive; FP, false-positive; TN, true-negative; FN, false-negative.  
<sup>a</sup>Accuracy, TP, FP, TN, and FN rates for individual classifications using an SVM classifier with the indicated number of selected features for the individual classification of PD versus Other. Note that the accuracy is calculated as the average accuracy of 10 repetitions using 10-fold cross-validation (average and SD).

The classification accuracy of approximately 97% across the 10 repetitions of the 10-fold cross-validation implies that on average, only 1 subject was incorrectly classified.

Note that SVM<sup>7</sup> analyses for individual classification are fundamentally different from the group-level voxelwise analyses discussed above. Such voxelwise analyses are univariate tests, which separately analyze each included voxel between 2 (or more) groups. Given the multiple tests, in our dataset of approximately 150,000 voxels, it is necessary to implement, as a second step, a correction for multiple comparisons. In contrast, individual-level SVM analyses are multivariate tools that originate from a field called “machine learning” or multivoxel pattern analysis, a branch of artificial intelligence. The aim is to identify patterns that allow the discrimination of individual subjects. There is only 1 resulting parameter per subject; hence, there is no need for corrections for multiple compari-

sons. For a more detailed discussion of SVM classifiers, see a recent review by Haller et al.<sup>8</sup>

There are only a few previous applications of SVM classification in the domain of PD. Most of these studies applied SVM classifiers to behavioral data of gait analysis,<sup>36</sup> fine-motor force tracking,<sup>37</sup> and analysis of wearable accelerometer sensors<sup>38</sup> or joint movement,<sup>39</sup> and even the recorded voice.<sup>40</sup>

The only previous SVM application to MR imaging data in the domain of PD analyzed VBM-preprocessed gray matter in 21 patients with PD, 11 with progressive multisystem atrophy and 10 with PSP, and 22 healthy controls.<sup>41</sup> The best classification accuracy up to 96.8% was obtained for PSP versus PD, while the accuracy was 71.9% for MSA versus PD. However, patients with PD could not be discriminated from controls. These classification accuracies are consistent with the clinical neuroradiologic experience because PSP has the most pronounced visible alterations in brain MR imaging with atrophy of the mesencephalon referred to as the “penguin” or “hummingbird” sign,<sup>42</sup> while changes in progressive multisystem atrophy are already less pronounced and, as discussed above, PD-associated changes are very subtle.

Neuroradiologic research has been dominated for decades by group studies. The patient groups for such studies should ideally be preselected to have homogeneous and matched groups with typical disease. This is fundamentally different for individual-level classification studies because the preselection of cases might systematically confound the performance of a classifier in a typical clinical setting consisting of unselected and consecutive cases. The preselection of an “artificially” homogeneous atypical Parkinsonism group would train the clas-



sifier to detect regions that best discriminate idiopathic PD versus the group of preselected atypical Parkinsonism, yet these regions are not necessarily those that best discriminate between idiopathic PD versus unselected and consecutive patients with suspected PD in a clinical setting. Note the prevalence of these diseases is very different. According to Medscape (<http://emedicine.medscape.com>), the prevalence in the United States of, for example, progressive multisystem atrophy is 1.9–4.9 cases per 100,000 population (<http://emedicine.medscape.com/article/1154583-overview#a0199>), yet around 120 (range, 18–328) in PD (<http://emedicine.medscape.com/article/1154583-overview>).

With respect to a potential clinical application of a classifier, the study populations should ideally match the prevalence of the diseases: A very high accuracy of detection of a very rare disease may overestimate, while the incorrect classification of a rare disease may underestimate, the classification accuracy in “real-world” data. Moreover, preselection of patients typically results in the inclusion of “classic” cases, which may have stronger disease-related alterations, while “real-world” data may contain fewer “classic” cases. In other words, the preselection of patients with specific diseases might represent a systematic confound with respect to the performance of a classifier in “real-world” data, and we consequently included consecutive unselected patients from our institution.

Most previous applications of the SVM classification to brain MR imaging data were performed on gray matter VBM data in the domain of Alzheimer disease<sup>43</sup> and mild cognitive impairment,<sup>44–46</sup> with classification accuracies between 75% and 85%. One recent investigation also assessed DTI data in the domain of mild cognitive impairment with accuracies over 95%,<sup>15</sup> implementing equivalent methodology to that used in the current investigation. This suggests that DTI might be a very sensitive brain MR imaging parameter. Consistent with this observation, several recent group-level investigations in various neurodegenerative disorders demonstrated that white matter DTI TBSS analysis is more sensitive than gray matter VBM.<sup>6,9–12</sup> This does not necessarily imply that WM pathology is more pronounced at a histopathologic level; it might simply be a methodologic difference in data acquisition and preprocessing sensitivity favoring white matter DTI TBSS over gray matter T1-weighted-based VBM. Note that FA is a directly assessed absolute parameter between 0 and 1. In contrast, VBM is based on relative 3D T1-weighted values. VBM consequently requires preprocessing that segments the brain into different compartments to provide an indirect probabilistic gray matter probability per voxel. Additionally, at least the major tracts of the white matter skeleton (TBSS) are generally more linear and have less interindividual variation compared with the much more complex superficial gyral and sulcal folding pattern (VBM), which might imply a different quality of the spatial normalization of the data.

### Limitations

The major limitation of the present investigation is the relatively small number of cases, which may affect the results of the SVM analysis, and we propose the current investigation as preliminary data. In fact, the very high accuracy rates of individual classification exceeded our expectations. Both training and testing were performed on the same dataset. A simple split

of the data into 2 halves, by using one-half for training and the other half for testing is problematic in small sample sizes such as in the current study because this decreases the number of instances to train the classifier, and the classification accuracy might depend on the division of cases. The reported values were obtained by a well-established 10-fold cross-validation in which 9 parts were used for training and the remaining part was used for testing the classifier. This procedure was repeated 10 times, so that each dataset was used once for testing. This approach increases the sample size for the training of the classifier and at the same time reduces variation of the classification results due to division of cases.

Even though this cross-validation approach is a standard method in the field of machine learning/multivoxel pattern analysis and appropriate for the number of subjects involved in our study, the present results are too optimistic, related to some degree of overfitting of the data. Future validation of the present findings is warranted in a larger and independent sample, which ideally should be acquired on different MR scanners. The consecutive and unselected composition of the Other group is another limitation, yet the rationale behind this selection is discussed in detail above. Additionally, the nonlinear (radial basis function-kernel) SVM does not provide an easy-to-interpret weight vector to identify the most discriminative brain areas. Another limitation is the retrospective nature of the present study.

### Conclusions

We propose the current study as the initial results that show the feasibility of performing SVM individual classification of DTI data in PD, which may merit future prospective and larger scale follow-up studies.

### References

1. Oikawa H, Sasaki M, Tamakawa Y, et al. **The substantia nigra in Parkinson disease: proton density-weighted spin-echo and fast short inversion time inversion-recovery MR findings.** *AJNR Am J Neuroradiol* 2002;23:1747–56
2. Chan LL, Rumpel H, Yap K, et al. **Case control study of diffusion tensor imaging in Parkinson's disease.** *J Neurol Neurosurg Psychiatry* 2007;78:1383–86
3. Tessa C, Giannelli M, Della Nave R, et al. **A whole-brain analysis in de novo Parkinson disease.** *AJNR Am J Neuroradiol* 2008;29:674–80
4. Nicoletti G, Manners D, Novellino F, et al. **Diffusion tensor MRI changes in cerebellar structures of patients with familial essential tremor.** *Neurology* 2010;74:988–94
5. Gattellaro G, Minati L, Grisoli M, et al. **White matter involvement in idiopathic Parkinson disease: a diffusion tensor imaging study.** *AJNR Am J Neuroradiol* 2009;30:1222–26
6. Karagulle Kendi AT, Lehericy S, Luciana M, et al. **Altered diffusion in the frontal lobe in Parkinson disease.** *AJNR Am J Neuroradiol* 2008;29:501–05
7. Noble WS. **What is a support vector machine?** *Nat Biotechnol* 2006;24:1565–67
8. Haller S, Lovblad KO, Giannakopoulos P. **Principles of classification analyses in mild cognitive impairment (MCI) and Alzheimer disease.** *J Alzheimers Dis* 2011;26(suppl 3):389–94
9. Della Nave R, Ginestroni A, Tessa C, et al. **Brain white matter tracts degeneration in Friedreich ataxia: an in vivo MRI study using tract-based spatial statistics and voxel-based morphometry.** *Neuroimage* 2008;40:19–25
10. Della Nave R, Ginestroni A, Tessa C, et al. **Brain white matter damage in SCA1 and SCA2: an in vivo study using voxel-based morphometry, histogram analysis of mean diffusivity and tract-based spatial statistics.** *Neuroimage* 2008;43:10–19
11. Haller S, Xekardaki A, Delaloye C, et al. **Combined analysis of grey matter voxel-based morphometry and white matter tract-based spatial statistics in late-life bipolar disorder.** *J Psychiatry Neurosci* 2011;36:391–401
12. Agosta F, Pievani M, Sala S, et al. **White matter damage in Alzheimer disease and its relationship to gray matter atrophy.** *Radiology* 2011;258:853–63
13. Smith SM, Jenkinson M, Johansen-Berg H, et al. **Tract-based spatial statistics: voxelwise analysis of multi-subject diffusion data.** *Neuroimage* 2006;31:1487–505

14. Ashburner J, Friston KJ. **Voxel-based morphometry: the methods.** *Neuroimage* 2000;11:805–21
15. Haller S, Nguyen D, Rodriguez C, et al. **Individual prediction of cognitive decline in mild cognitive impairment using support vector machine-based analysis of diffusion tensor imaging data.** *J Alzheimers Dis* 2010;22:315–27
16. Fazekas F, Chawluk JB, Alavi A, et al. **MR signal abnormalities at 1.5 T in Alzheimer's dementia and normal aging.** *AJR Am J Roentgenol* 1987;149:351–56
17. Smith SM, Johansen-Berg H, Jenkinson M, et al. **Acquisition and voxelwise analysis of multi-subject diffusion data with tract-based spatial statistics.** *Nat Protoc* 2007;2:499–503
18. Smith SM, Jenkinson M, Woolrich MW, et al. **Advances in functional and structural MR image analysis and implementation as FSL.** *Neuroimage* 2004;23(suppl 1):S208–19
19. Smith SM, Nichols TE. **Threshold-free cluster enhancement: addressing problems of smoothing, threshold dependence and localisation in cluster inference.** *Neuroimage* 2009;44:83–98
20. Kononenko I, Šimec E, Robnik-Šikonja M. **Overcoming the myopia of inductive learning algorithms with RELIEFF.** *Applied Intelligence* 1997;7:39–55
21. Platt J. **Sequential minimal optimization: a fast algorithm for training support vector machines.** Microsoft Research Technical Report MSR-TR-98, <http://research.microsoft.com/en-us/um/people/jplatt/smoTR.pdf> (Accessed April 21, 1998)
22. Schölkopf B, Sung KK, Burges CJ, et al. **Comparing support vector machines with Gaussian kernels to radial basis function classifiers.** *IEEE Transactions on Signal Processing* 1997;45:2758–65
23. Hoehn MM, Yahr MD. **Parkinsonism: onset, progression and mortality.** *Neurology* 1967;17:427–42
24. Gilman S, Low PA, Quinn N, et al. **Consensus statement on the diagnosis of multiple system atrophy.** *J Neurol Sci* 1999;163:94–98
25. Litvan I, Agid Y, Calne D, et al. **Clinical research criteria for the diagnosis of progressive supranuclear palsy (Steele-Richardson-Olszewski syndrome): report of the NINDS-SPSP international workshop.** *Neurology* 1996;47:1–9
26. McKeith IG, Dickson DW, Lowe J, et al. **Diagnosis and management of dementia with Lewy bodies: third report of the DLB Consortium.** *Neurology* 2005;65:1863–72
27. Roman GC, Tatemichi TK, Erkinjuntti T, et al. **Vascular dementia: diagnostic criteria for research studies: report of the NINDS-AIREN International Workshop.** *Neurology* 1993;43:250–60
28. Vaillancourt DE, Spraker MB, Prodoehl J, et al. **High-resolution diffusion tensor imaging in the substantia nigra of de novo Parkinson disease.** *Neurology* 2009;72:1378–84
29. Ibarretxe-Bilbao N, Junque C, Martí MJ, et al. **Olfactory impairment in Parkinson's disease and white matter abnormalities in central olfactory areas: a voxel-based diffusion tensor imaging study.** *Mov Disord* 2010;25:1888–94
30. Li W, Liu J, Skidmore F, et al. **White matter microstructure changes in the thalamus in Parkinson disease with depression: a diffusion tensor MR imaging study.** *AJNR Am J Neuroradiol* 2010;31:1861–66
31. Boelmans K, Bodammer NC, Suchorska B, et al. **Diffusion tensor imaging of the corpus callosum differentiates corticobasal syndrome from Parkinson's disease.** *Parkinsonism Relat Disord* 2010;16:498–502
32. Focke NK, Helms G, Pantel PM, et al. **Differentiation of typical and atypical Parkinson syndromes by quantitative MR imaging.** *AJNR Am J Neuroradiol* 2011;32:2087–92
33. Morgen K, Sammer G, Weber L, et al. **Structural brain abnormalities in patients with Parkinson disease: a comparative voxel-based analysis using T1-weighted MR imaging and magnetization transfer imaging.** *AJNR Am J Neuroradiol* 2011;32:2080–86
34. Thomalla G, Glauche V, Koch MA, et al. **Diffusion tensor imaging detects early Wallerian degeneration of the pyramidal tract after ischemic stroke.** *Neuroimage* 2004;22:1767–74
35. Haller S, Bartsch A, Nguyen D, et al. **Cerebral microhemorrhage and iron deposition in mild cognitive impairment: susceptibility-weighted MR imaging assessment.** *Radiology* 2010;257:764–73
36. Jeon HS, Han J, Yi WJ, et al. **Classification of Parkinson gait and normal gait using spatial-temporal image of plantar pressure.** *Conf Proc IEEE Eng Med Biol Soc* 2008;2008:4672–75
37. Brewer BR, Pradhan S, Carvell G, Delitto A. **Feature selection for classification based on fine motor signs of Parkinson's disease.** *Conf Proc IEEE Eng Med Biol Soc* 2009;2009:214–17
38. Patel S, Lorincz K, Hughes R, et al. **Monitoring motor fluctuations in patients with Parkinson's disease using wearable sensors.** *IEEE Trans Inf Technol Biomed* 2009;13:864–73
39. Chan J, Leung H, Poizner H. **Correlation among joint motions allows classification of Parkinsonian versus normal 3-D reaching.** *IEEE Trans Neural Syst Rehabil Eng* 2010;18:142–49
40. Ozcift A. **SVM feature selection based rotation forest ensemble classifiers to improve computer-aided diagnosis of Parkinson disease.** *J Med Syst* 2011 Mar 10. [Epub ahead of print]
41. Focke NK, Helms G, Scheewe S, et al. **Individual voxel-based subtype prediction can differentiate progressive supranuclear palsy from idiopathic Parkinson syndrome and healthy controls.** *Hum Brain Mapp* 2011;32:1905–15
42. Groschel K, Kastrup A, Litvan I, Schulz JB. **Penguins and hummingbirds: mid-brain atrophy in progressive supranuclear palsy.** *Neurology* 2006;66:949–50
43. Kloppel S, Stonnington CM, Chu C, et al. **Automatic classification of MR scans in Alzheimer's disease.** *Brain* 2008;131:681–89
44. Plant C, Teipel SJ, Oswald A, et al. **Automated detection of brain atrophy patterns based on MRI for the prediction of Alzheimer's disease.** *Neuroimage* 2010;50:162–74
45. Misra C, Fan Y, Davatzikos C. **Baseline and longitudinal patterns of brain atrophy in MCI patients, and their use in prediction of short-term conversion to AD: results from ADNI.** *Neuroimage* 2009;44:1415–22
46. Fan Y, Batmanghelich N, Clark CM, et al. **Spatial patterns of brain atrophy in MCI patients, identified via high-dimensional pattern classification, predict subsequent cognitive decline.** *Neuroimage* 2008;39:1731–43

## **Chapter 3.1.2**

### ***Differentiation between Parkinson disease and other forms of parkinsonism using support vector machine analysis of susceptibility-weighted imaging (SWI): initial results.***

S Haller S Badoud D Nguyen I Barnaure M-L Montandon K-O Lovblad

PR Burkhard

Published in European Radiology (2013)



# Differentiation between Parkinson disease and other forms of Parkinsonism using support vector machine analysis of susceptibility-weighted imaging (SWI): initial results

S Haller · S Badoud · D Nguyen · I Barnaure ·  
M-L Montandon · K-O Lovblad · PR Burkhard

Received: 7 April 2012 / Revised: 3 June 2012 / Accepted: 5 June 2012 / Published online: 15 July 2012  
© European Society of Radiology 2012

## Abstract

**Objectives** To diagnose Parkinson disease (PD) at the individual level using pattern recognition of brain susceptibility-weighted imaging (SWI).

**Methods** We analysed brain SWI in 36 consecutive patients with Parkinsonism suggestive of PD who had (1) SWI at 3 T, (2) brain  $^{123}\text{I}$ -ioflupane SPECT and (3) extensive neurological testing including follow-up (16 PD,  $67.4 \pm 6.2$  years, 11 female; 20 OTHER, a heterogeneous group of atypical

Parkinsonism syndromes  $65.2 \pm 12.5$  years, 6 female). Analysis included group-level comparison of SWI values and individual-level support vector machine (SVM) analysis.

**Results** At the group level, simple visual analysis yielded no differences between groups. However, the group-level analyses demonstrated increased SWI in the bilateral thalamus and left substantia nigra in PD patients versus other Parkinsonism. The inverse comparison yielded no supra-threshold clusters. At the individual level, SVM correctly classified PD patients with an accuracy above 86 %.

**Conclusions** SVM pattern recognition of SWI data provides accurate discrimination of PD among patients with various forms of Parkinsonism at an individual level, despite the absence of visually detectable alterations. This pilot study warrants further confirmation in a larger cohort of PD patients and with different MR machines and MR parameters.

## Key Points

- *Magnetic resonance imaging data offers new insights into Parkinson's disease*
- *Visual susceptibility-weighted imaging (SWI) analysis could not discriminate idiopathic from atypical PD*
- *However, support vector machine (SVM) analysis provided highly accurate detection of idiopathic PD*
- *SVM analysis may contribute to the clinical diagnosis of individual PD patients*
- *Such information can be readily obtained from routine MR data*

**Keywords** Parkinson disease · SWI · Brain iron deposition · SVM · Early diagnosis

## Abbreviations

AD	Alzheimer disease
DaTScan	$^{123}\text{I}$ -ioflupane SPECT
DN	dentate nucleus (of the cerebellum)
DTI	diffusion tensor imaging

S. Haller (✉) · K.-O. Lovblad  
Service neuro-diagnostique et neuro-interventionnel DISIM,  
Hôpitaux Universitaires de Genève,  
Rue Gabrielle Perret-Gentil 4,  
1211 Genève 14, Switzerland  
e-mail: sven.haller@hcuge.ch

S. Badoud · P. Burkhard  
Department of Neurology, Geneva University Hospitals,  
Geneva, Switzerland

S. Badoud · P. Burkhard  
Faculty of Medicine, University of Geneva,  
Geneva, Switzerland

D. Nguyen  
Centre Diagnostic Radiologique Carouge,  
1b Clos de la Fonderie,  
1227 Carouge, Switzerland

I. Barnaure  
Service de Radiologie, Geneva University Hospitals,  
Geneva, Switzerland

M.-L. Montandon  
Nuclear medicine and molecular imaging unit, DISIM,  
Geneva University Hospitals,  
Geneva, Switzerland

M.-L. Montandon  
Faculty of Medicine, University of Geneva,  
Geneva, Switzerland

FA	fractional anisotropy
GM	grey matter
MCI	mild cognitive impairment
MRI	magnetic resonance imaging
MSA-P	Parkinson variant of multiple system atrophy
PD	Parkinson disease
PSP	progressive supranuclear palsy
RBF	radial basis function
RN	red nucleus
ROI	region of interest
SMO	sequential minimal optimisation
SN	substantia nigra
SPECT	single-photon emission computed tomography
SVM	support vector machine
SWI	susceptibility-weighted imaging
TBSS	tract-based spatial statistics
TFCE	threshold free cluster enhancement
VBM	voxel-based morphometry
WM	white matter

## Introduction

Brain iron deposition has attracted increasing attention in neurodegeneration, occurring during normal aging [1] but being more marked in various neurodegenerative disorders [2], in particular in mild cognitive impairment (MCI) and Alzheimer disease (AD) [3–5]. Brain iron deposition has been proposed to play a key role in the pathogenesis of Parkinson disease (PD) [6, 7].

In the current investigation, we assessed recently introduced susceptibility-weighted imaging (SWI) [8] in PD. Brain MRI is routinely performed in the diagnostic work-up of suspected PD, mainly to exclude other confounding abnormalities. An uncommon alteration visible on conventional MRI involves narrowing or disappearance of the pars compacta of the substantia nigra (SN) on T2 weighted-imaging [9], yet this sign has low sensitivity and specificity, and contributes marginally to the diagnosis of PD, in particular at an early stage.

Based on the assumption that PD is associated with systematic brain SWI alteration, which is too subtle to be detected by visual analysis, we used an advanced computer-based analysis. It is important to distinguish PD from other degenerative or secondary forms of Parkinsonism, in view of its long disease duration, its relatively good prognosis and its remarkable response not only to dopaminergic agents but also to deep brain stimulation, providing relief of motor disability. This discrimination may sometimes be challenging based on clinical assessment alone, in particular in early stages of the disease [10]. In order to achieve a potentially clinically applicable diagnosis at the individual level, we implemented a pattern recognition approach, which can be illustrated by the example of face recognition. Individual

faces are not detected based on single features such as the tip of the nose, ears or eyes, but by a combination of multiple features, even though each individual feature may not be significantly different between groups (review [11]). As the most relevant clinical question is not the discrimination of PD versus healthy controls, but the diagnosis of PD versus other forms of Parkinsonism, we included 36 consecutive community-dwelling subjects with suspected PD. Inclusion criteria were brain  $^{123}\text{I}$ -ioflupane SPECT ('DaTScan') and extensive neurological testing including long-term follow-up as reference standard.

In particular, we addressed the question whether support vector machine (SVM) [12] pattern recognition of SWI data may contribute to the diagnosis of PD at an individual level.

## Methods

### Subjects

This retrospective study was approved by the local ethics committee. We included all consecutive patients seen in our institution between 2006 and 2010 with various forms of Parkinsonism who met the following criteria: (1) SWI at 3 T during clinical workup, (2) brain  $^{123}\text{I}$ -ioflupane SPECT ('DaTScan') as reference standard, (3) extensive neurological testing including clinical follow-up of at least 1 year and (4) absence of evident morphological findings on brain MRI.

The final sample included 16 PD patients (PD,  $67.4 \pm 6.2$  years, 9 female) and 20 patients with another form of Parkinsonism (OTHER,  $65.2 \pm 12.5$  years, 8 female). Age, sex and Fazekas score did not differ significantly between the two groups.

For the PD group, a diagnosis of PD was made in the presence of typical, asymmetrical and levodopa-responsive Parkinsonism meeting the UK Parkinson's Disease Society Brain Bank criteria, including at least two supportive criteria such as slow progression or peak-dose dyskinesia. PD was moderately advanced (mean Hoehn & Yahr stage [13]:  $2.3 \pm 0.6$ ), and none of these patients had atypical features, even after at least 1 year of follow-up (mean follow-up duration:  $6.4 \pm 3.3$  years). In addition, all had an asymmetrical decrease of  $^{123}\text{I}$ -ioflupane uptake in the posterior aspect of one or both putamen on SPECT. The OTHER group was more heterogeneous, reflecting the prevalence of common PD-mimicking conditions in the daily activity of a movement disorders clinic. All of these patients exhibited Parkinsonism defined as the presence of bradykinesia associated with resting tremor or rigidity. It included pathologies as varied as multiple system atrophy (MSA,  $n=4$ ), progressive supranuclear palsy (PSP,  $n=1$ ), dementia with Lewy body ( $n=2$ ), vascular Parkinsonism ( $n=1$ ), atypical tremors ( $n=5$ ) and psychogenic Parkinsonism ( $n=2$ ). In five cases, a firm



clinical diagnosis could not be established at last assessment, and these patients were labeled as having mixed Parkinsonism.

### MR Imaging

MR imaging was performed using a conventional clinical 3.0-T MR system (Magnetom Trio, Siemens, Erlangen, Germany). We used a standard SWI sequence [8]: field of view 352×448, 72 slices, voxel size 0.5×0.5×1.2 mm, echo time TE 20 ms, repetition time TR 34 ms and 1 average. Additional sequences (T1w, T2w, FLAIR) were acquired and analysed to exclude major brain abnormalities. White matter lesions were analysed according to the Fazekas score [14].

### Statistical analysis

Age, ROI volume and ROI mean signal intensity were analysed in parametric unpaired t-tests, and gender and visual rating of SWI in non-parametric unpaired Mann-Whitney tests. *P*-values <0.05 were considered significant.

### Visual Analyses

The presence of microbleeds was visually analysed because of the near-random distribution. A visual rating scale (0-3) analysis [15] was applied to the SN, red nucleus (RN), dentate nucleus (DN) of the cerebellum and putamen. The DN was not covered in the investigated SWI volume in six subjects.

### Voxel-wise analyses

The voxel-wise analyses were performed as in [5]. Pre-processing of the SWI data was done in the FSL software package [16]. All individual images were linearly transferred into Montreal Neurological Institute (MNI) standard space using FLIRT (part of FSL). Since SWI images are relative data, we performed intensity normalisation by normalising each individual image with respect to the average signal of the ventricular system [5].

### Group-level analyses

Voxel-wise statistical analysis was performed in RANDOMISE, part of FSL, corrected for multiple comparisons implementing threshold-free cluster enhancement (TFCE) considering fully corrected *P*-values <0.05 as significant [17]. Age and gender were used as non-explanatory co-regressors.

The linear spatial normalisation alignment of the infratentorial structures was less accurate than for the supratentorial regions. In combination with the small volumes of the SN and RN, these structures were additionally manually segmented and analysed with respect to volume and mean

signal intensity. This manual segmentation was performed on the spatially normalised data, which already compensate for differences in global brain volume.

### Individual-level SVM analysis

The individual SVM classification analysis is identical to previous studies [5, 18] and analysed in the freely available WEKA software package (<http://www.cs.waikato.ac.nz/ml/weka>, Version 3.6.1). In a first step, we performed a “Relief” [19] feature selection because not all voxels discriminate between groups. Both the inclusion of non-discriminative voxels and the exclusion of discriminative voxels reduce the classification accuracy. We selected the top 100, 250, 500, 750 and 1,000 features, implementing ten-fold cross validation. The second step consisted of the SVM classification sequential minimal optimisation (SMO) [20] with a radial basis function (RBF) kernel [21]. There are two fundamental parameters. GAMMA represents the width of the radial basis function, and C represents the error/trade-off parameter that adjusts the importance of the separation error in the creation of the separation surface. Based on our previous experience of similar analyses in the domain of mild cognitive impairment, which showed best results for C=1 [5, 18], GAMMA was iteratively explored from 0.01 to 0.09, with an increment of 0.01, while C was fixed to 1.00. We performed ten repetitions of a ten-fold cross validation technique.

## Results

### Visual analysis

Only one patient (of the PD group) had one microbleed. Due to the small number of microbleeds, no additional statistical analyses were performed.

There was no significant difference in the visual rating scale [15] between groups (Fig. 1).

### Group-level analyses

PD versus OTHER patients had increased SWI values in the bilateral, right-dominant thalamus (Fig. 2, Table 1). The inverse comparison yielded no supra-threshold clusters. The additional ROI analysis in SN and RN yielded no significant difference in volume between groups, yet significantly (*P*<0.05) increased signal intensity in PD versus OTHER in the left SN (Fig. 3).

### Individual-level SVM analysis

SVM analysis of SWI provided a correct classification of PD versus OTHER with an accuracy of up to 86.92±

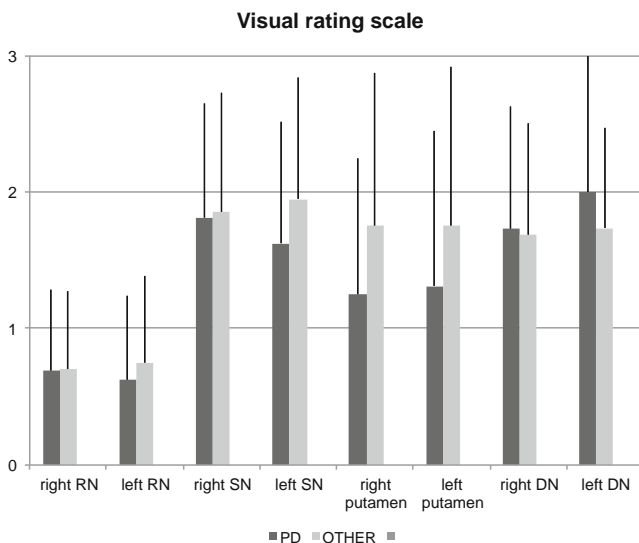


**Fig. 1** Visual rating of SWI in PD. In accordance with a previous investigation [15], the SWI in substantia nigra (SN), red nucleus (RN) and dentate nucleus (DN) of the cerebellum and putamen was visually assessed and graded from 0–3. There was no significant difference in this visual rating score between PD versus OTHER. Average visual rating score separated into left and right for PD (dark grey) and OTHER (light grey). Error bars indicate standard deviation

16.59 % (Table 2). The spatial distribution of the most discriminative voxels (features) overlapped substantially with the results of the group-level analysis in particular in thalamus bilaterally, while additional discriminative voxels were identified in bilateral head of caudate nucleus (Fig. 2).

## Discussion

Computer-based SVM analysis of brain SWI data provided an accurate individual detection of PD patients despite the absence of visually detectable differences. Given the extensive use of brain MRI during routine clinical workup of Parkinsonism and the operator-independent and almost automatic post-processing of the data, this analysis features easy applicability and significant benefit at the bedside. The method is not intended to replace but to complement existing tests, ideally as combined multi-modal assessment including other imaging parameters such as 3DT1 and DTI as well as laboratory, neurological testing, nuclear medicine, etc., to further improve accuracy and robustness of an individual diagnosis of PD.

### Visual analysis of SWI images in PD

In the investigated sample, only one microbleed was present. The presence of microbleeds thus does not represent a clinically useful parameter for the discrimination PD versus other forms of Parkinsonism.

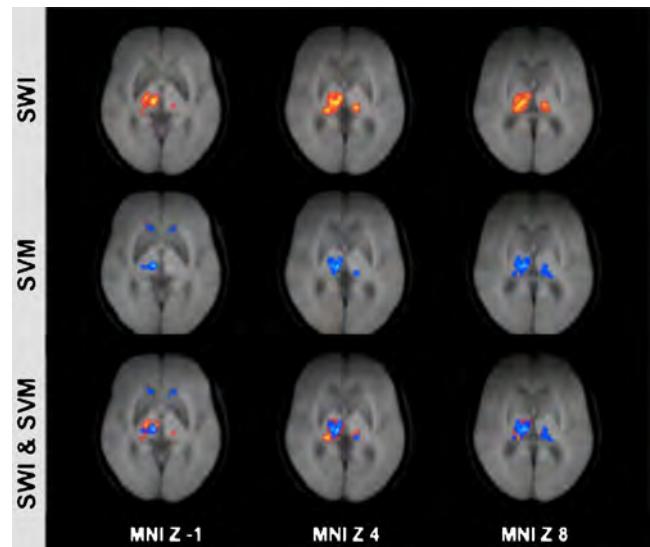


**Fig. 2** Voxel-wise SWI analysis in PD. PD patients versus OTHER had increased signal intensity in bilateral, right-dominant thalamus (red). The inverse comparison yielded no supra-threshold clusters. The most discriminative voxels (features) identified using the RELIEF feature selection algorithm, which are the basis for the individual-level SVM analysis, are illustrated for comparison in blue. Note the good overlap despite the fundamentally different methodology. Compared to the group-level voxel-wise analysis, the RELIEF additionally identified bilateral head of caudate nucleus as discriminative regions. These regions also displayed a trend in the group-level analysis, which did not reach multiple comparisons corrected significance. Axial slices at the indicated position in MNI (Montreal Neurological Institute) standard space coordinates (radiological convention with right hemisphere on left hand side). Grey: Mean SWI value. Threshold-free cluster enhancement (TFCE) corrected for multiple comparisons at  $P < 0.05$ . Supra-threshold voxels were enlarged using TBSS fill (part of FSL) for illustrative purposes

The previously proposed semi-quantitative visual rating scale in PD [15] found no significant difference between groups. The original study included 11 patients with PD, 12 with PSP, 12 with the Parkinson variant of MSA (MSA-P) and 11 healthy controls. The RN discriminated PSP from PD and MSA-P. The putamen differentiated PSP from PD. The rating score could however not differentiate MSA-P and PD. In conclusion, the score proposed in this study appeared best suited to detect PSP, while the visual rating was not sufficient to discriminate PD from the other forms of Parkinsonism. Our results are in agreement with these findings.

### Group-level analysis of SWI

The voxel-wise analysis of the SWI images yielded significantly increased SWI values in PD patients versus other Parkinsonism in bilateral, right-dominant thalamus. The additionally performed ROI analysis, which was performed because of the inaccuracy of automatic spatial normalisation in the infratentorial region in relation to the small size of SN and RN, demonstrated a significant increase of the physiological



**Table 1** Lists all significant voxels in SWI signal intensity between PD and OTHERS. Significant TFCE corrected differences were observed for PD versus OTHERS in bilateral thalamus, while the inverse comparison of OTHER versus PD yielded no supra-threshold clusters

Cluster index	Voxels	Z-MAX	Z-MAX X (mm)	Z-MAX Y (mm)	Z-MAX Z (mm)	Z-COG X (mm)	Z-COG Y (mm)	Z-COG Z (mm)	Side	Anatomic location
PD > OTHER										
1	1705	0.997	9	-21	-1	14.6	-21	5.16	right	thalamus
2	194	0.988	-11	-29	5	-12	-26	5.81	left	thalamus
3	14	0.964	-16	-32	7	-16.1	-29.8	7.5	left	thalamus
OTHER > PD										
No supra-threshold voxels										

Cluster index = number of cluster, voxels = number of supra-threshold voxels in cluster, Z-MAX = maximum Z value (or 1 - p-value) within each cluster, Z-MAX X,Y,Z = location of maximum p-value per cluster in MNI standard space (X, Y, Z) and Z-COG X,Y,Z = centre of gravity of the cluster in MNI standard space (X, Y, Z), side and anatomic location

low SWI signal in the left SN in PD patients, and a clear yet non-significant trend in the contralateral SN. This observation is in agreement with previous studies [15]. This asymmetry might be related to Parkinsonism being clinically more prominent on the right in the majority of PD patients (12 right versus 4 left dominant parkinsonism).

Only few previous studies used SWI to assess brain iron deposition in PD. The visual analysis study of SWI at 1.5 T discussed above showed brain iron in the putamen, SN, RN and DN in PD patients (and healthy controls) compared to MSA-P and PSP patients [15]. Another SWI study at 1.5 T in 16 PD, 8 MSA-P patients and 44 age-matched healthy controls used manually defined ROIs. MSA-P patients had higher iron deposition in the putamen and thalamus [22]. Both investigations are in principle agreement with our results.

SWI-derived phase shift values were analysed using a ROI approach in 40 patients with PD without dementia and 26 controls [23]. The SN was the only region that differed

between PD and controls. Huang et al. evaluated SWI at 3 T in 30 PD patients and 19 controls in a manual ROI analysis [24]. The mean phase values of both the SN and globus pallidum differed significantly between the PD group versus normal controls. Three studies focussed more on methodological aspects. A study in 51 patients with symptoms of PD compared several pulse sequences at 3 T to assess brain iron concentrations [25]. SWI contrast correlated well with brain iron concentration. One study assessed SWI-derived phase radians in 42 PD patients and 30 control subjects at 1.5 T, and demonstrated lower phase radians of the SN, caudate nucleus and RN in PD patients [26]. Finally, SWI-derived phase shift was assessed at 3 T in 12 PD patients and 5 controls [27]. Most of these studies provide group-level results; application of these findings in daily clinical neuroradiology is therefore limited.

The group-level comparisons in the current investigation should be interpreted with caution because of the composition

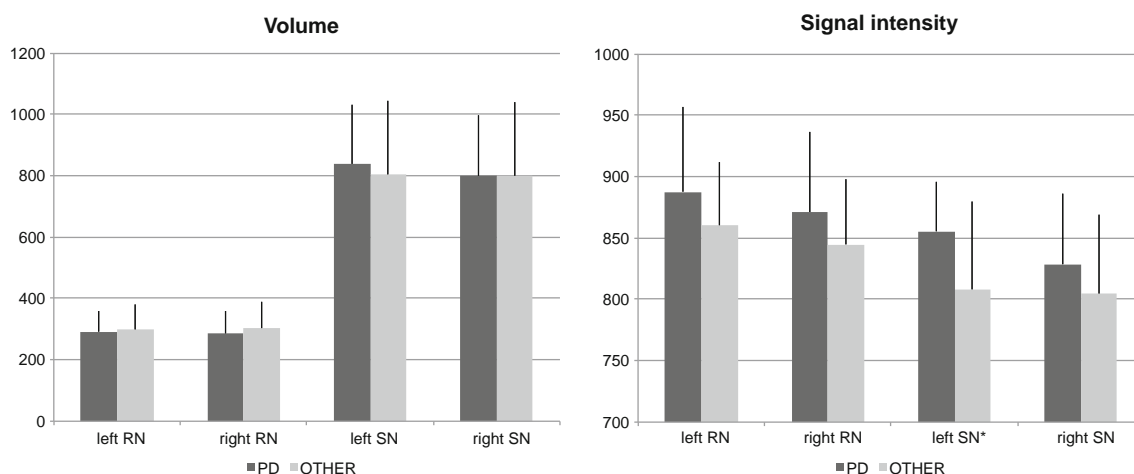


**Fig. 3** ROI analysis of red nucleus and substantia nigra. The region of interest analysis of red nucleus (RN) and substantia nigra (SN) yielded no significant difference in volume between groups (A). Concerning

signal intensity, there was a uniform tendency of increased signal intensity in PD (dark grey) versus OTHER (light grey), which was significant ( $P < 0.05$ ) in left SN

**Table 2** Individual SVM classification of PD based on SWI

SVM classification					
16 PD, 20 OTHER-NUL classification accuracy 55.6 % (20/36)					
No. of features	Accuracy	TP rate	FP rate	TN rate	FN rate
100	86.92(16.59)	0.87(0.28)	0.14(0.23)	0.87(0.23)	0.13(0.28)
250	82.83(18.38)	0.87(0.28)	0.21(0.28)	0.79(0.28)	0.13(0.28)
500	83.42(18.18)	0.87(0.28)	0.20(0.27)	0.80(0.27)	0.13(0.28)
750	81.58(18.44)	0.83(0.31)	0.20(0.26)	0.81(0.26)	0.18(0.31)
1000	82.25(18.98)	0.81(0.32)	0.17(0.26)	0.83(0.26)	0.19(0.32)

Accuracy, true positive (TP), false positive (FP), true negative (TN) and false negative (FN) rates for individual classifications using a SVM classifier using the indicated number of selected features for the individual classification of PD versus OTHER. Note that the accuracy is calculated as average accuracy of ten repetitions using ten-fold cross validation (average and standard deviation)

of the control group. The focus of the current investigation was the individual diagnosis of PD subjects. The clinically relevant analysis was thus oriented towards detection of PD in a group of individuals with a variety of PD-like conditions. The inclusion of healthy controls would have been irrelevant in this context. Even a classifier that perfectly discriminates between confirmed PD and healthy controls does not necessarily discriminate between PD and other forms of Parkinsonism. Indeed, the group composition of the control group may influence the performance of a classifier depending on the prevalence of each condition. For example, the frequency of PD (69.6 % of Parkinsonian syndromes) is approximately 22 times higher than the prevalence of MSA (3.2 %) [28]. This means that a “dummy” or null classifier that simply always gives the diagnosis of PD would obtain 95 % accuracy for the correct diagnosis of PD versus MSA in a community-dwelling sample. The pre-selection of patients with specific diseases might represent a systematic confound with respect to the performance of a classifier in the clinical setting, and we consequently included consecutive, unselected patients from our institution. Moreover, the presence of a  $^{123}\text{I}$ -ioflupane SPECT was an inclusion criterion in this study, but this is not available in healthy controls because of radiation exposure. The apparent disadvantage of using unselected consecutive patients is that it is difficult to interpret group-level results. We present these group-level results mainly to visualise detectable SWI changes between PD versus OTHER as the basis for the individual-level pattern recognition analysis.

#### Individual-level SVM classification analysis

In order to obtain an individual discrimination of PD subjects, we adopted a complex methodology including a spatial and intensity normalisation of SWI data, feature selection of the most discriminative voxels, and subsequent SVM classification [5, 18]. The best classification accuracy was about 86 %.

The already-discussed manual ROI analysis study by Huang et al. evaluated SWI at 3 T in 30 PD patients and 19 age-matched normal controls [24]. The best diagnostic accuracy for the detection of PD was 59.2 % (29/49), which is actually close to the null classification accuracy. The other study by Wang et al. [22] analysed SWI phase shift in manually defined ROIs in 16 PD, 8 MSA-P and 44 age-matched healthy controls. The putamen provided the best differentiation of MSA-P versus PD with an area under the curve of 0.92, which translates into a sensitivity of approximately 90 % and a specificity of approximately 82 %. The approach of voxel-wise data preprocessing followed by SVM classification described in this study is operator independent and nearly automatic, and yielded higher classification accuracy compared to these manual ROI investigations. Moreover, as discussed above, the pre-selection of specific diagnoses such as MSA-P, which do not mirror the prevalence of these conditions in a community-dwelling sample, may systematically confound the results of such classification analyses with respect to potential clinical applications in prospective, unselected cases.

It is noteworthy that SVM [12] analyses for individual classification are fundamentally different from the group-level ROI or voxel-wise analyses discussed above. Such voxel-wise analyses are univariate tests, which separately analyse each included ROI or voxel between two (or more) groups. Given the multiple tests for voxel-wise analyses, it is necessary to implement a correction for multiple comparisons as a second step. By comparison, individual-level SVM analyses are multivariate tools that originate from a field called “machine learning” or multi-voxel pattern analysis (MVPA), a branch of artificial intelligence. The aim is to identify patterns that allow for the discrimination of individual subjects. There is only one resulting parameter per subject; hence, there is no need for corrections for multiple comparisons (review [11]). There are only a few previous applications of SVM classification in the domain

of PD. The majority of these studies applied SVM classifiers to behavioral data of gait analysis [29], fine motor force tracking [30], analysis of wearable accelerometer sensors [31] or joint movement [32], and even voice recording [33]. The only previous SVM application to MRI data in the domain of PD analysed VBM pre-processed grey matter in 21 PD, 11 MSA-P and 10 PSP, and 22 healthy controls [34]. The best classification accuracy up to 96.8 % was obtained for PSP versus PD, while the accuracy was 71.9 % for MSA versus PD. PD could not be discriminated from controls. These classification accuracies are consistent with the clinical neuroradiological experience that PSP has the most pronounced visible alterations in brain MRI with selected atrophy of the mesencephalon, referred to as the “king penguin” or “hummingbird” sign [35], while changes in MSA-P are more subtle and PD-associated changes are almost always absent. Concerning analyses of white matter derived from diffusion tensor imaging (DTI) data, there are currently no SVM investigations in the domain of PD. However, a previous stepwise logistic regression analysis study discriminated PD versus PSP based on apparent diffusion coefficient (ADC) values in ROIs in the basal ganglia, notably the putamina, with a sensitivity of 90 % and a positive predictive value of 100 %, while this region did not discriminate between PSP and MSA-P [36]. Another related study demonstrated that ADC discriminates between MSA-P versus PD and controls, yet not between PD and controls [37]. Assessment of SWI may be a complimentary parameter with respect to the discussed VBM grey matter and DTI white matter data. Ideally, a classification analysis should integrate multiple imaging contrasts e.g., T1w VBM, DTI and SWI, preferably in combination with other parameters such as gait analysis, laboratory tests, neuropsychology, etc., with the intention to further increase the accuracy and robustness of individual diagnosis. It is however not trivial to optimise such multimodal classification analyses, which is a domain of current research. The SVM analysis can be performed on standard computer hardware within minutes using free software, which is thus eventually potentially applicable in a clinical routine setting.

### Limitations

The major limitation of this investigation is the relatively small sample size. The high accuracy rates of individual classification exceeded our expectations. These values were obtained by a well-established ten-fold cross validation where nine parts are used for training and the remaining part is used for testing the classifier. Even though this cross-validation approach is an appropriate method and for the number of subjects involved in our study, the present results seem too optimistic, probably related to some degree of overfitting of the data. Moreover, we first performed a

feature selection. The rationale behind this approach is that not all voxels discriminate between groups and the inclusion of non-discriminative voxels will decrease classification performance. Also, the number of voxels without feature selection clearly exceeds the number of subjects. This processing chain of feature selection followed by SVM classification was successfully applied in a few recent investigations [5, 18, 38], but it might still contribute to some degree of overfitting of the data. We present our data as a pilot study showing the feasibility of this methodology in the domain of Parkinson disease. Additional validation in larger independent data sets, which should be ideally acquired on different MR systems, field strengths and MR parameters, which might influence the image contrast [39], is warranted to confirm the present findings.

Most previous research-oriented SWI studies used phase images [40]. These phase images are not used for clinical diagnosis and are infrequently stored on image servers. We analysed SWI images taking into account that these SWI images correspond to relative values and that iron deposition is not the only origin for lower SWI values. Other origins of decreased SWI values include haemorrhage, calcifications, post-operative debris and deposition of other metals. We normalised the SWI images with respect to the water signal in the cerebrospinal fluid, inferring a constant SWI value in water [5]. A recent study compared several pulse sequences at 3-T MRI implementing a similar approach showed that SWI correlates well with brain iron content [25]. Although this approach is less direct than the analysis of the phase images, it allows for a wider application of the presented analysis strategy.

### References

1. Aquino D, Bizzi A, Grisoli M et al (2009) Age-related iron deposition in the basal ganglia: quantitative analysis in healthy subjects. *Radiology* 252:165–172
2. Thomas M, Jankovic J (2004) Neurodegenerative disease and iron storage in the brain. *Curr Opin Neurol* 17:437–442
3. Smith MA, Zhu X, Tabaton M et al (2010) Increased iron and free radical generation in preclinical Alzheimer disease and mild cognitive impairment. *J Alzheimers Dis* 19:363–372
4. Bishop GM, Robinson SR, Liu Q et al (2002) Iron: a pathological mediator of Alzheimer disease? *Dev Neurosci* 24:184–187
5. Haller S, Bartsch A, Nguyen D et al (2010) Cerebral microhemorrhage and iron deposition in mild cognitive impairment: susceptibility-weighted MR imaging assessment. *Radiology* 257:764–773
6. Dexter DT, Carayon A, Javoy-Agid F et al (1991) Alterations in the levels of iron, ferritin and other trace metals in Parkinson's disease and other neurodegenerative diseases affecting the basal ganglia. *Brain* 114:1953–1975
7. Youdim MB, Ben-Shachar D, Riederer P (1993) The possible role of iron in the etiopathology of Parkinson's disease. *Mov Disord* 8:1–12
8. Haacke EM, Xu Y, Cheng YC et al (2004) Susceptibility weighted imaging (SWI). *Magn Reson Med* 52:612–618

9. Oikawa H, Sasaki M, Tamakawa Y et al (2002) The substantia nigra in Parkinson disease: proton density-weighted spin-echo and fast short inversion time inversion-recovery MR findings. *AJNR Am J Neuroradiol* 23:1747–1756
10. Hughes AJ, Daniel SE, Ben-Shlomo Y et al (2002) The accuracy of diagnosis of parkinsonian syndromes in a specialist movement disorder service. *Brain* 125:861–870
11. Haller S, Lovblad KO, Giannakopoulos P (2011) Principles of classification analyses in mild cognitive impairment (MCI) and Alzheimer disease. *J Alzheimers Dis* 26:389–394
12. Noble WS (2006) What is a support vector machine? *Nat Biotechnol* 24:1565–1567
13. Hoehn MM, Yahr MD (1967) Parkinsonism: onset, progression and mortality. *Neurology* 17:427–442
14. Fazekas F, Chawluk JB, Alavi A et al (1987) MR signal abnormalities at 1.5 T in Alzheimer's dementia and normal aging. *AJR Am J Roentgenol* 149:351–356
15. Gupta D, Saini J, Kesavadas C et al (2010) Utility of susceptibility-weighted MRI in differentiating Parkinson's disease and atypical parkinsonism. *Neuroradiology* 52:1087–1094
16. Smith SM, Jenkinson M, Woolrich MW et al (2004) Advances in functional and structural MR image analysis and implementation as FSL. *NeuroImage* 23:S208–19
17. Smith SM, Nichols TE (2009) Threshold-free cluster enhancement: addressing problems of smoothing, threshold dependence and localisation in cluster inference. *NeuroImage* 44:83–98
18. Haller S, Nguyen D, Rodriguez C et al (2010) Individual prediction of cognitive decline in mild cognitive impairment using support vector machine-based analysis of diffusion tensor imaging data. *J Alzheimers Dis* 22:315–327
19. Kononenko I, Šimec E, Robnik-Šikonja M (1997) Overcoming the myopia of inductive learning algorithms with RELIEFF. *Appl Intell* 7:39–55
20. Platt J (1999) Sequential minimal optimization: A fast algorithm for training support vector machines. *Advances in Kernel methods-support vector learning* 208
21. Scholkopf B, Sung KK, Burges CJC et al (1997) Comparing support vector machines with Gaussian kernels to radialbasis function classifiers. *IEEE Trans Signal Process* 45:2758–2765
22. Wang Y, Butros S R, Shuai X et al (2011) Different iron-deposition patterns of multiple system atrophy with predominant parkinsonism and idiopathic parkinson diseases demonstrated by phase-corrected susceptibility-weighted imaging. *AJNR Am J Neuroradiol*
23. Zhang J, Zhang Y, Wang J et al (2010) Characterizing iron deposition in Parkinson's disease using susceptibility-weighted imaging: an in vivo MR study. *Brain Res* 1330:124–130
24. Huang XM, Sun B, Xue YJ et al (2010) Susceptibility-weighted imaging in detecting brain iron accumulation of Parkinson's disease. *Zhonghua Yi Xue Za Zhi* 90:3054–3058
25. Rossi M, Ruottinen H, Elovaara I et al (2010) Brain iron deposition and sequence characteristics in Parkinsonism: comparison of SWI, T\* maps, T-weighted-, and FLAIR-SPACE. *Invest Radiol* 45:795–802
26. Zhang W, Sun SG, Jiang YH et al (2009) Determination of brain iron content in patients with Parkinson's disease using magnetic susceptibility imaging. *Neurosci Bull* 25:353–360
27. Grabner G, Haubenberger D, Rath J et al (2010) A population-specific symmetric phase model to automatically analyze susceptibility-weighted imaging (SWI) phase shifts and phase symmetry in the human brain. *J Magn Reson Imaging* 31:215–220
28. Pezzoli G, Canesi M, Galli C (2004) An overview of parkinsonian syndromes: data from the literature and from an Italian data-base. *Sleep Med* 5:181–187
29. Jeon HS, Han J, Yi WJ et al (2008) Classification of Parkinson gait and normal gait using spatial-temporal image of plantar pressure. *Conf Proc IEEE Eng Med Biol Soc* 2008:4672–4675
30. Brewer BR, Pradhan S, Carvell G et al (2009) Feature selection for classification based on fine motor signs of Parkinson's disease. *Conf Proc IEEE Eng Med Biol Soc* 2009:214–217
31. Patel S, Lorincz K, Hughes R et al (2009) Monitoring motor fluctuations in patients with Parkinson's disease using wearable sensors. *IEEE Trans Inf Technol Biomed* 13:864–873
32. Chan J, Leung H, Poizner H (2010) Correlation among joint motions allows classification of Parkinsonian versus normal 3-D reaching. *IEEE Trans Neural Syst Rehabil Eng* 18:142–149
33. Ozcift A (2011) SVM feature selection based rotation forest ensemble classifiers to improve computer-aided diagnosis of Parkinson disease. *J Med Syst*
34. Focke NK, Helms G, Scheewe S et al (2011) Individual voxel-based subtype prediction can differentiate progressive supranuclear palsy from idiopathic parkinson syndrome and healthy controls. *Hum Brain Mapp* 32:1905–1915
35. Groschel K, Kastrup A, Litvan I et al (2006) Penguins and hummingbirds: midbrain atrophy in progressive supranuclear palsy. *Neurology* 66:949–950
36. Seppi K, Schocke MF, Esterhammer R et al (2003) Diffusion-weighted imaging discriminates progressive supranuclear palsy from PD, but not from the Parkinson variant of multiple system atrophy. *Neurology* 60:922–927
37. Schocke MF, Seppi K, Esterhammer R et al (2002) Diffusion-weighted MRI differentiates the Parkinson variant of multiple system atrophy from PD. *Neurology* 58:575–580
38. Plant C, Teipel SJ, Oswald A et al (2010) Automated detection of brain atrophy patterns based on MRI for the prediction of Alzheimer's disease. *NeuroImage* 50:162–174
39. Haacke EM, Mittal S, Wu Z et al (2009) Susceptibility-weighted imaging: technical aspects and clinical applications, part 1. *AJNR Am J Neuroradiol* 30:19–30
40. Hopp K, Popescu BF, McCrea RP et al (2010) Brain iron detected by SWI high pass filtered phase calibrated with synchrotron X-ray fluorescence. *J Magn Reson Imaging* 31:1346–1354

### ***Chapter 3.1.3***

## ***Distinct spatiotemporal patterns for disease duration and stage in Parkinson's disease.***

S. Badoud N. Nicastro V. Garibotto P.R. Burkhard S. Haller

Published in EUROPEAN JOURNAL OF NUCLEAR MEDICINE AND  
MOLECULAR IMAGING (2015)



# Distinct spatiotemporal patterns for disease duration and stage in Parkinson's disease

Simon Badoud<sup>1,2,3</sup> · Nicolas Nicastro<sup>1,3</sup> · Valentina Garibotto<sup>3,4</sup> · Pierre R. Burkhard<sup>1,3</sup> · Sven Haller<sup>3,5,6,7</sup>

Received: 12 May 2015 / Accepted: 12 August 2015  
© Springer-Verlag Berlin Heidelberg 2015

## Abstract

**Purpose** To assess correlations between the degree of dopaminergic depletion measured using single-photon emission computed tomography (SPECT) and different clinical parameters of disease progression in Parkinson's disease (PD).

**Methods** This retrospective study included 970 consecutive patients undergoing <sup>123</sup>I-ioflupane SPECT scans in our institution between 2003 and 2013, from which we selected a study population of 411 patients according to their clinical diagnosis: 301 patients with PD (69.4±11.0 years, of age, 163 men) and 110 patients with nondegenerative conditions included as controls (72.7±8.0 years of age, 55 men). Comprehensive and operator-independent data analysis included spatial normalization into standard space, estimation of the

mean uptake values in the striatum (caudate nucleus + putamen) and voxel-wise correlation between SPECT signal intensity and disease stage as well as disease duration in order to investigate the spatiotemporal pattern of the dopaminergic nigrostriatal degeneration. To compensate for potential interactions between disease stage and disease duration, one parameter was used as nonexplanatory coregressor for the other. **Results** Increasing disease stage was associated with an exponential decrease in <sup>123</sup>I-ioflupane uptake ( $R^2=0.1501$ ) particularly in the head of the ipsilateral caudate nucleus ( $p<0.0001$ ), whereas increasing disease duration was associated with a linear decrease in <sup>123</sup>I-ioflupane uptake ( $p<0.0001$ ;  $R^2=0.1532$ ) particularly in the contralateral anterior putamen ( $p<0.0001$ ).

**Keypoints** • Disease stage and disease duration have different spatiotemporal patterns of dopaminergic depletion in PD.

- <sup>123</sup>I-ioflupane uptake in the striatum decreases exponentially with disease stages.
- Disease stage correlates particularly with uptake in the head of the caudate nucleus with ipsilateral predominance.
- <sup>123</sup>I-ioflupane uptake in the striatum decreases linearly with disease duration.
- Disease duration correlates particularly with uptake in the anterior putamen with contralateral predominance.
- The operator-independent spatial normalization of <sup>123</sup>I-ioflupane SPECT scans provides a reference database for research and clinical studies based on a large sample of 411 patients.

✉ Sven Haller  
sven.haller@me.com

<sup>1</sup> Neurology Unit, Department of Clinical Neurosciences, Geneva University Hospitals, Geneva, Switzerland

<sup>2</sup> Neurophysiology Unit, Department of Medicine, University of Fribourg (CH), Fribourg, Switzerland

<sup>3</sup> Faculty of Medicine, University of Geneva, Geneva, Switzerland

<sup>4</sup> Nuclear Medicine and Molecular Imaging Unit, Department of Medical Imaging, Geneva University Hospitals, Geneva, Switzerland

<sup>5</sup> Centre de Diagnostique Radiologique de Carouge, Geneva, Switzerland

<sup>6</sup> Department of Surgical Sciences, Radiology, Uppsala University, Uppsala, Sweden

<sup>7</sup> Department of Neuroradiology, University Hospital Freiburg, Freiburg, Germany



**Conclusion** We observed two distinct spatiotemporal patterns of posterior to anterior dopaminergic depletion associated with disease stage and disease duration in patients with PD. The developed operator-independent reference database of 411  $^{123}\text{I}$ -ioflupane SPECT scans can be used for clinical and research applications.

**Keywords** Parkinson's disease ·  $^{123}\text{I}$ -ioflupane SPECT · Voxel-wise analysis · Disease duration · Disease stage

## Introduction

Over the last two decades,  $^{123}\text{I}$ -ioflupane SPECT has become a routinely used tool for the diagnosis of Parkinson's disease (PD). It has proved particularly useful in distinguishing PD and other degenerative forms of parkinsonism from nondegenerative movement disorders such as essential tremor, dystonia, drug-induced parkinsonism and many others [1–6]. It may also serve as a powerful instrument for the *in vivo* clinical investigation of the pathophysiological mechanisms underlying this neurodegenerative disorder. The technique involves a radioactive ligand ( $^{123}\text{I}$ -ioflupane) of the presynaptic dopamine transporter (DAT), which has been shown to reflect degeneration of the dopaminergic nigrostriatal pathway in PD [3, 7, 8]. More recently, several investigations have assessed a potential link between  $^{123}\text{I}$ -ioflupane SPECT data and progression of PD, and have shown a negative correlation between striatal  $^{123}\text{I}$ -ioflupane uptake and disease stage [3, 7, 9–11]. However, most of these studies included a relatively limited number of patients (16 PD vs. 10 controls [7], 41 PD [9], 32 PD vs. 24 controls [10], 19 PD [11], 103 PD [3]) and analysed manually defined regions of interest (ROI).

Our present study included a unique cohort of 301 PD and 110 control patients identified from among 970 consecutive patients scanned using the same SPECT apparatus and following the same acquisition protocol in our institution between 2003 and 2013. We conducted an operator-independent voxel-wise analysis in order to evaluate the correlation between striatal uptake of  $^{123}\text{I}$ -ioflupane and disease duration and disease stage in patients with PD at a high spatial resolution.

## Materials and methods

### Participants

The local ethics committee approved this retrospective study, which included 970 patients who had consecutively undergone a brain  $^{123}\text{I}$ -ioflupane SPECT scan in our institution between October 2003 and September 2013. From this cohort,

we identified 411 patients who met the following criteria: (1) a visually assessed brain  $^{123}\text{I}$ -ioflupane SPECT scan, (2) extensive neurological testing and follow-up, (3) a well-established diagnosis of PD (patient group) or a neurological disorder known to spare the nigrostriatal dopaminergic system (control group), and (4) the absence of structural abnormalities on brain MRI.

In the PD group, the diagnosis was established by a trained movement disorders specialist following the UK Parkinson's Disease Society Brain Bank criteria. Criteria included the presence of bradykinesia associated with at least one of the following three criteria: 4–6 Hz resting tremor, rigidity or postural instability. Supportive features included, among others, unilateral onset, progressive course, an excellent and sustained response to levodopa or typical levodopa-induced dyskinesia. Of note, patients exhibiting atypical features suggesting another form of degenerative parkinsonism, such as multiple system atrophy, progressive supranuclear palsy or corticobasal degeneration, or secondary parkinsonism such as vascular parkinsonism or normal pressure hydrocephalus were all excluded. Importantly, while  $^{123}\text{I}$ -ioflupane SPECT data were not used to establish a specific diagnosis of PD, an abnormal scan was required to confirm degenerative parkinsonism. Accordingly, in the PD group,  $^{123}\text{I}$ -ioflupane SPECT typically showed an asymmetrical reduction in striatal uptake more marked in the putamen than in the caudate nucleus. PD patients were staged according to the Hoehn and Yahr (H&Y) classification, from mild and unilateral (stage 1) to advanced and bilateral disease stages (stages 4 and 5) [12]. The control group included patients who had had a  $^{123}\text{I}$ -ioflupane SPECT scan to assess an unusual tremor, unclear parkinsonism or other movement disorder of uncertain origin, and whose scan turned out to be normal. This control group therefore included patients with essential tremor, drug-induced parkinsonism, psychogenic parkinsonism and various conditions known to be associated with an unaltered nigrostriatal pathway.

### Demographic and clinical data

The control group comprised 110 patients (age  $72.7 \pm 8.0$  years, 55 men). The patient group comprised 301 PD patients stratified as follows: H&Y stage 1 (43 patients), H&Y stage 2 (142 patients), H&Y stage 3 (83 patients), H&Y stage 4 (19 patients) and H&Y stage 5 (13 patients; Table 1). As expected, there were significant differences between adjacent groups regarding age except between group H&Y stage 3 and 4 ( $p=0.471$ ) and between H&Y stage 4 and 5 ( $p=0.965$ ). Statistical analysis did not reveal any significant differences among the groups in terms of gender.



**Table 1** Demographic and clinical characteristics

	Control group	Hoehn and Yahr stage				
		1	2	3	4	5
Sex (m/f)	55/55	18/25 (n.s. vs. control)	85/58 (n.s. vs. stage 1)	42/41 (n.s. vs. stage 2)	9/10 (n.s. vs. stage 3)	9/4 (n.s. vs. stage 4)
Age (years)	72.7±8.0	62.3±11.3 ( <i>p</i> <0.01 vs. control)	67.8±10.9 ( <i>p</i> <0.05 vs. stage 1)	73.5±8.9 ( <i>p</i> <0.001 vs. stage 2)	75.2±10.2 (n.s. vs. stage 3)	75±9.5 (n.s. vs. stage 4)
Disease duration (years)	–	2.1±2.3	3.8±5.0	5.1±4.4	5.3±4.7	7.1±6.0

*n.s.* not significant

### SPECT image acquisition

After blocking thyroid uptake with either Lugol solution or sodium perchlorate, about 185 MBq of  $^{123}\text{I}$ -FP-CIT was administered intravenously. SPECT images were acquired 4 h after injection on a triple-head gamma camera (Toshiba Medical Systems, Tokyo, Japan) and fan-beam, low-energy, high-resolution collimators. Images were acquired in steps of  $6^\circ$  over  $360^\circ$  and a  $128 \times 128$  matrix. Patients were positioned using a head holder to minimize head motion. Images were corrected for scatter using a triple-energy window method and for photon attenuation using a 0.15/cm uniform coefficient. Dopaminergic agents were not discontinued. All images were reconstructed using Toshiba GMS software version 5 with the same reconstruction algorithms and parameters. More details have been provided by Garibotto et al. [13].

### MR image acquisition

MR imaging was performed over a period of 10 years as part of routine clinical work-up. This explains the variable MR protocol, but all patients had at least T2 imaging, fluid attenuation inversion recovery imaging and diffusion-weighted imaging or diffusion tensor imaging to rule out structural brain lesions. Moreover, white matter lesions were assessed according to the Fazekas scale [14]. A group of 103 patients had an additional high-resolution Magnetization Prepared Rapid Gradient Echo (MPRAGE) 3D T1 brain magnetic resonance scan as part of clinical routine using a 3.0-T MR system (Magnetom Trio; Siemens, Erlangen Germany) with the following parameters  $256 \times 256$  matrix, 176 sections,  $1 \times 1 \times 1$  mm, TE=2.3 ms, TR=2.300 ms.

### Statistical analysis

Statistical analyses were performed with GraphPad Prism (version 6.0, [www.graphpad.com](http://www.graphpad.com)) and FSL

(FMRIB Software Library, version 5.0, <http://fsl.fmrib.ox.ac.uk/fsl/fslwiki>).

### Image postprocessing

In a first step, we created a  $^{123}\text{I}$ -ioflupane-specific template based on 103 patients who had both a  $^{123}\text{I}$ -ioflupane SPECT and a 3D T1 MPRAGE MRI scan. Each individual brain  $^{123}\text{I}$ -ioflupane scan was linearly registered to the same patient 3D T1 data using FLIRT (FMRIB's linear image registration tool, part of FSL) [15, 16] and  $6^\circ$  of motion. Additionally, the 3D T1 data from individual patients were nonlinearly registered to the Montreal neurological institute (MNI) standard space by running FNIRT (part of FSL). This nonlinear transformation matrix was then applied to the individual  $^{123}\text{I}$ -ioflupane scans. Finally, a  $^{123}\text{I}$ -ioflupane-specific template was generated by merging and averaging all  $^{123}\text{I}$ -ioflupane images (using *fslmerge* and *fslmeants*, parts of FSL). In summary, this procedure created a nonlinear spatial normalization of the  $^{123}\text{I}$ -ioflupane scan into standard space using the information from the 3D T1 high-resolution MRI imaging in individual patients. Similar procedures have been used successfully in previous investigations [17, 18].

In a second step, all individual  $^{123}\text{I}$ -ioflupane SPECT scans were spatially normalized to this  $^{123}\text{I}$ -ioflupane SPECT template. In addition to the spatial normalization, the  $^{123}\text{I}$ -ioflupane SPECT scans were also intensity normalized by subtracting the average signal in the occipital region as reference region to each individual  $^{123}\text{I}$ -ioflupane data by using *fslmaths* (part of FSL). The resulting images were then divided by the average signal of the occipital region as described by Garibotto et al. [13]. The occipital region mask was manually created using *fslview* (part of FSL) on the MNI152\_T1\_2mm\_brain template.

To take into account the asymmetrical nature of PD, using *fslswapdim* we flipped images in patients with predominantly left-sided clinical symptoms to have the clinical predominance of the disease on the same side, so that the right side of the images corresponded to the

clinically less affected body side and the left side to the more affected body side in all subjects including controls. This was done after spatial normalization.

### Analysis of mean $^{123}\text{I}$ -ioflupane uptake

The mean  $^{123}\text{I}$ -ioflupane uptake values were calculated using a mask of the striatum. This striatal mask was created using the Harvard Oxford subcortical atlas (included in FSL) by combining the regions of the left and right putamen and caudate nucleus using `fslmaths`. The patients were grouped according to disease stage (defined as the H&Y stage at the time of image acquisition) and disease duration according to the time elapsed between the appearance of the first PD symptom and image acquisition and as described below (Table 2). The mean  $^{123}\text{I}$ -ioflupane uptakes in the striatal mask were calculated for each group as well as for controls using `fslmeants`. Linear and nonlinear regression was applied to the mean values (exponential one-decay linear regression). Note that the control values were not taken into account by the software for the operations described above.

### Voxel-wise analysis of $^{123}\text{I}$ -ioflupane uptake

Voxel-wise analysis was performed by permutation testing ( $n=5,000$ ) using the `randomise` function (part of FSL) and Threshold-Free Cluster Enhancement (TFCE) error considering multiple comparison corrected  $p$  values  $<0.05$  corrected as significant [19]. The analysis was run for both disease stage according to the H&Y stage and disease duration in years since the first identified PD symptom, investigating positive and negative linear correlations. Note that for the correlation with disease duration, disease stage was used as a nonexplanatory coregressor to compensate for a potentially confounding effect of disease duration. The analysis was done similarly for disease stage. Moreover, age and gender were used as coregressors to compensate for potential effects of age and gender. To assess the laterality of these results, we compared the voxel values in the striatum between the ipsilateral (right) side and the contralateral

(left) side for disease stage and disease duration using unpaired  $t$  tests. In order not to bias the results, the statistical analysis did not include the control group.

## Results

### Analysis of mean $^{123}\text{I}$ -ioflupane uptake

Evolution of the average  $^{123}\text{I}$ -ioflupane uptake showed a posterior to anterior progression of the dopaminergic depletion in the striatum, particularly the putamen, related to disease stage (Fig. 1, top) and duration (Fig. 1, bottom), but with two distinct patterns. We found an exponential decrease in  $^{123}\text{I}$ -ioflupane uptakes with progressive disease stage ( $R^2=0.1509$ ). Conversely, the  $^{123}\text{I}$ -ioflupane uptakes decreased linearly with progressive disease duration ( $p<0.0001$ ;  $R^2=0.1532$ ).

### Voxel-wise analysis of $^{123}\text{I}$ -ioflupane uptake

The voxel-wise analysis revealed two different spatiotemporal patterns of  $^{123}\text{I}$ -ioflupane uptake with increasing disease duration and disease stage. Increasing disease duration correlated with decreased uptake particularly in the anterior part of the putamen with a contralateral predominance ( $p<0.0001$ ). Conversely, increasing disease stage was correlated with decreased  $^{123}\text{I}$ -ioflupane uptake particularly in the head of the caudate nucleus with an ipsilateral predominance ( $p<0.0001$ ). The voxel-wise analyses of disease duration and disease stage were performed using the other parameter as coregressor in order to exclude potentially confounding interactions between these two factors (Fig. 2).

## Discussion

We developed an operator-independent database of  $^{123}\text{I}$ -ioflupane scans for research and clinical studies based on a large sample of 301 consecutive PD patients and 110 controls who underwent extensive neurological evaluation and follow-up. Using this reference database, we demonstrated two

**Table 2** Patient grouping

Disease duration			Disease stage		
Duration (years)	Group	No. of patients	H&Y stage	Group	No. of patients
0–1	1	99	1	1	43
1.25–2	2	61	2	2	143
2.5–5	3	62	3	3	83
6–9	4	42	4	4	19
>10	5	37	5	5	13

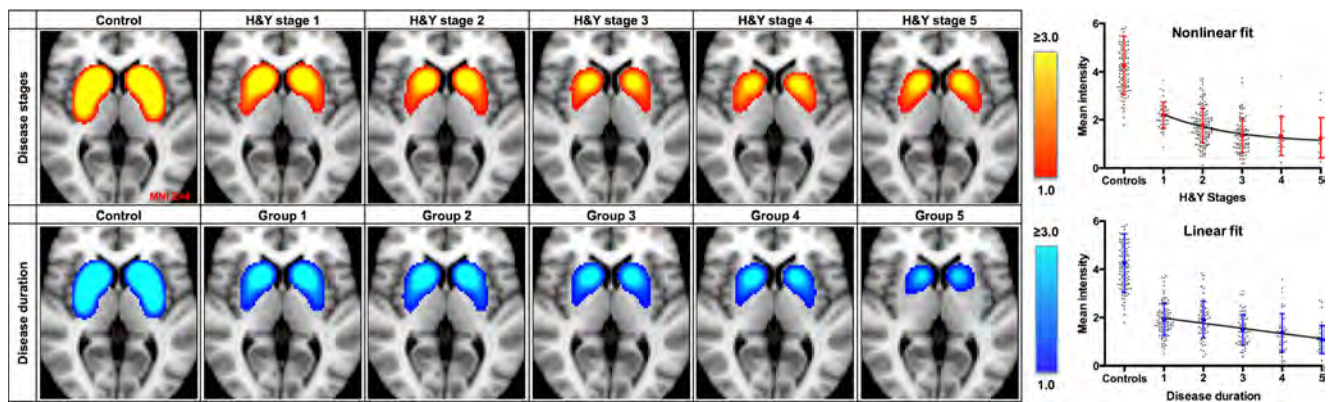


**Fig. 1** Mean <sup>123</sup>I-ioflupane uptake as a function of increasing Hoehn and Yahr disease stage (*top*) and increasing disease duration (*bottom*) superimposed on the Montreal Neurological Institute (MNI) standard space (T1 2-mm brain transverse section,  $z=4$ ). *Top* The normalized intensities range from 1 (low intensity, red) to 3 (high intensity, yellow).

<sup>123</sup>I-Ioflupane uptake decreases exponentially ( $R^2=0.1501$ ) with increasing Hoehn and Yahr stage. *Bottom* The normalized intensities range from 1 (dark blue) to 3 (light blue). <sup>123</sup>I-Ioflupane uptake decreases linearly with disease duration ( $p<0.0001$ ,  $R^2=0.1532$ ; group 1 short disease duration, group 5 long disease duration)

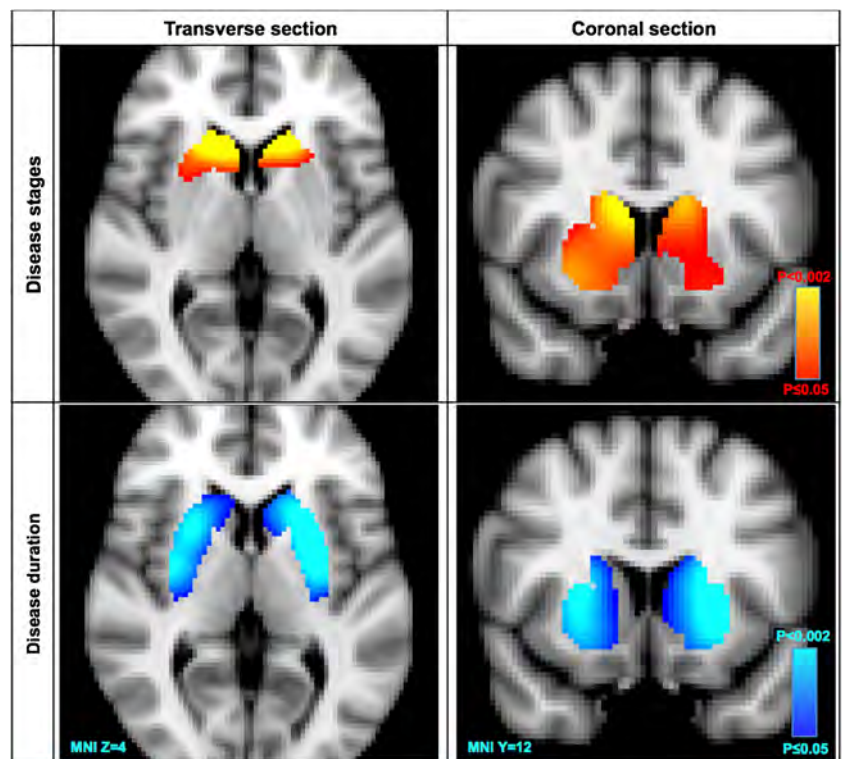
distinct spatiotemporal patterns of dopaminergic depletion in PD. Overall, both disease duration and disease stage were associated with progressive dopaminergic depletion in the striatum, particularly the putamen, with a posterior to anterior gradient, in accordance with the findings of many previous studies. Interestingly, we found that increasing disease stage was associated with an exponential dopaminergic depletion particularly in the ipsilateral head of the caudate nucleus, while increasing disease duration was associated with linear

dopaminergic depletion particularly in the contralateral anterior putamen.

**Disease stage**

During the past two decades, several molecular imaging studies have assessed the link between progression of PD and degeneration of the nigrostriatal dopaminergic system [3, 7, 9–11]. Most have observed a correlation between disease

**Fig. 2** Correlations corresponding to Hoehn and Yahr stage (red) and disease duration (blue) superimposed on the Montreal Neurological Institute (MNI) standard space (T1 2-mm brain transverse section,  $z=4$ , and coronal section,  $y=12$ )



stage and deterioration of the signal obtained by in vivo neuroimaging assessment of the dopaminergic system either with  $^{18}\text{F}$ -Dopa PET or with SPECT [3, 9, 10, 20–22], yet a few studies have failed to confirm this correlation [23, 24]. Overall, in our study, we definitely observed a clear posterior to anterior progression of dopaminergic depletion with increasing disease stage, in agreement with the findings of previous investigations [3, 25, 26]. Interestingly, Benamer et al. assessed 41 PD patients with Hoehn and Yahr stages I to IV and found a linear decrease in mean striatal uptake with increasing disease stage based on a ROI approach in a cross-sectional design [9]. Our results, obtained in a much larger cohort of 301 PD patients and an operator-independent voxel-wise analysis, in contrast demonstrated an exponential decrease in striatal uptake. This difference might be related to different scales for rating disease stage. Indeed, while Benamer et al. [9] used the Unified Parkinson's Disease Rating Score (UPDRS), we used the H&Y staging system, which is far less sensitive to the effects of levodopa and other antiparkinsonian medications.

The exponential decrease in striatal uptake with progressive disease stage indicates a faster dopaminergic depletion in early than in more advanced disease stages, following a steady percentage of neuronal loss or a variable absolute value of loss, more marked in the early phase of the condition. It is noteworthy that the few neuropathological investigations that have addressed this issue have indicated that the neuronal loss occurring in the PD substantia nigra pars compacta seems to follow a nonlinear exponential profile, as in our study, whereby neuronal loss within the nigrostriatal system is massive during the first few years after disease initiation and far less pronounced afterwards [27, 28]. The large variability in the data presented in Fig. 1b, d reflects the substantial interindividual variability of PD, as discussed by Benamer et al. [9].

In the majority of the investigations discussed above ROI analysis was used, and this, because of poor spatial resolution, may have biased the results. As a novel finding, the operator-independent voxel-wise analysis applied in this large cohort was able to show that uptake in the head of the caudate nucleus appears to be correlated with disease stage. This unexpected yet robust finding suggests that the anterior striatum is also the site of an intense and active degenerative process that takes place in more advanced stages of the disease, whereas the posterior striatum sustains massive neurodegeneration earlier in the disease course, as supported by the nonlinear decrease in the reduction of  $^{123}\text{I}$ -ioflupane uptake. In addition, at later stages, there might be a floor effect whereby ligand uptake is so low that a further reduction may no longer be captured. This finding is clinically meaningful as the caudate nucleus is essentially involved in the associative loop of the basal ganglia circuitry, and may well play an important role in late cognitive features of PD, including

executive dysfunction that is found in the vast majority of patients, apathy, memory loss, cognitive decline and, eventually, overt dementia.

### Disease duration

In contrast to disease stage, few previous studies have investigated the correlation between striatal uptake and disease duration. Overall, increasing disease duration was again associated with a posterior to anterior decrease in striatal  $^{123}\text{I}$ -ioflupane striatal uptake. In a longitudinal ROI-based study in 32 PD patients and 24 controls, Marek et al. found a linear decrease in striatal  $^{123}\text{I}$ - $\beta$ -CIT uptake [10]. Our operator-independent analysis reproduced this linear decrease in dopaminergic depletion in PD patients with increasing disease duration. As an additional finding, voxel-wise correlation analysis showed that the anterior part of the putamen was progressively impaired with increasing disease duration, which, as discussed in the previous section, can also be interpreted as a later step in the nigrostriatal degenerative process, whereby as structures become more affected with disease progression following a caudorostral gradient, the precommissural striatum undergoes rapid and severe degeneration later than the postcommissural striatum where the degenerative process has already slowed down.

### Laterality

While it is commonly accepted that there is a good correlation between the body side more affected by parkinsonism and a more marked contralateral decrease in striatal uptake, some previous investigations have shown partially conflicting results regarding the laterality of the dopaminergic depletion [4, 7, 9, 11]. In the current study, we disentangled the interaction of disease stage and duration. We were able to demonstrate that increasing disease stage was correlated with a predominantly ipsilateral dopaminergic depletion particularly in the head of the caudate nucleus, while increasing disease duration was correlated with predominantly contralateral dopaminergic depletion particularly in the anterior putamen. This complex interaction between disease stage and duration, which was not compensated for in the investigations discussed above, might explain the partially conflicting results among the previous studies.

### Strengths and limitations

The major strength of this study is the large sample size of 301 consecutive PD patients and 110 controls who were all scanned in the same institution using the same protocol and machine. Moreover, all postprocessing steps were operator-independent, resulting in a reference database for clinical and research applications. In order to compensate for



potentially confounding effects between disease duration and disease stage, we used the other parameter as a nonexplanatory coregressor, i.e. analysing duration and controlling for stage, and vice versa. Additionally, we used gender and age as additional coregressor to compensate for the well-known dopaminergic depletion linked to ageing [22, 24, 29, 30].

We used the H&Y scale [12] to assess disease stage. This scale was established in 1967 in a very large cohort of PD patients who were followed over 15 years at a time when no effective treatment for PD was available. Thus, the H&Y scale reflects the natural course of PD independently of any therapeutic intervention. This five-stage scale is easy to use and is therefore considered by many movement disorder experts a robust scale to follow disease progression, especially in later stages of the condition. On the other hand, the UPDRS [31] was developed as a comprehensive instrument for the evaluation of impairment and disability at a certain time point so that outcomes among different clinical trials or any therapeutic interventions could be directly compared. The UPDRS is highly sensitive to dopaminergic treatments and levodopa-responsive symptoms are particularly weighted. Consequently, as the vast majority of our patients were chronically treated with antiparkinsonian medications, and because an off-medication UPDRS score was not available at the time of the scan, we decided to rely on the H&Y staging system as a measure of disease progression as it better reflects the long-term stage of the disease and is less influenced by current medication. It is noteworthy, however, that there is as yet no ideal, validated and medication-insensitive clinical scale specifically dedicated to the measurement of disease progression in PD.

A limitation of the current investigation was its retrospective nature and the fact that patients were included from a clinical setting with a nonstandardized clinical work-up. The variable exposure to symptomatic medication in this clinical study might have been another potential bias. However, several studies have shown that standard antiparkinsonian treatment does not significantly affect the data obtained by  $^{123}\text{I}$ -ioflupane SPECT [32–34]. A previous multicentre study assessed 139 healthy controls [35] and another related study from the same multicentre database assessed 122 healthy controls focusing notably on ageing and gender differences [36]. In contrast to these studies, our database includes controls and patients, and provides a voxel-wise rather than a region-based analysis.

Finally, we believe that the findings of this study may be clinically useful and may help clarify some problematic situations at the bedside, for example discrepancies between the patient's perception of symptoms and the SPECT data, development of PD-related cognitive decline versus cognitive symptoms as side effects

of medication or even perhaps distinguishing between the various degenerative forms of parkinsonism.

#### Compliance with ethical standards

**Conflicts of interest** None.

**Ethical approval** All procedures performed in studies involving human participants were in accordance with the ethical standards of the institutional and/or national research committee and with the principles of the 1964 Declaration of Helsinki and its later amendments or comparable ethical standards.

**Informed consent** Informed consent was waived by the local ethics committee (retrospective analysis of imaging data acquired during clinical work-up).

#### References

1. Italian Neurological Society, Italian Society of Clinical Neurophysiology. Guidelines for the Treatment of Parkinson's Disease. The diagnosis of Parkinson's disease. *Neurol Sci.* 2003;24(3 Suppl):S157–64.
2. Scherfler C, Seppi K, Donnemiller E, Goebel G, Brenneis C, Virgolini I, et al. Voxel-wise analysis of [123I]beta-CIT SPECT differentiates the Parkinson variant of multiple system atrophy from idiopathic Parkinson's disease. *Brain.* 2005;128:1605–12.
3. Brücke PD, Asenbaum S, Pirker W, Djamshidian S, Wenger S, Wöber C, et al. Measurement of the dopaminergic degeneration in Parkinson's disease with [123I]β-CIT and SPECT. *J Neural Transm Suppl.* 1997;50:9–24.
4. Sixel-Döring F, Liepe K, Mollenhauer B, Trautmann E, Trenkwalder C. The role of 123I-FP-CIT-SPECT in the differential diagnosis of Parkinson and tremor syndromes: a critical assessment of 125 cases. *J Neurol.* 2011;258:2147–54.
5. Kägi G, Bhatia KP, Tolosa E. The role of DAT-SPECT in movement disorders. *J Neurol Neurosurg Psychiatr.* 2010;81:5–12.
6. Segovia F, Górriz JM, Ramirez J, Alvarez I, Jimenez-Hoyuela JM, Ortega SJ. Improved parkinsonism diagnosis using a partial least squares based approach. *Med Phys.* 2012;39:4395–403.
7. Tissingh G, Bergmans P, Booij J, Winogrodzka A, van Royen EA, Stoof JC, et al. Drug-naïve patients with Parkinson's disease in Hoehn and Yahr stages I and II show a bilateral decrease in striatal dopamine transporters as revealed by [123I]β-CIT SPECT. *J Neurol.* 1997;245:14–20.
8. Laruelle M, Wallace E, Seibyl JP, Baldwin RM, Zea Ponce Y, Zoghbi SS, et al. Graphical, kinetic, and equilibrium analyses of in vivo [123I] beta-CIT binding to dopamine transporters in healthy human subjects. *J Cereb Blood Flow Metab.* 1994;14:982–94.
9. Benamer HT, Patterson J, Wyper DJ, Hadley DM, Macphee GJ, Grosset DG. Correlation of Parkinson's disease severity and duration with 123I-FP-CIT SPECT striatal uptake. *Mov Disord.* 2000;15:692–8.
10. Marek K, Innis R, van Dyck C, Fussell B, Early M, Eberly S, et al. [123I]β-CIT SPECT imaging assessment of the rate of Parkinson's disease progression. *Neurology.* 2001;57:2089–94.
11. Djaldetti R, Treves TA, Ziv I, Melamed E, Lampl Y, Lorberboym M. Use of a single [123I]-FP-CIT SPECT to predict the severity of clinical symptoms of Parkinson disease. *Neurol Sci.* 2009;30:301–5.
12. Hoehn MM, Yahr MD. Parkinsonism: onset, progression and mortality. *Neurology.* 1967;17:427–42.

13. Garibotto V, Montandon ML, Viaud CT, Allaoua M, Assal F, Burkhard PR, et al. Regions of interest-based discriminant analysis of DaTSCAN SPECT and FDG-PET for the classification of dementia. *Clin Nucl Med*. 2013;38:e112–7.
14. Fazekas F, Chawluk JB, Alavi A, Hurtig HI, Zimmerman RA. MR signal abnormalities at 1.5 T in Alzheimer's dementia and normal aging. *AJR Am J Roentgenol*. 1987;149:351–6.
15. Jenkinson M, Smith S. A global optimisation method for robust affine registration of brain images. *Med Image Anal*. 2001;5:143–56.
16. Jenkinson M, Bannister P, Brady M, Smith S. Improved optimization for the robust and accurate linear registration and motion correction of brain images. *Neuroimage*. 2002;17:825–41.
17. García-Gómez FJ, García-Solís D, Luis-Simón FJ, Marín-Oyaga VA, Carrillo F, Mir P, et al. Elaboration of the SPM template for the standardization of SPECT images with 123I-Ioflupane. *Rev Esp Med Nucl Imagen Mol (Engl Ed)*. 2013;32:350–6.
18. Kas A, Payoux P, Habert M-O, Malek Z, Cointepas Y, El Fakhri G, et al. Validation of a standardized normalization template for statistical parametric mapping analysis of 123I-FP-CIT images. *J Nucl Med*. 2007;48:1459–67.
19. Smith SM, Nichols TE. Threshold-free cluster enhancement: addressing problems of smoothing, threshold dependence and localisation in cluster inference. *Neuroimage*. 2009;44:83–98.
20. Morrish PK, Sawle GV, Brooks DJ. An [F-18]dopa-PET and clinical study of the rate of progression in Parkinson's disease. *Brain*. 1996;119:585–91.
21. Seibyl JP, Marchek KL, Quinlan D, Sheff K, Zoghbi S, Zea Ponce Y, et al. Decreased single-photon emission computed tomographic {123I}β-CIT striatal uptake correlates with symptom severity in Parkinson's disease. *Ann Neurol*. 1995;38:589–98.
22. Ishikawa T, Dhawan V, Kazumata K, Chaly T, Mandel F, Neumeyer J, et al. Comparative nigrostriatal dopaminergic imaging with iodine-123-beta CIT-FP/SPECT and fluorine-18-FDOPA/PET. *J Nucl Med*. 1996;37:1760–5.
23. Booij J, Tissingh G, Winogrodzka A, Boer GJ, Stoof JC, Wolters EC, et al. Practical benefit of [123I]FP-CIT SPET in the demonstration of the dopaminergic deficit in Parkinson's disease. *Eur J Nucl Med*. 1997;24:68–71.
24. Tissingh G, Booij J, Bergmans P, Winogrodzka A, Janssen A, van Royen EA, et al. Iodine-123-N-omega-fluoropropyl-2 beta-carbomethoxy-3 beta-(4-iodophenyl)tropane SPECT in healthy controls and early-stage, drug-naive Parkinson's disease. *J Nucl Med*. 1998;39:1143–8.
25. Kish SJ, Shannak K, Hornykiewicz O. Uneven pattern of dopamine loss in the striatum of patients with idiopathic Parkinson's disease. Pathophysiologic and clinical implications. *N Engl J Med*. 1988;318:876–80.
26. Seibyl JP, Marek KL, Quinlan D, Sheff K, Zoghbi S. Decreased SPECT [123I]beta-CIT striatal uptake correlates with symptom severity in idiopathic Parkinson's disease. *Ann Neurol*. 1995;38:589–98.
27. Kordower JH, Olanow CW, Dodiya HB, Chu Y, Beach TG, Adler CH, et al. Disease duration and the integrity of the nigrostriatal system in Parkinson's disease. *Brain*. 2013;136:2419–31.
28. Fearnley JM, Lees AJ. Ageing and Parkinson's disease: substantia nigra regional selectivity. *Brain*. 1991;114(Pt 5):2283–301.
29. van Dyck CH, Seibyl JP, Malison RT, Laruelle M, Zoghbi SS, Baldwin RM, et al. Age-related decline in dopamine transporters: analysis of striatal subregions, nonlinear effects, and hemispheric asymmetries. *Am J Geriatr Psychiatry*. 2002;10:36–43.
30. Lavalaye J, Booij J, Reneman L, Habraken JB, van Royen EA. Effect of age and gender on dopamine transporter imaging with [123I]FP-CIT SPET in healthy volunteers. *Eur J Nucl Med*. 2000;27:867–9.
31. Martinez-Martin P, Gil-Nagel A, Gracia LM, Gómez JB, Martínez-Sarriés J, Bermejo F. Unified Parkinson's disease rating scale characteristics and structure. The Cooperative Multicentric Group. *Mov Disord*. 1994;9:76–83.
32. Laruelle M, Baldwin RM, Malison RT, Zea-Ponce Y, Zoghbi SS, al-Tikriti MS, et al. SPECT imaging of dopamine and serotonin transporters with [123I]β-CIT: pharmacological characterization of brain uptake in nonhuman primates. *Synapse*. 1993;13:295–309.
33. Innis RB, Marek KL, Sheff K, Zoghbi S, Castronuovo J, Feigin A, et al. Effect of treatment with L-dopa/carbidopa or L-selegiline on striatal dopamine transporter SPECT imaging with [123I]β-CIT. *Mov Disord*. 1999;14:436–42.
34. Ahlskog JE, Uitti RJ, O'Connor MK, Maraganore DM, Matsumoto JY, Stark KF, et al. The effect of dopamine agonist therapy on dopamine transporter imaging in Parkinson's disease. *Mov Disord*. 1999;14:940–6.
35. Varrone A, Dickson JC, Tossici-Bolt L, Sera T, Asenbaum S, Booij J, et al. European multicentre database of healthy controls for [123I]FP-CIT SPECT (ENC-DAT): age-related effects, gender differences and evaluation of different methods of analysis. *Eur J Nucl Med Mol Imaging*. 2012;40:213–27.
36. Nobili F, Naseri M, De Carli F, Asenbaum S, Booij J, Darcourt J, et al. Automatic semi-quantification of [123I]FP-CIT SPECT scans in healthy volunteers using BasGan version 2: results from the ENC-DAT database. *Eur J Nucl Med Mol Imaging*. 2012;40:565–73.

## ***Chapter 3.1.4***

### ***Individual differentiation between Parkinson's disease and atypical parkinsonian syndromes using <sup>123</sup>I- ioflupane SPECT.***

S. Badoud D. Van de Ville N. Nicastro V. Garibotto P.R. Burkhard S. Haller

Manuscript in preparation





**Abstract (246 words)****Background**

<sup>123</sup>I-ioflupane single photon emission tomography (SPECT) is a very sensitive and established imaging tool to detect alterations in the dopaminergic system in Parkinson's disease (PD) and atypical parkinsonian syndromes (APS), yet the discrimination between PD and APS is limited based on visual inspection or simple region of interest analyses. We applied advanced image analysis techniques to discriminate PD versus APS.

**Materials and Methods**

This study includes 392 consecutive patients: 306 PD, 24 multiple system atrophy (MSA), 32 progressive supranuclear palsy (PSP) and 30 corticobasal degeneration (CBD) patients undergoing <sup>123</sup>I-ioflupane SPECT. Data analysis included voxel-wise univariate statistical parametric mapping and multivariate pattern recognition using linear discriminant classifiers. Classification analysis was performed only within the striatum, only outside the striatum and using the entire brain.

**Results**

MSA and PSP had less dopaminergic metabolism in bilateral head of caudate nucleus as compared to PD and CBD, yet there was no difference between MSA and PSP. CBD had higher dopaminergic metabolism in bilateral putamen as compared to PD, MSA and PSP. Classification was significantly above chance level for PD 45% (chance 30%), PSP 60% (chance 40%) and CBD 47% (chance 34%) but not for MSA. PSP had the highest classification accuracy. **Striatal and extra-striatal regions contain classification information, yet the combination of both regions does not significantly improve classification accuracy.**

**Discussion**

PD, MSA, PSP and CBD have distinct patterns of dopaminergic depletion on <sup>123</sup>I-flupane SPECT and can be discriminated based on multi-vector pattern recognition with the exception of MSA.

**Abbreviations**

APS	atypical parkinsonian syndromes
CBD	corticobasal degeneration
MSA	multiple system atrophy
MVPA	Multi Voxel Pattern Analysis
PD	Parkinson's disease
PSP	progressive supranuclear palsy
ROI	region of interest
SPECT	single photon emission tomography
SVM	support vector machines

## ***Introduction***

Parkinson's Disease (PD) is the second most common neurodegenerative disorder after Alzheimer's Disease (AD) and has a prevalence ranging from 1-2% in the population above 65 years of age (Alves et al., 2008; Tanner and Goldman, 1996). In addition, several less common degenerative parkinsonian syndromes exist, named atypical parkinsonian syndromes (APS) including multiple system atrophy (MSA), progressive supranuclear palsy (PSP) and corticobasal degeneration (CBD). While clinical discrimination between these diseases can be done with high accuracy of about 90% by an experienced movement disorders specialist at later stages (Hughes et al., 2002; Italian Neurological Society et al., 2003), clinical symptoms may be overlapping notably in early stages of the diseases, impeding the differential diagnosis between PD and APS. This discrimination is however important with respect to both treatment and prognosis. While PD patients typically respond well to dopamine-based medication and have a slower progression, APS typically respond less to treatment and have a worse outcome.

Neuroimaging may complement the clinical assessment.  $^{123}\text{I}$ -FP-CIT single photon emission tomography (SPECT) is the most established clinical imaging tool to assess the integrity of the dopaminergic system (Brücke et al., 1997; Laruelle et al., 1994; Tissingh et al., 1997). This technique has a high sensitivity to detect PD versus controls even in early stages of the disease, however the pattern of alterations of the dopaminergic system are very similar between PD and APS (Benamer et al., 2000; Brücke et al., 1997; Italian Neurological Society et al., 2003; Kägi et al., 2010; Sixel-Döring et al., 2011). Consequently, simple visual or region of interest (ROI) analyses do not allow to differentiate PD patients from APS (Brooks, 2012; Kägi et al., 2010; Klaffke et al., 2006; Kupsch et al., 2013; Marek et al., 2000; Pirker et al., 2000a).

The current investigation is based on the assumption that systematic but subtle differences in  $^{123}\text{I}$ -ioflupane SPECT exist between PD and APS, which can be detected using advanced data analysis techniques. Accordingly,

previous investigations applying support vector machines (SVM), a type of Multi Voxel Pattern Analysis (MVPA), successfully discriminated PD from APS patients based on MRI diffusion tensor imaging (DTI) (Haller et al., 2012), MRI susceptibility weighted imaging (SWI) (Haller et al., 2013) and gait analysis (Tahir and Manap, 2012). This SVM classification technique was also applied to  $^{123}\text{I}$ -ioflupane SPECT data to discriminate 95 PD versus 94 controls (Segovia et al., 2012) and to discriminate 56 PD versus 34 non-PD (essential tremor and drug-induced parkinsonism) patients (Palumbo et al., 2014). A comparison between PD and APS was not performed.

The present study includes a large cohort of 392 consecutive patients with a clinical diagnosis of PD, MSA, PSP and CBD scanned on the same machine, in the same center and with similar image acquisition and processing protocol, over a period of 10 years. We performed univariate statistical parametric mapping and multivariate pattern recognition classification analyses to test the hypothesis that PD and APS have distinct patterns of dopaminergic depletion on  $^{123}\text{I}$ -FP-CIT SPECT, which allows a clinically useful discrimination between groups.

## ***Materials and methods***

### ***Participants***

The present retrospective study was approved by the local ethical committee and includes 970 consecutive patients undergoing  $^{123}\text{I}$ -ioflupane SPECT scanning in our institution between October 2003 and September 2013. Out of this cohort, 392 participants met our inclusion criteria: 1)  $^{123}\text{I}$ -ioflupane SPECT of good image quality, 2) extensive neurological assessment and 3) follow-up and 4) absent morphological findings on structural images based on magnetic resonance imaging (MRI). UK Parkinson's disease society brain bank criteria were used for PD (Hughes et al., 1992). The presence of bradykinesia

associated with one of the following criteria: rest tremor (4-6Hz), postural instability or rigidity was necessary. Among others, a very good and sustained response to Levodopa with or without appearance of typical Levodopa-induced dyskinesia, unilateral onset and progressive course were considered as supportive characteristics. This assessment was achieved by an experienced movement disorder specialist.

Regarding APS, we used the second consensus statement for the diagnosis of MSA (Gilman et al., 2008), the National Institute of Neurological Disorders Society (NINDS) clinical research criteria for PSP (Litvan et al., 1996) and the criteria for the diagnosis of CBD proposed by Boeve and colleagues (Boeve et al., 2003).

It is important to keep in mind that the  $^{123}\text{I}$ -ioflupane SPECT was not used to confirm a specific diagnosis but to exclude non-neurodegenerative parkinsonisms (eg. Drug-induced parkinsonism).

The final sample included 306 PD (age  $69.42 \pm 11$ , disease duration  $2.4 \pm 0.9$ , 164 males) 24 MSA (age  $64.58 \pm 10.03$ , disease duration  $3.2 \pm 3.1$ , 13 males), 32 PSP (age  $72.94 \pm 8.26$ , disease duration  $1.9 \pm 1.2$ , 21 males) and 30 CBD (age  $73.93 \pm 7.09$ , disease duration  $2.4 \pm 1.8$ , 16 males). According to the ANOVA multiple comparison test, there was no significant difference between groups concerning the sex ratio. The ANOVA test revealed significant differences between groups in terms of age ( $p=0.019$ ) and disease duration ( $p=0.007$ ) (see table 1).

**Table 1: Demographic and clinical characteristics**

	PD	Atypicals			Stat.
		MSA	PSP	CBD	
<b>Sexe (m/f)</b>	164/142	13/11	21/11	16/14	n.s
<b>Age (yr)</b>	$69.4 \pm 11$	$64.6 \pm 10$	$72.9 \pm 8.3$	$73.9 \pm 7.1$	**
<b>Disease duration (yr)</b>	$2.4 \pm 0.9$	$3.2 \pm 3.1$	$1.9 \pm 1.2$	$2.4 \pm 1.8$	*

Table 1 summarized the essential demographic data of the patient groups

## ***SPECT image acquisition***

Sodium perchlorate or Lugol solution were preventively administered to the patients in order to block thyroid uptake. Then, the patients were scanned on a triple-head gamma-camera (Toshiba Medical Systems, Tokyo, Japan) with fan-beam, low-energy, high-resolution collimators, 4 hours after intravenous injection of about 184 MBq of  $^{123}\text{I}$ -FP-CIT. The images acquisitions were performed in frames of 6 degrees over 360 degrees with a matrix of 128 x 128. A head holder was used to prevent movement's artifacts. The correction for scatters was performed with a triple-energy window method. A 0.15/cm uniform coefficient was applied for photon attenuation. The more detailed procedure can be found in (Garibotto et al., 2013).

## ***MR image acquisition***

Variable MRI protocols were performed following clinical routine procedure due to the fact that they were acquired over a period of 10 years. However a minimum of a T2, fluid attenuation inversion recovery (FLAIR) and diffusion weighted imaging (DWI) or diffusion tensor imaging (DTI) were available in all participants to exclude structural brain lesions. In addition, the integrity of white matter was checked regarding to the Fazekas score (Fazekas et al., 1987).

103 patients had in addition a high-resolution Magnetization Prepared Rapid Gradient Echo (MPRAGE) 3DT1brain scan performed on 3.0 tesla MR system (Magnetom Trio, Siemens, Erlangen Germany) as part of clinical routine protocol (256x256 matrix, 176 sections, 1x1x1 mm<sup>3</sup>, TE=2.3ms, TR=2300ms.). This subsample was used to build a  $^{123}\text{I}$ -ioflupane SPECT template in Montreal Neurological Institute (MNI) standard space as described earlier (García-Gómez et al., 2013; Kas et al., 2007)

## ***Statistical analyses***

FSL (FMRIB Software Library version 5.0 <http://fsl.fmrib.ox.ac.uk/fsl/fslwiki>), Graphpad Prim (version 6.0, [www.graphpad.com](http://www.graphpad.com)), and Matlab (version R2014a) were used for statistical analyses and classification.

## ***Image post-processing***

The initial step was to generate a  $^{123}\text{I}$ -Ioflupane specific template using a group of patients having both a normal  $^{123}\text{I}$ -Ioflupane scan and a high-resolution 3DT1 MPRAGE MRI. The SPECT images were linearly registered to the MRI images of each patient by running the FLIRT function in FSL (FMRIB's linear image registration tool, part of FSL) with 6 degrees of freedom (Jenkinson et al., 2002; Jenkinson and Smith, 2001). Then, the structural data were normalized by non-linearly registration to the Montreal Neurological Institute (MNI) standard space using the FNIRT function (part of FSL). This matrix was then applied to the functional data of each individual patient. The last step of the template creation was to merge all the normalized SPECT images by running `fslmerge` and `fslmeants` (parts of FSL). Similar approaches have been used in (García-Gómez et al., 2013; Kas et al., 2007). The spatial normalization of all individual  $^{123}\text{I}$ -Ioflupane data was then achieved using the FLIRT function and the  $^{123}\text{I}$ -Ioflupane SPECT specific template described above as reference. Moreover, the intensity was normalized at the individual level with respect to the occipital region.

Due to the asymmetrical degeneration of the nigrostriatal pathways in PD and APS, we decided to flip all patients presenting predominant clinical symptoms on the left side of the body.

## ***Voxel-wise statistical analysis***

The voxel-wise statistical analysis was done using the randomize function of FSL by permutation testing ( $n=5000$ ) and Threshold-Free Cluster enhancement (TFCE) error multiple comparisons correction at  $p < 0.05$  considered as significant (Smith and Nichols, 2009). Age and gender were used as non-explanatory co-regressors to eliminate potential bias linked to age or gender. The analyses described in this paragraph were performed inside a striatal mask including the putamen and the caudate nuclei. The mask was created using the Harvard subcortical atlas included in FSL.

## ***Classification analysis***

We applied a robust ensemble classifier as implemented in the Matlab Statistics Toolbox by using linear discriminant classifiers as weak learners on random subspace projections. The total number of learners was set to 1'500 and the prior probabilities of the patient labels were assumed uniformly distributed to compensate for the unequal number of subjects in each category. To reduce the dimensionality and exploit spatial correlation - the total number of voxels was 4'916 in the striatum mask and 253'454 in the whole-brain mask (without striatum) - we applied the singular value decomposition to the data of each patient group (within the cross-validation fold) and retained 20 and 30 components that corresponded to 94% and 99% of the explained variance for the striatum and whole-brain mask, respectively. All training subjects were then projected onto the principal components of each group, which led to a total number of features of 80 and 120 for classification based on the striatum and whole-brain mask, respectively. The classification accuracy was evaluated using leave-one-subject-out cross-validation with strict separation of training and test data. Chance level was at 25%. We established the 5% confidence interval on the chance level by using the same algorithms on the same data but with random labels.



## Results

### Voxel-wise group-level statistical analysis

#### APS versus PD

The voxel-wise analysis revealed a significantly lower  $^{123}\text{I}$ -loflupane uptake in all APS versus PD in the head of caudate nucleus ( $p < 0.002$ ). The inverse comparison showed a cluster located on the ipsilateral putamen with increased  $^{123}\text{I}$ -loflupane in APS versus PD ( $p < 0.05$ ).

Concerning the subtypes of APS, MSA and PSP exhibit a significantly lower  $^{123}\text{I}$ -loflupane uptake in the head of the caudate nucleus ( $p < 0.002$ ). The inverse comparison led to no significant results.

CBD versus PD revealed increased  $^{123}\text{I}$ -loflupane uptake in the bilateral putamen, while the inverse comparison revealed no significant differences (see figure 1).

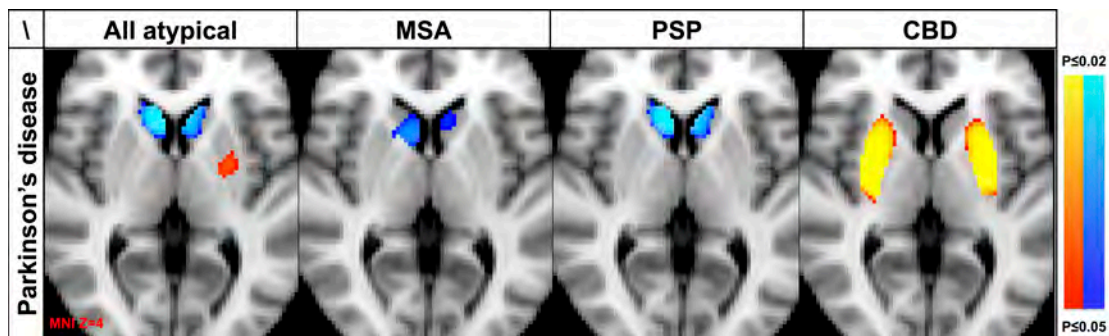


Figure 1 illustrates the comparison between all APS confounded, only MSA, only PSP and only CBD versus PD. APS versus PD had decreased  $^{123}\text{I}$ -loflupane uptake in bilateral head of caudate nucleus yet increased  $^{123}\text{I}$ -loflupane uptake in ipsilateral putamen. MSA and PSP versus PD had decreased  $^{123}\text{I}$ -loflupane uptake in bilateral head of caudate nucleus. CBD versus PD had increased  $^{123}\text{I}$ -loflupane uptake in bilateral head of caudate nucleus.  $^{123}\text{I}$ -loflupane uptake maps superimposed on axial T1 weighted MRI in Montreal Neurological Institute (MNI) standard space with the clinically dominant symptomatic side on the right hemisphere. Threshold-Free Cluster enhancement (TFCE) error multiple comparisons correction at  $p < 0.05$

## ***APS versus APS***

The comparison within the group of APS, i.e. MSA versus PSP versus CBD revealed significantly lower  $^{123}\text{I}$ -Ioflupane uptake in MSA and PSP compared to CBD in bilateral putamen and the posterior part of the head of the caudate nucleus, with the head of the caudate nucleus more affected in PSP (see **figure 2**). The inverse comparison did not yield any supra-threshold clusters. The comparison between MSA versus PSP revealed no supra-threshold clusters.

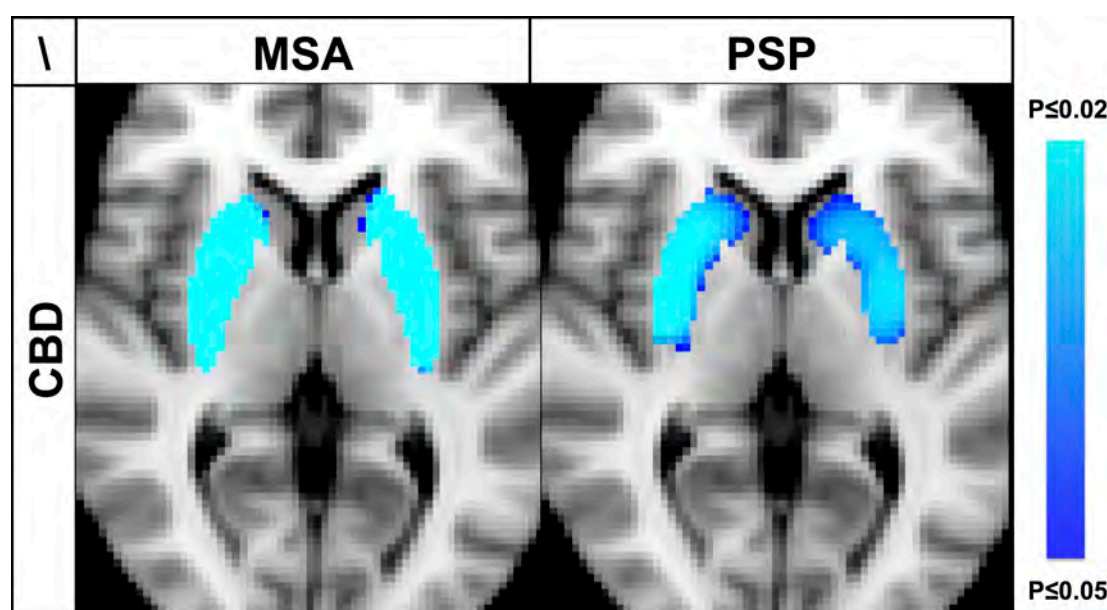


Figure 2. MSA and PSP versus CBD had decreased  $^{123}\text{I}$ -Ioflupane uptake in bilateral putamen and head of caudate nucleus. The inverse comparison between CBD versus MSA or PSP as well as the comparison between MSA versus PSP revealed no supra-threshold clusters. Illustration equivalent to figure 1.

## ***Classification analysis***

Classification of all patients groups was significantly above chance level except for MSA. PSP had the highest classification accuracy.

Voxels in the striatum mask was most informative for the classification; however, the use of the whole-brain mask without the striatum was still informative, although with slightly reduced accuracies. The whole-brain mask with striatum did not improve accuracies, which might indicate that information was redundant inside and outside the striatum mask, but not complementary. The accuracies for prediction of the patient label are illustrated in Table 2.

**Table 2:**

	PD	Atypicals		
		MSA	PSP	CBD
<b>Striatum only</b>	45% (30%)	25% (41%)	60% (40%)	47% (34%)
<b>Extra-striatum</b>	35% (30%)	25% (41%)	53% (40%)	47% (34%)
<b>Whole-brain</b>	42% (30%)	29% (41%)	60% (40%)	47% (34%)

Table 2. Classification results in terms of cross-validation accuracy and 5% confidence interval by chance (between parentheses). Classification was significant for all groups except MSA.

## ***Discussion***

The current investigation assessed the detailed spatial distribution of dopaminergic depletion based on  $^{123}\text{I}$ -ioflupane SPECT in a sample of 392 consecutive patients with PD and APS using advanced and operator-independent data analysis. We were able to demonstrate distinct patterns of dopaminergic depletion for PD, MSA, PSP and CBD and that these diseases can be discriminated at the individual level based on multi-vector pattern recognition with the exception of MSA.

### ***PD versus APS***

Our results show that the atypical forms of parkinsonism, notably MSA, PSP and CBD, affect the dopaminergic  $^{123}\text{I}$ -ioflupane uptake notably in the striatum in a topographic distinct way, which is different from PD. MSA and PSP have significantly lower  $^{123}\text{I}$ -ioflupane uptake in bilateral head of the caudate nucleus as compared to PD. In contrast, CBD has increased  $^{123}\text{I}$ -ioflupane uptake indicating less pronounced dopaminergic depletion in the bilateral putamen as compared to PD.

As we demonstrate that the various subtypes of APS have distinct patterns of dopaminergic depletion, the analysis of all APS confounded versus PD should be interpreted with care. The direct comparison between PD and all APS taken together is thus confounded by the differences in the spatial pattern of dopaminergic depletion in MSA, PSP and CBD and consequently potentially confounded by the group size composition.

### ***Specific patterns of dopaminergic depletion in APS***

The MSA group had significantly stronger dopaminergic depletion in the bilateral head of caudate nucleus as compared to PD. This result is consistent

with a previous [ $^{123}\text{I}$ ]- $\beta$ -CIT SPECT study in 8 MSA versus 11 PD patients, demonstrating a significant decrease of SPECT signal in the head of the caudate nucleus and anterior part of the putamen in MSA group (Nocker et al., 2012). Moreover, and in line with the current results, several previous investigations reported decreased  $^{123}\text{I}$ -Ioflupane uptake in MSA as compared to PD (Pirker et al., 2000a; Scherfler et al., 2005; Varrone et al., 2001). However, at variance with our study, the results presented by Pirker et al. were obtained by calculating values in hand drawn ROI that could introduce important variability in the data (Pirker et al., 2000a). Similarly, Varrone and colleagues did not perform spatial normalization before setting their ROI template. This method did also risk to introduce a bias in measures (Varrone et al., 2001). Finally, Scherfler and colleagues, chosen to conduct voxel-wise analysis using statistical parametric mapping software (SPM) on the same line with our protocol (Scherfler et al., 2005). Nevertheless, they achieved spatial normalization through an indirect method consisting in transferring the [ $^{123}\text{I}$ ]- $\beta$ -CIT SPECT images to a  $^{18}\text{F}$ -DOPA PET template whereas we decided to create a study specific functional template for the exact modality needed ( $^{123}\text{I}$ -flupane SPECT).

The asymmetrical pattern that can be seen on figure 1 (PD vs. MSA), showing a more significant decrease on the contralateral side, can be related to the fact that the contra/ipsilateral signal asymmetry is supposed to be more pronounced in PD than in MSA (Varrone et al., 2001).

Concerning PSP, the dopaminergic depletion is also more pronounced in the head of the caudate nucleus as compared to PD. This pattern is similar to MSA discussed above

Previous investigations demonstrated that PSP is characterized by a more uniform reduction of the striatal dopaminergic uptake in the caudate nucleus and putamen and by low left/right asymmetry (Antonini et al., 2003; Brooks, 2010). Globally, the dopaminergic striatal functions seem to be more severely affected in PSP than in PD (Brooks et al., 1990). In agreement with our results, a previous [ $^{123}\text{I}$ ]- $\beta$ -CIT SPECT study in 14 PSP patients and 17 PD patients demonstrates a significantly lower signal in the caudate nuclei in the PSP group (Seppi et al., 2006).

Concerning CBD, there is increased  $^{123}\text{I}$ -loflupane uptake representing less dopaminergic depletion in bilateral putamen as compared to PD. These results indicate that CBD affects the dopaminergic system less severely in the putamen and are consistent with the observation that the dopaminergic system is less severely affected in CBD as compared PD (Pirker et al., 2000a).

### ***MSA versus PSP versus CBD***

MSA and PSP exhibit significantly stronger dopaminergic depletion in the bilateral head of caudate nucleus and putamen as compared to CBD. These results are not in line with the study published by Pirker and colleagues suggesting no significant difference between CBD, PSP and MSA in terms of dopaminergic denervation (Pirker et al., 2000b). However, the authors conducted an analysis comparing the average striatal activities and included only four CBD patients.

### ***Classification***

All patient groups were classified above chance level except for MSA. Notably PSP had the best classification accuracy. Two previous investigations by Palumbo et al. and by Segovia et al. assessed classification performance of PD versus controls (Palumbo et al., 2014; Segovia et al., 2012). Note that the classification accuracies of 73.9% and 94.7%, respectively, exceed the classification accuracy of the current investigation due to the fact that the discrimination of a disease with clear dopaminergic depletion versus a control group is evidently much easier than the classification of several diseases which significantly affect the dopaminergic system. Even if some subtle differences in  $^{123}\text{I}$ -loflupane uptake between PD and APS were previously reported, there is a general agreement that these differences are subtle and

consequently the visual inspection of  $^{123}\text{I}$ -loflupane uptake maps does not allow for an accurate diagnosis (Brooks, 2012; Kägi et al., 2010; Klaffke et al., 2006; Kupsch et al., 2013; Marek et al., 2000; Pirker et al., 2000a). The presented operator-independent classification analysis of the complex pattern of dopaminergic depletion, which provided above-chance classification accuracy is therefore an added value for clinical diagnosis of individual patients.

### ***Striatal versus extra-striatal signal***

The  $^{123}\text{I}$ -loflupane uptake is most pronounced in the striatal system (Booij et al., 1997a; 1997b). Consequently, most previous investigations have focused on this region of the brain. Based on the assumption that PD and APS might also affect the  $^{123}\text{I}$ -loflupane uptake outside the striatum, we performed the classification analysis three times, once only within the striatum, once in the remaining brain outside the striatum, and once using the entire brain. The striatum was most informative for the classification. Nevertheless, above-chance classification was possible even when considering only the regions outside the striatum. This indicates that PD and APS also affect extra-striatal brain regions. The observation that the classification accuracy was lower outside the striatum as compared to within the striatum is consistent with the known dopaminergic distribution and depletion notably of the striatum. In addition, the whole-brain analysis did not improve accuracies, which might indicate that information was redundant inside and outside the striatum, but not complementary. While previous studies suggested that the striatum was the only region to provide relevant information regarding the state of the nigro-striatal (Booij et al., 1997b; Catafau and Tolosa, 2004; Gaig et al., 2006; Seibyl et al., 2013), our results indicate that extra-striatal regions also convey relevant information. For example, one recent investigation indicates that extra-striatal  $^{123}\text{I}$ -loflupane modification can be observed in the context of addiction (Leroy et al., 2012).

## ***Strength and limitation***

The large cohort used for this study (392 patients) represents its major asset. Additionally, all patients were scanned consecutively on the same machine using the same protocol of acquisition. In order to avoid operator-linked variability, all post-processing procedures were conducted in an operator-independent manner including the creation of a study specific template. Sex and age data were used as non-explanatory co-regressors in order to compensate their well-known impact on the nigrostriatal pathway (Lavalaye et al., 2000; van Dyck et al., 2002).

The retrospective nature of this study is an important limitation. Even if the sequences of acquisition were always the same, the operational procedure applied to clinical routine is not standardized. Moreover, an impact of anti-parkinsonian medications on the images cannot be totally excluded even if several studies haven't showed significant consequences regarding  $^{123}\text{I}$ -ioflupane SPECT acquisition (Ahlskog et al., 1999; Innis et al., 1999; Laruelle et al., 1993).

## ***Conclusions***

PD, MSA, PSP and CBD have distinct patterns of dopaminergic depletion on  $^{123}\text{I}$ -flupane SPECT. Advanced and operator-independent multi-vector pattern recognition analysis allows for the individual classification of all groups with the exception of MSA. Future methodological developments might further improve classification accuracy, taking into account also complimentary information e.g. derived from MRI which is performed in most cases, to further improve classification accuracy and robustness.



## References

- Ahlskog, J.E., Uitti, R.J., O'Connor, M.K., Maraganore, D.M., Matsumoto, J.Y., Stark, K.F., Turk, M.F., Burnett, O.L., 1999. The effect of dopamine agonist therapy on dopamine transporter imaging in Parkinson's disease. *Movement Disorders* 14, 940–946. doi:10.1002/1531-8257(199911)14:6<940::AID-MDS1005>3.0.CO;2-Y
- Alves, G., Forsaa, E.B., Pedersen, K.F., Dreetz Gjerstad, M., Larsen, J.P., 2008. Epidemiology of Parkinson's disease. *Journal of Neurology* 255, 18–32. doi:10.1007/s00415-008-5004-3
- Antonini, A., Benti, R., De Notaris, R., Tesei, S., Zecchinelli, A., Sacilotto, G., Meucci, N., Canesi, M., Mariani, C., Pezzoli, G., Gerundini, P., 2003. I-123-loflupane/SPECT binding to striatal dopamine transporter (DAT) uptake in patients with Parkinson's disease, multiple system atrophy, and progressive supranuclear palsy. *Neurol Sci* 24, 149–150. doi:10.1007/s10072-003-0103-5
- Benamer, H.T.S., Patterson, J., Grosset, D.G., Booij, J., de Bruin, K., van Royen, E., Speelman, J.D., Horstink, M.H.I.M., Sips, H.J.W.A., Dierckx, R.A., Versijpt, J., Decoo, D., Van Der Linden, C., Hadley, D.M., Doder, M., Lees, A.J., Costa, D.C., Gacinovic, S., Oertel, W.H., Pogarell, O., Hoeffken, H., Joseph, K., Tatsch, K., Schwarz, J., Ries, V., 2000. Accurate differentiation of parkinsonism and essential tremor using visual assessment of [123I]-FP-CIT SPECT imaging: The [123I]-FP-CIT study group. *Movement Disorders* 15, 503–510. doi:10.1002/1531-8257(200005)15:3<503::AID-MDS1013>3.0.CO;2-V
- Boeve, B.F., Lang, A.E., Litvan, I., 2003. Corticobasal degeneration and its relationship to progressive supranuclear palsy and frontotemporal dementia. *Ann.Neurol* 54 Suppl 5, S15–9. doi:10.1002/ana.10570
- Booij, J., Andringa, G., Rijks, L.J., Vermeulen, R.J., de Bruin, K., Boer, G.J., Janssen, A.G., van Royen, E.A., 1997a. [123I]FP-CIT binds to the

- dopamine transporter as assessed by biodistribution studies in rats and SPECT studies in MPTP-lesioned monkeys. *Synapse* 27, 183–190. doi:10.1002/(SICI)1098-2396(199711)27:3<183::AID-SYN4>3.0.CO;2-9
- Booij, J., Tissingh, G., Winogrodzka, A., Boer, G.J., Stoof, J.C., Wolters, E.C., van Royen, E.A., 1997b. Practical benefit of [123I]FP-CIT SPET in the demonstration of the dopaminergic deficit in Parkinson's disease. *Eur J Nucl Med* 24, 68–71. doi:10.1007/BF01728311
- Brooks, D.J., 2012. Can imaging separate multiple system atrophy from Parkinson's disease? *Movement Disorders* 27, 3–5. doi:10.1002/mds.24046
- Brooks, D.J., 2010. Imaging dopamine transporters in Parkinson's disease. *Biomark Med* 4, 651–660. doi:10.2217/bmm.10.86
- Brooks, D.J., IBANEZ, V., Sawle, G.V., Quinn, N., Lees, A.J., MATHIAS, C.J., BANNISTER, R., Marsden, C.D., Frackowiak, R., 1990. Differing Patterns of Striatal F-18 Dopa Uptake in Parkinsons-Disease, Multiple System Atrophy, and Progressive Supranuclear Palsy. *Ann.Neurol* 28, 547–555. doi:10.1002/ana.410280412
- Brücke, P.D.T., Asenbaum, S., Pirker, W., Djamshidian, S., Wenger, S., Wöber, C., Müller, C., Podreka, I., 1997. Measurement of the dopaminergic degeneration in Parkinson's disease with [123I]β-CIT and SPECT, in: *Advances in Research on Neurodegeneration, Journal of Neural Transmission. Supplementa*. Springer Vienna, Vienna, pp. 9–24. doi:10.1007/978-3-7091-6842-4\_2
- Catafau, A.M., Tolosa, E., 2004. Impact of dopamine transporter SPECT using 123I-loflupane on diagnosis and management of patients with clinically uncertain parkinsonian syndromes. *Movement Disorders* 19, 1175–1182. doi:10.1002/mds.20112
- Fazekas, F., Chawluk, J.B., Alavi, A., Hurtig, H.I., Zimmerman, R.A., 1987. MR signal abnormalities at 1.5 T in Alzheimer's dementia and normal aging. *AJR Am J Roentgenol* 149, 351–356. doi:10.2214/ajr.149.2.351
- Gaig, C., Martí, M.J., Tolosa, E., Valldeoriola, F., Paredes, P., Lomeña, F.J., Nakamae, F., 2006. 123I-loflupane SPECT in the diagnosis of suspected psychogenic parkinsonism. *Movement Disorders* 21, 1994–1998.

- doi:10.1002/mds.21062
- García-Gómez, F.J., García-Solís, D., Luis-Simón, F.J., Marín-Oyaga, V.A., Carrillo, F., Mir, P., Vázquez-Albertino, R.J., 2013. Elaboration of the SPM template for the standardization of SPECT images with 123I-iodoflupane. *Revista Española de Medicina Nuclear e Imagen Molecular (English Edition)* 32, 350–356. doi:10.1016/j.remnie.2013.09.003
- Garibotto, V., Montandon, M.L., Viaud, C.T., Allaoua, M., Assal, F., Burkhard, P.R., Ratib, O., Zaidi, H., 2013. Regions of interest-based discriminant analysis of DaTSCAN SPECT and FDG-PET for the classification of dementia. *Clin Nucl Med* 38, e112–7. doi:10.1097/RLU.0b013e318279b991
- Gilman, S., Wenning, G.K., Low, P.A., Brooks, D.J., MATHIAS, C.J., Trojanowski, J.Q., Wood, N.W., Colosimo, C., Dürr, A., Fowler, C.J., Kaufmann, H., Klockgether, T., Lees, A., Poewe, W., Quinn, N., Revesz, T., Robertson, D., Sandroni, P., Seppi, K., Vidailhet, M., 2008. Second consensus statement on the diagnosis of multiple system atrophy., in: Presented at the Neurology, Lippincott Williams & Wilkins, pp. 670–676. doi:10.1212/01.wnl.0000324625.00404.15
- Haller, S., Badoud, S., Nguyen, D., Barnaure, I., Montandon, M.-L., Lovblad, K.O., Burkhard, P.R., 2013. Differentiation between Parkinson disease and other forms of parkinsonism using support vector machine analysis of susceptibility-weighted imaging (SWI): initial results. *Eur Radiol* 23, 12–19. doi:10.1007/s00330-012-2579-y
- Haller, S., Badoud, S., Nguyen, D., Garibotto, V., Lovblad, K.O., Burkhard, P.R., 2012. Individual Detection of Patients with Parkinson Disease using Support Vector Machine Analysis of Diffusion Tensor Imaging Data: Initial Results. *AJNR Am J Neuroradiol*. doi:10.3174/ajnr.A3126
- Hughes, A., Daniel, S., Kilford, L., 1992. Accuracy of clinical diagnosis of idiopathic Parkinson's disease: a clinico-pathological study of 100 cases. *Journal of Neurology*.
- Hughes, A.J., Daniel, S.E., Ben-Shlomo, Y., Lees, A.J., 2002. The accuracy of diagnosis of parkinsonian syndromes in a specialist movement disorder service. *Brain* 125, 861–870.
- Innis, R.B., Marek, K.L., Sheff, K., Zoghbi, S., Castronuovo, J., Feigin, A.,

- Seibyl, J.P., 1999. Effect of treatment with L-dopa/carbidopa or L-selegiline on striatal dopamine transporter SPECT imaging with [123I]β-CIT. *Movement Disorders* 14, 436–442. doi:10.1002/1531-8257(199905)14:3<436::AID-MDS1008>3.0.CO;2-J
- Italian Neurological Society, Italian Society of Clinical Neurophysiology, Guidelines for the Treatment of Parkinson's Disease 2002, 2003. The diagnosis of Parkinson's disease., in: Presented at the Neurological sciences : official journal of the Italian Neurological Society and of the Italian Society of Clinical Neurophysiology, pp. S157–64. doi:10.1001/archinte.144.11.2146
- Jenkinson, M., Bannister, P., Brady, M., Smith, S., 2002. Improved Optimization for the Robust and Accurate Linear Registration and Motion Correction of Brain Images. *Neuroimage* 17, 825–841. doi:10.1006/nimg.2002.1132
- Jenkinson, M., Smith, S., 2001. A global optimisation method for robust affine registration of brain images. *Med Image Anal* 5, 143–156.
- Kas, A., Payoux, P., Habert, M.-O., Malek, Z., Cointepas, Y., Fakhri, El, G., Chaumet-Riffaud, P., Itti, E., Remy, P., 2007. Validation of a standardized normalization template for statistical parametric mapping analysis of 123I-FP-CIT images. *J. Nucl. Med.* 48, 1459–1467. doi:10.2967/jnumed.106.038646
- Kägi, G., Bhatia, K.P., Tolosa, E., 2010. The role of DAT-SPECT in movement disorders. *J Neurol Neurosurg Psychiatr* 81, 5–12. doi:10.1136/jnnp.2008.157370
- Klaffke, S., Kuhn, A.A., Plotkin, M., Amthauer, H., Harnack, D., Felix, R., Kupsch, A., 2006. Dopamine transporters, D2 receptors, and glucose metabolism in corticobasal degeneration. *Mov Disord* 21, 1724–1727. doi:10.1002/mds.21004
- Kupsch, A., Bajaj, N., Weiland, F., Tartaglione, A., Klutmann, S., Copp, R., Sherwin, P., Tate, A., Grachev, I.D., 2013. Changes in clinical management and diagnosis following DaTscan SPECT imaging in patients with clinically uncertain parkinsonian syndromes: a 12-week follow-up study. *Neurodegener Dis* 11, 22–32. doi:10.1159/000337351

- Laruelle, M., Baldwin, R.M., Malison, R.T., Zea Ponce, Y., Zoghbi, S.S., Tikeriti, Al, M.S., Sybiriska, E.H., Zimmermann, R.C., Wisniewski, G., Neumeyer, J.L., Milius, R.A., Wang, S., Smith, E.O., Roth, R.H., Charney, D.S., Hoffer, P.B., Innis, R.B., 1993. SPECT imaging of dopamine and serotonin transporters with [ $^{123}\text{I}$ ] $\beta$ -CIT: Pharmacological characterization of brain uptake in nonhuman primates. *Synapse* 13, 295–309. doi:10.1002/syn.890130402
- Laruelle, M., Wallace, E., Seibyl, J.P., Baldwin, R.M., Zea Ponce, Y., Zoghbi, S.S., Neumeyer, J.L., Charney, D.S., Hoffer, P.B., Innis, R.B., 1994. Graphical, kinetic, and equilibrium analyses of in vivo [ $^{123}\text{I}$ ] beta-CIT binding to dopamine transporters in healthy human subjects. *J. Cereb. Blood Flow Metab.* 14, 982–994. doi:10.1038/jcbfm.1994.131
- Lavalaye, J., Booij, J., Reneman, L., Habraken, J.B.A., van Royen, E.A., 2000. Effect of age and gender on dopamine transporter imaging with [ $^{123}\text{I}$ ]FP-CIT SPET in healthy volunteers. *Eur J Nucl Med* 27, 867–869. doi:10.1007/s002590000279
- Leroy, C., Karila, L., Martinot, J.L., Lukasiewicz, M., Duchesnay, E., Comtat, C., Dollé, F., Benyamina, A., Artiges, E., Ribeiro, M.J., Reynaud, M., Trichard, C., 2012. Striatal and extrastriatal dopamine transporter in cannabis and tobacco addiction: a high-resolution PET study. *Addiction Biology* 17, 981–990. doi:10.1111/j.1369-1600.2011.00356.x
- Litvan, I., Agid, Y., Jankovic, J., Goetz, C., Brandel, J.P., Lai, E.C., Wenning, G., D'Olhaberriague, L., Verny, M., Chaudhuri, K.R., McKee, A., Jellinger, K., Bartko, J.J., Mangone, C.A., Pearce, R.K., 1996. Accuracy of clinical criteria for the diagnosis of progressive supranuclear palsy (Steele-Richardson-Olszewski syndrome). *Neurology* 46, 922–930.
- Marek, K., Seibyl, J., Holloway, R., Kieburtz, K., Oakes, D., Lang, A., Yim, J., Dey, H., Cellar, J., Fussell, B., Broshjeit, S., Early, M., Smith, E.O., Sudarsky, L., Johnson, K.A., Corwin, C., Johnson, D., Lajoie, S., Reich, S.G., Frost, J.J., Goldberg, P., Flesher, J.E., Feigin, A., Mazurkiewicz, J., Castronuovo, J., Joseph, F., DiRocco, A., Olanow, C.W., Machac, J., Cotei, D., Webner, P., Rudolph, A., Day, D., Casaceli, C., Freimuth, A., Orme, C., Hodgeman, K., Eberly, S., Henry, E., Morgan, G., Haley, J.B.,

- Grp, P.S., 2000. A multicenter assessment of dopamine transporter imaging with DOPASCAN/SPECT in parkinsonism. *Neurology* 55, 1540–1547.
- Nocker, M., Seppi, K., Donnemiller, E., Virgolini, I., Wenning, G.K., Poewe, W., Scherfler, C., 2012. Progression of dopamine transporter decline in patients with the Parkinson variant of multiple system atrophy: a voxel-based analysis of [123I]β-CIT SPECT. *Eur J Nucl Med Mol Imaging* 39, 1012–1020. doi:10.1007/s00259-012-2100-5
- Palumbo, B., Fravolini, M.L., Buresta, T., Pompili, F., Forini, N., Nigro, P., Calabresi, P., Tambasco, N., 2014. Diagnostic Accuracy of Parkinson Disease by Support Vector Machine (SVM) Analysis of 123I-FP-CIT Brain SPECT Data. *Medicine* 93, e228. doi:10.1097/MD.0000000000000228
- Pirker, W., Asenbaum, S., Bencsits, G., Prayer, D., Gerschlager, W., Deecke, L., Brücke, T., 2000a. [123I]beta-CIT SPECT in multiple system atrophy, progressive supranuclear palsy, and corticobasal degeneration. *Mov Disord* 15, 1158–1167.
- Pirker, W., Asenbaum, S., Bencsits, G., Prayer, D., Gerschlager, W., Deecke, L., Brücke, T., 2000b. [123I]β-CIT spect in multiple system atrophy, progressive supranuclear palsy, and corticobasal degeneration. *Movement Disorders* 15, 1158–1167. doi:10.1002/1531-8257(200011)15:6<1158::AID-MDS1015>3.0.CO;2-0
- Scherfler, C., Seppi, K., Donnemiller, E., Goebel, G., Brenneis, C., Virgolini, I., Wenning, G.K., Poewe, W., 2005. Voxel-wise analysis of [123I]beta-CIT SPECT differentiates the Parkinson variant of multiple system atrophy from idiopathic Parkinson's disease. *Brain* 128, 1605–1612. doi:10.1093/brain/awh485
- Segovia, F., Górriz, J.M., Ramirez, J., Alvarez, I., Jimenez-Hoyuela, J.M., Ortega, S.J., 2012. Improved parkinsonism diagnosis using a partial least squares based approach. *Med Phys* 39, 4395–4403. doi:10.1118/1.4730289
- Seibyl, J., Jennings, D., Grachev, I., Coffey, C., Marek, K., 2013. 123-I Ioflupane SPECT measures of Parkinson disease progression in the Parkinson Progression Marker Initiative (PPMI) trial. *J Nucl Med*.

- Seppi, K., Scherfler, C., Donnemiller, E., Virgolini, I., Schocke, M.F.H., Goebel, G., Mair, K.J., Boesch, S., Brenneis, C., Wenning, G.K., Poewe, W., 2006. Topography of Dopamine Transporter Availability in Progressive Supranuclear Palsy: A Voxelwise [ $^{123}\text{I}$ ] $\beta$ -CIT SPECT Analysis. *Archives of neurology* 63, 1154–1160. doi:10.1001/archneur.63.8.1154
- Sixel-Döring, F., Liepe, K., Mollenhauer, B., Trautmann, E., Trenkwalder, C., 2011. The role of  $^{123}\text{I}$ -FP-CIT-SPECT in the differential diagnosis of Parkinson and tremor syndromes: a critical assessment of 125 cases. *Journal of Neurology* 258, 2147–2154. doi:10.1007/s00415-011-6076-z
- Smith, S.M., Nichols, T.E., 2009. Threshold-free cluster enhancement: addressing problems of smoothing, threshold dependence and localisation in cluster inference. *Neuroimage* 44, 83–98. doi:10.1016/j.neuroimage.2008.03.061
- Tahir, N.M., Manap, H.H., 2012. Parkinson Disease Gait Classification based on Machine Learning Approach. *Journal of Applied Sciences*.
- Tanner, C.M., Goldman, S.M., 1996. Epidemiology of Parkinson's disease. *Neurol Clin* 14, 317–335.
- Tissingh, G., Bergmans, P., Booij, J., Winogrodzka, A., van Royen, E.A., Stoof, J.C., Wolters, E.C., 1997. Drug-naive patients with Parkinson's disease in Hoehn and Yahr stages I and II show a bilateral decrease in striatal dopamine transporters as revealed by [ $^{123}\text{I}$ ] $\beta$ -CIT SPECT. *Journal of Neurology* 245, 14–20. doi:10.1007/s004150050168
- van Dyck, C.H., Seibyl, J.P., Malison, R.T., Laruelle, M., Zoghbi, S.S., Baldwin, R.M., Innis, R.B., 2002. Age-related decline in dopamine transporters: analysis of striatal subregions, nonlinear effects, and hemispheric asymmetries. *Am J Geriatr Psychiatry* 10, 36–43.
- Varrone, A., Marek, K.L., Jennings, D., Innis, R.B., Seibyl, J.P., 2001. [ $^{123}\text{I}$ ] $\beta$ -CIT SPECT imaging demonstrates reduced density of striatal dopamine transporters in Parkinson's disease and multiple system atrophy. *Movement Disorders* 16, 1023–1032. doi:10.1002/mds.1256





## ***3.2 – Pre-clinical aspects***



## **Chapter 3.2.1**

### ***Effects of dorsolateral prefrontal cortex lesion on motor habit and performance assessed with manual grasping and control of force behavioral tasks in macaque monkeys.***

S. Badoud\*, S. Borgognon\*, J. Cottet\*, P. Chatagny, V. Moret, M. Fregosi, M. Kaeser, E. Fortis, E. Schmidlin, J. Bloch, J.F. Brunet and E.M. Rouiller

Manuscript in preparation



## ***Introduction***

During the last decades the dorsolateral prefrontal cortex (dlPFC) has been extensively studied, revealing its role in the integration of multiple cognitive attributes in the context of working memory, as well as its implication in risk related decision making (e.g. (Barber et al., 2013; Goldmanrakis et al., 1987; Owen et al., 1998; Petrides, 1994; Petrides & Pandya, 1999; Watanabe & Sakagami, 2007; Ye et al., 2015)). Several investigations conducted on non-human primates also emphasized an implication of dlPFC in the execution of spatiotemporal motor sequences, as well as in grip force's control (Barone & Joseph, 1989; Berdyeva & Olson, 2010; Ninokura et al., 2004; Shima et al., 2007). However, while its role in motor learning is well established, dlPFC's activation seems to progressively vanish when a motor task becomes more and more "automatic", possibly reflecting delegation of responsibility to "lower" brain structures (Halsband & Lange, 2006).

More recently, Kaeser and colleagues reported original data underlying the role of dlPFC in motor habit representation (Kaeser et al., 2013). In this study, the authors performed cortical biopsies in dlPFC on two macaque monkeys (*Macaca fascicularis*) and assessed their impact on sequential motor behavior (habit). More specifically, the "modified Brinkman board" task was used to quantify "free-will" spatiotemporal retrieval of pellets, performed with precision grip movements executed unimanually (Brinkman & Kuypers, 1973; Kaeser et al., 2013; Liu & Rouiller, 1999; Schmidlin et al., 2011). In comparison to control monkeys, dlPFC (area 46) lesioned animals exhibited a significant impact on the spatiotemporal sequences (order to visit the wells), whereas the motor performance per se (score) remained unaffected (Kaeser et al., 2013). Moreover, there was a first indication of a relationship between the size of the dlPFC biopsies and the extent of motor habit changes, as a small biopsy impacted less on motor sequences than a larger biopsy (Kaeser et al., 2013). Nevertheless, due to their limited number of cases (n=2), clearly more data are required to support this hypothesis, both in terms of number of cases as well as variability in precise location of dlPFC lesions.

Additionally, functional magnetic resonance imaging (fMRI) investigations conducted on human subjects also emphasized a role of dlPFC in the execution of motor tasks requiring some control (prediction) of the grip force to be exerted (Neely et al., 2013; Wasson et al., 2010).

The present report corresponds to the initial step of a broader study aiming at testing a novel therapeutic strategy based on autologous adult neural cell ecosystem (ANCE) transplantation (e.g. (Bloch et al., 2014; Brunet et al., 2005; Kaeser et al., 2011)) in a non-human primate 1-methyl-4-phenyl-1,2,3,6-tetrahydropyridine (MPTP) model of Parkinson's disease. In this context, unilateral biopsies in dlPFC were performed in four intact adult female macaque monkeys (several months before MPTP treatment) in order to provide the cellular material needed to produce the ANCE. The monkeys were previously trained to perform quantitative motor (manual dexterity) tasks, including the "modified Brinkman board" task and the "reach and grasp drawer" task (see Kaeser et al., 2014; Schmidlin et al., 2011). The aim of the present study was thus to extent preliminary data on the role of the prefrontal cortex (PFC) in motor habit and test the hypothesis that dlPFC indeed contributes to predict the grip force required when a precise level of force to be generated is known beforehand.

## ***Material and methods***

### ***Subjects***

For the present study, the data were collected from a group of four adult females macaque monkeys (*Macaca fascicularis*) weighting from 3.0 kg to 5.0 kg (Mk-MY, Mk-LY, Mk-MI, and Mk-LL) and aged between 4 and 8 years old at the beginning of the behavioral training. They were housed in a 45m<sup>3</sup> room, in which they were free to move and interact with each other. In addition, the room was equipped with different enrichment features (including an external

room) and free access to water (see [www.unifr.ch/spccr/about/housing](http://www.unifr.ch/spccr/about/housing)). Each monkey worked every day with an experimenter on one or two different behavioral tasks. Before being transferred to the behavioral laboratory each animal was first transferred in a free-will manner into a primate chair and was weighted in order to monitor its health condition. In addition, the appetite, the social behavior and the fur state were controlled daily during the entire experiment. After performing the behavioral tests, the monkey received its daily ration of food composed of cereal croquettes, vegetables and fruits. All surgical and behavioral procedures were approved by the local ethical committee in accordance to the guidelines for the Care and Use of Laboratory Animals and approved by local (Canton of Fribourg) and federal (Swiss) veterinary authorities (authorization number FR 22010).

### ***Behavioural tasks***

Manual dexterity assessment was based first on the “modified-Brinkman board” task (adapted from the original task of Brinkman & Kuypers, 1973), which consisted of pellets retrieval from 25 horizontal and 25 vertical wells, randomly distributed in a Plexiglas plate, each containing a banana-flavored food pellet (Rouiller et al., 1998; Schmidlin et al., 2011). The size and the shape of the wells forced the monkey to use the precision grip (opposition of the thumb and the index finger) to successfully retrieve the food pellets. The task was performed for each hand separately, three days a week. The number of pellets correctly retrieved within the first 30 seconds corresponded to the score, reflecting the motor performance (in Mk-MY, Mk-LY and Mk-MI). The motor performance in Mk-LL was assessed in a different manner. Indeed, Mk-LL adopted a mix of two behaviors, either grasping one pellet after the other as expected or by sometimes retrieving several pellets in a row to store them into the hand palm before bringing all of them to the mouth (as illustrated in Kaeser et al., 2014). Due to such random variation, MK-LL motor performance was thus calculated by summing the total number of single

pellets correctly retrieved and the multiple pellets correctly retrieved during the entire task, corresponding to the “total score”.

In addition, the motor strategy (habit) was assessed based on the temporal picking sequence (order to visit the 50 wells one after the other). However, the motor strategy given by the sequential order to visit the slots remains a qualitative assessment of the motor habit. In order to quantify the motor habit data, the same statistical approach as used by Kaeser et al. (2013) was applied. Each well received a spatial position number according to the left-right axis (left corresponded to small number and right to great number). The spatial position of each well was subtracted from the temporal sequence. The absolute values of the 50 differences were summed up giving an index of systematic motor sequence. This index permitted to assess whether the monkey repeated the same sequence along the daily sessions or not. For instance, a great variability in this index reflects changes in the picking sequence from one daily session to the next, whereas a small variability reflects stable picking sequence along the consecutive daily sessions. Note that the motor strategy of Mk-LL could not be assessed as the monkey did not perform the “modified Brinkman board” task following the standard individual pellet grasping procedure (see above).

The second motor task was the “reach and grasp drawer” task, used to quantify the production of controlled grip and load forces, as well as their time course (see Kaeser et al., 2013; Schmidlin et al., 2011). This task was designed so that the monkey had to pull open a drawer against different resistances, using one hand at the time (as derived from previous versions: (Kazennikov et al., 1999; 1994; Kermadi et al., 1997; Kermadi et al., 1998)). The “reach and grasp drawer” task required holding firmly the drawer knob between the thumb and index finger (grip force), as well as exerting a force to pull the drawer (load force), which were both monitored. One standard session consisted of ten consecutive trials at each different resistance ( $R_0 = 0$  Newton,  $R_3 = 1.25$  Newton and  $R_5 = 2.75$  Newton), performed with each hand. Each session started with the smallest resistance ( $R_0$ ) corresponding to almost no resistance. Once ten correct trials were performed at  $R_0$ , the monkey received an extra reward (a piece of almond) and the resistance was then raised to  $R_3$ . After ten correct trials at  $R_3$ , again extra-rewarded, the



resistance was increased to R5. Once the three resistances have been performed with one hand, the same paradigm was followed for the other hand. Two different parameters were analyzed in the present report. The first one was the **maximal grip force** developed in each trial. The second one was the **maximal load force**, also measured in each trial. The first trial at each resistance was removed from the analysis, as it represents an outlier (unknown resistance at the onset of a new series of trials). The four monkeys performed this task two to three times a week.

One of the monkeys (Mk-MI) performed the drawer task correctly with the left hand only (due to an injury of the right hand). Indeed, Mk-MI did not use a precision grip movement to hold the drawer's knob with its right hand, but used an alternative strategy (single finger push on the upper side of the knob), preventing any measurement of grip force. Despite of this, Mk-MI performed the "modified Brinkman board" task correctly with both hands.

### ***Surgical procedure (cortical biopsy)***

Before surgery, each animal was first lightly sedated under ketamine (Ketasol®, 10mg/kg), midazolam (Dormicum®, 0.1mg/kg) and methadone (0.2mg/kg), and prepared for the surgery. Additionally, each animal received an intramuscular dose of methadone (Methadon®; Streuli; 0.2 mg/kg) and were treated with analgesic Carprofen (Rymadil®; Pfizer; 4 mg/kg; subcutaneously), atropine (atropine; 0.05 mg/kg; intramuscularly) in order to reduce bronchial secretions, antibiotics (Synulox®; Pfizer; 8.75 mg/kg; subcutaneously) and dexamethasone (Dexadreson®; Intervet; 0.3 ml/kg; diluted 1:1 in saline; intramuscularly). Once the animal was in the surgery room, it was put under intravenous (femoral vein) perfusion with 1 % propofol (Fresenius®) diluted with ringer lactate solution and 125 mg of ketamine hydrochloride (20ml of propofol for 40ml of Ringer lactate and 1.25ml of ketamine), to ensure deep anesthesia. The infusion rate was modulated to maintain an optimal level of anesthesia. During the entire surgical procedure, the level of anesthesia and physiological state was controlled through the

arterial oxygen saturation, heart rate (ECG), ventilation (rate and expired CO<sub>2</sub>) and body temperature. The animal was then placed in a stereotaxic framework to fix its head with ear bars for the surgery. To reduce possible pain resulting from the fixation points, ear bars were coated with a local analgesic cream (LidoHex®). Local injections of lidocaine (Rapidocain®) were used to anesthetize the incision site. After the incision, the muscle tissue was pushed on the side to expose the skull, allowing craniotomy above dIPFC. In three monkeys the skull opening was made on the left side (Mk-LY, Mk-MI and Mk-LL) whereas it was on the right side in Mk-MY. After bone removal, the dura mater was incised and a piece of dIPFC cortical tissue was removed and directly placed into storage medium. The injured blood vessel were cauterized, the bone flap put back in place and fixed with histological glue (Histoacryl®). The muscle tissue and the skin were sutured. After the surgery, each animal was surveyed until its total awakening. It was considered as stable when the monkey started to eat and drink again. A posology composed of Caprofen (Rymadil®, ½ pill twice a day) and antibiotics (Clavubactin®, 1 pill twice a day) was followed during ten days.

### ***Magnetic resonance imaging (MRI)***

MRI was used to determine the precise position of the biopsies while the monkeys were still alive, before engaged in the MPTP subsequent protocol. Each animal was first lightly sedated with ketamine (Ketasol®, 10mg/kg) and midazolam (Dormicum®, 0.1mg/kg). After being transported to the MRI facility (radiology, Hospital of Fribourg, Switzerland), each monkey was anesthetized via an intravenous perfusion of 1 % propofol (Fresenius®) diluted with ringer lactate solution and 125 mg of ketamine hydrochloride (20ml of propofol for 20ml ringer lactate and 1.25ml of ketamine). The infusion rate was adjusted to ensure an optimal level of anesthesia (ECG and O<sub>2</sub> saturation were continuously monitored). In addition, gloves filled with hot water were placed around monkey's body to maintain its body temperature. The monkey was placed in the magnet in a prone position with a flow of oxygen (3l/min) in front

of the nose. Data were acquired on a GE 3T magnet using 3D transverse T1 weighted acquisition protocol. The parameters were as follows: field of view: 256 \* 256, TR: 7.248, TE: 3.032 and FS: 3. Images were then rotated because of the prone position of the animal (FSLview V3.2.0). After the proper rotation, brains were extracted from the skull and represented in a three dimensional view before being schematized. The positions of each biopsy and their volumes were estimated based on the MRI images. Note that histological verification of the biopsy could not take place, as a second dlPFC biopsy took place in the vicinity of the first one when the MPTP treatment was ongoing. It was therefore not possible to distinguish the two biopsies and only the first one is relevant for the present behavioral study, before MPTP treatment.

## ***Results***

### ***Location and size of the biopsies***

Based on MRI, as explained in the methods, the extent and position of the cortical biopsies were identified and reconstructed. Transposed to the surface of the corresponding brains, the biopsies are illustrated in Figure 1, for Mk-MY, Mk-LY, Mk-MI and Mk-LL. The biopsy size was 7 mm<sup>3</sup>, 14 mm<sup>3</sup>, 16mm<sup>3</sup> and 7 mm<sup>3</sup>, respectively. In Mk-MY, the biopsy is located at the most rostral part of dlPFC, about 5 mm from the midline, most likely overlapping the transition zone between Brodmann's cortical area 9 and area 10. Also about 5 mm lateral with respect to the midline, but somewhat more caudal, the biopsy in Mk-LY appears to be located in the rostral part of area 9. The lesion in Mk-MI is located in a zone of dlPFC comparable to that of Mk-LY, though somewhat more lateral. In the fourth monkey (Mk-LL), the biopsy is located clearly more caudally, slightly anterior to the genu of the arcuate sulcus and at a medio-lateral level consistent with a location in the premotor dorsal rostral area (PMd-r, area F7), close to the more medial pre-supplementary motor area (SMA, area F6). In other words, Mk-LL should be treated here as an outlier, considering that its biopsy did not involve dlPFC. The four monkeys

included in the present study differ from the two animals subjected to dIPFC lesion in Kaeser et al. (2013), as in the latter study the two biopsies were located in area 46.

### ***Modified Brinkman board task***

The data derived from the score, given by the number of pellets retrieved in 30 seconds, showed that the monkeys exhibited a largely stable manual dexterity performance before dIPFC biopsy, as illustrated for Mk-MY in Figure 2A. The score data for all 4 monkeys and the two hands are shown in the supplementary Figure 1, together with the results of statistical analyses. Similarly, the data obtained from the temporal picking sequence analysis show that the monkeys followed a largely reproducible strategy (motor habit) to empty the board before the biopsy, in other words the temporal sequence to visit the 50 wells, along the left-right axis (Fig. 2B, illustrated for Mk-MY; see supplementary Figures 2 for a comprehensive presentation of the motor sequence data). Interestingly, neither the score nor the temporal sequences to visit the wells were affected by the dIPFC or PMd-r biopsy, as illustrated for Mk-MY in Figure 2A and B. Indeed, statistical analyses (see Kaeser et al., 2013) comparing pre versus post-biopsy scores and temporal sequences did not show any statistically significant difference ( $p > 0.05$ ). These conclusions apply for both the ipsilesional and contralesional arms in the four monkeys, with however the exceptions of the contralesional hand in Mk-MY and the contralesional hand in Mk-LY for the score (Suppl. Fig. 1A). In addition, the index of systematic motor sequence for the contralesional hand of Mk-MI showed a significant modification related to the biopsy (Suppl. Fig. 3F). At that step, we can conclude that the dIPFC biopsies, with the characteristics as performed in the present study (size and/or precise location), did not systematically impact on performance and motor habit in the “modified Brinkman board” task, in contrast to larger and differently located biopsies (area 46) performed earlier (Kaeser et al., 2013).

## ***Reach and grasp drawer task***

The results obtained from the reach and grasp drawer task were separated into the three resistances opposing drawer opening, namely R0, R3 and R5 (Fig. 3). For each resistance the data were split into pre-biopsy and post-biopsy periods. Each box and whisker plot encompassed all correct trials for the corresponding period. For each hand, the pre- and post-biopsy periods were represented next to each other in order to facilitate direct comparison. The quantitative data show that the resistance had an impact on the maximal grip force and the maximal load force during both the pre-biopsy and the post-biopsy periods. Indeed, and as expected, both maximal forces increased in parallel with the resistances, the higher the resistance the higher the force required to grasp the knob or to pull the drawer.

When comparing pre-biopsy versus post-biopsy periods (grey versus next black box), a statistically significant decrease of **maximal grip force** was observed post-biopsy for both hands in the two animals subjected to dIPFC biopsy in areas 9/10 (Mk-MY and Mk-LY), with the exception of the right (contralesional) hand of Mk-LY at resistance R0 (Fig. 3A and C). Mk-MI, subjected to dIPFC biopsy in the same rostro-caudal position than Mk-LY but somewhat more lateral (area 9), exhibited a statistically significant increase of the maximal grip force at all 3 resistances (data available for ipsilesional hand only, as explained earlier) (Fig. 3 E). In Mk-LL subjected to PMd-r biopsy, in some contrast with the other 2 monkeys, the maximal grip force varied less systematically post-biopsy, as a decrease was limited to the left (ipsilesional) hand at resistances R3 and R5 (Fig. 3G).

As far as the **maximal load force** is concerned, the subjects were differentially affected (Fig. 3B, D, F and H). In Mk-MY (Fig. 3B), the maximal load force was not at all affected by the dIPFC biopsy whereas, in Mk-LY, the dIPFC biopsy impacted on the maximal load force exerted by the right (contralesional) hand at all resistances (Fig. 3D), the left (ipsilesional) hand being not influenced. In Mk-MI, following dIPFC biopsy, there was a decrease of the load force at resistances R3 and R5 (Fig. 3F) for the ipsilesional hand. In Mk-LL (PMd-r lesion), a decrease of the maximal load force was observed

for the left (ipsilesional) hand at all resistance and for the right (contralesional) hand at R5 only (Fig. 3H).

To sum up, following a kind of rostro-caudal biopsy gradient, Mk-MY with the most rostral biopsy exhibited post-biopsy a decrease of the maximal grip force at all resistances and for both hands (Fig. 3A), without effect on the maximal load force. In Mk-LY, subjected to a somewhat more caudal (and bigger) lesion in area 9, the maximal grip force was also affected (decrease) by the biopsy on both hands (with one exception however, Fig. 3C), whereas some effect on the maximal load force amplitude appeared, but limited to the contralesional hand (Fig. 3D). In Mk-MI (ipsilesional hand only), the biopsy impacted on the maximal grip force at all the resistances, though in the form of an increase, as well as on the load force (but decrease) at R3 and R5. Finally, in Mk-LL subjected to a lesion caudal to dlPFC, namely in PMd-r, the effects appeared more lateralized, with the ipsilesional hand more affected (both maximal load and grip forces) than the contralesional hand (only the maximal load force at R5; Fig. 3H).

## ***Discussion***

In a general manner, the present study led to four main conclusions with respect to the role of the dlPFC in motor control:

- 1) Lesions resulting from small biopsies in dlPFC and/or when located in areas 9/10 did not affect either the motor habit (spatiotemporal sequential strategies) or the motor performance (score) of manual dexterity in the “modified Brinkman board” task. The same conclusion holds true for a lesion located in PMd-r (area F7).
- 2) In sharp contrast, as revealed by the “reach and grasp drawer” task, significant modifications in the control of the maximal grip force were observed as a result of a lesion in areas 9/10, whereas the maximal load force was also affected, but to a lesser extent and only as a consequence of a more caudal lesion in area 9.

- 3) A lesion more caudal to dIPFC, in PMd-r (area F7), led to more lateralized hand (predominantly ipsilesional) and less systematic changes for both maximal grip and load forces.
- 4) Although limited to four cases, a rostro-caudal gradient of biopsy location appears to dictate the specific effects of the lesions (Fig. 4).

The above conclusion 1 valid for areas 9/10 and PMd-r is coherent with previous lesions in dIPFC targeted to area 46 (Kaeser et al., 2013) as far as the absence of effect on performance (score in the “modified Brinkman board” task) is concerned. On the other hand, a biopsy of 44 mm<sup>3</sup> in area 46 led to a massive change of motor habit whereas a medium size biopsy of 20 mm<sup>3</sup> induced a moderate change of motor habit (Kaeser et al., 2013). This is in contrast with the present area 9/10 (7 mm<sup>3</sup>, 14 mm<sup>3</sup> and 16mm<sup>3</sup>) or PMd-c (7 mm<sup>3</sup>) lesions, which did not (or very little) impact on the “modified Brinkman board” data (neither score nor motor habit). At that step, it cannot be distinguished whether these differences related to the “modified Brinkman board” task between the present study and the study of Kaeser et al. (2013) is due to a difference in lesion size or to the location of the lesion, or to both.

In the context of cell therapy strategies, in particular regarding the ANCE approach, Kaeser et al. (2013) recommended to not exceed a dIPFC biopsy of 10 mm<sup>3</sup> in order to limit deleterious effects on the motor habit and motor performance, as reflected by the “modified Brinkman board” task. The present results suggest that this upper limit of 10 mm<sup>3</sup> may easily be raised up to 16 mm<sup>3</sup> without significant impact on motor habit and performance. This observation has clinical implication, implying a reduced concern to apply the ANCE strategy to patients (stroke or Parkinson’s disease), as the present macaque monkey experiments suggest that unwanted motor consequences are unlikely, at least as far as motor habit and motor performance are concerned in the context of a sequential grasping a small objects, which does not require the development of significant force levels. Indeed, in the case of strokes or edema, surgical procedure is often required. The removed cortical material during this kind of surgery could be sorted and cryopreserved for

possible subsequent ANCE production and treatment in case of poor functional recovery (see: Brunet et al., 2002; Brunet et al., 2003).

Unfortunately, due to the absence of significant spatiotemporal patterns' modification or motor habit (Fig. 2), it was not possible to assess a potential hemispheric lateralization of such motor representations as suggested in some papers (Baker et al., 1996; Kaeser et al., 2013; McCarthy et al., 1996; Reuter-Lorenz et al., 2000).

In contrast to the study of Kaeser et al. (2013), limited to the “modified and rotating Brinkman board” tasks (thus focused on grasping of small objects), the originality of the present study was to extend the consequences of dIPFC lesion to a substantially different motor control, involving the precise development of two forces, namely grip force and load force. The above conclusions 2, 3 and 4 are consistent with the notion that dIPFC is involved in the precise control of predicted force, though more for the grip force than the load force. Indeed, as the trials on the “reach and grasp drawer” task are grouped according to the resistance level, after the first trial in each group of resistances (excluded from the analysis), the monkey knew the level of force required for each resistance and therefore could predict how much force was required in the subsequent trials. The observed decrease of maximal grip force amplitude post-biopsy suggests that, after dIPFC or PMd-r lesion (to a lesser extent for the latter), there is a decrease in the margin of security to successfully grasp the drawer's knob with enough force to prevent the fingers from slipping away from the knob. This phenomenon may favor an economy of energy, beneficial in case of brain lesion, but at the cost to increase the risk of incorrect (unsuccessful) trials. Note however the case of Mk-MI (ipsilesional hand only) which also showed an impact of the biopsy on the maximal grip force, but in the other direction (increase post-biopsy), suggesting a possible loss in grip force control (to maximize effort as in the other monkeys). This divergent result in Mk-MI may be due the position of the biopsy (more lateral than in Mk-LY), and/or a different recovery strategy from the lesion, and/or the asymmetry between both hands in the execution of the “reach and grasp drawer” task (as mentioned earlier).



The present data in the macaque monkey (except for Mk-MI) related to the prediction of grip force is well in line with previous fMRI data reported for human subjects. Indeed, the role of pre-frontal cortices (such as dlPFC), the cingulate motor area (CMA) as well as the ventral pre-motor area (PMv) have been widely reported to play a role in the control of grip force control in fMRI studies on human subjects (Ehrsson et al., 2001; Kutz et al., 2001; Rowe et al., 2000). Furthermore, Vaillancourt and colleagues reported that the dlPFC and the anterior cingulate cortex (ACC) exhibited an increase of blood-oxygen-level dependent (BOLD) signal when the task consisted of selecting the force amplitude (Vaillancourt et al., 2007). In addition, Wasson et al. (2010) demonstrated an activation of dlPFC, pre-SMA and PMv in a task based on predictable grip force amplitude. In addition to cortical regions, the ventral thalamus, the cerebellum and the anterior nuclei of the basal ganglia were activated suggesting a network encompassing all these regions to successfully execute grip force that require prediction. Moreover, Neely et al. (2013) emphasized the role of the dlPFC in the production of dynamic grip force as well as static grip force with a more pronounced effect for the latter. In our study, the behavioral paradigm seems to be closer to the dynamic grip force reported by Neely et al., 2013. However, in both cases the dlPFC is involved in the grip force production. Taken together, our data are consistent with previous reports on human subjects and strengthen the role of the dlPFC in the control (prediction) of the grip force and its role in working memory (Pochon et al., 2001).

The case of monkey MK-LL, subjected to biopsy located not in the aimed dlPFC but in the adjacent PMd-r, illustrates that functional properties do not vary abruptly from one cortical area to the next, but rather exhibit a progressive transition. Indeed the effect on maximal grip force was less present and less prominent than after lesion of area 9/10 (Fig. 3). Reciprocally, the effect on the maximal load force was somewhat more affected by the biopsy in PMd-r than in dlPFC (Fig. 3). This observation related to load force control for PMd-r is consistent with previously reported roles of PMd in the control of proximal forelimb muscles (Fink et al., 1997; Freund, 1985; Freund & Hummelsheim, 1985).

To summarize, the present study provides new and complementary functional data regarding the role of dlPFC in motor habit representations and manual dexterity performances that support and extend the data and conclusions recently published by Kaeser and colleagues (Kaeser et al., 2013). Moreover, due to its integrative conception, the “reach and grasp drawer” task developed by our laboratory allowed us to track subtle behavioral modifications in terms of grip and load forces’ control and their prediction. These data offer new interpretations related to lesions’ size and their precise location (e.g. area 46 versus areas 9/10) in dlPFC, as well as on the spatial functional organization of dlPFC along the rostro-caudal extent, with spread to the adjacent PMd-r area. However, due to the limited number of animal included in the present investigation, the interpretation of the data remains limited. Further investigations on a larger pool of monkeys are required to consolidate our hypotheses and conclusions at that step. Furthermore, the present data argue for the pertinence of the ANCE approach as cell therapy to treat brain lesion or neurodegeneration, based on biopsies targeted to dlPFC, although the size of the biopsy needs to be reduced as much as possible, to also avoid effects on the prediction and control of grip force levels.

### ***Authors’ contributions***

Simon Badoud, Simon Borgognon, Jérôme Cottet and Eric M. Rouiller designed the study, conducted the experiments, acquired, analyzed, and interpreted the data, and drafted the manuscript. Pauline Chatagny and Véronique Moret acquired and analyzed some of the data. Michela Fregosi analyzed some of the data. Mélanie Kaeser, Ekaterina Fortis, Eric Schmidlin and Eric M. Rouiller developed the “reach and grasp drawer” task. Jocelyne Bloch performed the biopsies. Jean-François Brunet put the cortical biopsies in culture. All authors critically revised the text and significantly contributed to the final version of the manuscript.

## ***Acknowledgments***

The authors wish to thank Professor Henri-Marcel Hoogewoud and Eric Daflon from the radiology of the Hospital of Fribourg for providing the MRI machinery. In addition, the authors wish to thank the technical assistance of Laurent Bossy, Jacques Maillard (animal house keeping), André Gaillard (mechanics), Bernard Aebischer (electronics) and Laurent Monney (informatics).

Grant Sponsors: Swiss National Science Foundation, grants No 31-61857.00, 310000-110005 and 31003A-132465 (EMR), No 3100A0-103924 (JB), the Novartis Foundation; the National Centre of Competence in Research (NCCR) on "Neural plasticity and repair" and the Christopher Reeves Foundation (Springfield, NJ).

The authors have no conflict of interest in relation to the present study.

## **Bibliography**

- Baker, S. C., Rogers, R. D., Owen, A. M., Frith, C. D., Dolan, R. J., Frackowiak, R., & Robbins, T. W. (1996). Neural systems engaged by planning: A PET study of the Tower of London task. *Neuropsychologia*, *34*(6), 515–526.
- Barber, A. D., Caffo, B. S., Pekar, J. J., & Mostofsky, S. H. (2013). Effects of Working Memory Demand on Neural Mechanisms of Motor Response Selection and Control. *Journal of Cognitive Neuroscience*, *25*(8), 1235–1248. [http://doi.org/10.1162/jocn\\_a\\_00394](http://doi.org/10.1162/jocn_a_00394)
- Barone, P., & Joseph, J. P. (1989). Prefrontal Cortex and Spatial Sequencing in Macaque Monkey. *Experimental Brain Research*, *78*(3), 447–464.
- Berdyeva, T. K., & Olson, C. R. (2010). Rank signals in four areas of macaque frontal cortex during selection of actions and objects in serial order. *Journal of Neurophysiology*, *104*(1), 141–159. <http://doi.org/10.1152/jn.00639.2009>
- Bloch, J., Brunet, J.-F., McEntire, C. R. S., & Redmond, D. E. (2014). Primate adult brain cell autotransplantation produces behavioral and biological recovery in 1-methyl-4-phenyl-1,2,3,6-tetrahydropyridine-induced parkinsonian St. Kitts monkeys. *The Journal of Comparative Neurology*, *522*(12), 2729–2740. <http://doi.org/10.1002/cne.23579>
- Brinkman, J., & Kuypers, H. G. (1973). Cerebral control of contralateral and ipsilateral arm, hand and finger movements in the split-brain rhesus monkey. *Brain : a Journal of Neurology*, *96*(4), 653–674.
- Brunet, J.-F., Pellerin, L., Arsenijevic, Y., Magistretti, P., & Villemure, J.-G. (2002). A Novel Method for In Vitro Production of Human Glial-Like Cells from Neurosurgical Resection Tissue. *Laboratory Investigation*, *82*(6), 809–812. <http://doi.org/10.1097/01.LAB.0000017166.26718.BB>
- Brunet, J.-F., Pellerin, L., Magistretti, P., & Villemure, J.-G. (2003). Cryopreservation of human brain tissue allowing timely production of viable adult human brain cells for autologous transplantation. *Cryobiology*, *47*(2), 179–183.
- Brunet, J. F., Rouiller, E., Wannier, T., Villemure, J. G., & Bloch, J. (2005). Primate adult brain cell autotransplantation, a new tool for brain repair? *Experimental Neurology*, *196*(1), 195–198. <http://doi.org/10.1016/j.expneurol.2005.04.005>
- Ehrsson, H. H., Fagergren, E., & Forssberg, H. (2001). Differential fronto-parietal activation depending on force used in a precision grip task: an fMRI study. *Journal of Neurophysiology*, *85*(6), 2613–2623.
- Fink, G. R., Frackowiak, R., Pietrzyk, U., & Passingham, R. E. (1997). Multiple nonprimary motor areas in the human cortex. *Journal of Neurophysiology*, *77*(4), 2164–2174.
- Freund, H. J. (1985). Clinical aspects of premotor function. *Behavioural Brain Research*, *18*(2), 187–191.
- Freund, H. J., & Hummelsheim, H. (1985). Lesions of premotor cortex in man. *Brain : a Journal of Neurology*, *108* ( Pt 3), 697–733.
- Goldmandrakic, P. S. (1987). Motor Control Function of the Prefrontal Cortex.

- Ciba Foundation Symposia*, 132, 187–200.
- Halsband, U., & Lange, R. K. (2006). Motor learning in man: A review of functional and clinical studies. *Journal of Physiology-Paris*, 99(4-6), 414–424. <http://doi.org/10.1016/j.jphysparis.2006.03.007>
- Kaesler, M., Brunet, J.-F., Wyss, A., Belhaj-Saif, A., Liu, Y., Hamadjida, A., et al. (2011). Autologous adult cortical cell transplantation enhances functional recovery following unilateral lesion of motor cortex in primates: a pilot study. *Neurosurgery*, 68(5), 1405–16– discussion 1416–7. <http://doi.org/10.1227/NEU.0b013e31820c02c0>
- Kaesler, M., Chatagny, P., Gindrat, A. D., Savidan, J., Badoud, S., Fregosi, M., et al. (2014). Variability of manual dexterity performance in non-human primates (). *International Journal of Comparative Psychology*, 27(2).
- Kaesler, M., Wannier, T., Brunet, J.-F., Wyss, A., Bloch, J., & Rouiller, E. M. (2013). Representation of motor habit in a sequence of repetitive reach and grasp movements performed by macaque monkeys: Evidence for a contribution of the dorsolateral prefrontal cortex. *Cortex*, 49(5), 1404–1419. <http://doi.org/10.1016/j.cortex.2012.05.025>
- Kazennikov, O., Hyland, B., Corboz, M., Babalian, A., Rouiller, E. M., & Wiesendanger, M. (1999). Neural activity of supplementary and primary motor areas in monkeys and its relation to bimanual and unimanual movement sequences. *Neuroscience*, 89(3), 661–674. [http://doi.org/10.1016/S0306-4522\(98\)00348-0](http://doi.org/10.1016/S0306-4522(98)00348-0)
- Kazennikov, O., Wicki, U., Corboz, M., Hyland, B., Palmeri, A., Rouiller, E. M., & Wiesendanger, M. (1994). Temporal Structure of a Bimanual Goal-directed Movement Sequence in Monkeys. *European Journal of Neuroscience*, 6(2), 203–210. <http://doi.org/10.1111/j.1460-9568.1994.tb00262.x>
- Kermadi, I., Liu, Y., Tempini, A., & Rouiller, E. M. (1997). Effects of reversible inactivation of the supplementary motor area (SMA) on unimanual grasp and bimanual pull and grasp performance in monkeys. *Somatosensory and Motor Research*, 14(4), 268–280. <http://doi.org/10.1080/08990229770980>
- Kermadi, I., Liu, Y., Tempini, A., Calciati, E., & Rouiller, E. M. (1998). Neuronal activity in the primate supplementary motor area and the primary motor cortex in relation to spatio-temporal bimanual coordination. *Somatosensory and Motor Research*, 15(4), 287–308.
- Kuhtz Buschbeck, J. P., Ehrsson, H. H., & Forssberg, H. (2001). Human brain activity in the control of fine static precision grip forces: an fMRI study. *European Journal of Neuroscience*, 14(2), 382–390. <http://doi.org/10.1046/j.0953-816x.2001.01639.x>
- Liu, Y., & Rouiller, E. M. (1999). Mechanisms of recovery of dexterity following unilateral lesion of the sensorimotor cortex in adult monkeys. *Experimental Brain Research*, 128(1-2), 149–159.
- McCarthy, G., Puce, A., Constable, R. T., Krystal, J. H., Gore, J. C., & Goldman-Rakic, P. (1996). Activation of human prefrontal cortex during spatial and nonspatial working memory tasks measured by functional MRI. *Cerebral Cortex (New York, NY : 1991)*, 6(4), 600–611.
- Neely, K. A., Coombes, S. A., Planetta, P. J., & Vaillancourt, D. E. (2013). Segregated and overlapping neural circuits exist for the production of static and dynamic precision grip force. *Human Brain Mapping*, 34(3),

- 698–712. <http://doi.org/10.1002/hbm.21467>
- Ninokura, Y., Mushiake, H., & Tanji, J. (2004). Integration of temporal order and object information in the monkey lateral prefrontal cortex. *Journal of Neurophysiology*, *91*(1), 555–560. <http://doi.org/10.1152/jn.00694.2003>
- Owen, A. M., Stern, C. E., Look, R. B., Tracey, I., Rosen, B. R., & Petrides, M. (1998). Functional organization of spatial and nonspatial working memory processing within the human lateral frontal cortex. *Proceedings of the National Academy of Sciences*, *95*(13), 7721–7726.
- Petrides, M. (1994). Frontal lobes and behaviour. *Current Opinion in Neurobiology*, *4*(2), 207–211. [http://doi.org/10.1016/0959-4388\(94\)90074-4](http://doi.org/10.1016/0959-4388(94)90074-4)
- Petrides, M., & Pandya, D. N. (1999). Dorsolateral prefrontal cortex: comparative cytoarchitectonic analysis in the human and the macaque brain and corticocortical connection patterns. *The European Journal of Neuroscience*, *11*(3), 1011–1036.
- Pochon, J. B., Levy, R., Poline, J. B., Crozier, S., Lehericy, S., Pillon, B., et al. (2001). The role of dorsolateral prefrontal cortex in the preparation of forthcoming actions: an fMRI study. *Cerebral Cortex (New York, NY : 1991)*, *11*(3), 260–266.
- Reuter-Lorenz, P. A., Jonides, J., Smith, E. E., Hartley, A., Miller, A., Marshuetz, C., & Koeppe, R. A. (2000). Age differences in the frontal lateralization of verbal and spatial working memory revealed by PET. *Journal of Cognitive Neuroscience*, *12*(1), 174–187.
- Rouiller, E. M., Yu, X. H., Moret, V., Tempini, A., Wiesendanger, M., & Liang, F. (1998). Dexterity in adult monkeys following early lesion of the motor cortical hand area: the role of cortex adjacent to the lesion. *The European Journal of Neuroscience*, *10*(2), 729–740.
- Rowe, J. B., Toni, I., Josephs, O., Frackowiak, R. S., & Passingham, R. E. (2000). The prefrontal cortex: response selection or maintenance within working memory? *Science (New York, NY)*, *288*(5471), 1656–1660.
- Schmidlin, E., Kaeser, M., Gindrat, A. D., Savidan, J., Chatagny, P., Badoud, S., et al. (2011). Behavioral Assessment of Manual Dexterity in Non-Human Primates. *Journal of Visualized Experiments*, (57), e3258–e3258. <http://doi.org/10.3791/3258>
- Shima, K., Isoda, M., Mushiake, H., & Tanji, J. (2007). Categorization of behavioural sequences in the prefrontal cortex. *Nature*, *445*(7125), 315–318. <http://doi.org/10.1038/nature05470>
- Vaillancourt, D. E., Yu, H., Mayka, M. A., & Corcos, D. M. (2007). Role of the basal ganglia and frontal cortex in selecting and producing internally guided force pulses. *Human Brain Mapping Journal*, *36*(3), 793–803. <http://doi.org/10.1016/j.neuroimage.2007.03.002>
- Wasson, P., Prodoehl, J., Coombes, S. A., Corcos, D. M., & Vaillancourt, D. E. (2010). Predicting grip force amplitude involves circuits in the anterior basal ganglia. *NeuroImage*, *49*(4), 3230–3238. <http://doi.org/10.1016/j.neuroimage.2009.11.047>
- Watanabe, M., & Sakagami, M. (2007). Integration of cognitive and motivational context information in the primate prefrontal cortex. *Cerebral Cortex (New York, NY : 1991)*, *17*(suppl 1), I101–I109. <http://doi.org/10.1093/cercor/bhm067>
- Ye, H., Chen, S., Huang, D., Wang, S., & Luo, J. (2015). Modulating activity in

the prefrontal cortex changes decision-making for risky gains and losses: A transcranial direct current stimulation study. *Behavioural Brain Research*, 286, 17–21. <http://doi.org/10.1016/j.bbr.2015.02.037>





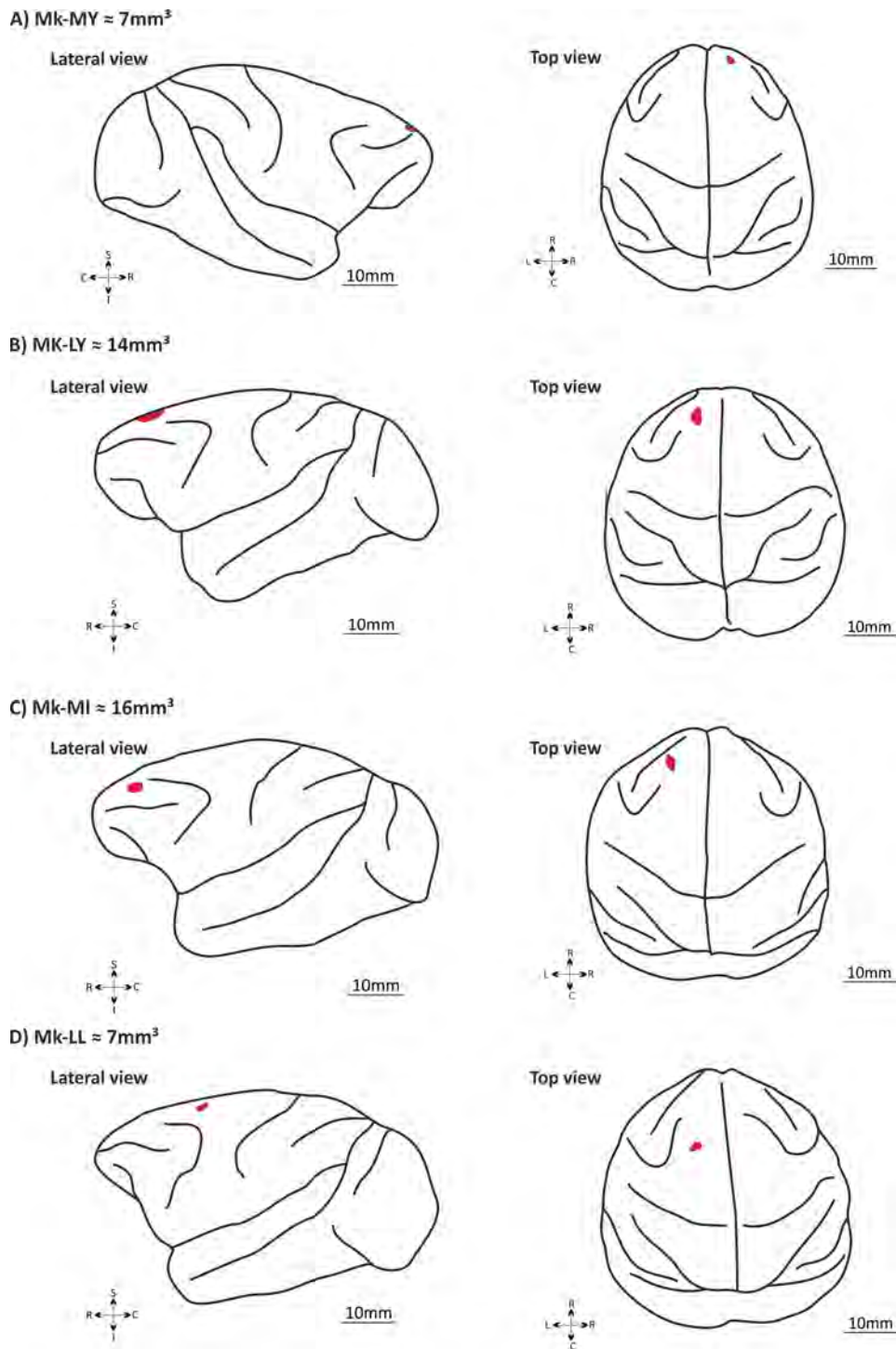
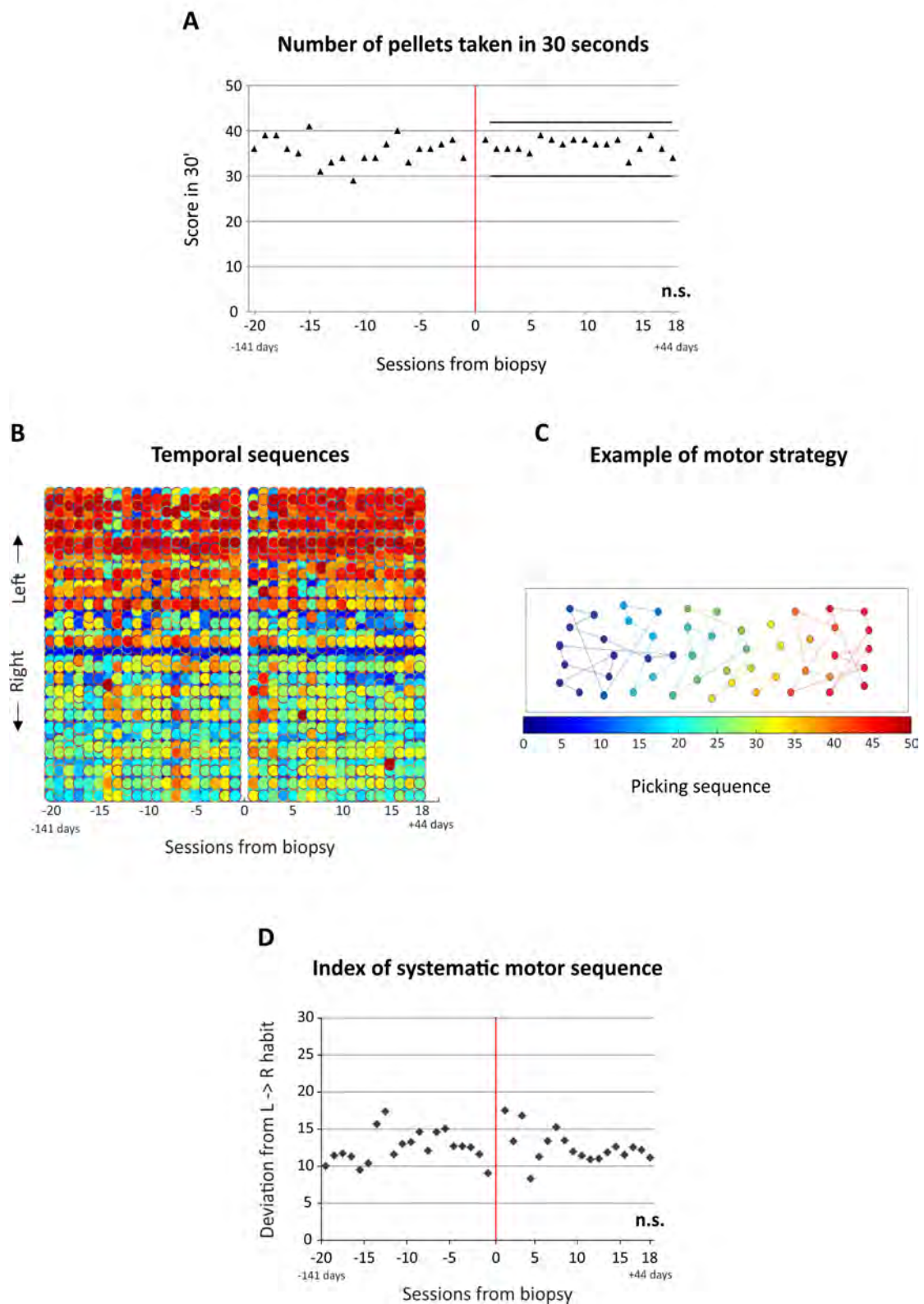


**Fig. 1.** On schematic representations of the brain of the four monkeys, the dLPFC biopsies' location and extent are represented by a red spot. Each biopsy's volume and position was estimated from MRI images using the software FSLView v3.2.0. The panel **(A)** represents the lateral (left) and the top view (right) of Mk-MY's brain with the biopsy in red (volume =  $7\text{mm}^3$ ). The panel **(B)** represents the lateral (left) and the top view (right) of Mk-LY's brain with the biopsy in red (volume =  $14\text{mm}^3$ ). The panel **(C)** represents the lateral (left) and the top view (right) of Mk-MI's brain with the biopsy in red (volume =  $16\text{mm}^3$ ). The panel **(D)** represents the lateral (left) and the top view (right) of Mk-LL's brain with the biopsy in red (volume =  $7\text{mm}^3$ ).

Legends: **(A,B,C,D)** lateral view of the brain: S=superior (medial), I=inferior (lateral), R=rostral, C=caudal; top view of the brain: R=rostral, C=caudal, L=left, R=right.

## Mk-MY - Right (ipsilesional) Hand



first 30 seconds. The X axis corresponds to the behavioral sessions (note that the time is represented as “sessions from biopsy” because in the pre-biopsy phase one session per week during 4 months was analyzed as the monkeys were considered to be on a plateau of motor performance, whereas during the post-biopsy phase, all sessions were analyzed. This is also true for the picking sequence and the “reach and grasp drawer” task data). The Y axis corresponds to the numbers of pellets (horizontal and vertical slots) retrieved during the first 30 seconds (total score in 30’). The red line corresponds to the day at which the cortical biopsy took place. The two black horizontal lines indicate superior and inferior limits, defined as mean pre-biopsy value plus 2 standard deviations (SDs) and mean pre-lesion value minus 2 SDs, respectively). The panel **(B)** represents the picking sequence along the left-right axis of the board. The X axis represents the daily behavioral sessions, so that one column corresponds to one individual session. The Y axis represents the 50 wells of the board, ordered according to the left-right axis. The colors correspond to the temporal picking sequence. The first pellet retrieved is represented in dark blue and the last one in dark red. The entire sequence is thus represented in a color gradient fashion, ranging from the darkest blue (first pellet retrieved) to the darkest red (last pellet retrieved). The session 0 corresponds to the time point of the cortical biopsy. The panel **(C)** is a schematic representation of an individual “modified Brinkman board” session. In this example, the subject began to pick up the pellets from the left extremity of the board (blue dots) to progressively move towards the right extremity (red symbols). The panel **(D)** represents the quantitative assessment of motor sequence in the “modified Brinkman board” task. The black dots represent the index of systemic motor sequence. The X axis corresponds to the behavioral daily sessions starting at the time of the biopsy (0 in the abscissa). Negative days are pre-biopsy and positive days are post-biopsy. The Y axis represents the extent of deviation from an “ideal” systematic motor sequence starting from the left of the board and finishing at the right side of the board. In other words, a picking sequence going from left to right gives a low score whereas a picking sequence going from right to left gives a high score. The indexes were compared pre- versus post-biopsy, based on the non-parametric Mann and Whitney test (MW) or the parametric unpaired Student t-test). The results for each statistical comparison is indicated on the bottom right of each graph: n.s. = non-significant difference ( $p > 0.05$ ). Comprehensive data for the “modified Brinkman board” task are shown in the supplementary figures 1-3.

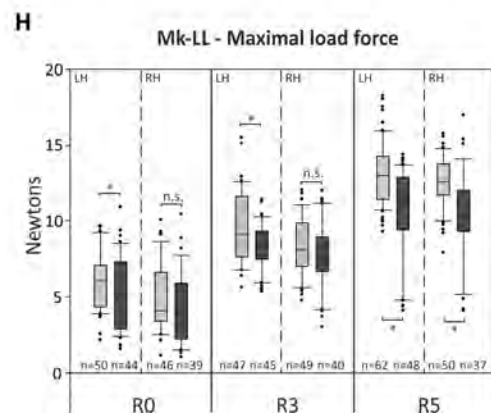
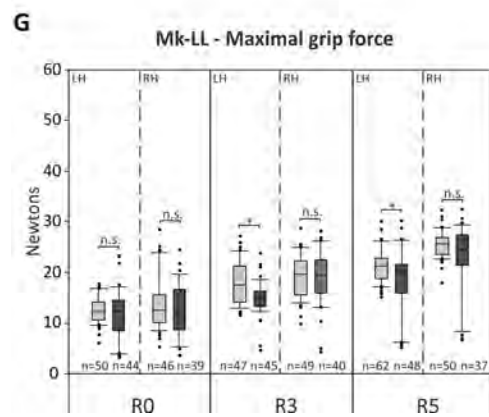
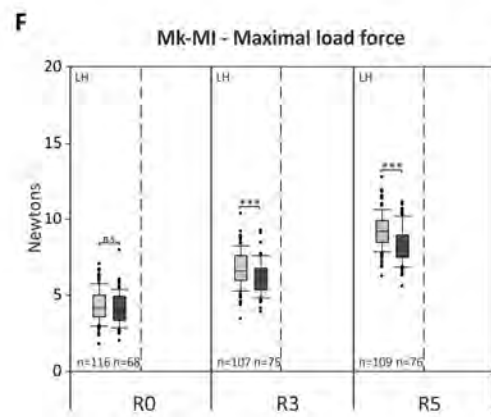
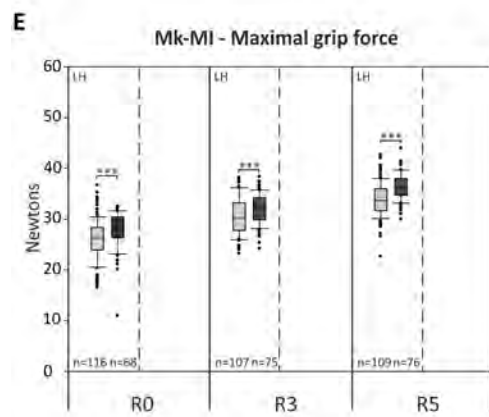
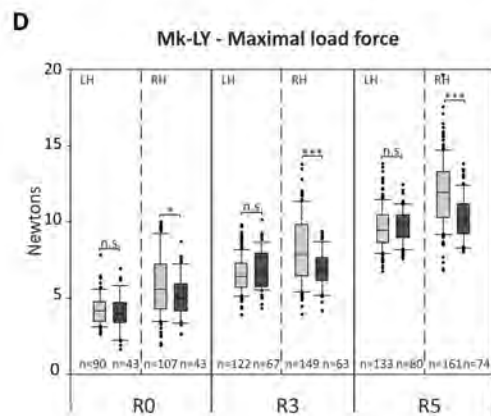
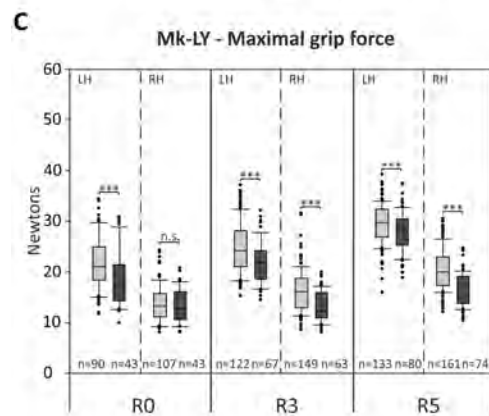
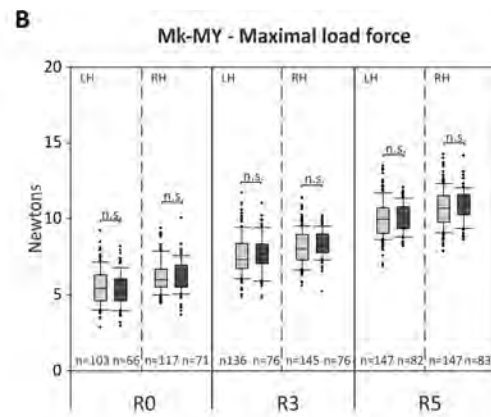
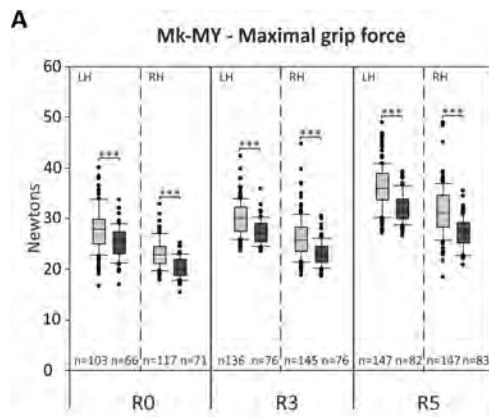


**Fig. 3.** The box and whiskers graphs show the quantitative assessments in the “reach and grasp drawer” task, separately for the 3 resistances namely R0, R3 and R5. For each resistance, the left hand (LH) and the right hand (RH) are represented. Box plots are composed of all correct trials before (pre-, represented in grey) and after (post-, represented in black) the cortical biopsies. The total number of correct trials composing each box and whiskers is indicated under it (n=). Statistical analyses (parametric Student unpaired t-test/Mann-Whitney test) compare maximal grip and load forces between pre-biopsy and post-biopsy sessions, for each resistance and for each hand. Statistically significant differences are indicated: \* is for  $p \leq 0.05$ , \*\* for  $p \leq 0.01$ , \*\*\* for  $p \leq 0.001$ , «n.s.» meaning statistically non-significant ( $p > 0.05$ ). The panels **(A and B)** show the maximal grip force and maximal load force for Mk-MY, in which the right hand is the ipsilesional hand. The panels **(C and D)** show the maximal grip force and maximal load force for Mk-LY, in which the right hand is the contralesional hand. The panels **(E and F)** show the maximal grip force and maximal load force for Mk-MI, in which the left hand is the ipsilesional hand. For Mk-MI only the left hand was analyzed (not able to perform precision grip with the right hand). The panels **(G and H)** show the maximal grip force and maximal load force for Mk-LL, in which the right hand is the contralesional hand.

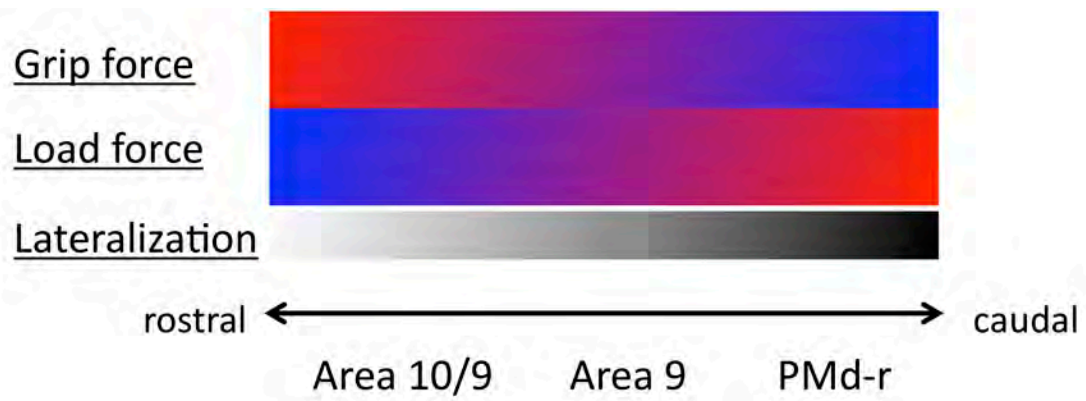
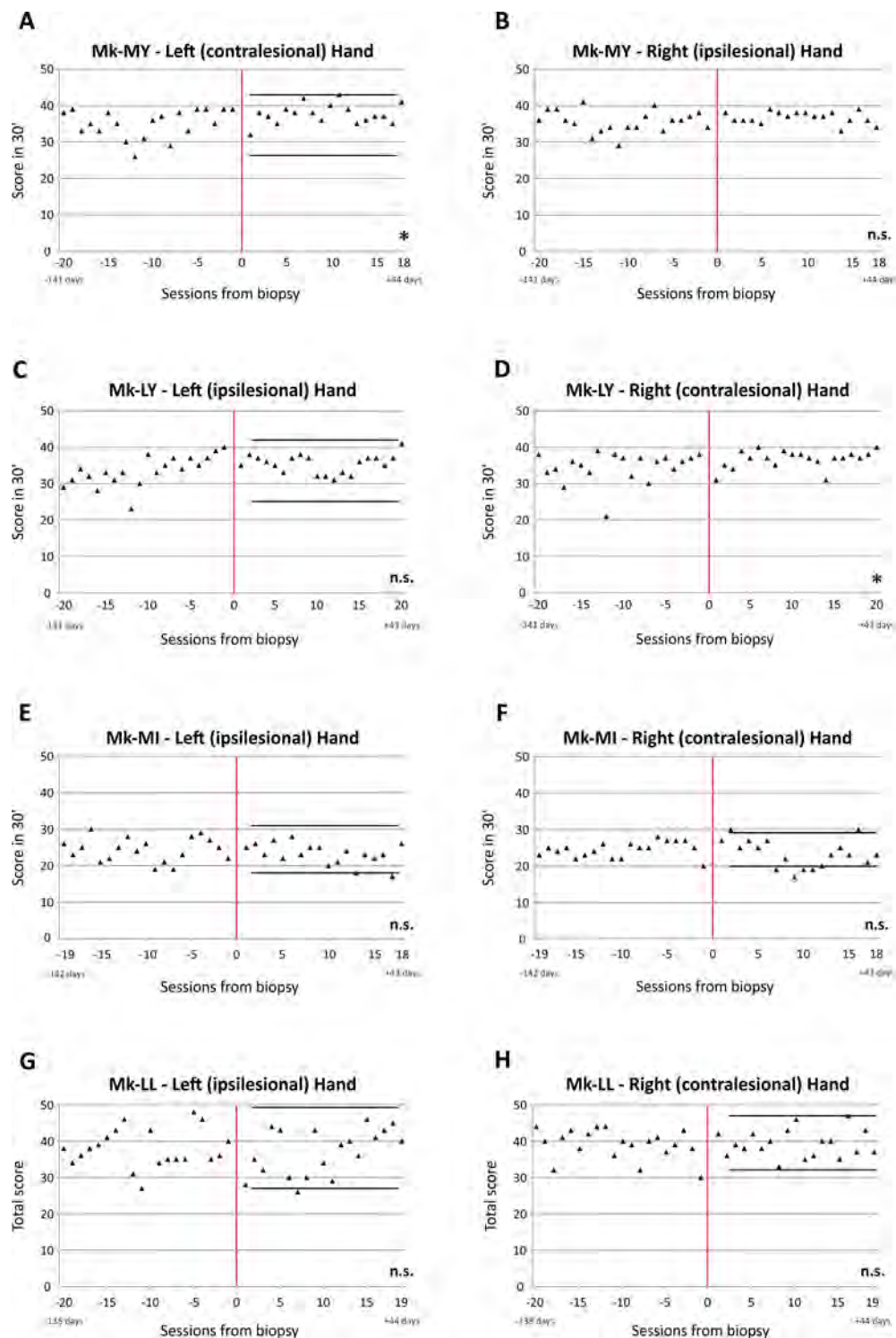
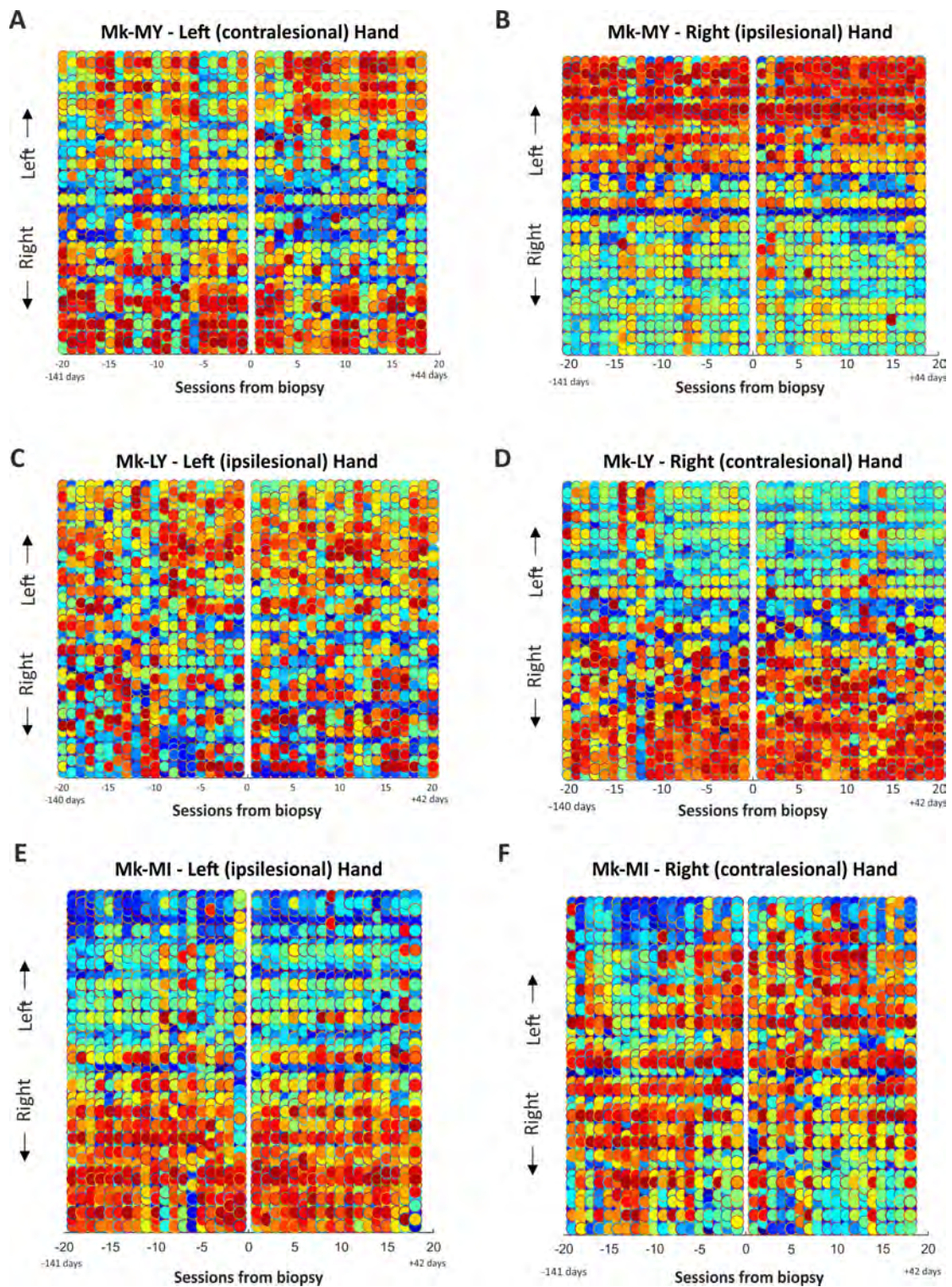


**Fig. 4.** Schematic representation of the rostro-caudal gradient of impact of unilateral lesions of the dIPFC (areas 10 and 9) or PMd-r on the control – prediction of grip and load forces and the lateralization of the effects on the load force, measured with the “reach and grasp drawer” task. The red to blue gradient represents the impact extent of the lesion according to the rostro-caudal position of the biopsy in dIPFC – PMd-r: in red, a strong impact and in blue a poor or absence of impact. In addition, the white to black gradient represents the lateralization of the effects on the load force according to the rostro-caudal position of the biopsy: in white, poor or no lateralized effect and in black stronger lateralized effect.



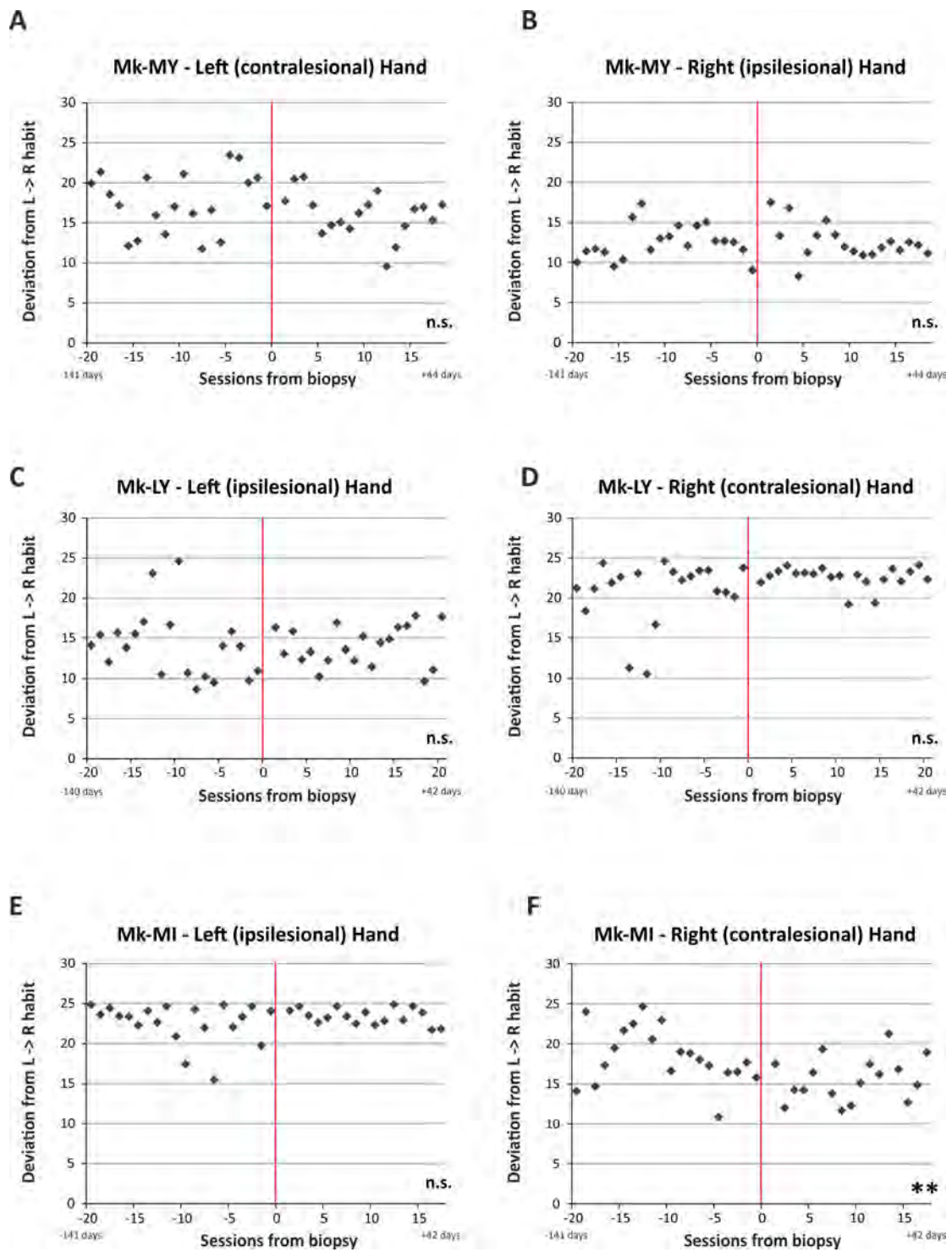
**Supplementary Figure 1.** Same conventions as in Fig. 2A. The scores were compared pre- versus post-biopsy, based on the parametric Student unpaired t-test, except for panel (D). The results for each statistical comparison is indicated on the bottom right of each graph: n.s. = non-significant difference ( $p > 0.05$ ); \* is for  $p \leq 0.05$ ; \*\* is for  $p \leq 0.01$ ; \*\*\* is for  $P \leq 0.001$ .





**Supplementary Figure 2.** Same conventions as in Fig. 2B Note that for Mk-LL the strategy analyses could not be performed due to its special task execution (see methods).





**Supplementary Figure 3.** Same conventions as in Fig. 2D. Note that for Mk-LL the strategy analyses could not be performed due to its special task execution. The indexes were compared pre- versus post-biopsy, based on the non-parametric Mann and Whitney test or the parametric Student unpaired t-test. The results for each statistical comparison is indicated on the bottom right of each graph: n.s. = non-significant difference ( $p > 0.05$ ); \* is for  $p \leq 0.05$ ; \*\* is for  $p \leq 0.01$ ; \*\*\* is for  $P \leq 0.001$ .



## **Chapter 3.2.2**

### ***Adult neural progenitor cells autotransplantation in a non-human primate model of Parkinson's disease: a pre-clinical study.***



## ***Introduction***

Over the last decades, dozens of pre-clinical studies have been conducted in the field of PD. Their aims? To investigate the therapeutic potential of cellular transplantations in animal models exhibiting PD-like symptoms and to assess their limitations in terms of both safety and efficacy. In this highly specialized domain, the MPTP non-human primate models are still, nowadays, considered as gold standards to tackle the points mentioned above (M. E. Emborg, 2007). As exposed in chapter 1.4, this model reproduces most of the motor disabilities that progressively appear in PD patients (Forno et al., 1993). The evolutionary proximity between the monkeys and the human beings, especially in regards with their motor system, allows to investigate, in a reliable manner, the potential corrective effect of a treatment and its possible side-effects, in a way that would not be possible in other species like rodents (J. P. Capitanio and M. E. Emborg, 2008; Courtine et al., 2007; Porras et al., 2012; Potts et al., 2013). However, as no model is perfect, the MPTP monkey models encompass several limitations that are mainly linked to the variability of the lesion's responses and to ethical controversies (J. Capitanio and M. Emborg, 2008; Potts et al., 2013).

Among the most common tools used by researchers to address the impact of the MPTP lesions and the potential effects of a treatment in non-human primate (NHP), the "clinical rating scales" have always occupied a special place (Imbert et al., 2000). Those scales that allow to rate different items (mainly motor aspects) in a semi-quantitative manner, have been used in almost all transplantation studies conducted in NHP (Bloch et al., 2014; M. E. Emborg et al., 2008; 2013; Hallett et al., 2015; Kordower et al., 2000; Kriks et al., 2011; Redmond et al., 2013). However, their important differences in terms of sensitivity, combined with the relatively subjective assessment of their different items make inter-studies comparisons difficult to achieve (Imbert et al., 2000).

Since the end of the 90's, Prof. E.M. Rouiller's lab acquired an extensive expertise in the assessment of manual dexterity in macaque monkeys. By training the animals to performed motor tasks including, among others, the modified Brinkman board and a reach and grasp drawer task, they were able to finely monitor the effects of spinal and cortical lesions on different motor parameters (Freund et al., 2009; Hoogewoud et al., 2013; Kaeser et al., 2011; Y. Liu and Rouiller, 1999; Rouiller et al., 1998; Schmidlin et al., 2011; Wyss et al., 2013). In those studies, a therapeutic agent was administered and a functional recovery measured.

The literature has extensively described the impact of the nigro-striatal denervation on motor functions, including rigidity, bradykinesia and akinesia, in both human pathology and NHP MPTP models (Blesa et al., 2010; Davie, 2008; Forno et al., 1993; Gerlach et al., 1991; Hoehn and Yahr, 1967; Olanow, 1999; Porras et al., 2012). Moreover, several investigations were conducted on the impact of PD on different arm movement's parameters including proximal and distal muscles control (Fellows and Noth, 2004; Fellows et al., 1998; Weiss et al., 2009). Fellows and colleagues described, among other things, an increase of the timing when lifting object using the precision grip (Fellows et al., 1998).

In humans, the pegboards are widely used by clinicians and therapists to assess manual dexterity deficits and/or to promote functional adaptations (Earhart et al., 2011; STERNE, 1969). This test consists in filling a board composed of small holes with cylindrical objects called pegs, as fast as possible. In the context of PD, it has been demonstrated that the degree of dopaminergic depletion correlates very well with the scores obtained in the pegboard task (Sage et al., 2012; Vingerhoets et al., 1996). According to Bohnen and colleagues, this manual dexterity test could even be considered as a good biomarker of nigro-striatal denervation's level (Bohnen et al., 2007). In NHP models of PD, several items of the existing rating scales are referring to manual dexterity impairments as for example the ability to manipulate food (Schneider et al., 1995). However, and as previously mentioned, the interpretation of those scales is not exhaustive, the data hardly reproducible.

In the present study, we decided to take advantage of the in-house expertise in matter of motor control to evaluate the influence on manual dexterity of ANCE transplantation in four MPTP intoxicated macaque monkeys (ANCE approach is introduced in chapter 1.3.5.3.3). In this sense, the modified brinkman board task and the reach and grasp drawer task would allow to obtain new quantitative data during the three main phases of the protocol.

As the gold standard regarding the behavioral assessment of NHP MPTP models remains the clinical scales, we assessed in parallel the animal's health state using the Schneider scale (Schneider et al., 1995). Additionally, the spontaneous activity of each monkey was also closely monitored using the VigiePrimate software developed by Viewpoint behavioral technology (Lyon, France).

To complete those behavioral tests, the state of the dopaminergic system was evaluated at each important step by  $^{18}\text{F}$ -DOPA PET that has been broadly used in PD related investigations (Blesa et al., 2010; Garnett et al., 1983; Kortekaas et al., 2013; Melega et al., 1996; Olanow et al., 2003b)

Finally, histological analysis would provide crucial information regarding the fate of the transplanted cells and, *in fine*, would allow to raise some hypotheses with respect to their mode of action.

## **Materials and methods**

### **PET scans**

#### **PET acquisitions**

The PET acquisitions were conducted at the service of nuclear medicine at

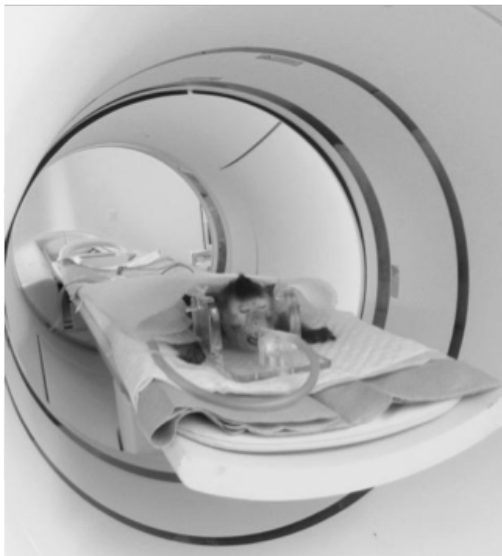


Figure 1. Monkey placed in the stereotaxic frame inside the scanner.

the HFr (Hôpital fribourgeois). The animals were positioned in the PET setup in pronation position with the head placed in a custom made Plexiglas® stereotaxic frame (figure 1). The PET acquisitions were performed on a Philips Ingenuity TF scanner according to the following protocol: dynamic, 4x30sec; 3x60sec; 2x120sec, 7x180sec; 12x300sec, 128 slices per frame. The  $^{18}\text{F}$ -DOPA was administered i.v. at the very start of the data collection (about

125MBq; Radiopharmazie, Klinik für nuklearmedizin, Zürich CH). In order to maximize the bioavailability of the  $^{18}\text{F}$ -DOPA and to augment its brain concentration, the animal received 50mg of carbidopa (a DDC inhibitor) *per os*, one hour before the scan. Prior to the functional acquisitions, anatomical references were obtained by computer tomography scanner (CT scan) subsequent analysis.

During the whole procedure, the monkeys were anesthetized according to the same protocol as for MRI procedures, as described in chapter 2.2.4.



## ***Data post-processing and analysis***

The different steps of the post processing and analysis protocols were conducted on Pmod software (v3.605). The first one consisted in converting and flipping the original images from DICOM to NIFI format. The CT images were then co-registered (rigid matching) on the previously acquired structural T1-weighted images and the transformation matrix saved. The next step consisted in applying each individual transformation matrix to the PET dynamic images. The aim of this procedure was to align the functional images on the anatomical data for each monkey. Regions of interest (ROIs) were then manually defined on the basis of individual anatomical images and adjusted on functional images in order to compensate small miss-registration errors. ROIs were placed on left/right striatum and left/right caudate nuclei. The occipital cortex, known for its poor dopaminergic innervation, was used as reference area. The average values of each ROI were then calculated by the software and the mean signal of each structure of interest calculated with excel software. The “kinetic” function of Pmod was then used to obtain the influx constant ( $K_i$ ) by applying the Patlak algorithm on our data using the occipital values as references (PATLAK et al., 1983). The different percentages were generated on excel (Microsoft office 2011) and the figure on GraphPad Prism 6.

PET images were finally generated by averaging the frames 10 to 28 and dividing the values by the mean signal of the occipital region for intensity normalization purposes. At the end, the scale was arbitrarily set between 0 and 1.7 for all images.

## ***Behavioral assessment***

### ***Schneider MPTP scale***

All four monkey's behaviors were closely monitored using the Schneider scale (Schneider et al., 1995). This scale encompasses eight items rated from 0 (absent) to 3 (severe) that allow to assess the evolution of the symptoms (upper limb movement, lower limb movement, ability to manipulate food, range of arm movement, bradykinesia / akinesia, hyperkinesia, tremor and dystonia). Each individual subject was followed by a single experimenter that was previously used to work with this particular animal. The behavioral evaluation was performed on a regular basis in the animal housing facility by periods of about 20 min. The scores were then reported in an excel file and the total scores obtained by summation of the different elements of the scale.

### ***Spontaneous movements' activity***

The spontaneous movements' activity was recorded on a daily basis for each monkey individually. Prior to each behavioral session, the monkeys were placed in a smaller cage (52.5 cm x 115 cm x 82 cm) located in a separated room for a period of 40 minutes. This period was composed of a first habituation phase of 10 minutes, followed by a 30minutesrecording session. The spontaneous movements' activity was filmed by a camera placed in front of the cage and the data processed in real time by the VigiePrimate software (ViewPoint® behavior technology, Lyon, France). This software allowed estimating the amount of movements generated by the animal trough the changes of gray levels (256 gray levels) for each pixel in a defined region of interest. The number of changes per second was then categorized into three classes of spontaneous activity according to different thresholds that were specifically set to meet our needs: freezing (< 500), middle (>500, < 2000) and burst (> 2000) activities. The data were finally exported in a excel file for each session.

For this thesis the time spent by the animals within each of the above mentioned categories during each experimental phases were statistically compared with GraphPad Prism (version 6.0)

## ***The modified Brinkman board task***

Modified by Rouiller and colleagues (1998) from the initial version of Brinkman and Kuypers (1973), the modified Brinkman board task is composed by 50 slots (15mm x 8mm x 6mm), 25 oriented vertically and 25 horizontally (figure 2) (Brinkman and Kuypers, 1973; Rouiller et al., 1998; Schmidlin et al., 2011). In this task, the monkey has to retrieve small banana pellets from the slots, firstly with both hands free and, in a second step unimanually, with the left or the right hand independently. By its conception, the modified Brinkman board task obliges the animal to use the precision grip (opposition of the thumb and index finger) to obtain the rewards (Schmidlin et al., 2011).

During each behavioral session, the motor performances of the monkeys were recorded with a video camera filming at 50 frames/sec. Those videos were then subsequently analyzed by an experimenter using the Dartfish software (v. 7.0) in order to quantify the motor performances for each experimental phase. In the present report, the following information was considered: the score in 30 seconds, the contact time and the strategy (temporal sequence to visit the 50 pellets).

- The score in 30 second correspond to the number of pellets correctly retrieved during half a minute (30 seconds). The scores were established separately for the vertical and the horizontal slots. A total score value was derived from the sum of the vertical score and the horizontal score. In Mk-LL, the score was not limited to the first 30 seconds, but representing the overall number of slots visited independently of the time.

- The contact time refers to the time difference between the time point when the animal entered its finger inside the slot and the time point when the fingers were completely out of the slot (with the pellet). They were calculated for the first five vertical and the first five horizontal slots visited.

- To obtain the strategies' information, each slot was numerated from 1 to 50. The temporal sequences of prehension were then associated to each slot for each session. Finally, the data were processed in Matlab to obtain a graphical representation of the strategies' evolution over the different experimental phases. The quantitative comparisons between the different experimental phases were conducted as described in chapter 3.2.1

N.B. Due to a particular behavior, the total score was used to assess the performances of Mk-LL. Moreover, because of an injury to its left hand, the data of Mk-MI were obtained for its right hand only.

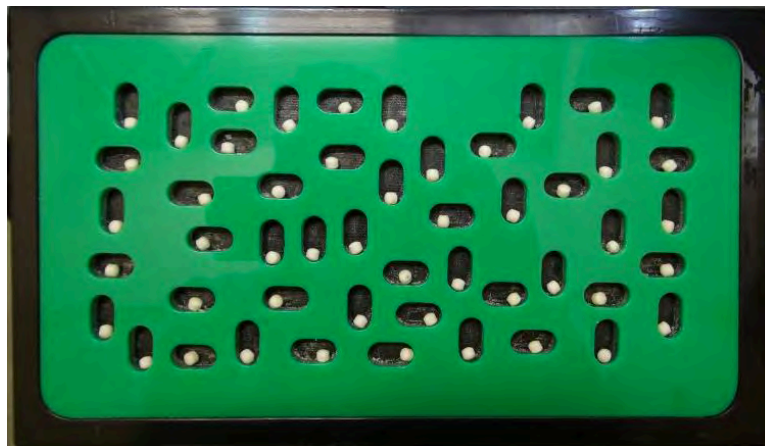


Figure 2. Modified Brinkman board filled with the pellets (rewards).

### ***The reach and grasp drawer task***

The reach and grasp drawer task used in this study was adapted from the bimanual setups originally designed by Kazennikov and colleagues and Kermadi and colleagues (Kazennikov et al., 1999; 1994; Kermadi et al., 1998; 1997). In the present version of the task, the monkeys work one hand at a time. Multiple sensors allowed to record, in real time, different information related to the timing of the different trial phases, to the force applied by the animal to grasp the knob and to pull the drawer (figure 3) (Schmidlin et al., 2011).

When performing the task, the animal has to open the drawer against three different resistances ( $R_0=0N$ ,  $R_3=1.25N$ ,  $R_5=2.75N$ ) to get a reward (banana pellet), placed inside the drawer. For each resistance the monkey had to execute ten correct trials before moving to the next one. Bad (erroneous) trials' marker was manually added to the raw data file by the experimenter by pressing a button. The raw data were then processed following the protocol presented in annex 1.

For this thesis, the trial duration parameter, which corresponds to the time interval between the start-open event and the pick-out event, was considered as the most relevant and the most informative in regards to MPTP effects on the motor system. The analyses were conducted separately for both hands except in Mk-MI for the previously mentioned reason (injury to the left hand). Statistical analyses were conducted using GraphPad Prism to assess intra-individual variation during the three experimental phases.

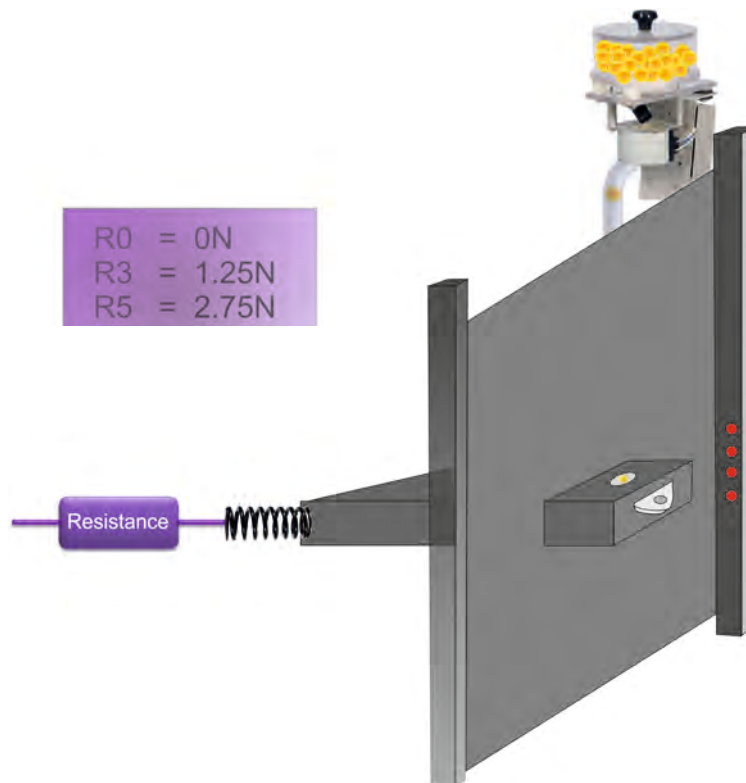


Figure 3. Schematic representation of the drawer setup with the three resistances indicated in the purple square.

## ***Histology***

In the present thesis, three series out of the ten series of histological sections were used for histological analyses.

The first series of each animal was used for anatomical observation and stained according to a Nissl protocol that is detailed in annex 2.

A second series for the observation of PKH67 positive cell was direct set on microscope slides. Yet, due to important autofluorescence, the slides were treated in a second step with Sudan black (Sudan Black B, Fluka 86015). The protocol can be found in annex 2.

Finally, immunohistological analyses were performed in order to assess the state of the nigrostriatal system using anti-Tyrosine Hydroxylase (TH) antibodies as primary antibody (AB152, anti-TH polyclonal antibody, Millipore, LOT 2552365) and Alexa Fluor 488 as secondary antibody (Alexa Fluor 488, goat anti-rabbit IgG, Molecular prob; LOT 1670152). Full protocol can be found in annex 2.

Observations and photographic acquisitions were performed using a conventional light and fluorescence microscope Olympus BX40 (camera, mbf bioscienc, Q imaging, colour 12 bit) and Neurolucida software (version 11.0).

## ***Statistics***

All statistical analyses were performed on GraphPad Prims (version 6.0). The normality of the data distributions was firstly checked with the D'Agostino-Pearson omnibus test. A p-value superior or equal to 0.05 was required to consider the distribution as normal. Then the Student's t or the Mann-Whitney *U* tests were used to compare the different groups (intra-individual: pre-lesion, post-lesion, post-implantation). P-value <0.05 were considered as statistically significant. The "levels of significance" were indicated on the box plots by stars "\*". One star "\*" p-value = 0.01 to 0.05, two stars "\*\*" p-value = 0.001 to 0.01, three stars "\*\*\*" p-value = 0.0001 to 0.001 and four stars "\*\*\*\*" p-value = <0.0001. "n.s." refers to non-statistically significant results ( $p \geq 0.05$ ).

The PET striatal  $K_i$  values along the three experimental phases (i.e. Pre-lesion, post-lesion and post-implantation) were compared with a linear random slope and intercept model (lme, package nlme in "R", version 3.2.1). The experimental phases were considered as the fixed effects and the x identities (monkeys) as the random effects. Significant threshold was set at  $p=0.05$ .



## **Results**

### ***Positron Emission Tomography (PET)***

During the pre-lesion phase, all four monkeys exhibited similar Ki values, ranging from 0.00736 to 0.00858 respectively for Mk-LY and Mk-MI (table 1). About seven weeks after the last toxin injection (MPTP), the second PET acquisitions were performed. The data showed that three out of four monkeys experienced dramatic dopaminergic depletion reflected by a very important decrease of the PET values of about 80% compared to normal values (figure 5). Surprisingly, the Ki values of Mk-LY were much less affected with a fall of only 17% with respect to the pre-lesion phase (figure 4 and 5, table 1). As it can be seen in figure 4, the lesion impacted the striatum in a relatively global manner with minimal left/right asymmetry. Additionally, the figure 4 reveals that the head of the caudate nuclei and the most anterior part of the putamen seems to be slightly less affected by the dopaminergic depletion than the posterior part of the putamen.

About six months after ANCE implantations, a new batch of <sup>18</sup>F-DOPA PET scans was performed in all monkeys. The analysis of the data revealed a clear augmentation of the PET signal in all four animals (figure 5, table 1). Nevertheless, even if those augmentations in terms of Ki were relatively modest, they varied by a factor of two from one animal to another. For instance, Mk-MI showed a recovery of the striatal uptake of only 10.82% whereas Mk-MY exhibited an augmentation of Ki values of 21.37%, following ANCE transplantation (figure 5).

Globally, statistical analyses revealed significant differences between the three experimental phases regarding the striatal Ki values ( $p < 0.05$ ; linear random slope and intercept model) (figure 6).

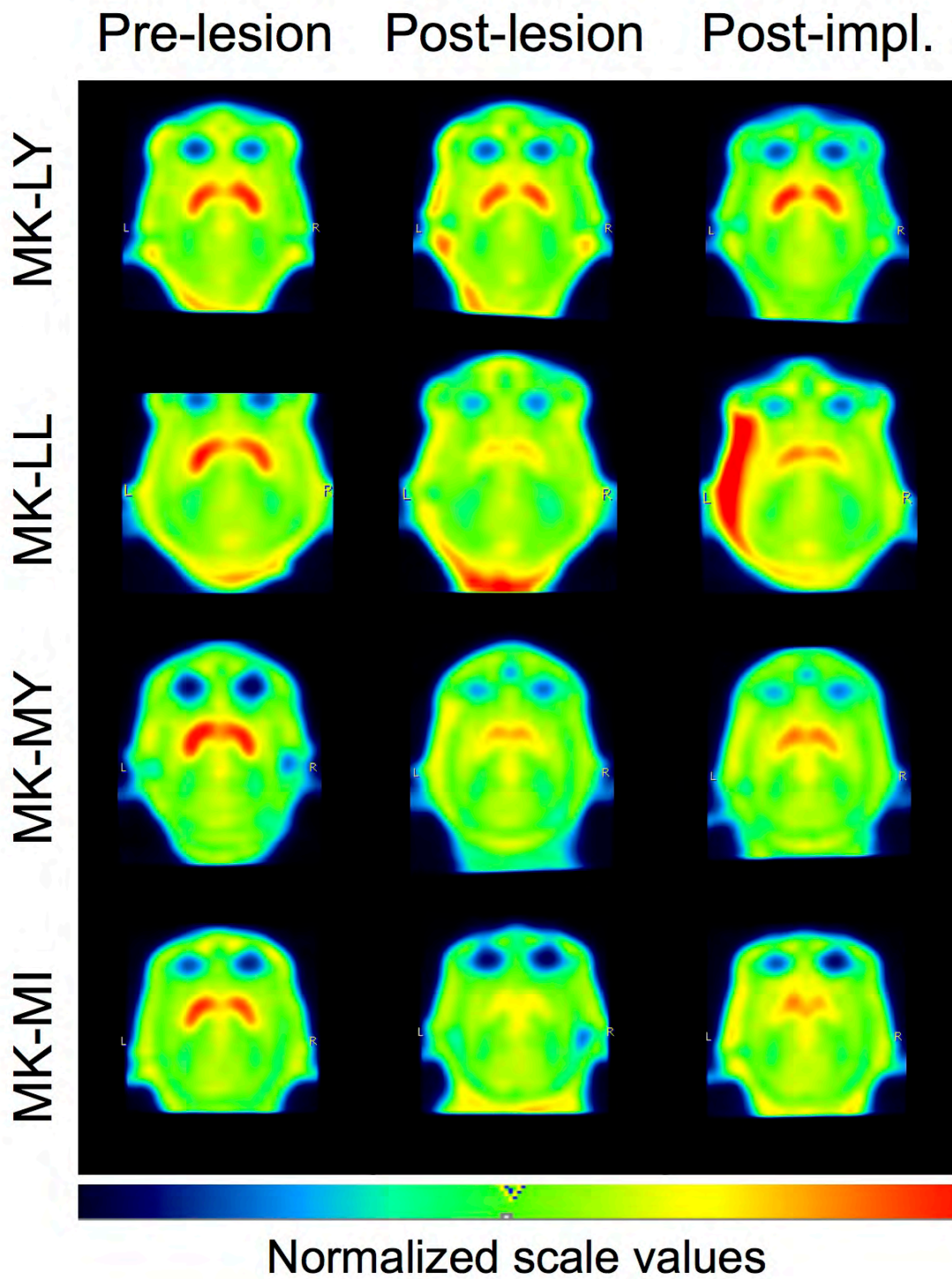


Figure 4. Transverse slice of the four monkeys' head cut at striatal level at the three main experimental phases (pre-lesion, post-lesion, post-treatment). The values were normalized by dividing each individual scan by their mean occipital signal. Black color corresponds to an absence of signal and red to the strongest signal. L=left, R=right. N.B.: The figure representing the results of MK-LL post-implantation exhibits an important artifact of its left side due to postoperative inflammatory process.

<b>Influx constant (Ki) - Mk-LL</b>						
	<b>Pre-lesion</b>		<b>Post-lesion</b>		<b>Post-implantation</b>	
	L	R	L	R	L	R
<b>Caudate</b>	0.00735	0.00805	0.00093	0.00138	0.00106	0.00194
<b>Putamen</b>	0.00840	0.00769	0.00120	0.00147	0.00236	0.00347
<b>Striatum</b>	0.00787		0.00125		0.00221	
<b>% of pre-lesion</b>			<b>15.82</b>		<b>28.03</b>	

<b>Influx constant (Ki) - Mk-LY</b>						
	<b>Pre-lesion</b>		<b>Post-lesion</b>		<b>Post-implantation</b>	
	L	R	L	R	L	R
<b>Caudate</b>	0.00600	0.00646	0.00550	0.00442	0.00712	0.00675
<b>Putamen</b>	0.00856	0.00840	0.00710	0.00740	0.00785	0.00786
<b>Striatum</b>	0.00736		0.00611		0.00739	
<b>% of pre-lesion</b>			<b>83.00</b>		<b>100.53</b>	

<b>Influx constant (Ki) - Mk-MI</b>						
	<b>Pre-lesion</b>		<b>Post-lesion</b>		<b>Post-implantation</b>	
	L	R	L	R	L	R
<b>Caudate</b>	0.00831	0.00836	0.00160	0.00179	0.00274	0.00196
<b>Putamen</b>	0.00949	0.00815	0.00163	0.00210	0.00278	0.00336
<b>Striatum</b>	0.00858		0.00178		0.00271	
<b>% of pre-lesion</b>			<b>20.75</b>		<b>31.57</b>	

<b>Influx constant (Ki) - Mk-MY</b>						
	<b>Pre-lesion</b>		<b>Post-lesion</b>		<b>Post-implantation</b>	
	L	R	L	R	L	R
<b>Caudate</b>	0.00718	0.00836	0.00156	0.00142	0.00275	0.00343
<b>Putamen</b>	0.00861	0.00862	0.00198	0.00111	0.00346	0.00343
<b>Striatum</b>	0.00819		0.00152		0.00327	
<b>% of pre-lesion</b>			<b>18.52</b>		<b>39.89</b>	

Table 1. Table summarizing the Ki values obtained from the analysis of the 18F-DOPA PET data with Patlak algorithm in Pmod software. The values presented in red are corresponding to the percentage of pre-lesion Ki values for the striatum. L=left, R=right, Caudate= caudate nucleus.

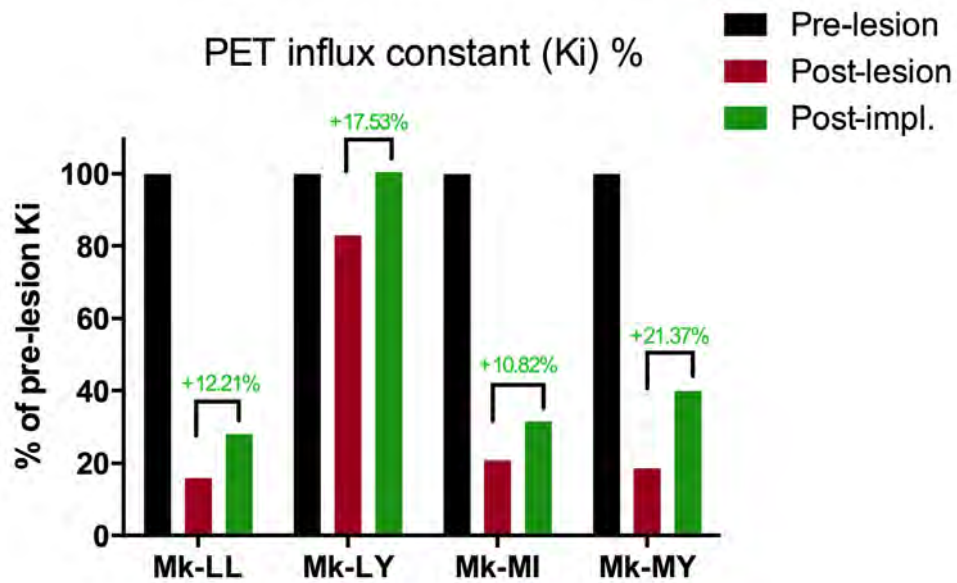


Figure 5. Graphic representing the evolution of the Ki values across the consecutive experimental phases in percentage of the pre-lesion values. The numbers in green correspond to the differences between the post-lesion and the post-implantation phases.

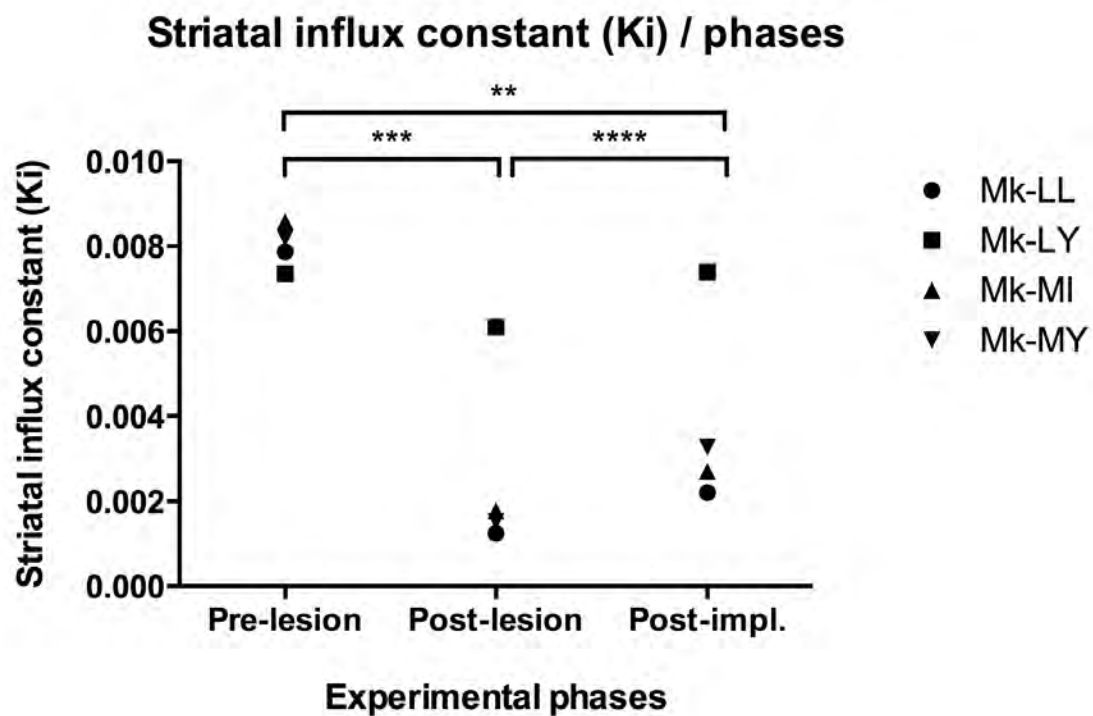


Figure 6. Graphic representing the individual striatal Ki values at each experimental phase. Statistical results are displayed by stars <sup>\*\*\*</sup> (linear random slope and intercept model).

## ***Schneider MPTP scale***

Globally, all animals were affected differently by the MPTP lesions. Two out of the four monkeys spontaneously recovered almost completely few days after the end on the injection's protocol (Mk-LL, Mk-LY) (figure 7). The two other animals were more severely affected with symptoms that remained relatively high until the implantation to the cells (Mk-MI, Mk-MY). Those monkeys progressively recovered their motor functions after ANCE implantations. Nevertheless, Mk-MI, which was the most affected, recovered only partially with a total score of two that remained stable until sacrifice.

In a general manner, there was very important day-to-day variability in terms of symptom's severity.

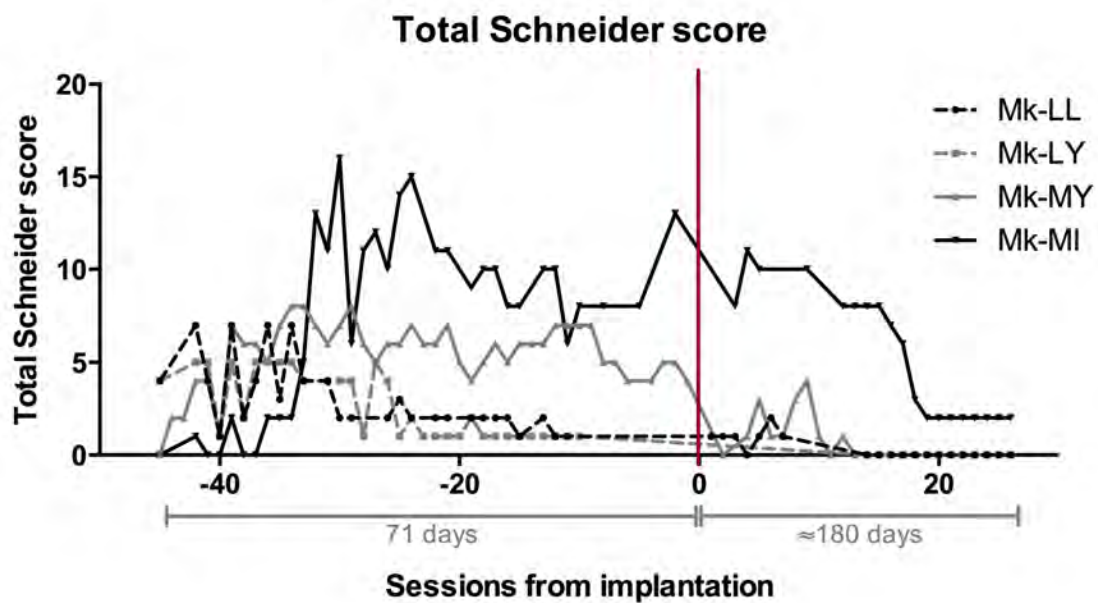


Figure 7. Figure representing the evolution of the total Schneider score per session. The 0 (X axis) corresponds to the time of the cells implantation (red vertical bar). The time periods are indicated below the X axis (in gray).

## ***Spontaneous movement activity***

In a general manner, all four monkeys exhibited significant modifications of their spontaneous movement activity patterns following the MPTP lesions with p-values ranging from 0.001 to  $<0.0001$ . In more details, there was a significant augmentation of the freezing activity in all four animals post-lesion ( $p < 0.001$ ) (figure 8). However, if those modifications were extreme for Mk-MI and Mk-MY (figure 8, C and D), the increases of the freezing activity were more moderate for Mk-LL and even more for Mk-LY (figure 8, A and B). The behavioral modifications induced by the MPTP injections were opposite regarding the middle and burst activity ranges, with significant decreases of the time spent into those two categories ( $p$ -values = 0.001 to  $<0.0001$ ) (figure 8). As for the freezing activity, Mk-LL and Mk-LY were affected less than Mk-MI and Mk-MY (figure 8, A and B).

The comparisons between the post-lesional states and the post-implantation periods (April until sacrifice) exhibited a normalization of all three activity's categories, with a statistically significant decrease of the freezing duration and a statistically significant increase of the middle and burst activity durations ( $p < 0.05$ ). However, the analyses comparing the pre-lesion and the post-implantation phases were statistically significant for all monkeys as well, indicating that the recovery post-implantation was incomplete ( $p < 0.05$ ), except for the middle activity time in Mk-LY ( $p = 0.404$ ) (figure 8).

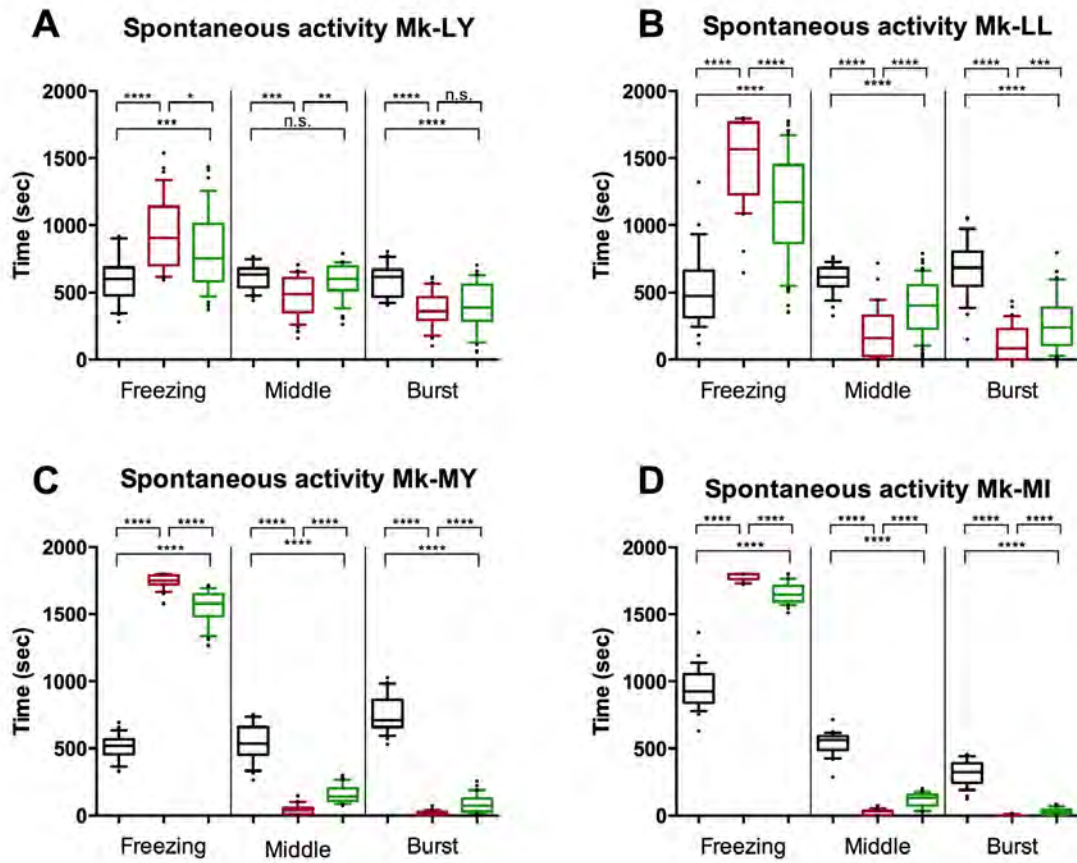


Figure 8. Box and whiskers representation of the spontaneous movement activity durations (in seconds). The lower and upper limits of the boxes correspond respectively to the 25th percentile and 75th percentile while the lower and upper limits of the whiskers are showing the 10th and 90th percentiles. The median value (50th percentile) is represented by a bar in the middle of the box. The points outside of the whiskers are showing the “extreme values”. The black boxes correspond to the pre-lesion phase (June 2014 to September 2014), the red boxes correspond to the post-lesion phase (October 2014 to December 2014) and the green boxes to the post-implantation phase (April 2015 to sacrifice). The statistical values are indicated by “stars” and “n.s.”. One star “\*” p-value = 0.01 to 0.05, two stars “\*\*” p-value = 0.001 to 0.01, three stars “\*\*\*” p-value = 0.0001 to 0.001 and four stars “\*\*\*\*” p-value = <0.0001. “n.s.” refers to non-statistically significant results ( $p \geq 0.05$ ).

## ***Modified Brinkman board task***

### ***Scores in 30 seconds***

In a general manner, the performance of the animals at the modified Brinkman board task was significantly affected by the MPTP lesions with a decrease of the score in 30 seconds (total score for Mk-LL) in three out of the four monkeys for both hands (figure 10). Among these 3 monkeys affected by the MPTP lesion both Mk-MI and Mk-MY exhibited a statistically significant improvement of performance from the post-lesion phase to the post-implantation phase (figure 10, C and D).

Globally, Mk-LY was not significantly affected regarding the scores in 30 seconds ( $p \geq 0.05$ ) (figure 10, A). Moreover, the cells' transplantation did not trigger any significant modification of motor performances as reflected by score ( $p \geq 0.05$ ) (figure 10, A). On a qualitative point of view, during the pre-lesion phase, Mk-LY exhibited a relatively large variability of its motor performance for its left and right hands. Surprisingly, this variability was slightly reduced during the post-implantation phase (figure 9, A and B).

Due to a particular behavior, the total scores of Mk-LL for its right and left hands were considered as the most relevant. Over the whole experiment, Mk-LL was extremely variable at performing the modified Brinkman board task. This variability can be qualitatively assessed for both hands on figure 9 F. The scores obtained with the right and left hands were significantly affected by the MPTP lesion with an average reduction of respectively 14.6% and 11.3% with respect to the pre-lesion values ( $p < 0.05$ ) (figure 10, B). Yet, when comparing the post-lesion and post-implantation phases, the statistical analyses did not show any significant modification of the total scores (left and right hands), ( $p \geq 0.05$ ) (figure 10, B).

Globally, during the pre-lesion phase, Mk-MY exhibited very stable performances regarding its scores in 30 seconds with relatively little variability



(figure 9, C and D). The qualitative assessment of the post-lesion phase revealed a progressive, but limited, normalization of the motor performances (figure 9,C and D). Following ANCE implantation, a progressive augmentation of the scores can be seen until reaching a plateau. Quantitative analyses revealed a statistically significant reduction of the scores in 30 seconds for both hands during the post-lesion phase, with respectively 62.3% (right hand) and 70.7% (left hand) of the average pre-lesion values ( $p < 0.0001$ ) (figure 10, C). The post-implantation data (April to sacrifice) were statistically significantly higher than the post-lesion data ( $p < 0.0001$ ), reaching 95% of the reference values (pre-lesion) for the left hand and 94.5% for the right hand (figure 10, C). Nevertheless, the post-implantation scores were still significantly lower than the pre-lesion values ( $p < 0.05$ ) (figure 10, C).

Mk-MI was the most affected animal in terms of motor performances. During the pre-lesion phase, it showed a very large variability in terms of score. Following the MPTP injections, Mk-MI almost completely lost its ability to perform the modified Brinkman board task. About six weeks post-implantation, Mk-MI recovered the ability to execute the task and exhibited a progressive improvement of its fine manual dexterity score (figure 9, E). However, this recovery remained incomplete until the end of the experiment. The statistical comparison between the three experimental phases confirmed the qualitative observations with a dramatic decrease of the score following the lesion ( $p < 0.0001$ , 13.8% of the pre-lesional data), followed by a significant improvement of the motor performance ( $p = 0.003$ ) with an average score at 46.6% of the reference values (figure 10, D).

The qualitative assessment of the vertical and horizontal scores taken separately did not reveal obvious modifications regarding the slot's orientations' preferences (figure 9).

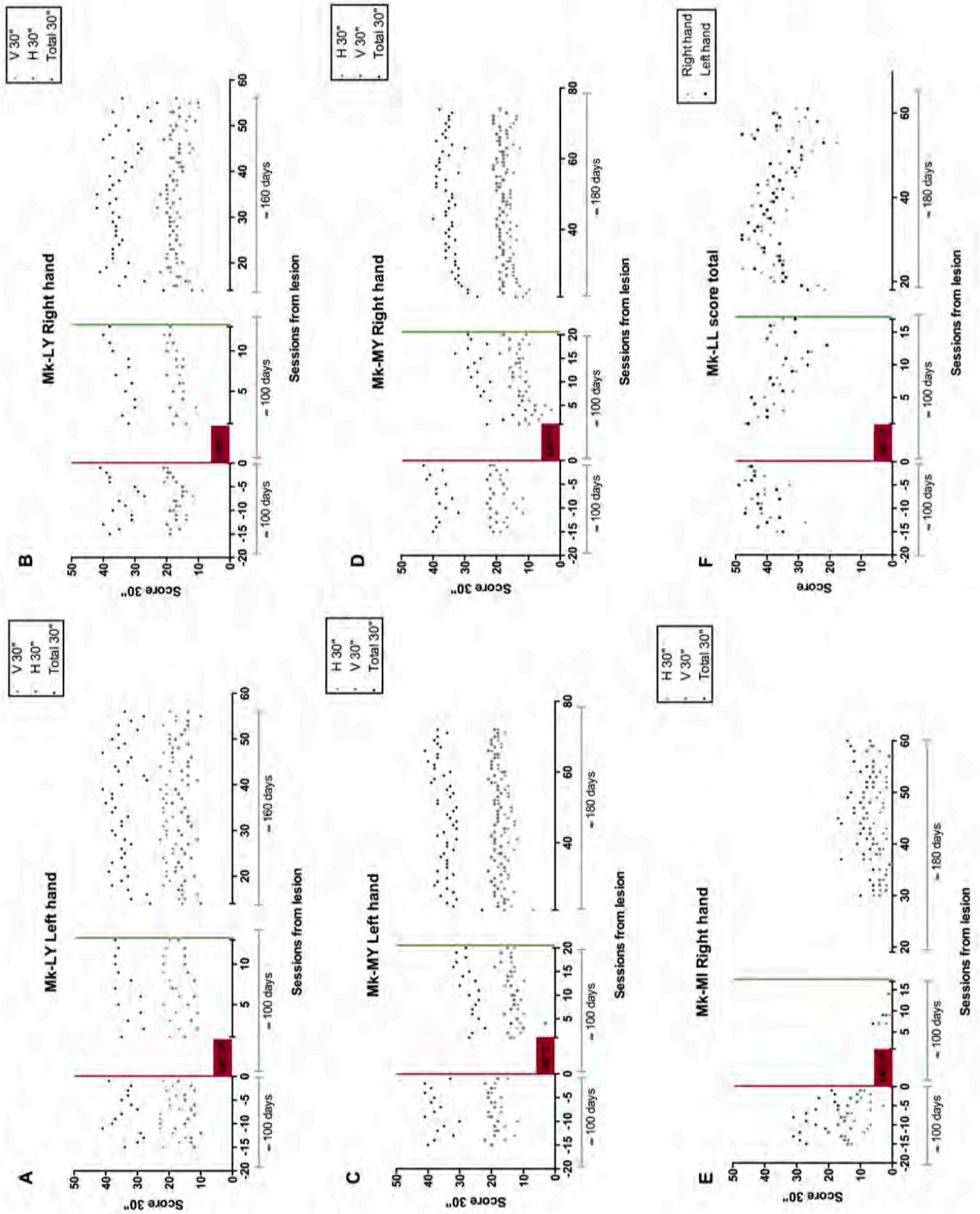


Figure 9. Representation of the scores obtained along modified Brinkman board task daily sessions. The X axis is split into three sectors representing the sessions in the three experimental phases (pre-lesion, post-lesion, post-implantation). Spaces between the three axes correspond to period of inactivity. Below the session's axis (in black), the approximate time course of each period is indicated in days (gray bars). The red bars represent the beginning of the MPTP treatments and the green bars correspond to the time point of the cellular (ANCE) implantations.

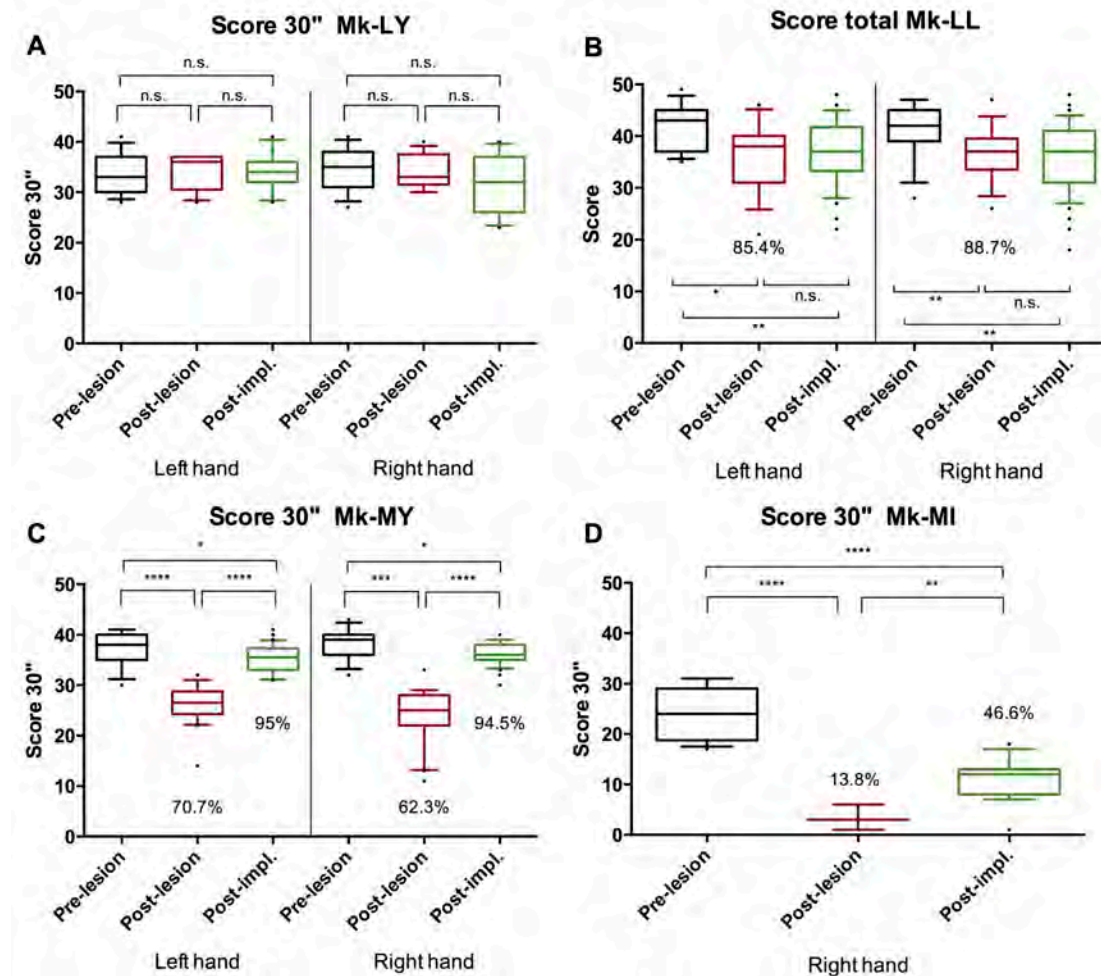


Figure 10. Box and whiskers representation of the scores in 30 seconds, cumulating the vertical and horizontal slots. In Mk-LL, the score was not limited to the first 30 seconds, but representing the overall number of slots visited independently of the time. The lower and upper limits of the boxes correspond respectively to the 25th percentile and 75th percentile while the lower and upper limits of the whiskers show the 10th and 90th percentiles. The median value (50th percentile) is represented by a bar in the middle of the box. The points outside of the whiskers are showing the "extreme values". The black boxes correspond to the pre-lesion phases (June 2014 to September 2014), the red boxes correspond to the post-lesion phase (October 2014 to December 2014) and the green boxes to the post-implantation phase (April 2015 to sacrifices). The statistical values are indicated by "stars" and "n.s.". One star "\*" p-value = 0.01 to 0.05, two stars "\*\*" p-value = 0.001 to 0.01, three stars "\*\*\*" p-value = 0.0001 to 0.001 and four stars "\*\*\*\*" p-value = <0.0001. "n.s." refers to non-significant results ( $p \geq 0.05$ ). The percentages are representing the evolution of the average scores compared to the pre-lesional state.

## **Contact times**

In a general way, the contact time (CT), referring to the time spent by the monkeys' hand inside the slots using the precision grip, was significantly affected by the MPTP lesion. Two out of the four animals were affected bilaterally while in the two other monkeys the lesion impacted only some parameters.

The CT in Mk-LY and Mk-LL remained globally unaffected by the MPTP lesion with non-significant differences between the pre-lesion and post-lesion phases (figure 11, A, B, C and D). However, two exceptions can be seen in figure 11 A and D. Actually, Mk-LY showed a significant increase of its CT for its left hand, though restricted to the vertical slots ( $p < 0.0001$ ), whereas Mk-LL exhibited a significant increase of CT following the MPTP lesion for its right hand (horizontal slots only).

Mk-MY showed significant increases of its CT in the post-lesion phase for both hands, regardless of the slots' orientation ( $p < 0.0001$ ) (figure 11, E and F). Following the implantation of the cells, all parameters came back to the pre-lesion state with statistically non-significant differences between pre-lesion scores and post-implantation scores ( $p > 0.05$ ) (figure 11, E and F).

Concerning Mk-MI, there were not enough trials performed correctly to measure the contact times during the post-lesion phase as the monkey was almost not able to perform the task anymore (figure 11, G). Despite of that, it regained this capacity few weeks after ANCE implantation. This recovery was only limited, with CT significantly higher in the post-implantation phase than in the pre-lesion phase ( $p < 0.0001$ ).

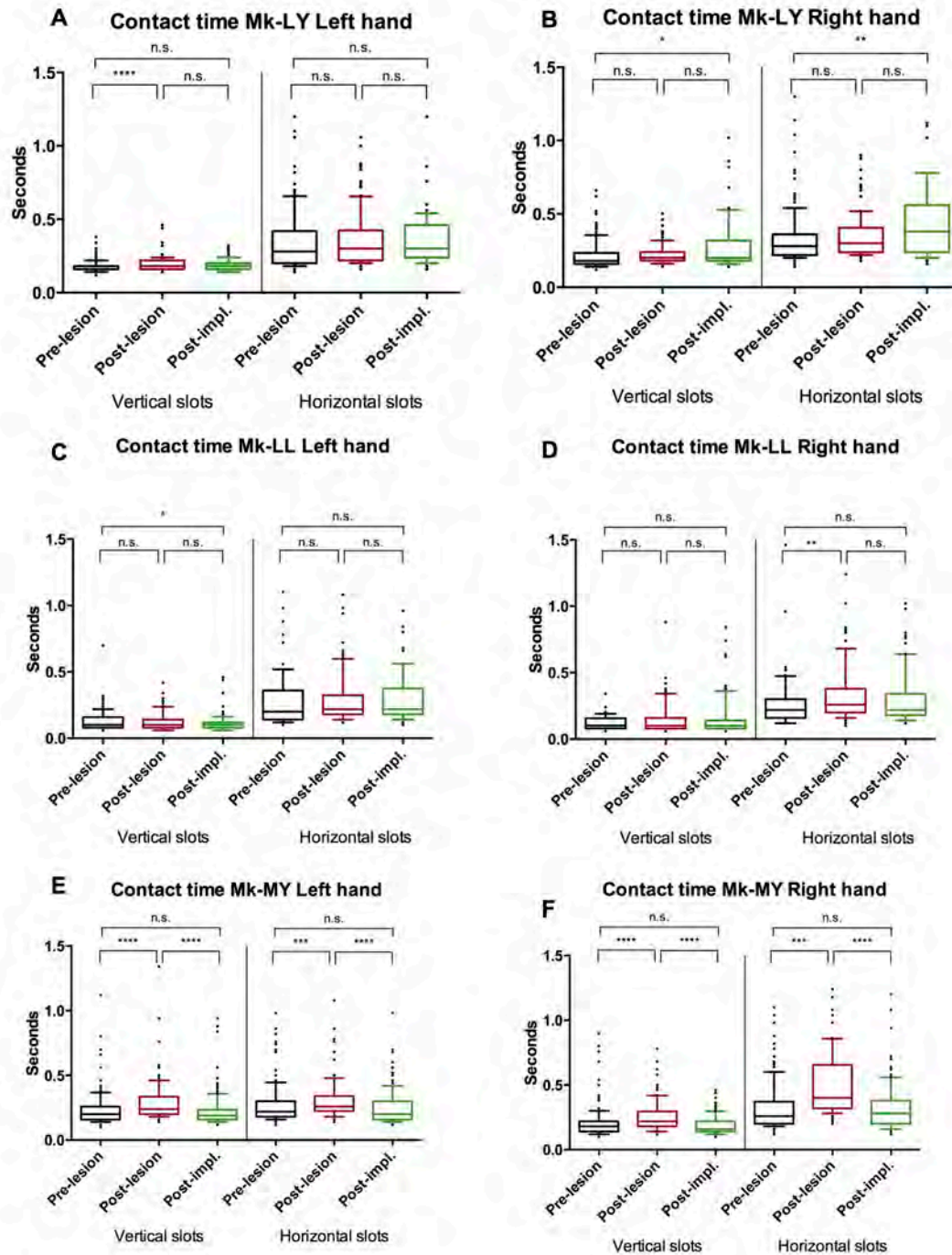
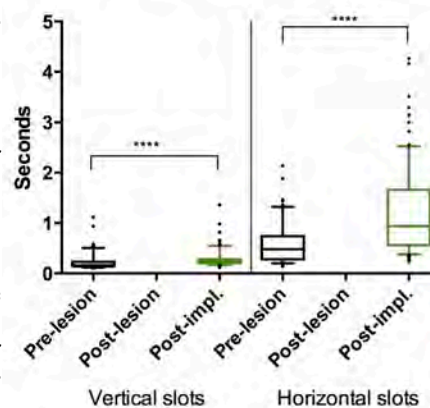


Figure 11. Box and whiskers representation of the contact times (CT) in seconds. The lower and upper limits of the boxes correspond respectively to the 25th percentile and 75th percentile while the lower and upper limits of the whiskers show the 10th and 90th percentiles. The median value (50th percentile) is represented by a bar in the middle of the box. The points outside of the whiskers show the “extreme values”. The black boxes correspond to the pre-lesion phases (June 2014 to September 2014), the red boxes correspond to the post-lesion phase (October 2014 to December 2014) and the green boxes to the post-implantation phase (April 2015 to sacrifices). Each graph presents separately the values for the horizontal and vertical slots. The statistical values are indicated by “stars” and “n.s.”. One star “\*” p-value = 0.01 to 0.05, tow stars “\*\*” p-value = 0.001 to 0.01, three stars “\*\*\*” p-value = 0.0001 to 0.001 and four stars “\*\*\*\*” p-value = <0.0001. “n.s.” refers to non-significant results (p≥0.05).

**G Contact time Mk-MI Right hand**



## ***Strategies***

All three monkeys analyzed for the picking temporal sequences exhibited a relatively good regularity regarding their motor strategies during the pre-lesion phase. Qualitative assessment revealed some subtle modifications following the lesion protocol and a normalization of the picking sequences during the post-implantation phase (figure 12).

The picking sequences used by Mk-LY remained very stable over the whole experiment for its right hand, starting on the right of the board and progressively moving to the left side without evident perturbation, neither after the lesion nor after cells' implantation (figure 12, B). The invert strategy was used when performing the task with its left hand, with a transient modification of the picking sequence following the MPTP injections (figure 12, A). Nevertheless, the quantitative analyses revealed that, although subtle, those modifications of the left/right strategies are significant (figure 13, A and B).

Concerning Mk-MY, similar strategies were used regardless of the hand. The animal started generally the task by grasping pellets located in the middle of the modified Brinkman board with a tendency to continue on the left side to finally end on the right side of the board (figure 12, C and D). During the first sessions of the post-lesion phase, the spatio-temporal sequences were slightly disturbed but came back to the normal state during the post-implantation phase (figure 12, C and D). Those observations were confirmed for the left hand by the quantitative analysis but the strategy for the right hand between pre-lesion phase and post-implantation phase remained significantly different (figure 13, C and D).

As previously mentioned Mk-MI was only able to perform the task with its right hand due to an injury to its left hand. This monkey exhibited a relatively different strategy than the two others by starting at different locations of the board before completing the "gaps" in-between. Nevertheless, it seems that, even if the first slots visited were spread on the board, the animal started

always with the same group of slots as indicated by the blue pearl lines that are very regular (figure 12, E). As Mk-MI almost completely lost its capacity to execute the task after the MPTP lesions, very few data are available during the post-lesion phase. The gaps in the “pearl necklace” are indicating slots that were not visited by the monkey. During the post-lesion phase, Mk-MI progressively regained its motor capacities and, during the last sessions before sacrifice, the pearl necklaces were again complete (figure 12, E).

Due to the very few data available during the post-lesion phase, it was not possible to statistical quantify the impact of the MPTP lesion of the motor sequence for this animal. However, pre-lesion and post-implantation data were significantly different (figure 13, E).



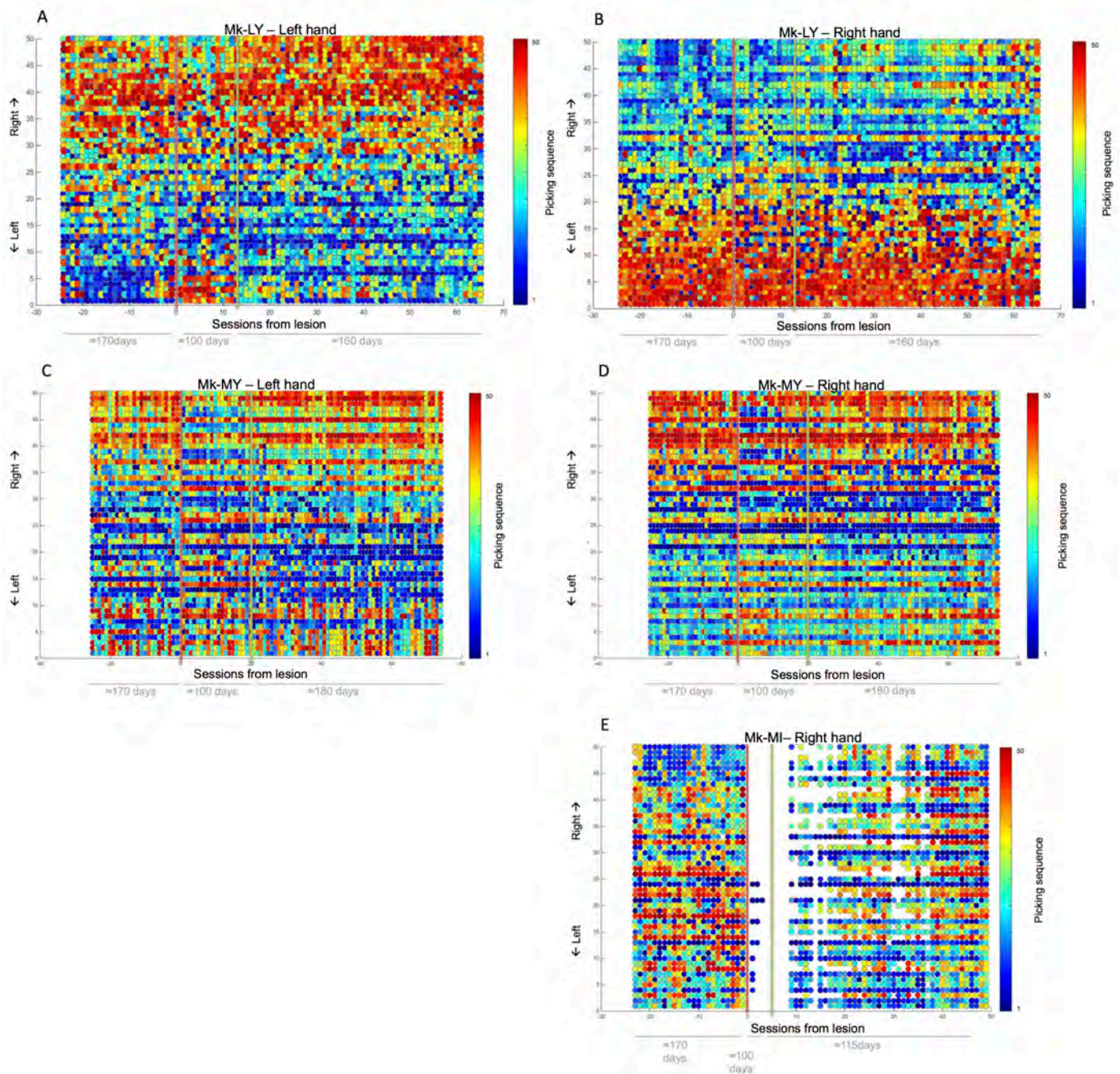


Figure 12. Representation of the spatio-temporal picking sequences by daily sessions. The Y axis represents the positions of the slots on the board (0= extreme left, 50= extreme right). The X axis represents the analyzed daily sessions from the MPTP lesion (0= lesion). Below the X axis, the approximate time course is indicated in days (gray). The vertical red bars indicate the MPTP lesions and the green lines indicate the time point of the ANCE implantations. The color scales indicate the temporal picking sequence (deep blue = first pellet picked out, dark red = last pellet picked out).



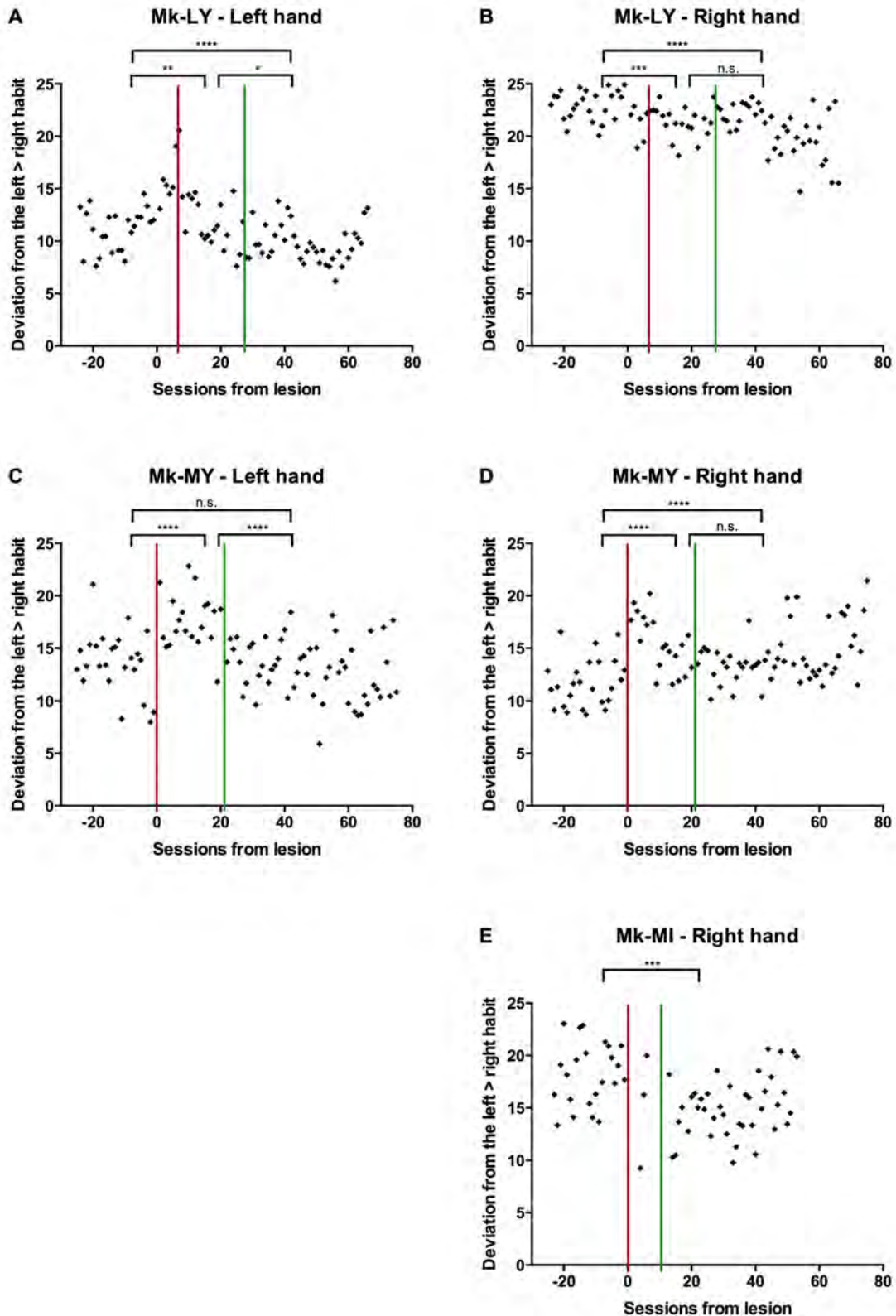


Figure 13. Figure representing the quantitative data of the left/right motor sequences. The Y axis represent the deviation from the left to right habit. The X axis represents the analyzed daily sessions from the MPTP lesion (0= lesion). The vertical red bars indicate the MPTP lesions and the green lines indicate the time point of the ANCE implantations. The statistical values are indicated by "stars" and "n.s.". One star "\*" p-value = 0.01 to 0.05, tow stars "\*\*" p-value = 0.001 to 0.01, three stars "\*\*\*" p-value = 0.0001 to 0.001 and four stars "\*\*\*\*" p-value = <0.0001. "n.s." refers to non-significant results (p≥0.05).

## ***Reach and grasp drawer task***

### ***Trial durations***

The trial durations, which correspond to the time differences between the time point when the monkey start to open the drawer and the time point when the pellet was correctly picked-out of the drawer's slot, were relatively similar for all monkeys during the pre-lesion phase. Following the MPTP injections, the modifications of the trial durations values were relatively different from one animal to the next (figure 14). In the same way, post-implantation data were quite variable.

In a general manner, Mk-LY exhibited a statistically significant modification of its trial durations values for both hands with an augmentation of the values during post-lesion phases at resistance R3, right hand ( $p < 0.0001$ ) and at R5 both hands ( $p < 0.001$ ) (figure 14, A and B). R0 values were significantly decreased for the left hand and remained unaffected for the right hand (figure 14, A and B). The post-lesion / post-implantation comparisons showed a significant decrease for the trial durations at all three resistances for the left hand ( $p < 0.0001$ ) but was limited to R5 for the right hand ( $p < 0.05$ ) (figure 14, A and B).

At one exception, Mk-LL did not exhibit any significant changes of its trial durations consecutive to the MPTP injections (figure 14, C and D). Nevertheless, the implantation of the cells was followed by a significant decrease of the trial duration's values for the left hand (at all resistances) while the right hand did not exhibit any significant modifications in terms of durations (figure 14, C and D).

The post-lesion values of Mk-MY were all significantly higher than the pre-lesion ones ( $p < 0.001$ ). About three months post-implantation, the trial durations were significantly reduced compared to the post-lesion phase for both hands, at all resistances ( $p < 0.0001$ ) (figure 14, E and F). Moreover, post-implantation values did not significantly differ from the normal (pre-lesion) values (left hand; at R5, right hand; at R3 and at R5). At R0, R3 (left hand) and R0 (right hand), the trial duration's values were even smaller than during the pre-lesion phase (figure 14, E and F).

Concerning Mk-MI, this monkey was not able to perform the reach and grasp drawer task after the MPTP lesion. Consequently, no data were available for the post-lesion phase. At about six weeks post-implantation, this animal started again to execute the task. However, the post-implantation values were still significantly higher than the reference values (pre-lesion) (figure 14, G).

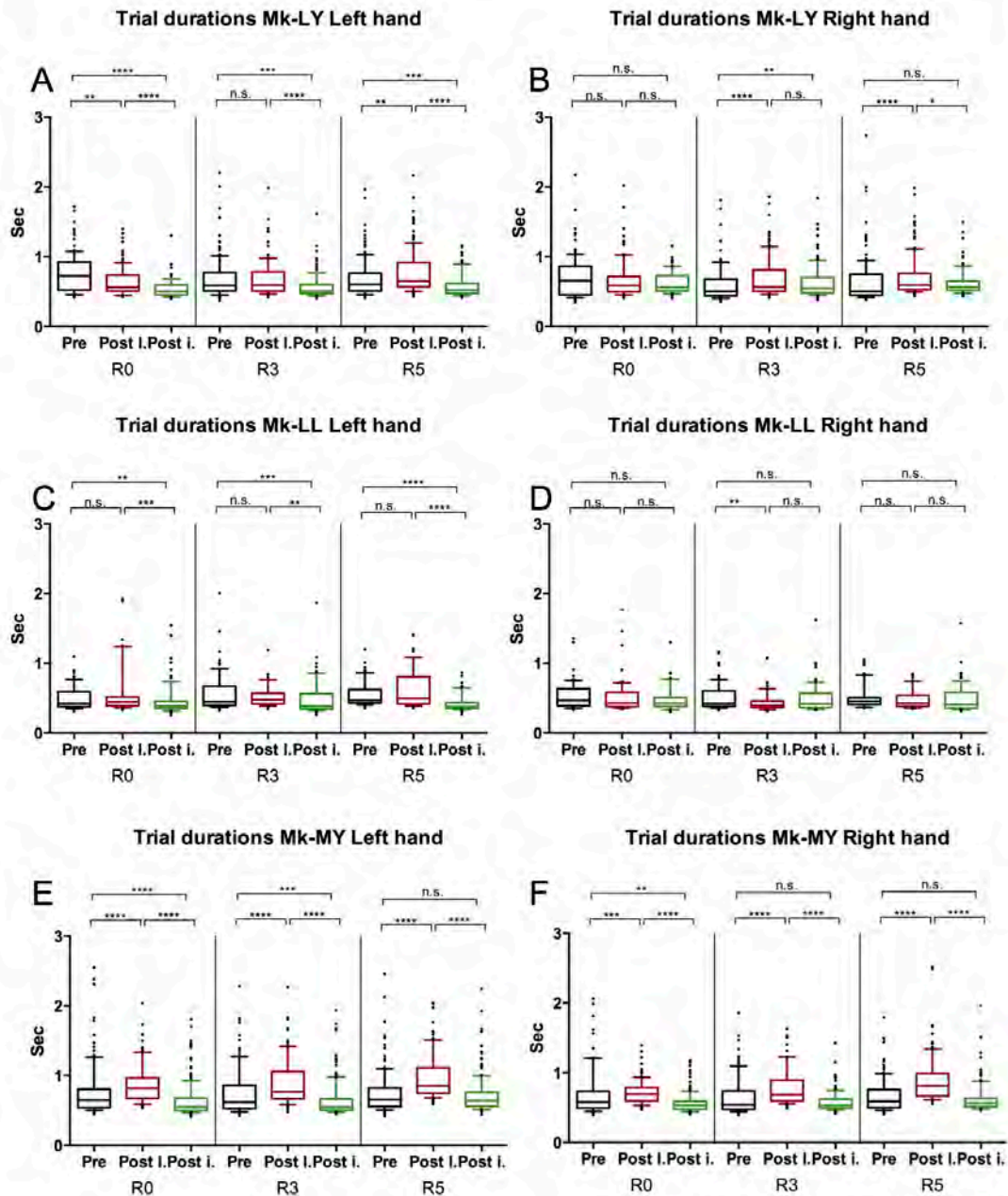
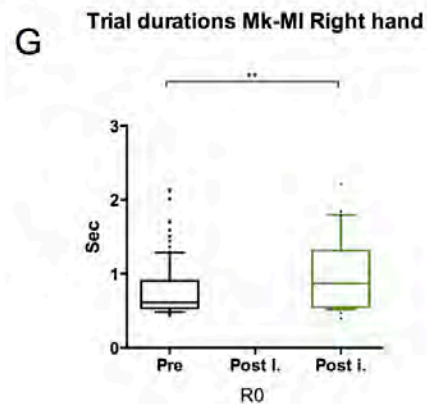


Figure 14. Box and whiskers representation of the trial durations in seconds. The lower and upper limits of the boxes correspond respectively to the 25th percentile and 75th percentile while the lower and upper limits of the whiskers show the 10th and 90th percentiles. The median value (50th percentile) is represented by a bar in the middle of the box. The points outside of the whiskers show the “extreme values”. The black boxes correspond to the pre-lesion phases (June 2014 to September 2014), the red boxes correspond to the post-lesion phase (October 2014 to December 2014) and the green boxes to the post-implantation phase (April 2015 to sacrifices). Each graph presents separately the values for the three resistances (R0, R3, R5). The statistical values are indicated by “stars” and “n.s.”. One star “\*” p-value = 0.01 to 0.05, tow stars “\*\*” p-value = 0.001 to 0.01, three stars “\*\*\*” p-value = 0.0001 to 0.001 and four stars “\*\*\*\*” p-value = <0.0001. “n.s.” refers to non-significant results ( $p \geq 0.05$ ).



## ***Histology***

Regarding the Nissl staining, we were able to detect at low magnification (10x) the tracts consequent to the stereotactic implantations of the cells. In Mk-MI the needle tracts were clearly visible and located in the targeted structures as aimed based on MRI stereotaxic coordinates (1 caudate nucleus, 1 anterior putamen, 1 posterior putamen; bilaterally) (figure 15, A, D and G). Most of the penetration tracts exhibited a slightly darker coloration. Moreover the general assessment of the brain's structures did not reveal any evident structural aberration. The observation of the other three subjects provided very similar results (data not shown).

The qualitative examination with the fluorescence microscope allowed to detect the implanted cells that were stained with PKH67 dye prior to their injection into the striatum. Similarly to what was observed in Mk-LL, Mk-MY and Mk-LY, Mk-MI exhibited the presence of numerous PKH67 positive cells. Those cells were mainly located around the injection tracts but were also visible at more remote areas (figure 15, B, E, and H). Unfortunately, and for technical reasons it was not possible, at the time, to perform stereotaxic counting and, consequently, to estimate the survival rate of the transplanted cells.

Finally, the TH immunohistochemistry analysis provided qualitative information regarding the quantity of dopaminergic fibers and neurons remaining in the substantia nigra. Mk-MI, which was severely affected with a very important decrease of its dopaminergic activity on the PET, exhibited few spread TH+ fibers in the SN (figure 15, C). Similar results were visible in Mk-MY and Mk-LL. The observation of Mk-LY's SN revealed a more abundant TH immunoreactivity with an important number of TH+ cells (figure 15, F). Finally the figure 15 I shows the SN of a control animal.



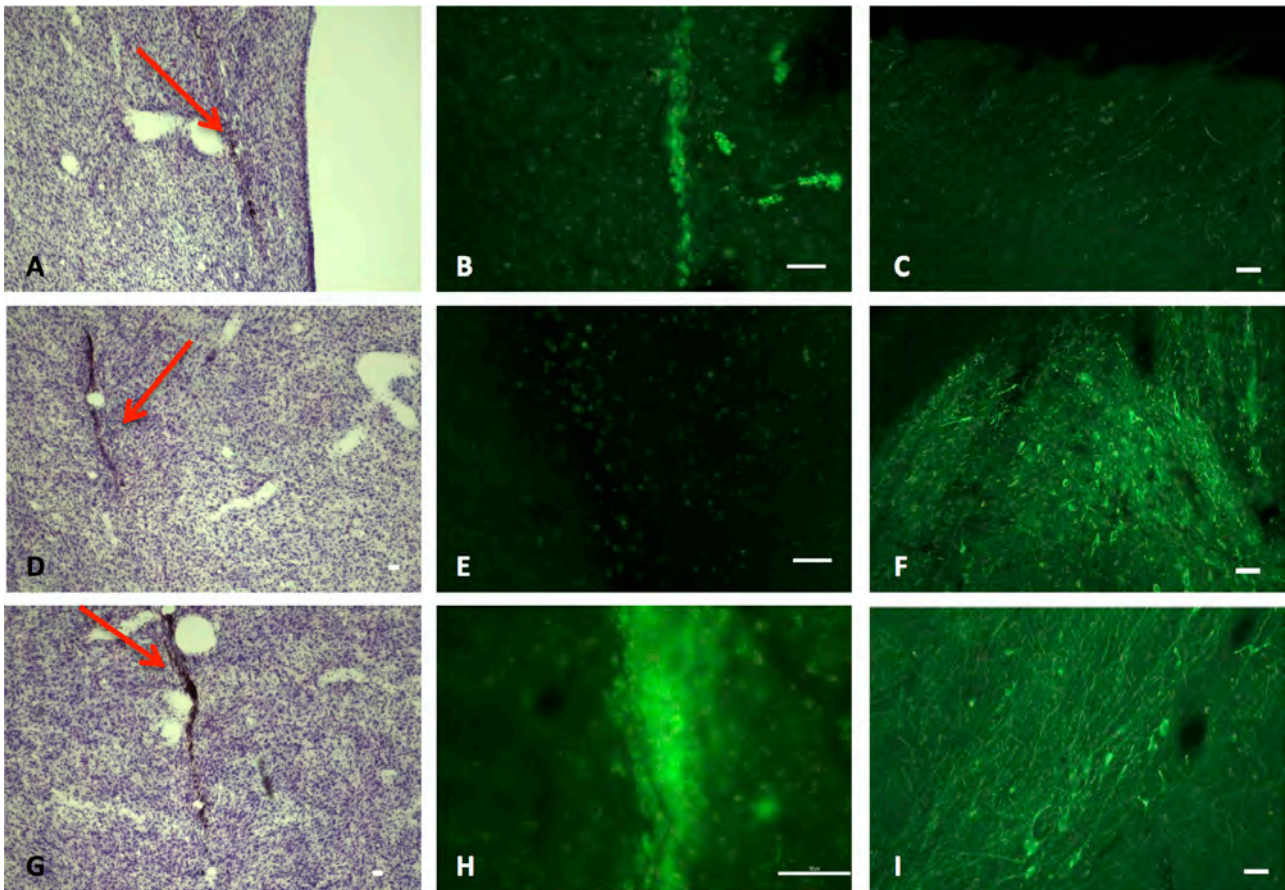


Figure 15. Summary of the histological results for Mk-MI (the first two columns) and Mk-MI, Mk-LY and a control monkey (last column). The left column corresponds to the Nissl coloration. The injection tracts are indicated by the red arrows. A= caudate nucleus, D= putamen (anterior part), G= putamen (posterior part). The middle column corresponds to the PHK67 labeled cells (in green). Pictures B and H were both taken on the injection site located in the putamen at two different magnifications (10x and 20x). Picture E was taken in the putamen but remotely from the injection tracks. The right column displays the results of the TH immunoreaction in the substantia nigra. C= Mk-MI, F= Mk-LY, I= control monkey. The scales are indicated by the white rectangles on the bottom right of the images and correspond to 50 $\mu$ m.

## ***Discussion***

In the context of therapeutic approaches for neurodegenerative disorders, cells transplantations are seen as a promising tool for the development of the next generation of treatments (Morizane and Li, 2008). Over the last decades, many laboratories have intensively dig this paradigm and brought crucial information regarding these novel methods. As mentioned in the introduction, the main cell sources used for the investigations of cell therapies in PD are the hESC and the fetal tissues. However, even if promising results have been published, pre-clinical and clinical investigations have raised some important issues and have shown some limitations linked to immunological reactions, limited donors' availability and to ethical controversies. Moreover, double-blind controlled clinical trials failed to support fetal tissues efficacy to restore motor function in PD patients (Freed et al., 2001; Olanow et al., 2003a). In this situation, autologous cell where seen as intrinsically solving those problems (Arias-Carrión and Yuan, 2009).

In the present study we assessed the impact of ANCE implantation in a NHP MPTP model. This novel approach was developed by Brunet and colleagues and has been shown to promote functional recovery in MPTP treated monkeys (Bloch et al., 2014; J.-F. Brunet et al., 2002; J. F. Brunet et al., 2005). Nevertheless, in addition to the classical behavioral assessment, we used different tools allowing to measure quantitatively different parameters of the behavior and in particular of the manual dexterity (Schmidlin et al., 2011). Moreover, the integrity of the dopaminergic system was closely monitored with  $^{18}\text{F}$ -DOPA PET during the principal phases of the study.

In a general manner, all four monkeys were differently affected by the MPTP lesions. Two of them almost completely recovered few days after the last MPTP injection while the two other exhibited more severe and stable symptoms. Yet, by their sensitivity, the methods used to quantify the spontaneous activity of the animals (VigiePrimate) and their manual dexterity (reach and grasp drawer task and modified Brinkman board task (MBB)) were able to detect subtle modifications, even in apparently asymptomatic

monkeys. Six months following the stereotaxic injections of the ANCE, almost all analyzed parameters were significantly improved with animals exhibiting partial to complete functional recovery.

Moreover, the different data recorded along this study revealed new information regarding the impact of a nigro-striatal lesion on the motor system of NHP and more particularly on the control of the manual dexterity.

### ***Pre-lesion versus post-lesion phases***

#### ***PET, Schneider MPTP scale and spontaneous activity.***

The  $^{18}\text{F}$ -DOPA PET scan has been extensively used in animal models investigation but also in clinical frame as a diagnostic tool (Blesa et al., 2010; Calne et al., 1985; Doudet et al., 1992; Garnett et al., 1983; Guttman et al., 1988; Snow et al., 1993).

Our pre-lesion data showed relatively similar uptake values in the four animals, with  $K_i$  ranging from 0.0073 to 0.0085 (Mk-LY, Mk-MI). Those quantitative results are in line with the data available in the literature where  $K_i$  values range between 0.007 and 0.011 (Blesa et al., 2010; 2012; Doudet et al., 1989; Melega et al., 1996; 1991).

Seven weeks after the end of the MPTP protocol, a second PET scan was performed in order to assess, *in vivo*, the impact of the lesion in each animal. Those post-lesion scans revealed that the striatal  $^{18}\text{F}$ -DOPA uptakes were clearly diminished in all four monkeys. However, those data also underline important inter-individual discrepancies regarding the impact of the toxin on their dopaminergic systems. Out of the four subjects, three exhibited dramatic striatal  $K_i$  decreases (minus  $\approx 80\%$ ) compared to pre-lesion states (Mk-LL, Mk-MI, Mk-MY), while the last one was less affected with a decrease limited to about 17% of its reference value (Mk-LY). Despite important variations and



limited data, statistical analysis revealed that the pre-lesion versus post-lesion differences are statistically related to the MPTP lesions ( $p=0.0002$ ).

It is interesting to notice the particular pattern of degeneration, where the posterior parts of the putamen seemed to be more affected than the anterior part and the caudate nucleus. Those observations are in line with what is known from the human pathology and from some human MPTP intoxication cases (Marek et al., 2001; Snow et al., 2000). Blesa and colleagues have shown similar patterns in MPTP monkeys (Blesa et al., 2012; 2010).

Behaviorally, the symptoms of each animal were closely followed during the different experimental phases with the Schneider MPTP scale (Schneider et al., 1995). Globally, two groups of two animal presented very distinct symptomatic evolutions. On one hand, Mk-LL and Mk-LY exhibited very early quite marked symptoms including bradykinesia and tremors. Those motor impairments were present until the end of the MPTP protocol but rapidly and almost completely vanished few days after the last injection. On the other hand, Mk-MY and Mk-MI were more severely affected by the toxin with symptoms that were sustained during the whole post-lesion phase. The symptoms of Mk-MI, which were clearly the most severe, remained prominent during the whole post-lesion phase. Interestingly, this animal was the last to show deterioration of its motor capacity and actually required additional injections of MPTP.

Regarding the spontaneous activity, the data were collected using the VigiePrimate system developed by ViewPoint technology (Lyon, France). This system offers a reliable and standardized method to assess the global activity of the monkeys and was used in several publications (Chassain et al., 2001; N. Liu et al., 2009; Mounayar et al., 2007b; Worbe et al., 2009). Similarly to the results of the Schneider MPTP scale, the spontaneous activities of the four monkeys were significantly impacted by the lesions in all animals but in two different ways, with an increase of the freezing activity and a decrease of the middle and burst activity. Mk-LL and Mk-LY were moderately affected while Mk-MI and Mk-MY were dramatically altered. Yet, regarding Mk-LL and Mk-LY, although the modification of spontaneous activity was not evident

when observing the animals freely behaving, the VigiePrimate system allowed revealing some subtle but statistically significant changes.

Globally, those different data are pointing out that the MPTP protocol that we adapted from Mounayar and Colleagues, generated parkinsonian behaviors in in all four monkeys according to the methods that are commonly used to assess the global behaviors in similar models (Bloch et al., 2014; Chassain et al., 2001; M. E. Emborg et al., 2008; N. Liu et al., 2009; Mounayar et al., 2007b; Ren et al., 2013; Schneider and Kovelowski, 1990). Moreover, those behavioral results were supported by in vivo data regarding the integrity of the dopaminergic system obtained with 18F-DOPA PET scans.

### ***Lesion variability and compensatory mechanisms***

Yet, the data presented above have raised an important point that has to be addressed. Despite of identical intoxication protocols, there was important inter-individual variability in terms of MPTP susceptibilities. This point has extensively been discussed in the literature and has been stressed out to constitute one major limitation of the NHP MPTP model (Collier et al., 2003; EIDELBERG et al., 1986; Mounayar et al., 2007a; Potts et al., 2013). Porras and colleagues suggested that the age of the monkeys as well as genetic variations can constitute an important source of variations of the MPTP model (Porras et al., 2012). Those two elements could explain why the two younger animals (Mk-LY, MK-LL) that were also close genetically (same father) did recover in few days while the two other monkeys remained more severely affected (Mk-MI, Mk-MY).

The mechanisms underlying spontaneous recovery in NHP, even if fascinating, are still largely unknown. Yet several hypotheses do exist. Song and Haber (2000) and later Mounayar and colleagues (2007) suggested that a sprouting of the dopaminergic fibers spared by the degenerative process would compensate the lack of dopaminergic inputs (Mounayar et al., 2007b;

Song and Haber, 2000). This sprouting phenomenon is believed to originate from both sensory-motor and associative territories of the striatum (Mounayar et al., 2007b). Moreover, Song and Haber emphasized a possible reactivation of some dopaminergic neurons that would have been down-regulated during the MPTP treatment (Song and Haber, 2000). Another hypothesis associates an increase of non-dopaminergic neurotransmitters such as serotonin as suggested by Boulet et al. (Boulet et al., 2008). A new NHP model developed by Beaudoin and colleagues in which they sequentially performed a dopaminergic lesion (using MPTP) and a lesion of the serotonergic neurons (using MDMA), allowed to underline the role of the serotonergic system in the muscular rigidity as well as its implication in the appearance of levodopa induced dyskinesia (Beaudoin-Gobert et al., 2015).

Among others, those elements are suspected to play a compensatory role during the preclinical phase of PD (Song and Haber, 2000; Zigmond et al., 1984).

In the present study, the profile exhibited by Mk-LL, with a Schneider score close to 0 at the end of the post lesion phase and only 15.8% of  $^{18}\text{F}$ -DOPA striatal uptake compared to its pre-lesional state, would go in the direction of a non-dopaminergic compensation (Boulet et al., 2008). In contrast, Mk-LY showing initially relatively marked parkinsonian symptoms and then spontaneously recovered with striatal Ki values decreased by only 17% would rather support the dopaminergic theory. However, the huge difference between those two animals seems to be hardly explainable exclusively by the sprouting of spared fibers. Potts and colleagues pointed out some form of resistance to the MPTP in some monkeys that could possibly fit to the profile of Mk-LY (Potts et al., 2013). Several molecular mechanisms have been suspected to be implicated in the resistance processes against MPTP induced dopaminergic depletion, including an overexpression of VMAT2 (vesicular monoamine transporter 2) or SOD1 (superoxide dismutase1) that would play a role in ROS protection (Y. Liu et al., 1992; Przedborski et al., 1992).

In their paper, Mounayar and colleagues (2007) showed that an acute injection protocol, such as the one used in the present study, would generate more pronounced and stable symptoms (Mounayar et al., 2007b). Moreover,

they advice to inject an extra-acute dose to stabilize or reveal the motor deficits if needed. We followed their recommendation for Mk-MI that was the last to express parkinsonian symptoms by injecting an extra 0.75 mg/kg amount of MPTP. Unfortunately, Mk-LL and Mk-LY that were showing marked and stable parkinsonism at the end of the MPTP protocol, recovered after the end of the quarantine when the facility was not equipped for MPTP treatment anymore.

## ***PET / behaviour correlation***

The cardinal symptoms of PD have early been associated to the depletion of the dopaminergic neurons in the SNpc and consequently to a decrease of the dopamine in the striatum (Forno, 1982; Hornykiewicz, 1982). Several papers have also underlined, both in human and NHP MPTP model, that a destruction of 60% to 80% of the nigro-striatal projection was necessary before the progressive appearance of the motor signs (Agid, 1991; Fearnley and Lees, 1991; 1990; Tabbal et al., 2012). With the development of the neuroimaging techniques such as  $^{123}\text{I}$ -ioflupane SPECT or  $^{18}\text{F}$ -DOPA PET, it was possible to assess, *in vivo*, the state of the dopaminergic system at different stages of the disease (Garnett et al., 1983; Tissingh et al., 1997). Globally there is a good correlation between the motor deficits and the PET/SPECT signal in PD (Benamer et al., 2000; Djaldetti et al., 2009; Marek et al., 2001; Tissingh et al., 1997). Several groups reported similar conclusions in regards with the NHP PD models (Blesa et al., 2012; 2010; Doudet et al., 1998; Kortekaas et al., 2013).

Our results seem to show a poor correlation between the Schneider score and the striatal uptake values (figure 16). Actually, if the results of Mk-LY, Mk-MI and Mk-MY could more or less fit the literature, the case of Mk-LL appears more problematic. At the time of the second scan, Mk-LL exhibited a very low Schneider score, due to an almost complete spontaneous recovery, while its striatal  $K_i$  was very low. However, Blesa et al (2010, 2012), as well as other authors, reported strong inter-individual variability in terms of striatal uptakes (Blesa et al., 2012; 2010; Doudet et al., 1998; Kortekaas et al., 2013). The same is true concerning the human pathology (Marek et al., 2000; Tissingh et al., 1997). Taken together with the very limited number of animals included in this study, this strong variability could explain the lack of correlation between those two parameters. Additionally, an experimenter (rater) bias must be considered, as the assessment of the Schneider score remains a relatively subjective measurement.

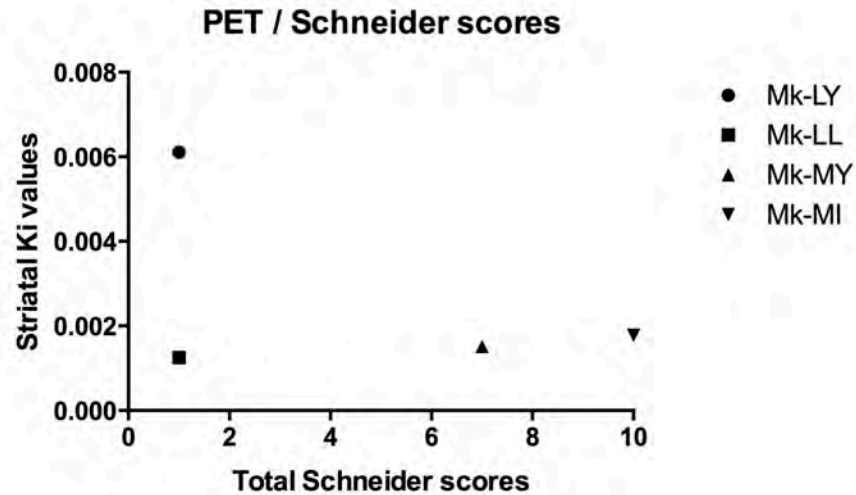


Figure 16. Representation of the score and PET values for each animal. The Y axis gives the average striatal Ki values and the X axis gives the total Schneider score at the time of the second  $^{18}\text{F}$ -DOPA PET scan.

### ***Modified Brinkman Board task and reach and grasp drawer task***

One current manifestation of PD is a decrease of hand dexterity. Actually, if the patient's ability to control their proximal muscles (arms) remains relatively spared, their capacity to perform fine movements with their fingers get more and more deteriorated with the disease progression (Agostino et al., 1998; Castiello and Bennett, 1997; Jackson et al., 2000; Jankovic, 1987; Knopp et al., 1970; Whishaw et al., 2002). It has been hypothesized that this motor manifestation would be linked to the fact that the pallidal outputs are projecting on the ventrolateral thalamus that itself innervates selectively the hand representation of M1 (Holsapple and Preston, 1991; Nambu et al., 1988). In the movement disorder society unified Parkinson's disease rating scale (MDS-UPDRS), which is the most frequently used scale to assess the state of PD patients, several items are directly or indirectly linked to manual dexterity. This includes daily life task such as eating, dressing, handwriting or

more standardized assessments of the hands' movements (Martinez-Martin et al., 1994).

In addition to these semi-quantitative methods, some tasks allow to assess more specifically the forelimbs' deficits and more particularly the hands' impairments. The Pegboard, which consists in a board with holes and small cylindrical objects (pegs), has been widely used in clinics and for research purposes in different pathologies including PD (Sage et al., 2012; Vingerhoets et al., 1996). In this task, the patients have to insert the pegs in the holes as fast as possible. Vingerhoets and colleagues have shown that the pegboard score correlated the best with the nigrostriatal depletion and considered this task as a good biomarker of the PD evolution (Vingerhoets et al., 1996; 1997). This quantitative measure is closely linked to the bradykinesia of the patients which is one of the cardinal symptoms of PD (Hietanen et al., 1987).

Similarly to the UPDRS scale, several MPTP scales in NHP rate items dependent on the ability of the monkeys to use their hands, such as grooming or manipulating food (Imbert et al., 2000; Schneider et al., 1995). However very few studies have investigated the modification of manual dexterity consequent to a lesion of the dopaminergic system in animal models of PD (Annett et al., 1994; Ellis et al., 1992). In a paper, Whishaw and colleagues claimed that the hand control deficits seen in PD patients are similar to those expressed by rat or monkey models (Whishaw et al., 2002).

The modified Brinkman board task and the reach and grasp drawer task are both providing quantitative information regarding the manual dexterity of the subjects (Y. Liu and Rouiller, 1999; Rouiller et al., 1998; Schmidlin et al., 2011).

The MBB task has been used and validated in several studies that were, among others, investigating the impact of therapeutic strategies on spinal and cortical lesions in NHP (Freund et al., 2009; Kaeser et al., 2011; Y. Liu and Rouiller, 1999; Rouiller et al., 1998). By its construction, the task is very close to the pegboard task used in clinics. Both force the subjects to perform fine hand movements. In the two cases, the subject has to generate an "transport movement", mostly involving proximal muscles, and a "grasp movement" that

requires fine control of the distal muscles (Jeannerod, 1984; Jeannerod et al., 1995).

At the exception of Mk-LY, in all monkeys the MBB score in 30 seconds (total score for Mk-LL) were significantly reduced after the MPTP lesions with post-lesional score ranging from 85.4% to 13.8% of the pre-lesion values. Similarly to what is known in PD patients, the deficits in the MBB score were more pronounced in animals with a higher Schneider score.

Regarding the contact time that corresponds the “grasp phase” in the MBB, significant increases were observed in the two most affected monkeys (Mk-MI and Mk-MY) but globally not in the two others. Due to a quite total incapacity of Mk-MI to execute the task, not enough data were available to perform statistical analyses.

Taken together, those two parameters provide precious information. In a general manner, the MBB task’s results show that following the MPTP lesions, the monkeys are slower to execute the task. Those results are relatively in line with some studies conducted on human subjects showing that the reach and grasp movements are generally slower in PD patients compared to controls, suggesting that this would be due to global bradykinesia and rigidity (Bohnen et al., 2007; Hietanen et al., 1987; Sage et al., 2012; Vingerhoets et al., 1996; 1997).

Our data also suggest that the control of the proximal muscles controlling the arms were globally more affected, with three out of four monkeys affected, than the ability to perform the precision grip, i.e. to retrieve the pellet inside the slots with an increase of the CT visible in the two most affected animals only. Those results are in contradiction with the conclusions of Whishaw et al. and Agostino and colleagues (Agostino et al., 1998; Whishaw et al., 2002). Yet, those differences could possibly be linked to the differences between the tasks, the shape and the weight of the objects to grasp. A refinement of our video analysis, more focused on the “quality” of the finger movements, may possibly lead to different conclusions.



Qualitatively, the general patterns of the movements were relatively unchanged (based on visual observations) in the same way than previously reported in PD (Castiello et al., 1999; 2000; Tresilian et al., 1997).

Regarding the motor strategies in the MBB (temporal sequence to visit the slots), quantitative analyses of the left to right motor sequences revealed that all analyzed animals were significantly affected by the MPTP protocol. Two different hypotheses could explain those changes in terms of strategy. On one side, the motor disability consequent the lesion of the nigro-striatal projections could force the animal to adapt its behavioral strategy in order to achieve its goal (adaptive strategy). On the other side, a modification of the motor sequences could be explained by the fact that the basal ganglia are interconnected to the supplementary motor area (SMA) that has been shown to play an important role in the generation of motor sequences in both NHP and humans (Berdyeva and Olson, 2010; Clower and Alexander, 1998; Goldberg, 1985; Kennerley et al., 2004; Mushiake et al., 1990). Moreover, Kaeser and colleagues (2013) argued that the dorsolateral prefrontal cortex (dlPFC) was implicated in motor habits' representations (Kaeser et al., 2013) and a recent functional instigation using PET and conducted by Tian et al (2015) revealed a reduced dopaminergic activity in the dlPFC of MPTP treated monkeys that is supposed to be due to the destruction of some dopaminergic neurons in the ventral tegmental area (VTA) (Tian et al., 2015). Thus, it is possible that the dopaminergic depletion in our model could impact on the motor habits of our monkeys directly or indirectly.

Presently, the observation in Mk-LY that the performance at the MBB was not altered by the lesion but exhibited a significant modification of its strategy seems to fit better with the "cognitive hypothesis", as the modification of the strategy could not be explained by an impairment of the motor function. Regarding the two more affected animals, both hypotheses are potentially plausible but further investigation appears necessary to discriminate the different factors implicated.

In contrary to the MBB task, the execution of the reach and grasp drawer task required the animal to perform always the same movement in order to reach the target (drawer's knob), to generate a certain amount of force to open the drawer and get the reward and allow to finely quantify a specific motor action (Schmidlin et al., 2011) This task also demands the involvement of relatively more different groups of muscles than the MBB.

Similarly to the MBB task's results, Mk-MI and Mk-MY, which exhibited the more severe parkinsonian symptoms, were also the more seriously impaired in term of trial durations. In Mk-MY, the time to execute the task was significantly increased in the post-lesion phase for both hands at all resistances, while Mk-MI was once again almost completely unable to perform the task after the MPTP injections due to a severe akinetic state and to important tremors. Surprisingly, Mk-LL that was significantly affected for the other task (MBB) was not impacted in the reach and grasp drawer task. The reverse is true for Mk-LY, but to a lesser extent than for Mk-MY and Mk-MI.

In the literature, an analogous task during which the patient has to grasp a knob and to lift it was used to assess the grip parameters in PD patients (Fellows and Noth, 2004). Fellows and colleagues reported a prolonged time to lift the charge in PD patients compared to age matched controls (Fellows et al., 1998). They claimed that this was certainly associated with bradykinesia.

The observation that Mk-LL was affected in the MBB but not in the reach and grasp drawer task looks paradoxical. One aspect that could explain this dichotomy is linked to the fact that the movements necessary to perform the two tasks are very different. On one hand, the score of the MBB encompasses the transport movement from the board to the mouth and involves the biceps and supinator muscles while, on the other hand, the movement to execute the drawer task is linear and involve more the triceps and pronator muscles (during the recorded phase). Fellow and colleagues (1998) reported that PD was associated with a deterioration of the supinatory and pronatory movements (Fellows et al., 1998). They moreover suggested that those impairments of the motor function were analogue to those seen in rodents and NHP models of PD. As its is now known that the MPTP lesions are quite variable, it is possible to hypothesize that subtle variability in the

destruction of the nigro-striatal projections could lead to different deficits that could *de facto* be revealed by different motor tasks.

### ***Post-implantation versus pre-lesion phase***

Globally, the data of the post-implantation phase were significantly improved as compared to post-lesion data. However, while all four monkeys exhibited functional recovery, there were important inter-individual disparities depending on the nature of the data obtained.

### ***PET, Schneider MPTP scale and spontaneous activity.***

About six months after the implantation of the ANCE, a third and final  $^{18}\text{F}$ -DOPA PET scan was performed for each animal in order to assess the evolution of the dopaminergic function.

Our data revealed an increase of the striatal Ki values in the four monkeys ranging from 10.8% to 21.4% (Mk-MI and Mk-MY) with respect to the data obtained before the stereotaxic surgery. This increase was statistically significant ( $p < 0.0001$ ; linear random slope and intercept model) but remained significantly different from the pre-lesion values ( $p = 0.007$ ).

Several papers published over the past years have assessed the evolution of the dopaminergic function in NHP MPTP models after the end of the MPTP intoxications (Y. Liu et al., 2013; Melega et al., 1996; Schneider et al., 1995). None of them described an increase of the striatal uptake after the last MPTP injection. Melega and colleagues (1996) conducted a longitudinal study in which they performed several  $^{18}\text{F}$ -DOPA PET scans at different time-points (Melega et al., 1996). Their results showed either stable striatal Ki or a progressive decrease of the  $^{18}\text{F}$ -DOPA uptake over a period of one year. Vezoli and colleagues showed a transient increase of the dopaminergic transporter (DAT) striatal density, using functional neuroimaging tool

([<sup>11</sup>C]PE2I), during the pre-motor stage (Vezoli et al., 2014). However, this phenomenon emphasized as an early compensatory mechanism rapidly vanished with the appearance of the symptoms and so could be excluded in our monkeys.

On a behavioral point of view, the longitudinal follow-up of the Schneider MPTP score displayed two different patterns. As mentioned previously, Mk-LY and Mk-LL that were considered as recovered monkeys, exhibited very light symptoms with a total score of 1 at the time of the ANCE implantation. Few weeks after surgery, those two animals came back to a normal state with a total score of 0. Mk-MI and Mk-MY that were more severely affected before the cellular implantation (total score 5 to 14), progressively recovered after the implantation. Mk-MY, that was affected less than MK-MI, fully recovered within four weeks, while Mk-MI started to regain about two months after cells implantation. About eleven weeks after the implantation, Mk-MI showed a stable score of 2, while light bradykinesia and tremors lasted until its sacrifice.

As already criticized, the use of clinical scales in non-human primates could be a relatively subjective measurement, particularly when the number of observations is quite limited. Moreover, the fact that the experimenters were unblinded could introduce an important bias in the data. For those reasons, the use of the video monitoring software to evaluate the spontaneous activity of each animal represents an objective and unbiased methods to acquire quantitative data. This method was already used in previous studies and correlated with the clinical score (N. Liu et al., 2009; Mounayar et al., 2007b). As formerly exposed, Mk-LL and Mk-LY were moderately impacted in terms of spontaneous activity while Mk-MI and Mk-MY were extremely akinetic during the recording sessions. The data obtained from the last three months of the post-implantation phase, just before the sacrifice, were significantly improved in all four subjects. Interestingly during the later part of the post-lesion phase, Mk-MY, Mk-LL and Mk-LY were considered as totally recovered with a Schneider score of 0, while the recovery in terms of spontaneous activity was only partial (at the exception of Mk-LY middle activity range). This disparity could be partially explained by a greater sensitivity of the VigiePrimate system

to detect the behavioral changes even if our results are not in line with the data presented by Liu and colleagues showing a good clinical score and spontaneous activity correlation (N. Liu et al., 2009).

However, the different behaviors that can be detected visually in those two environmental conditions, even in Mk-MI, must trigger some more explanations. One of them could be linked to the environment itself. On one hand, the Schneider scores were rated in the monkeys' housing facility (45 cubic meters) in which they had social interactions and access to a rich environment. On the other hand, for the recording of the spontaneous activity, the animals were placed for 30 minutes in a smaller cage in a separated room with no social contact or external stimulus.

In a paper published by Currà et al. (1997), the authors suggested that the PD patients were more impaired in the "internally" generated actions than when the actions were triggered by external stimuli (Currà et al., 1997). Even if our paradigm is relatively far from the one of Currà and colleagues, we could hypothesize that the enriched social and environmental composition of the homeroom is more prone to stimulate a motor activity than a limited and poor environment such as in the recording cage.

### ***MBB task and reach and grasp drawer task***

Regarding the post-implantation data obtained with the MBB task, Mk-LY that was not significantly affected for this task and Mk-LL that showed significant but limited impairment after the MPTP lesion, both exhibited non-significant modifications of their scores and CT during the post-implantation phase. On the contrary, Mk-MI and Mk-MY (the most affected) exhibited a significant but incomplete functional recovery for this task.

Concerning the reach and grasp drawer task, Mk-MY showed significant improvement of its trial duration during the last part of the post-implantation phase. Some data were even statistically equal or better than the normal values. Mk-MI that was unable to perform the task after the MPTP injections

regained this capacity few weeks after ANCE transplantation. This recovery was nevertheless partial with significantly slower performances compared to the pre-lesion state. Mk-LL and Mk-LY both showed significant diminution of their trial durations compared to pre-lesion data but this effect was generally limited to their left hand. This means that during the post-implantation phase, those two subjects were even better than before the MPTP lesions. Those unexpected results are difficult to explain. Nevertheless, several hypotheses can be proposed. Firstly, a variability of the performance cannot totally be excluded. Actually, during some periods the monkeys could be very focused on the tasks while, during another period, they could be very forgetful. Secondly, the fact that the left hand shows significant modifications, while the right one did not, could be linked to the lateralization of the monkeys as discussed in annex 5. Finally, it is not totally impossible that the ANCE implantation could be responsible of these particular behavioral modifications.

## ***Histological analyses***

Globally, the histological analyses revealed several important information that is crucial for the validity of this study.

First of all, the observation at low magnification (10x) of the Nissl stained slices confirmed that the implantations of the ANCE were indeed performed in the targeted anatomical structures (one in the caudate nucleus and two in the putamen (anterior and posterior), bilaterally) in all four animals. The penetration tracts exhibited a slightly darker coloration certainly due to some micro bleeding at the time of the surgeries.

Secondly, the general assessment of the anatomy did not reveal any evident anatomical aberration suggesting an absence of tumor formation, as it was the case in previous investigations on ANCE transplantation (Bloch et al., 2014; Brunet et al., 2009; Kaeser et al., 2011). This problematic that represents one of the major limitation to the use of hESC for clinical

application has been intensively debated in the literature (Brederlau et al., 2006; Hwang et al., 2010; Morizane et al., 2008; Politis and Lindvall, 2012).

Thirdly, the qualitative assessment of the brain slices with the fluorescence microscope underline the presence of multiple PKH67 labeled cells. They were located around the implantation tracts but also in more remote parts of the striatum. As the quantification of the cells has not been performed so far, it is not yet possible to evaluate the survival rate of the transplanted cells.

In several studies the survival rate of the implanted cells was very low and so, it was an important point to consider for hoping a therapeutically effect (Brundin and Bjorklund, 1987; Brundin et al., 2000; Hagell and Brundin, 2001). In contrast, the transplantation of ANCE in an MPTP models similar to ours showed an impressive survival rate reaching up to 50% at four months post-implantations (Brunet et al., 2009).

Finally, TH positive fibers were present in a much reduced extent in the SNpc of the MPTP treated monkeys than in a control animal. These qualitative observations seem to confirm the PET data but further quantitation are now required to perform any correlation.

## ***Place of ANCE implantations in the functional and behavioural recovery***

In 2014, Bloch and colleagues published a similar study in which they implanted ANCE produced according to the exact same protocol as ours in a similar NHP MPTP model (Bloch et al., 2014). They were able to show a significant motor improvement in four out of five treated monkeys while the control subjects (no cells or killed cells) remained parkinsonian. For this reason, the present investigation did not aim at providing a proof of efficacy of ANCE transplantation but more to bring complementary information.

In a general manner, the post-implantation results discussed above exhibited significant improvement in comparison to the post-lesion phase. Yet, in the absence of control due to the very limited number of animal included in this study, it is not possible to definitively conclude to a therapeutic effect of the ANCE implantation. Nevertheless, there are some indications that the compensatory mechanisms described in the literature cannot be considered as the unique contributors responsible for this functional recovery.

As the generation of stable motor symptoms is mandatory for the assessment of the efficacy of a new treatment, several laboratories have tackled this important question (Mounayar et al., 2007b; Smith et al., 1993; Soderstrom et al., 2006; Taylor et al., 1997). Taylor and colleagues (1997) reported that the most severely affected monkeys exhibited stable symptoms that lasted for months (Taylor et al., 1997). Soderstrom et al. (2006) estimated that stable motor symptoms were possible with a striatal dopaminergic depletion of at least 80% (Soderstrom et al., 2006).

In our case, it is evident that Mk-LL and Mk-LY underwent functional recovery, certainly due to some compensatory mechanisms (see (Emborg, 2007)). However, Mk-MY and Mk-MI were both more severely affected by the MPTP intoxication with a decrease of at least 80% of the <sup>18</sup>F-DOPA striatal uptake. Actually, without our intervention, Mk-MI would have succumbed to the lesion due to an almost complete incapacity to feed itself. Those evidences are



supporting that the recovery of Mk-MI and Mk-MY is unlikely due to spontaneous compensatory mechanisms only.

In addition to the behavioral elements exposed above, the results of the PET scans provide some important clues supporting that the ANCE implantation has had an effect on the striatal dopaminergic function and consequently on the behavior. As discussed in the previous chapter, the MPTP lesions trigger stable dopaminergic deficits assessable with functional neuroimaging techniques that are lasting over time (Y. Liu et al., 2013; Melega et al., 1996). This permanent diminution of dopaminergic function has also been described in recovered monkeys (Schneider et al., 1995). Yet, the cellular mechanisms sustaining this behavioral and functional recovery are still largely unknown and need to be further investigated.

In their papers, Brunet et al. (2009) and Bloch et al. (2014) stressed out the fact that the neural progenitors transplanted did not generate dopaminergic neurons as only very few cells were co-labeled PKH67 and TH (Bloch et al., 2014; J.-F. Brunet et al., 2009). They emphasized that glial derived neurotrophic factor (GDNF) and brain derived neurotrophic factor (BDNF), which were both present in *in vitro* culture and at histological analyses, could be responsible of those recoveries (Bloch et al., 2014; J.-F. Brunet et al., 2009).

The potential of GDNF as a treatment for PD has been extensively investigated over the last decades (Choi-Lundberg et al., 1997; Gash et al., 1996; Gill et al., 2003; Kordower et al., 2000; Lang et al., 2006; Patel et al., 2005; Patel and Gill, 2007; Ren et al., 2013; Slevin et al., 2005). Several papers reported both a neuroprotective and a restorative effect in PD animal model (Ren et al., 2013; Sinclair et al., 1996; Tomac et al., 1995). On a behavioral point of view, GDNF delivery was accompanied with a significant improvement (or preservation) of the parkinsonian symptoms in both NHP MPTP models and rodent models (M. E. Emborg et al., 2008; Gash et al., 1996; Georgievska et al., 2002; Kordower et al., 2000; Redmond et al., 2009; Ren et al., 2013; Tomac et al., 1995).

Those promising preclinical studies opened the way to the first clinical trials in PD patients (Gill et al., 2003; Patel et al., 2005; Slevin et al., 2005). However, if those open-label trials were showing significant improvement of the motor symptoms, a randomized controlled clinical trial conducted by Lang and colleagues reported more limited improvements and underlined the importance of the placebo effect as already discussed in the introduction (Lang et al., 2006). BDNF has also be put in light as a neurotrophic factor stimulating the dopaminergic growth (Beck et al., 1993; Hyman et al., 1991).

In our case, although the presence of GDNF and/or BDNF has not been yet checked on our monkeys, the results published by Brunet et al. (2009) with the same protocol of cell development let us presume that our grafts may also produce such factors. Consequently, based on the elements presented above, we can reasonably support that ANCE transplantations most likely played a role in the functional recovery exhibited by our monkeys.

## ***Strengths and limitations***

The extensive behavioral follow-up of the animal together with the longitudinal use of *in vivo* functional neuroimaging represent certainly one of the major asset of the present study. From its conception, it was built around the idea to combine the classical approaches (clinical scale and spontaneous activity recording) with two manual dexterity tasks (MBB and reach and grasp drawer task) already validated in other models of lesions of the motor system (Schmidlin et al., 2011). Those methods allowed to track fine behavioral modifications during the whole experimental procedure from the pre-lesion state until the sacrifice. Additionally to the use of  $^{18}\text{F}$ -DOPA PET scans to assess the state of the dopaminergic system in each animal at specific time points, MRI technology was used to precisely target the structures of interest (caudate nuclei and putamen) in order to plan and adapt the stereotaxic surgery to each subject's anatomy. Moreover, the protocols of culture of the ANCE used for the implantation were conducted in strict accordance to good manufacture practices (GMP) in a Swissmedic accredited facility. The GMP implementation is a crucial and necessary step to move towards future clinical applications.

One of the major limitations of this study is linked to the very small number of animals. Taken together with the intrinsic behavioral variability of the NHP (see annex 4) and the inter-individual variations in terms of MPTP sensitivity, no direct statistical comparison between subjects could be performed. The second limitation of the present investigation is associated to the absence of control subject in the same conditions. However, as mentioned above, control subjects were involved in a recent largely comparable ANCE experiment conducted on MPTP monkeys (Bloch et al., 2014). Yet, and for the same reasons as mentioned above, a cohort limited to only four monkeys can not allow to generate relevant group to group statistical comparisons. Actually, a much larger number of animals would be required to achieve such comparison that would not be feasible in terms of infrastructure and would be ethically questionable. This problematic was already tackled in several articles

from our laboratory (Freund et al., 2009; Kaeser et al., 2011). Nevertheless, and as mentioned in the introduction, the proof of efficacy of the ANCE transplantation was already made (Bloch et al., 2014) and therefore we aimed more at refining the knowledge regarding the impact of the implanted cells on the motor system than at providing statistical evidences of efficacy.

## **References**

- Agid, Y., 1991. Parkinson's disease: pathophysiology. *Lancet* 337, 1321–1324. doi:10.1016/0140-6736(91)92989-F
- AGOSTINO, R., Berardelli, A., Currà, A., 1998. Clinical impairment of sequential finger movements in Parkinson's disease. *Movement ....*
- ANNETT, L.E., MARTEL, F.L., ROGERS, D.C., RIDLEY, R.M., BAKER, H.F., Dunnett, S.B., 1994. Behavioral-Assessment of the Effects of Embryonic Nigral Grafts in Marmosets with Unilateral 6-Ohda Lesions of the Nigrostriatal Pathway. *Exp Neurol* 125, 228–246. doi:10.1006/exnr.1994.1026
- Arias-Carrión, O., Yuan, T.-F., 2009. Autologous neural stem cell transplantation: a new treatment option for Parkinson's disease? *Med Hypotheses* 73, 757–759. doi:10.1016/j.mehy.2009.04.029
- Beaudoin-Gobert, M., Epinat, J., Météreau, E., Duperrier, S., Neumane, S., Ballanger, B., Lavenne, F., Liger, F., Tourvielle, C., Bonnefoi, F., Costes, N., Bars, D.L., Broussolle, E., Thobois, S., Tremblay, L., Sgambato-Faure, V., 2015. Behavioural impact of a double dopaminergic and serotonergic lesion in the non-human primate. *Brain* 138, 2632–2647. doi:10.1093/brain/awv183
- Beck, K.D., Knüsel, B., Hefti, F., 1993. The nature of the trophic action of brain-derived neurotrophic factor, des (1-3)-insulin-like growth factor-1, and basic fibroblast growth factor on mesencephalic .... *Neuroscience*.
- Benamer, H.T.S., Patterson, J., Wyper, D.J., Hadley, D.M., Macphee, G.J.A., Grosset, D.G., 2000. Correlation of Parkinson's disease severity and duration with 123I-FP-CIT SPECT striatal uptake. *Movement Disorders* 15, 692–698. doi:10.1002/1531-8257(200007)15:4<692::AID-MDS1014>3.0.CO;2-V
- Berdyeva, T.K., Olson, C.R., 2010. Rank signals in four areas of macaque frontal cortex during selection of actions and objects in serial order. *J Neurophysiol* 104, 141–159. doi:10.1152/jn.00639.2009
- Blesa, J., Juri, C., Collantes, M., Peñuelas, I., Prieto, E., Iglesias, E., Martí-Clement, J., Arbizu, J., Zubieta, J.L., Rodríguez-Oroz, M.C., García-García, D., Richter, J.A., Cavada, C., Obeso, J.A., 2010. Progression of dopaminergic depletion in a model of MPTP-induced parkinsonism in non-human primates. An 18F-DOPA and 11C-DTBZ PET study. *Neurobiol Dis*

- 38, 456–463. doi:10.1016/j.nbd.2010.03.006
- Blesa, J., Piffl, C., Sánchez-González, M.A., Juri, C., García-Cabezas, M.A., Adánez, R., Iglesias, E., Collantes, M., Penuelas, I., Sánchez-Hernández, J.J., Rodríguez-Oroz, M.C., Avendaño, C., Hornykiewicz, O., Cavada, C., Obeso, J.A., 2012. The nigrostriatal system in the presymptomatic and symptomatic stages in the MPTP monkey model: a PET, histological and biochemical study. *Neurobiol Dis* 48, 79–91. doi:10.1016/j.nbd.2012.05.018
- Bloch, J., Brunet, J.-F., McEntire, C.R.S., Redmond, D.E., 2014. Primate adult brain cell autotransplantation produces behavioral and biological recovery in 1-methyl-4-phenyl-1,2,3,6-tetrahydropyridine-induced parkinsonian St. Kitts monkeys. *J Comp Neurol* 522, 2729–2740. doi:10.1002/cne.23579
- Bohnen, N.I., Kuwabara, H., Constantine, G.M., Mathis, C.A., Moore, R.Y., 2007. Grooved pegboard test as a biomarker of nigrostriatal denervation in Parkinson's disease. *Neurosci Lett* 424, 185–189. doi:10.1016/j.neulet.2007.07.035
- Boulet, S., Mounayar, S., Poupard, A., Bertrand, A., Jan, C., Pessiglione, M., Hirsch, E.C., Feuerstein, C., François, C., Féger, J., Savasta, M., Tremblay, L., 2008. Behavioral recovery in MPTP-treated monkeys: neurochemical mechanisms studied by intrastriatal microdialysis. *Journal of Neuroscience* 28, 9575–9584. doi:10.1523/JNEUROSCI.3465-08.2008
- Brederlau, A., Correia, A.S., Anisimov, S.V., Elmi, M., Paul, G., Roybon, L., Morizane, A., Bergquist, F., Riebe, I., Nannmark, U., Carta, M., Hanse, E., Takahashi, J., Sasai, Y., Funa, K., Brundin, P., Eriksson, P.S., Li, J.-Y., 2006. Transplantation of human embryonic stem cell-derived cells to a rat model of Parkinson's disease: effect of in vitro differentiation on graft survival and teratoma formation. *Stem Cells* 24, 1433–1440. doi:10.1634/stemcells.2005-0393
- Brinkman, J., Kuypers, H.G., 1973. Cerebral control of contralateral and ipsilateral arm, hand and finger movements in the split-brain rhesus monkey. *Brain* 96, 653–674.
- Brundin, P., Bjorklund, A., 1987. Survival, growth and function of dopaminergic neurons grafted to the brain. *Prog Brain Res* 71, 293–308.
- Brundin, P., Karlsson, J., Emgård, M., Schierle, G.S., Hansson, O., Petersén, A., Castilho, R.F., 2000. Improving the survival of grafted dopaminergic neurons: a review over current approaches. *Cell Transplant.* 9, 179–195.
- Brunet, J.-F., Redmond, D.E., Bloch, J., 2009. Primate adult brain cell autotransplantation, a pilot study in asymptomatic MPTP-treated monkeys. *Cell Transplant.* 18, 787–799. doi:10.3727/096368909X470847
- Brunet, J.-F.C.O., Pellerin, L., Arsenijevic, Y., Magistretti, P., Villemure, J.-G., 2002. A Novel Method for In Vitro Production of Human Glial-Like Cells from Neurosurgical Resection Tissue. *Laboratory Investigation* 82, 809–812. doi:10.1097/01.LAB.0000017166.26718.BB
- Brunet, J.F., Rouiller, E., Wannier, T., Villemure, J.G., Bloch, J., 2005. Primate adult brain cell autotransplantation, a new tool for brain repair? *Exp Neurol* 196, 195–198. doi:10.1016/j.expneurol.2005.04.005
- Calne, D.B., Langston, J.W., Martin, W.R., Stoessl, A.J., Ruth, T.J., Adam, M.J., Pate, B.D., Schulzer, M., 1985. Positron emission tomography after MPTP: observations relating to the cause of Parkinson's disease. *Nature* 317, 246–248.

- Capitano, J., Emborg, M., 2008. Contributions of non-human primates to neuroscience research. *Lancet* 371, 1126–1135.
- Capitano, J.P., Emborg, M.E., 2008. Contributions of non-human primates to neuroscience research. *The Lancet* 371, 1126–1135. doi:10.1016/S0140-6736(08)60489-4
- Castiello, U., Bennett, K., 1997. The bilateral reach-to-grasp movement of Parkinson's disease subjects. *Brain* 120, 593–604. doi:10.1093/brain/120.4.593
- Castiello, U., Bennett, K., Bonfiglioli, C., Lim, S., Peppard, R.F., 1999. The reach-to-grasp movement in Parkinson's disease: response to a simultaneous perturbation of object position and object size. *Exp. Brain Res.* 125, 453–462.
- Castiello, U., Bonfiglioli, C., Peppard, R., 2000. Dopaminergic effects on the implicit processing of distracter objects in Parkinson's disease. *Exp. Brain Res.* 135, 251–258.
- Chassain, C., Eschalièr, A., Durif, F., 2001. Assessment of motor behavior using a video system and a clinical rating scale in parkinsonian monkeys lesioned by MPTP. *J Neurosci Methods* 111, 9–16.
- Choi-Lundberg, D.L., Lin, Q., Chang, Y.N., Chiang, Y.L., Hay, C.M., Mohajeri, H., Davidson, B.L., Bohn, M.C., 1997. Dopaminergic neurons protected from degeneration by GDNF gene therapy. *Science* 275, 838–841.
- Clower, W.T., Alexander, G.E., 1998. Movement sequence-related activity reflecting numerical order of components in supplementary and presupplementary motor areas. *J Neurophysiol.*
- Collier, T., Steece-Collier, K., Kordower, J., 2003. Primate models of Parkinson's disease. *Exp Neurol* 183, 258–262.
- Courtine, G., Bunge, M.B., Fawcett, J.W., Grossman, R.G., Kaas, J.H., Lemon, R., Maier, I., Martin, J., Nudo, R.J., Ramon-Cueto, A., Rouiller, E.M., Schnell, L., Wannier, T., Schwab, M.E., Edgerton, V.R., 2007. Can experiments in nonhuman primates expedite the translation of treatments for spinal cord injury in humans? *Nat Med* 13, 561–566. doi:10.1038/nm1595
- Currà, A., Berardelli, A., AGOSTINO, R., Modugno, N., Puorger, C.C., ACCORNERO, N., Manfredi, M., 1997. Performance of sequential arm movements with and without advance knowledge of motor pathways in Parkinson's disease. *Mov Disord* 12, 646–654. doi:10.1002/mds.870120505
- Davie, C., 2008. A review of Parkinson's disease. *British medical bulletin.*
- Djaldetti, R., Treves, T.A., Ziv, I., Melamed, E., Lampl, Y., Lorberboym, M., 2009. Use of a single [123I]-FP-CIT SPECT to predict the severity of clinical symptoms of Parkinson disease. *Neurol Sci* 30, 301–305. doi:10.1007/s10072-009-0100-4
- Doudet, D.J., Aigner, T.G., McLellan, C.A., Cohen, R.M., 1992. Positron Emission Tomography with F-18 Dopa - Interpretation and Biological Correlates in Nonhuman-Primates. *Psychiatry Research: Neuroimaging* 45, 153–168. doi:10.1016/0925-4927(92)90023-W
- Doudet, D.J., Chan, G., Holden, J.E., McGeer, E.G., 1998. 6-[18 F] Fluoro-L-DOPA PET studies of the turnover of dopamine in MPTP-induced parkinsonism in monkeys. *Synapse.*
- Doudet, D.J., Miyake, H., Finn, R.T., McLellan, C.A., Aigner, T.G., Wan, R.Q.,

- Adams, H.R., Cohen, R.M., 1989. 6-18F-L-DOPA imaging of the dopamine neostriatal system in normal and clinically normal MPTP-treated rhesus monkeys. *Exp. Brain Res.* 78, 69–80. doi:10.1007/BF00230688
- Earhart, G.M., Cavanaugh, J.T., Ellis, T., Ford, M.P., Foreman, K.B., Dibble, L., 2011. The 9-Hole Peg Test of Upper Extremity Function: Average Values, Test-Retest Reliability, and Factors Contributing to Performance in People With Parkinson Disease. *J Neurol Phys Ther* 35, 157–163. doi:10.1097/NPT.0b013e318235da08
- EIDELBERG, E., BROOKS, B.A., MORGAN, W.W., WALDEN, J.G., KOKEMOOR, R.H., 1986. Variability and Functional Recovery in the N-Methyl-4-Phenyl-1,2,3,6-Tetrahydropyridine Model of parkinsonism in Monkeys. *Neuroscience* 18, 817–822.
- Ellis, J.E., Byrd, L.D., Bakay, R.A.E., 1992. A method for quantitating motor deficits in a nonhuman primate following MPTP-induced hemiparkinsonism and Co-grafting. *Exp Neurol* 115, 376–387. doi:10.1016/0014-4886(92)90202-2
- Emborg, M.E., 2007. Nonhuman primate models of Parkinson's disease. *ILAR.J.* 48, 339–355.
- Emborg, M.E., Ebert, A.D., Moirano, J., Peng, S., Suzuki, M., Capowski, E., Joers, V., Roitberg, B.Z., Aebischer, P., Svendsen, C.N., 2008. GDNF-secreting human neural progenitor cells increase tyrosine hydroxylase and VMAT2 expression in MPTP-treated cynomolgus monkeys. *Cell Transplant.* 17, 383–395.
- Emborg, M.E., Liu, Y., Xi, J., Zhang, X., Yin, Y., Lu, J., Joers, V., Swanson, C., Holden, J.E., Zhang, S.-C., 2013. Induced Pluripotent Stem Cell-Derived Neural Cells Survive and Mature in the Nonhuman Primate Brain. *Cell Reports* 1–7. doi:10.1016/j.celrep.2013.02.016
- Fearnley, J.M., Lees, A.J., 1991. Ageing and Parkinson's disease: substantia nigra regional selectivity. *Brain* 114 ( Pt 5), 2283–2301.
- Fearnley, J.M., Lees, A.J., 1990. Striatonigral degeneration. A clinicopathological study. *Brain* 113 ( Pt 6), 1823–1842.
- Fellows, S.J., Noth, J., 2004. Grip force abnormalities in de novo Parkinson's disease. *Mov Disord* 19, 560–565. doi:10.1002/mds.10710
- Fellows, S.J., Noth, J., Schwarz, M., 1998. Precision grip and Parkinson's disease. *Brain* 121 ( Pt 9), 1771–1784.
- Forno, L.S., 1982. Pathology of Parkinson's disease. *Movement disorders.*
- Forno, L.S., DeLanney, L.E., Irwin, I., Langston, J.W., 1993. Similarities and differences between MPTP-induced parkinsonism and Parkinson's disease. *Neuropathologic considerations.* *Adv Neurol* 60, 600–608.
- Freed, C., Greene, P., Breeze, R., 2001. Transplantation of embryonic dopamine neurons for severe Parkinson's disease. ... *England Journal of*  
....
- Freund, P., Schmidlin, E., Wannier, T., Bloch, J., Mir, A., Schwab, M.E., Rouiller, E.M., 2009. Anti-Nogo-A antibody treatment promotes recovery of manual dexterity after unilateral cervical lesion in adult primates - re-examination and extension of behavioral data. *European Journal of Neuroscience* 29, 983–996. doi:10.1111/j.1460-9568.2009.06642.x
- Garnett, E.S., Firnau, G., Nahmias, C., 1983. Dopamine visualized in the basal ganglia of living man. *Nature* 305, 137–138. doi:10.1038/305137a0
- Gash, D.M., Zhang, Z., Ovadia, A., Cass, W.A., Yi, A., Simmerman, L.,

- Russell, D., Martin, D., Lapchak, P.A., Collins, F., Hoffer, B.J., Gerhardt, G.A., 1996. Functional recovery in parkinsonian monkeys treated with GDNF. *Nature* 380, 252–255. doi:10.1038/380252a0
- Georgievska, B., Kirik, D., Rosenblad, C., Lundberg, C., Bj rklund, A., 2002. Neuroprotection in the rat Parkinson model by intrastriatal GDNF gene transfer using a lentiviral vector. *NeuroReport* 13, 75–82.
- Gerlach, M., Riederer, P., Przuntek, H., 1991. MPTP mechanisms of neurotoxicity and their implications for Parkinson's disease. *European Journal of ...*
- Gill, S.S., Patel, N.K., Hotton, G.R., O'Sullivan, K., McCarter, R., Bunnage, M., Brooks, D.J., Svendsen, C.N., Heywood, P., 2003. Direct brain infusion of glial cell line-derived neurotrophic factor in Parkinson disease. *Nat Med* 9, 589–595. doi:10.1038/nm850
- GOLDBERG, G., 1985. Supplementary Motor Area Structure and Function - Review and Hypotheses. *Behavioral and Brain Sciences* 8, 567–588.
- Guttman, M., Yong, V.W., Kim, S.U., Calne, D.B., Martin, W.R.W., Adam, M.J., Ruth, T.J., 1988. Asymptomatic striatal dopamine depletion: PET scans in unilateral MPTP monkeys. *Synapse* 2, 469–473. doi:10.1002/syn.890020502
- Hagell, P., Brundin, P., 2001. Cell survival and clinical outcome following intrastriatal transplantation in Parkinson disease. *J.Neuropathol.Exp.Neurol.* 60, 741–752.
- Hallett, P.J., Deleidi, M., Astradsson, A., Smith, G.A., Cooper, O., Osborn, T.M., Sundberg, M., Moore, M.A., Perez-Torres, E., Brownell, A.-L., Schumacher, J.M., Spealman, R.D., Isacson, O., 2015. Successful Function of Autologous iPSC-Derived Dopamine Neurons following Transplantation in a Non-Human Primate Model of Parkinson's Disease. *Stem Cell* 1–7. doi:10.1016/j.stem.2015.01.018
- Hietanen, M., Teravainen, H., Tsui, J.K., McLennan, D., 1987. The pegboard as a measurement of parkinsonian motor deficit. *Neurology*.
- Hoehn, M.M., Yahr, M.D., 1967. parkinsonism: onset, progression and mortality. *Neurology* 17, 427–442.
- Holsapple, J.W., Preston, J.B., 1991. The origin of thalamic inputs to the“ hand” representation in the primary motor cortex. *The journal of ....*
- Hoogewoud, F., Hamadjida, A., Wyss, A.F., Mir, A., Schwab, M.E., Belhaj-Saif, A., Rouiller, E.M., 2013. Comparison of Functional Recovery of Manual Dexterity after Unilateral Spinal Cord Lesion or Motor Cortex Lesion in Adult Macaque Monkeys. *Frontiers in Neurology* 4, 101. doi:10.3389/fneur.2013.00101
- Hornykiewicz, O., 1982. Brain neurotransmitter changes in Parkinson's disease. *Movement Disorders*.
- Hwang, D.-Y., Kim, D.-S., Kim, D.-W., 2010. Human ES and iPS cells as cell sources for the treatment of Parkinson's disease: current state and problems. *J Cell Biochem* 109, 292–301. doi:10.1002/jcb.22411
- Hyman, C., Hofer, M., Barde, Y.A., Juhasz, M., 1991. BDNF is a neurotrophic factor for dopaminergic neurons of the substantia nigra. *Nature*.
- Imbert, C.C., Bezard, E.E., Guitraud, S.S., Boraud, T.T., Gross, C.E.C., 2000. Comparison of eight clinical rating scales used for the assessment of MPTP-induced parkinsonism in the Macaque monkey. *J Neurosci Methods* 96, 71–76.



- Jackson, G.M., Jackson, S.R., Hindle, J.V., 2000. The control of bimanual reach-to-grasp movements in hemiparkinsonian patients. *Exp. Brain Res.* 132, 390–398.
- Jankovic, J., 1987. Pathophysiology and clinical assessment of motor symptoms in Parkinson's disease. *Handbook of Parkinson's Disease* (pp. 99–126). New York: ...
- Jeannerod, M., 1984. The timing of natural prehension movements. *J Mot Behav* 16, 235–254.
- Jeannerod, M., ARBIB, M.A., Rizzolatti, G., SAKATA, H., 1995. Grasping Objects - the Cortical Mechanisms of Visuomotor Transformation. *Trends in Neurosciences* 18, 314–320.
- Kaesler, M., Brunet, J.-F., Wyss, A., Belhaj-Saif, A., Liu, Y., Hamadjida, A., Rouiller, E.M., Bloch, J., 2011. Autologous adult cortical cell transplantation enhances functional recovery following unilateral lesion of motor cortex in primates: a pilot study. *Neurosurgery* 68, 1405–16–discussion 1416–7. doi:10.1227/NEU.0b013e31820c02c0
- Kaesler, M., Wannier, T., Brunet, J.-F., Wyss, A., Bloch, J., Rouiller, E.M., 2013. Representation of motor habit in a sequence of repetitive reach and grasp movements performed by macaque monkeys: Evidence for a contribution of the dorsolateral prefrontal cortex. *Cortex* 49, 1404–1419. doi:10.1016/j.cortex.2012.05.025
- Kazennikov, O., Hyland, B., Corboz, M., Babalian, A., Rouiller, E.M., Wiesendanger, M., 1999. Neural activity of supplementary and primary motor areas in monkeys and its relation to bimanual and unimanual movement sequences. *Neuroscience* 89, 661–674. doi:10.1016/S0306-4522(98)00348-0
- Kazennikov, O., Wicki, U., Corboz, M., Hyland, B., Palmeri, A., Rouiller, E.M., Wiesendanger, M., 1994. Temporal Structure of a Bimanual Goal-directed Movement Sequence in Monkeys. *European Journal of Neuroscience* 6, 203–210. doi:10.1111/j.1460-9568.1994.tb00262.x
- Kennerley, S.W., Sakai, K., Rushworth, M.F.S., 2004. Organization of Action Sequences and the Role of the Pre-SMA. *J Neurophysiol* 91, 978–993. doi:10.1152/jn.00651.2003
- Kermadi, I., Liu, Y., Tempini, A., Calciati, E., Rouiller, E.M., 1998. Neuronal activity in the primate supplementary motor area and the primary motor cortex in relation to spatio-temporal bimanual coordination. *Somatosens Mot Res* 15, 287–308.
- Kermadi, I., Liu, Y., Tempini, A., Rouiller, E.M., 1997. Effects of reversible inactivation of the supplementary motor area (SMA) on unimanual grasp and bimanual pull and grasp performance in monkeys. *Somatosens Mot Res* 14, 268–280. doi:10.1080/08990229770980
- KNOPP, W., PAULSON, G., ALLEN, J.N., SMELTZER, D., BROWN, F.D., KOSE, W., 1970. Parkinsons Disease - L-Dopa Treatment and Handwriting Area. *Curr Ther Res Clin Exp* 12, 115–&.
- Kordower, J., Emborg, M., Bloch, J., Ma, S., Chu, Y., 2000. Neurodegeneration prevented by lentiviral vector delivery of GDNF in primate models of Parkinson's disease. *Science*.
- Kortekaas, R., Eshuis, S.A., Andringa, G., Cools, A.R., Leenders, K.L., 2013. Motor behavior correlates with striatal [F-18]-DOPA uptake in MPTP-lesioned primates. *Neurochemistry International* 62, 349–353.

- doi:10.1016/j.neuint.2013.01.021
- Kriks, S., Shim, J.-W., Piao, J., Ganat, Y.M., Wakeman, D.R., Xie, Z., Carrillo-Reid, L., Auyeung, G., Antonacci, C., Buch, A., Yang, L., Beal, M.F., Surmeier, D.J., Kordower, J.H., Tabar, V., Studer, L., 2011. Dopamine neurons derived from human ES cells efficiently engraft in animal models of Parkinson's disease. *Nature* 1–7. doi:10.1038/nature10648
- Lang, A.E., Gill, S., Patel, N.K., Lozano, A., Nutt, J.G., Penn, R., Brooks, D.J., Hotton, G., Moro, E., Heywood, P., Brodsky, M.A., Burchiel, K., Kelly, P., Dalvi, A., Scott, B., Stacy, M., Turner, D., Wooten, V.G.F., Elias, W.J., Laws, E.R., Dhawan, V., Stoessel, A.J., Matcham, J., Coffey, R.J., Traub, M., 2006. Randomized controlled trial of intraputamenal glial cell line-derived neurotrophic factor infusion in Parkinson disease. *Ann.Neurol* 59, 459–466. doi:10.1002/ana.20737
- Liu, N., Yue, F., Tang, W.P., Chan, P., 2009. An objective measurement of locomotion behavior for hemiparkinsonian cynomolgus monkeys. *J Neurosci Methods* 183, 188–194. doi:10.1016/j.jneumeth.2009.06.037
- Liu, Y., Peter, D., Roghani, A., Schuldiner, S., Prive, G.G., 1992. A cDNA that suppresses MPP+ toxicity encodes a vesicular amine transporter. *Cell*.
- Liu, Y., Rouiller, E.M., 1999. Mechanisms of recovery of dexterity following unilateral lesion of the sensorimotor cortex in adult monkeys. *Exp.Brain Res.* 128, 149–159.
- Liu, Y., Yue, F., Tang, R., Tao, G., Pan, X., Zhu, L., Kung, H.F., Chan, P., 2013. Progressive loss of striatal dopamine terminals in MPTP-induced acute parkinsonism in cynomolgus monkeys using vesicular monoamine transporter type 2 PET imaging ([18F]AV-133). *Neurosci. Bull.* 30, 409–416. doi:10.1007/s12264-013-1374-3
- Marek, K., Innis, R., van Dyck, C., Fussell, B., Early, M., Eberly, S., Oakes, D., Seibyl, J., 2001. [123I]β-CIT SPECT imaging assessment of the rate of Parkinson's disease progression. *Neurology* 57, 2089–2094. doi:10.1212/WNL.57.11.2089
- Marek, K., Seibyl, J., Holloway, R., Kieburtz, K., Oakes, D., Lang, A., Yim, J., Dey, H., Cellar, J., Fussell, B., Broshjeit, S., Early, M., Smith, E.O., Sudarsky, L., Johnson, K.A., Corwin, C., Johnson, D., Lajoie, S., Reich, S.G., Frost, J.J., Goldberg, P., Flesher, J.E., Feigin, A., Mazurkiewicz, J., Castronuovo, J., Joseph, F., DiRocco, A., Olanow, C.W., Machac, J., Cotei, D., Webner, P., Rudolph, A., Day, D., Casaceli, C., Freimuth, A., Orme, C., Hodgeman, K., Eberly, S., Henry, E., Morgan, G., Haley, J.B., Grp, P.S., 2000. A multicenter assessment of dopamine transporter imaging with DOPASCAN/SPECT in parkinsonism. *Neurology* 55, 1540–1547.
- Martinez-Martin, P., Gil-Nagel, A., Gracia, L.M., Gómez, J.B., Martínez-Sarriés, J., Bermejo, F., 1994. Unified Parkinson's Disease Rating Scale characteristics and structure. The Cooperative Multicentric Group. *Mov Disord* 9, 76–83. doi:10.1002/mds.870090112
- Melega, W.P., Hoffman, J.M., Schneider, J.S., Phelps, M.E., BARRIO, J.R., 1991. 6-[F-18]Fluoro-L-Dopa Metabolism in Mptp-Treated Monkeys - Assessment of Tracer Methodologies for Positron Emission Tomography. *Brain Res* 543, 271–276. doi:10.1016/0006-8993(91)90037-V
- Melega, W.P., Raleigh, M.J., Stout, D.B., DeSalles, A.A., Cherry, S.R., Blurton-Jones, M., Morton, G.G., Huang, S.C., Phelps, M.E., 1996.

- Longitudinal behavioral and 6-[18F]fluoro-L-DOPA-PET assessment in MPTP-hemiparkinsonian monkeys. *Exp Neurol* 141, 318–329. doi:10.1006/exnr.1996.0167
- Morizane, A., Li, J., 2008. From bench to bed: the potential of stem cells for the treatment of Parkinson's disease. *Cell and tissue research*.
- Morizane, A., Li, J.-Y., Brundin, P., 2008. From bench to bed: the potential of stem cells for the treatment of Parkinson's disease. *Cell and tissue research* 331, 323–336. doi:10.1007/s00441-007-0541-0
- Mounayar, S., Boulet, S., Tande, D., Jan, C., Pessiglione, M., Hirsch, E.C., Féger, J., Savasta, M., François, C., Tremblay, L., 2007a. A new model to study compensatory mechanisms in MPTP-treated monkeys exhibiting recovery. *Brain* 130, 2898–2914. doi:10.1093/brain/awm208
- Mounayar, S., Boulet, S., Tandé, D., Jan, C., Pessiglione, M., Hirsch, E.C., Féger, J., Savasta, M., François, C., Tremblay, L., 2007b. A new model to study compensatory mechanisms in MPTP-treated monkeys exhibiting recovery. *Brain* 130, 2898–2914. doi:10.1093/brain/awm208
- Mushiake, H., Inase, M., Tanji, J., 1990. Selective coding of motor sequence in the supplementary motor area of the monkey cerebral cortex. *Experimental brain research*.
- Nambu, A., Yoshida, S., Jinnai, K., 1988. Projection on the motor cortex of thalamic neurons with pallidal input in the monkey. *Experimental brain research*.
- Olanow, C., 1999. Etiology and pathogenesis of Parkinson's disease. *Annual review of neuroscience*.
- Olanow, C., Goetz, C., Kordower, J., Stoessl, A., Sossi, V., Brin, M., Shannon, K., Nauert, G., Perl, D., Godbold, J., Freeman, T., 2003a. A double-blind controlled trial of bilateral fetal nigral transplantation in Parkinson's disease. *Ann.Neurol* 54, 403–414.
- Olanow, C.W., Goetz, C.G., Kordower, J.H., Stoessl, A.J., Sossi, V., Brin, M.F., Shannon, K.M., Nauert, G.M., Perl, D.P., Godbold, J., Freeman, T.B., 2003b. A double-blind controlled trial of bilateral fetal nigral transplantation in Parkinson's disease. *Ann.Neurol* 54, 403–414. doi:10.1002/ana.10720
- Patel, N.K., Bunnage, M., Plaha, P., Svendsen, C.N., Heywood, P., Gill, S.S., 2005. Intraputamenal infusion of glial cell line-derived neurotrophic factor in PD: a two-year outcome study. *Ann.Neurol* 57, 298–302. doi:10.1002/ana.20374
- Patel, N.K., Gill, S.S., 2007. GDNF delivery for Parkinson's disease. *Acta Neurochir. Suppl.* 97, 135–154.
- PATLAK, C.S., BLASBERG, R.G., FENSTERMACHER, J.D., 1983. Graphical Evaluation of Blood-to-Brain Transfer Constants From Multiple-Time Uptake Data. *J. Cereb. Blood Flow Metab.* 3, 1–7. doi:10.1038/jcbfm.1983.1
- Politis, M., Lindvall, O., 2012. Clinical application of stem cell therapy in Parkinson's disease. *BMC Med* 10, 1. doi:10.1186/1741-7015-10-1
- Porrás, G., Li, Q., Bezard, E., 2012. Modeling Parkinson's Disease in Primates: The MPTP Model. *Cold Spring Harb Perspect Med* 2, a009308. doi:10.1101/cshperspect.a009308
- Potts, L.F., Wu, H., Singh, A., Marcilla, I., Luquin, M.R., Papa, S.M., 2013. *Experimental Neurology*. *Exp Neurol* 1–11.

- doi:10.1016/j.expneurol.2013.09.014
- Przedborski, S., Kostic, V., Jackson-Lewis, V., 1992. Transgenic mice with increased Cu/Zn-superoxide dismutase activity are resistant to N-methyl-4-phenyl-1, 2, 3, 6-tetrahydropyridine-induced neurotoxicity.
- Redmond, D., Elsworth, J., Roth, R., Leranath, C., Collier, T., Blanchard, B., Bjugstad, K., Samulski, R., Aebischer, P., Sladek, J., 2009. Embryonic substantia nigra grafts in the mesencephalon send neurites to the host striatum in non-human primate after overexpression of GDNF. *J Comp Neurol* 515, 31–40. doi:10.1002/cne.22028 [doi]
- Redmond, D.E., Jr, McEntire, C.R., Kingsbery, J.P., Leranath, C., Elsworth, J.D., Bjugstad, K.B., Roth, R.H., Sladek, R.J.S.J.R., Jr, 2013. Comparison of Fetal Mesencephalic Grafts, AAV-delivered GDNF, and Both Combined in an MPTP-induced Nonhuman Primate Parkinson's Model 1–9. doi:10.1038/mt.2013.180
- Ren, Z., Wang, J., Wang, S., Zou, C., Li, X., Guan, Y., Chen, Z., Zhang, Y.A., 2013. Autologous transplantation of GDNF-expressing mesenchymal stem cells protects against MPTP-induced damage in cynomolgus monkeys. *Sci Rep* 3. doi:10.1038/srep02786
- Rouiller, E.M., Yu, X.H., Moret, V., Tempini, A., Wiesendanger, M., Liang, F., 1998. Dexterity in adult monkeys following early lesion of the motor cortical hand area: the role of cortex adjacent to the lesion. *European Journal of Neuroscience* 10, 729–740. doi:10.1046/j.1460-9568.1998.00075.x
- Sage, M.D., Bryden, P.J., Roy, E.A., Almeida, Q.J., 2012. The Relationship Between the Grooved Pegboard Test and Clinical Motor Symptom Evaluation Across the Spectrum of Parkinson's Disease Severity. *J Parkinsons Dis* 2, 207–213. doi:10.3233/JPD-2012-012093
- Schmidlin, E., Kaeser, M., Gindrat, A.D., Savidan, J., Chatagny, P., Badoud, S., Hamadjida, A., Beaud, M.-L., Wannier, T., Belhaj-Saif, A., Rouiller, E.M., 2011. Behavioral Assessment of Manual Dexterity in Non-Human Primates. *JoVE* e3258–e3258. doi:10.3791/3258
- Schneider, J.S., Kovelowski, C.J., 1990. Chronic exposure to low doses of MPTP. I. Cognitive deficits in motor asymptomatic monkeys. *Brain Res* 519, 122–128.
- Schneider, J.S., Lidsky, T.I., Hawks, T., Mazziotta, J.C., Hoffman, J.M., 1995. Differential recovery of volitional motor function, lateralized cognitive function, dopamine agonist-induced rotation and dopaminergic parameters in monkeys made hemi-parkinsonian by intracarotid MPTP infusion. *Brain Res* 672, 112–117.
- Sinclair, S.R., Svendsen, C.N., Torres, E.M., Martin, D., Fawcett, J.W., Dunnett, S.B., 1996. GDNF enhances dopaminergic cell survival and fibre outgrowth in embryonic nigral grafts. *NeuroReport* 7, 2547–2552.
- Slevin, J.T., Gerhardt, G.A., Smith, C.D., Gash, D.M., Kryscio, R., Young, B., 2005. Improvement of bilateral motor functions in patients with Parkinson disease through the unilateral intraputaminial infusion of glial cell line-derived neurotrophic factor. *J.Neurosurg.* 102, 216–222. doi:10.3171/jns.2005.102.2.0216
- Smith, R.D., Zhang, Z., Kurlan, R., McDermott, M., Gash, D.M., 1993. Developing a stable bilateral model of parkinsonism in rhesus monkeys. *Neuroscience*.

- Snow, B.J., Tooyama, I., McGeer, E.G., Yamada, T., Calne, D.B., Takahashi, H., Kimura, H., 1993. Human positron emission tomographic [18F]Fluorodopa studies correlate with dopamine cell counts and levels. *Ann.Neurol* 34, 324–330. doi:10.1002/ana.410340304
- Snow, B.J., Vingerhoets, F., Langston, J.W., Tetrud, J.W., Sossi, V., Calne, D.B., 2000. Pattern of dopaminergic loss in the striatum of humans with MPTP induced parkinsonism. *J Neurol Neurosurg Psychiatr* 68, 313–316. doi:10.1136/jnnp.68.3.313
- Soderstrom, K., O'Malley, J., Steece-Collier, K., Kordower, J.H., 2006. Neural repair strategies for Parkinson's disease: insights from primate models. *Cell Transplant.* 15, 251–265.
- Song, D.D., Haber, S.N., 2000. Striatal responses to partial dopaminergic lesion: evidence for compensatory sprouting. *Journal of Neuroscience* 20, 5102–5114.
- STERNE, D.M., 1969. Purdue Pegboard and Macquarrie Tapping and Dotting Tasks as Measures of Motor Functioning. *Perceptual and Motor Skills* 28, 556–&.
- Tabbal, S.D., Tian, L., Karimi, M., Brown, C.A., Loftin, S.K., Perlmutter, J.S., 2012. Low nigrostriatal reserve for motor parkinsonism in nonhuman primates. *Exp Neurol* 237, 355–362. doi:10.1016/j.expneurol.2012.07.008
- Taylor, J.R., Elsworth, J.D., Roth, R.H., Sladek, J.R., Redmond, D.E., 1997. Severe long-term 1-methyl-4-phenyl-1,2,3,6-tetrahydropyridine-induced parkinsonism in the vervet monkey (*Cercopithecus aethiops sabaeus*). *Neuroscience* 81, 745–755.
- Tian, L., Xia, Y., Flores, H.P., Campbell, M.C., Moerlein, S.M., Perlmutter, J.S., 2015. Neuroimaging Analysis of the Dopamine Basis for Apathetic Behaviors in an MPTP-Lesioned Primate Model. *PLoS ONE* 10, e0132064. doi:10.1371/journal.pone.0132064
- Tissingh, G., Bergmans, P., Booij, J., Winogrodzka, A., van Royen, E.A., Stoof, J.C., Wolters, E.C., 1997. Drug-naïve patients with Parkinson's disease in Hoehn and Yahr stages I and II show a bilateral decrease in striatal dopamine transporters as revealed by [123I]β-CIT SPECT. *Journal of Neurology* 245, 14–20. doi:10.1007/s004150050168
- Tomac, A., Lindqvist, E., Lin, L.F.H., Ögren, S.O., Young, D., Hoffer, B.J., Olson, L., 1995. Protection and repair of the nigrostriatal dopaminergic system by GDNF in vivo. , Published online: 26 January 1995; | doi:10.1038/373335a0 373, 335–339. doi:10.1038/373335a0
- Tresilian, J.R., Stelmach, G.E., Adler, C.H., 1997. Stability of reach-to-grasp movement patterns in Parkinson's disease. *Brain* 120, 2093–2111.
- Vezoli, J., Dzahini, K., Costes, N., Wilson, C.R.E., Fifel, K., Cooper, H.M., Kennedy, H., Procyk, E., 2014. Increased DAT binding in the early stage of the dopaminergic lesion: A longitudinal [11C]PE2I binding study in the MPTP-monkey. *Neuroimage* 102, 249–261. doi:10.1016/j.neuroimage.2014.07.059
- Vingerhoets, F., Uitti, R.J., Schulzer, M., Caine, D.B., 1996. The purdue pegboard task reliably reflects the nigrostriatal deficit in Parkinson's disease. *Neurology* 46, 1099–1099.
- Vingerhoets, F.J., Schulzer, M., Calne, D.B., Snow, B.J., 1997. Which clinical sign of Parkinson's disease best reflects the nigrostriatal lesion? *Ann.Neurol* 41, 58–64. doi:10.1002/ana.410410111

- Weiss, P.H., Dafotakis, M., Metten, L., Noth, J., 2009. Distal and proximal prehension is differentially affected by Parkinson's disease. *Journal of Neurology* 256, 450–456. doi:10.1007/s00415-009-0113-1
- Whishaw, I., Suchowersky, O., Davis, L., Sarna, J., Metz, G., Pellis, S., 2002. Impairment of pronation, supination, and body co-ordination in reach-to-grasp tasks in human Parkinson's disease (PD) reveals homology to deficits in animal models. *Behav. Brain Res.* 133, 165–176.
- Worbe, Y., Baup, N., Grabli, D., Chaigneau, M., Mounayar, S., McCairn, K., Feger, J., Tremblay, L., 2009. Behavioral and Movement Disorders Induced by Local Inhibitory Dysfunction in Primate Striatum. *Cereb Cortex* 19, 1844–1856. doi:10.1093/cercor/bhn214
- Wyss, A.F., Hamadjida, A., Savidan, J., Liu, Y., Bashir, S., Mir, A., Schwab, M.E., Rouiller, E.M., Belhaj-Saif, A., 2013. Long-term motor cortical map changes following unilateral lesion of the hand representation in the motor cortex in macaque monkeys showing functional recovery of hand functions. *Restor. Neurol. Neurosci.* 31, 733–760. doi:10.3233/RNN-130344
- Zigmond, M.J., Acheson, A.L., Stachowiak, M.K., Stricker, E.M., 1984. Neurochemical compensation after nigrostriatal bundle injury in an animal model of preclinical parkinsonism. *Archives of neurology* 41, 856–861.

## ***4 – General considerations and conclusion.***





## ***General considerations***

As exposed previously, PD is an age-linked pathology affecting 1 to 2% of the population over 65 years old and up to 5 % above 85 (Alves et al., 2008a). The socio-economical costs that can be attributed to this neurodegenerative disorder are massive. In our aging societies, the necessity of bringing new solutions for PD management has become a public health issue. By tackling this problematic from two different angles, this thesis brought new relevant information regarding the understanding of PD's pathophysiological processes, the feasibility of computer-aided diagnosis (CAD) and opened new perspective in terms of cell-based therapies.

### ***4.1 - Clinical aspects***

#### ***4.1.1 -Pathophysiological data***

Regarding the clinical aspects presented in the chapter 3.1, the creation of a neuroimaging database build around an exceptional pool of almost 1000 patients, allowed to conduct robust analyses that would not have been possible with small populations.

The group-level comparisons performed on MRI data including diffusion tensor imaging (DTI) and susceptibility weighted imaging (SWI) revealed new pathophysiological clues regarding the neurodegeneration of PD (chap. 3.1.1 and 3.1.2).

Yet, the originality of our approach was that, in contrary to most of the studies published at the time that were comparing PD patients with healthy controls, we decided to investigate the potential differences between PD and atypical forms of parkinsonism (Chan et al., 2007; Gattellaro et al., 2009; Karagulle Kendi et al., 2008). Despite of different paradigms, our results obtained on DTI data were globally in line with the observations of Kendi and colleagues (2008) showing an alteration of the white matter in the frontal lobe (Karagulle Kendi et al., 2008).

Similarly, the SWI investigation gave new information regarding the role of iron deposition into the brain during the neurodegenerative process, as suggested in the literature (Aquino et al., 2009; Thomas and Jankovic, 2004).

In a second time, we decided to conduct voxel-wise analyses on brain functional data. One of the inclusion criteria in our database was the availability of  $^{123}\text{I}$ -ioflupane SPECT images that are frequently performed to assess the integrity of the dopaminergic system in the clinical frame in order to exclude non-degenerative conditions of parkinsonisms like drug induced or vascular parkinsonism (Bajaj et al., 2013; Kägi et al., 2010; Sixel-Döring et al., 2011). This time, and in contrast to the SWI and DTI sequences, the important number of patients having a  $^{123}\text{I}$ -ioflupane SPECT furnished enough data to conduct spatial statistical analyses between the different forms of atypical parkinsonisms (multiple systems atrophy (MSA), parasupranuclear palsy (PSP) and cortico-basal degeneration (CBD)). Our results have underlined spatial differences in terms of striatal  $^{123}\text{I}$ -ioflupane SPECT signals, which were specific to each pathology. This suggests disparities regarding the dopaminergic depletion patterns (chapter 3.1.4).

Several investigations have tackled this problem and have emphasized that atypical parkinsonian syndromes (APS) were slightly different from PD regarding the dopaminergic activity (Brooks et al., 1990; Nocker et al., 2012; Pirker et al., 2000b; Seppi et al., 2006; Varrone et al., 2001). Yet, most of those studies included relatively limited number of patients and operator-dependent procedure while our results were built on a much larger number of cases in a very standardized manner.

Regarding the PD pathology itself, we were able to bring new information in front of the scene with respect to the spatiotemporal dopaminergic degeneration (chapter 3.1.3). Actually our data suggest a discrepancy in terms of nigro-striatal depletion between the stages of the disease and the duration of the disease. In fact, the duration seems to be associated with a linear decrease of the striatal uptake while the stage looks to be more linked to an exponential pattern. Moreover, using those two information as co-regressors for each other, the voxel-wise analysis showed different spatial

statistical clusters that correlates more specifically with the duration or with the stage.

Globally, those results were in line with the literature, showing a negative-correlation between the advancement of the pathology and the diminution of the dopaminergic striatal activity (Benamer et al., 2000; Brücke et al., 1997; Djaldetti et al., 2009; Marek et al., 2001; Tissingh et al., 1997). Nevertheless, those studies did not investigate the spatiotemporal evolution of the pathology and in contrary to our research, used manually defined regions of interest (ROI) for the quantification of the signal with the risk to induce a bias in the data.

#### **4.1.2 - Clinical relevance**

If the results summarized above are certainly of primary interest in regards with pathophysiological investigations and bring new insight in the processes underling the symptoms exerted by the patients affected by those disorders, they are unfortunately of little significance regarding their utility in the clinical frame. For those reasons, we decided to take advantage of the exact same database to perform individual patient classification using machine learning interface, in our case, support vector machine (SVM) and similar algorithm (Noble, 2006). Briefly, the SVM approach aims at finding the line that discriminates the best between two or more populations based on data of different nature (Haller et al., 2011; Noble, 2006). The classification is generally conducted in two steps: the first one consists in training the classifier with some data (e.g. length of the hairs for males and females) and, in a second step, to ask the classifier to assign the label male or female to a new data set (is it a male or a female?).

Relatively recently, several papers came out in which the authors used SVM technics to discriminate patients with neurological disorders from healthy controls based on brain structural or functional data (Haller et al., 2011; 2009; Klöppel et al., 2008; Magnin et al., 2009; Plant et al., 2010). Yet very few

studies investigated the potential of SVM in PD (Focke et al., 2011; Palumbo et al., 2014).

As the most clinically relevant question was not to discriminate PD patients from healthy controls, we decided to conduct our investigations using on one hand a group of PD patients and on another hand a group of patients affected by other forms of parkinsonisms including degenerative pathologies notably MSA, PSP and CBD.

Using the newly introduced susceptibility weighted imaging sequence that is sensitive to iron concentration, the classifier was able to discriminate PD cases from the others with an accuracy for 86% (chapter 3.1.2). In a study published in 2010, Huang and colleagues used SWI for diagnostic purpose in PD but were able to reach a limited accuracy of 59.2% (Huang et al., 2010). Based on tract-based spatial statistics (TBSS) data, we were even able to reach an accuracy of 97% (chapter 3.1.1).

Those results suggest that both sequences are providing relevant information for the distinction between those pathological conditions. Moreover, the differences in terms of accuracy indicate a higher sensitivity of DTI compared to SWI sequence.

As mentioned previously, the 123I-ioflupane SPECT are frequently used as a diagnostic tool in PD for the exclusion of non-degenerative pathologies. Yet, based on visual inspection only, it is not possible to set a diagnosis (Kägi et al., 2009). Based on the presumption that different patterns of dopaminergic degeneration occur in PD and atypical parkinsonian syndromes (APS) but that those modifications are discrete and *de facto* hardly visible at individual level, we chose to perform automated individual classification on our data (chapter 3.1.4). The results revealed that, at the exception of MSA, all groups were correctly classified above chance level (up to 60% for PSP). They also emphasized that extra-striatal signals are also provide relevant information. Yet the relatively limited seize of APS groups taken together with relatively important inter-individual variability in terms of 123I-ioflupane SPECT signal should be considered as an important limitation to the interpretation of those results.

In the future developments in neuroimaging and the probable decrease of the associated costs, I personally think that CAD will play an increasing role in the management of neurological disorders. Even if the aim is certainly not to replace the conventional clinical approaches, this technology could offer to small health structures the possibility to reorient patients with suspected pathologies to bigger structures that have access to specialists and so, to decrease the risk of misdiagnosis and inappropriate treatments related to important side-effects and consequences. Such techniques would also potentially allow to setup diagnosis at early stage of the pathology, when the symptoms could be misleading or even during the preclinical phase and so, help to provide the best therapeutic strategy to the patients.

This futuristic perspective would require the creation of large neuroimaging databases necessary to train efficiently the algorithm. To achieve this aim, the issues regarding the standardization of the acquisition (different protocols, different scanners, etc.) would need to be solved. In this sense, we conducted our investigations in an operator-free manner, decreasing the risk to introduce a human bias in the results.

Finally, and as suggested by Haller and colleagues, the combination of multi-modal sequences could certainly help to refine the computer-aided diagnosis even if further investigations and improvements are still required (Haller et al., 2014).

## ***4.2 - Pre-clinical evaluation of ANCE transplantation in a MPTP NHP model of PD***

The pre-clinical part of the present thesis that aimed at assessing the therapeutic potential of ANCE transplantation in a NHP model of PD, revealed a significant improvement of the motor functions following ANCE transplantation in all four MPTP monkeys (chapter 3.2.2). This recovery was especially eloquent in the two most affected animals. Globally, all specimens have seen their spontaneous activity significantly corrected while the improvements in terms of manual dexterity differed from one subject to another. These behavioral recoveries were accompanied with a significant increase of the  $^{18}\text{F}$ -DOPA striatal uptakes.

Histological investigations underlined an important number of PKH67 positive cells suggesting a high survival rate after transplantation as already shown by Brunet and colleagues (Bloch et al., 2014; Brunet et al., 2009). Moreover, no evident structural aberration was visible on the Nissl stained slices at six months post implantations. This poor carcinogenicity emphasize the good safety profile of those cells as claimed in previous publications (Bloch et al., 2014; Brunet et al., 2009; 2005; Kaeser et al., 2011).

Yet, if this study provides important clues indicating a positive effect of ANCE transplantation on the behavior and dopaminergic function (see chapter 3.2.2), the very limited number of animals and the absence of control prohibits to formally conclude to a causal link between functional recovery and cell implantation.

However, as repeated all along this thesis, the proof of efficacy of ANCE transplantation was already brought by Bloch and colleagues in a former publication and our goal was thus more to refine the knowledge regarding their behavioral and functional impacts using quantitative tools such as the MBB, the reach and grasp drawer task and the PET scan (Bloch et al., 2014).

In the landscape of cellular therapies for PD, autologous cell transplantations overcome important issues raised by the use of alternative cell sources, such

as fetal tissues and hESC. Indeed, by their nature, the problematic linked to immunological rejections as well as to ethical concerns are *de facto* solved. The ANCE approach is also for advantage, in contrary to the iPSC ones, to exhibit a low proliferation profile (Bloch et al., 2011; Brunet et al., 2009). Consequently, ANCE transplantations are much less prone to form tumors, which is recognized as one of the major concerns seen for iPSC / hPSC based therapies for translation to clinical trials (Björklund and Kordower, 2013; de Munter et al., 2014; A. S. Lee et al., 2009; Morizane and Li, 2008; Politis and Lindvall, 2012).

Now, one limitation of our paradigm resides in the fact that the development of the ANCE requires to perform a small cortical biopsy. Even if withdrawn from a region considered as “none-eloquent” by the neurosurgeons, this biopsy could potentially have consequences. However, and as suggested by the results presented in chapter 3.2.1, the biopsies below a certain critical size seems to have very limited behavioral consequences in regards with the dramatic disabilities associated with PD. Nevertheless, the possibility to cryopreserve cortical tissues as described by Brunet et al. (2003) open new possibilities (Brunet et al., 2003). We can easily imagine the creation of a brain tissues biobank that would preserve cortical tissues obtained during, for example, traumatic or epilepsy surgeries for future therapeutic applications.

In addition to the therapeutic aspects summarized above, the results presented in chapter 3.2.2 bring new information on front of the scene with respect to the impact of dopaminergic lesions on the control of manual dexterity in NHP MPTP model. Actually, if those aspects were extensively investigated in PD patients, very few studies have tackled this problematic in macaque monkey that are considered as the gold standards for PD research (Castiello and Bennett, 1997; Fellows et al., 1998; Vingerhoets et al., 1996; Whishaw et al., 2002).

### ***4.3 - Inter-species translation***

One of the objectives of this thesis that was built around clinical and pre-clinical aspects, was to underline new potential links between the NHP MPTP model and the human pathology especially in terms of neuroimaging. Unfortunately, due to the very important variability in terms of the lesion, it was very difficult to achieve this goal. Yet, this variability itself can be considered as a similarity. In fact, our results in macaque monkeys showed that for the same clinical score, two animals could express very large discrepancies in terms of striatal uptakes (chapter 3.2.2). On the same way one PD patient can have severe parkinsonian symptoms with  $^{123}\text{I}$ -loflupane SPECT values that could be the same in a “normal” subject (chap 3.1.3).

The postero-anterior evolution of the nigro-striatal depletion that was underlined in chapter 3.1.3 was also suggested by the results presented in monkeys in chapter 3.2.2, even if no conclusion can be made on the basis of this simple observation.

Over these “intra-thesis” points, the aspects regarding the impact of a dopaminergic lesion on the manual dexterity are making echo to this important clinical aspect of PD. The results related to the MBB and to the reach and grasp drawer task provide complementary information to an already well-established model and those tools offer new possibilities to investigate fine manual dexterity dysfunctions in PD, even if the inclusion of more animals would be required to refine the present data.



## ***4.4 - Conclusion and perspectives***

By tackling clinical and pre-clinical aspects that are, to my sense, representing two necessary and complementary approaches, the present thesis allowed to generate new data relevant for the understanding of PD's pathophysiology.

On one hand, we were able to support, in an original manner, that existing neuroimaging data that are largely underexploited, can provide relevant information specific to a certain pathology. Following a pragmatic approach, we succeeded to differentiate various forms of parkinsonism using classifier algorithms. Taken together, those results represent an additional proof a feasibility regarding the application of computer-aided diagnosis in the clinical frame.

On another hand, the pre-clinical assessment of ANCE transplantation in a NHP MPTP model consolidate the arguments in favor of a future clinical application published by Brunet and colleagues and Bloch and colleagues (Bloch et al., 2014; Brunet et al., 2009). Indeed, our study reveals that a functional recovery occurred few weeks after cell implantations in all four treated monkeys. Yet, the limited number of animal and the absence of control still represent an important limitation that has to be overcome.

In conclusion, even if the way to the patients' beds is still long, the different elements presented in this thesis contribute to bring concrete solutions necessary for the improvement of PD patients' management. Based on this evidences, further investigations are now required in order to fulfill the safety and efficacy requirements necessary for future potential clinical applications. Hopefully, the present results will bring some fuel the global effort to overcome this major public health challenge.



## 5- Bibliography

- Ahlskog, J.E., Uitti, R.J., O'Connor, M.K., Maraganore, D.M., Matsumoto, J.Y., Stark, K.F., Turk, M.F., Burnett, O.L., 1999. The effect of dopamine agonist therapy on dopamine transporter imaging in Parkinson's disease. *Movement Disorders* 14, 940–946. doi:10.1002/1531-8257(199911)14:6<940::AID-MDS1005>3.0.CO;2-Y
- Alexander, G.E., DeLong, M.R., STRICK, P.L., 1986. Parallel organization of functionally segregated circuits linking basal ganglia and cortex. *Annual review of neuroscience* 9, 357–381. doi:10.1146/annurev.ne.09.030186.002041
- Alves, G., Forsaa, E.B., Pedersen, K.F., Dreetz Gjerstad, M., Larsen, J.P., 2008a. Epidemiology of Parkinson's disease. *Journal of Neurology* 255, 18–32. doi:10.1007/s00415-008-5004-3
- Alves, G., Forsaa, E.B., Pedersen, K.F., Dreetz Gjerstad, M., Larsen, J.P., 2008b. Epidemiology of Parkinson's disease. *Journal of Neurology* 255, 18–32. doi:10.1007/s00415-008-5004-3
- Aquino, D., Bizzi, A., Grisoli, M., Garavaglia, B., Bruzzone, M.G., Nardocci, N., Savoardo, M., Chiapparini, L., 2009. Age-related iron deposition in the basal ganglia: quantitative analysis in healthy subjects. *Radiology* 252, 165–172. doi:10.1148/radiol.2522081399
- Arias-Carrión, O., Yuan, T.-F., 2009. Autologous neural stem cell transplantation: a new treatment option for Parkinson's disease? *Med Hypotheses* 73, 757–759. doi:10.1016/j.mehy.2009.04.029
- Ascherio, A., Zhang, S.M., Hernán, M.A., Kawachi, I., Colditz, G.A., Speizer, F.E., Willett, W.C., 2001. Prospective study of caffeine consumption and risk of Parkinson's disease in men and women. *Ann.Neurol* 50, 56–63.
- Astradsson, A., Cooper, O., Vinuela, A., 2008. Recent advances in cell-based therapy for Parkinson disease. *J.Neurosurg.*
- Bajaj, N., Hauser, R.A., Grachev, I.D., 2013. Clinical utility of dopamine transporter single photon emission CT (DaT-SPECT) with (123I) ioflupane in diagnosis of parkinsonian syndromes. *J Neurol Neurosurg Psychiatr* 84, 1288–1295. doi:10.1136/jnnp-2012-304436
- Baldwin, R.M., Zea Ponce, Y., al-Tikriti, M.S., Zoghbi, S.S., Seibyl, J.P., Charney, D.S., Hoffer, P.B., Wang, S., Milius, R.A., Neumeyer, J.L., 1995. Regional brain uptake and pharmacokinetics of [123I]N-omega-fluoroalkyl-2 beta-carboxy-3 beta- (4-iodophenyl)nortropine esters in baboons. *Nucl. Med. Biol.* 22, 211–219.
- Baron, J.A., 1986. Cigarette smoking and Parkinson's disease. *Neurology* 36, 1490–1490. doi:10.1212/WNL.36.11.1490
- Barraud, Q., Lambrecq, V., Forni, C., McGuire, S., Hill, M., Bioulac, B., Balzamo, E., Bezard, E., Tison, F., Ghorayeb, I., 2009. Sleep disorders in Parkinson's disease: the contribution of the MPTP non-human primate model. *Exp Neurol* 219, 574–582. doi:10.1016/j.expneurol.2009.07.019
- Bartels, A.L., Leenders, K.L., 2009. Parkinson's disease: The syndrome, the pathogenesis and pathophysiology. *Cortex* 45, 915–921. doi:10.1016/j.cortex.2008.11.010
- Ben-Hur, T., Idelson, M., Khaner, H., Pera, M., Reinhartz, E., Itzik, A.,

- Reubinoff, B.E., 2004. Transplantation of human embryonic stem cell-derived neural progenitors improves behavioral deficit in Parkinsonian rats. *Stem Cells* 22, 1246–1255. doi:10.1634/stemcells.2004-0094
- Benabid, A., 2003. Deep brain stimulation for Parkinson's disease. *Curr.Opin.Neurobiol.* 13, 696–706.
- Benabid, A.-L., Chabardes, S., Mitrofanis, J., Pollak, P., 2009. Deep brain stimulation of the subthalamic nucleus for the treatment of Parkinson's disease. *Lancet Neurol* 8, 67–81. doi:10.1016/S1474-4422 (08)70291-6
- BENABID, A.L., Pollak, P., Louveau, A., Henry, S., de Rougemont, J., 1987. Combined (Thalamotomy and Stimulation) Stereotactic Surgery of the VIM Thalamic Nucleus for Bilateral Parkinson Disease. *Stereotact Funct Neurosurg* 50, 344–346. doi:10.1159/000100803
- Benamer, H.T.S., Patterson, J., Wyper, D.J., Hadley, D.M., Macphee, G.J.A., Grosset, D.G., 2000. Correlation of Parkinson's disease severity and duration with 123I-FP-CIT SPECT striatal uptake. *Movement Disorders* 15, 692–698. doi:10.1002/1531-8257 (200007)15:4<692::AID-MDS1014>3.0.CO;2-V
- Bergman, H., Wichmann, T., DeLong, M.R., 1990. Reversal of experimental parkinsonism by lesions of the subthalamic nucleus. *Science* 249, 1436–1438.
- Betarbet, R., Sherer, T., MacKenzie, G., 2000. Chronic systemic pesticide exposure reproduces features of Parkinson's disease. *Nature*.
- Bjorklund, A., Brundin, P., Isacson, O., 1988. Neuronal replacement by intracerebral neural implants in animal models of neurodegenerative disease. *Adv Neurol* 47, 455–492.
- Björklund, A., Kordower, J.H., 2013. Cell therapy for Parkinson's disease: what next? *Movement Disorders* 28, 110–115. doi:10.1002/mds.25343
- Blesa, J., Juri, C., Collantes, M., Peñuelas, I., Prieto, E., Iglesias, E., Martí-Climent, J., Arbizu, J., Zubieta, J.L., Rodríguez-Oroz, M.C., García-García, D., Richter, J.A., Cavada, C., Obeso, J.A., 2010. Progression of dopaminergic depletion in a model of MPTP-induced parkinsonism in non-human primates. An 18F-DOPA and 11C-DTBZ PET study. *Neurobiol Dis* 38, 456–463. doi:10.1016/j.nbd.2010.03.006
- Blesa, J., Piffl, C., Sánchez-González, M.A., Juri, C., García-Cabezas, M.A., Adánez, R., Iglesias, E., Collantes, M., Penuelas, I., Sánchez-Hernández, J.J., Rodríguez-Oroz, M.C., Avendaño, C., Hornykiewicz, O., Cavada, C., Obeso, J.A., 2012. The nigrostriatal system in the presymptomatic and symptomatic stages in the MPTP monkey model: a PET, histological and biochemical study. *Neurobiol Dis* 48, 79–91. doi:10.1016/j.nbd.2012.05.018
- Bloch, J., Brunet, J.-F., McEntire, C.R.S., Redmond, D.E., 2014. Primate adult brain cell autotransplantation produces behavioral and biological recovery in 1-methyl-4-phenyl-1,2,3,6-tetrahydropyridine-induced parkinsonian St. Kitts monkeys. *J Comp Neurol* 522, 2729–2740. doi:10.1002/cne.23579
- Bloch, J., Kaeser, M., Sadeghi, Y., Rouiller, E.M., Redmond, D.E., Brunet, J.-F., 2011. Doublecortin-positive cells in the adult primate cerebral cortex and possible role in brain plasticity and development. *J Comp Neurol* 519, 775–789. doi:10.1002/cne.22547
- Booij, J., Andringa, G., Rijks, L.J., Vermeulen, R.J., de Bruin, K., Boer, G.J., Janssen, A.G., van Royen, E.A., 1997a. [123I]FP-CIT binds to the

- dopamine transporter as assessed by biodistribution studies in rats and SPECT studies in MPTP-lesioned monkeys. *Synapse* 27, 183–190. doi:10.1002/(SICI)1098-2396(199711)27:3<183::AID-SYN4>3.0.CO;2-9
- Booij, J., Tissingh, G., Winogrodzka, A., Boer, G.J., Stoof, J.C., Wolters, E.C., van Royen, E.A., 1997b. Practical benefit of [<sup>123</sup>I]FP-CIT SPET in the demonstration of the dopaminergic deficit in Parkinson's disease. *Eur J Nucl Med* 24, 68–71. doi:10.1007/BF01728311
- Braak, H., Braak, E., 2000. Pathoanatomy of Parkinson's disease. *Journal of Neurology* 247 Suppl 2, II3–10.
- Braak, H., Del Tredici, K., Rüb, U., de Vos, R.A.I., Jansen Steur, E.N.H., Braak, E., 2003a. Staging of brain pathology related to sporadic Parkinson's disease. *Neurobiol Aging* 24, 197–211.
- Braak, H., Tredici, K.D., Rüb, U., de Vos, R.A.I., Jansen Steur, E.N.H., Braak, E., 2003b. Staging of brain pathology related to sporadic Parkinson's disease. *Neurobiol Aging* 24, 197–211. doi:10.1016/S0197-4580(02)00065-9
- Brederlau, A., Correia, A.S., Anisimov, S.V., Elmi, M., Paul, G., Roybon, L., Morizane, A., Bergquist, F., Riebe, I., Nannmark, U., Carta, M., Hanse, E., Takahashi, J., Sasai, Y., Funa, K., Brundin, P., Eriksson, P.S., Li, J.-Y., 2006. Transplantation of human embryonic stem cell-derived cells to a rat model of Parkinson's disease: effect of in vitro differentiation on graft survival and teratoma formation. *Stem Cells* 24, 1433–1440. doi:10.1634/stemcells.2005-0393
- Brinkman, C., 1981. Lesions in supplementary motor area interfere with a monkey's performance of a bimanual coordination task. *Neurosci Lett* 27, 267–270.
- Brinkman, J., Kuypers, H.G., 1973. Cerebral control of contralateral and ipsilateral arm, hand and finger movements in the split-brain rhesus monkey. *Brain* 96, 653–674.
- Brooks, D.J., 2012. Can imaging separate multiple system atrophy from Parkinson's disease? *Movement Disorders* 27, 3–5. doi:10.1002/mds.24046
- Brooks, D.J., 2010. Imaging approaches to Parkinson disease. *J Nucl Med* 51, 596–609. doi:10.2967/jnumed.108.059998
- Brooks, D.J., IBANEZ, V., Sawle, G.V., Quinn, N., Lees, A.J., MATHIAS, C.J., BANNISTER, R., Marsden, C.D., Frackowiak, R., 1990. Differing Patterns of Striatal F-18 Dopa Uptake in Parkinsons-Disease, Multiple System Atrophy, and Progressive Supranuclear Palsy. *Ann.Neurol* 28, 547–555. doi:10.1002/ana.410280412
- Brooks, D.J., Pavese, N., 2011. ScienceDirect.com - Progress in Neurobiology - Imaging biomarkers in Parkinson's disease. *Prog Neurobiol*.
- Brown, J.P., Couillard-Després, S., Cooper-Kuhn, C.M., Winkler, J., Aigner, L., Kuhn, H.G., 2003. Transient expression of doublecortin during adult neurogenesis. *J. Comp. Neurol.* 467, 1–10. doi:10.1002/cne.10874
- Brundin, P., Bjorklund, A., 1987. Survival, growth and function of dopaminergic neurons grafted to the brain. *Prog Brain Res* 71, 293–308.
- Brundin, P., Pogarell, O., Hagell, P., Piccini, P., Widner, H., Schrag, A., Kupsch, A., Crabb, L., Odin, P., Gustavii, B., Bjorklund, A., Brooks, D.J., Marsden, C.D., Oertel, W.H., Quinn, N.P., Rehncrona, S., Lindvall, O.,

2000. Bilateral caudate and putamen grafts of embryonic mesencephalic tissue treated with lazaroïds in Parkinson's disease. *Brain* 123 ( Pt 7), 1380–1390.
- Brundin, P., Strecker, R.E., Lindvall, O., Isacson, O., Nilsson, O.G., Barbin, G., Prochiantz, A., Forni, C., Nieoullon, A., Widner, H., 1987. Intracerebral grafting of dopamine neurons. Experimental basis for clinical trials in patients with Parkinson's disease. *Ann. N. Y. Acad. Sci.* 495, 473–496.
- Brunet, J.-F., Pellerin, L., Magistretti, P., Villemure, J.-G., 2003. Cryopreservation of human brain tissue allowing timely production of viable adult human brain cells for autologous transplantation. *Cryobiology* 47, 179–183. doi:10.1016/j.cryobiol.2003.08.005
- Brunet, J.-F., Redmond, D.E., Bloch, J., 2009. Primate adult brain cell autotransplantation, a pilot study in asymptomatic MPTP-treated monkeys. *Cell Transplant.* 18, 787–799. doi:10.3727/096368909X470847
- Brunet, J.-F.C.O., Pellerin, L., Arsenijevic, Y., Magistretti, P., Villemure, J.-G., 2002. A Novel Method for In Vitro Production of Human Glial-Like Cells from Neurosurgical Resection Tissue. *Laboratory Investigation* 82, 809–812. doi:10.1097/01.LAB.0000017166.26718.BB
- Brunet, J.F., Rouiller, E., Wannier, T., Villemure, J.G., Bloch, J., 2005. Primate adult brain cell autotransplantation, a new tool for brain repair? *Exp Neurol* 196, 195–198. doi:10.1016/j.expneurol.2005.04.005
- Brücke, P.D.T., Asenbaum, S., Pirker, W., Djamshidian, S., Wenger, S., Wöber, C., Müller, C., Podreka, I., 1997. Measurement of the dopaminergic degeneration in Parkinson's disease with [123I]β-CIT and SPECT, in: *Advances in Research on Neurodegeneration, Journal of Neural Transmission. Supplementa.* Springer Vienna, Vienna, pp. 9–24. doi:10.1007/978-3-7091-6842-4\_2
- Burn, D.J., Sawle, G.V., Brooks, D.J., 1994. Differential diagnosis of Parkinson's disease, multiple system atrophy, and Steele-Richardson-Olszewski syndrome: discriminant analysis of striatal 18F-dopa PET data. *J Neurol Neurosurg Psychiatr* 57, 278–284.
- Carlsson, A., LINDQVIST, M., MAGNUSSON, T., 1957. 3,4-Dihydroxyphenylalanine and 5-Hydroxytryptophan as Reserpine Antagonists. *Nature* 180, 1200–1200. doi:10.1038/1801200a0
- Castiello, U., Bennett, K., 1997. The bilateral reach-to-grasp movement of Parkinson's disease subjects. *Brain* 120, 593–604. doi:10.1093/brain/120.4.593
- Celada, P., Paladini, C.A., Tepper, J.M., 1999. Gabaergic control of rat substantia nigra dopaminergic neurons: Role of globus pallidus and substantia nigra pars reticulata. *Neuroscience* 89, 813–825. doi:10.1016/S0306-4522 (98)00356-X
- Chan, L.L., Rumpel, H., Yap, K., Lee, E., Loo, H.V., 2007. Case control study of diffusion tensor imaging in Parkinson's disease. *Journal of Neurology.*
- Charcot, J.M., 1897. La foi qui guérit.
- Ciehanover, A., Hod, Y., Hershko, A., 1978. A heat-stable polypeptide component of an ATP-dependent proteolytic system from reticulocytes. *Biochem.Biophys.Res.Commun.* 81, 1100–1105.
- Collier, T., Steece-Collier, K., Kordower, J., 2003. Primate models of Parkinson's disease. *Exp Neurol* 183, 258–262.
- Comoli, E., Coizet, V., Boyes, J., BOLAM, J.P., Canteras, N.S., Quirk, R.H.,

- Overton, P.G., Redgrave, P., 2003. A direct projection from superior colliculus to substantia nigra for detecting salient visual events. *Nature Neuroscience* 6, 974–980. doi:10.1038/nn1113
- Corrigan, F.M., Murray, L., Wyatt, C.L., Shore, R.F., 1998. Diorthosubstituted polychlorinated biphenyls in caudate nucleus in Parkinson's disease. *Exp Neurol* 150, 339–342. doi:10.1006/exnr.1998.6776
- Courtine, G., Bunge, M.B., Fawcett, J.W., Grossman, R.G., Kaas, J.H., Lemon, R., Maier, I., Martin, J., Nudo, R.J., Ramon-Cueto, A., Rouiller, E.M., Schnell, L., Wannier, T., Schwab, M.E., Edgerton, V.R., 2007. Can experiments in nonhuman primates expedite the translation of treatments for spinal cord injury in humans? *Nat Med* 13, 561–566. doi:10.1038/nm1595
- Curtis, M.A., Eriksson, P.S., Faull, R.L., 2007. PROGENITOR CELLS AND ADULT NEUROGENESIS IN NEURODEGENERATIVE DISEASES AND INJURIES OF THE BASAL GANGLIA. *Clinical and Experimental Pharmacology and Physiology* 34, 528–532. doi:10.1111/j.1440-1681.2007.04609.x
- Da Cunha, C., Boschen, S.L., Gómez-A, A., Ross, E.K., Gibson, W.S.J., Min, H.-K., Lee, K.H., Blaha, C.D., 2015. Toward sophisticated basal ganglia neuromodulation: Review on basal ganglia deep brain stimulation. *Neuroscience and Biobehavioral Reviews*. doi:10.1016/j.neubiorev.2015.02.003
- Darcourt, J., Schiavza, A., Sapin, N., Dufour, M., Ouvrier, M.J., Benisvy, D., Fontana, X., Koulibaly, P.M., 2014. 18F-FDOPA PET for the diagnosis of parkinsonian syndromes. *Q J Nucl Med Mol Imaging* 58, 355–365.
- Dauer, W., 2003. Parkinson's Disease:: Mechanisms and Models. *Neuron*.
- Davie, C., 2008. A review of Parkinson's disease. *British medical bulletin*.
- de Munter, J.P.J.M., Melamed, E., Wolters, E.C., 2014. Stem cell grafting in parkinsonism--why, how and when. *parkinsonism.Relat Disord.* 20 Suppl 1, S150–3. doi:10.1016/S1353-8020 (13)70036-1
- DeLong, M.R., Alexander, G.E., Georgopoulos, A.P., Crutcher, M.D., Mitchell, S.J., Richardson, R.T., 1984. Role of basal ganglia in limb movements. *Hum Neurobiol* 2, 235–244.
- DeLong, M.R., Coyle, J.T., 1979. Globus Pallidus lesions in the monkey produced by kainic acid: histologic and behavioral effects. *Appl Neurophysiol* 42, 95–97.
- DeLong, M.R., Crutcher, M.D., Georgopoulos, A.P., 1985. Primate globus pallidus and subthalamic nucleus: functional organization. *J Neurophysiol* 53, 530–543.
- DeLong, M.R., Wichmann, T., 2007. Circuits and circuit disorders of the basal ganglia. *Archives of neurology* 64, 20–24. doi:10.1001/archneur.64.1.20
- Djaldetti, R., Treves, T.A., Ziv, I., Melamed, E., Lampl, Y., Lorberboym, M., 2009. Use of a single [123I]-FP-CIT SPECT to predict the severity of clinical symptoms of Parkinson disease. *Neurol Sci* 30, 301–305. doi:10.1007/s10072-009-0100-4
- Djang, D.S.W., Janssen, M.J.R., Bohnen, N., Booij, J., Henderson, T.A., Herholz, K., Minoshima, S., Rowe, C.C., Sabri, O., Seibyl, J., Van Berckel, B.N.M., Wanner, M., 2012. SNM Practice Guideline for Dopamine Transporter Imaging with 123I-Ioflupane SPECT 1.0. *J. Nucl. Med.* 53, 154–163. doi:10.2967/jnumed.111.100784

- Doi, D., Samata, B., Katsukawa, M., Kikuchi, T., Morizane, A., Ono, Y., Sekiguchi, K., Nakagawa, M., Parmar, M., Takahashi, J., 2014. Isolation of human induced pluripotent stem cell-derived dopaminergic progenitors by cell sorting for successful transplantation. *Stem Cell Reports* 2, 337–350. doi:10.1016/j.stemcr.2014.01.013
- Doty, R.L., 2012. Olfactory dysfunction in Parkinson disease. *Nat.Rev.Neurol* 8, 329–339. doi:10.1038/nrneurol.2012.80
- DOUDET, D., CORNFELDT, M., HONEY, C., SCHWEIKERT, A., ALLEN, R., 2004. PET imaging of implanted human retinal pigment epithelial cells in the MPTP-induced primate model of Parkinson's disease. *Exp Neurol* 189, 361–368. doi:10.1016/j.expneurol.2004.06.009
- Emborg, M.E., 2007. Nonhuman primate models of Parkinson's disease. *ILAR.J.* 48, 339–355.
- Farrer, M., Maraganore, D.M., Lockhart, P., Singleton, A., Lesnick, T.G., de Andrade, M., West, A., de Silva, R., Hardy, J., Hernandez, D., 2001. alpha-Synuclein gene haplotypes are associated with Parkinson's disease. *Hum. Mol. Genet.* 10, 1847–1851.
- Fellows, S.J., Noth, J., Schwarz, M., 1998. Precision grip and Parkinson's disease. *Brain* 121 ( Pt 9), 1771–1784.
- Fink, G.R., Frackowiak, R., Pietrzyk, U., Passingham, R.E., 1997. Multiple nonprimary motor areas in the human cortex. *J Neurophysiol* 77, 2164–2174.
- Flaherty, A.W., Graybiel, A.M., 1993. Two input systems for body representations in the primate striatal matrix: experimental evidence in the squirrel monkey. *J Neurosci* 13, 1120–1137.
- Focke, N.K., Helms, G., Scheewe, S., Pantel, P.M., 2011. Individual voxel-based subtype prediction can differentiate progressive supranuclear palsy from idiopathic parkinson syndrome and healthy controls. *Human brain ....*
- Follett, K.A., Weaver, F.M., Stern, M., Hur, K., Harris, C.L., Luo, P., Marks, W.J., Rothlind, J., Sagher, O., Moy, C., Pahwa, R., Burchiel, K., Hogarth, P., Lai, E.C., Duda, J.E., Holloway, K., Samii, A., Horn, S., Bronstein, J.M., Stoner, G., Starr, P.A., Simpson, R., Baltuch, G., De Salles, A., Huang, G.D., Reda, D.J., CSP 468 Study Group, 2010. Pallidal versus subthalamic deep-brain stimulation for Parkinson's disease. *N Engl J Med* 362, 2077–2091. doi:10.1056/NEJMoa0907083
- Forno, L.S., DeLanney, L.E., Irwin, I., Langston, J.W., 1993. Similarities and differences between MPTP-induced parkinsonism and Parkinson's disease. Neuropathologic considerations. *Adv Neurol* 60, 600–608.
- Forster, E., Lewy, F.H., 1912. Paralysis agitans. ... *Anatomie. Handbuch der Neurologie.* Berlin: Springer ....
- Francis, F., Koulakoff, A., Boucher, D., Chafey, P., Schaar, B., Vinet, M.-C., Friocourt, G., McDonnell, N., Reiner, O., Kahn, A., McConnell, S.K., Berwald-Netter, Y., Denoulet, P., Chelly, J., 1999. Doublecortin Is a Developmentally Regulated, Microtubule-Associated Protein Expressed in Migrating and Differentiating Neurons. *Neuron* 23, 247–256. doi:10.1016/S0896-6273(00)80777-1
- Freed, C., Greene, P., Breeze, R., 2001. Transplantation of embryonic dopamine neurons for severe Parkinson's disease. ... *England Journal of ....*
- Freed, C.R., Breeze, R.E., Fahn, S., Eidelberg, D., 2004. Preoperative



- response to levodopa is the best predictor of transplant outcome. *Ann.Neurol* 55, 896; author reply 896–7. doi:10.1002/ana.20085
- Freed, C.R., Breeze, R.E., Rosenberg, N.L., Schneck, S.A., Kriek, E., Qi, J.X., Lone, T., Zhang, Y.B., Snyder, J.A., Wells, T.H., 1992. Survival of implanted fetal dopamine cells and neurologic improvement 12 to 46 months after transplantation for Parkinson's disease. *N Engl J Med* 327, 1549–1555. doi:10.1056/NEJM199211263272202
- Freeman, T.B., Vawter, D.E., Leaverton, P.E., 1999. The use of a surgical placebo-control in evaluating cellular-based therapy for Parkinson's disease. *N Engl J Med*.
- Freund, H.J., 1985. Clinical aspects of premotor function. *Behav.Brain Res.* 18, 187–191.
- Freund, H.J., Hummelsheim, H., 1985. Lesions of premotor cortex in man. *Brain* 108 ( Pt 3), 697–733.
- Freund, P., Schmidlin, E., Wannier, T., Bloch, J., Mir, A., Schwab, M.E., Rouiller, E.M., 2009. Anti-Nogo-A antibody treatment promotes recovery of manual dexterity after unilateral cervical lesion in adult primates - re-examination and extension of behavioral data. *European Journal of Neuroscience* 29, 983–996. doi:10.1111/j.1460-9568.2009.06642.x
- Gaig, C., Martí, M.J., Tolosa, E., Valldeoriola, F., Paredes, P., Lomeña, F.J., Nakamae, F., 2006. 123I-loflupane SPECT in the diagnosis of suspected psychogenic parkinsonism. *Movement Disorders* 21, 1994–1998. doi:10.1002/mds.21062
- Garnett, E.S., Firnau, G., Nahmias, C., 1983. Dopamine Visualized in the Basal Ganglia of Living Man. *Nature* 305, 137–138. doi:10.1038/305137a0
- Gattellaro, G., Minati, L., Grisoli, M., Mariani, C., Carella, F., Osio, M., Ciceri, E., Albanese, A., Bruzzone, M.G., 2009. White Matter Involvement in Idiopathic Parkinson Disease: A Diffusion Tensor Imaging Study. *AJNR Am J Neuroradiol* 30, 1222–1226. doi:10.3174/ajnr.A1556
- Gerfen, C.R., 1995. Dopamine-Receptor Function in the Basal Ganglia. *Clin Neuropharmacol* 18, S162–S177.
- Gerfen, C.R., 1992a. D1 and D2 dopamine receptor regulation of striatonigral and striatopallidal neurons. *Seminars in Neuroscience* 4, 109–118. doi:10.1016/1044-5765(92)90009-Q
- Gerfen, C.R., 1992b. The neostriatal mosaic: multiple levels of compartmental organization in the basal ganglia. *Annual review of neuroscience* 15, 285–320. doi:10.1146/annurev.ne.15.030192.001441
- Geyer, S., Ledberg, A., Schleicher, A., Kinomura, S., Schormann, T., Bürgel, U., Klingberg, T., Larsson, J., Zilles, K., Roland, P.E., 1996. Two different areas within the primary motor cortex of man. *Nature* 382, 805–807. doi:10.1038/382805a0
- Goetz, C.G., Wu, J., McDermott, M.P., Adler, C.H., Fahn, S., Freed, C.R., Hauser, R.A., Olanow, W.C., Shoulson, I., Tandon, P.K., Parkinson Study Group, Leurgans, S., 2008. Placebo response in Parkinson's disease: comparisons among 11 trials covering medical and surgical interventions. *Movement Disorders* 23, 690–699. doi:10.1002/mds.21894
- Grealish, S., Diguët, E., Kirkeby, A., Mattsson, B., Heuer, A., Bramoulle, Y., Van Camp, N., Perrier, A.L., Hantraye, P., Björklund, A., Parmar, M., 2014. Human ESC-Derived Dopamine Neurons Show Similar Preclinical Efficacy and Potency to Fetal Neurons when Grafted in a Rat Model of

- Parkinson's Disease. *Stem Cell* 15, 653–665.  
doi:10.1016/j.stem.2014.09.017
- Greffard, S., VERNY, M., BONNET, A.-M., BEINIS, J.-Y., GALLINARI, C., MEAUME, S., PIETTE, F., HAUW, J.-J., DUYSCKAERTS, C., 2006. Motor Score of the Unified Parkinson Disease Rating Scale as a Good Predictor of Lewy Body–Associated Neuronal Loss in the Substantia Nigra. *Archives of neurology* 63, 584–588. doi:10.1001/archneur.63.4.584
- Guttman, M., YONG, V.W., KIM, S.U., CALNE, D.B., MARTIN, W.R.W., ADAM, M.J., RUTH, T.J., 1988. Asymptomatic striatal dopamine depletion: PET scans in unilateral MPTP monkeys. *Synapse* 2, 469–473.  
doi:10.1002/syn.890020502
- Haacke, E.M., XU, Y.B., CHENG, Y., REICHENBACH, J.R., 2004. Susceptibility weighted imaging (SWI). *Magn Reson Med* 52, 612–618.  
doi:10.1002/mrm.20198
- Haber, S.N., 2014. The place of dopamine in the cortico-basal ganglia circuit. *Neuroscience* 282C, 248–257. doi:10.1016/j.neuroscience.2014.10.008
- Hall, V.J., LI, J.-Y., BRUNDIN, P., 2007. Restorative cell therapy for Parkinson's disease: a quest for the perfect cell. *Semin. Cell Dev. Biol.* 18, 859–869.  
doi:10.1016/j.semcdb.2007.09.004
- Haller, S., LOVBLAD, K.O., GIANNAKOPOULOS, P., 2011. Principles of classification analyses in mild cognitive impairment (MCI) and Alzheimer disease. *J. Alzheimers Dis.* 26 Suppl 3, 389–394. doi:10.3233/JAD-2011-0014
- Haller, S., LÖVBLAD, K.O., GIANNAKOPOULOS, P., VILLE, D., 2014. Multivariate Pattern Recognition for Diagnosis and Prognosis in Clinical Neuroimaging: State of the Art, Current Challenges and Future Trends. *Brain Topogr* 1–9.  
doi:10.1007/s10548-014-0360-z
- Haller, S., NGUYEN, D., RODRIGUEZ, C., EMCH, J., 2009. Individual prediction of cognitive decline in mild cognitive impairment using support vector machine-based analysis of diffusion tensor imaging data. *Journal of Alzheimer's ....*
- Hallett, P.J., DELEIDI, M., ASTRADSSON, A., SMITH, G.A., COOPER, O., OSBORN, T.M., SUNDBERG, M., MOORE, M.A., PEREZ-TORRES, E., BROWNELL, A.-L., SCHUMACHER, J.M., SPEALMAN, R.D., ISACSON, O., 2015. Successful Function of Autologous iPSC-Derived Dopamine Neurons following Transplantation in a Non-Human Primate Model of Parkinson's Disease. *Stem Cell* 1–7. doi:10.1016/j.stem.2015.01.018
- Halliday, G.M., STEVENS, C.H., 2011. Glia: Initiators and progressors of pathology in Parkinson's disease. *Movement Disorders* 26, 6–17.  
doi:10.1002/mds.23455
- Hammond, C., BERGMAN, H., BROWN, P., 2007. Pathological synchronization in Parkinson's disease: networks, models and treatments. *Trends in Neurosciences* 30, 357–364. doi:10.1016/j.tins.2007.05.004
- Hauser, R.A., FREEMAN, T.B., SNOW, B.J., NAUERT, M., GAUGER, L., KORDOWER, J.H., OLANOW, C.W., 1999. Long-term evaluation of bilateral fetal nigral transplantation in Parkinson disease. *Archives of neurology* 56, 179–187.
- Haynes, W.I.A., HABER, S.N., 2013. The organization of prefrontal-subthalamic inputs in primates provides an anatomical substrate for both functional specificity and integration: implications for Basal Ganglia models and deep brain stimulation. *Journal of Neuroscience* 33, 4804–4814.

- doi:10.1523/JNEUROSCI.4674-12.2013
- Heimer, L., Wilson, R.D., 1975. The subcortical projections of the allocortex: similarities in the neural associations of the hippocampus, the piriform cortex, and the neocortex. *Golgi centennial symposium* ....
- Hepp-Reymond, Trouche, E., Wiesendanger, M., 1974. Effects of unilateral and bilateral pyramidotomy on a conditioned rapid precision grip in monkeys (*Macaca fascicularis*). *Exp. Brain Res.* 21, 519–527.
- HERRERO, M.T., Hirsch, E.C., JAVOYAGID, F., Obeso, J.A., Agid, Y., 1993. Differential Vulnerability to 1-Methyl-4-Phenyl-1,2,3,6-Tetrahydropyridine of Dopaminergic and Cholinergic Neurons in the Monkey Mesopontine Tegmentum. *Brain Res* 624, 281–285.
- Hirsch, E., Graybiel, A.M., Agid, Y.A., 1988. Melanized dopaminergic neurons are differentially susceptible to degeneration in Parkinson's disease. *Nature* 334, 345–348. doi:10.1038/334345a0
- Hirsch, E.C., Hunot, S., 2000. Nitric oxide, glial cells and neuronal degeneration in parkinsonism. *Trends in Pharmacological Sciences*.
- Hoogewoud, F., Hamadjida, A., Wyss, A.F., Mir, A., Schwab, M.E., Belhaj-Saif, A., Rouiller, E.M., 2013. Comparison of Functional Recovery of Manual Dexterity after Unilateral Spinal Cord Lesion or Motor Cortex Lesion in Adult Macaque Monkeys. *Frontiers in Neurology* 4, 101. doi:10.3389/fneur.2013.00101
- Huang, X.M., Sun, B., Xue, Y.J., Duan, Q., 2010. [Susceptibility-weighted imaging in detecting brain iron accumulation of Parkinson's disease]. *Zhonghua yi xue za zhi*.
- Imbert, C.C., Bezard, E.E., Guitraud, S.S., Boraud, T.T., Gross, C.E.C., 2000. Comparison of eight clinical rating scales used for the assessment of MPTP-induced parkinsonism in the Macaque monkey. *J Neurosci Methods* 96, 71–76.
- Innis, R.B., Marek, K.L., Sheff, K., Zoghbi, S., Castronuovo, J., Feigin, A., Seibyl, J.P., 1999. Effect of treatment with L-dopa/carbidopa or L-selegiline on striatal dopamine transporter SPECT imaging with [<sup>123</sup>I]β-CIT. *Movement Disorders* 14, 436–442. doi:10.1002/1531-8257(199905)14:3<436::AID-MDS1008>3.0.CO;2-J
- Isacson, O., Pritzel, M., Dawbarn, D., Brundin, P., Kelly, P.A., Wiklund, L., Emson, P.C., Gage, F.H., Dunnett, S.B., Bjorklund, A., 1987. Striatal neural transplants in the ibotenic acid-lesioned rat neostriatum. Cellular and functional aspects. *Ann. N. Y. Acad. Sci.* 495, 537–555.
- Johansson, C.B., Momma, S., Clarke, D.L., Risling, M., Lendahl, U., Frisén, J., 1999. Identification of a Neural Stem Cell in the Adult Mammalian Central Nervous System. *Cell* 96, 25–34. doi:10.1016/S0092-8674(00)80956-3
- Jones, E.G., Coulter, J.D., Burton, H., Porter, R., 1977. Cells of origin and terminal distribution of corticostriatal fibers arising in the sensory-motor cortex of monkeys. *J. Comp. Neurol.* 173, 53–80. doi:10.1002/cne.901730105
- Kaaser, M., Brunet, J.-F., Wyss, A., Belhaj-Saif, A., Liu, Y., Hamadjida, A., Rouiller, E.M., Bloch, J., 2011. Autologous adult cortical cell transplantation enhances functional recovery following unilateral lesion of motor cortex in primates: a pilot study. *Neurosurgery* 68, 1405–16–discussion 1416–7. doi:10.1227/NEU.0b013e31820c02c0

- Kamp, F., Exner, N., Lutz, A.K., Wender, N., Hegermann, J., Brunner, B., Nuscher, B., Bartels, T., Giese, A., Beyer, K., Eimer, S., Winklhofer, K.F., Haass, C., 2010. Inhibition of mitochondrial fusion by  $\alpha$ -synuclein is rescued by PINK1, Parkin and DJ-1. *EMBO J.* 29, 3571–3589. doi:10.1038/emboj.2010.223
- Karagulle Kendi, A.T., Lehericy, S., Luciana, M., Ugurbil, K., Tuite, P., 2008. Altered Diffusion in the Frontal Lobe in Parkinson Disease. *AJNR Am J Neuroradiol* 29, 501–505. doi:10.3174/ajnr.A0850
- KAUFMAN, M.J., MADRAS, B.K., 1991. Severe Depletion of Cocaine Recognition Sites Associated with the Dopamine Transporter in Parkinsons-Diseased Striatum. *Synapse* 9, 43–49. doi:10.1002/syn.890090107
- Kawasaki, H., Mizuseki, K., Nishikawa, S., Kaneko, S., Kuwana, Y., Nakanishi, S., Nishikawa, S.I., Sasai, Y., 2000. Induction of midbrain dopaminergic neurons from ES cells by stromal cell-derived inducing activity. *Neuron* 28, 31–40.
- Kazennikov, O., Hyland, B., Corboz, M., Babalian, A., Rouiller, E.M., Wiesendanger, M., 1999. Neural activity of supplementary and primary motor areas in monkeys and its relation to bimanual and unimanual movement sequences. *Neuroscience* 89, 661–674. doi:10.1016/S0306-4522(98)00348-0
- Kazennikov, O., Hyland, B., Wicki, U., Perrig, S., Rouiller, E.M., Wiesendanger, M., 1998. Effects of lesions in the mesial frontal cortex on bimanual co-ordination in monkeys. *Neuroscience* 85, 703–716. doi:10.1016/S0306-4522(97)00693-3
- Kägi, G., Bhatia, K.P., Tolosa, E., 2010. The role of DAT-SPECT in movement disorders. *J Neurol Neurosurg Psychiatr* 81, 5–12. doi:10.1136/jnnp.2008.157370
- Kägi, G., Bhatia, K.P., Tolosa, E., 2009. The role of DAT-SPECT in movement disorders. *J Neurol Neurosurg Psychiatr* 81, 5–12. doi:10.1136/jnnp.2008.157370
- Kefalopoulou, Z., Politis, M., Piccini, P., Mencacci, N., Bhatia, K., Jahanshahi, M., Widner, H., Rehncrona, S., Brundin, P., Björklund, A., Lindvall, O., Limousin, P., Quinn, N., Foltynie, T., 2014. Long-term Clinical Outcome of Fetal Cell Transplantation for Parkinson Disease. *JAMA Neurol* 71, 83–5. doi:10.1001/jamaneurol.2013.4749
- Keller, G.M., 1995. In vitro differentiation of embryonic stem cells. *Curr. Opin. Cell Biol.* 7, 862–869.
- Kermadi, I., Liu, Y., Rouiller, E.M., 2000. Do bimanual motor actions involve the dorsal premotor (PMd), cingulate (CMA) and posterior parietal (PPC) cortices? Comparison with primary and supplementary motor cortical areas. *Somatosens Mot Res* 17, 255–271. doi:10.1080/08990220050117619
- Kermadi, I., Liu, Y., Tempini, A., Calciati, E., Rouiller, E.M., 1998. Neuronal activity in the primate supplementary motor area and the primary motor cortex in relation to spatio-temporal bimanual coordination. *Somatosens Mot Res* 15, 287–308.
- Kermadi, I., Liu, Y., Tempini, A., Rouiller, E.M., 1997. Effects of reversible inactivation of the supplementary motor area (SMA) on unimanual grasp and bimanual pull and grasp performance in monkeys. *Somatosens Mot*

- Res 14, 268–280. doi:10.1080/08990229770980
- KINDT, M.V., HEIKKILA, R.E., NICKLAS, W.J., 1987. Mitochondrial and metabolic toxicity of 1-methyl-4- (2'-methylphenyl)-1,2,3,6-tetrahydropyridine. *J Pharmacol Exp Ther* 242, 858–863.
- Kitada, T., Asakawa, S., Hattori, N., Matsumine, H., Yamamura, Y., Minoshima, S., Yokochi, M., Mizuno, Y., Shimizu, N., 1998. Mutations in the parkin gene cause autosomal recessive juvenile parkinsonism. *Nature* 392, 605–608. doi:10.1038/33416
- Klöppel, S., Stonnington, C.M., Chu, C., Draganski, B., Scahill, R.I., Rohrer, J.D., Fox, N.C., Jack, C.R., Ashburner, J., Frackowiak, R.S.J., 2008. Automatic classification of MR scans in Alzheimer's disease. *Brain* 131, 681–689. doi:10.1093/brain/awm319
- Kopin, I., Markey, S., 1988. MPTP toxicity: implications for research in Parkinson's disease. *Annual review of neuroscience*.
- Kriks, S., Shim, J.-W., Piao, J., Ganat, Y.M., Wakeman, D.R., Xie, Z., Carrillo-Reid, L., Auyeung, G., Antonacci, C., Buch, A., Yang, L., Beal, M.F., Surmeier, D.J., Kordower, J.H., Tabar, V., Studer, L., 2011. Dopamine neurons derived from human ES cells efficiently engraft in animal models of Parkinson's disease. *Nature* 1–7. doi:10.1038/nature10648
- Krüger, R., Kuhn, W., Müller, T., Woitalla, D., Graeber, M., Kösel, S., Przuntek, H., Epplen, J.T., Schöls, L., Riess, O., 1998. Ala30Pro mutation in the gene encoding alpha-synuclein in Parkinson's disease. *Nat Genet* 18, 106–108. doi:10.1038/ng0298-106
- Kuypers, H.G., 1962. Corticospinal connections: postnatal development in the rhesus monkey. *Science* 138, 678–680. doi:10.1126/science.138.3541.678
- Kuypers, H.G.J.M., 1981. *Anatomy of the Descending Pathways*. John Wiley & Sons, Inc., Hoboken, NJ, USA. doi:10.1002/cphy.cp010213
- Langston, J., Ballard, P., Tetrud, J., 1983. Chronic parkinsonism in humans due to a product of meperidine-analog synthesis. *Science*.
- Lawrence, D.G., Kuypers, H., 1968. The functional organization of the motor system in the monkey. *Brain*.
- Lee, A.S., Tang, C., Cao, F., Xie, X., van der Bogt, K., Hwang, A., Connolly, A.J., Robbins, R.C., Wu, J.C., 2009. Effects of cell number on teratoma formation by human embryonic stem cells. *Cell Cycle* 8, 2608–2612.
- Lee, S., Lumelsky, N., Studer, L., Auerbach, J., 2000. Efficient generation of midbrain and hindbrain neurons from mouse embryonic stem cells. *Nature*.
- Lemon, R., 2004. Cortico-motoneuronal system and dexterous finger movements. *J Neurophysiol* 92, 3601; author reply 3601–3. doi:10.1152/jn.00624.2004
- Lemon, R.N., 1999. Neural control of dexterity: what has been achieved? *Exp.Brain Res.* 128, 6–12.
- Lemon, R.N., Johansson, R.S., Westling, G., 1995. Corticospinal control during reach, grasp, and precision lift in man. *J Neurosci* 15, 6145–6156.
- Limousin, P., Pollak, P., Benazzouz, A., HOFFMANN, D., LEBAS, J.F., BROUSSOLLE, E., PERRET, J.E., BENABID, A.L., 1995. Effect on Parkinsonian Signs and Symptoms of Bilateral Subthalamic Nucleus Stimulation. *Lancet* 345, 91–95.
- Lindvall, O., 1999. Engineering neurons for Parkinson's disease. *Nat*

- Biotechnol.
- Lindvall, O., Brundin, P., Widner, H., Rehncrona, S., Gustavii, B., Frackowiak, R., Leenders, K.L., Sawle, G., Rothwell, J.C., Marsden, C.D., 1990. Grafts of fetal dopamine neurons survive and improve motor function in Parkinson's disease. *Science* 247, 574–577.
- Lindvall, O., Rehncrona, S., Brundin, P., Gustavii, B., Astedt, B., Widner, H., Lindholm, T., Bjorklund, A., Leenders, K.L., Rothwell, J.C., Frackowiak, R., Marsden, D., Johnels, B., Steg, G., Freedman, R., Hoffer, B.J., Seiger, A., Bygdeman, M., Strömberg, I., Olson, L., 1989. Human fetal dopamine neurons grafted into the striatum in two patients with severe Parkinson's disease. A detailed account of methodology and a 6-month follow-up. *Archives of neurology* 46, 615–631.
- Liu, Y., Rouiller, E.M., 1999. Mechanisms of recovery of dexterity following unilateral lesion of the sensorimotor cortex in adult monkeys. *Exp. Brain Res.* 128, 149–159.
- Luppino, G., Rizzolatti, G., 2000. The organization of the frontal motor cortex. *News Physiol. Sci.* 15, 219–224.
- Madhavan, L., Collier, T.J., 2010. A synergistic approach for neural repair: cell transplantation and induction of endogenous precursor cell activity. *Neuropharmacology* 58, 835–844. doi:10.1016/j.neuropharm.2009.10.005
- Magnin, B., Mesrob, L., Kinkingnéhun, S., Péligrini-Issac, M., Colliot, O., Sarazin, M., Dubois, B., Lehericy, S., Benali, H., 2009. Support vector machine-based classification of Alzheimer's disease from whole-brain anatomical MRI. *Neuroradiology* 51, 73–83. doi:10.1007/s00234-008-0463-x
- Maier, M.A., Armand, J., Kirkwood, P.A., Yang, H.W., Davis, J.N., Lemon, R.N., 2002. Differences in the corticospinal projection from primary motor cortex and supplementary motor area to macaque upper limb motoneurons: An anatomical and electrophysiological study. *Cereb Cortex* 12, 281–296. doi:10.1093/cercor/12.3.281
- Malach, R., Graybiel, A.M., 1986. Mosaic architecture of the somatic sensory-recipient sector of the cat's striatum. *J Neurosci* 6, 3436–3458.
- Marek, K., Innis, R., van Dyck, C., Fussell, B., Early, M., Eberly, S., Oakes, D., Seibyl, J., 2001. [<sup>123</sup>I]β-CIT SPECT imaging assessment of the rate of Parkinson's disease progression. *Neurology* 57, 2089–2094. doi:10.1212/WNL.57.11.2089
- Marek, K., Seibyl, J., Holloway, R., Kieburtz, K., Oakes, D., Lang, A., Yim, J., Dey, H., Cellar, J., Fussell, B., Broshjeit, S., Early, M., Smith, E.O., Sudarsky, L., Johnson, K.A., Corwin, C., Johnson, D., Lajoie, S., Reich, S.G., Frost, J.J., Goldberg, P., Flesher, J.E., Feigin, A., Mazurkiewicz, J., Castronuovo, J., Joseph, F., DiRocco, A., Olanow, C.W., Machac, J., Cotei, D., Webner, P., Rudolph, A., Day, D., Casaceli, C., Freimuth, A., Orme, C., Hodgeman, K., Eberly, S., Henry, E., Morgan, G., Haley, J.B., Grp, P.S., 2000. A multicenter assessment of dopamine transporter imaging with DOPASCAN/SPECT in parkinsonism. *Neurology* 55, 1540–1547.
- Markey, S.P., Johannessen, J.N., Chiueh, C.C., Burns, R.S., Herkenham, M.A., 1984. Intraneuronal generation of a pyridinium metabolite may cause drug-induced parkinsonism. *Nature* 311, 464–467.
- Marshall, V., Grosset, D., 2003. Role of dopamine transporter imaging in

- routine clinical practice. *Mov Disord* 18, 1415–1423.  
doi:10.1002/mds.10592
- Matsuo, N., Kawamoto, S., Matsubara, K., Okubo, K., 1998. Cloning and developmental expression of the murine homolog of doublecortin. *Biochem.Biophys.Res.Comm.* 252, 571–576.  
doi:10.1006/bbrc.1998.9698
- Mayer, R.A., Kindt, M.V., Heikkila, R.E., 1986. Prevention of the Nigrostriatal Toxicity of 1-Methyl-4-Phenyl-1,2,3,6-Tetrahydropyridine by Inhibitors of 3,4-Dihydroxyphenylethylamine Transport. *J.Neurochem.* 47, 1073–1079.  
doi:10.1111/j.1471-4159.1986.tb00722.x
- McGeer, P.L., McGeer, E.G., 2008. Glial reactions in Parkinson's disease. *Movement Disorders* 23, 474–483. doi:10.1002/mds.21751
- McNaught, K.S., Olanow, C.W., Halliwell, B., Isacson, O., Jenner, P., 2001. Failure of the ubiquitin-proteasome system in Parkinson's disease. *Nature Publishing Group* 2, 589–594. doi:10.1038/35086067
- Molinuevo, J.L., Valldeoriola, F., Tolosa, E., Rumia, J., Valls-Sole, J., Roldan, H., Ferrer, E., 2000. Levodopa withdrawal after bilateral subthalamic nucleus stimulation in advanced Parkinson disease. *Archives of neurology* 57, 983–988.
- Morizane, A., Li, J., 2008. From bench to bed: the potential of stem cells for the treatment of Parkinson's disease. *Cell and tissue research.*
- Morizane, A., Li, J.-Y., Brundin, P., 2008. From bench to bed: the potential of stem cells for the treatment of Parkinson's disease. *Cell and tissue research* 331, 323–336. doi:10.1007/s00441-007-0541-0
- Morrish, P.K., Sawle, G.V., Brooks, D.J., 1996. An [F-18]dopa-PET and clinical study of the rate of progression in Parkinson's disease. *Brain* 119, 585–591.
- Morrish, P.K., Sawle, G.V., Brooks, D.J., 1995. Clinical and [18F] dopa PET findings in early Parkinson's disease. *J Neurol Neurosurg Psychiatr* 59, 597–600. doi:10.1136/jnnp.59.6.597
- Mounayar, S., Boulet, S., Tandé, D., Jan, C., Pessiglione, M., Hirsch, E.C., Féger, J., Savasta, M., François, C., Tremblay, L., 2007. A new model to study compensatory mechanisms in MPTP-treated monkeys exhibiting recovery. *Brain* 130, 2898–2914. doi:10.1093/brain/awm208
- Muir, R.B., Lemon, R.N., 1983. Corticospinal neurons with a special role in precision grip. *Brain Res* 261, 312–316. doi:10.1016/0006-8993(83)90635-2
- Murray, E.A., Coulter, J.D., 1981. Organization of corticospinal neurons in the monkey. *J. Comp. Neurol.* 195, 339–365. doi:10.1002/cne.901950212
- Nakagawa, M., Taniguchi, Y., Senda, S., Takizawa, N., Ichisaka, T., Asano, K., Morizane, A., Doi, D., Takahashi, J., Nishizawa, M., Yoshida, Y., Toyoda, T., Osafune, K., Sekiguchi, K., Yamanaka, S., 2014. A novel efficient feeder-free culture system for the derivation of human induced pluripotent stem cells. *Sci Rep* 4. doi:10.1038/srep03594
- Nakano, K., Kayahara, T., Tsutsumi, T., Ushiro, H., 2000. Neural circuits and functional organization of the striatum. *Journal of Neurology* 247, V1–V15. doi:10.1007/PL00007778
- Nambu, A., 2011. Somatotopic organization of the primate Basal Ganglia. *Front Neuroanat* 5, 26. doi:10.3389/fnana.2011.00026
- NICKLAS, W.J., YOUNGSTER, S.K., KINDT, M.V., HEIKKILA, R.E., 1987.

- Mptp, Mpp+ and Mitochondrial-Function. *Life Sci.* 40, 721–729. doi:10.1016/0024-3205 (87)90299-2
- Noble, W.S., 2006. What is a support vector machine? *Nat Biotechnol* 24, 1565–1567.
- Nocker, M., Seppi, K., Donnemiller, E., Virgolini, I., Wenning, G.K., Poewe, W., Scherfler, C., 2012. Progression of dopamine transporter decline in patients with the Parkinson variant of multiple system atrophy: a voxel-based analysis of [123I]β-CIT SPECT. *Eur J Nucl Med Mol Imaging* 39, 1012–1020. doi:10.1007/s00259-012-2100-5
- Obeso, J.A., Marin, C., Rodriguez-Oroz, C., Blesa, J., Benitez-Temiño, B., Mena-Segovia, J., Rodríguez, M., Olanow, C.W., 2009. The basal ganglia in Parkinson's disease: Current concepts and unexplained observations. *Ann.Neurol* 64, S30–S46. doi:10.1002/ana.21481
- Odekerken, V.J.J., van Laar, T., Staal, M.J., Mosch, A., Hoffmann, C.F.E., Nijssen, P.C.G., Beute, G.N., van Vugt, J.P.P., Lenders, M.W.P.M., Contarino, M.F., Mink, M.S.J., Bour, L.J., van den Munckhof, P., Schmand, B.A., de Haan, R.J., Schuurman, P.R., de Bie, R.M.A., 2013. Subthalamic nucleus versus globus pallidus bilateral deep brain stimulation for advanced Parkinson's disease (NSTAPS study): a randomised controlled trial. *Lancet Neurol* 12, 37–44. doi:10.1016/S1474-4422 (12)70264-8
- Olanow, C., Goetz, C., Kordower, J., Stoessl, A., Sossi, V., Brin, M., Shannon, K., Nauert, G., Perl, D., Godbold, J., Freeman, T., 2003. A double-blind controlled trial of bilateral fetal nigral transplantation in Parkinson's disease. *Ann.Neurol* 54, 403–414.
- Olanow, C.W.C., Kordower, J.H.J., Freeman, T.B.T., 1996. Fetal nigral transplantation as a therapy for Parkinson's disease. *Trends in Neurosciences* 19, 102–109. doi:10.1016/S0166-2236 (96)80038-5
- Palacios, N., Gao, X., McCullough, M.L., Schwarzschild, M.A., Shah, R., Gapstur, S., Ascherio, A., 2012. Caffeine and risk of Parkinson's disease in a large cohort of men and women. *Movement Disorders* 27, 1276–1282. doi:10.1002/mds.25076
- Palumbo, B., Fravolini, M.L., Buresta, T., Pompili, F., Forini, N., Nigro, P., Calabresi, P., Tambasco, N., 2014. Diagnostic Accuracy of Parkinson Disease by Support Vector Machine (SVM) Analysis of 123I-FP-CIT Brain SPECT Data. *Medicine* 93, e228. doi:10.1097/MD.0000000000000228
- Parent, A., 2012. The History of the Basal Ganglia: The Contribution of Karl Friedrich Burdach. *NM* 03, 374–379. doi:10.4236/nm.2012.34046
- Parkinson, J., 1817. *An Essay on the Shaking Palsy*. London: Whittingham & Rowland.
- Paxinos, G., Huang, X.F., Toga, A.W., 1999. The rhesus monkey brain in stereotaxic coordinates.
- Penfield, W., Boldrey, E., 1937. Somatic motor and sensory representation in the cerebral cortex of man as studied by electrical stimulation. *Brain* 60, 389–443. doi:10.1093/brain/60.4.389
- Penfield, W., Rasmussen, T., 1950. *Secondary sensory and motor representation. The cerebral cortex of man*. New York: Macmillan.
- Percheron, G., Yelnik, J., Francois, C., 1984. A Golgi analysis of the primate globus pallidus. III. Spatial organization of the striato-pallidal complex. *J. Comp. Neurol.* 227, 214–227. doi:10.1002/cne.902270207



- Picard, N., STRICK, P.L., 1996. Motor areas of the medial wall: A review of their location and functional activation. *Cereb Cortex* 6, 342–353. doi:10.1093/cercor/6.3.342
- Pifl, C., SCHINGNITZ, G., Hornykiewicz, O., 1991. Effect of 1-Methyl-4-Phenyl-1,2,3,6-Tetrahydropyridine on the Regional Distribution of Brain Monoamines in the Rhesus-Monkey. *Neuroscience* 44, 591–605. doi:10.1016/0306-4522(91)90080-8
- Pirker, W., Asenbaum, S., Bencsits, G., Prayer, D., Gerschlager, W., Deecke, L., Brücke, T., 2000a. [123I]beta-CIT SPECT in multiple system atrophy, progressive supranuclear palsy, and corticobasal degeneration. *Mov Disord* 15, 1158–1167.
- Pirker, W., Asenbaum, S., Bencsits, G., Prayer, D., Gerschlager, W., Deecke, L., Brücke, T., 2000b. [123I]β-CIT spect in multiple system atrophy, progressive supranuclear palsy, and corticobasal degeneration. *Movement Disorders* 15, 1158–1167. doi:10.1002/1531-8257(200011)15:6<1158::AID-MDS1015>3.0.CO;2-0
- Plant, C., Teipel, S.J., Oswald, A., Böhm, C., Meindl, T., Mourao-Miranda, J., Bokde, A.W., Hampel, H., Ewers, M., 2010. Automated detection of brain atrophy patterns based on MRI for the prediction of Alzheimer's disease. *Neuroimage* 50, 162–174. doi:10.1016/j.neuroimage.2009.11.046
- Politis, M., 2014. Neuroimaging in Parkinson disease: from research setting to clinical practice. *Nat.Rev.Neurol* 10, 708–722. doi:10.1038/nrneurol.2014.205
- Politis, M., Lindvall, O., 2012. Clinical application of stem cell therapy in Parkinson's disease. *BMC Med* 10, 1. doi:10.1186/1741-7015-10-1
- Politis, M.M., 2010. Optimizing functional imaging protocols for assessing the outcome of fetal cell transplantation in Parkinson's disease. *CORD Conference Proceedings* 9, 50–50. doi:10.1186/1741-7015-9-50
- Polymeropoulos, M., Lavedan, C., Leroy, E., Ide, S., 1997. Mutation in the {alpha}-synuclein gene identified in families with Parkinson's disease. *Science*.
- Polymeropoulos, M.H., 1998. Autosomal dominant Parkinson's disease and alpha-synuclein. *Ann.Neurol* 44, S63–4.
- Porras, G., Li, Q., Bezard, E., 2012. Modeling Parkinson's Disease in Primates: The MPTP Model. *Cold Spring Harb Perspect Med* 2, a009308. doi:10.1101/cshperspect.a009308
- Prodoehl, J., Li, H., Planetta, P.J., Goetz, C.G., Shannon, K.M., Tangonan, R., Comella, C.L., Simuni, T., Zhou, X.J., Leurgans, S., Corcos, D.M., Vaillancourt, D.E., 2013. Diffusion Tensor Imaging of Parkinson's Disease, Atypical parkinsonism, and Essential Tremor. *Mov Disord* 28, 1816–1822. doi:10.1002/mds.25491
- Przedborski, S., Jackson-Lewis, V., Naini, A.B., Jakowec, M., Petzinger, G., Miller, R., Akram, M., 2001. The parkinsonian toxin 1-methyl-4-phenyl-1,2,3,6-tetrahydropyridine (MPTP): a technical review of its utility and safety. *J.Neurochem.* 76, 1265–1274.
- Rascol, O., Brooks, D.J., Korczyn, A.D., De Deyn, P.P., Clarke, C.E., Lang, A.E., 2000. A five-year study of the incidence of dyskinesia in patients with early Parkinson's disease who were treated with ropinirole or levodopa. *N Engl J Med* 342, 1484–1491. doi:10.1056/NEJM200005183422004
- Richardson, J.R., Shalat, S.L., Buckley, B., Winnik, B., O'Suilleabhain, P.,

- Diaz-Arrastia, R., Reisch, J., German, D.C., 2009. Elevated serum pesticide levels and risk of Parkinson disease. *Archives of neurology* 66, 870–875. doi:10.1001/archneurol.2009.89
- Rodriguez, M.C., Guridi, O.J., Alvarez, L., Mewes, K., Macias, R., Vitek, J., DeLong, M.R., Obeso, J.A., 1998. The subthalamic nucleus and tremor in Parkinson's disease. *Mov Disord* 13 Suppl 3, 111–118.
- Roland, P.E., Zilles, K., 1996. Functions and structures of the motor cortices in humans. *Curr.Opin.Neurobiol.* 6, 773–781. doi:10.1016/S0959-4388(96)80027-4
- Rouiller, E.M., Moret, V., Tanne, J., Boussaoud, D., 1996. Evidence for direct connections between the hand region of the supplementary motor area and cervical motoneurons in the macaque monkey. *Eur J Neurosci* 8, 1055–1059. doi:10.1111/j.1460-9568.1996.tb01592.x
- Rouiller, E.M., Yu, X.H., Moret, V., Tempini, A., Wiesendanger, M., Liang, F., 1998. Dexterity in adult monkeys following early lesion of the motor cortical hand area: the role of cortex adjacent to the lesion. *Eur J Neurosci* 10, 729–740.
- Roy, N.S., Cleren, C., Singh, S.K., Yang, L., Beal, M.F., Goldman, S.A., 2006. Functional engraftment of human ES cell-derived dopaminergic neurons enriched by coculture with telomerase-immortalized midbrain astrocytes. *Nat Med* 12, 1259–1268. doi:10.1038/nm1495
- Sadato, N., Yonekura, Y., Waki, A., Yamada, H., Ishii, Y., 1997. Role of the supplementary motor area and the right premotor cortex in the coordination of bimanual finger movements. *J Neurosci* 17, 9667–9674.
- Sanes, J.N., Donoghue, J.P., Thangaraj, V., Edelman, R.R., Warach, S., 1995. Shared neural substrates controlling hand movements in human motor cortex. *Science* 268, 1775–1777.
- Schapira, A., Cooper, J., Dexter, D., 1990. Mitochondrial complex I deficiency in Parkinson's disease. *Journal of ...*
- Schapira, A., COOPER, J.M., Dexter, D., Jenner, P., CLARK, J.B., Marsden, C.D., 1989. Mitochondrial Complex I Deficiency in Parkinsons-Disease. *Lancet* 1, 1269–1269.
- Schapira, A.H.V., 2009. Etiology and Pathogenesis of Parkinson Disease. *Neurol Clin* 27, 583–603. doi:10.1016/j.ncl.2009.04.004
- Schieber, M.H., 2001. Constraints on somatotopic organization in the primary motor cortex. *J Neurophysiol* 86, 2125–2143.
- Schneider, J.S., Kovelowski, C.J., 1990. Chronic exposure to low doses of MPTP. I. Cognitive deficits in motor asymptomatic monkeys. *Brain Res* 519, 122–128.
- Schneider, J.S., Lidsky, T.I., Hawks, T., Mazziotta, J.C., Hoffman, J.M., 1995. Differential recovery of volitional motor function, lateralized cognitive function, dopamine agonist-induced rotation and dopaminergic parameters in monkeys made hemi-parkinsonian by intracarotid MPTP infusion. *Brain Res* 672, 112–117.
- Schrag, A., Quinn, N., 2000. Dyskinesias and motor fluctuations in Parkinson's disease - A community-based study. *Brain* 123, 2297–2305.
- Schwarz, S.T., Afzal, M., Morgan, P.S., Bajaj, N., Gowland, P.A., Auer, D.P., 2014. The “Swallow Tail” Appearance of the Healthy Nigrosome – A New Accurate Test of Parkinson's Disease: A Case-Control and Retrospective Cross-Sectional MRI Study at 3T. *PLoS ONE* 9, e93814–8.

- doi:10.1371/journal.pone.0093814
- Semchuk, K.M., Love, E.J., Lee, R.G., 1992. Parkinson's disease and exposure to agricultural work and pesticide chemicals. *Neurology* 42, 1328–1335.
- Seppi, K., Scherfler, C., Donnemiller, E., Virgolini, I., Schocke, M.F.H., Goebel, G., Mair, K.J., Boesch, S., Brenneis, C., Wenning, G.K., Poewe, W., 2006. Topography of Dopamine Transporter Availability in Progressive Supranuclear Palsy: A Voxelwise [<sup>123</sup>I]β-CIT SPECT Analysis. *Archives of neurology* 63, 1154–1160. doi:10.1001/archneur.63.8.1154
- Serrien, D.J., Strens, L.H.A., Oliviero, A., Brown, P., 2002. Repetitive transcranial magnetic stimulation of the supplementary motor area (SMA) degrades bimanual movement control in humans. *Neurosci Lett* 328, 89–92.
- Shastri, B.S., 2001. Parkinson disease: etiology, pathogenesis and future of gene therapy. *Neurosci. Res.*
- Sixel-Döring, F., Liepe, K., Mollenhauer, B., Trautmann, E., Trenkwalder, C., 2011. The role of 123I-FP-CIT-SPECT in the differential diagnosis of Parkinson and tremor syndromes: a critical assessment of 125 cases. *Journal of Neurology* 258, 2147–2154. doi:10.1007/s00415-011-6076-z
- SMITH, A.D., BOLAM, J.P., 1990. The Neural Network of the Basal Ganglia as Revealed by the Study of Synaptic Connections of Identified Neurons. *Trends in Neurosciences* 13, 259–265. doi:10.1016/0166-2236(90)90106-K
- Spillantini, M.G., Schmidt, M.L., Lee, V.M., Trojanowski, J.Q., Jakes, R., Goedert, M., 1997. Alpha-synuclein in Lewy bodies. *Nature* 388, 839–840. doi:10.1038/42166
- Stern, M.B., Follett, K.A., Weaver, F.M., 2013. Randomized trial of deep brain stimulation for Parkinson disease: thirty-six-month outcomes; turning tables: should GPi become the preferred DBS target for Parkinson disease? Author response. *Neurology* 80, 225–225. doi:10.1212/WNL.0b013e3182804657
- Takagi, Y., Takahashi, J., Saiki, H., Morizane, A., Hayashi, T., Kishi, Y., Fukuda, H., Okamoto, Y., Koyanagi, M., Ideguchi, M., Hayashi, H., Imazato, T., Kawasaki, H., Suemori, H., Omachi, S., Iida, H., Itoh, N., Nakatsuji, N., Sasai, Y., Hashimoto, N., 2005. Dopaminergic neurons generated from monkey embryonic stem cells function in a Parkinson primate model. *J Clin Invest* 115, 102–109. doi:10.1172/JCI21137
- Takahashi, K., Yamanaka, S., 2006. Induction of pluripotent stem cells from mouse embryonic and adult fibroblast cultures by defined factors. *Cell* 126, 663–676. doi:10.1016/j.cell.2006.07.024
- Tanner, C., Langston, J., Klawans, H., 1990. Do environmental toxins cause Parkinson's disease?. A critical review. Discussion. *Neurology*.
- Tanner, C.M., 1992. Occupational and environmental causes of parkinsonism. *Occup Med* 7, 503–513.
- Tanner, C.M., Ottman, R., Goldman, S.M., Ellenberg, J., Chan, P., Mayeux, R., Langston, J.W., 1999. Parkinson disease in twins: an etiologic study. *JAMA* 281, 341–346.
- Temel, Y., Blokland, A., Steinbusch, H., Visser-Vandewalle, V., 2005. The functional role of the subthalamic nucleus in cognitive and limbic circuits. *Prog Neurobiol* 76, 393–413. doi:10.1016/j.pneurobio.2005.09.005

- Thobois, S., Guillouet, S., BROUSSOLLE, E., 2001. Contributions of PET and SPECT to the understanding of the pathophysiology of Parkinson's disease. *Neurophysiol Clin* 31, 321–340.
- Thomas, M., Jankovic, J., 2004. Neurodegenerative disease and iron storage in the brain. *Curr. Opin. Neurol.* 17, 437–442.  
doi:10.1097/01.wco.0000137534.61244.d1
- Tissingh, G., Bergmans, P., Booij, J., Winogrodzka, A., van Royen, E.A., Stoof, J.C., Wolters, E.C., 1997. Drug-naive patients with Parkinson's disease in Hoehn and Yahr stages I and II show a bilateral decrease in striatal dopamine transporters as revealed by [<sup>123</sup>I]β-CIT SPECT. *Journal of Neurology* 245, 14–20. doi:10.1007/s004150050168
- Toyoshima, K., Sakai, H., 1982. Exact cortical extent of the origin of the corticospinal tract (CST) and the quantitative contribution to the CST in different cytoarchitectonic areas. A study with horseradish peroxidase in the monkey. *J Hirnforsch* 23, 257–269.
- Uchida, N., Buck, D.W., He, D., Reitsma, M.J., Masek, M., Phan, T.V., Tsukamoto, A.S., Gage, F.H., Weissman, I.L., 2000. Direct isolation of human central nervous system stem cells. *PNAS* 97, 14720–14725.  
doi:10.1073/pnas.97.26.14720
- Valente, E.M., Abou-Sleiman, P.M., Caputo, V., Muqit, M.M.K., Harvey, K., Gispert, S., Ali, Z., Del Turco, D., Bentivoglio, A.R., Healy, D.G., Albanese, A., Nussbaum, R., González-Maldonado, R., Deller, T., Salvi, S., Cortelli, P., Gilks, W.P., Latchman, D.S., Harvey, R.J., Dallapiccola, B., Auburger, G., Wood, N.W., 2004. Hereditary early-onset Parkinson's disease caused by mutations in PINK1. *Science* 304, 1158–1160.  
doi:10.1126/science.1096284
- Van Den Eeden, S.K., Tanner, C.M., Bernstein, A.L., Fross, R.D., Leimpeter, A., Bloch, D.A., Nelson, L.M., 2003. Incidence of Parkinson's disease: variation by age, gender, and race/ethnicity. *Am. J. Epidemiol.* 157, 1015–1022. doi:10.1093/aje/kwg068
- VARASTET, M., RICHE, D., MAZIERE, M., Hantraye, P., 1994. Chronic Mptp Treatment Reproduces in Baboons the Differential Vulnerability of Mesencephalic Dopaminergic-Neurons Observed in Parkinsons-Disease. *Neuroscience* 63, 47–56.
- Varrone, A., Marek, K.L., Jennings, D., Innis, R.B., Seibyl, J.P., 2001. [<sup>123</sup>I]β-CIT SPECT imaging demonstrates reduced density of striatal dopamine transporters in Parkinson's disease and multiple system atrophy. *Movement Disorders* 16, 1023–1032. doi:10.1002/mds.1256
- Viallet, F., Massion, J., Massarino, R., Khalil, R., 1992. Coordination between posture and movement in a bimanual load lifting task: putative role of a medial frontal region including the supplementary motor area. *Exp. Brain Res.* 88, 674–684.
- Vingerhoets, F., Uitti, R.J., Schulzer, M., Caine, D.B., 1996. The purdue pegboard task reliably reflects the nigrostriatal deficit in Parkinson's disease. *Neurology* 46, 1099–1099.
- Wakabayashi, K., Tanji, K., Mori, F., Takahashi, H., 2007. The Lewy body in Parkinson's disease: molecules implicated in the formation and degradation of alpha-synuclein aggregates. *Neuropathology* 27, 494–506.
- Wannier, T., Schmidlin, E., Bloch, J., Rouiller, E.M., 2005. A unilateral section of the corticospinal tract at cervical level in primate does not lead to

- measurable cell loss in motor cortex. *J Neurotrauma* 22, 703–717.  
doi:10.1089/neu.2005.22.703
- Whishaw, I., Suchowersky, O., Davis, L., Sarna, J., Metz, G., Pellis, S., 2002. Impairment of pronation, supination, and body co-ordination in reach-to-grasp tasks in human Parkinson's disease (PD) reveals homology to deficits in animal models. *Behav. Brain Res.* 133, 165–176.
- Wichmann, T., DeLONG, M., 2003. Pathophysiology of Parkinson's disease: the MPTP primate model of the human disorder. *Ann NY Acad Sci.*
- Wichmann, T., DeLong, M.R., 2011. Deep-Brain Stimulation for Basal Ganglia Disorders. *Basal Ganglia* 1, 65–77. doi:10.1016/j.baga.2011.05.001
- Wichmann, T., DeLong, M.R., 2007. Anatomy and physiology of the basal ganglia: relevance to Parkinson's disease and related disorders. *Handb Clin Neurol* 83, 1–18. doi:10.1016/S0072-9752 (07)83001-6
- Wichmann, T., DeLong, M.R., 1996. Functional and pathophysiological models of the basal ganglia. *Curr. Opin. Neurobiol.* 6, 751–758.  
doi:10.1016/S0959-4388 (96)80024-9
- Williams, N.R., Okun, M.S., 2013. Deep brain stimulation (DBS) at the interface of neurology and psychiatry. *J Clin Invest* 123, 4546–4556.  
doi:10.1172/JCI68341
- Wolters, E.C., Braak, H., 2006. Parkinson's disease: premotor clinico-pathological correlations, in: *Parkinson's Disease and Related Disorders, Journal of Neural Transmission. Supplementa.* Springer Vienna, pp. 309–319. doi:10.1007/978-3-211-45295-0\_47
- Wyss, A.F., Hamadjida, A., Savidan, J., Liu, Y., Bashir, S., Mir, A., Schwab, M.E., Rouiller, E.M., Belhaj-Saif, A., 2013. Long-term motor cortical map changes following unilateral lesion of the hand representation in the motor cortex in macaque monkeys showing functional recovery of hand functions. *Restor. Neurol. Neurosci.* 31, 733–760. doi:10.3233/RNN-130344
- Zhang, Z.-X., Dong, Z.-H., Román, G.C., 2006. Early descriptions of Parkinson disease in ancient China. *Archives of neurology* 63, 782–784.  
doi:10.1001/archneur.63.5.782



## **6 - Annexes**





## ***Annex 1***

***(Drawer's data post-processing)***



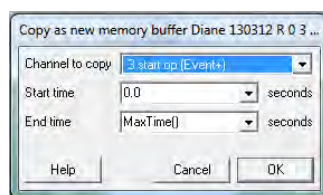
# Protocole d'utilisation de Spike dans l'analyse des données de la tâche du tiroir

## 1. «Purifier» les essais («purifier» les «start open» pour la «load force» et les «knob touch» pour la «grip force»)

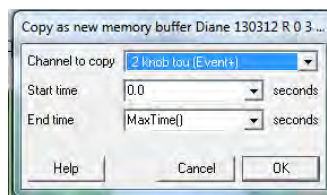
### 1.1. Créer des copies des canaux «start open» et «knob touch»

1.1.1. Ouvrir un fichier

1.1.2. Analysis -> Memory Buffer -> Create Channel Copy -> 3 start op (Event+) -> OK

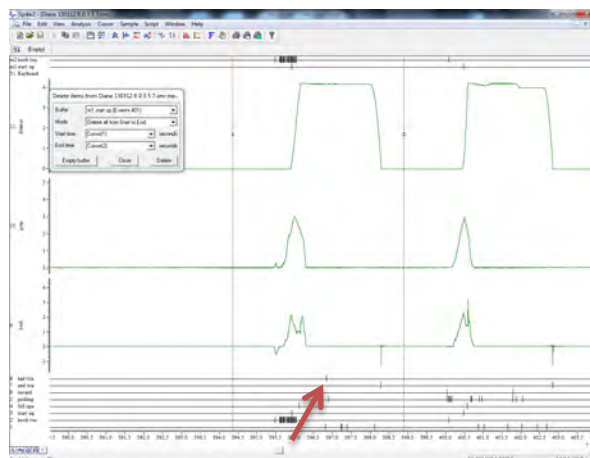


1.1.3. Analysis -> Memory Buffer -> Create Channel Copy -> 2 knob tou (Event+) -> OK

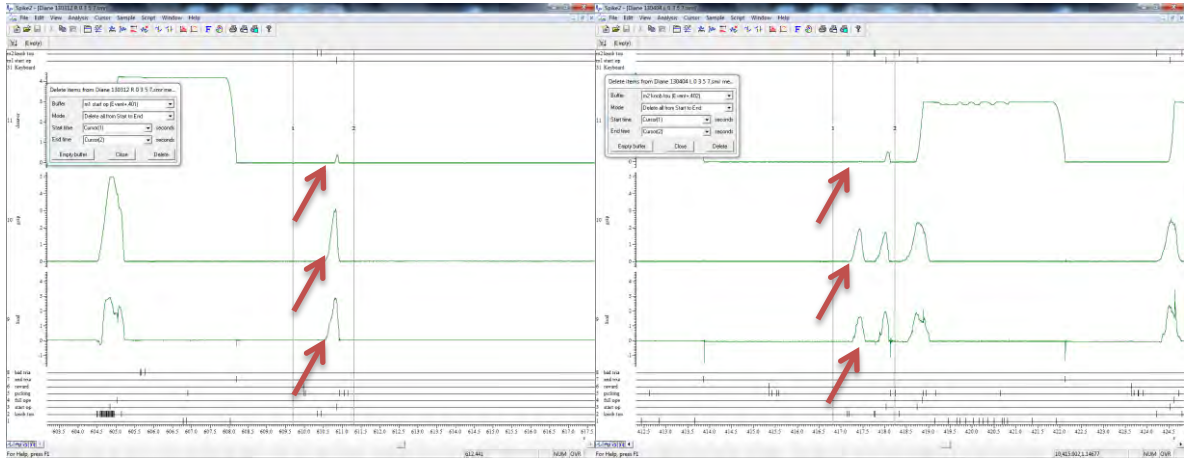


### 1.2. Eliminer les «bad trials» et les «knob touch» en surplus

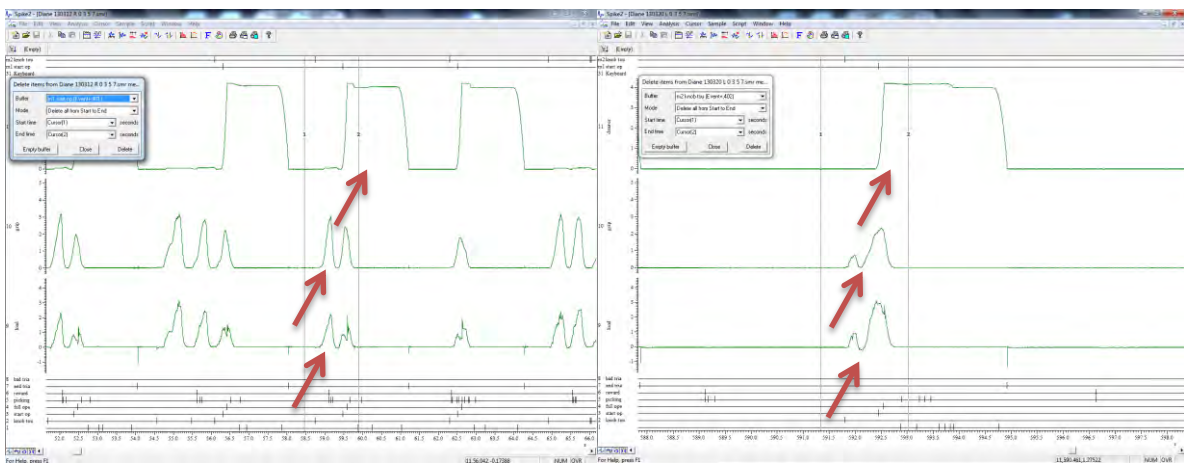
«Bad trial» : - essai considéré comme «bad trial» par l'expérimentateur (en cas de doute, vérifier avec la vidéo)



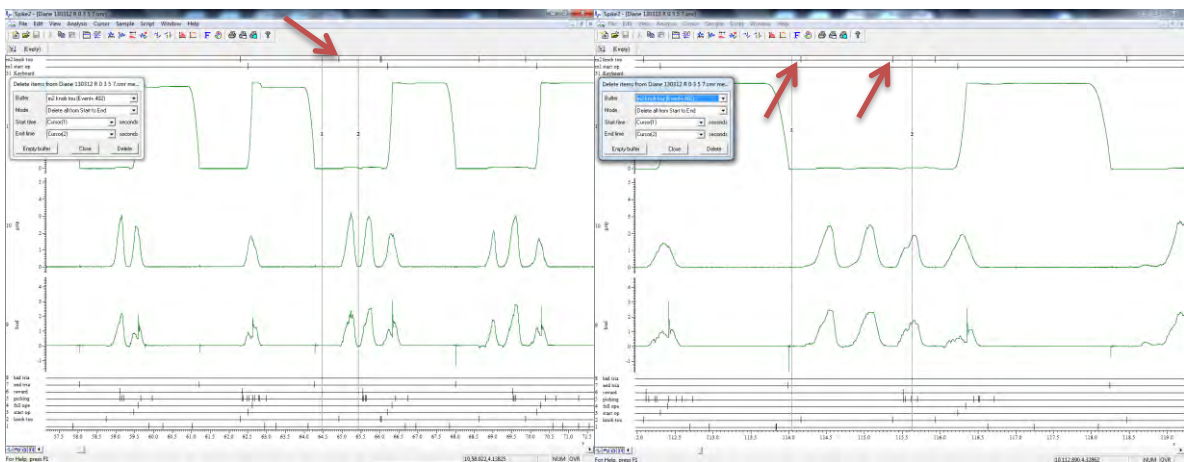
- absence de réponse pour «drawer displacement» alors qu'il y a une réponse pour la «grip force» et la «load force»



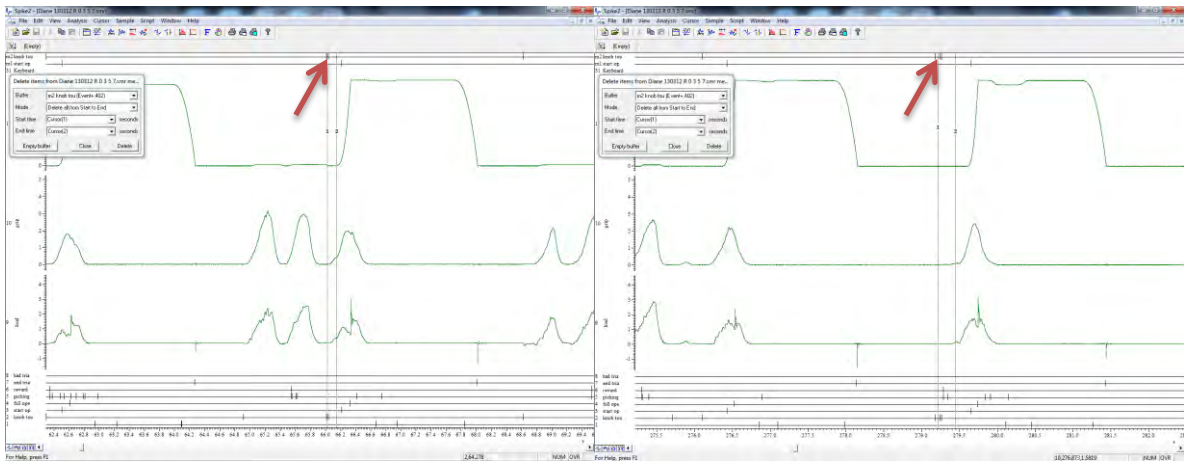
- plusieurs réponses très proches pour la «grip force» et la «load force», alors qu'une seule réponse pour «drawer displacement» est présente



«Knob touch» en surplus : -dans le cas de «bad trials» (trait vertical absent dans «m1 start op»)  
 -> éliminer tous les «knob touch» correspondants aux «bad trials»

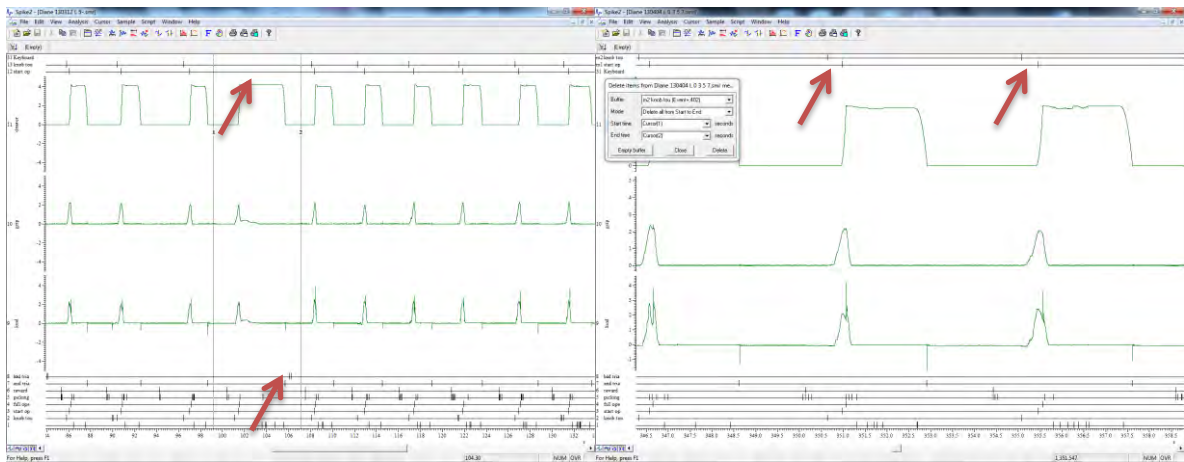


- dans le cas de «bons» essais (trait vertical présent dans «m1 start op») -> éliminer les «knob touch» en surplus (ceux qui se trouvent après le premier «knob touch» du «bon» essai)



**But :** Avoir une session «pure» :

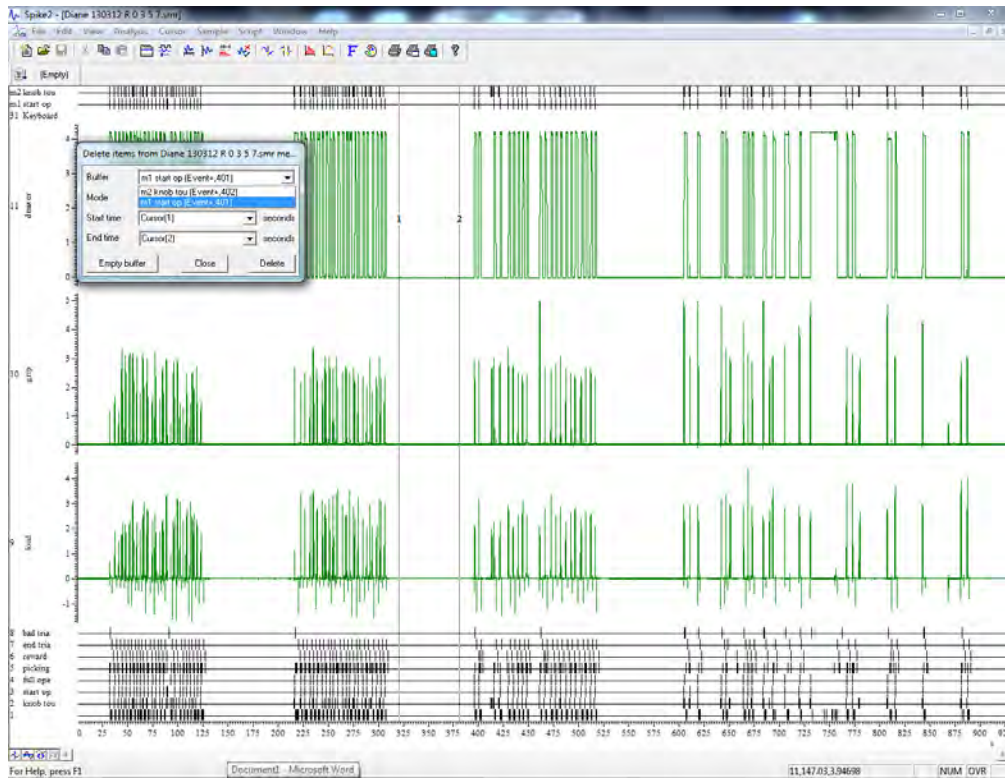
- absence de trait dans le canal «m1 start op» et dans le canal «m2 knob tou» pour chaque «bad trial»
- présence d'un trait dans le canal «m1 start op» et d'un trait dans le canal «m2 knob tou» pour chaque «bon» essai



1.2.1. Créer deux curseurs verticaux (1 et 2)

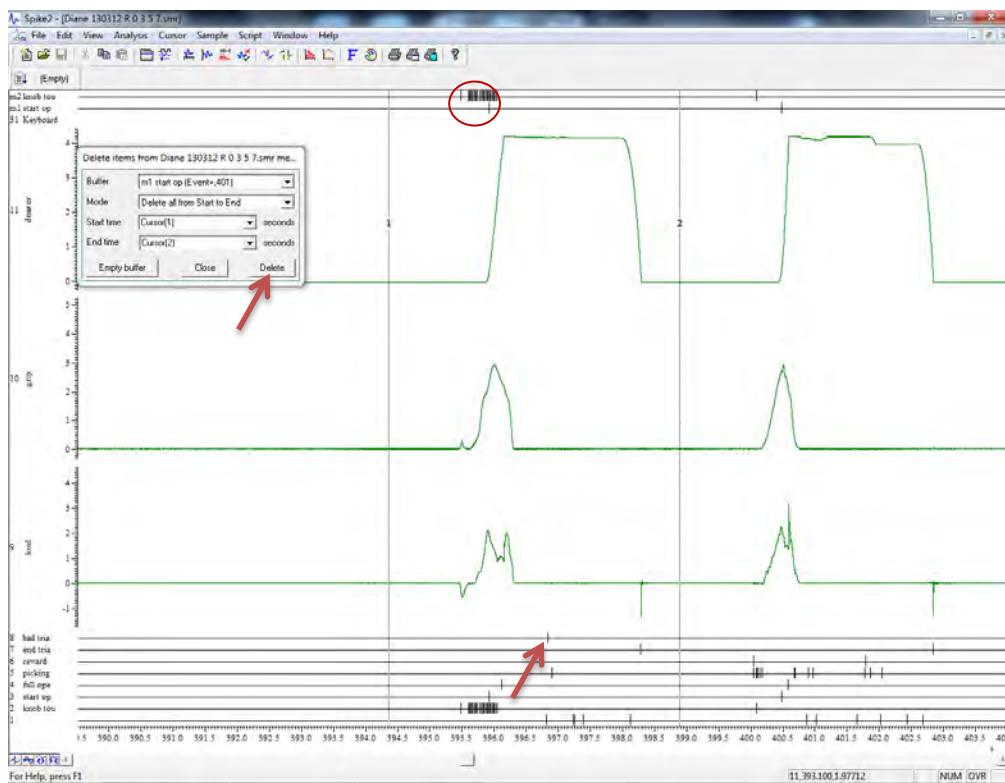
1.2.2. Analysis -> Memory Buffer -> Delete Items -> m1 start op... -> Delete all from Start to End -> Cursor(1) -> Cursor(2)

Garder la fenêtre ouverte



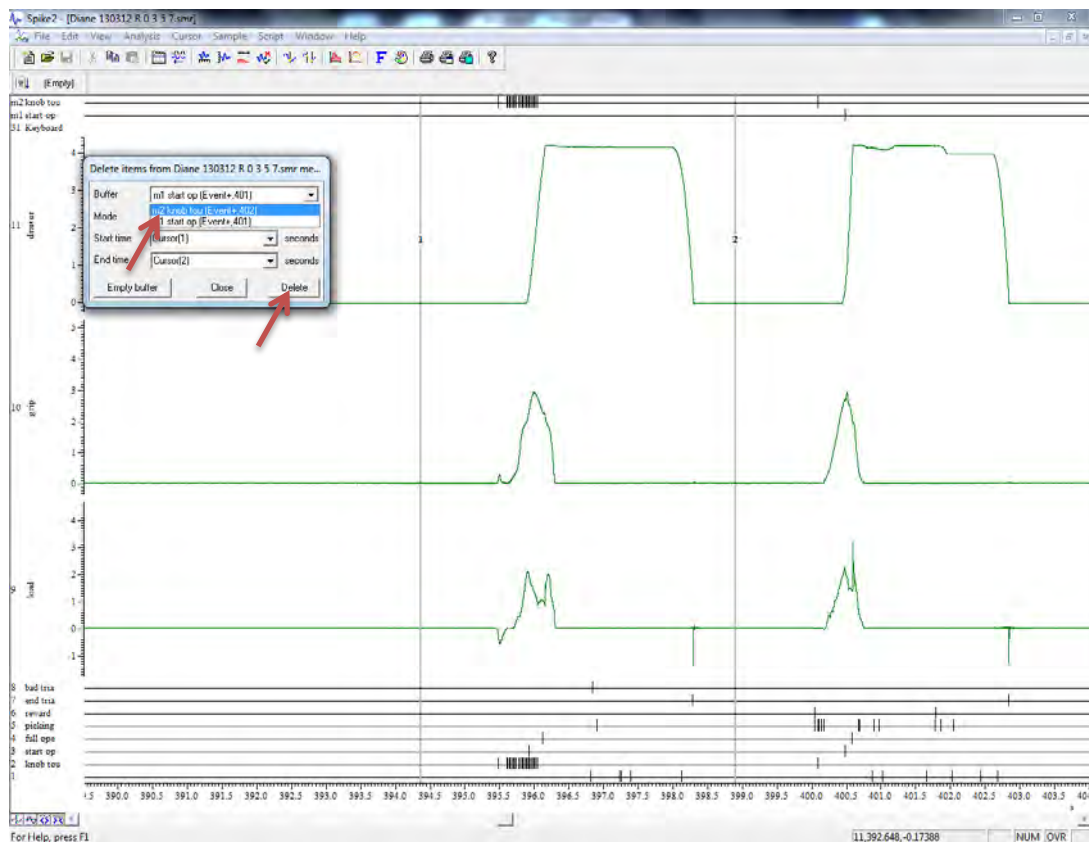
### 1.2.3. Eliminer les essais considérés comme «bad trials» par l'expérimentateur

Parcourir la session (sans trop agrandir les essais) et délimiter avec les deux curseurs verticaux les traits présents dans les nouveaux canaux créés («m1 start op» et «m2 knob tou»), correspondant au «bad trial» -> *Delete* (le trait dans «m1 start op» va disparaître)





-> changer le «Buffer» en *m2 knob tou...* -> *Delete* (les traits dans «m2 knob tou» vont disparaître)

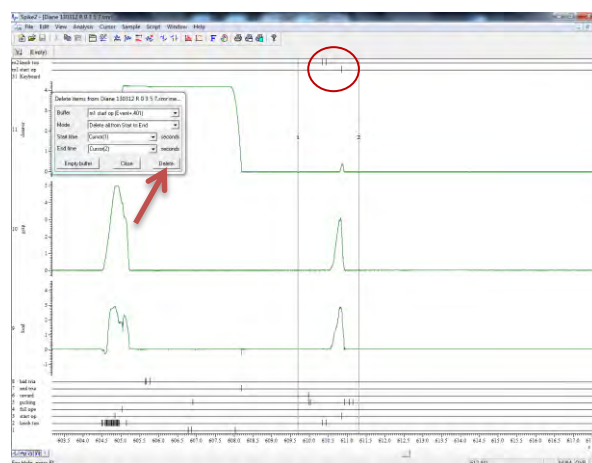


Garder la fenêtre ouverte et presser la touche *Delete* («Buffer» *m1 start op...* puis *m2 knob tou...*) après avoir délimité le prochain «bad trial» par les curseurs 1 et 2 et ainsi de suite

1.2.4. Eliminer les autres «bad trials» et les «knob touch» en surplus

Revenir au début de la session et agrandir les essais, parcourir la session en suivant la procédure pour les cas suivants :

- Absence de réponse pour «drawer displacement» alors qu'il y a une réponse pour la «grip force» et la «load force» -> éliminer tous les traits correspondants à l'essai dans les nouveaux canaux

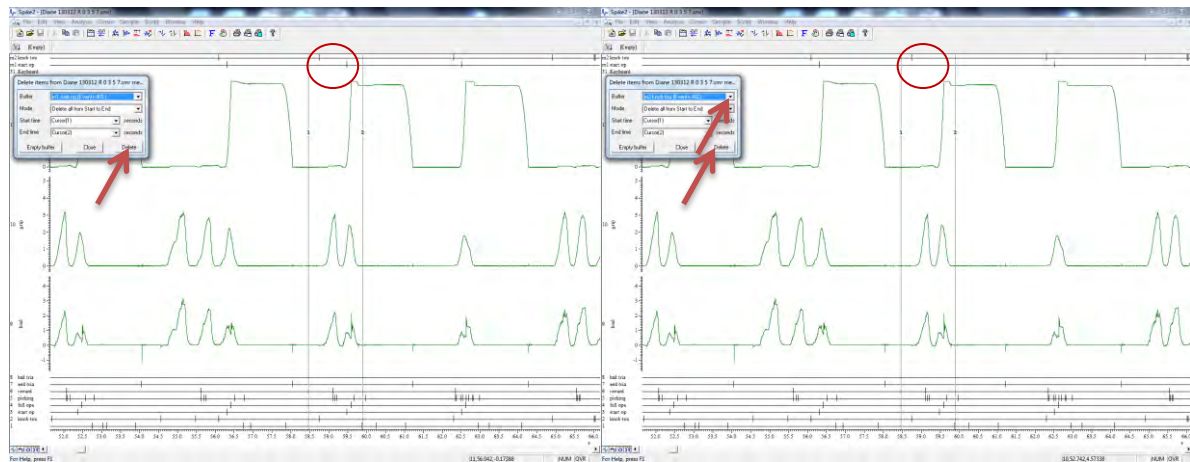


Délimiter avec les deux curseurs verticaux tous les traits correspondants à l'essai dans les nouveaux canaux -> *Delete* -> changer le «Buffer» -> *Delete*

- Plusieurs réponses très proches pour la «grip force» et la «load force», alors qu'une seule réponse pour «drawer displacement» est présente -> éliminer tous les traits correspondants aux «bad trials» dans les nouveaux canaux



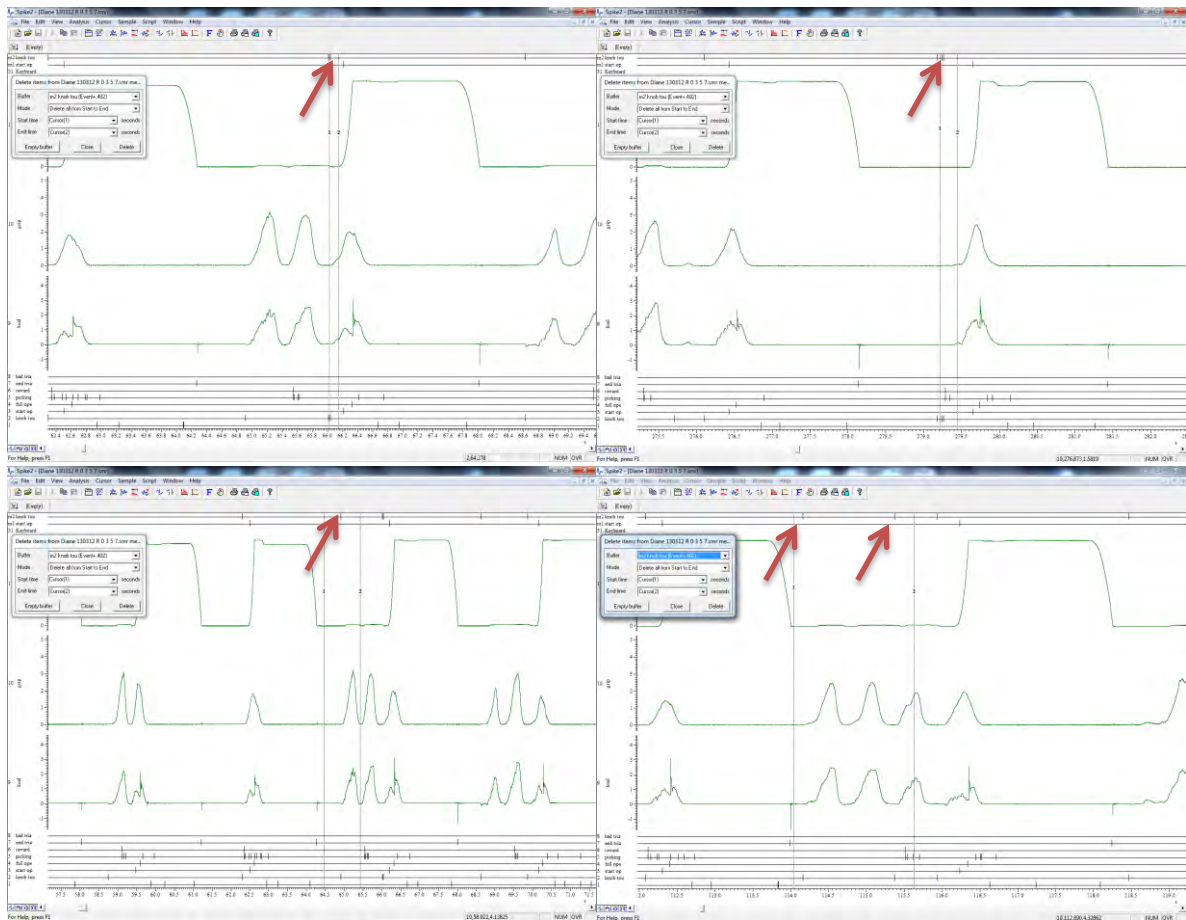
Délimiter avec les deux curseurs verticaux tous les traits correspondants aux «bad trials» dans les nouveaux canaux -> *Delete* -> changer le «Buffer» -> *Delete*



Dans ce cas, le trait du «knob touch» ne correspond pas au bon essai (celui juste en dessous de la réponse pour «drawer displacement») -> délimiter avec les deux curseurs verticaux tous les traits dans les nouveaux canaux -> *Delete* -> changer le «Buffer» -> *Delete*



-«Knob touch» en surplus



Délimiter les «knob touch» en surplus (après le premier «knob touch» de l'essai) avec les curseurs verticaux (dans le cas d'un «bad trial», délimiter tous les «knob touch» de l'essai) -> *m2 knob tou...*  
-> Delete

Ne pas fermer le fichier, sinon toutes les modifications seront perdu

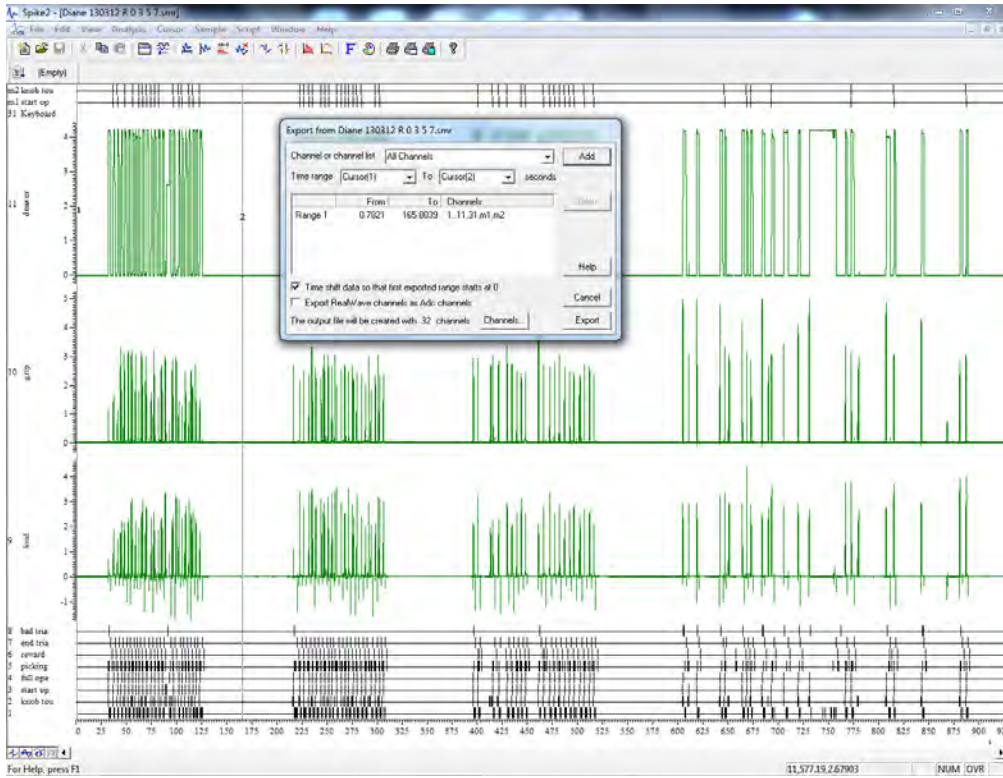
### 1.3. Sauvegarder les modifications apportées au fichier

Dans le cas d'un fichier contenant les quatre résistances

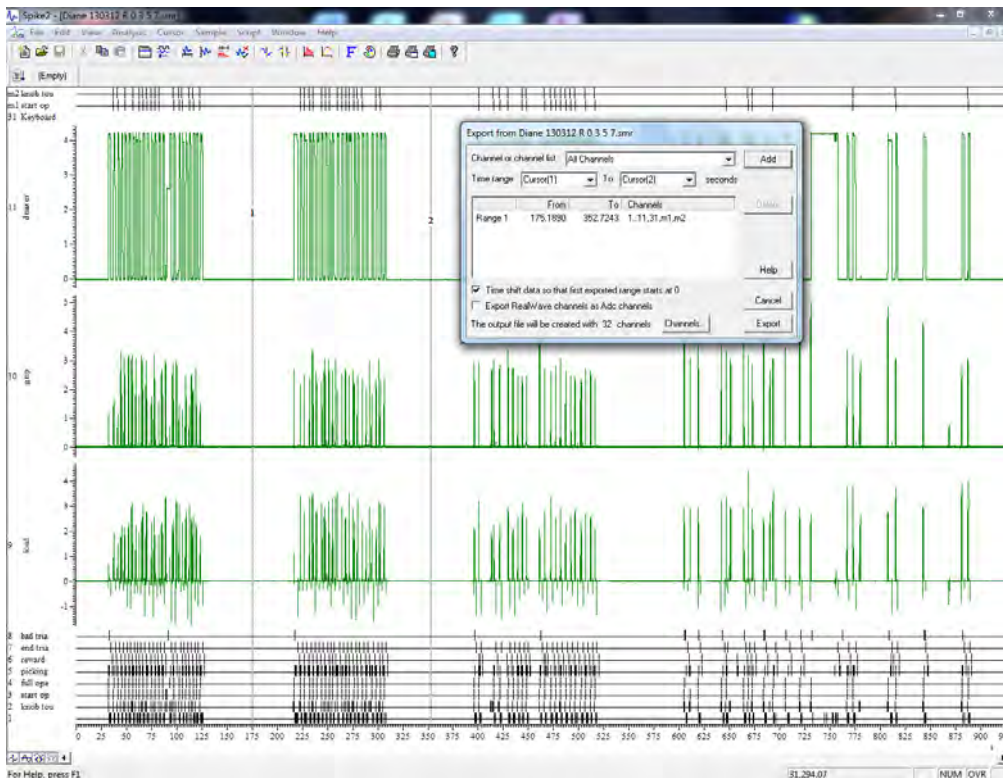
1.3.1. Presser la touche << (en bas à gauche de l'écran) jusqu'à avoir une vue d'ensemble sur la session avec les différentes résistances, délimitées en général par des espaces

1.3.2. Délimiter R0 avec deux curseurs verticaux

-> File -> Export As -> File name ... -> Save as type Data file (\*.smr) -> Save -> All Channels -> Cursor (1) to Cursor (2) -> Add-> Export



Même procédure pour les autres résistances (R3, R5, R7) pour la main gauche (L)



Même procédure pour le fichier de la main droite (R) après purification (1.3.1.-1.3.2.)

Pour un fichier Diane121026 L 0 3 5 7.smr nous obtenons quatre fichiers «purifiés» :

Diane121026 L 0.smr

Diane121026 L 3.smr

Diane121026 L 5.smr

Diane121026 L 7.smr

Pour un fichier Diane121026 R 0 3 5 7.smr nous obtenons quatre fichiers «purifiés» :

Diane121026 R 0.smr

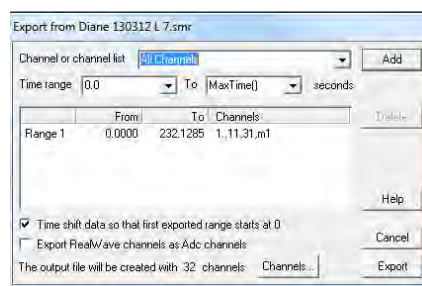
Diane121026 R 3.smr

Diane121026 R 5.smr

Diane121026 R 7.smr

### Dans le cas d'un fichier contenant une résistance

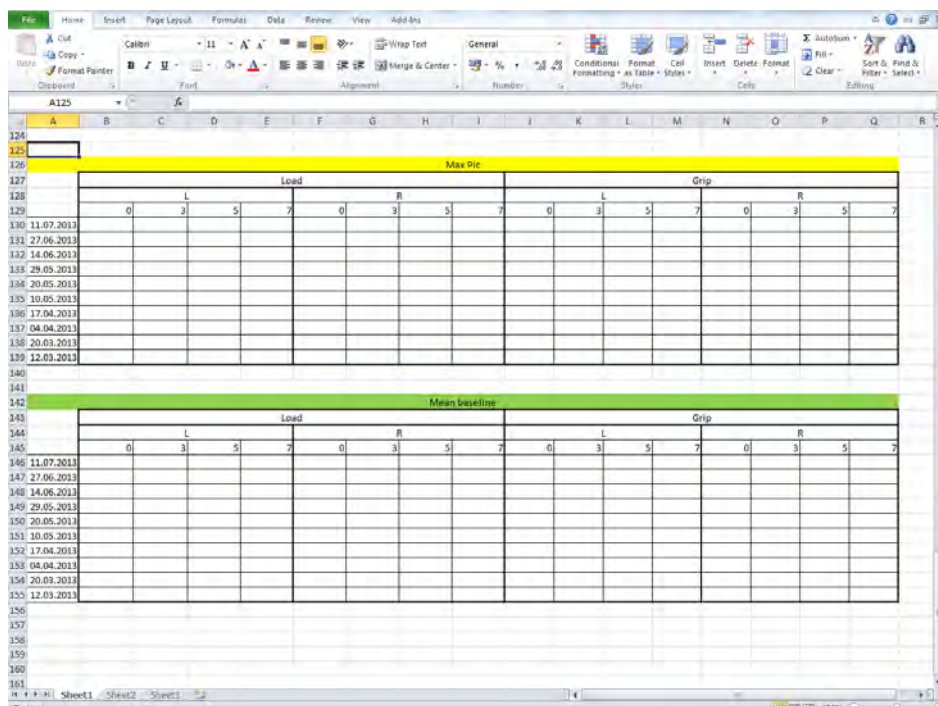
File -> Export As -> Renommer le fichier -> Save -> All Channels -> 0.0 to Max Time() -> Add -> Export



## 1.4. Utiliser les fichiers «purifiés» pour les prochaines analyses

## 2. Créer un document Excel pour pouvoir récolter des données

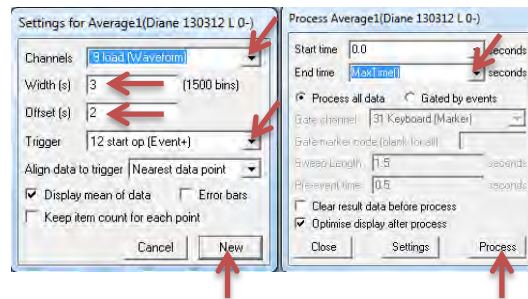
Un exemple :



### 3. Récolter les données pour pouvoir définir la hauteur des pics et la valeur moyenne de la «baseline»

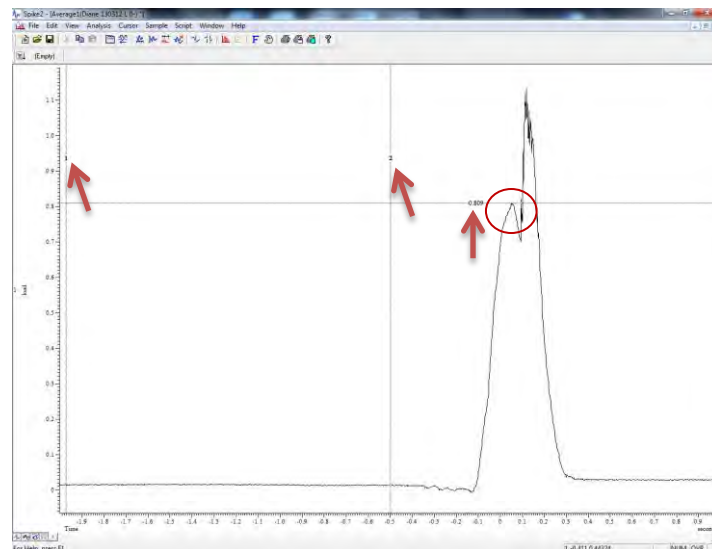
#### 3.1. Ouvrir un fichier («purifié»)

3.1.1. Analysis -> New Result View -> Waveform Average ->



#### 3.2. Situation d'une «baseline» «stable»

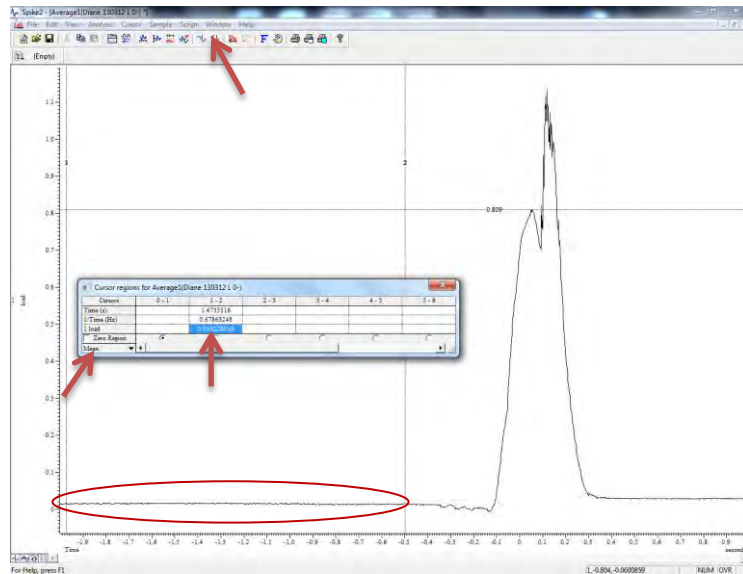
3.2.1. Placer deux curseurs verticaux (délimiter la «baseline» la plus stable avant la réponse) et un curseur horizontal (sur le maximum du pic de la «load force»)



3.2.2. La valeur max du pic pour la «load force» est de 0.809 dans cet exemple, la reporter dans le tableau Excel

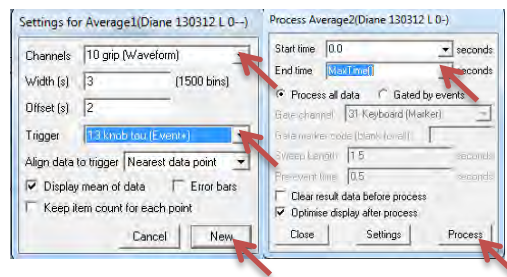
3.2.3. Pour avoir la valeur moyenne de la «baseline» pour la «load force» ->



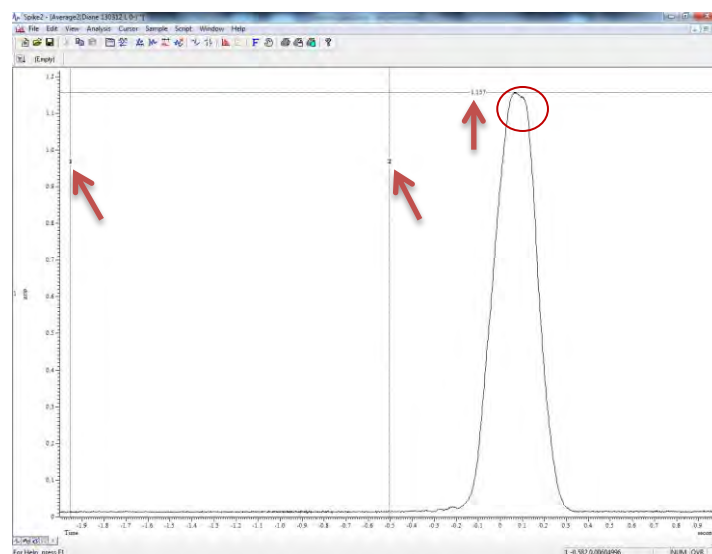


-> Copier-coller la valeur en bleu dans le tableau Excel

3.2.4. Analysis -> New Result View -> Waveform Average ->

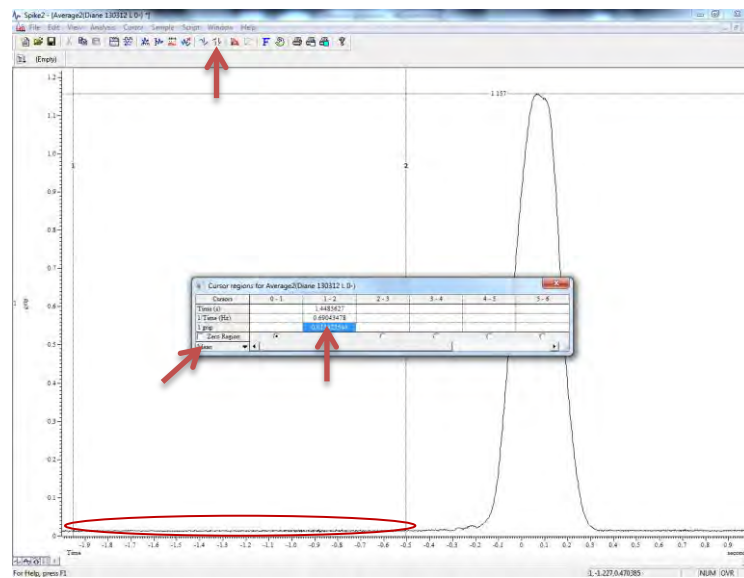


3.2.5. Placer deux curseurs verticaux (délimiter la «baseline» la plus stable avant la réponse) et un curseur horizontal (sur le maximum du pic de la «grip force»)



3.2.6. La valeur max du pic pour la «grip force» est de 1.157 dans cet exemple, la reporter dans le tableau Excel

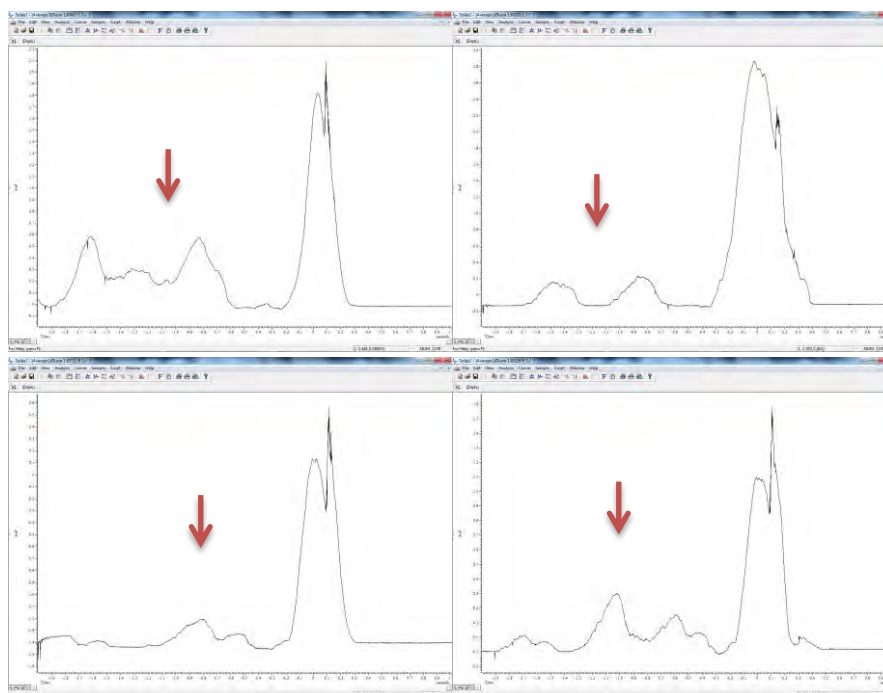
3.2.7. Pour avoir la valeur moyenne de la «baseline» pour la «grip force» ->



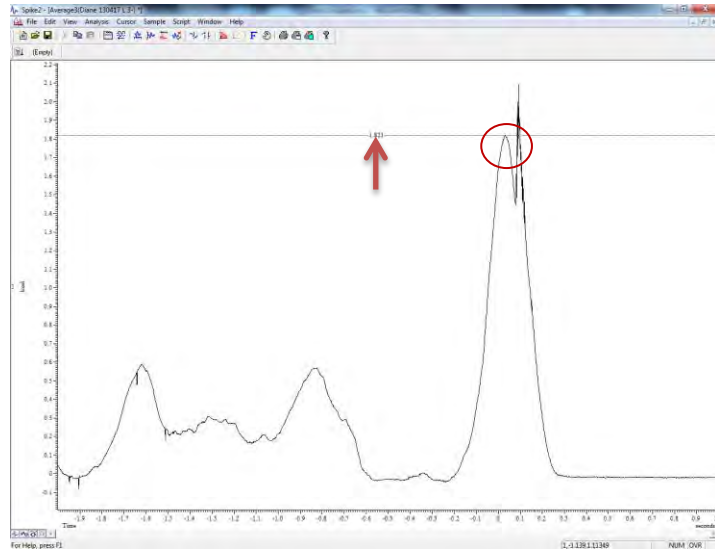
Copier-coller la valeur en bleu dans le tableau Excel

### 3.3. Situation d'une «baseline» «instable»

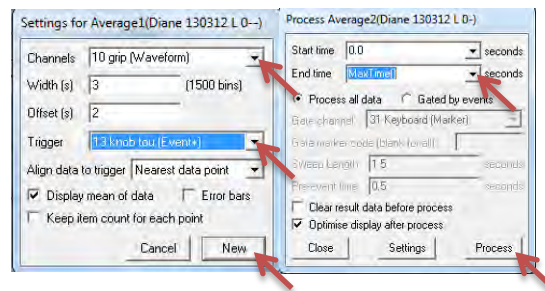
Exemples :



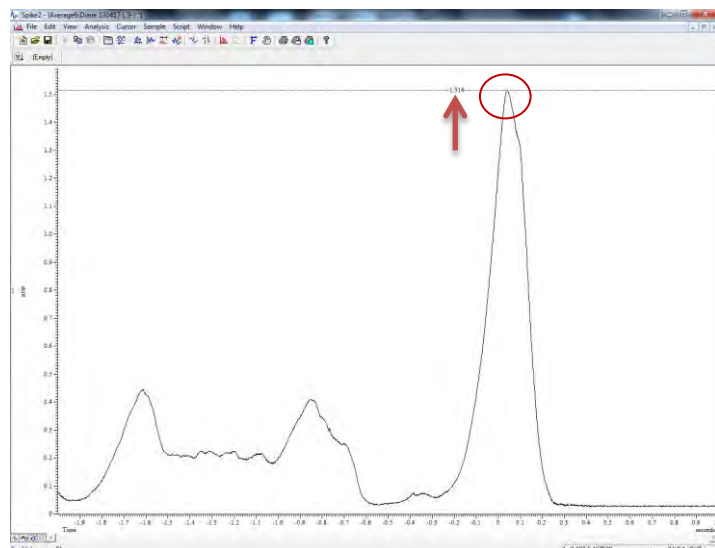
3.3.1. Placer le curseur horizontal sur le max du pic de la «load force» et la reporter dans le tableau Excel



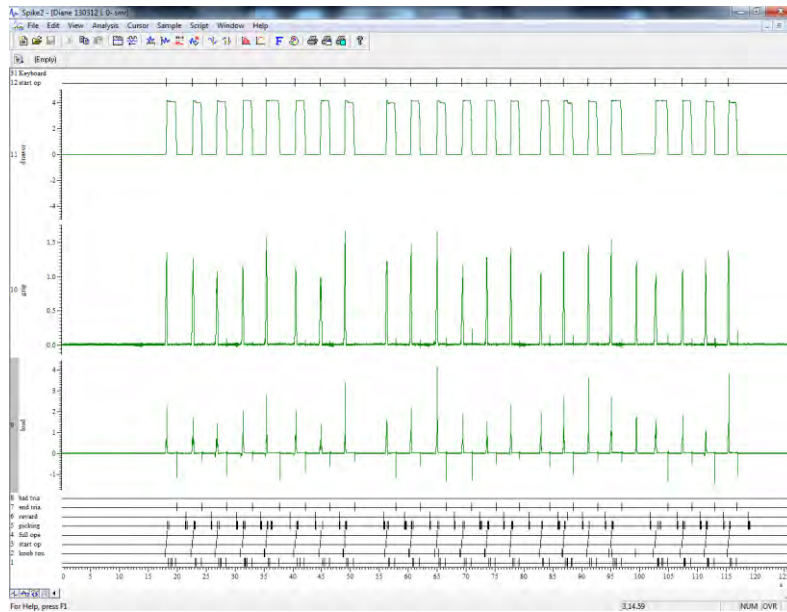
3.3.2. Analysis -> New Result View -> Waveform Average ->



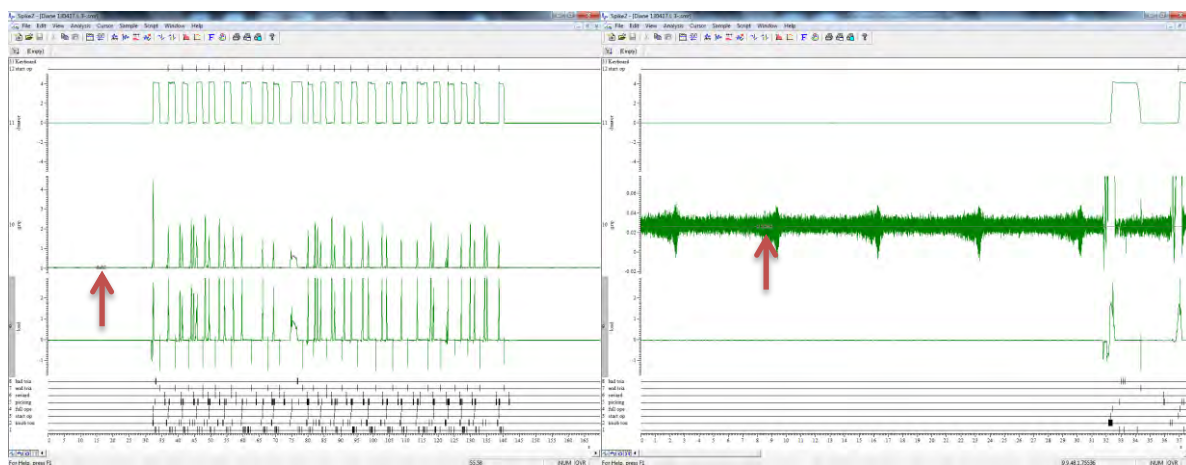
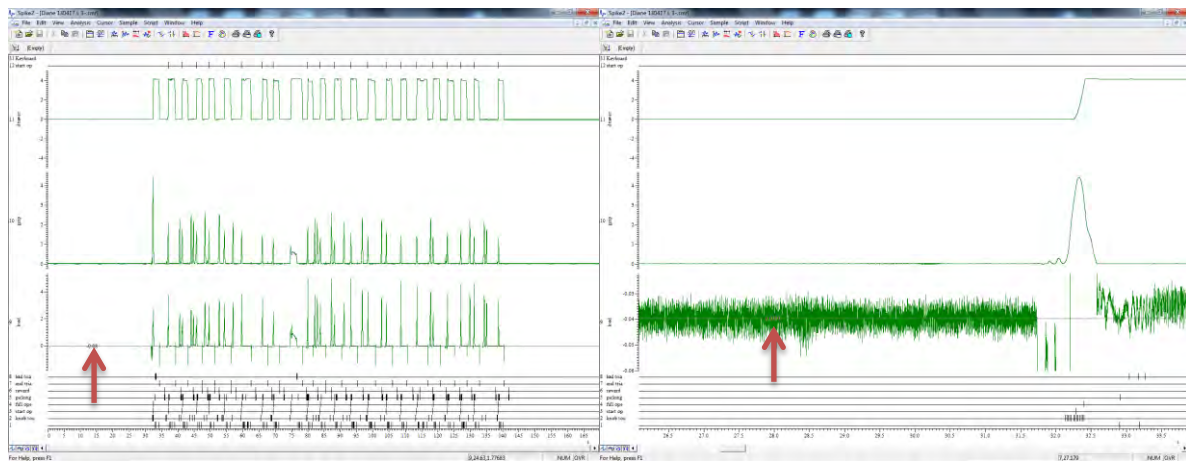
3.3.3. Placer le curseur horizontal sur le max du pic de la «grip force» et la reporter dans le tableau Excel



3.3.4. Pour avoir la valeur moyenne de la «baseline» pour la «load force» et la «grip force» -> Windows -> Choisir le fichier d'origine (sans «Average») ->



-> Placer un curseur horizontal sur la «baseline» de la «load force» puis agrandir pour voir la valeur (même démarche pour la «grip force»)->



-> Reporter les valeurs dans le tableau Excel



## 4. Calculs pour trouver la valeur du seuil de la «baseline»

Exemple :

	A	B	C	D	E	F	G	H	I	J	K	L	M	N	O	P	Q	
1	Max pic																	
2	Load									Grip								
3	L				R					L				R				
4		0	3	5	7	0	3	5	7	0	3	5	7	0	3	5	7	
5	11.07.2013	-0.555	0.121	1.021	1.852	-0.491	0.132	0.826	1.6374	1.483	1.839	2.429	2.498	1.532	2.331	2.598	2.991	
6	27.06.2013	0.729	1.312	2.21	2.983	0.4801	1.14	1.983	2.877	1.481	2.038	2.476	3.124	1.576	2.458	2.814	3.028	
7	14.06.2013	0.5	0.963	1.72	2.632	0.364	0.743	1.49	2.725	1.801	2.027	2.468	2.78	1.852	2.594	2.963	3.028	
8	29.05.2013	0.6217	1.211	1.934	2.994	0.714	1.1	1.795	2.745	1.498	2.166	2.719	2.905	1.865	2.271	2.591	2.932	
9	20.05.2013	0.6325	1.205	2.007	2.869	0.4649	1.065	1.807	2.305	1.344	2.331	2.641	2.737	1.333	2.219	2.505	3.017	
10	10.05.2013	1.035	1.616	2.419	3.075	0.609	1.03	2.109	2.975	1.654	1.832	2.279	2.336	1.843	2.51	2.865	2.9	
11	17.04.2013	1.002	1.824	2.596	3.35	0.641	1.097	1.993	2.849	1.369	1.516	1.889	2.179	1.824	2.561	2.865	3.38	
12	04.04.2013	0.78	1.442	2.117	2.936	0.546	1.346	2.032	2.738	1.556	1.838	2.239	2.598	1.781	2.098	2.571	3.328	
13	20.03.2013	0.738	1.326	2.167	3.094	0.535	1.263	2.059	2.882	0.9852	1.373	2.015	2.24	1.459	2.367	2.834	3.212	
14	12.03.2013	0.811	1.386	2.24	3.1	0.977	1.574	2.227	2.277	1.159	1.712	2.213	2.196	1.747	2.292	2.573	2.555	
15																		
16																		
17	Mean baseline																	
18	Load									Grip								
19	L				R					L				R				
20		0	3	5	7	0	3	5	7	0	3	5	7	0	3	5	7	
21	11.07.2013	-1.4564437	-1.4546254	-1.453687	-1.444073	-1.4515	-1.4451	-1.43609	-1.430256	0.155493	0.154762	0.153495	0.151384	0.148	0.147412	0.146533	0.141931	
22	27.06.2013	-0.12747	-0.1261463	-0.11789	-0.116271	-0.127564	-0.123773	-0.126575	-0.123583	0.038671	0.038975	0.039865	0.04056	0.041982	0.04165	0.040147	0.039132	
23	14.06.2013	-0.2711718	-0.270141	-0.266438	-0.261885	-0.245806	-0.257892	-0.265034	-0.268831	0.091332	0.088105	0.08589	0.082934	0.072462	0.082926	0.088428	0.090843	
24	29.05.2013	-0.0800417	-0.0867723	-0.090273	-0.092865	-0.096246	-0.0949	-0.097263	-0.09903	0.040256	0.04635	0.049839	0.050028	0.047623	0.0477	0.048042	0.048391	
25	20.05.2013	-0.1216463	-0.1316275	-0.131831	-0.1524	-0.1191	-0.139775	-0.133665	-0.131322	0.019173	0.029438	0.031981	0.033	0.0304	0.029351	0.03031	0.028914	
26	10.05.2013	-0.1275517	-0.1249139	-0.124855	-0.117752	-0.115094	-0.122332	-0.126999	-0.127729	0.051185	0.051154	0.050762	0.050092	0.038305	0.047766	0.051183	0.051435	
27	17.04.2013	-0.0427509	-0.039	-0.03277	-0.030099	-0.054532	-0.050037	-0.046199	-0.045299	0.027428	0.029	0.027123	0.027464	0.02534	0.025919	0.02784	0.027624	
28	04.04.2013	-0.0642147	-0.0542308	-0.052424	-0.049397	-0.097354	-0.082958	-0.067794	-0.070213	0.009671	0.009638	0.010727	0.010332	0.004961	0.006723	0.007692	0.010602	
29	20.03.2013	-0.0482464	-0.0490023	-0.050506	-0.042803	-0.031414	-0.034076	-0.040721	-0.049113	-0.00769	-0.009089	-0.008747	-0.008389	-0.017351	-0.01254	-0.010801	-0.009514	
30	12.03.2013	0.0142226	0.0159719	0.0201272	0.0374631	0.0314612	0.0360644	0.028004	0.0285746	0.013519	0.016074	0.016244	0.02592	0.016529	0.016304	0.018547	0.018517	
31																		

### 4.1. Calculer la différence entre «Max pic» et «Mean baseline» (-> hauteur du pic par rapport à la «baseline»)

	A	B	C	D	E	F	G	H	I	J	K	L	M	N	O	P	Q	
31																		
32																		
33	Max pic-Mean baseline																	
34	Load									Grip								
35	L				R					L				R				
36		0	3	5	7	0	3	5	7	0	3	5	7	0	3	5	7	
37	11.07.2013	0.9014437	1.5756254	2.4746866	3.2960727	0.9605	1.5771	2.2620901	3.0676559	1.327507	1.684238	2.275505	2.346616	1.384	2.183588	2.451467	2.849069	
38	27.06.2013	0.85647	1.4381463	2.32789	3.0992714	0.6076638	1.263773	2.1095753	3.0005835	1.442329	1.999025	2.436135	3.08344	1.534018	2.41635	2.773853	3.038868	
39	14.06.2013	0.7711718	1.233141	1.986438	2.8938851	0.6098056	1.0008922	1.7550344	2.9938307	1.709668	1.938895	2.38211	2.697066	1.779538	2.511074	2.874572	2.937157	
40	29.05.2013	0.7017417	1.2977723	2.024273	3.0868648	0.8102456	1.1949	1.8922635	2.84403	1.457744	2.11965	2.669161	2.854972	1.817377	2.2233	2.542958	2.883609	
41	20.05.2013	0.7541463	1.3366275	2.1388309	3.0214	0.584	1.2047748	1.9406652	2.4363224	1.324827	2.301562	2.609019	2.704	1.3026	2.189649	2.47469	2.988086	
42	10.05.2013	1.1625517	1.7409139	2.5438549	3.1927517	0.7240938	1.152332	2.2359995	3.1027291	1.602815	1.780846	2.228238	2.285908	1.804695	2.462234	2.813817	2.848565	
43	17.04.2013	1.0447509	1.863	2.6287702	3.3800991	0.6955316	1.1470375	2.039199	2.894299	1.341572	1.487	1.861877	2.151536	1.79866	2.535081	2.83716	3.352376	
44	04.04.2013	0.8442147	1.4962308	2.1694243	2.9853971	0.6433535	1.4289579	2.0997942	2.8082134	1.546329	1.828362	2.228273	2.587668	1.776039	2.091277	2.563308	3.317398	
45	20.03.2013	0.7862464	1.3750023	2.2175065	3.1368025	0.5664139	1.2970755	2.0997213	2.9311129	0.99289	1.382089	2.023747	2.248389	1.476351	2.37954	2.844801	3.221514	
46	12.03.2013	0.7967774	1.3700281	2.2198728	3.0625369	0.9455388	1.5379356	2.198996	2.2484254	1.145481	1.695926	2.196756	2.17008	1.730471	2.275696	2.554453	2.536483	

Pour la B37 : =B5-B21

Pour la B38 : =B6-B22

...

## 4.2. Calculer la moyenne des hauteurs des pics de toutes les sessions pour chaque résistance (load L/R, grip L/R), puis calculer le 10% des moyennes obtenues

	A	B	C	D	E	F	G	H	I	J	K	L	M	N	O	P	Q
31																	
32																	
33	Max pic-Mean baseline																
34	Load								Grip								
35	L				R				L				R				
36	0	3	5	7	0	3	5	7	0	3	5	7	0	3	5	7	
37	11.07.2013	0.9014437	1.5756254	2.4746866	3.2960727	0.9605	1.5771	2.2620901	3.0676559	1.327507	1.684238	2.275505	3.346616	1.384	2.183588	2.451467	2.849069
38	27.06.2013	0.85647	1.4381463	2.32789	3.0992714	0.6076638	1.263773	2.1095753	3.0005835	1.442329	1.999025	2.436135	3.08344	1.534018	2.41635	2.773853	3.038868
39	14.06.2013	0.7711718	1.233141	1.986438	2.8938851	0.6098056	1.0008922	1.7550344	2.9938307	1.709668	1.938895	2.38211	2.697066	1.779538	2.511074	2.874572	2.937157
40	29.05.2013	0.7017417	1.2977723	2.024273	3.0868648	0.8102456	1.1949	1.8922635	2.84403	1.457744	2.11965	2.669161	2.854972	1.817377	2.2233	2.542958	2.883609
41	20.05.2013	0.7541463	1.3366275	2.1388309	3.0214	0.584	1.2047748	1.9406652	2.4363224	1.324827	2.301562	2.609019	2.704	1.3026	2.189649	2.47469	2.988086
42	10.05.2013	1.1625517	1.7409139	2.5438549	3.1927517	0.7240938	1.152332	2.2359955	3.1027291	1.602815	1.780846	2.228238	2.285908	1.804695	2.462234	2.813817	2.848565
43	17.04.2013	1.0447509	1.863	2.6287702	3.3800991	0.6955316	1.1470375	2.039199	2.894299	1.341572	1.487	1.861877	2.151536	1.79866	2.535081	2.83716	3.352376
44	04.04.2013	0.8442147	1.4962308	2.1694243	2.9853971	0.6433535	1.4289579	2.0997942	2.8082134	1.546329	1.828362	2.228273	2.587668	1.776039	2.091277	2.563308	3.317398
45	20.03.2013	0.7862464	1.3750023	2.2175065	3.1368025	0.5664139	1.2970755	2.0997213	2.9311129	0.99289	1.382089	2.023747	2.248389	1.476351	2.37954	2.844801	3.221514
46	12.03.2013	0.7967774	1.3700281	2.2198728	3.0625369	0.9455388	1.5379356	2.198996	2.2484254	1.145481	1.695926	2.196756	2.17008	1.730471	2.275696	2.554453	2.536483
47	Mean	0.8619515	1.4726488	2.2731547	3.1155081	0.7147147	1.2804778	2.0633338	2.8327202	1.389116	1.821759	2.291082	2.512967	1.640375	2.326779	2.673108	2.997312
48	10%	0.08619515	0.1472649	0.2273155	0.3115508	0.0714715	0.1280478	0.2063334	0.283272	0.138912	0.182176	0.229108	0.251297	0.164037	0.232678	0.267311	0.299731

## 4.3. Calculer la valeur du seuil : additionner le 10% de la moyenne des hauteurs des pics à la valeur de la «Mean baseline»

	A	B	C	D	E	F	G	H	I	J	K	L	M	N	O	P	Q
49																	
50																	
51	Seuil (Mean baseline+(10% (Max pic-Mean baseline)))																
52	Load								Grip								
53	L				R				L				R				
54	0	3	5	7	0	3	5	7	0	3	5	7	0	3	5	7	
55	11.07.2013	-1.3702486	-1.3073605	-1.2263711	-1.1325219	-1.3800285	-1.3170522	-1.2297567	-1.1469839	0.2944051	0.3369382	0.3826033	0.4026805	0.3120375	0.3800899	0.4138440	0.4416626
56	27.06.2013	-0.0412748	0.0211186	0.1094255	0.1952794	-0.0560923	0.0042748	0.0797581	0.1596886	0.1775827	0.2211507	0.2689734	0.2918572	0.2060195	0.2743281	0.3074577	0.3388635
57	14.06.2013	-0.1849767	-0.1228761	-0.0391226	0.0496657	-0.1743341	-0.1298444	-0.0587010	0.0144413	0.2302432	0.2702808	0.3149984	0.3342306	0.2364990	0.3156036	0.3557389	0.3905747
58	29.05.2013	0.0061534	0.0604926	0.1370424	0.2186861	-0.0247741	0.0331478	0.1090699	0.1842421	0.1791676	0.2285261	0.2789476	0.3013250	0.2116604	0.2803779	0.3153532	0.3481219
59	20.05.2013	-0.0354512	0.0156374	0.0954846	0.1591508	-0.0476285	-0.0117270	0.0726681	0.1519496	0.1580851	0.2116136	0.2610895	0.2842967	0.1944375	0.2620285	0.2976204	0.3286454
60	10.05.2013	-0.0413566	0.0223510	0.1024606	0.1937991	-0.0436224	0.0057158	0.0793339	0.1555429	0.1900962	0.2333295	0.2798699	0.3013890	0.2023428	0.2804443	0.3184940	0.3511666
61	17.04.2013	0.0434443	0.1082649	0.1945453	0.2814517	0.0169398	0.0780103	0.1601344	0.2379730	0.1666397	0.2111759	0.2562311	0.2787603	0.1893772	0.2585973	0.2951511	0.3273552
62	04.04.2013	0.0219804	0.0930341	0.1748912	0.2621537	-0.0258821	0.0450899	0.1385392	0.2130586	0.1485823	0.1918135	0.2398356	0.2616289	0.1689986	0.2394008	0.2750029	0.3103331
63	20.03.2013	0.0379487	0.0982626	0.1768090	0.2687483	0.0400576	0.0939722	0.1656120	0.2341591	0.1312213	0.1730866	0.2203614	0.2429082	0.1466865	0.2201375	0.2565102	0.2902173
64	12.03.2013	0.1004178	0.1632368	0.2474426	0.3490139	0.1029327	0.1641122	0.2343374	0.3118466	0.1524305	0.1982497	0.2453523	0.2772168	0.1805663	0.2489817	0.2858578	0.3182485

Pour la B55 : =B21+B48

Pour la B56 : =B22+B48

Pour la C55 : =C21+C48

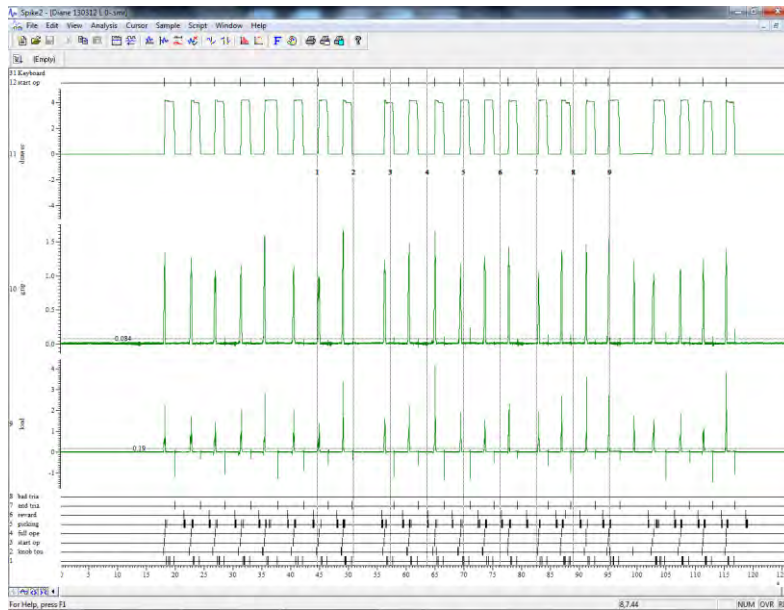
...

## 5. Créer un script

Ce script unique sera utilisé pour tous les fichiers «purifiés» à analyser

### 5.1. Ouvrir un fichier «purifié»

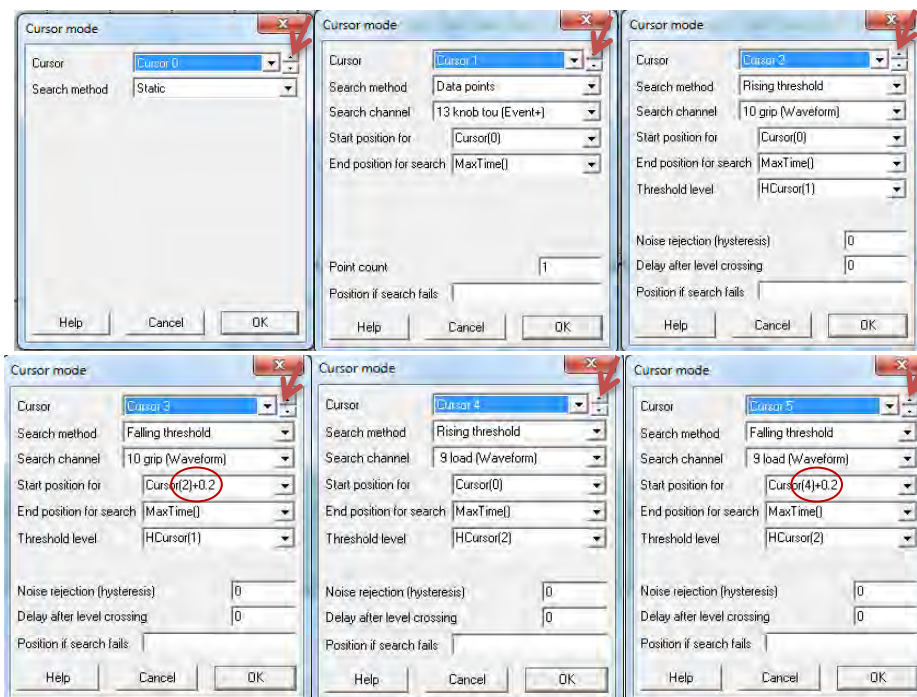
5.1.1. Script -> Turn recording On -> placer le 1<sup>er</sup> curseur horizontal (HC 1) en dessus de la baseline de la «grip force» -> placer le 2<sup>ème</sup> curseur horizontal (HC 2) en dessus de la «baseline» de la «load force» -> ajouter 9 curseurs verticaux

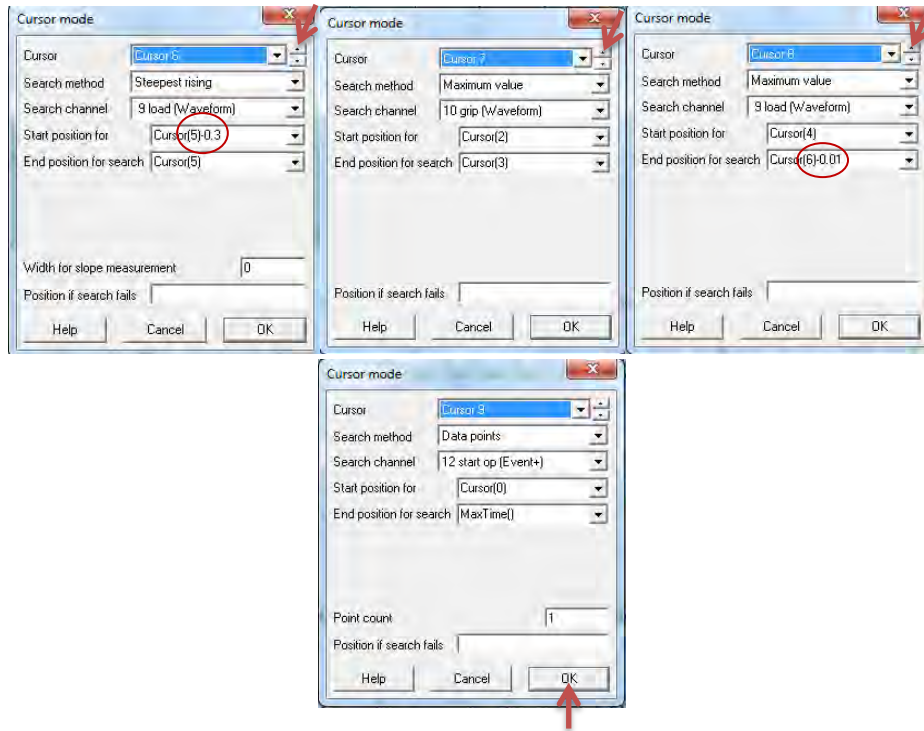


## 5.2. Définir les curseurs

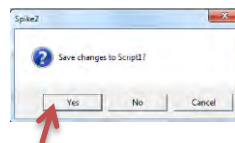
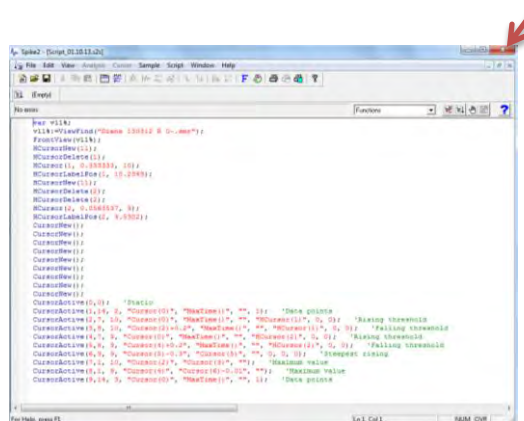
Les valeurs entourées pour les curseurs 3, 5, 6, 8 ne sont pas fixes, elles peuvent varier d'un sujet à l'autre -> redéfinir ces valeurs si au point 6.2.4., les curseurs ne se placent pas aux bons endroits : examiner la durée des réponses pour la «load/grip force» (intervalle de temps entre le début et la fin de la réponse) lors de l'analyse des «Waveform Averages» au point 4.

-> Cursor -> Active Modes ->





-> Script -> Turn Recording Off ->



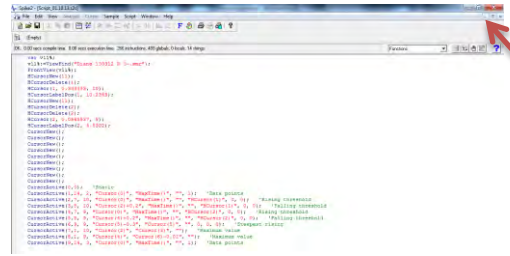
-> Save

## 6. Appliquer les valeurs de seuil dans Spike

### 6.1. Ouvrir un fichier («purifié»)

6.1.1. Script -> Run Script -> Load and run... -> Choisir le script crée dans 5. -> Open -> Minimize ->

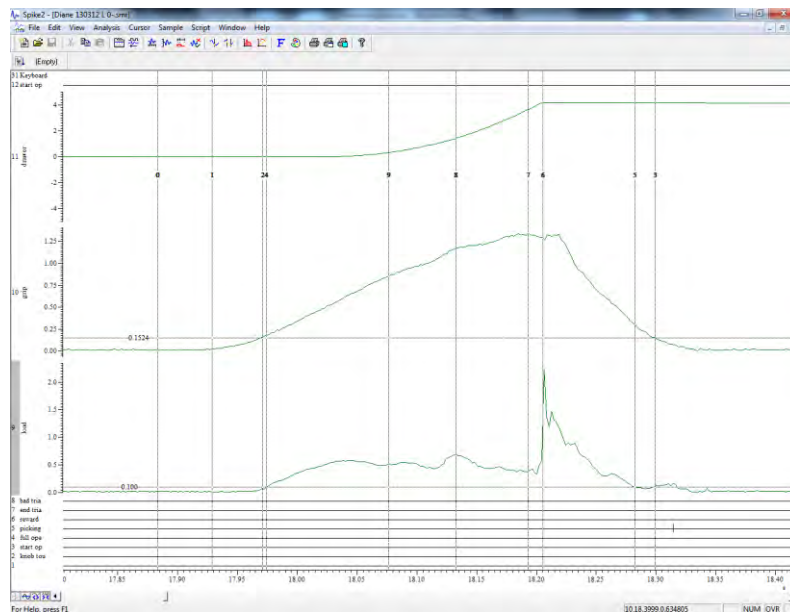




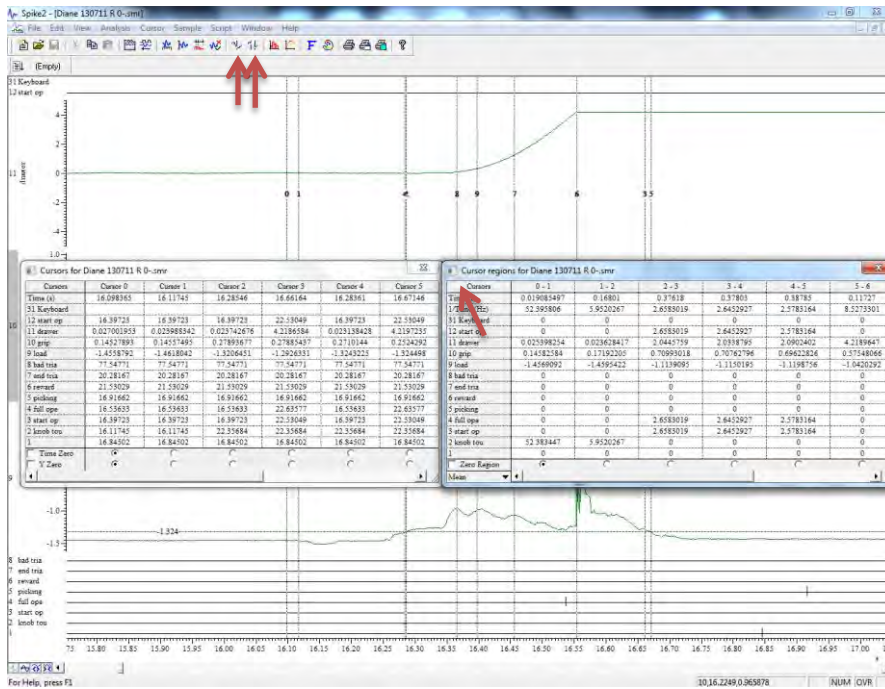
- 6.1.2. Placer le curseur horizontal existant (HC 1) en dessus de la «baseline» de la «grip force»
- 6.1.3. Placer un nouvel curseur horizontal (HC 2) en dessus de la «baseline» de la «load force»
- 6.1.4. Clic droit sur le curseur horizontal de la «grip force»-> *HCursor 1* -> *Set position...* -> Copier la valeur du seuil calculé (depuis le tableau Excel) et la coller dans *Cursor Position* -> *OK*
- 6.1.5. Clic droit sur le curseur horizontal de la «load force» -> *HCursor 2* -> *Set position...* -> Copier la valeur du seuil calculé (depuis le tableau Excel) et la coller dans *Cursor Position* -> *OK*

## 6.2. Agrandir le premier essai

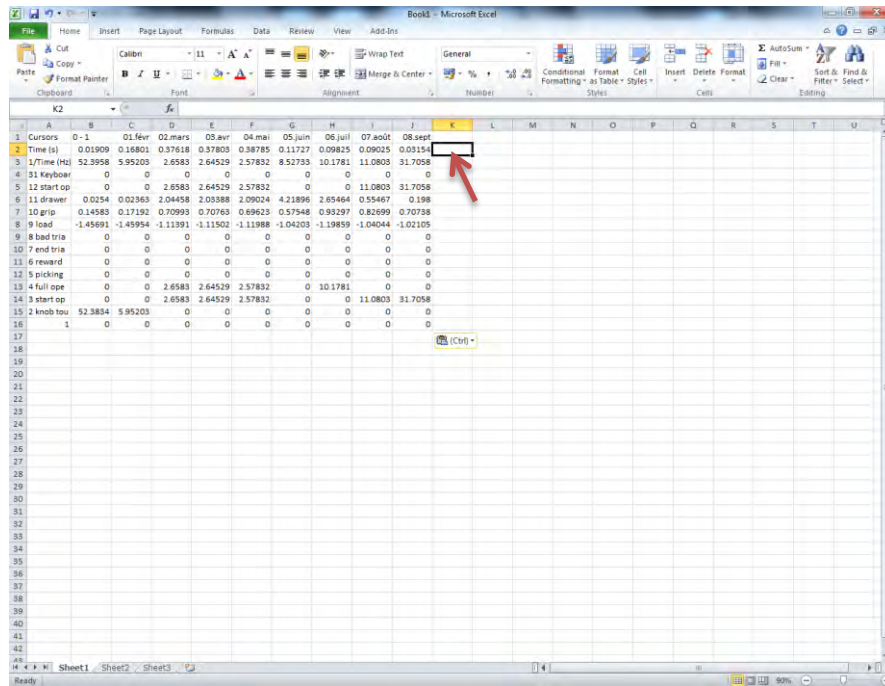
- 6.2.1. Si nécessaire, clic droit sur 9 -> *Channel 9* -> *Optimise Y range* (même chose pour «channel 10»)
- 6.2.2. Si un trait est présent dans «12 start op» et dans «13 knob tou», les réponses peuvent être analysées (dans le cas contraire, c'est un «bad trial», il faut passer à la réponse suivante et ainsi de suite)
- 6.2.3. *Cursor* -> *Fetch* -> *Cursor 0* -> Placer le curseur 0 juste avant le trait du «knob touch»



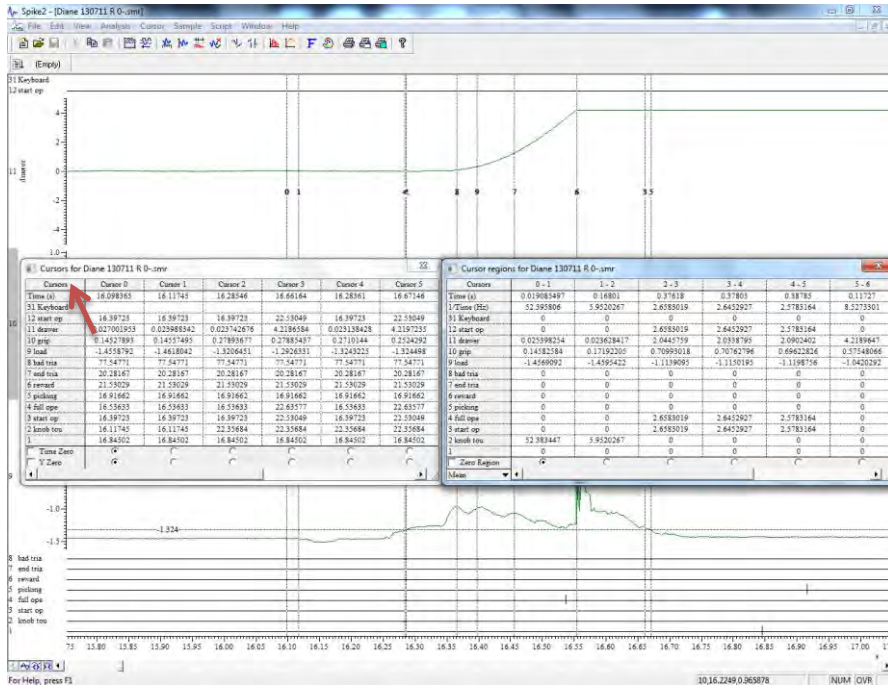
- 6.2.4. S'assurer que tous les curseurs sont présent et qu'ils sont positionnés aux bons endroits (dans le cas contraire, considérer l'essai comme un «bad trial», passer à l'essai suivant)
- 6.2.5. Prélever les valeurs des curseurs dans le tableau Excel



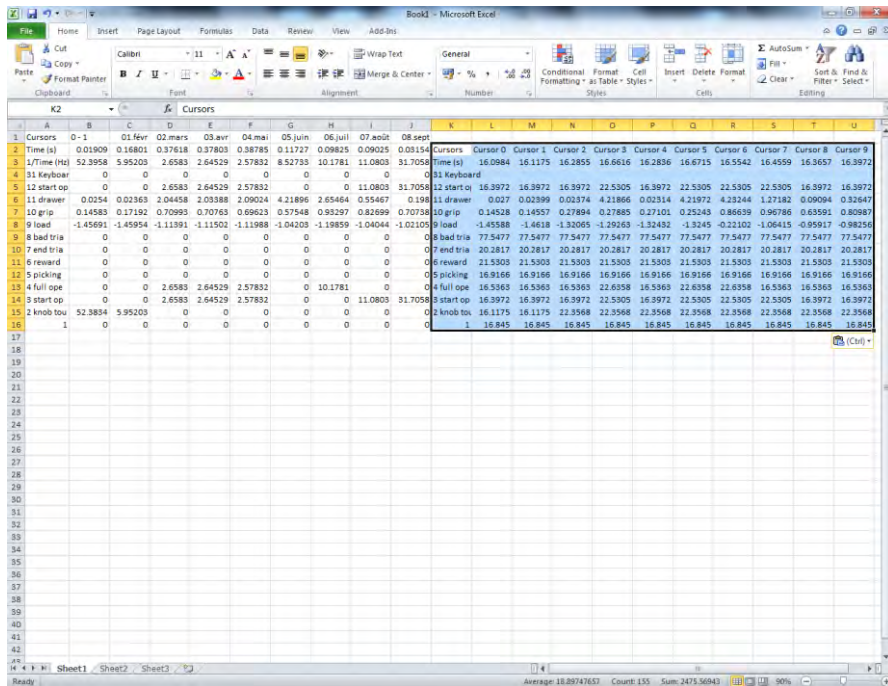
-> Copier -> Coller dans Excel-> Sélectionner la cellule comme indiqué ->



-> Copier le deuxième tableau



-> Coller dans Excel



-> Vérifier que les numéros des curseurs sont alignés pour les deux tableaux (-> utile pour les prochaines analyses)

### 6.3. Passer aux essais suivants et répéter les étapes 6.2.1.-6.2.5.

### 6.4. Sauver le fichier Excel

Un minimum de 5 « bons » essais par résistance est souhaitable

Garder un intervalle régulier entre les sessions analysées (analyser 1 session par semaine par ex.)





***Annex 2***  
***(Histological procedures)***



## Violet de Crésyl (juin 2009)

Solutions : Violet de Crésyl 0.5%

- 1000 ml H<sub>2</sub>O dist.
- 5.444 Na acétate (tri-hydrate de Merck)
- 5 g violet de Crésyl (Merck)

Mélanger 2 heures => 2 jours

Ajouter 9.606 ml acide acétique (100%)

Filtrer 3 à 5 fois

### Alcool-acide

Alcool 80%	1000 ml
Acide acétique conc.	20 ml

Technique: Dégraissage préalable comme suit :

Chloroforme-alcool 100 (1/1) 1h.

Alcool 100 2x 3 min.

Alcool 95 3 min.

Sécher à l'étuve à 37 °C puis :

- alcool 70 2 min.

- alcool 50 1 min.

- H<sub>2</sub>O dist. 30 sec.

- V.C. 2 => 7 min. à 40°C

- H<sub>2</sub>O dist. 2-3x total 1 min.30 sec.

- alcool 70 1 => 3 min.

- alcool-acide env. 1=>6 min.

- alcool 95 1 min.

- alcool 100 2x total 1 min.

- butanol 5=>45 min.

- xylol 2x 5 min.

Monter avec Eukit

## Coloration Noir de Soudan (Sudan Black B) – Protocole J.-F Brunet

### Coloration :

- 1) PBS 1x – rinçage 30 secondes
- 2) Noir de Soudan B 1 % 5 minutes
- 3) Alcool 70 % - rinçage 2 minutes
- 4) PBS 1x – rinçage 30 secondes
- 5) Monter la lame (**Glemoun, Vectashield, à tester**). Fluoromount aqueous Mounting Sigma F4680

### Préparation :

1 % Noir de Soudan B à diluer dans l'alcool 70%  
(1 g dans 100 ml d'éthanol 70 %)

Mettre une nuit sous agitation. **Filtrer ?**

Refaire régulièrement cette solution (toutes les semaines)

Eventuellement de 0.1 à 10 %, dépend des structures autofluorescentes à masquer

Attention solution très colorante.

### Référence :

Sudan Black B, Fluka 86015

Environ 90 CHF la boîte

---

### Phosphate Buffer 0.2M

NaH <sub>2</sub> PO <sub>4</sub>	10.48 g
Na <sub>2</sub> HPO <sub>4</sub> (x12 H <sub>2</sub> O)	57.68 g
Distilled water	1800 ml

### **Adjust pH to 7.4**

Add distilled water <b>until</b>	2000 ml
----------------------------------	---------

### PBS 1x :

NaCl	9 g
PB 0.2M	50 ml
Add distilled water <b>until</b>	1000 ml

## DAY 1

- **Rinçages:** Phosphate Buffer (50RPM) -
- **Rinçages:** PBS 1x 1x rapide + 2x 10'

Sous agitation circulaire 50 RPM

- **Blocage sites non spé :** PBS-BSA 0.25% + Triton 0.3% + NGS 5% 1h-RT

Sous agitation circulaire 50 RPM

1.5ml/puit précisément

- **Anticorps primaire :** Voir plan des coupes !!!

### 1. Polyclonal Rabbit anti-TH (ref : Millipore, Polyclonal antibody, AB152)

Dilution **1/500** et **1/1000** (1.5ml/puit précisément)

Dans PBS-BSA 0.25% + Triton 0.3%

#### Incubation

Durant la nuit à 4°C, sous agitation circulaire à 50 RPM et à l'abri de la lumière (alu)

- **Neutralisation Ac secondaire :** avec 1 coupe de Mörly (coupe de singe) **un lobe suffit !**

**!! un par anticorps secondaire !!**

Goat anti rabbit Alexa 488 (IgG(H+L)), A11034, 8148 → 1/300

Goat anti mouse Alexa fluor 594 (IgG(γ1), A21125, 753763 → 1/300

Dans PBS 1x

#### Incubation

**Durant la nuit à 4°C** Sous agitation circulaire 50 RPM et à l'abri de la lumière (alu)

## **DAY 2**

- Rinçages: PBS 1x 1x rapide + 2x 10'

- NNG: 1 :1000

**Neurotrace Nissl Green (NNG) (ref. Molecular Probes N21480-lot 1218003)**

- Anticorps secondaire (dans mörly): **Voir plan des coupes !!!**

**Goat anti rabbit Alexa 488 (IgG(H+L)), A11034, 8148 →1/300**

**Goat anti mouse Alexa fluor 594 (IgG(γ1), A21125, 753763 →1/300**

**1.5ml/puit précisément**

Dans PBS 1x

### Incubation

**1h à RT, sous agitation circulaire 50RPM**

- Rinçages: PBS 1x 3x5'

Sous agitation circulaire 50RPM

\*\*\*\*\*

- Montage et séchage:

**Milieu de montage aqueux (ref : Sigma F.4680 (25mL)\_lot :060M1527)**

Montage dans Petri dish (100ml dist. H<sub>2</sub>O + 100ml PBS)

Attendre 1 à 2h avant de coller lamelle

**Conservé au Frigo**

## ***Annex 3***

### ***Behavioral Assessment of Manual Dexterity in Non-Human Primates.***

Eric Schmidlin\*, Mélanie Kaeser\*, Anne- Dominique Gindrat, Julie Savidan,  
Pauline Chatagny, Simon Badoud, Adjia Hamadjida, Marie-  
Laure Beaud, Thierry Wannier, Abderraouf Belhaj-Saif, Eric M. Rouiller

Published in Journal of Visualized Experiments (2011)





## Video Article

# Behavioral Assessment of Manual Dexterity in Non-Human Primates

Eric Schmidlin<sup>1</sup>, Mélanie Kaeser<sup>1</sup>, Anne-Dominique Gindrat<sup>1</sup>, Julie Savidan<sup>1</sup>, Pauline Chatagny<sup>1</sup>, Simon Badoud<sup>1</sup>, Adja Hamadjida<sup>1</sup>, Marie-Laure Beaud<sup>1</sup>, Thierry Wannier<sup>1</sup>, Abderraouf Belhaj-Saif<sup>1</sup>, Eric M. Rouiller<sup>1</sup>

<sup>1</sup>Department of Medicine, University of Fribourg

\*These authors contributed equally

Correspondence to: Eric M. Rouiller at [Eric.Rouiller@unifr.ch](mailto:Eric.Rouiller@unifr.ch)

URL: <http://www.jove.com/video/3258>

DOI: [doi:10.3791/3258](https://doi.org/10.3791/3258)

Keywords: Neuroscience, Issue 57, monkey, hand, spinal cord lesion, cerebral cortex lesion, functional recovery

Date Published: 11/11/2011

Citation: Schmidlin, E., Kaeser, M., Gindrat, A.D., Savidan, J., Chatagny, P., Badoud, S., Hamadjida, A., Beaud, M.L., Wannier, T., Belhaj-Saif, A., Rouiller, E.M. Behavioral Assessment of Manual Dexterity in Non-Human Primates. *J. Vis. Exp.* (57), e3258, doi:10.3791/3258 (2011).

## Abstract

The corticospinal (CS) tract is the anatomical support of the exquisite motor ability to skillfully manipulate small objects, a prerogative mainly of primates<sup>1</sup>. In case of lesion affecting the CS projection system at its origin (lesion of motor cortical areas) or along its trajectory (cervical cord lesion), there is a dramatic loss of manual dexterity (hand paralysis), as seen in some tetraplegic or hemiplegic patients. Although there is some spontaneous functional recovery after such lesion, it remains very limited in the adult. Various therapeutic strategies are presently proposed (e.g. cell therapy, neutralization of inhibitory axonal growth molecules, application of growth factors, etc), which are mostly developed in rodents. However, before clinical application, it is often recommended to test the feasibility, efficacy, and security of the treatment in non-human primates. This is especially true when the goal is to restore manual dexterity after a lesion of the central nervous system, as the organization of the motor system of rodents is different from that of primates<sup>1,2</sup>. Macaque monkeys are illustrated here as a suitable behavioral model to quantify manual dexterity in primates, to reflect the deficits resulting from lesion of the motor cortex or cervical cord for instance, measure the extent of spontaneous functional recovery and, when a treatment is applied, evaluate how much it can enhance the functional recovery.

The behavioral assessment of manual dexterity is based on four distinct, complementary, reach and grasp manual tasks (use of precision grip to grasp pellets), requiring an initial training of adult macaque monkeys. The preparation of the animals is demonstrated, as well as the positioning with respect to the behavioral set-up. The performance of a typical monkey is illustrated for each task. The collection and analysis of relevant parameters reflecting precise hand manipulation, as well as the control of force, are explained and demonstrated with representative results. These data are placed then in a broader context, showing how the behavioral data can be exploited to investigate the impact of a spinal cord lesion or of a lesion of the motor cortex and to what extent a treatment may enhance the spontaneous functional recovery, by comparing different groups of monkeys (treated versus sham treated for instance). Advantages and limitations of the behavioral tests are discussed. The present behavioral approach is in line with previous reports emphasizing the pertinence of the non-human primate model in the context of nervous system diseases<sup>2,3</sup>.

## Video Link

The video component of this article can be found at <http://www.jove.com/video/3258/>

## Protocol

The overall scheme of the experiment is depicted in Figure 1.

### 1. Animal preparation and transfer to the behavioral laboratory

1. In the laboratory, prepare the behavioral set-up: fill the wells of the different test boards (tests 1 to 3 below) with the pellets, which serve as reward during the behavioral tests.
2. Transfer the monkey from the group housing room into a transfer cage. The monkey is trained to enter a tunnel giving access to the primate chair, with subsequent positioning of the head. The monkey's weight is measured, before transfer in the primate chair to the laboratory.

### 2. Test 1: Modified Brinkman board

1. This test, modified and adapted from previous reports<sup>4,5</sup>, is the basic behavioral task of reference, to be conducted on every behavioral session. Initiate the video recording with the digital camera above the set-up (possibility also to place 2 additional cameras, one on each side of the board) and place the monkey in front of the Brinkman board.
2. Open for instance the right window on the primate chair to give access to the right hand. Using the right hand, the monkey retrieves the food pellets from the 50 slots (25 vertical and 25 horizontal).
3. After completion of the test, close the right window and refill the board with pellets.

4. Open the left window and repeat the test for the left hand.
5. Reward the animal at the end of the test with a few dried raisins or an almond, a procedure to be repeated at the end of each test to maintain the motivation during the whole daily session.

Additional information: Three digital video cameras are used to record the sequence for off-line processing, placed one above the board and one on each side of the board (to precisely assess the position of the fingers while performing the grasping). Within the same daily session, the monkey can perform another task (either task 2, and/or task 3 and/or task 4; to be distributed among the different days of the week). For the test 1, if the monkey started with the right hand on day 1, start with the left hand on day 2 and so on.

6. Optional: While the test performed above with one or the other hand separately allows comparing the performance of the left hand to the right hand (to identify the "dominant hand"), it is also possible at an early stage of the training to let the monkey perform the task with both hands simultaneously. If one hand is used more often than the other to grasp pellets, then it may be considered as the "preferred hand".

### 3. Test 2: Brinkman box (with and without visual control)

1. The Brinkman box comprises 20 wells (10 vertical and 10 horizontal). As compared to test 1, the monkey has to control the hand in a limited space, with reduced degrees of freedom to perform the precision grip movement. Fill the board with pellets and close the upper facet of the box, in order to conduct first the test in absence of visual control (relying on tactile exploration).
2. Place the monkey in front of the Brinkman box. Open the left window of the primate chair to test the left hand in absence of visual control. The monkey tries to retrieve the 20 pellets, while the sequence is recorded from a digital camera placed below the box.
3. Close the left window of the primate chair. Refill the board with pellets. Open the right window of the primate chair. The monkey repeats the test with the right hand in absence of visual control. Close the right window of the primate chair.
4. To test the ability to grasp pellets in the Brinkman box under visual control, open the top facet of the box.
5. Refill the box with pellets and the monkey performs the test using the right hand.
6. Close the right window of the primate chair. Refill the box with pellets.
7. Open the left window of the primate chair. The monkey performs the test using the left hand. Repeat step 2.5.

### 4. Test 3: Rotating Brinkman board

1. This test is comparable to the Brinkman board task (test 1), except that the board is rotating, forcing the monkey to anticipate the displacement of the board in one (clockwise) or the other (counter-clockwise) direction. Fill the board with pellets. The sequence is recorded with a digital camera placed above the set-up (possibility also to place 2 additional cameras, one on each side).
2. Open the right window of the primate chair. The monkey retrieves the pellets from the 32 wells, distributed on four concentric rows, while the board is turning clockwise.
3. Close the right window. Refill the board with pellets.
4. Open the left window of the primate chair. The monkey performs the test as in 4.2 with the left hand.
5. Repeat points 4.2 to 4.4, while the board is turning counterclockwise (one hand after the other). Repeat step 2.5.

### 5. Test 4: Reach and grasp drawer task

1. To combine prehension ability with the capacity to generate force, this test (derived from previous versions<sup>6-11</sup>) was designed so that the monkey has to open a drawer by exerting first a grip force on the knob of the drawer, followed by a load force to open the drawer, giving access to a pellet placed inside the drawer. The pellet is retrieved with the same hand while the drawer remains open, again using the precision grip. A digital camera is placed on top of the drawer, to record the trials for off-line control of the data (e.g. detection of erroneous trials).
2. Open the right window of the primate chair. The monkey performs 10 trials at each of the 5 different levels of resistance, using the right hand (to have at least 5 correct trials for each resistance level).
3. Repeat the test (50 trials) with the left hand. Repeat step 2.5.

Additional information: On the next behavioral daily session, alternate the hand with which the animal did the test first on the previous session.

### 6. End of behavioral session

1. After completion of the tests foreseen on that day, feed and reward the monkey with food in addition to the pellets received during the tests. Typically, the monkey receives cereals and fruits.
2. The monkey is returned to the group housing room with the mates.

The precise temporal sequence of the various tests performed is written on the protocol form.

### 7. Representative Results

The four behavioral tests illustrated above (**Figure 1**) have been used extensively in our laboratory in the context of studies aimed at investigating the functional recovery from lesion of the cervical spinal cord (**Figure 2A**) or of the motor cortex (**Figure 2B**), in absence or in presence of a treatment applied to enhance the spontaneous recovery<sup>12-19</sup>.

For test 1 (*modified Brinkman board*), the analysis is focused on two parameters (**Figures 3 and 4A**): i) the score, given by the number of pellets retrieved by the monkey in the first 30 seconds, counted separately for the vertical slots and the horizontal slots (by replaying off-line the

recorded video sequence); ii) the contact time (CT), defined as the time (duration) of contact between the fingers and the pellet (see also Figure 6, bottom series of pictures). It is the time interval between the insertion of the first finger (usually the index finger) into the slot to touch the pellet and the onset of retrieval of the pellet out of the well. The time interval is measured by replaying frame by frame the video sequence. The CT is measured for the first five vertical slots and the first five horizontal slots aimed by the monkey<sup>16-18</sup>. The graphs of the score illustrate the initial training phase, the pre-lesion plateau, the dramatic drop of score (usually to zero) immediately after the lesion, the progressive (spontaneous) functional recovery towards the post-lesion plateau. The functional recovery is expressed in % by the ratio of the median post-lesion score at plateau divided by the median pre-lesion score (plateau)  $\times 100$  (Figures 3 and 4A). For the CT, as an increase reflects a deficit, the functional recovery expressed in % is the ratio of the median pre-lesion CT (plateau) divided by the median post-lesion CT at plateau  $\times 100$ . The effect of treatments post-lesion, demonstrated based on the test 1, are illustrated in detail in previous reports from this laboratory<sup>14,15,17</sup>. A further analysis may address the issue of the strategy, namely the temporal sequence of slots visited by the monkey (Figure 4B).

For test 2 (*Brinkman box*), although the score can also be established as in test 1, a more meaningful parameter is the "total time", defined as the time interval between the picking of the pellet in the first slot and the picking of the pellet in the last (20<sup>th</sup>) slot (Figure 5). A functional recovery can be computed and expressed in %. It is calculated using the median total time pre-lesion (plateau after training phase) divided by the median total time post-lesion at plateau  $\times 100$ .

For test 3 (*rotating Brinkman board*), although the score can also be established as above (test 1), a sensitive parameter is the contact time (CT, defined as above in test 1), measured for the first ten slots (Figure 6).

For test 4 (*reach and grasp drawer task*), the set-up comprises several detectors, recording discrete events such as trial initiation (the hand interrupts a light beam placed in front of the panel), hand touching the knob, onset of drawer pulling, end of drawer opening, hand entering the slot (pick-in time), hand withdrawal from the slot (pick-out time). Force transducers on the knob allow measuring the grip force (exerted by the thumb and index finger pressing on the knob) and the load force (exerted to pull the drawer, to counteract different levels of resistance imposed on the drawer opening). The different levels of resistance opposing the opening of the drawer were obtained by changing the intensity of current applied to a rotative electromagnetic motor attached to the back of the drawer. The set-up is designed to apply a resistive force in parallel to the orientation of the opening of the drawer. Detailed scheme of the drawer set-up is available on request to the corresponding author. All these data are collected with the interface and software *Spike 2* and displayed as illustrated in Figure 7.

As previously reported<sup>14,15</sup>, these tasks represent the behavioral basis to investigate whether the spontaneous recovery from a lesion of the cervical cord may be enhanced with a specific treatment aimed at promoting axonal regeneration (Figure 8).

The retrieval score and the contact time parameters reflect different components of the manual dexterity: the first one includes the entire motor sequence (reaching, grasping, withdrawal of the hand, transport of the pellet to the mouth), whereas the second one is focused on the grasping phase only. These two parameters are particularly accurate and complementary for the modified and the rotating Brinkman board tasks. Whereas the score represents largely redundant information in these two tasks, the contact time in contrast provides more task-specific information due to the variability of the slots' positions in the rotating Brinkman board task, as compared to their static position in the modified Brinkman board task. The Brinkman box task differs from the two above mentioned tasks, as the degrees of freedom of movements with the hand are limited by the closed space. As a consequence, the positions of the different slots on the board within the Brinkman box play an important role in terms of difficulty to perform the manual prehension, due to the exiguity of the box. For instance, the grasping with the hand from the slots located on the right side of the box interferes with right lateral wall.

Consequently, the assessment of retrieval score limited to 30 seconds as in the modified Brinkman board would be biased depending on the position of the slots actually visited by the monkey during this restricted time period, generating a substantial variability from one session to another. For this reason, it is more appropriate to involve all slots ( $n=20$ ) and therefore the parameter total time was chosen. In the modified Brinkman board, the total time was not considered, as the monkey may in some case loose motivation (for instance post-lesion) due to the large number of slots to be performed ( $n=50$ ). Along the same line, the analysis of the contact time would implicate to take all the slots of the Brinkman box into consideration (whereas only the first five slots in the modified Brinkman board were considered as the position of the selected slots has little, if no impact on this parameter). Therefore, for the Brinkman box, we recommend in a first approach to determine the total time, as it was observed to be a highly pertinent and informational parameter, at least in our studies with monkeys subjected to a motor cortex lesion (no data available for spinal cord lesioned monkeys). Nevertheless, the contact time may be considered for the Brinkman box, but in a second step including all twenty slots, separately however for the horizontal and vertical slots (not shown).

## Four manual dexterity tasks

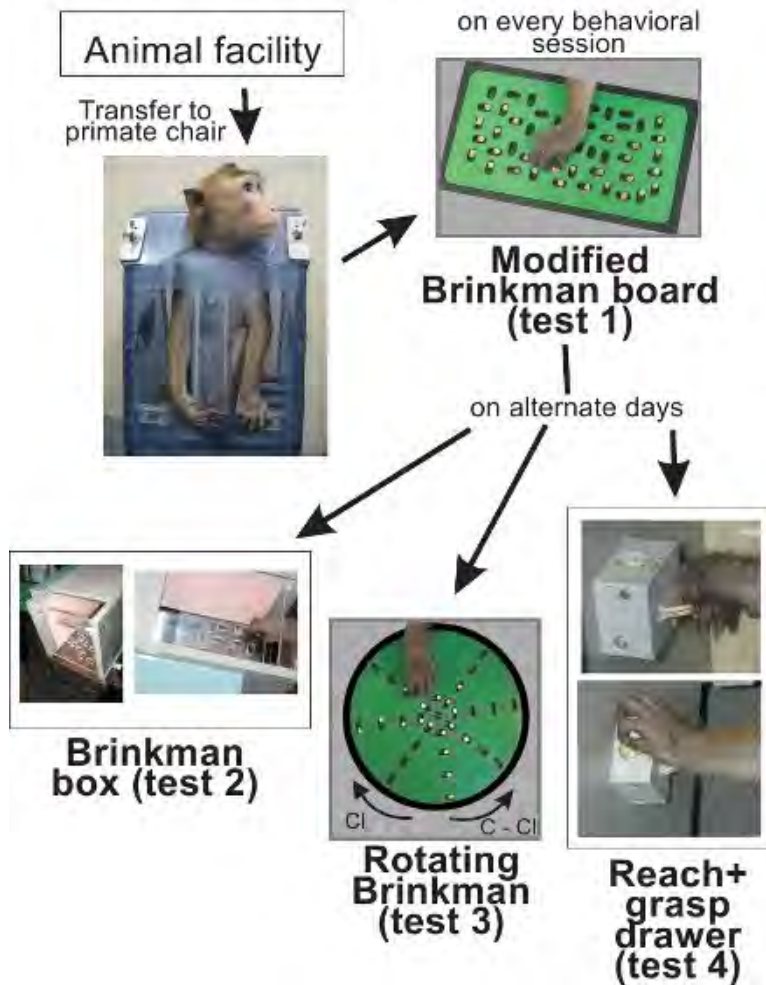


**Figure 1.** Overall scheme of the experiment. The animal is transferred from the animal facility into the primate chair, transported then to the behavioral laboratory. On each daily session, the monkey performs the test 1. On alternate days, the monkey then performs test 2, and/or test 3, and/or test 4. Some monkeys (especially motivated) may perform all tests on the same daily session. Food pellets (used as reward) were made of dried banana or glucose powder that is compressed in a round shape of about 4 mm in diameter. In all our behavioral tests, we use dustless precision pellets (45 mg) provided by BioServ, One 8th street, Suite One, Frenchtown, NJ 08825, USA.

The dimension of the modified Brinkman board is 240mm long and 140 mm wide, whereas the dimension of the slots is 15 mm long, 8 mm wide and 6 mm deep. The diameter of the board in the rotative Brinkman board is 114 mm.

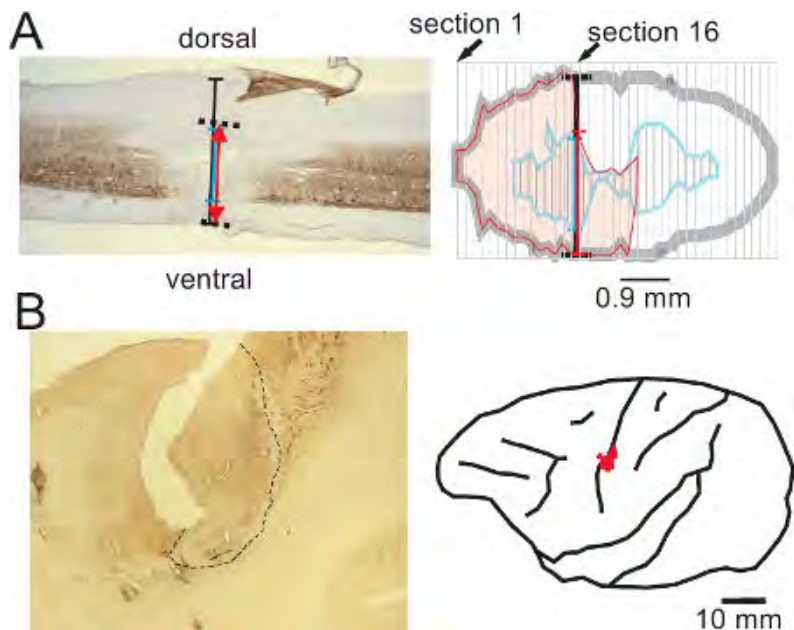


**Figure 2.** Representative (surgical) lesion of the cervical cord (panel A; modified from<sup>15</sup>) and (chemical) lesion of the motor cortex (panel B; modified from<sup>16</sup>), derived from corresponding histological sections, processed for SMI-32 staining. The maximal extent of the cervical cord lesion has been reconstructed from consecutive sagittal sections of the spinal cord (panel A), whereas the extent and position of the motor cortex lesion has been reconstructed from consecutive frontal sections of the brain and re-positioned on a lateral view of the corresponding brain hemisphere (red spot in panel B). The cervical cord lesion resulted from a transection with a surgery blade at the level C7-C8, resulting in a sub-hemisection interrupting unilaterally the main CS tract component in the dorsolateral funiculus, above the motoneurons controlling hand muscles<sup>14,15,20</sup>. The permanent cortical lesion was produced by infusion of ibotenic acid<sup>13,16,17</sup>, at sites covering the hand representation previously established using intracortical microstimulation (ICMS, see<sup>16,21,22</sup>). The cortical lesion territory appears as an abrupt interruption of the SMI-32 staining of neurons in layers III and V in the rostral bank of the central sulcus (area delineated with the dashed line in panel B).

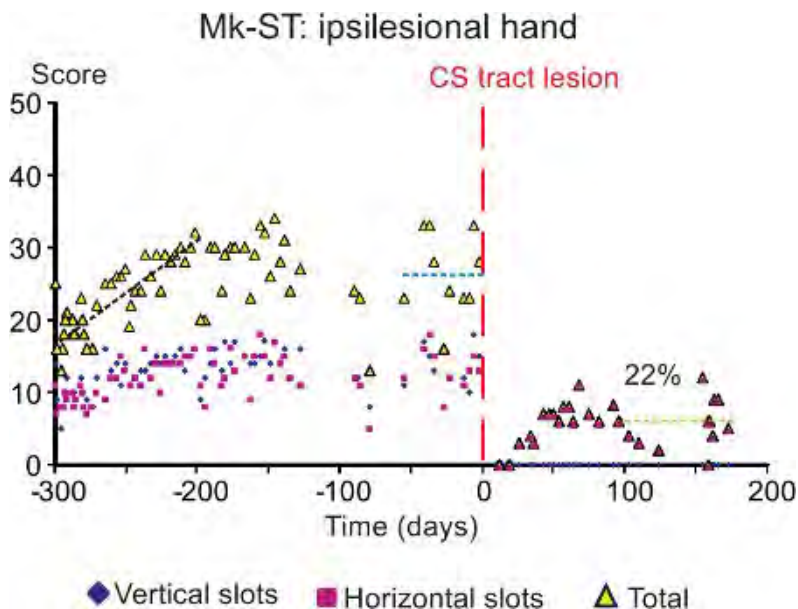


**Figure 3.** Representative data derived from the modified Brinkman board task (test 1) performed by a monkey subjected to a lesion of the spinal cord (as illustrated in Figure 2A). The graph shows the score (ordinate), separately for the vertical slots (blue symbols) and the horizontal slots (red symbols). The yellow symbols are for the sum of vertical and horizontal scores on a given daily session. In the abscissa, the time is for the consecutive days of the behavioral sessions. The vertical dashed redline (day 0) is the day at which the lesion was performed. Three different periods are highlighted: the first one (black dashed line) corresponds to the training period, the second one (blue dashed line) to the plateau of performance before the lesion, and the third one (green dashed line) to the plateau of recovered performance. Data modified from<sup>15</sup>.



**Figure 4A.** Same as in Figure 3 (test 1), but in a monkey subjected to a lesion of the motor cortex (as illustrated in Figure 2B). The graphs show the score (panel A; same conventions as in Figure 3) and the contact time (CT; panel B) data. In the abscissa, the time is for the consecutive days of the behavioral sessions. The vertical dashed redline (day 0) is the day at which the lesion was performed. In panel B, each dot corresponds to the time of contact between the finger and the pellet in one slot (5 trials per orientation for each session; the grey bar represents the median value). Note that for the trials in which the animal could not perform the task (immediately after the lesion), the CT appears as a saturated value at 5 seconds. Data modified from<sup>16,17</sup>.

**Figure 4B.** Analysis of strategy adopted in the modified Brinkman board task performed with the contralesional hand, before lesion of the motor cortex (Pre), during the recovery phase (Recovery) and post-lesion at plateau (Post). The color of each slot indicates the sequential order of the slots visited by the monkey in one session (the first slot visited is depicted by the darkest blue and the last slot visited by the darkest red). Note that pre-lesion, the monkey started on the left side of the board and scanned systematically towards right. During the recovery, the sequential order was changed. At plateau post-lesion, the strategy adopted pre-lesion re-appeared (systematic scan from left to right).

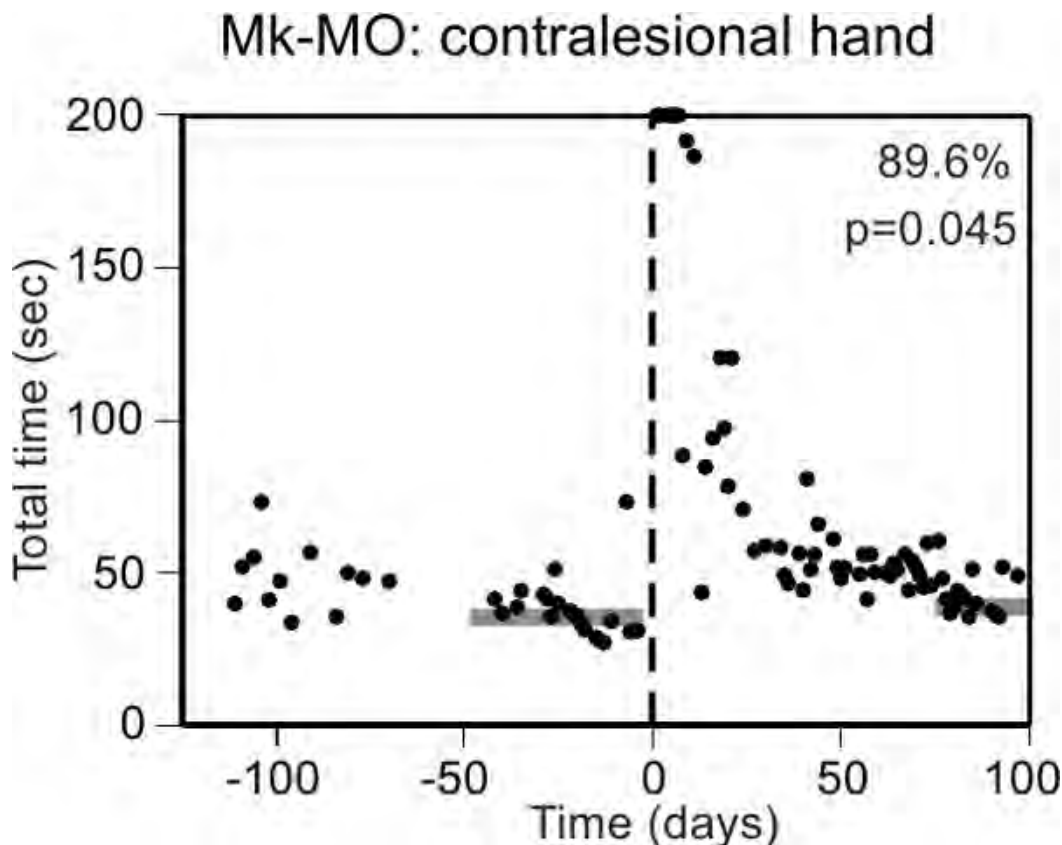


**Figure 5.** Representative data derived from the Brinkman box (test 2), for a monkey performing the task under visual control. The ordinate is the total time needed to empty the 20 wells along the daily sessions (abscissa), conducted before and after a lesion of the motor cortex (vertical dashed line). The dimensions of the accessible volume within the box are 1360 cm<sup>3</sup> (120mm\*110mm\*103mm). Note an initial phase of training, characterized by a larger variability of the total time from one session to the next. Immediately after the cortical lesion, the monkey was not able to perform the task (data points saturated at 200 seconds). The p value is statistically significant for the difference between the median total time pre-lesion (middle of the horizontal gray rectangle at the left) and the median total time post-lesion in the last sessions (middle of the horizontal gray rectangle at the right). The percentage of functional recovery is 89.6% whereas the volume of the motor cortex lesion was 41.8 mm<sup>3</sup>. Data modified from<sup>19</sup>.

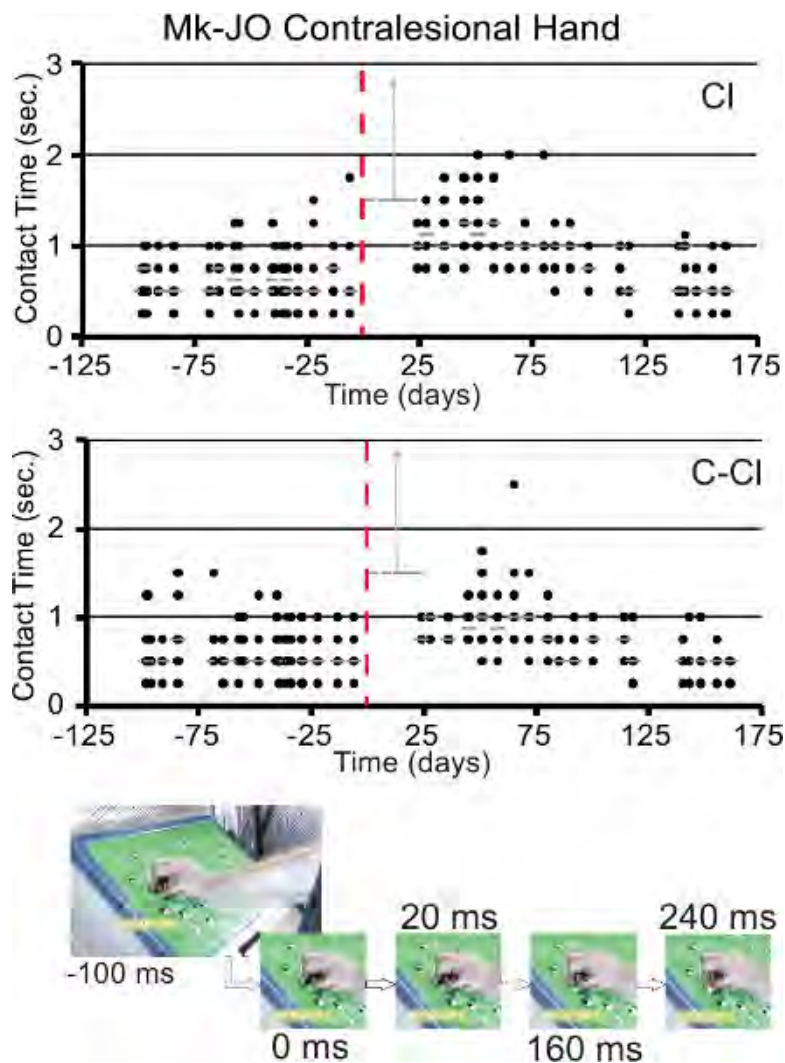


**Figure 6.** Representative results (top two graphs) derived from the rotative Brinkman board task (**test 3**), with illustration of the contact time measured pre-lesion and post-lesion, with the same conventions as in Figure 4A (panel B), for a monkey subjected to a lesion of the motor cortex (data modified from<sup>17</sup>). The top graph is for a clockwise ("CI") rotation of the board, whereas the bottom graph is for a counterclockwise ("C-CI") rotation of the board. The two vertical gray arrows indicate that the contact time was infinitely long in few sessions immediately after the lesion, as the monkey was unable to perform the task with the contralesional hand. The series of pictures at the bottom of the figure illustrate the method to measure the contact time (valid for both the modified Brinkman board and the rotating Brinkman board). The leftmost picture shows the hand approaching the slot containing the pellet (100 ms before contact between the index finger and the pellet). The next frame on the right corresponds to the time point of contact (0 ms). Then the contact time is defined as the time interval (in ms) running until reaching the frame (rightmost one) corresponding to the time point at which the pellet is taken out of the slot. The contact time here is 240 ms.

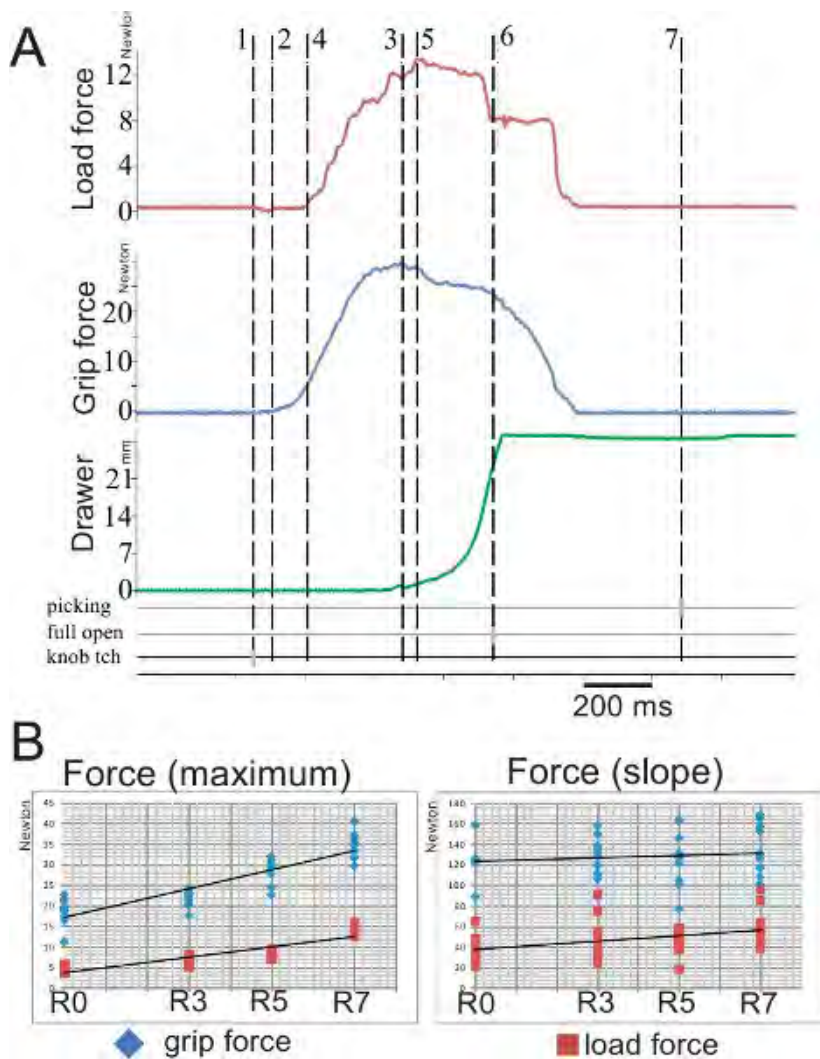


**Figure 7.** Representative data derived from a session performed by one monkey on the reach and grasp drawer task (test 4).

Panel A: Raw data corresponding to three parameters acquired online during a single trial: load force in red, grip force in blue and displacement of the drawer in green. Several markers were also acquired during the task: picking time corresponds to the time of the reward grasping, full open to the full opening of the drawer and knob touch (tch) to the time point when the animal first touches the knob. For the analysis, seven cursors were placed at critical time points in the unfolding task (e.g. 3 gray cursors on the bottom three horizontal lines): 1) time locked to the touch of the knob by the animal; 2) onset of grip force; 3) maximal grip force; 4) onset of load force; 5) maximal load force; 6) time locked when the drawer is fully open; 7) time locked to the picking time.

Panel B: Representation of the quantitative results for two parameters recorded during the task: the grip force (force used to grasp the knob between the index finger and the thumb) and the load force (force used to open the drawer) in two diagrams: the maximal value (left graph) and the slope value (from the onset to the max.; right graph).

Four out of the five different relative levels of resistance have been illustrated here: R0 (0 Newton), R3 (1.4 N), R5 (2.75 N) to R7 (5 N). The knob of the drawer has a triangular and flat shape. The base of the triangle attached to the drawer measures 20mm and the top (15 mm from the base) consists in a circular contour of 7 mm of diameter. The drawer itself has the following dimensions: length=50 mm; width=27 mm and height= 45mm.



## Effect of anti-Nogo-A antibody treatment on functional recovery from spinal cord injury

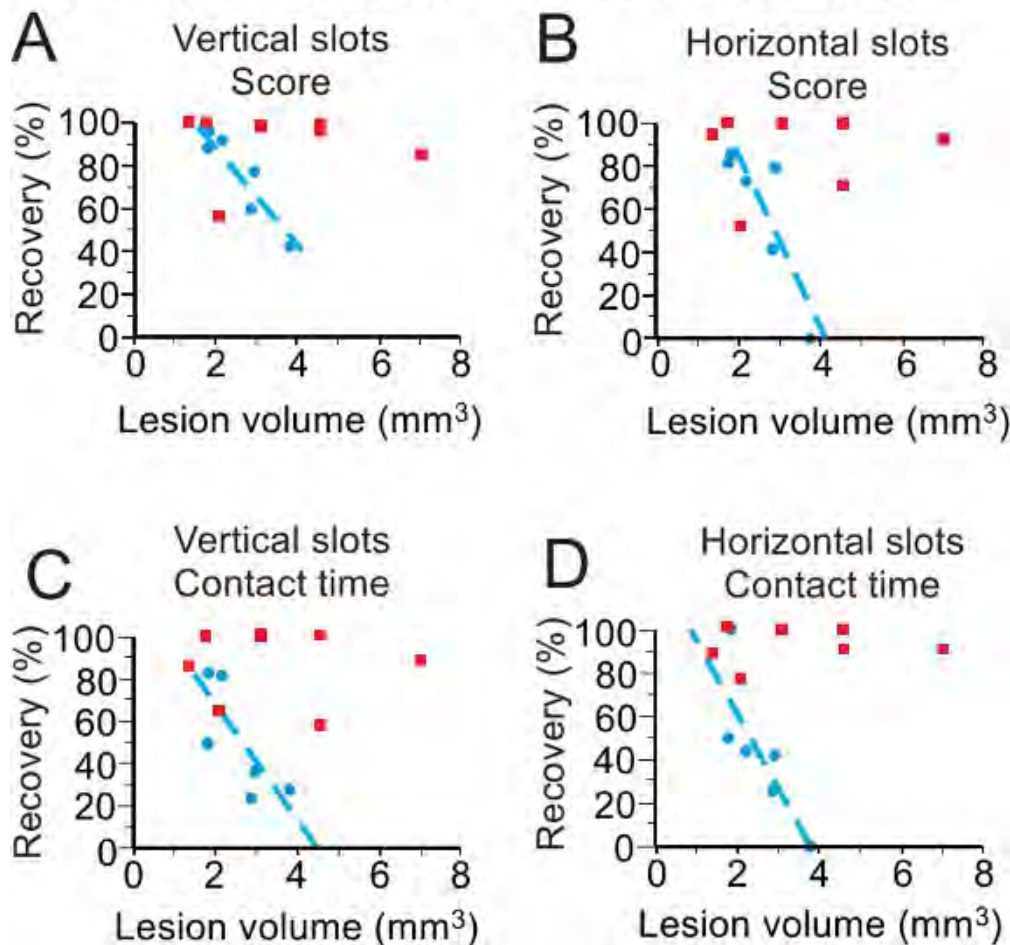


**Figure 8.** Reminder (modified from<sup>15</sup>) of the use of the behavioral **test 1** to investigate the possible effect of a treatment (anti-Nogo-A antibody) on the functional recovery from cervical cord lesion. For both scores and contact time, as well as for both slot orientations, the group of control antibody treated monkeys (blue symbols; n=6) recovers manual dexterity less well than the group of anti-Nogo-A antibody treated monkeys (red symbols; n=7), especially for large volumes of lesion. The 2 groups differ significantly with  $p=0.035$  (panel A),  $p=0.022$  (panel B),  $p=0.035$  (panel C) and  $p=0.008$  (panel D).

### Discussion

Although the present behavioral tasks have been considered so far in our laboratory in the context of studies related to lesion of the cervical cord or to lesion of the motor cortex with the aim to test various treatments (see<sup>14,15,17</sup> and <http://www.unifr.ch/neuro/rouiller> >select "research" in the top bar menu, then > "motor system" > "recovery after lesion"), they may also have a broader application, as manual dexterity is also an aspect to consider in other pathologies, such as Parkinson disease (MPTP monkeys) or in case of sensory de-afferentation affecting proprioception and/or the sense of touch (especially the **test 2** in absence of visual control).

The behavioral tests proposed here are suitable to investigate the motor control of distal movements of the forelimb, as involved in manual dexterity. The specificity of the tests is demonstrated by the absence of deficit (except for a couple of days) in case of a lesion which does not impair relevant components of the control system: indeed, in case of a lesion placed more caudal than the motoneurons controlling hand muscles, there was no deficit. The pertinence of the test 1 can be appreciated by comparing on video sequences taken at two time points of the post-lesion recovery curve, which differ by an enhancement of functional recovery of 25%, possibly in relation to a cell therapy treatment<sup>17</sup>.

In spite of some initial, relatively short training phase at beginning (lasting generally 2-3 months), the behavioral tests proposed here are relatively "natural" and straightforward, as compared to complex (e.g. conditional) tasks for which the training of the monkey may take nearly a year or more. The positive reinforcement is based on solid food, which is less sensitive on the ethical point of view than water deprivation, usually used in more complex tasks<sup>23</sup>. There is no need to deprive the monkeys from food to obtain stable and consistent results. The pellets

received during the tasks represent the first access to the food on the day of the behavioral session (assuming that the monkey does not eat during the preceding night; however additional food may be given until the end of the afternoon of the preceding day). It is crucial that each monkey performs the behavioral session at the same time of the day, as well as respecting the same sequential order between the different monkeys forming a group in the housing room. As the monkeys are sensitive to external disturbing events, the behavioral tasks should be conducted in presence of background music, masking potential disturbing noise coming from neighboring rooms or laboratories. It is crucial that during the whole duration of the experiment (from initial training up to the last daily experimental session, a period of several months if not years), a given monkey is placed daily under the supervision of the same experimenter.

The present behavioral tests, used since several years in our laboratory to quantify manual dexterity, are to some extent comparable to other tests of manual dexterity recently reported in the literature<sup>24-28</sup>. There is however a crucial need to standardize tests across different laboratories (for better comparison), which is a tentative goal of the present report. On demand, the detailed properties of the set-ups illustrated here for tests 1-4 can be provided by the corresponding author, in order to replicate them. Beyond the issue of regenerative medicine (recovery from lesion of spinal cord or cerebral cortex), the present palette of tests may be suitable to address in normal non-human primates developmental issues (e.g. time course of motor development of dexterous movements), to investigate lateralization aspects (hand preference/dominance) and to decipher evolutionary questions by comparing the motor abilities of different species of primates, including human subjects. Note however that the dimensions of the apparatuses should be adapted according to the digits' size (thickness and length) of the primate species, as it may influence the task performance. In the present study, the tests were conducted on macaca fascicularis monkeys, ranging from 2.5 to 8 years old and weighing between 2.5 and 8 kg. The length of the index finger (used first to manipulate the pellets) ranges from 32 to 35 mm, whereas the circumference of the distal phalanx (tip) of the index finger was between 22 and 25 mm in the monkeys included in our studies. As tested in previous experiments, the same grasping tests are suitable for macaca mulatta as well.

All experiments were conducted in accordance with the *Guide for the Care and Use of Laboratory Animals* (1996) and approved by local (Swiss) veterinary authorities. All experimental procedures on the monkeys, as well as the detention conditions in the animal facility, were described in detail in recent reports from our laboratory: see references 12-18.

## Disclosures

No conflicts of interest declared.

## Acknowledgements

The authors would like to thank Prof. M.E. Schwab, Dr. P. Freund, Dr. A. Wyss, Dr. S. Bashir, Dr. A. Mir, Dr. J. Bloch, Dr. J.F. Brunet, Dr. J. Aebischer, Dr. A. Meszaros, Dr. V. Goetschman for their contribution to previous experiments and analyses. The experimental set-ups were constructed by André Gaillard, Bernard Aebischer and Laurent Monney. In the animal facility, the monkeys were placed under the supervision of professional animal caretakers: Josef Corpataux, Laurent Bossy and Jacques Maillard. The behavioral tests and analysis of the data, as well as histology, were conducted with the highly valuable contributions of laboratory technicians: Véronique Moret (also web master), Françoise Tinguely, Christine Roulin, Monica Bennefeld, Christiane Marti and Georgette Fischer. This work was supported by the Swiss National Science Foundation, grants No 31-61857.00, 310000-110005, 31003A-132465 (EMR), 310030-118357, 31003A-104061 (TW), 310030-120411 (ABS), PZ00P3\_121646 (ES), Novartis Foundation; The National Centre of Competence in Research (NCCR) on "Neural plasticity and repair".

## References

1. Lemon, R.N. Descending pathways in motor control. *Annu. Rev. Neurosci.* **31**, 195-218 (2008).
2. Courtine, G., *et al.* Can experiments in nonhuman primates expedite the translation of treatments for spinal cord injury in humans? *Nat. Med.* **13**, 561-566 (2007).
3. Capitanio, J.P. & Emborg, M.E. Contributions of non-human primates to neuroscience research. *Lancet.* **371**, 1126-1135 (2008).
4. Brinkman, C. Supplementary motor area of the monkey's cerebral cortex: short- and long-term deficits after unilateral ablation and the effects of subsequent callosal section. *J. Neurosci.* **4**, 918-929 (1984).
5. Brinkman, J. & Kuypers, H.G. Cerebral control of contralateral and ipsilateral arm, hand and finger movements in the split-brain rhesus monkey. *Brain.*, 653-674 (1973).
6. Kazennikov, O., *et al.* Temporal structure of a bimanual goal-directed movement sequence in monkeys. *Eur. J. Neurosci.* **6**, 203-210 (1994).
7. Kazennikov, O., *et al.* Neural activity of supplementary and primary motor areas in monkeys and its relation to bimanual and unimanual movement sequences. *Neuroscience.* **89**, 661-674 (1999).
8. Kermadi, I., Liu, Y., Tempini, A., & Rouiller, E.M. Effects of reversible inactivation of the supplementary motor area (SMA) on unimanual grasp and bimanual pull and grasp performance in monkeys. *Somatosens. Mot. Res.* **14**, 268-280 (1997).
9. Kermadi, I., Liu, Y., Tempini, A., Calciati, E., & Rouiller, E.M. Neuronal activity in the primate supplementary motor area and the primary motor cortex in relation to spatio-temporal bimanual coordination. *Somatosens. Mot. Res.* **15**, 287-308 (1998).
10. Kermadi, I., Liu, Y., & Rouiller, E.M. Do bimanual motor actions involve the dorsal premotor (PMd), cingulate (CMA) and posterior parietal (PPC) cortices? Comparison with primary and supplementary motor cortical areas. *Somatosensory and Motor Research.* **17**, 255-271 (2000).
11. Wannier, T., Liu, J., Morel, A., Joffrais, C. & Rouiller, E.M. Neuronal activity in primate striatum and pallidum related to bimanual motor actions. *NeuroReport.* **13**, 143-147 (2002).
12. Rouiller, E.M. *et al.* Dexterity in adult monkeys following early lesion of the motor cortical hand area: the role of cortex adjacent to the lesion. *Eur. J. Neurosci.* **10**, 729-740 (1998).
13. Liu, Y., & Rouiller, E.M. Mechanisms of recovery of dexterity following unilateral lesion of the sensorimotor cortex in adult monkeys. *Exp. Brain. Res.* **128**, 149-159 (1999).
14. Freund, P. *et al.* Nogo-A-specific antibody treatment enhances sprouting and functional recovery after cervical lesion in adult primates. *Nature. Med.* **12**, 790-792 (2006).

15. Freund, P. *et al.* Anti-Nogo-A antibody treatment promotes recovery of manual dexterity after unilateral cervical lesion in adult primates--re-examination and extension of behavioral data. *Eur. J. Neurosci.* **29**, 983-996 (2009).
16. Kaeser, M. *et al.* Effects of Unilateral Motor Cortex Lesion on Ipsilesional Hand's Reach and Grasp Performance in Monkeys: Relationship With Recovery in the Contralesional Hand. *J. Neurophysiol.* **103**, 1630-1645 (2010).
17. Kaeser, M. *et al.* Autologous adult cortical cell transplantation enhances functional recovery following unilateral lesion of motor cortex in primates: a pilot study. *Neurosurgery.* **68**, 1405-1417 (2011).
18. Bashir, S. *et al.* Short-term effects of unilateral lesion of the primary motor cortex (M1) on Ipsilesional hand dexterity in adult macaque monkeys. *Brain Structure and Function.* (In Press, 2011).
19. Hamadjida, A. *et al.* Influence of anti-Nogo-A treatment on the reorganization of callosal connectivity of the premotor cortical areas following unilateral lesion of primary motor cortex (M1) in adult macaque monkeys (Submitted, 2011).
20. Jenny, A.B. & Inukai, J. Principles of motor organization of the monkey cervical spinal cord. *J. Neurosci.* **3**, 567-575 (1983).
21. Schmidlin, E., *et al.* Progressive plastic changes in the hand representation of the primary motor cortex parallel incomplete recovery from a unilateral section of the corticospinal tract at cervical level in monkeys. *Brain Research.* **1017**, 172-183 (2004).
22. Schmidlin, E., *et al.* Reduction of the hand representation in the ipsilateral primary motor cortex following unilateral section of the corticospinal tract at cervical level in monkeys. *BMC Neuroscience.* **6:56**, (2005).
23. Prescott, M.J., *et al.* Refinement of the use of food and fluid control as motivational tools for macaques used in behavioural neuroscience research: report of a Working Group of the NC3Rs. *J. Neurosci. Methods.* 193,167-188 (2010).
24. Darling, W.G., *et al.* Volumetric effects of motor cortex injury on recovery of dexterous movements. *Exp. Neurol.* **220**, 90-108 (2009).
25. Darling, W.G., *et al.* Minimal forced use without constraint stimulates spontaneous use of the impaired upper extremity following motor cortex injury. *Exp. Brain. Res.* **202**, 529-542 (2010).
26. McNeal, D.W., *et al.* Selective long-term reorganization of the corticospinal projection from the supplementary motor cortex following recovery from lateral motor cortex injury. *J. Comp. Neurol.* **518**, 586-621 (2010).
27. Nishimura, Y., *et al.* Time-dependent central compensatory mechanisms of finger dexterity after spinal cord injury. *Science.* 318, 1150-1155 (2007).
28. Pizzimenti, M.A., *et al.* Measurement of reaching kinematics and prehensile dexterity in nonhuman primates. *J. Neurophysiol.* **98**, 1015-1029 (2007).



## ***Annex 4***

# ***Variability of manual dexterity performance in non-human primates (Macaca fascicularis).***

Mélanie Kaeser, Pauline Chatagny Anne- Dominique Gindrat, Julie Savidan,  
Simon Badoud, Michela Fregosi, Verinique Moret, Christine Roulin, Eric  
Schmidlin, Eric M. Rouiller

Published in International Journal of Comparative Psychology (2014)





## **Variability of manual dexterity performance in non-human primates (*Macaca fascicularis*)**

**Mélanie Kaeser\***, **Pauline Chatagny\***, **Anne-Dominique Gindrat**, **Julie Savidan**, **Simon Badoud**,  
**Michela Fregosi**, **Véronique Moret**, **Christine Roulin**, **Eric Schmidlin<sup>#</sup>** and **Eric M. Rouiller<sup>#</sup>**  
*Domain of Physiology, Department of Medicine and Fribourg Center for Cognition, University of  
Fribourg, Chemin du Musée 5, CH-1700 Fribourg, Switzerland.*

The goal of this study was to quantify the inter-individual and intra-individual variability of manual (digits) skill in adult macaque monkeys, over a motor learning phase and, later on, when motor skills were consolidated. The hypothesis is that several attributes of the stable manual dexterity performance can be predicted from learning characteristics. The behavioral data were collected from 20 adult *Macaca fascicularis*, derived from their dominant hand, defined as the hand exhibiting a better performance than the other. Two manual dexterity tasks were tested: (i) the “modified Brinkman board” task, consisting in the retrieval of food pellets placed in 50 slots in a board, using the precision grip (opposition of the thumb and index finger); (ii) the “reach and grasp drawer” task, in which the grip force and the load force were continuously monitored while the monkey opened a drawer against a resistance, before grasping a pellet inside the drawer. The hypothesis was verified for the performance of manual dexterity after consolidation, correlated with the initial score before learning. Motor habit, reflected by the temporal order of sequential movements executed in the modified Brinkman board task, was established very early during the learning phase. As mostly expected, motor learning led to an optimization of manual dexterity parameters, such as score, contact time, as well as a decrease in intra-individual variability. Overall, the data demonstrate the substantial inter-individual variability of manual dexterity in non-human primates, to be considered for further pre-clinical applications based on this animal model.

In the common language, some people are described as clumsy whereas others have recognized talents to practice challenging motor tasks with great manual (digits) dexterity, such as musicians, top sports performers, as well as in some professional activities requiring high degree of precision in motor control (e.g., handmade watchmakers). Such inter-individual variability of motor skill is accompanied by some degree of intra-individual variability as the manual dexterity of a human being is subjected to variations from one day to the next, as well as to improvement resulting from motor practice. Manual dexterity corresponds to the skill to control independently and precisely each finger. From an evolutionary point of view, exquisite manual dexterity is largely considered as a prerogative of primates, as other mammalian orders do not exhibit such a high degree of manual dexterity, in spite of some recent findings providing evidence in favor of some manual skill in rodents for instance (see e.g., Sacrey, Alaverdashvili, & Whishaw, 2009; Whishaw, Whishaw, & Gorny, 2008; Whishaw, Travis, Koppe, Sacrey, Gholamrezaei, & Gorny, 2010; but see also Klein, Sacrey, Whishaw, & Dunnett, 2012). The specialty of primates for manual dexterity is based on the specific anatomical organization of the primate motor system, comprising the direct cortico-spinal projection called the cortico-motoneuronal (CM) system (see Lawrence & Hopkins, 1976; Lawrence, Porter, & Redman, 1985;

\* shared first authorship, <sup>#</sup> shared senior authorship

Please send correspondence to Prof. Eric M. Rouiller, Domain of Physiology, Department of Medicine and Fribourg Center for Cognition, University of Fribourg, Chemin du Musée 5, CH-1700 Fribourg, Switzerland, Phone: +41 26 300 86 09; Fax: +41 26 300 96 75. (Email: [eric.rouiller@unifr.ch](mailto:eric.rouiller@unifr.ch))



Lemon, 2008). The progressive evolution of the CM system across mammalian species is correlated with an increasing manual skill (see e.g., Courtine et al., 2007). Consequently, the non-human primates represent a unique animal model to study mechanisms involved in manual dexterity, which are also applicable to human subjects. For instance, monkeys have been used extensively to investigate experimentally the consequences on manual dexterity of various types of lesions affecting the motor system (e.g., Bashir et al., 2012; Beaud et al., 2008; Beaud et al., 2012; Bihel et al., 2010; Brinkman, 1984; Brinkman & Kuypers, 1973; Dancause & Nudo, 2011; Dancause et al., 2005; Dancause et al., 2006; Darling et al., 2009; Darling et al., 2010; Darling et al., 2011; Darling et al., 2013; Eisner-Janowicz et al., 2008; Friel & Nudo, 1998; Friel, Heddings & Nudo, 2000; Frost, Barbay, Friel, Plautz & Nudo, 2003; Galea & Darian-Smith 1997; Glees & Cole, 1950; Hoogewoud et al., 2013; Kaeser et al., 2010; Kaeser et al., 2013; Liu & Rouiller 1999; Marshall et al., 2003; McNeal et al., 2010; Murata et al., 2008; Nishimura et al., 2007; Nudo & Milliken, 1996; Nudo, Wise, SiFuentes, & Milliken, 1996; Ogden & Franz, 1917; Passingham, Perry, & Wilkinson, 1983; Pizzimenti et al., 2007; Roitberg et al., 2003; Rouiller et al., 1998; Sasaki & Gemba, 1984; Schmidlin, Wannier, Bloch, & Rouiller, 2004; Schmidlin et al., 2005; Schmidlin et al., 2011; Travis, 1955; Wannier, Schmidlin, Bloch, & Rouiller, 2005) and, in some cases, also to test the potential of various treatments after such lesions (e.g., Freund et al., 2006; Freund et al., 2007; Freund et al., 2009; Hamadjida et al., 2012; Kaeser et al., 2011; Plautz et al., 2003; Sugiyama et al., 2013; Wyss et al., 2013).

Numerous studies shed light on the anatomical, physiological and developmental aspects underlying manual dexterity in monkeys (e.g., Alstermark et al., 2011, Alstermark & Isa, 2002, 2012; Armand, Edgley, Lemon, & Olivier, 1994; Armand, Olivier, Edgley, & Lemon, 1997; Borra, Belmalih, Gerbella, Rozzi, & Luppino, 2010; Bortoff & Strick, 1993; Darian-Smith, Galea, & Darian-Smith, 1996; Darian-Smith et al., 1996; Darian-Smith, Burman, & Darian-Smith, 1999; Flament, Hall, & Lemon, 1992; Galea & Darian-Smith, 1994, 1995; Iwaniuk, Pellis, & Whishaw, 1999; Kinoshita et al., 2012; Lacroix et al., 2004; Lemon, Johansson, & Westling, 1996; Lemon, 1999; Maier et al., 2002; Manoel & Connolly, 1995; Ogiwara & Oishi, 2012; Olivier, Edgley, Armand, & Lemon, 1997; Padberg et al., 2007; Rathelot & Strick, 2009; Rouiller, Moret, Tanné, & Boussaoud, 1996; Sasaki et al., 2004). Furthermore, various aspects linked with manual dexterity were studied, such as manual coordination and strategies, handedness and tool use, as well as phylogenetic characteristics (e.g., Chalmeau, Visalberghi, & Gallo, 1997; Chatagny et al., 2013; Christel & Billard, 2002; Costello & Frigaszy, 1988; Falk, Pyne, Helmkamp, & DeRousseau, 1988; Fragaszy & Adams-Curtis, 1997; Gash et al., 1999; Fragaszy, 1998; Iwaniuk & Whishaw, 1999, 2000; King, 1986; King & Landau, 1993; Lacreuse & Fragaszy, 1999; Leca, Gunst, & Huffman, 2011; Lemon & Griffiths, 2005; Lindshield & Rodrigues, 2009; Nahallage & Huffman, 2007; Pouydebat, Laurin, Gorce, & Bels, 2008; Pouydebat, Gorce, Coppens, & Bels, 2009; Pouydebat, Reghem, Borel, & Gorce, 2011; Van Schaik, Deaner, & Merrill, 1999; Spinozzi, Castorina, & Truppa, 1998; Spinozzi, Truppa, & Lagana, 2004; Spinozzi, Lagana, & Truppa, 2007; Wiesendanger, 1999; Zhao, Hopkins, & Li, 2012).

In the present study, our goal was to use two complementary manual dexterity tasks, namely the *modified Brinkman board* task and the *reach and grasp drawer* task, to quantify the inter-individual variability of manual skill in adult macaque monkeys, as well as the intra-individual variations along a motor learning phase and, later on, during motor skills consolidation. More specifically, our main hypothesis is that manual dexterity performance and variability in the modified Brinkman board task, when acquired, can be predicted from the duration of the learning phase, and/or from the learning slope and/or from the initial score before any training took place. For the two tasks, it is also expected that the learning phase contributes: (i) to significantly reduce the intra-individual variability of manual skills, when a plateau of performance is reached; (ii) to optimize several attributes of manual dexterity, underlying the better motor performance reached at plateau. Nevertheless, in line with the principle of motor equivalence (see Lashley, 1930), the same motor goals with comparable levels of performance can be achieved using highly different motor strategies, as reflected by a wide inter-individual variability in manual skill parameters exhibited by adult macaque monkeys.



## Method

### Subjects

The behavioral experiments were conducted on 20 adult macaque monkeys (see Table 1 for individual parameters related to sex, weight, age, etc). Detailed information about the detention conditions of the monkeys, the veterinary authorizations, reward procedures and inclusion of the monkeys in previous studies can be found in the supplementary Methods and Results. As illustrated previously in the form of a video sequence (Schmidlin et al., 2011), the first experimental step (lasting 1-3 months) was to habituate the monkeys to be transferred into a primate chair, without direct manipulation of the animals by the experimenters, a procedure reducing the stress on the animals and the risks for the experimenters. Placed in the primate chair, the monkeys were weighed, and then transferred to the behavioral set-up in the laboratory.

### Procedure

On each behavioral session (3-5 days a week), the monkeys systematically performed the modified Brinkman board task (derived from the initial task of Brinkman & Kuypers, 1973; Brinkman, 1984), representing the basic manual dexterity task on which the present data are based. In addition, shifting from one session to the next, the monkeys performed additional tasks (rotating Brinkman board task; Brinkman box task; reach and grasp drawer task; as illustrated in Schmidlin et al., 2011). In the present report, only the reach and grasp drawer task is considered as an additional behavioral test to the modified Brinkman board task and in a subgroup of the monkeys only as this quantitative test was introduced fairly recently.

Taking advantage of two separate windows in front of the primate chair, each hand was tested separately and the first hand tested was alternated at each session. Typically, a daily behavioral session lasted about one hour, to test separately each hand. All behavioral tests were videotaped for off-line analysis. The present report is however restricted to data derived from the **dominant hand**, defined as the hand exhibiting the highest score in the modified Brinkman board task at plateau, to be distinguished from the preferred hand defined as the hand preferably chosen to perform a task when the monkey had the choice to use one or the other hand, irrespective of the performance (see Chatagny et al., 2013).

### Materials and Measures

The modified Brinkman board task requires the precision grip (opposition of thumb and index finger) to grasp food pellets from 50 slots dug in a perspex board (see Schmidlin et al., 2011), placed in front of the monkey (see also Figure 5D). The 50 slots are divided into 25 vertically oriented slots and 25 horizontally oriented slots, randomly distributed on the board. Banana flavor 45 mg pellets were used (*Bio-Serv, US and Canada: www.bio-serv.com*).

As previously reported (Schmidlin et al., 2011), the following 4 parameters were analyzed in the modified Brinkman board task: i) the **score** (number of food pellets retrieved during the first 30 seconds); ii) the **contact time** (CT = duration in seconds of contact between the fingers and the food pellets in the slot), determined for the first 5 vertical slots and the first 5 horizontal slots; iii) the **temporal sequence** followed by the monkey's hand to visit the 50 slots of the board; iv) the **types of movements** and **strategies** used to retrieve the pellets from the slots, as well as the quantification of errors of grasping.

The reach and grasp drawer task also measures the ability to unimanually catch a food pellet in a well, but this action is preceded by the opening of a drawer, requiring to counteract a variable resistance opposing the pulling. The test thus allows quantifying via sensors the force applied to hold the knob of the drawer in between the thumb and the index finger (grip force), as well as the load force (applied to pull the drawer). Moreover, several other sensors allow quantifying distinct consecutive phases of the task (Figure 6A; Schmidlin et al., 2011). In the reach and grasp drawer task, emphasis was put on aspects not covered by the modified Brinkman board task, namely the ability of the monkey to generate different levels of force to counteract the resistances opposing the opening of the drawer (load force), while precisely controlling the grip force between the thumb and index finger to prevent the loss of contact with the drawer knob (see Schmidlin et al., 2011). The following parameters were specifically analyzed in the reach and grasp drawer task: i) the **maximal grip force**; ii) the **maximal load force**; iii) the **duration of the grip force** application; iv) the **duration of the load force** application. The load force is believed to be initiated only when the grip force has reached a sufficient level to prevent sliding of the fingers on the knob due to the resistance opposing the opening of the drawer. Further details about the behavioral set-ups were described earlier (Schmidlin et al., 2011).

The behavioral data were represented graphically and analyzed statistically using the Sigmaplot 12.0 software package (*www.sigmaplot.com*). Accordingly, group comparisons were based on parametric tests (paired or unpaired t-tests) when the normality criteria were satisfied or, if not, on non-parametric tests (Wilcoxon rank-sum test or Mann-Whitney U test). Relationships between two behavioral parameters were assessed based on the Pearson correlation test.

## Results

### Modified Brinkman Board Task

The modified Brinkman board task is largely intuitive in the sense that an experimentally-naïve monkey placed in front of the board rapidly starts to grasp flavored food pellets, thus representing a fairly *natural* motor task. However, as a result of practice, the performance measured by the number of pellets retrieved in 30 seconds (score) increased from one session to the next, during the learning phase (Figure 1 and Supplementary Figure 1). The use of the precision grip to perform the task is also naturally adopted by all monkeys, although there may be subtle variations in the prehension pattern itself (see below). Furthermore, as there is no time constraint imposed to visit the 50 slots, the monkeys perform the task at their own pace depending on their motivation, a task thus assimilated to a voluntary behavior. In absence of strong constraints imposing a learning schedule and a level of performance on the monkeys, there is the possibility to assess the inter-individual variability related to manual skill, both during the learning phase and the plateau phase. The data will be first, and mainly, described based on the total score.

**Learning phase: Total score.** The learning phase of the modified Brinkman board task appeared quite variable from one animal to the next. A unique case is Mk-RO (Figure 1), exhibiting more a substantial decrease in variability along the 146 days of practice than a true increase in performance (modest regression line slope; see also Table 1). Another particular case is Mk-MO (Figure 1), with an impressive score from beginning, maintained during more than 100 days, before a moderate enhancement of score taking place at day 110, considered as the end of the learning phase. The regression line with a slightly negative slope is meaningless (Table 1), reflecting the absence of progressive improvement of score during the first 110 days.

All other monkeys exhibited a progressive increase in score, although the slope and the duration of the corresponding learning period were highly variable across animals (see Figure 1 and Supplementary Figure 1; Table 1). Four monkeys were characterized by a very steep learning slope (Figure 2 panel A; Table 1): Mk-AT (see also Figure 1), Mk-DI (see also Supplementary Figure 1), Mk-WI and Mk-CE. In the rest of the monkeys, the learning slope ranged from low to medium values (Figure 2 panel A), as illustrated for instance by Mk-JO (Figure 1; Table 1).

Another parameter of interest in relation to the learning phase is the intercept of the learning regression line with the y-axis (score), yielding an estimate of the initial performance at the onset of the training. As shown in Figure 2 (panel B: filled circles), the intercept values are quite variable from one monkey to the next, without however forming separate clusters. In Figure 1, three monkeys illustrate a low initial value (Mk-AN), a medium initial score (Mk-JA) and a high initial value (Mk-MO), respectively.

Highly variable also was the duration of the learning phase (Figure 2 panel C). With the exception of Mk-RO (as discussed above), the end of the learning phase was defined using the following criterion (as already used in a recent study on hand dominance/preference: Chatagny et al., 2013): when the progressive increase in score approached a plateau perceived by visual inspection, as observed in most monkeys, the first score value considered as the onset of the plateau is the score which is not exceeded by another value among the five next score values. Consequently, the end of the learning phase, indicated by the vertical dashed line in

Table 1  
List of monkeys and relevant parameters for the modified Brinkman board task

	Sex+	Weight*	Age*	Learning phase (days)&	Plateau (days)&	First score value& $\zeta$	Median plateau value&	Mean plateau value&	SD plateau value&	Slope learning phase&	Score plateau# Comparison H vs V slots	Median contact time at plateau V slots	Median contact time at plateau H slots	Mean errors (learning; plateau)
<b>Mk-AN</b>	f <sup>1,b</sup>	3.2	6	151	44	8.894	22	21.889	1.987	0.0795	H>V	0.32	0.48	5; 0 (c)
<b>Mk-AT</b>	f <sup>1,b</sup>	3.4	7	32	129	18.266	30	29.507	3.521	0.418	<b>V&gt;H (W)</b>	0.16	0.26	4.5; 1.2 (c)
<b>Mk-CA</b>	f <sup>1,b</sup>	3.7	7	210	30	12.177	28	26.875	4.303	0.0598	<b>V&gt;H (t)</b>	0.2	0.36	3.8; 2.1 (e)
<b>Mk-LO</b>	f <sup>1,b</sup>	3	7	97	92	12.302	22	21.528	2.408	0.0827	<b>V&gt;H (t)</b>	0.32	0.8	2.3; 0.4 (c)
<b>Mk-MA</b>	f <sup>1,b</sup>	3.2	7	89	133	17.416	33	33.179	2.984	0.176	<b>V&gt;H (t)</b>	0.24	0.2	16; 0.7 (c)
<b>Mk-MI</b>	f <sup>1,b</sup>	3.1	7	86	85	19.846	26	25.465	3.397	0.0611	<b>V&gt;H (t)</b>	0.2	0.36	9.8; 1.4 (c)
<b>Mk-TH</b>	f <sup>1,b</sup>	3.9	6	101	26	16.77	31.5	30.938	4.389	0.15	<b>V&gt;H (t)</b>	0.2	0.32	7; 0.5 (c)
<b>Mk-DI</b>	f <sup>1,b</sup>	3.4	7	41	109	20.516	31	31.154	3.294	0.410	<b>H&gt;V (W)</b>	0.2	0.2	4.8; 1 (c)
<b>Mk-EN</b>	m <sup>3,a</sup>	4.2	5	213	216	27.816	33	32.78	2.339	0.0095	<b>V&gt;H (W)</b>	0.2	0.32	2.4; 0.4 (c)
<b>Mk-AV</b>	m <sup>2,b</sup>	3.2	3	31	120	20.132	31	30.35	2.854	0.198	H>V	0.24	0.44	0; 0 (d)
<b>Mk-JO</b>	m <sup>2,b</sup>	3.2	3	63	34	24.52	34.5	34.25	2.817	0.121	<b>V&gt;H (W)</b>	0.16	0.28	1; 0.7 (d)
<b>Mk-JA</b>	m <sup>2,b</sup>	2.5	3	163	60	22.75	28	28.2	2.783	0.0199	<b>V&gt;H (t)</b>	0.333	0.867	0; 0.7 (d)
<b>Mk-WI</b>	m <sup>2,b</sup>	2.7	3.5	16	234	30.116	35	34.95	3.306	0.409	<b>V&gt;H (W)</b>	0.24	0.32	3.8; 0.2 (c)
<b>Mk-VA</b>	m <sup>2,a</sup>	3.4	3.5	64	404	24.12	26.5	26.875	4.463	0.0937	<b>V&gt;H (W)</b>	0.333	0.6	2.3; 0 (c)
<b>Mk-BI</b>	m <sup>2,a</sup>	3.7	4.5	163	142	29.567	34.5	33.817	3.362	0.0336	<b>V&gt;H (W)</b>	0.18	0.32	0.7; 0.3 (d)
<b>Mk-MO</b>	m <sup>2,a</sup>	4	4.5	110	114	33.318	35	34.424	2.681	-0.00370	<b>V&gt;H (t)</b>	0.133	0.267	1; 0.5 (c)
<b>Mk-GE</b>	f <sup>2,a</sup>	3.5	5	70	447	17.751	21	20.955	4.817	0.0516	<b>V&gt;H (t)</b>	0.34	0.56	1.9; 0.1 (c)
<b>Mk-RO</b>	m <sup>2,a</sup>	3.7	3	146	181	23.651	28	27.667	2.087	0.0288	<b>V&gt;H (W)</b>	0.44	0.52	6.1; 0.9 (c)
<b>Mk-CE</b>	m <sup>2,a</sup>	3.5	4	21	77	21.75	25.5	23.5	4.468	0.274	<b>V&gt;H (t)</b>	0.667	0.8	0.8; 0.9 (d)
<b>Mk-DG</b>	m <sup>3,a</sup>	5.2	4	107	64	20.58	31	31.68	4.13	0.119	<b>V&gt;H (t)</b>	0.23	0.32	2.3; 1.8 (e)

Notes. + f = female; m = male. The following number (1, 2 or 3) indicates the housing conditions: 1 = 45 m<sup>3</sup> housing facility; 2 = 15 m<sup>3</sup> facility; 3 = transfer from 15 m<sup>3</sup> to 45 m<sup>3</sup> (data acquired however after transfer). The following letter (a, b) indicates whether the animal has been subjected to preliminary habituation to the behavioral set-up (a) or not (b), before data collection.

\* at beginning of training (age rounded 0.5).

& established for total score in the modified Brinkman board task (all monkeys).

$\zeta$  intercept of regression line with y-axis in score plot.

# **Bold** characters are for statistically significant differences between H (horizontal slots) and V (vertical slots): paired t-test (t) or Wilcoxon (W) test; see also text for learning phase.

In the rightmost column, c, d and e correspond to three different error profiles (see text).

Figure 1 and Supplementary Figure 1, precedes the first score value defined as the onset of the plateau. Mk-AV is representative of a very quick learning (Supplementary Figure 1), with a plateau reached after only 31 days. At the other extremity, Mk-EN exhibited a very long learning phase, with a weak slope, completed after 213 days (Supplementary Figure 1). An average duration of learning phase is illustrated by Mk-MA (Supplementary Figure 1), with a plateau reached after about 3 months.

The difference between the average score at plateau and the initial score before training yields an estimate of the score enhancement obtained during the learning phase. This value is represented for the total score by crosses in Figure 2 (panel B). As one might have expected, there is a trend towards a larger improvement of score during the learning phase in the monkeys with a low initial score as compared to those with a higher initial score characterized by a limited score progression. The two (interdependent to some extent) parameters of initial score and score improvement during learning appear to present a difference with respect to sex. As shown in Figure 2 panel B, the nine females (identified by “f” the x-axis) exhibit lower initial values than most males. The average initial score was 15.99 pellets in 30 seconds in females ( $SD = 3.95$ ) whereas, in males, it was 25.3 pellets in 30 seconds ( $SD = 4.3$ ). This difference between females and males is statistically significant ( $p < 0.001$ ; unpaired t-test). Consequently, females exhibited a larger margin of score progression during learning (average 10.84 pellets in 30 seconds;  $SD = 4.23$ ) than males (average 5.47 pellets in 30 seconds;  $SD = 3.42$ ); this difference related to sex is also statistically significant ( $p = 0.006$ ; unpaired t-test). The other two parameters related to learning (learning slope and duration of training) did not differ between the sex groups (Figure 2 panels A and C).

**Plateau phase: Total score.** As illustrated in Figure 1 and Supplementary Figure 1, the plateau phase starts after the vertical dashed line. The average and median score values reached at plateau were also variable among monkeys, ranging from 21 to 35 pellets (Figure 2 panels E and F; Table 1). A relevant parameter at plateau is the intra-individual variability from one daily session to the next, estimated by the standard deviation ( $SD$ ) of the score values during the entire plateau phase (Table 1). The  $SD$  was highly variable across monkeys (Figure 2 panel D), ranging from 1.99 to 4.82. A “typical” monkey is represented by Mk-AN (Figure 1), whereas a monkey exhibiting an atypical performance at plateau is illustrated by Mk-MI (Supplementary Figure 1).

To assess whether the performance reached at plateau (score and variability) depends on learning properties, such as the duration of the learning phase, the slope of the learning regression line or the initial score before training, the average score at plateau and its  $SD$  were plotted for the 20 monkeys as a function of the corresponding learning parameters (Supplementary Figure 2). There was correlation neither between the learning duration (in days) and the average score at plateau, nor between the learning duration and the  $SD$  of the score at plateau (top two panels in Supplementary Figure 2). The same absence of correlations was found during the first five learning sessions. Similarly, the speed of learning, estimated by the slope of the learning regression line, was not correlated with the manual performance at plateau (score or  $SD$ ; bottom two panels in Supplementary Figure 2). In contrast, the initial score before training was to some extent a predictor of the score at plateau, as there was a statistically significant correlation between these two parameters (top right panel in Figure 3; Pearson correlation test). On the other hand, there was no correlation between the initial score before training and the variability ( $SD$ ) of the score at plateau (middle right panel in Supplementary Figure 2).

Both the inter-individual and intra-individual variations of the total score can be better visualized when displayed in the form of box and whisker plots (Figure 3 top left panel). Some animals exhibited a fairly small variability of their total score at plateau, from one daily session to the next (Mk-AN, Mk-CA, Mk-LO, Mk-JO and Mk-RO). In these monkeys, the distance between the 25 and 75 percentiles was equal to or smaller than

3.6 pellets. At the other extreme, some monkeys were characterized by a large variability across daily sessions (Mk-GE and Mk-WI), with a distance between the 25 and 75 percentiles equal to or larger than 10 pellets.

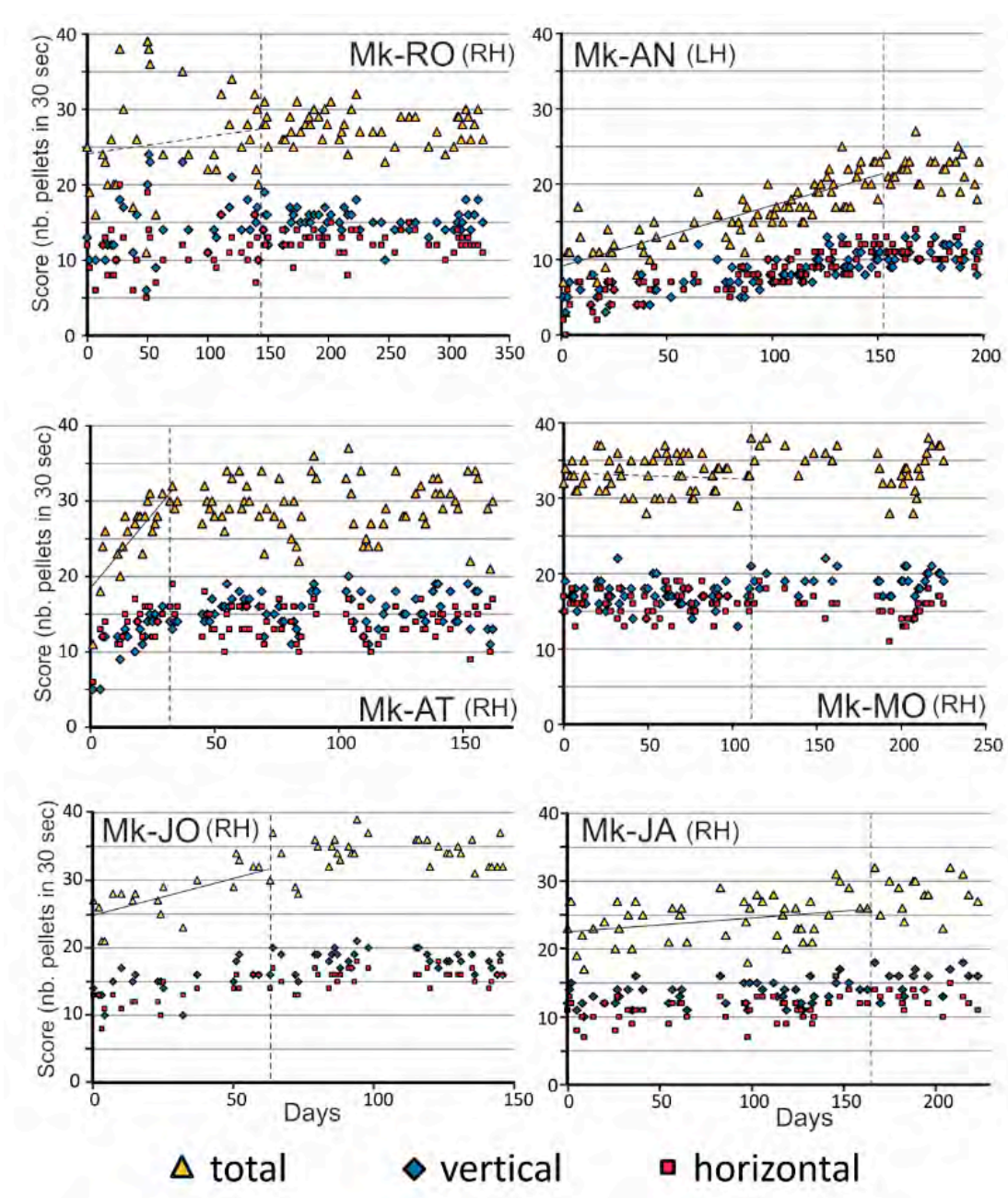
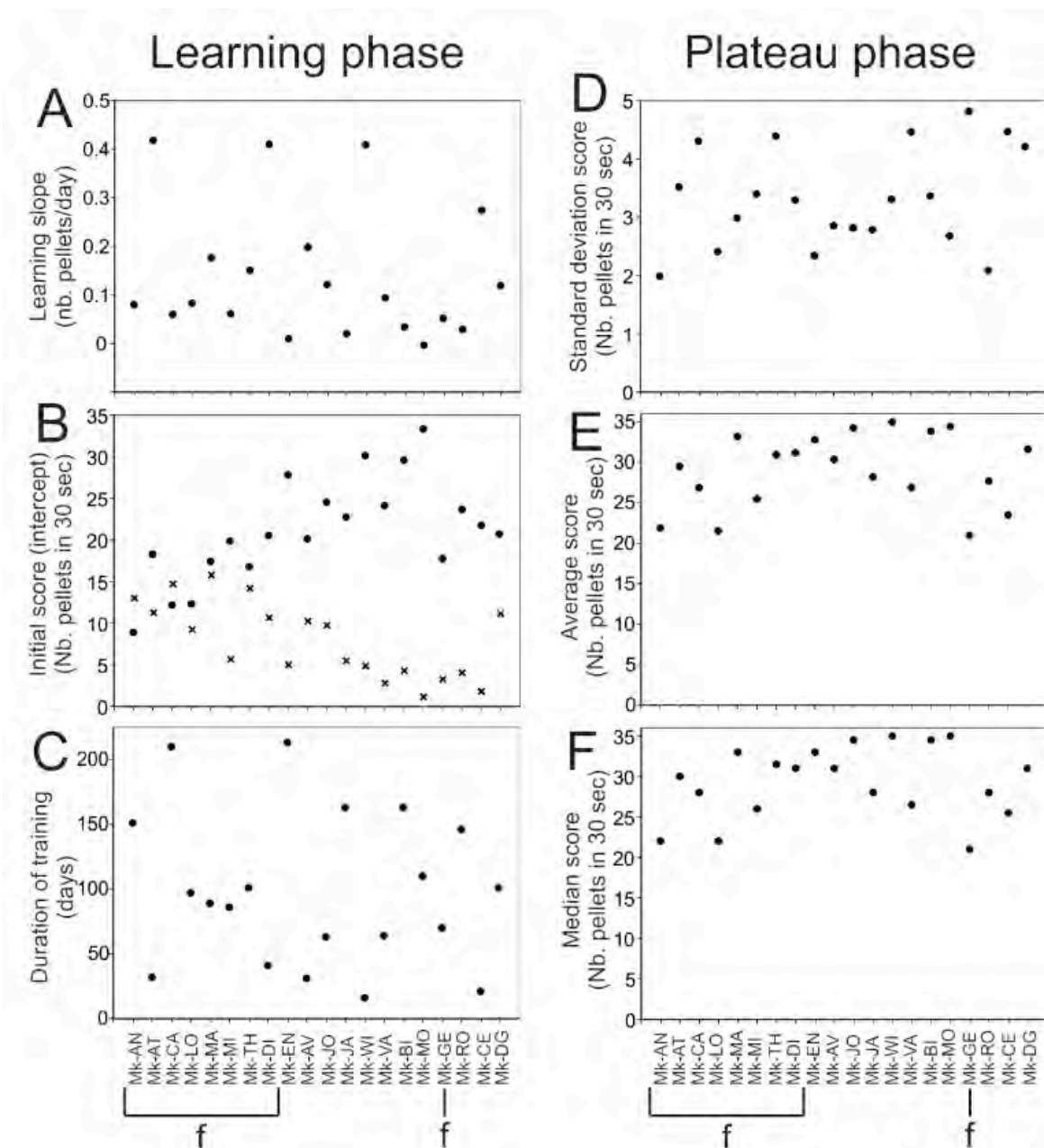


Figure 1. Plots showing the score obtained by 6 monkeys (Mk-RO, Mk-AT, Mk-JO, Mk-AN, Mk-MO, MK-JA) in the modified Brinkman board task for the dominant hand (RH=right hand; LH=left hand). Yellow triangles represent the total score, whereas the separate scores in vertical and horizontal slots are displayed by blue diamonds and purple squares, respectively. The time in days from the first day of testing is represented on the x-axis. For instance, in absence of test during the weekend, there is a delta of 3 days between tests conducted on Friday and then on next Monday. The vertical dashed lines represent the end of the learning phase and consequently the onset of the plateau phase (see text). A learning regression line on the total score is displayed for each animal (see text). The regression lines for Mk-RO and Mk-MO are represented with dashed lines as they are special cases (see text).





*Figure 2.* Plots showing relevant parameters for motor performance by all monkeys during the learning phase and the plateau phase of the modified Brinkman board task. The data concern the total score. The ID name of the monkeys appears below each bottom graphs. The 9 females monkeys are identified by “F” below the ID names. The other 11 monkeys are males. In panel B, crosses represent the progress of score obtained during the learning phase: it is the average score at plateau minus the initial score (also expressed as a number of pellets in 30 seconds; see text).

**Score in vertical and horizontal slots.** Pellet retrieval from the horizontal slots is more challenging than from the vertical ones (see Chatagny et al., 2013; Freund et al., 2009; Hoogewoud et al., 2013; Schmidlin et al., 2011), as the precision grip is usually accompanied by a deviation of the wrist/arm, not necessary for the vertical slots, corresponding either to an ulnar deviation or a radial deviation (see below, Variable Patterns of

Food Pellet Grasping). Below, the data are presented first at plateau, where they are more stable, and then, for comparison, during the learning phase.

At plateau, the scores were in most cases lower in the horizontal slots than in the vertical slots (Figure 1 and Supplementary Figure 1; Table 1): this difference was statistically significant in 17 monkeys ( $p < 0.001$  in 15 monkeys;  $p = 0.016$  in Mk-CE and  $p = 0.011$  in Mk-TH; see Table 1). In contrast, in three monkeys, the horizontal scores were higher than the vertical scores, but the difference was not statistically significant ( $p > 0.05$ ) in two monkeys (Mk-AN, see Figure 1; Mk-AV, see Supplementary Figure 1). In the third monkey (Mk-DI), the horizontal score was significantly higher than the vertical score ( $p < 0.001$ ; see Supplementary Figure 1 and Table 1). At the plateau phase, there was no statistically significant difference between females and males in the median score for the vertical and horizontal slots taken separately, as well as for the variability of both of them (Figure 3).

The variability of the scores at plateau taken separately for the horizontal and the vertical slots can be visualized when the scores are displayed in the form of box and whisker plots (Figure 3 bottom two panels). In this way, the 20 monkeys can be distributed in three subgroups. First, in eight monkeys the variability of scores at plateau was comparable for both slot orientations. Second, the variability of scores at plateau was lower in the vertical slots in six monkeys. Third, it was the other way around in six monkeys with a lower variability in the horizontal slots.

In the learning phase, there was a positive correlation between vertical and horizontal mean scores ( $r = 0.79$ ), indicating that the learning performance for one slot orientation is consistent with that for the other orientation. Nevertheless, no significant correlation appeared neither between vertical and horizontal *SDs*, nor between mean and *SD* for both slots orientations. However, differences between the scores observed in the vertical slots and in the horizontal slots at plateau were already visible during the learning phase (see all monkeys illustrated in Figure 1 and Supplementary Figure 1, except Mk-AT). In the three monkeys (Mk-AN, Mk-AV and Mk-DI) with a higher score in the horizontal slots at plateau, this difference was already present during the learning phase. However, it was only a trend as the differences were not statistically significant ( $p > 0.05$ , paired t-test or Wilcoxon rank-sum test). In the 17 monkeys exhibiting higher scores in the vertical slots at plateau, this difference was already present and statistically significant in 13 of them during the learning phase ( $p < 0.05$ , paired t-test or Wilcoxon rank-sum test); it was only a trend in two monkeys (Mk-CE and Mk-EN;  $p > 0.05$ , paired t-test or Wilcoxon rank-sum test); there was a statistically non-significant trend towards a better score in the horizontal slots during learning in Mk-GE ( $p > 0.05$ , paired t-test); surprisingly, in Mk-AT, there were statistically better scores in the horizontal slots during the learning phase ( $p = 0.023$ , Wilcoxon rank-sum test), whereas this was the opposite at plateau (Figure 1).

**Contact time (CT).** The score data of the modified Brinkman board task described above involve motor components that are not purely part of the precision grip itself, such as the time of transport of the arm first towards and then away from the board. The contact time (CT) represents the time interval used by the monkey's hand to retrieve the pellets from the slots (see Method). As the precision grip movement is different with respect to slot orientation, the CT was measured separately in the horizontal and in the vertical slots in all 20 monkeys during the plateau phase (Figure 4; same plateau phase as defined for the score data). As expected, in the vast majority of monkeys ( $n = 18$ ), the median CT at plateau was shorter in the vertical slots than in the horizontal slots (Table 1). The median CT was equal in both slot orientations in Mk-DI (0.2 second), and it was shorter in the horizontal slots in Mk-MA (Table 1). At plateau, the median CTs ranged from 0.13 sec to 0.67 sec across the 20 monkeys in the vertical slots and from 0.20 sec to 0.87 sec in the horizontal slots (see Table 1 and left panels of Figures 4A and B). The variability of the CTs at plateau (Figure 4) was greater for the horizontal slots in all monkeys. Three monkeys (Mk-CE, Mk-JA and Mk-RO) exhibited consistent highly variable CTs at plateau in both horizontal and vertical slots (Figure 4).

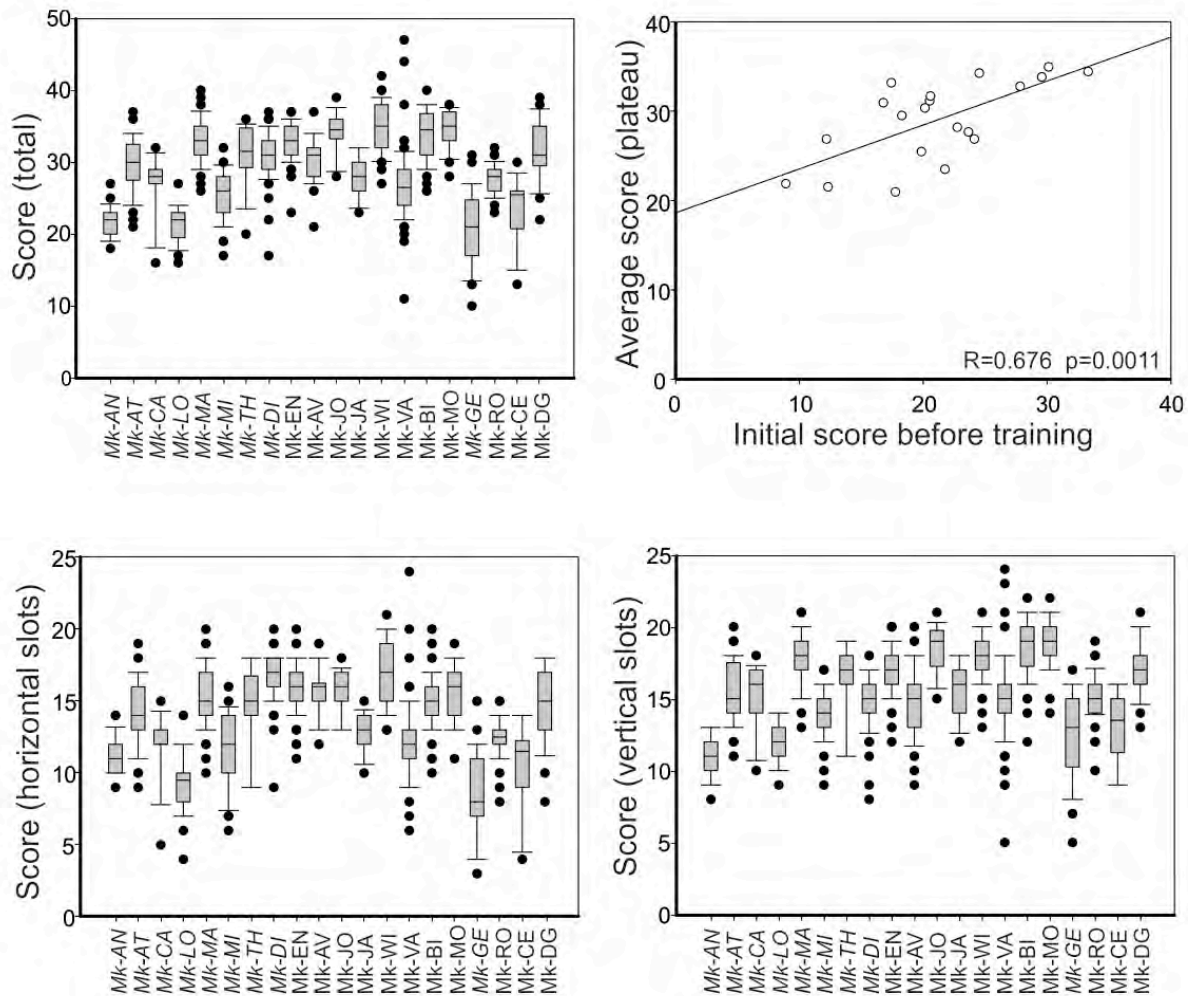


Figure 3. Scores obtained by all monkeys at **plateau phase** in the modified Brinkman board task, represented in the form of box and whisker plots. The horizontal line in the boxes represents the median value. The top and bottom of the boxes are for the 75 and 25 percentiles, respectively. The top and bottom of the whiskers represent the 90 and 10 percentiles, respectively. Black dots are for individual values above and below the 90 and 10 percentiles, respectively. The top left graph displays the total score, whereas the scores in the horizontal and vertical slots are shown in the bottom left and bottom right graphs, respectively. The ID names of females are shown in italics. The plot on the top right shows the statistically significant correlation between the average total score at plateau and the initial score before training, with the regression line. The corresponding coefficient of correlation (R) is given at the bottom right of the plot, followed by the p value (Pearson correlation test).

The CTs established at plateau were compared with those at the onset of the learning phase. The CT was assessed during the first four daily behavioral sessions (right panel in Figures 4A and B, for the horizontal and vertical slots, respectively), based on previous evidence that individual differences and intra-individual variations are greatest during the first four practice trials during motor learning (e.g., Carron & Leavitt, 1968; Marteniuk, 1974). The median CT values at onset of learning are clearly longer than those measured at plateau (Figure 4), reflecting a decrease in CT during the learning phase, corresponding to an enhancement of precision grip performance. An in-depth comparison of CTs at plateau with those at onset of learning is presented in the supplementary Methods and Results, together with supplementary Figure 3. Moreover, how



the CTs progressively decrease during the first four days of learning is also reported in the supplementary Methods and Results.

**Temporal sequence of grasping (motor habit).** As the modified Brinkman board task is a voluntary motor task, there was no constraint on the monkey on how to perform the task, for instance in which temporal order to visit the 50 slots. However, as previously reported (Kaeser et al., 2013; Schmidlin et al., 2011), most monkeys did not visit the 50 slots randomly at plateau, but they generally adopted a preferential temporal sequence, for instance starting to empty the slots at one extremity of the board (right side for instance) and then scanning the board progressively and systematically towards the opposite extremity (left side in this example), as illustrated by the bottom inset in Figure 5A.

Such preferential temporal sequence, generally maintained at plateau from one daily session to the next, was considered as a **motor habit** and was found to be affected by a unilateral lesion of the dorsolateral prefrontal cortex (Kaeser et al., 2013; as assessed in five monkeys). In the present study, these data were extended by investigating variability of motor habit across 20 monkeys and by assessing whether the motor habit was already introduced at the beginning of the learning phase.

Overall, the comparison of the temporal sequence at the beginning of the learning phase with that at plateau yielded a distribution of the monkeys into four profiles (Figure 5 panels A and B). Profile 1, illustrated by Mk-AV, is characterized by variable temporal sequences to visit the 50 slots across daily sessions, without significant difference between the learning phase and the plateau phase. Several monkeys ( $n = 10$  including Mk-AV) exhibited a similar sequence pattern (Mk-AT, Mk-BI, Mk-EN, Mk-GE, Mk-LO, Mk-MA, Mk-MI, Mk-RO, Mk-TH). Profile 2, illustrated by Mk-MO, is shared by three monkeys (Mk-AN, Mk-CE, Mk-MO) also exhibiting variable daily temporal sequences to visit the 50 slots but, in addition to a daily variability, the general pattern during the learning phase appears different from the one adopted during the plateau phase. Profile 3 includes four monkeys (Mk-JA, Mk-JO, Mk-VA, Mk-WI), and is characterized by a systematic temporal sequence to visit the 50 slots, present already during the learning phase and maintained during the plateau phase (illustrated by Mk-JA in Figure 5A). Finally, Profile 4 comprises three monkeys (Mk-CA, Mk-DG, Mk-DI), in which there was also a systematic daily temporal sequence to visit the 50 slots, but the sequence was significantly different during the learning phase from the one during the plateau phase (illustrated by Mk-DG in Figure 5A). The four profiles of motor habit are illustrated quantitatively in Figure 5B, where the positions of the 50 slots were given increasing numbers going from the left extremity of the Brinkman board to the right. Then, these numbers were subtracted from the temporal order (first slot visited, second, third, etc), cumulating their absolute values yielded a low cumulative value for a systematic scan from left to right; on the contrary, a systematic scan from right to left yielded a high cumulative value.

In the above four profiles of temporal sequences to visit the 50 slots, Profiles 1 and 3 exhibited comparable patterns at both learning phase and plateau phase, corresponding quantitatively to an absence of statistically significant difference between the two phases (*ns* in Figure 5B for Mk-AV and Mk-VA for instance). In contrast, the other two profiles (2 and 4) exhibited statistically significant differences in patterns of temporal sequences between the learning phase and the plateau phase (Figure 5B, *stars*, Mk-MO and Mk-DG for instance; see legend for a description of the statistical tests used).

**Variable patterns of food pellet grasping.** Although the monkeys generally used the standard precision grip (opposition of thumb and index finger) to grasp the food pellets in the modified Brinkman board task, there was some subtle variability in the precise pattern of grasping. For instance, already at the beginning

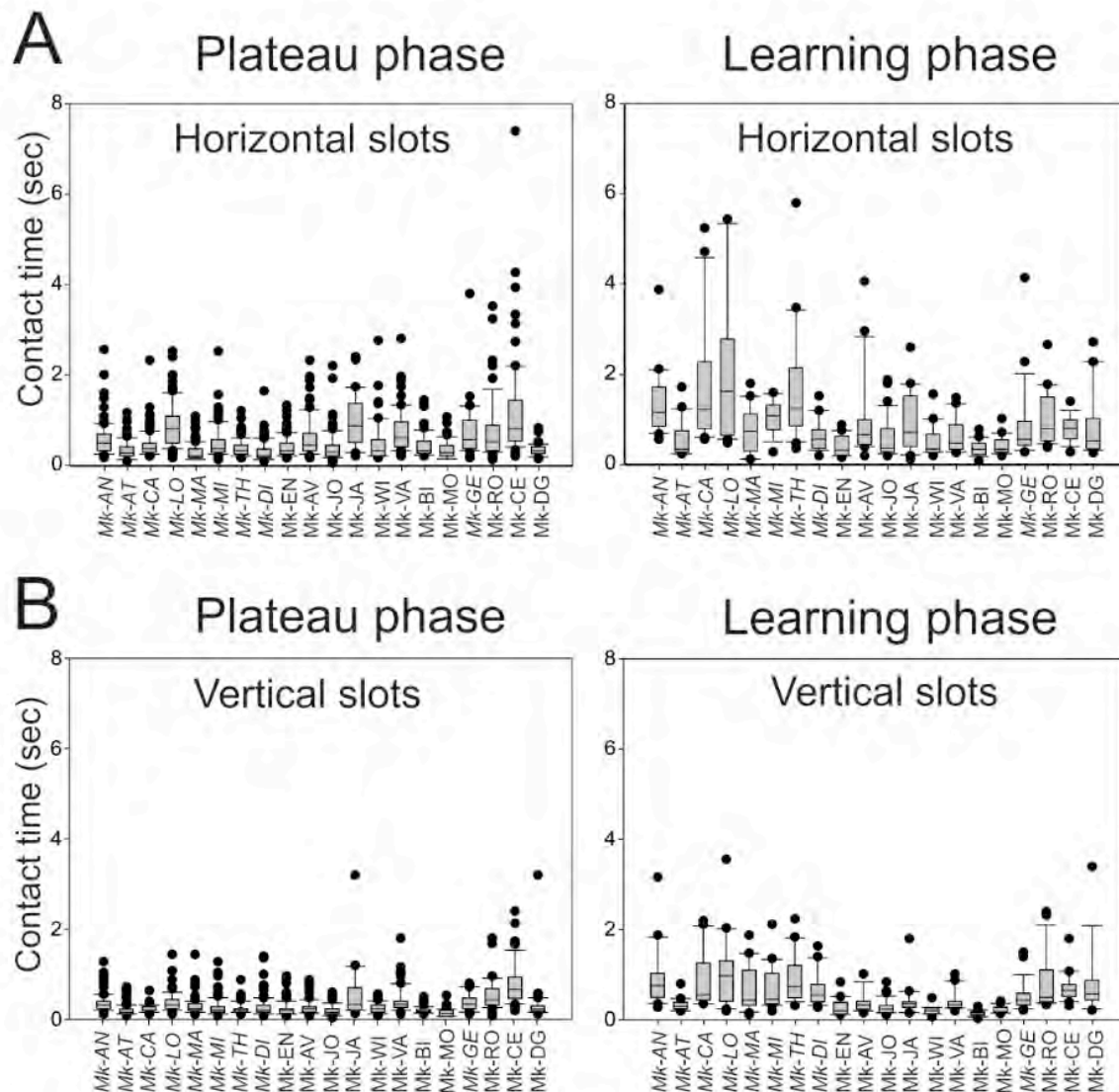


Figure 4. Contact times measured at **plateau phase** and at the **onset of the learning phase** for all monkeys in the modified Brinkman board task, in the horizontal (panel A) and vertical (panel B) slots, represented in the form of box and whiskers plots. The ID names of females are shown in italics. Same conventions as in Figure 3.

of practice, Mk-EN did not grasp a single food pellet with the left hand at a time to bring it to the mouth, as seen in the other monkeys, but grasped a first pellet, stored it in the palm of the hand, and then grasped a second pellet, before transporting both of them together to the mouth (see video sequence at <http://www.unifr.ch/neuro/rouiller/ijcp/fr0.html>). Conversely, single pellets were transported to the mouth with the right hand at the beginning of the learning phase. After about 10 months of practice, Mk-EN adopted frequently the strategy to collect two pellets at the same time with the left hand (Figure 5C). At the same time point, this strategy was also present for the right hand, but less systematically than for the left hand. Later, after two years of practice, Mk-EN systematically exhibited the prehension of two pellets at the same time with the left hand, extending it even to the grasping of three pellets together on a few trials (<http://www.unifr.ch/neuro/rouiller/ijcp/fr0.html>). This strategy to collect two pellets at the same time was also observed in few other monkeys, but more occasionally, for instance in Mk-JO and Mk-WI (Figure 5C)

during the plateau phase only, and in Mk-AV and Mk-JA, both during the learning phase and the plateau phase.

The standard grasping from the vertical slots (one single pellet after the other) was highly stereotyped among the monkeys with the use of the standard precision grip (opposition of thumb and index finger). The temporal sequence of movement was such that the monkeys first established contact between the index finger and the pellet, moved the pellet toward the bottom extremity of the vertical slot and finally put the thumb in contact with the pellet to perform the retrieval itself from the slot.

The pattern of grasping was more variable for the horizontal slots. The first contact might be performed with the index finger first (as for the vertical slots) but also sometimes with the thumb first (see a few examples in Mk-EN at <http://www.unifr.ch/neuro/rouiller/ijcp/fr0.html>). Seven monkeys used the strategy to contact the pellet only with index finger first (Mk-BI, Mk-CA, Mk-GE, Mk-JO, Mk-LO, Mk-MO, Mk-VA). Episodic first contacts with the thumb were observed in six monkeys (Mk-AV, Mk-CE, Mk-EN, Mk-JA, Mk-MI, Mk-WI). Finally, first contacts with the thumb were frequent in seven monkeys, amounting to about 30% of trials in Mk-DG, Mk-RO and Mk-TH; in the other four monkeys, first contact established with the thumb were as frequent (Mk-AN) or even more frequent (Mk-AT, Mk-DI, Mk-MA) than with the index finger. In two of these seven monkeys with frequent first contacts with the thumb, this behavior appeared only at the plateau phase (Mk-MA, Mk-TH), whereas for the other five monkeys it was present already during the learning phase, with increasing frequency of occurrence over time.

To retrieve pellets from the horizontal slots, in part depending on their position on the Brinkman board, the monkeys performed the precision grip with the wrist/arm either in a radial deviation posture or in an ulnar deviation posture (Figure 5D; nomenclature derived from Hoffman and Strick, 1986). In 11 monkeys, the ulnar deviation was highly predominant (Mk-AN, Mk-AT, Mk-BI, Mk-GE, Mk-LO, Mk-MA, Mk-MI, Mk-MO, Mk-RO, Mk-TH, Mk-WI; see Figure 5E for Mk-LO). In one of them, the wrist/arm in radial deviation posture occurred only during the learning phase (Mk-MA), whereas in Mk-MI and Mk-RO the radial deviation posture was observed only at the plateau phase. In the other nine monkeys, ulnar and radial deviation postures of the wrist/arm were mixed with usually fewer radial deviations (ranging mostly from 20 to 40%) than ulnar deviations in eight of them (Mk-AV, Mk-CA, Mk-DG, Mk-DI, Mk-EN, Mk-JA, Mk-JO, Mk-VA; Figure 5E for Mk-JA and Mk-DG), whereas radial deviations were as frequent as ulnar deviations in Mk-CE. Overall, in the nine monkeys using a mix of radial and ulnar deviation postures, this behavior was in most cases already present during the learning phase (Figure 5E).

**Errors of food pellet grasping.** In the modified Brinkman board task, the monkeys made episodic errors in the form of unsuccessful trials, for instance when the pellet was ejected from the slot instead of being grasped, or when the pellet was dropped before transport to the mouth. Three profiles were identified among the 20 monkeys. The first profile (in 13 monkeys; see (c) in the rightmost column of Table 1) is defined by a progressive decrease in the number of errors from one day to the next during the few days at onset of learning followed by a further decrease at plateau, as expected. The second profile was observed in five monkeys (see (d) in Table 1), with a surprising constant and low number of errors both at onset of the learning phase and at plateau. The third profile included two monkeys (see (e) in Table 1), in which the errors occurred randomly (low to moderate number of errors), irrespective of the phase (onset of learning or plateau). As shown in Table 1, the mean number of errors at the onset of the learning phase ranged across monkeys from 0 to 16 and at plateau from 0 to 2. There was no correlation between the mean number of errors at onset of learning and the mean number of errors at plateau.

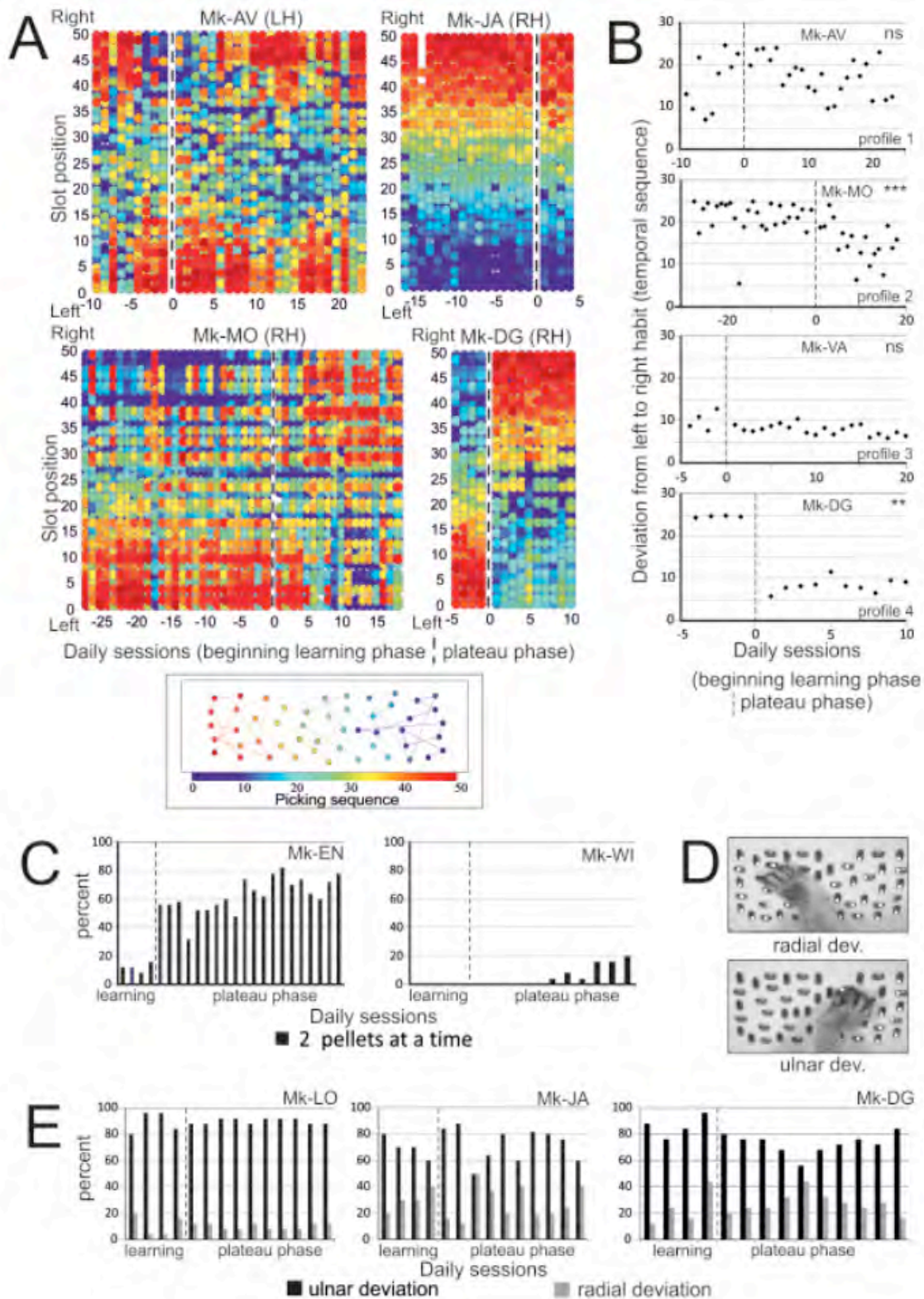


Figure 5. **Panel A:** Temporal sequence used by the monkeys to visit the 50 slots in the modified Brinkman board task. The picking sequence is shown by a color scale in the bottom inset, in which the first-visited slots are represented in blue, whereas the last visited



ones are represented in red (board scanning from right (blue slots) to left (red slots) in this example). In the top and middle displays, the temporal sequence was established for 4 monkeys, each representative of a behavioral profile (see text), both during the beginning of the learning phase (negative session numbers) and the plateau phase (positive session numbers). The x-axis displays the time in daily sessions, irrespective of the time interval (in days) between two consecutive sessions (different from the time scale in Figures 1 and Supplementary Figure 1). Each vertical column corresponds to a daily session of the modified Brinkman board task. Along each column, dots at the bottom are for slots located at the left extremity of the board, whereas dots at the top are for slots at the right extremity. RH=Right hand; LH=Left hand. **Panel B:** Quantitative assessment of the temporal sequence used to visit the 50 slots in the modified Brinkman board task for four monkeys, representative of the four profiles reported in the text. An index of systematic motor sequence (habit) was computed, indicating the extent of deviation from a systematic sequence starting from the left extremity of the board and terminating at its right extremity (corresponding to a low value for this precise sequence), and plotted in the y-axis as a function of behavioral daily sessions. The mirror sequence (systematic right to left scan) yields a high value. A small variability from one daily behavioral session to the next, indicating a reproducible motor sequence, reflects motor habit. The temporal sequence is shown qualitatively for the same monkeys Mk-AV, Mk-MO and Mk-DG in panel A. See text for detailed description of the results. The index of motor sequence was compared between the learning phase and the plateau phase with the non-parametric Mann-Whitney U test. The result of the statistical comparison is indicated at the top right of each graph: ns = statistically non-significant difference ( $p > 0.05$ ); \*\* is for  $p \leq 0.01$ ; \*\*\* is for  $p \leq 0.001$ . **Panel C:** Percentage of grasping patterns (at the beginning of learning and at plateau) in which two pellets were retrieved at the same time instead of a single one, in the modified Brinkman board task. In other words, the monkey grasped two pellets before transport to the mouth. In the other trials, the monkey retrieved a single pellet and brought it to the mouth. For this analysis, the vertical and horizontal slots were cumulated. **Panel D:** Usually, to retrieve pellets from the horizontal slots and depending on their position in the modified Brinkman board, the monkeys used a precision grip movement associated with a complementary wrist/arm movement. As illustrated for a right hand, on the left part of the Brinkman board, there was a trend to perform a radial deviation of the wrist/arm (top picture) whereas, on the right part of the Brinkman board, the trend was in favour of an ulnar deviation (bottom picture). **Panel E:** The distribution of wrist/arm radial deviation and ulnar deviation postures for pellet retrieval from the horizontal slots is illustrated for three monkeys over consecutive daily sessions, at the beginning of the learning phase and at plateau. For each daily session, the black bar and the gray one indicate the percentage of ulnar deviations and radial deviations, respectively. The sum of the radial and ulnar deviations is 100% in each daily session. Mk-LO is representative of 11 monkeys exhibiting a clear prevalence of ulnar deviations, during both the learning phase and the plateau phase. Mk-JA and Mk-DG also preferred ulnar deviations, but to a lesser extent.

Based on multiple correlation analyses (not shown), it turned out that the mean number of errors both at onset of the learning phase and at plateau was correlated with none of the following parameters: learning duration, slope of learning regression line, initial score value at onset of learning, median score value at plateau, *SD* of score at plateau, difference between the initial score at learning onset, or average score at plateau. Nevertheless, there was a positive correlation between the gain of score performance during practice and the mean number of errors at onset of learning ( $p = 0.029$ ): monkeys with larger mean numbers of errors at onset of learning exhibited a larger gain of performance provided by the learning phase.

## Reach and Grasp Drawer Task

Typical traces of grip force and load force recorded during a single trial of the reach and grasp drawer task are illustrated in Figure 6A, in parallel to the displacement of the drawer and discrete events, such as *touch knob*, *open onset*, *full open* and *picking*. Four monkeys were included in the analysis of the drawer task (Mk-LO, Mk-TH, Mk-DI and Mk-AT). Based on five daily sessions recorded both at the beginning of the learning phase and at plateau, the maximal grip force was measured for five correct trials at each resistance tested ( $R1 = 0$  Newton,  $R2 = 1.25$  N,  $R3 = 2.75$  N,  $R4 = 5$  N) and plotted in the form of box and whisker plots (Figure 6C). Two of the monkeys (Mk-DI and Mk-TH) exhibited a systematic and statistically significant increase in the maximal grip force applied on the drawer knob when the task was performed at plateau as compared to the

learning phase (Mann-Whitney U test). A comparable result was obtained in Mk-LO for the lowest two resistances, whereas there was no statistically significant difference between the learning and plateau phases at higher resistances (R3 and R4). A reverse behavior was found in Mk-AT, exhibiting in contrast a lower maximal grip force at plateau than during the learning phase at R1, R2 and R3, although the difference was statistically significant at R2 only (Figure 6C). At R4, Mk-AT used a statistically higher maximal grip force at plateau than during the learning phase, as Mk-TH.

The maximal load force was measured from the same trials, as shown in Figure 7A, and no difference between the learning and plateau phases appeared in Mk-AT and Mk-TH with the exception in the latter of the resistance R2, at which the maximal load force was significantly higher at plateau. Mk-DI used a lower maximal load force at plateau as compared to the learning phase (Figure 7A), but the difference was statistically significant only at the resistances R2 and R3. Mk-LO presented a more variable behavior, with a higher maximal load force at plateau at R1 and R2, but statistically significant at R1 only and a lower maximal load force at plateau as compared to the learning phase at R3 and R4, but statistically significant at R4 only. As illustrated for Mk-AT and for Mk-LO (Figure 7B), in the four monkeys enrolled in the reach and grasp drawer task the transition from the learning phase to the plateau phase was accompanied by a statistically significant decrease in both the grip force duration and the load force duration (Figure 7B), except at the highest level of resistance (R4). In Mk-TH, at resistance R4 as well, both durations were also statistically shorter at plateau than at the beginning of the learning phase.

The difference in grip force (solid lines in Figure 6B left column) and in load force (solid lines in Figure 6B right column) between the beginning of the learning phase and the end of the plateau phase is illustrated in Mk-DI, together with their variability (dashed lines representing plus and minus *SDs*). These data are representative of the observation (Figure 6C) that grip force was usually stronger at plateau phase than at the beginning of the learning phase, except in Mk-AT. However, variability was clearly larger at the onset of the learning phase than at the end of the plateau. Duration of grip application was shorter at plateau phase (as seen in Figure 7B). There was less difference between the two phases in the amplitude of the load force (Figure 6B right column), as compared to the grip force. However, load force duration was shorter and less variable at the end of the plateau than at onset of the learning phase, as shown in Figure 7B (right panel).

## Discussion

### Survey of the Main Results

Our main hypothesis that acquired manual (digits) dexterity performance and variability can be predicted from the duration of the learning phase, from the learning slope and from the initial score before any training was not verified for the most part, based on the modified Brinkman board data. Indeed, both performance and variability of manual dexterity, precision grip in the present case, were not related to the duration of training and to the slope of the learning regression line (Supplementary Figure 2). Only the performance of manual dexterity at plateau was correlated with the initial score before learning, the higher the initial score before training, the better the score at plateau (Figure 3, top right panel). On the other hand, the initial score of manual dexterity before learning was a poor predictor of intra-individual variability at plateau (Supplementary Figure 2).

As mostly expected, motor learning led to an optimization of manual dexterity parameters in the modified Brinkman board task, such as score, CT, as well as a substantial decrease in intra-individual variability, especially for the CT (Figures 1, 4 and Supplementary Figures 1, 3), in line with current theories

(see e.g., Marteniuk 1974). The present study also demonstrates the considerable inter-individual variations in precision grip skills, reflected across monkeys both by wide ranges of motor parameters (score, CT, learning properties) and disparate qualitative characteristics of grasping patterns (e.g., grip type, hand posture, strategy, motor habit). Such large inter-individual variability is in line with the theory of motor equivalence claiming that a given motor goal can be achieved via multiple strategies. In relation to motor habit, reflected by the temporal order in which sequential movements were executed in the modified Brinkman board task, the data (Figure 5A and B) support the notion that motor habit is established very early during the learning phase in most animals. These data suggest that macaque monkeys, as most human subjects would do, adopt motor habits early, reflecting the capability to organize motor sequences following a strategy perceived as optimal, as opposed to a random scan of the board augmenting the probability of neglecting a slot and requiring more attention to detect yet unvisited slots. The early emergence of a preferential prehension sequence is present also in children (3-5 years old), as observed in the Pegboard with 12 pegs test (Kakebeeke, Caflisch, Chaouch, Rousson, Largo & Jenni, 2013; T. Kakebeeke, personal communication). In adult human subjects performing the modified Brinkman board task, a preferential prehension sequence is most often already present at first trial and then maintained over 10 repetitions of the test (data derived from Chatagny et al., 2013).

In the reach and grasp drawer task, the expectation that the monkeys would use exaggerated maximal grip and load forces to make sure to open the drawer during learning phase, then reduced at plateau to just exceed the minimal forces required, representing an energy conservation and behavioral optimization, was not verified, at least in three out of four monkeys tested (Figures 6 and 7: Mk-LO, Mk-TH and Mk-AT). This principle of optimization was observed only in one monkey (Mk-DI), for the load force but not for the grip force. On the other hand, the duration of application of both the grip force and load force was reduced at plateau as compared to the learning phase (Figure 7), as expected.

## **Methodological Considerations and Limitations**

In the present study, emphasis was put on an individual analysis of 20 adult macaques. This individual (*differential*) strategy was prompted by the notion that “averaging data over participants (the *experimental* approach) can mask the actual individual participant and trial functions of change, as well as it can also produce learning curves that are not representative of any single individual in the group” (Adi-Japha, Karni, Parnes, Loewenschuss & Vakil, 2008; Newell, Liu & Mayer-Kress, 2001; Schmidt & Lee, 2011: Chapter 9). These concerns emitted in relation to the learning curves apply also most likely to the motor performance at plateau. Indeed the data shown in all Figures of the present study emphasize the considerable inter-individual variability of manual dexterity performance across our population of 20 macaque monkeys, although they were housed for many years in groups in the same environment and performed the same motor tasks in well controlled and reproducible laboratory conditions.

Our study presents weaknesses in the data gathering due to variations in the experimental protocol, inherent to this type of non-human primate study and its related constraints. First, as expected for a study conducted over a long period of time (15 years), several conditions changed from one animal to the next. One example is the size of the housing facility and its degree of enrichment (Table 1), adapted over the years according to changes in the legislation dealing with the protection of animals involved in scientific research. A second confounding factor is the supervision of the monkeys by different experimenters: a given experimenter is devoted to the very same monkeys every day and therefore cannot supervise more than two monkeys daily.

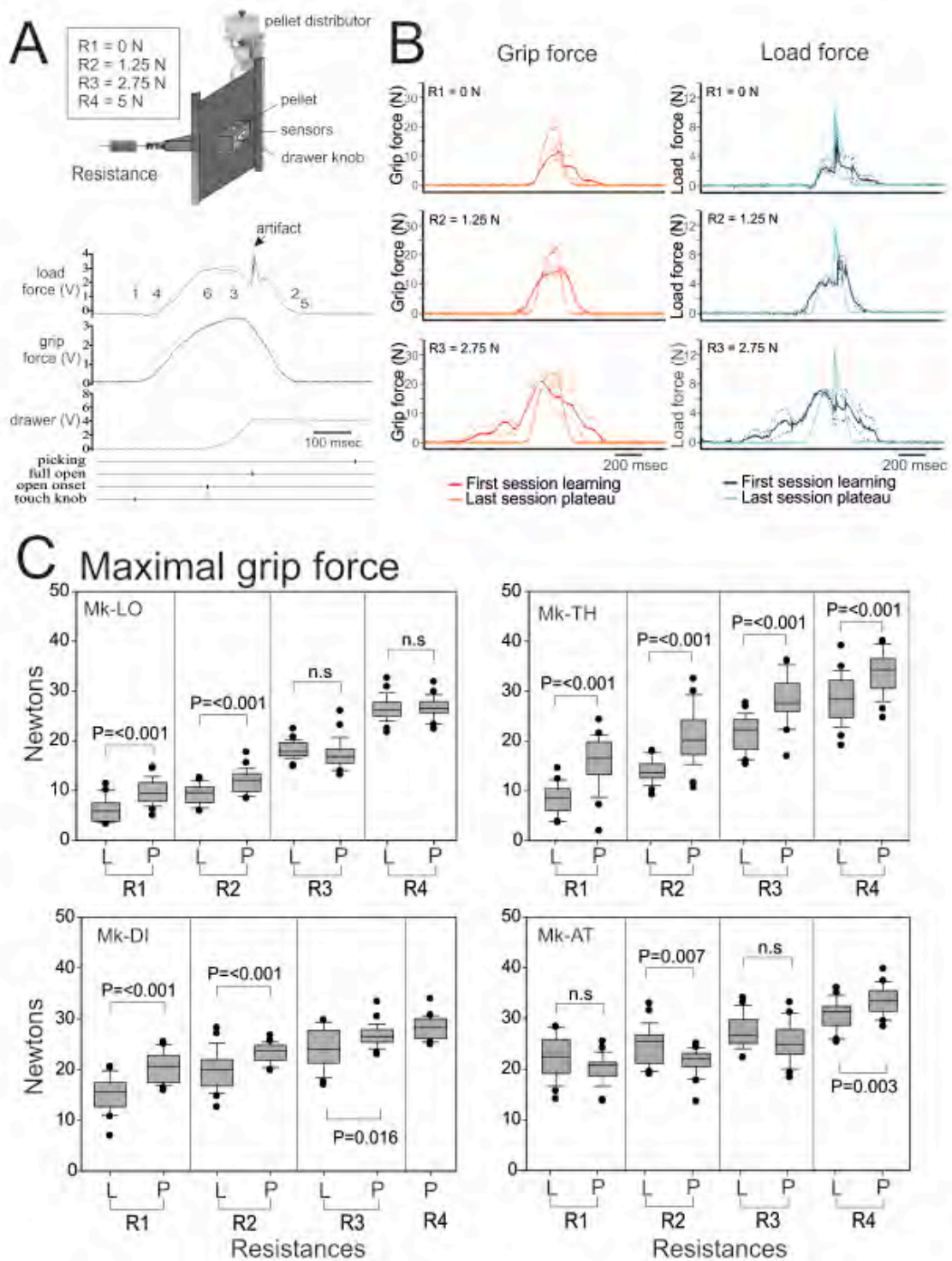


Figure 6. **Panel A:** Typical traces of the load force, grip force and drawer displacement as a function of time (from top to bottom) when a monkey executed a trial in the reach and grasp drawer task. The time occurrence of four discrete events is shown below (vertical tics). A schematic representation of the drawer set-up is shown on the top, with the four increasing resistances opposing the opening of the drawer (R1 to R4). The vertical dashed lines with numbers correspond to: *onset of grip force* (1), *offset of grip force* (2), *maximal grip*



force (3), onset of load force (4), offset of load force (5) and maximal load force (6). An artifact in the load force trace occurred when the drawer was blocked at its maximal opening. **Panel B:** Average traces (over 5 trials) and their variability ( $\pm 1 SD$ ) in Newtons (N) for the grip force (left column) and load force (right column), recorded in Mk-DI. In each column, the two colors distinguish traces obtained at the beginning of the learning phase and at the end of the plateau phase. The traces are shown for three levels of resistances (R1, R2, R3; see panel A). For each curve, the variability is represented by the envelope in dashed lines. **Panel C:** Box and whisker plots (same conventions as in Fig. 3) of the maximal grip force recorded during the learning phase (L) and during the plateau phase (P), in the four monkeys involved in the reach and grasp drawer task, as a function of 4 increasing resistance levels opposing the opening of the drawer (R1, R2, R3, R4). The results of the statistical comparison between “L” and “P” are given with the corresponding p value or n.s when statistically non-significant ( $p > 0.05$ ). Note that Mk-DI performed the task at resistance level R4 only during the plateau phase, after learning.

Moreover, the duration of the entire experiment on a given monkey may last up to two to three years and may consequently be conducted by several successive experimenters. Equally important, each experimenter develops his/her own approach to train each animal, depending also on the *personal* traits of the latter. In particular, some monkeys required a longer preliminary habituation phase than others before being actively involved in the experiment, before collecting the behavioral data for subsequent analysis (Table 1). Over the years, the monkeys originated from different sources, such as our own breeding colony (before 2010) or from different authorized suppliers (China, Mauritius Island, Vietnam), via various quarantine European centers. In spite of these multiple parameters influencing our monkey data, which cannot be strictly controlled over a 15 year period, it remains that they have most likely less impact than the even more numerous confounding factors associated with human studies, such as genetic variability, socio-cultural background, education, economical status, motivation, professional occupation, hobbies and so on.

The vast majority of lesion studies dealing with manual dexterity in non-human primates (see introduction) provide behavioral data restricted to two time points, namely before a lesion of the motor system (after reaching a plateau of performance) and after the lesion. In these studies, the data related to the learning phase of the motor tasks were rarely, if not at all, reported. The originality of the present study was to compare the manual dexterity properties of adult macaque monkeys at their plateau (before subsequent lesion) with those derived earlier from the acquisition of manual performance for two motor tasks, in the same animals. Furthermore, as the behavioral sessions took place three to five days a week, it was possible to precisely follow progressive changes in each monkey in order to assess intra-individual and inter-individual variability over a very long time frame. As the motor tests took place in the laboratory with the monkeys sitting in a primate chair, confounding factors such as the position of the monkeys with respect to the set-up and the separate use of each hand were well controlled.

### Initial Score Before Training

The statistically significant correlation between the initial score before training and the score reached in the modified Brinkman board task at plateau (Figure 3, top right panel) suggests that there is a limited margin of progression during learning, meaning a ceiling effect. When the initial score was high (above 25 pellets; in four monkeys, see Table 1), the increase in score during the learning phase was modest (1-5 pellets at most; Figure 2B: crosses), corresponding to the ceiling effect, with a maximal score in the most dexterous monkeys ranging from about 30 to 35 pellets in 30 seconds. A few other monkeys ( $n = 5$ ), in spite of a lower initial score before training (ranging from 18 to 24 pellets), also exhibited a limited gain of score during the learning phase (below 6 pellets; Figure 2B: crosses). Overall, 10 monkeys improved relatively modestly during the learning phase. In the other 10 monkeys, the margin of score progression during learning was more prominent (ranging from 9 to 16; Figure 2B: crosses). The latter monkeys were predominantly females (7 out of 10). In comparison with human subjects performing the modified Brinkman board task in 10 consecutive sessions on

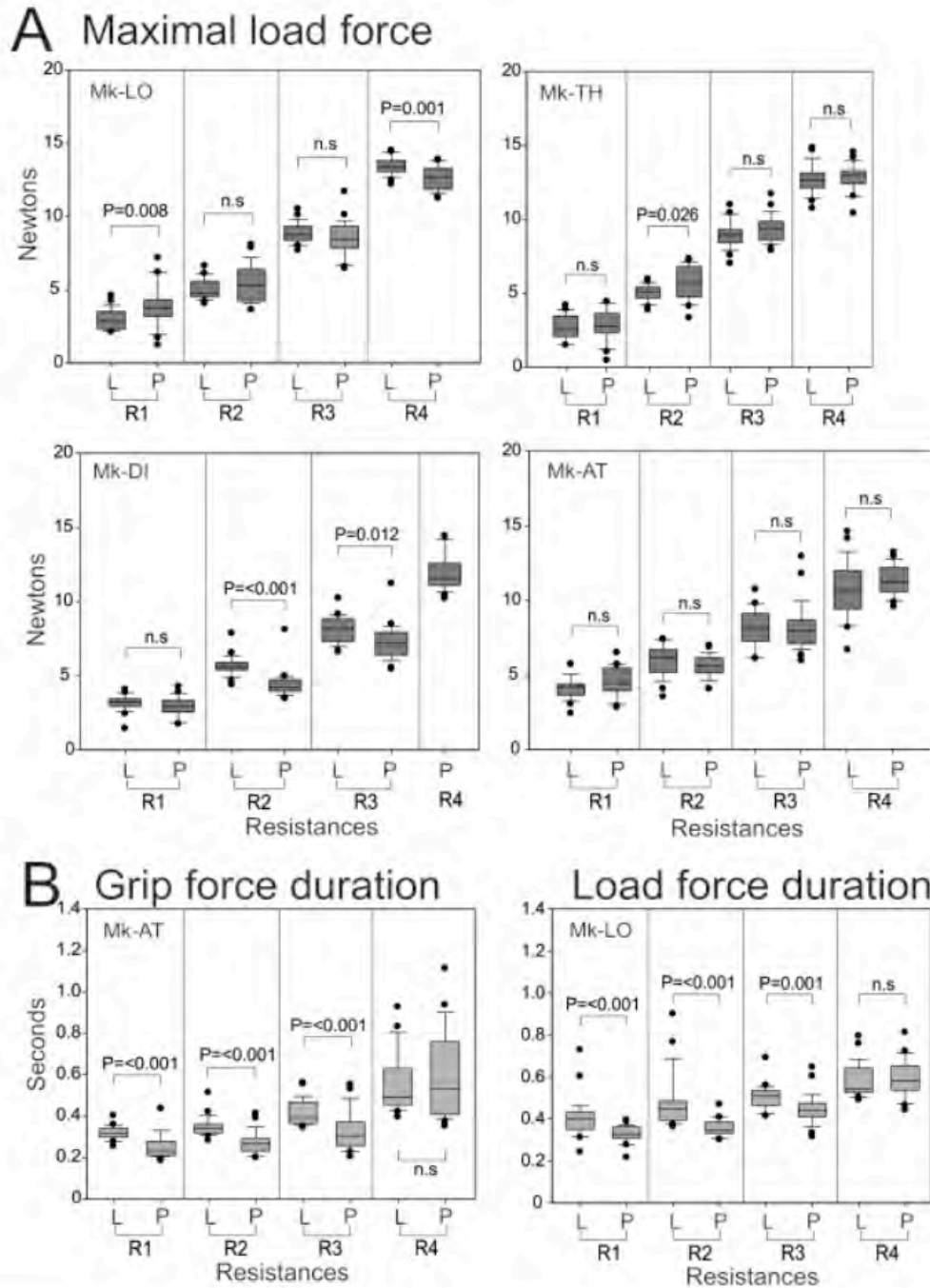


Figure 7. **Panel A:** Box and whisker plots (same conventions as in Fig. 3) of the maximal load force during the learning phase (L) and during the plateau phase (P), in the same four monkeys as in Figure 6. Same conventions as in Figure 6. **Panel B:** Grip force duration and load force duration measured in 2 animals during the learning phase (L) and the plateau phase (P), as a function of the resistance levels opposing the opening of the drawer (R1, R2, R3, R4). Same conventions as in Figure 6.

the same day, the training effect was less prominent than in monkeys (Chatagny et al., 2013), suggesting that humans started closer to the ceiling of performance.

The statistically significant lower scores in females than males (Figure 2B) is consistent with the lack of a few habituating sessions before collecting data in females, as opposed to the majority of males (Table 1). Moreover, other confounding factors might have played a role in this sex difference as well (e.g., size of housing facility, degree of enrichment; see Table 1). However, later on, when females were more familiar with the new environment and the tasks, their score increased more than in males so that the two groups exhibited largely overlapping mean or median scores at plateau (Figure 2, panels E and F). The absence of sex difference for the score at plateau in the macaque monkeys enrolled in the present study contrasts with the significantly better performance observed in women than in men in a human adapted version of the modified Brinkman board task (Chatagny et al., 2013).

### **Application to Lesion Studies**

The large inter-individual variability of the average score at plateau (Table 1) may be considered as an inconvenience in comparing two groups of monkeys subjected to a lesion, one group receiving a treatment and the other not. Nevertheless, this drawback is actually attenuated because, in such studies and in contrast to clinical trials (see e.g., Kaeser et al., 2010), the most relevant comparison is made within the same monkey, between the pre-lesion score and the post-lesion score at plateau after functional recovery (usually incomplete; see e.g., Freund et al., 2009; Hamadjida et al., 2012). Thus, the comparison between two groups of animals is based on the percentage of functional recovery individually determined for each animal (see e.g., Freund et al., 2009; Hamadjida et al., 2012; Hoogewoud et al., 2013; Kaeser et al., 2010, 2011), which is less affected by inter-individual variability than group comparisons in clinical trials.

### **Learning Curves**

As reviewed by Newell and collaborators (2001), the forms of the learning curves, defined as “plots of the outcome performance as a function of practice”, can be highly variable: “learning curves of almost every conceivable shape can and have been found”, corresponding to various mathematical functions, such as exponential, power law, S-shaped, hyperbolic, accelerating functions, etc. In the present case, one would have intuitively expected an exponential rise of performance (score) to a maximum (ceiling; see Schmidt & Lee, 2011: Chapter 10, their Figure 10.8). As illustrated in Figure 1 and Supplementary Figure 1 however, the majority of monkeys ( $n = 16$  out of 20) exhibited a progression of performance during the learning phase that was rather better approximated by a regression line than by an exponential function. The exceptions are Mk-RO (Figure 1), Mk-DI, Mk-LO (Supplementary Figure 1) and Mk-TH (not shown). This linear learning progression observed here may be specific to the modified Brinkman board task, as well as to each monkey, in line with the proposition that the “learning rate is individual and task dependent” (Newell et al., 2001). In the same line, unlike recent studies in humans (e.g., Rosenblatt, Hurt, Latash, & Grabiner, 2014 in locomotor tasks; Wu et al., 2014 in arm movements tasks) demonstrating that a greater variability at the beginning of practice allows a faster learning rate, no such correlation was found in our monkeys performing unconditioned voluntary tasks requiring fine manual dexterity. Individual differences in motor skill learning are likely to be related to variations in the function and structure of specific brain regions, such as prefrontal, premotor and parietal cortices, as well as basal ganglia and cerebellum (Tomassini et al., 2011).

An important parameter here is the time scale when attempting to characterize the change in behavior resulting from motor learning (Newell et al., 2001). In most cases, especially in human subjects, the time range of observation of the learning phase was narrow (an hour to a single day most often; e.g., Chatagny et al., 2013). Longitudinal studies, though conducted in relation to infant motor development, are relatively rare

and therefore the present study is original thanks to the long time period of observation during the learning phase (over weeks to months). Short daily sessions, during such a long time scale, may explain the very progressive and regular improvement of performance with practice observed in the majority of monkeys. In the present learning data on macaque monkeys, the learning phase may appear rather long for a relatively natural motor task, such as the precision grip performed in the modified Brinkman board task, at least in some individuals (Table 1). This underlies the fact that precision grip is an exquisite motor function subjected to very fine and progressive adjustments with practice. For instance, it was reported that the even more sophisticated skill in rolling cigars may still improve after many years (up to seven) of practice (Crossman, 1959).

### Comparison with Previous Studies

Comparing the present behavioral data with the literature is limited to some extent, as the manual dexterity performance and variability strongly depends on the animal/primate species, on practice schedule (Stelmach, 1968), on expertise level (Schorer, Baker, Fath, & Jaitner, 2007), as well as on the type of task. Individual differences are indeed strongly task specific, corresponding to the theory of specificity (see e.g., Marteniuk, 1974). Even close species such as *Macaca fascicularis* and *Macaca mulatta* have different hand size (e.g., finger length), larger for the latter, corresponding consequently to different manual dexterity abilities (see e.g., Darling et al., 2013 for more details). A direct comparison of the present macaque data with rodent data (mainly rats) remains questionable, due to the strong difference between the pincer grasp (or precision grip) in primates and the arpeggio/power grasp in rodents (Klein et al., 2012). In the context of motor specificity, a strong influence is exerted by the size and shape of the object to be manipulated, as well as by the size of the well containing the object, when applicable. In a human study focused on precision grasps (Wong & Whishaw, 2004), it was shown that there was a high degree of variability of grasping pattern within and between subjects, like in our group of monkeys. Wong and Whishaw (2004) reported up to seven grasp types in human subjects, involving the thumb and various combinations of other digits, depending on the size of the bead being held. The proper precision grip (opposition of thumb and index finger only) was highly predominant when grasping the smallest beads, whereas the involvement of other fingers increased when progressively larger beads were grasped. In the present study on monkeys, only the proper precision grip was observed (opposition of thumb and index finger) because the food pellet was small compared to the finger size. Wong and Whishaw (2004) reported also in human subjects a large variability of first contact strategy with an object, depending on which and how the first finger contacted the object. This observation is in line with the large inter-individual variability observed here for the monkeys in the first digit used to contact the pellet in the horizontal slots (see results paragraph Variable Patterns of Food Pellet Grasping). The large inter- and intra-individual variability of grasping patterns observed in our monkeys and in humans (Wong & Whishaw, 2004) is consistent with the exquisitely complex somatotopic organization in mosaics of the primary motor cortex in primates (e.g., Schieber, 2001) as well as with complex movements synergies elicited in primates by microstimulation of the primary motor cortex (Graziano, Taylor, & Moore, 2002).

In two studies conducted on *Macaca fascicularis* (Brinkman, 1984) and *Macaca mulatta* (Brinkman & Kyupers, 1973), using a very comparable task (the original Brinkman board task), the data were mostly reported in a qualitative manner (movement pattern), preventing a direct comparison with the present quantitative data. The same limitation applies to other macaque studies using different manual tasks (e.g., Glees & Cole, 1950; Ogden & Franz, 1917; Passingham et al., 1983). In several studies on non-human primates (as listed in the introduction) involving a lesion of the motor system followed by functional recovery, the pre-lesion behavioral data were often limited to very few baseline data points, if not a single one, thus strongly limiting the comparison with the present progressive training phase over weeks, followed then by a long period of performance stabilization at plateau.

An exception is the study by Pizzimenti et al. (2007) conducted on *Macaca mulatta* and using a somewhat different behavioral apparatus, modified from the often used dexterity *Kliver* board. Although different from our modified Brinkman board, the wells A and B in the dexterity board used by Pizzimenti et al. (2007) had a size comparable to our slots. The manual dexterity was assessed quantitatively in three monkeys, using the so-called performance ratio, defined as the average score divided by the *SD* of the score, derived from five pre-lesion sessions (plateau). For the preferred hand, the performance ratios ranged from 2.5 to 3.0 in well A and from 3.5 to 8 in well B, the latter being the least difficult. Taking our data from the modified Brinkman board at plateau (Table 1) and computing similarly the performance ratio, values ranging from 4.4 to 14.0 (average = 9.3) among the 20 monkeys were obtained, thus corresponding to a generally better manual dexterity performance in our monkeys. However, such direct comparison may be biased due to important differences, such as species, manual task, duration of the considered plateau phase, scoring, as well as the time interval between the sessions (1-2 weeks in Pizzimenti et al., 2007 versus 1-3 days in our study). Furthermore, the monkeys of Pizzimenti et al. (2007) worked from their home cage (in a primate chair here).

As far as the reach and grasp drawer task is concerned, slightly different versions of the original set-up (Kazennikov et al., 1994) were used along the years (Kazennikov et al., 1998; Kazennikov et al., 1999; Kermadi, Liu, Tempini, & Rouiller, 1997; Kermadi, Liu, Tempini, Calciati, & Rouiller, 1998; Kermadi, Liu, & Rouiller, 2000), with special emphasis put on the issue of inter-limb coordination. In the current report, the reach and grasp drawer task was used in its unimanual version only, with focus on the assessment of the grip and load forces, a situation more closely related to studies on human subjects performing the reach and grasp drawer task (e.g., Grichting, Hediger, Kaluzny, & Wiesendanger, 2000; Serrien & Wiesendanger, 1999; Serrien, Kaluzny, Wicki & Wiesendanger, 1999). Interestingly, as compared to intact human subjects, cerebellar patients overestimated the proactive grip force requested to pull the drawer (Serrien & Wiesendanger, 1999). It can thus be expected that the reach and grasp drawer task will also be pertinent in macaque monkeys to evaluate deficits related to various motor dysfunctions (e.g., Parkinson disease, cortical lesion, spinal cord lesion) and to follow the time course and extent of functional recovery. In particular, it will be interesting to compare the properties of the initial learning phase of a motor task with those of the re-learning phase of the same task in the same animals following a lesion, in absence (spontaneous recovery) or presence of a specific treatment (induced recovery).

### Acknowledgements

The authors wish to thank the technical assistance of Françoise Tinguely, Josef Corpataux, Laurent Bossy, Jacques Maillard (animal care taking), André Gaillard (mechanics), Bernard Aebischer (electronics), Laurent Monney (informatics). Over the years, previous members of the laboratory were involved in some of the experiments: Dr. Alexander Wyss, Dr. Shahid Bashir, Dr. Yu Liu and Dr. Abderraouf Belhaj-Saif.

**Informative video material:** <http://www.unifr.ch/neuro/rouiller/ijcp/fr0.html>.

### References

Adi-Japha, E., Karni, A., Parnes, A., Loewenschuss, I., & Vakil, E. (2008). A shift in task routines during the learning of a motor skill: group-averaged data may mask critical phases in the individuals' acquisition of skilled performance. *Journal of Experimental Psychology: Learning, Memory, and Cognition*, *34*, 1544-1551.



- Alstermark, B., & Isa, T. (2002). Premotoneuronal and direct corticomotoneuronal control in the cat and macaque monkey. *Advances in experimental medicine and biology*, 508, 281-297.
- Alstermark, B., Pettersson, L. G., Nishimura, Y., Yoshino-Saito, K., Tsuboi, F., Takahashi, M., & Isa, T. (2011). Motor command for precision grip in the macaque monkey can be mediated by spinal interneurons. *Journal of Neurophysiology*, 106, 122-126.
- Alstermark, B., & Isa, T. (2012). Circuits for skilled reaching and grasping. *Annual Review of Neuroscience*, 35, 559-578.
- Armand, J., Edgley, S. A., Lemon, R. N., & Olivier, E. (1994). Protracted postnatal development of corticospinal projections from the primary motor cortex to hand motoneurons in the macaque monkey. *Experimental Brain Research*, 101, 178-182.
- Armand, J., Olivier, E., Edgley, S. A., & Lemon, R. N. (1997). Postnatal development of corticospinal projections from motor cortex to the cervical enlargement in the macaque monkey. *Journal of Neuroscience*, 17, 251-266.
- Bashir, S., Kaeser, M., Wyss, A., Hamadjida, A., Liu, Y., Bloch, J., . . . Rouiller, E. M. (2012). Short-term effects of unilateral lesion of the primary motor cortex (M1) on ipsilesional hand dexterity in adult macaque monkeys. *Brain Structure and Function*, 217, 63-79.
- Beaud, M. L., Schmidlin, E., Wannier, T., Freund, P., Bloch, J., Mir, A., . . . Rouiller, E. M. (2008). Anti-Nogo-A antibody treatment does not prevent cell body shrinkage in the motor cortex in adult monkeys subjected to unilateral cervical cord lesion. *BMC Neuroscience*, 9, 5.
- Beaud, M. L., Rouiller, E. M., Bloch, J., Mir, A., Schwab, M. E., Wannier, T., & Schmidlin, E. (2012). Invasion of lesion territory by regenerating fibers after spinal cord injury in adult macaque monkeys. *Neuroscience*, 227, 271-282.
- Bihel, E., Pro-Sistiaga, P., Letourneur, A., Toutain, J., Saulnier, R., Insausti, R., . . . Touzani, O. (2010). Permanent or transient chronic ischemic stroke in the non-human primate: behavioral, neuroimaging, histological, and immunohistochemical investigations. *Journal of Cerebral Blood Flow and Metabolism*, 30, 273-285.
- Borra, E., Belmalih, A., Gerbella, M., Rozzi, S., & Luppino, G. (2010). Projections of the hand field of the macaque ventral premotor area F5 to the brainstem and spinal cord. *Journal of Comparative Neurology*, 518, 2570-2591.
- Bortoff, G. A., & Strick, P. L. (1993). Corticospinal terminations in two new-world primates: further evidence that corticomotoneuronal connections provide part of the neural substrate for manual dexterity. *Journal of Neuroscience*, 13, 5105-5118.
- Brinkman, C. (1984). Supplementary motor area of the monkey's cerebral cortex: short- and long-term deficits after unilateral ablation and the effects of subsequent callosal section. *Journal of Neuroscience*, 4, 918-929.
- Brinkman, J., & Kuypers, H. G. J. M. (1973). Cerebral control of contralateral and ipsilateral arm, hand and finger movements in the split-brain rhesus monkey. *Brain*, 96, 653-674.
- Carron, A. V., & Leavitt, J. L. (1968). Individual differences in two motor learning tasks under massed practice. *Perceptual and Motor Skills*, 27, 499-504.
- Chalmeau, R., Visalberghi, E., & Gallo, A. (1997). Capuchin monkeys, *Cebus apella* fail to understand a cooperative task. *Animal Behaviour*, 54, 1215-1225.
- Chatagny, P., Badoud, S., Kaeser, M., Gindrat, A. D., Savidan, J., Fregosi, M., . . . Rouiller, E. M. (2013). Distinction between hand dominance and hand preference in primates: a behavioral investigation of manual dexterity in nonhuman primates (macaques) and human subjects. *Brain and Behavior*, 3, 575-595.
- Christel, M. I., & Billard, A. (2002). Comparison between macaques' and humans' kinematics of prehension: the role of morphological differences and control mechanisms. *Behavioural Brain Research*, 131, 169-184.

- Costello, M. B., & Fragaszy, D. M. (1988). Prehension in *Cebus* and *Saimiri*: I. Grip type and hand preference. *American Journal of Primatology*, *15*, 235-245.
- Courtine, G., Bunge, M. B., Fawcett, J. W., Grossman, R. G., Kaas, J. H., Lemon, R., . . . Edgerton, V. R. (2007). Can experiments in nonhuman primates expedite the translation of treatments for spinal cord injury in humans? *Nature Medicine*, *13*, 561-566.
- Crossman, E. R. F. W. (1959) A theory of the acquisition of speed-skill. *Ergonomics* *2*, 153-166.
- Dancause, N., Barbay, S., Frost, S. B., Plautz, E. J., Chen, D. F., Zoubina, E. V., . . . Nudo, R. J. (2005). Extensive cortical rewiring after brain injury. *Journal of Neuroscience*, *25*, 10167-10179.
- Dancause, N., Barbay, S., Frost, S. B., Zoubina, E. V., Plautz, E. J., Mahnken, J. D., & Nudo, R. J. (2006). Effects of small ischemic lesions in the primary motor cortex on neurophysiological organization in ventral premotor cortex. *Journal of Neurophysiology*, *96*, 3506-3511.
- Dancause, N., & Nudo, R. J. (2011). Shaping plasticity to enhance recovery after injury. *Progress in Brain Research*, *192*, 273-295.
- Darian-Smith, I., Galea, M. P., & Darian-Smith, C. (1996). Manual dexterity: how does the cerebral cortex contribute? *Clinical and Experimental Pharmacology and Physiology*, *23*, 948-956.
- Darian-Smith, I., Galea, M. P., Darian-Smith, C., Sugitani, M., Tan, A., & Burman, K. (1996). The anatomy of manual dexterity. The new connectivity of the primate sensorimotor thalamus and cerebral cortex. *Advances in Anatomy, Embryology and Cell Biology*, *133*, 1-140.
- Darian-Smith, I., Burman, K., & Darian-Smith, C. (1999). Parallel pathways mediating manual dexterity in the macaque. *Experimental Brain Research*, *128*, 101-108.
- Darling, W. G., Pizzimenti, M. A., Rotella, D. L., Peterson, C. R., Hynes, S. M., Ge, J., . . . Morecraft, R. J. (2009). Volumetric effects of motor cortex injury on recovery of dexterous movements. *Experimental Neurology*, *220*, 90-108.
- Darling, W. G., Pizzimenti, M. A., Rotella, D. L., Hynes, S. M., Ge, J., Stilwell-Morecraft, K. S., . . . Morecraft, R. J. (2010). Minimal forced use without constraint stimulates spontaneous use of the impaired upper extremity following motor cortex injury. *Experimental Brain Research*, *202*, 529-542.
- Darling, W. G., Pizzimenti, M. A., Hynes, S. M., Rotella, D. L., Headley, G., Ge, J., . . . Morecraft, R. J. (2011). Volumetric effects of motor cortex injury on recovery of ipsilesional dexterous movements. *Experimental Neurology*, *231*, 56-71.
- Darling, W. G., Helle, N., Pizzimenti, M. A., Rotella, D. L., Hynes, S. M., Ge, J., . . . Morecraft, R. J. (2013). Laterality affects spontaneous recovery of contralateral hand motor function following motor cortex injury in rhesus monkeys. *Experimental Brain Research*, *228*, 9-24.
- Eisner-Janowicz, I., Barbay, S., Hoover, E., Stowe, A. M., Frost, S. B., Plautz, E. J., & Nudo, R. J. (2008). Early and late changes in the distal forelimb representation of the supplementary motor area after injury to frontal motor areas in the squirrel monkey. *Journal of Neurophysiology*, *100*, 1498-1512.
- Falk, D., Pyne, L., Helmkamp, R. C., & DeRousseau, C. J. (1988). Directional asymmetry in the forelimb of *Macaca mulatta*. *American Journal of Physical Anthropology*, *77*, 1-6.
- Flament, D., Hall, E. J., & Lemon, R. N. (1992). The development of cortico-motoneuronal projections investigated using magnetic brain stimulation in the infant macaque. *Journal of Physiology*, *447*, 755-768.
- Fragaszy, D. M., & Adams-Curtis, L. E. (1997). Developmental changes in manipulation in tufted capuchins (*Cebus apella*) from birth through 2 years and their relation to foraging and weaning. *Journal of Comparative Psychology*, *111*, 201-211.
- Fragaszy, D. M. (1998). How non-human primates use their hands. In K. J. Connolly (Ed.), *The psychobiology of the hand* (pp. 77-96). London, UK: Mac Keith Press.
- Freund, P., Schmidlin, E., Wannier, T., Bloch, J., Mir, A., Schwab, M. E., & Rouiller, E. M. (2006). Nogo-A-specific antibody treatment enhances sprouting and functional recovery after cervical lesion in adult primates. *Nature Medicine*, *12*, 790-792.

- Freund, P., Wannier, T., Schmidlin, E., Bloch, J., Mir, A., Schwab, M. E., & Rouiller, E. M. (2007). Anti-Nogo-A antibody treatment enhances sprouting of corticospinal axons rostral to a unilateral cervical spinal cord lesion in adult macaque monkey. *Journal of Comparative Neurology*, *502*, 644-659.
- Freund, P., Schmidlin, E., Wannier, T., Bloch, J., Mir, A., Schwab, M. E., & Rouiller, E. M. (2009). Anti-Nogo-A antibody treatment promotes recovery of manual dexterity after unilateral cervical lesion in adult primates--re-examination and extension of behavioral data. *European Journal of Neuroscience*, *29*, 983-996.
- Friel, K. M., & Nudo, R. J. (1998). Recovery of motor function after focal cortical injury in primates: compensatory movement patterns used during rehabilitative training. *Somatosensory and Motor Research*, *15*, 173-189.
- Friel, K. M., Heddings, A. A., & Nudo, R. J. (2000). Effects of postlesion experience on behavioral recovery and neurophysiologic reorganization after cortical injury in primates. *Neurorehabilitation and Neural Repair*, *14*, 187-198.
- Frost, S. B., Barbay, S., Friel, K. M., Plautz, E. J., & Nudo, R. J. (2003). Reorganization of remote cortical regions after ischemic brain injury: A potential substrate for stroke recovery. *Journal of Neurophysiology*, *89*, 3205-3214.
- Galea, M. P., & Darian-Smith, I. (1994). Multiple corticospinal neuron populations in the macaque monkey are specified by their unique cortical origins, spinal terminations, and connections. *Cerebral Cortex*, *4*, 166-194.
- Galea, M. P., & Darian-Smith, I. (1995). Postnatal maturation of the direct corticospinal projections in the macaque monkey. *Cerebral Cortex*, *5*, 518-540.
- Galea, M. P. & Darian-Smith, I. (1997). Corticospinal projection patterns following unilateral section of the cervical spinal cord in the newborn and juvenile macaque monkey. *Journal of Comparative Neurology*, *381*, 282-306.
- Gash, D. M., Zhang, Z. M., Umberger, G., Mahood, K., Smith, M., Smith, C., & Gerhardt, G. A. (1999). An automated movement assessment panel for upper limb motor functions in rhesus monkeys and humans. *Journal of Neuroscience Methods*, *89*, 111-117.
- Glees, P., & Cole, J. (1950). Recovery of skilled motor function after small repeated lesions of motor cortex in macaque. *Journal of Neurophysiology*, *13*, 137-148.
- Graziano, M. S., Taylor, C. S., & Moore, T. (2002). Complex movements evoked by microstimulation of precentral cortex. *Neuron*, *34*, 841-851.
- Grichting, B., Hediger, V., Kaluzny, P., & Wiesendanger, M. (2000). Impaired proactive and reactive grip force control in chronic hemiparetic patients. *Clinical Neurophysiology*, *111*, 1661-1671.
- Hamadjida, A., Wyss, A. F., Mir, A., Schwab, M. E., Belhaj-Saif, A., & Rouiller, E. M. (2012). Influence of anti-Nogo-A antibody treatment on the reorganization of callosal connectivity of the premotor cortical areas following unilateral lesion of primary motor cortex (M1) in adult macaque monkeys. *Experimental Brain Research*, *223*, 321-340.
- Hoffman, D. S., & Strick, P. L. (1986). Step-tracking movements of the wrist in humans. I. Kinematic analysis. *Journal of Neuroscience*, *6*, 3309-3318.
- Hoogewoud, F., Hamadjida, A., Wyss, A. F., Mir, A., Schwab, M. E., Belhaj-Saif, A., & Rouiller, E. M. (2013). Comparison of functional recovery of manual dexterity after unilateral spinal cord lesion or motor cortex lesion in adult macaque monkeys. *Frontiers in Neurology*, (in press).
- Iwaniuk, A. N., Pellis, S. M., & Whishaw, I. Q. (1999). Is digital dexterity really related to corticospinal projections?: a re-analysis of the Heffner and Masterton data set using modern comparative statistics. *Behavioural Brain Research*, *101*, 173-187.
- Iwaniuk, A. N., & Whishaw, I. Q. (1999). How skilled are the skilled limb movements of the raccoon (*Procyon lotor*)? *Behavioural Brain Research*, *99*, 35-44.
- Iwaniuk, A. N., & Whishaw, I. Q. (2000). On the origin of skilled forelimb movements. *Trends in Neuroscience*, *23*, 372-376.



- Kaeser, M., Wyss, A. F., Bashir, S., Hamadjida, A., Liu, Y., Bloch, J., . . . Rouiller, E. M. (2010). Effects of unilateral motor cortex lesion on ipsilesional hand's reach and grasp performance in monkeys: Relationship with recovery in the contralesional hand. *Journal of Neurophysiology*, *103*, 1630-1645.
- Kaeser, M., Brunet, J. F., Wyss, A., Belhaj-Saif, A., Liu, Y., Hamadjida, A., . . . & Bloch, J. (2011). Autologous adult cortical cell transplantation enhances functional recovery following unilateral lesion of motor cortex in primates: a pilot study. *Neurosurgery*, *68*, 1405-1416.
- Kaeser, M., Wannier, T., Brunet, J. F., Wyss, A., Bloch, J., & Rouiller, E. M. (2013). Representation of motor habit in a sequence of repetitive reach and grasp movements performed by macaque monkeys: Evidence for a contribution of the dorsolateral prefrontal cortex. *Cortex*, *49*, 1404-1419.
- Takebeke, T. H., Cafilisch, J., Chaouch, A., Rousson, V., Largo, R. H., & Jenni, O. G. (2013). Neuromotor development in children. Part 3: motor performance in 3- to 5-year olds. *Developmental Medicine and Child Neurology*, *55*, 248-256.
- Kazennikov, O., Wicki, U., Corboz, M., Hyland, B., Palmeri, A., Rouiller, E. M., & Wiesendanger, M. (1994). Temporal structure of a bimanual goal-directed movement sequence in monkeys. *European Journal of Neuroscience*, *6*, 203-210.
- Kazennikov, O., Hyland, B., Wicki, U., Perrig, S., Rouiller, E. M., & Wiesendanger, M. (1998). Effects of lesions in the mesial frontal cortex on bimanual co-ordination in monkeys. *Neuroscience*, *85*, 703-716.
- Kazennikov, O., Hyland, B., Corboz, M., Babalian, A., Rouiller, E. M., & Wiesendanger, M. (1999). Neural activity of supplementary and primary motor areas in monkeys and its relation to bimanual and unimanual movement sequences. *Neuroscience*, *89*, 661-674.
- Kermadi, I., Liu, Y., Tempini, A., & Rouiller, E. M. (1997). Effects of reversible inactivation of the supplementary motor area (SMA) on unimanual grasp and bimanual pull and grasp performance in monkeys. *Somatosensory and Motor Research*, *14*, 268-280.
- Kermadi, I., Liu, Y., Tempini, A., Calciati, E., & Rouiller, E. M. (1998). Neuronal activity in the primate supplementary motor area and the primary motor cortex in relation to spatio-temporal bimanual coordination. *Somatosensory and Motor Research*, *15*, 287-308.
- Kermadi, I., Liu, Y., & Rouiller, E. M. (2000). Do bimanual motor actions involve the dorsal premotor (PMd), cingulate (CMA) and posterior parietal (PPC) cortices? Comparison with primary and supplementary motor cortical areas. *Somatosensory and Motor Research*, *17*, 255-271.
- King, B. J. (1986). Extractive foraging and the evolution of primate intelligence. *Journal of Human Evolution*, *1*, 361-372.
- King, J., & Landau, V. (1993). Manual preference in varieties of reaching in squirrel monkeys. In J. Ward & W. Hopkins (Eds.), *Primate laterality* (pp. 107-124). New York, NY: Springer.
- Kinoshita, M., Matsui, R., Kato, S., Hasegawa, T., Kasahara, H., Isa, K., . . . Isa, T. (2012). Genetic dissection of the circuit for hand dexterity in primates. *Nature*, *487*, 235-238.
- Klein, A., Sacrey, L. A., Whishaw, I. Q., & Dunnett, S. B. (2012). The use of rodent skilled reaching as a translational model for investigating brain damage and disease. *Neuroscience and Biobehavioral Reviews*, *36*, 1030-1042.
- Lacreuse, A., & Frigaszy, D. M. (1999). Left hand preferences in capuchins (*Cebus apella*): role of spatial demands in manual activity. *Laterality*, *4*, 65-78.
- Lacroix, S., Havton, L. A., McKay, H., Yang, H., Brant, A., Roberts, J., & Tuszynski, M. H. (2004). Bilateral corticospinal projections arise from each motor cortex in the macaque monkey: A quantitative study. *Journal of Comparative Neurology*, *473*, 147-161.
- Lashley, K. S. (1930) Basic neural mechanisms in behavior. *Psychological Review*, *37*, 1-24.
- Lawrence, D. G., & Hopkins, D. A. (1976). The development of motor control in the rhesus monkey: evidence concerning the role of corticomotoneuronal connections. *Brain*, *99*, 235-254.
- Lawrence, D. G., Porter, R., & Redman, S. J. (1985). Corticomotoneuronal synapses in the monkey: light microscopic localization upon motoneurons of intrinsic muscles of the hand. *Journal of Comparative Neurology*, *232*, 499-510.

- Leca, J. B., Gunst, N., & Huffman, M. (2011). Complexity in object manipulation by Japanese macaques (*Macaca fuscata*): A cross-sectional analysis of manual coordination in stone handling patterns. *Journal of Comparative Psychology, 125*, 61-71.
- Lemon, R. N., Johansson, R. S., & Westling, G. (1996). Modulation of corticospinal influence over hand muscles during gripping tasks in man and monkey. *Canadian Journal of Physiology and Pharmacology, 74*, 547-558.
- Lemon, R. N. (1999). Neural control of dexterity: what has been achieved? *Experimental Brain Research, 128*, 6-12.
- Lemon, R. N., & Griffiths, J. (2005). Comparing the function of the corticospinal system in different species: organizational differences for motor specialization? *Muscle Nerve, 32*, 261-279.
- Lemon, R. N. (2008). Descending pathways in motor control. *Annual Review of Neuroscience, 31*, 195-218.
- Lindshield, S. M., & Rodrigues, M. A. (2009). Tool use in wild spider monkeys (*Ateles geoffroyi*). *Primates, 50*, 269-272.
- Liu, Y., & Rouiller, E. M. (1999). Mechanisms of recovery of dexterity following unilateral lesion of the sensorimotor cortex in adult monkeys. *Experimental Brain Research, 128*, 149-159.
- Maier, M. A., Armand, J., Kirkwood, P. A., Yang, H. W., Davis, J. N., & Lemon, R. N. (2002). Differences in the corticospinal projection from primary motor cortex and supplementary motor area to macaque upper limb motoneurons: an anatomical and electrophysiological study. *Cerebral Cortex, 12*, 281-296.
- Manoel, E. J., & Connolly, K. J. (1995). Variability and the development of skilled actions. *International Journal of Psychophysiology, 19*, 129-147.
- Marshall, J. W., Ridley, R. M., Baker, H. F., Hall, L. D., Carpenter, T. A., & Wood, N. I. (2003). Serial MRI, functional recovery, and long-term infarct maturation in a non-human primate model of stroke. *Brain Research Bulletin, 61*, 577-585.
- Marteniuk, R. G. (1974). Individual differences in motor performances and learning. *Exercise and Sport Sciences Reviews, 2*, 103-130.
- McNeal, D. W., Darling, W. G., Ge, J., Stilwell-Morecraft, K. S., Solon, K. M., Hynes, S. M., . . . Morecraft, R. J. (2010). Selective long-term reorganization of the corticospinal projection from the supplementary motor cortex following recovery from lateral motor cortex injury. *Journal of Comparative Neurology, 518*, 586-621.
- Murata, Y., Higo, N., Oishi, T., Yamashita, A., Matsuda, K., Hayashi, M., & Yamane, S. (2008). Effects of motor training on the recovery of manual dexterity after primary motor cortex lesion in macaque monkeys. *Journal of Neurophysiology, 99*, 773-786.
- Nahallage, C. A. D., & Huffman, M. A. (2007). Acquisition and development of stone handling behavior in infant Japanese macaques. *Behaviour, 144*, 1193-1215.
- Newell, K. M., Liu, Y. T., & Mayer-Kress, G. (2001). Time scales in motor learning and development. *Psychological Review, 108*, 57-82.
- Nishimura, Y., Onoe, H., Morichika, Y., Perfiliev, S., Tsukada, H., & Isa, T. (2007). Time-dependent central compensatory mechanisms of finger dexterity after spinal cord injury. *Science, 318*, 1150-1155.
- Nudo, R. J., Wise, B. M., SiFuentes, F., & Milliken, G. W. (1996). Neural substrates for the effects of rehabilitative training on motor recovery after ischemic infarct. *Science, 272*, 1791-1794.
- Nudo, R. J., & Milliken, G. W. (1996). Reorganization of movement representations in primary motor cortex following focal ischemic infarcts in adult squirrel monkeys. *Journal of Neurophysiology, 75*, 2144-2149.
- Ogden, R., & Franz, S. I. (1917). On cerebral motor control: the recovery from experimentally produced hemiplegia. *Psychobiology, 1*, 33-49.
- Ogihara, N., & Oishi, M. (2012). Muscle dimensions in the Japanese macaque hand. *Primates, 53*, 391-396.
- Olivier, E., Edgley, S. A., Armand, J., & Lemon, R. N. (1997). An electrophysiological study of the postnatal development of the corticospinal system in the macaque monkey. *Journal of Neuroscience, 17*, 267-276.

- Padberg, J., Franca, J. G., Cooke, D. F., Soares, J. G., Rosa, M. G., Fiorani, M. Jr., . . . Krubitzer, L. (2007). Parallel evolution of cortical areas involved in skilled hand use. *Journal of Neuroscience*, *27*, 10106-10115.
- Passingham, R. E., Perry, V. H., & Wilkinson, F. (1983). The long-term effects of removal of sensorimotor cortex in infant and adult rhesus monkeys. *Brain*, *106* (Pt 3), 675-705.
- Pizzimenti, M. A., Darling, W. G., Rotella, D. L., McNeal, D. W., Herrick, J. L., Ge, J., . . . Morecraft, R. J. (2007). Measurement of reaching kinematics and prehensile dexterity in nonhuman primates. *Journal of Neurophysiology*, *98*, 1015-1029.
- Plautz, E. J., Barbay, S., Frost, S. B., Friel, K. M., Dancause, N., Zoubina, E. V., . . . Nudo, R. J. (2003). Post-infarct cortical plasticity and behavioral recovery using concurrent cortical stimulation and rehabilitative training: a feasibility study in primates. *Neurological Research*, *25*, 801-810.
- Pouydebat, E., Laurin, M., Gorce, P., & Bels, V. (2008). Evolution of grasping among anthropoids. *Journal of Evolutionary Biology*, *21*, 1732-1743.
- Pouydebat, E., Gorce, P., Coppens, Y., & Bels, V. (2009). Biomechanical study of grasping according to the volume of the object: human versus non-human primates. *Journal of Biomechanisms*, *42*, 266-272.
- Pouydebat, E., Reghem, E., Borel, A., & Gorce, P. (2011). Diversity of grip in adults and young humans and chimpanzees (*Pan troglodytes*). *Behavioural Brain Research*, *218*, 21-28.
- Rathelot, J. A., & Strick, P. L. (2009). Subdivisions of primary motor cortex based on cortico-motoneuronal cells. *Proceedings of the National Academy of Sciences of the United States of America*, *106*, 918-923.
- Roitberg, B., Khan, N., Tuccar, E., Kompoliti, K., Chu, Y., Alperin, N., . . . Emborg, M. E. (2003). Chronic ischemic stroke model in cynomolgus monkeys: behavioral, neuroimaging and anatomical study. *Neurological Research*, *25*, 68-78.
- Rosenblatt, N. J., Hurt, C. P., Latash, M. L., & Grabiner, M. D. (2014) An apparent contradiction: increasing variability to achieve greater precision? *Experimental Brain Research*, *232*, 403-413.
- Rouiller, E. M., Moret, V., Tanné, J., & Boussaoud, D. (1996). Evidence for direct connections between the hand region of the supplementary motor area and cervical motoneurons in the macaque monkey. *European Journal of Neuroscience*, *8*, 1055-1059.
- Rouiller, E. M., Yu, X. H., Moret, V., Tempini, A., Wiesendanger, M., & Liang, F. (1998). Dexterity in adult monkeys following early lesion of the motor cortical hand area: the role of cortex adjacent to the lesion. *European Journal of Neuroscience*, *10*, 729-740.
- Sacrey, L. A., Alaverdashvili, M., & Whishaw, I. Q. (2009). Similar hand shaping in reaching-for-food (skilled reaching) in rats and humans provides evidence of homology in release, collection, and manipulation movements. *Behavioural Brain Research*, *204*, 153-161.
- Sasaki, K., & Gemba, H. (1984). Compensatory motor function of the somatosensory cortex for dysfunction of the motor cortex following cerebellar hemispherectomy in the monkey. *Experimental Brain Research*, *56*, 532-538.
- Sasaki, S., Isa, T., Pettersson, L. G., Alstermark, B., Naito, K., Yoshimura, K., . . . Ohki, Y. (2004). Dexterous finger movements in primate without monosynaptic corticomotoneuronal excitation. *Journal of Neurophysiology*, *92*, 3142-3147.
- Schieber, M. H. (2001). Constraints on somatotopic organization in the primary motor cortex. *Journal of Neurophysiology*, *86*, 2125-2143.
- Schmidlin, E., Wannier, T., Bloch, J., & Rouiller, E. M. (2004). Progressive plastic changes in the hand representation of the primary motor cortex parallel incomplete recovery from a unilateral section of the corticospinal tract at cervical level in monkeys. *Brain Research*, *1017*, 172-183.
- Schmidlin, E., Wannier, T., Bloch, J., Belhaj-Saïf, A., Wyss, A., & Rouiller, E. M. (2005). Reduction of the hand representation in the ipsilateral primary motor cortex following unilateral section of the corticospinal tract at cervical level in monkeys. *BMC Neuroscience*, *6*:56.

- Schmidlin, E., Kaeser, M., Gindrat, A. D., Savidan, J., Chatagny, P., Badoud, S., . . . Rouiller, E. M. (2011). Behavioral assessment of manual dexterity in non-human primates. *Journal of Visualized Experiments*, 57: 3258.
- Schmidt, R. A., & Lee, T. D. (2011). Individual differences and capabilities. In *Motor control and learning: a behavioral emphasis* (5<sup>th</sup> ed., pp. 297-324). Champaign, IL: Human Kinetics.
- Schmidt, R. A., & Lee, T. D. (2011). Motor learning concepts and research methods. In *Motor control and learning: a behavioral emphasis* (5<sup>th</sup> ed., pp. 327-346). Champaign, IL: Human Kinetics.
- Schorer, J., Baker, J., Fath, F., & Jaitner, T. (2007). Identification of interindividual and intraindividual movement patterns in handball players of varying expertise levels. *Journal of Motor Behavior*, 39, 409-421.
- Serrien, D. J., & Wiesendanger, M. (1999). Grip-load force coordination in cerebellar patients. *Experimental Brain Research*, 128, 76-80.
- Serrien, D. J., Kaluzny, P., Wicki, U., & Wiesendanger, M. (1999). Grip force adjustments induced by predictable load perturbations during a manipulative task. *Experimental Brain Research*, 124, 100-106.
- Spinozzi, G., Castorina, M. G., & Truppa, V. (1998). Hand preferences in unimanual and coordinated-bimanual tasks by tufted capuchin monkeys (*Cebus apella*). *Journal of Comparative Psychology*, 112, 183-191.
- Spinozzi, G., Truppa, V., & Lagana, T. (2004). Grasping behavior in tufted capuchin monkeys (*Cebus apella*): grip types and manual laterality for picking up a small food item. *American Journal of Physical Anthropology*, 125, 30-41.
- Spinozzi, G., Lagana, T., & Truppa, V. (2007). Hand use by tufted capuchins (*Cebus apella*) to extract a small food item from a tube: digit movements, hand preference, and performance. *American Journal of Primatology*, 69, 336-352.
- Stelmach, G. E. (1968). Distribution of practice in individual differences and intra-variability. *Perceptual and Motor Skills*, 26, 727-730.
- Sugiyama, Y., Higo, N., Yoshino-Saito, K., Murata, Y., Nishimura, Y., Oishi, T., & Isa, T. (2013). Effects of early versus late rehabilitative training on manual dexterity after corticospinal tract lesion in macaque monkeys. *Journal of Neurophysiology*, 109, 2853-2865.
- Tomassini, V., Jbabdi, S., Kincses, Z. T., Bosnell, R., Douaud, G., Pozzilli, C., . . . Johansen-Berg, H. (2011). Structural and functional bases for individual differences in motor learning. *Human Brain Mapping*, 32, 494-508.
- Travis, A. M. (1955). Neurological deficiencies after ablation of the precentral motor area in *Macaca mulatta*. *Brain*, 78, 155-173.
- Van Schaik, C. P., Deaner, R. O., & Merrill, M. Y. (1999). The conditions for tool use in primates: implications for the evolution of material culture. *Journal of Human Evolution*, 36, 719-741.
- Wannier, T., Schmidlin, E., Bloch, J., & Rouiller, E. M. (2005). A unilateral section of the corticospinal tract at cervical level in primate does not lead to measurable cell loss in motor cortex. *Journal of Neurotrauma*, 22, 703-717.
- Whishaw, I. Q., Whishaw, P., & Gorny, B. (2008). The structure of skilled forelimb reaching in the rat: a movement rating scale. *Journal of Visualized Experiments*, 18: 816.
- Whishaw, I. Q., Travis, S. G., Koppe, S. W., Sacrey, L. A., Gholamrezaei, G., & Gorny, B. (2010). Hand shaping in the rat: conserved release and collection vs. flexible manipulation in overground walking, ladder rung walking, cylinder exploration, and skilled reaching. *Behavioural Brain Research*, 206, 21-31.
- Wiesendanger, M. (1999). Manual dexterity and the making of tools - an introduction from an evolutionary perspective. *Experimental Brain Research*, 128, 1-5.
- Wong, Y. J., & Whishaw, I. Q. (2004). Precision grasps of children and young and old adults: individual differences in digit contact strategy, purchase pattern, and digit posture. *Behavioural Brain Research*, 154, 113-123.

- Wu, H. G., Miyamoto, Y. R., Gonzalez Castro, L. N., Ölveczky, B. P., & Smith, M. A. (2014) Temporal structure of motor variability is dynamically regulated and predicts motor learning ability. *Nature Neuroscience*, *17*, 312-321.
- Wyss, A. F., Hamadjida, A., Savidan, J., Liu, Y., Bashir, S., Mir, A., . . . Belhaj-Saif, A. (2013). Long-term motor cortical map changes following unilateral lesion of the hand representation in the motor cortex in macaque monkeys showing functional recovery of hand functions. *Restorative Neurology and Neuroscience*, *31*, 733-760.
- Zhao, D., Hopkins, W. D., & Li, B. (2012). Handedness in nature: first evidence on manual laterality on bimanual coordinated tube task in wild primates. *American Journal of Physical Anthropology*, *148*, 36-44.

**Financial Support:** Swiss National Science Foundation, Grants No 31-61857.00, 310000-110005, 31003A-132465, 310030B-149643 (EMR), the National Centre of Competence in Research (NCCR) on *Neural plasticity and repair*; Novartis Foundation; The Christopher Reeves Foundation (Springfield, NJ, USA); The Swiss Primate Competence Centre for Research (SPCCR): <http://www.unifr.ch/neuro/rouiller/SPCCR>; Consortium Grant Sinergia CRSI33-125408.

**Conflict of interest:** none.

**Submitted:** August 31<sup>st</sup>, 2013  
**Resubmitted:** December 14<sup>th</sup>, 2013  
**Accepted:** January 22<sup>nd</sup>, 2014



## ***Annex 5***

### ***Distinction between hand dominance and hand preference in primates: a behavioral investigation of manual dexterity in nonhuman primates (macaques) and human subjects.***

Pauline Chatagny\*, Simon Badoud\*, Mélanie Kaeser, Anne-Dominique Gindrat, Julie Savidan, Michela Fregosi, Véronique Moret, Christine Roulin,  
Eric Schmidlin & Eric M. Rouiller

Published in Brain and Behavior (2013)





## Distinction between hand dominance and hand preference in primates: a behavioral investigation of manual dexterity in nonhuman primates (macaques) and human subjects

Pauline Chatagny\*, Simon Badoud\*, Mélanie Kaeser, Anne-Dominique Gindrat, Julie Savidan, Michela Fregosi, Véronique Moret, Christine Roulin, Eric Schmidlin & Eric M. Rouiller

Unit of Physiology, Department of Medicine, Faculty of Sciences and Fribourg Center for Cognition, University of Fribourg, Chemin du Musée 5, CH-1700 Fribourg, Switzerland

### Keywords

Bimanual coordination, handedness, intermanual difference, motor performance, precision grip

### Correspondence

Eric M. Rouiller, Unit of Physiology, Department of Medicine, Faculty of Sciences and Fribourg Center for Cognition, University of Fribourg, Chemin du Musée 5, CH-1700 Fribourg, Switzerland.  
Tel: +41 26 300 86 09; Fax: +41 26 300 96 75;  
E-mail: eric.rouiller@unifr.ch

### Funding Information

This study was supported by Swiss National Science Foundation, grants No. 31-61857.00, 310000-110005, 31003A-132465, and FZFS-0\_144990 (E. M. R.), 31-121646 (E. S.); the Novartis Foundation; the National Centre of Competence in Research (NCCR) on "Neural plasticity and repair" and the Christopher Reeves Foundation (Springfield, NJ).

Received: 2 January 2013; Revised: 29 June 2013; Accepted: 30 June 2013

doi: 10.1002/brb3.160

\*Equal first authorship.

## Introduction

How is handedness defined? Commonly, handedness means hand preference. For most people, the preferred hand is the hand which is most efficient to perform specific manual dexterity tasks (e.g., writing, manipulating objects or tools, etc.). In the present study, in line with a previously proposed concept (e.g., Hopkins et al. 1992; Triggs et al. 2000), we propose to emphasize the distinction between two hand attributes: hand preference and hand dominance.

## Abstract

**Background:** The present study aimed to determine and confront hand preference (hand chosen in priority to perform a manual dexterity task) and hand dominance (hand with best motor performance) in eight macaques (*Macaca fascicularis*) and in 20 human subjects (10 left-handers and 10 right-handers). **Methods:** Four manual dexterity tests have been executed by the monkeys, over several weeks during learning and stable performance phases (in controlled body position): the modified Brinkman board, the reach and grasp drawer, the tube and the bimanual board tasks. Three behavioral tests, adapted versions from the monkeys tasks (modified Brinkman board, tube and bimanual board tasks), as well as a handedness questionnaire, have been conducted in human subjects. **Results:** In monkeys, there was a large disparity across individuals and motor tasks. For hand dominance, two monkeys were rather right lateralized, three monkeys rather left lateralized, whereas in three monkeys, the different parameters measured were not consistent. For hand preference, none of the eight monkeys exhibited a homogeneous lateralization across the four motor tasks. *Macaca fascicularis* do not exhibit a clear hand preference. Furthermore, hand preference often changed with task repetition, both during training and plateau phases. For human subjects, the hand preference mostly followed the self-assessment of lateralization by the subjects and the questionnaire (in the latter, right-handers were more lateralized than left-handers), except a few discrepancies based on the tube task. There was no hand dominance in seven right-handers (the other three performed better with the right hand) and in four left-handers. Five left-handers showed left-hand dominance, whereas surprisingly, one left-hander performed better with the right hand. In the modified Brinkman board task, females performed better than males, right-handers better than left-handers. **Conclusions:** The present study argues for a distinction between hand preference and hand dominance, especially in macaque monkeys.

The hand of preference is defined as the hand with which subjects prefer to work on a specific task, instinctively and without concern whether this hand is actually the most efficient one. In bimanual tasks for instance (e.g., tapping a nail with a hammer, knitting, eating with a fork, and a knife, etc.), the preferred hand is the hand which executes the most complex action or the manipulative role, whereas the nonpreferred hand acts mainly as postural support. In the above mentioned bimanual tasks, they need to be learned, whereas other bimanual tasks are

more instinctive and they are also observed in nonhuman primates (e.g., peeling a fruit, cracking a nut with a stone, etc.). In contrast to hand preference, hand dominance refers to the hand which shows the best efficiency to perform a particular unimanual action (Serrien *et al.* 2006), thus reflecting an intermanual difference of motor performance. The general aim of the present study was to assess separately hand preference and hand dominance in eight adult long-tailed macaque monkeys (*Macaca fascicularis*) and in 20 young adult human subjects.

Population-level right-handedness (preference for the right hand) was considered for a long time as a feature of human being (Raymond *et al.* 1996). During the last 20 years, several studies demonstrated that handedness for specific manual tasks is also present in nonhuman primates, from prosimians to great apes (e.g., Masataka 1989; Ward *et al.* 1990, 1993; Fagot and Vauclair 1991; Spinozzi *et al.* 1998; Lacreuse *et al.* 1999; Hopkins *et al.* 2011). Whereas 90% of humans are right-handed (Coren and Porac 1977; Raymond and Pontier 2004), the percentage and the direction of the lateralization vary among the nonhuman primates (see e.g., Papademetriou *et al.* 2005; mainly for reaching tasks). Concerning the great apes, a recent study by Hopkins *et al.* (2011) showed population right-handedness, except for Orangutans, which tend to use preferentially the left hand. These results are consistent with other studies (Lacreuse *et al.* 1999; Wesley *et al.* 2001; Hopkins *et al.* 2002, 2003, 2004, 2005; Sherwood *et al.* 2007). Baboons were also found to be right-handed at population level (Fagot and Vauclair 1988; Vauclair *et al.* 2005). However, some divergent observations were reported (Pouydebat *et al.* 2010), concluding to the difficulty to establish a stable handedness among Gorillas, based on different behavioral tasks. In Old World monkeys, handedness seems to be less consistent among the family (Westergaard *et al.* 1997, 2001a,b), as it appears to depend on the species, especially in Macaques. Although some macaques, such as *Macaca mulatta*, exhibited population-level left-handedness when they performed a specific task (also *Macaca fuscata*, see Murata *et al.* 2008), other species like *M. fascicularis* did not exhibit any manual bias at the population-level for the same tasks (tube task, reaching to food morsel; Westergaard *et al.* 1997, 2001a,b; see also Lehman 1980b). The above data for *M. mulatta* are not consistent with previous observations derived from food reaching tests (Lehman 1978a), which showed roughly equal numbers of right- and left-handed individuals. Furthermore, the latter author and others reported that handedness was accentuated with monkeys' age, as well as with task repetition (e.g., Lehman 1978a,b, 1980a,b; Westergaard and Suomi 1996; Westergaard and Lussier 1999; Zhao *et al.* 2012). Similarly, Hopkins (2004) found

a less prominent handedness among Old and New World monkeys in comparison to the great apes. It is, however, interesting to highlight that, for some investigators (e.g., Lehman 1980a, 1989; Hopkins *et al.* 1989; Fagot and Vauclair 1991; Uomini 2009), these disparate results may depend on the task used to determine handedness (see also Spinozzi *et al.* 1998, 2007). Indeed, these authors showed that the complexity of the task plays an important role. A high-level manual activity involves, most of the time, a manual bias at the population-level, whereas a simple and low-level task does not. A typical example of high-level manual performance is the precision grip (opposition of thumb and usually index finger to grasp an object), requiring the cooperation of several muscles of hand and arm, tendons, ligaments, and the stabilization of the upper limb to ensure a better effectiveness (e.g., Lemon 1993, 2008; Porter and Lemon 1993). Bimanual tasks are considered as high-level ones, involving a coordination of different limbs and movements. As demonstrated in squirrel monkeys, hand preference is correlated to an asymmetry in functional topography of motor cortex between the two hemispheres, with a greater distal forelimb representation in the dominant hemisphere, opposite the preferred hand (Nudo *et al.* 1992). Asymmetries in the primary motor cortex related to handedness was reported in great apes (Hopkins and Pilcher 2001; Hopkins *et al.* 2002, 2010; Hopkins and Cantalupo 2004; Dadda *et al.* 2006; Sherwood *et al.* 2007) and in humans (e.g., Dassonville *et al.* 1997).

Hand preference and hand dominance were each determined based on three adapted manual tasks, which belong to high-level manual activities, for both human subjects and monkeys (*M. fascicularis*). Two tests are bimanual coordinated tasks: the bimanual Brinkman board task (Mark and Sperry 1968) and the tube task (Hopkins 1995), whereas the third test is the modified Brinkman board task (original test: Brinkman and Kuypers 1973; see also Brinkman 1984), performed either unimanually or with both hands at the same time. Monkeys had to perform an additional task, the reach and grasp drawer task, whereas humans had to answer a handedness questionnaire, which allowed us to confirm the self-assessment of each subject and, then, to compare the self-assessment with the results derived from the manual dexterity tests. More specifically, the aim of the study was to test the hypothesis that, in *M. fascicularis*, hand preference is variable across tasks and individuals, the dominant hand does not systematically correspond to the preferred hand, whereas human subjects exhibit more systematic lateralization (hand preference) and the preferred hand generally corresponds to the most dexterous hand (dominant hand).

## Material and Methods

### Nonhuman primate subjects

The experiments were conducted on eight adult female monkeys (*M. fascicularis*), aged between 6 and 7 years old at the beginning of the tests (weight: 3–3.9 kg) and housed in 45 m<sup>3</sup> rooms with four other animals. The monkeys were neither food nor water deprived (see e.g., Kaeser et al. 2010; Schmidlin et al. 2011). None of the animals had executed the different manual dexterity tasks before, so they were totally naïve. The experimental protocol has been approved by the local ethical committee on animal experimentation and it was in accordance with the *Guidelines for the Care and Use of Laboratory Animals* (ISBN 0-309-05377-3; 1996), as well as authorized by local (Canton of Fribourg) and federal (Swiss) veterinary authorities. The present experiments were covered by the official authorization numbers FR 192/07E, FR 206/08, FR 17/09, FR 18/10, FR 22010. The experimental procedures were designed to minimize pain and suffering for the animals. In the part of the present study on monkeys, the protocol was restricted to behavioral assessment, without any surgical or pharmacological intervention. The macaque monkeys originate initially from an officially recognized breeding center in China and were imported via a quarantine center in Europe (Harlan, Milano, Italy), where they stayed during a few months within a large group of a couple of dozen animals from the same origin. After arrival in our animal facility, the animals were habituated during 1–2 months to the new environment, before starting the habituation procedure (2–3 months duration) aimed at transferring the monkey on a free-will basis to the primate chair (see Schmidlin et al. 2011). The present behavioral experiments were then initiated when the monkeys were comfortable with the primate chair.

During each behavioral test, the monkey sat in a primate chair (see Schmidlin et al. 2011), made of Plexiglas<sup>®</sup> (Transparent PVC, Notz Plastik AG, Biel, Switzerland), with an adjustable opening on top allowing free head movements although the monkey is restrained. The primate chair also comprises two independent sliding doors at the front, allowing execution of manual dexterity tasks with both hands, separately or simultaneously (Schmidlin et al. 2011). Each experimental session was recorded with one to three digital video cameras, depending on the task (drawer, tube, and bimanual board tasks with one camera; modified Brinkman board task with three cameras; Schmidlin et al. 2011). The duration of a typical daily behavioral session was about 60 min and the experiments were conducted with background music to cover possible disturbing, external noise. At the end of the session, the animals received their daily ration of food, composed of

cereals, fruits, and vegetables, in addition to the rewards (food pellets) received during the tests.

### Human subjects

The human subjects were 20 persons (students) aged between 18 and 30 years old. The human experiments were conducted in the context of practical courses for students at the University of Fribourg and the subjects gave their full consent to the experimental protocol. They agreed that the data may be used anonymously for the present study. The human subjects first declared themselves either as left- or as right-handers and it corresponded to the hand they used to write. Based on this initial self-declaration, there were ten left-handers (six men and four women) and ten right-handers (four men and six women). The size of each of these two groups ( $n = 10$ ) was chosen as to approximately match the group size of monkeys ( $n = 8$ ). Given the human population bias for right-hand preference (about 90%), self-declared left-handers were deliberately recruited, thanks to a large pool of students available on the campus. It is expected that the self-declared left-handers are less lateralized than the self-declared right-handers.

Each human subject was enrolled in a single behavioral session (lasting about 60–90 min) and he/she executed three manual dexterity tasks, before responding to the handedness questionnaire at the end of the session. The set-ups for the three manual dexterity tasks were positioned on a table and the behavioral session was recorded with a digital video camera. The subjects began with the modified Brinkman board task, followed by the bimanual board task, and finally, the tube task. Before the beginning of the tests, the subjects sat on a chair in the middle and in front of the experimental table. They had to adjust the height of the chair to feel comfortable.

### Behavioral tasks

The assessment of handedness was based on a palette of behavioral manual dexterity tasks, in which macaque monkeys ( $n = 8$ ) and human subjects ( $n = 20$ ) were enrolled. For both monkeys and human subjects, typical video sequences illustrating the various behavioral tasks described below can be visualized on the following website: <http://www.unifr.ch/neuro/rouiller/research/PM/pm1.html>.

### Modified Brinkman board task

The modified Brinkman board and its different adapted versions from the original test of Brinkman and Kuypers (1973) were used routinely for behavioral and motor control studies in macaques (Brinkman 1984; Rouiller

et al. 1998; Liu and Rouiller 1999; Freund et al. 2009; Kaeser et al. 2010, 2011, 2013; Schmidlin et al. 2011). The modified Brinkman board for monkeys (Fig. 1A, left panel) is made of a rectangular board of Perspex® with 50 rounded rectangular slots: 25 slots are oriented horizontally and 25 vertically. Each slot measures 6 mm deep, 14 mm long, and 7 mm wide. The board itself measures 22 cm length, 12 cm wide, and 1.2 cm thick. At the beginning of the test, each slot is filled with a banana or sugar flavored pellet (diameter 4 mm). The size of slots permits the monkeys to grasp the pellets only by performing the precision grip, generally using the thumb and the index finger (or rarely another finger, with a flexion of the distal phalanx). Retrieval from the horizontal slots is more difficult than from the vertical ones, because it involves also a rotation of the wrist, either a radial deviation or an ulnar deviation, depending on the position of the corresponding slot on the board (Freund et al. 2009). The board was positioned in front of the monkey with 40° of inclination from horizontal. During each daily session, the animal has used firstly both hands, then each individual hand successively by alternating daily the hand used first. The daily protocol for this task thus comprises three consecutive tests, with retrieval of 50 pellets in each,

lasting overall about 10 min, including the time interval to refill the modified Brinkman board with pellets in between the three tests. With respect to the board, the monkey was placed in a middle position (when performing the task with both hand simultaneously), or slightly at the left, or at the right, when using only the right or the left hand, respectively, in such a manner that the hand performing the task is aligned to the set-up. Video sequences illustrating this task can be visualized on the website: <http://www.unifr.ch/neuro/rouiller/research/PM/pm1.html> (video sequences 1–3) or in a recent visualized experimental report (Schmidlin et al. 2011).

The Brinkman board model, adapted for human subjects (Fig. 1A, right panel), is made of a wooden board of 58 cm long and 28.5 cm wide and it comprises 50 rounded rectangular slots of 4.3 cm long, 2.2 cm wide, and 1.8 cm deep (25 oriented vertically and 25 oriented horizontally). It is tilted with a 30-degree angle from horizontal. Before the beginning of a session, each slot is filled with a bolt (external diameter: 1.8 cm, internal diameter: 1 cm). The bolts replace the food pellets used for the same tests on monkeys. The slots were designed in a manner that subjects have to use the precision grip to retrieve the bolts, and their spatial arrangement is identical to that of the modified Brinkman

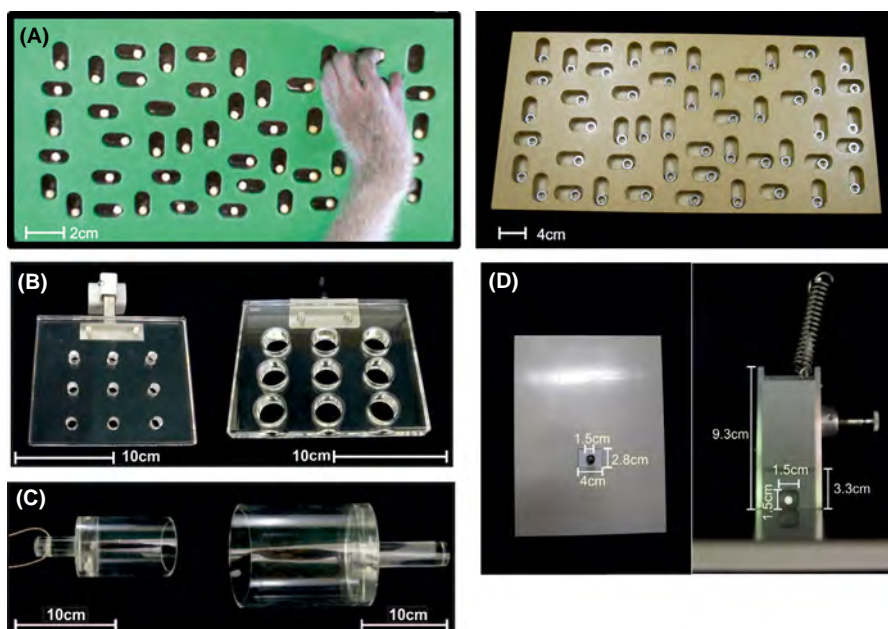


**Figure 1.** Pictures illustrate the experimental set-ups used in the different behavioral tasks for monkeys and for human subjects. In panel (A), the modified Brinkman board used for monkeys is shown on the left, with each slots filled with a banana pellet, whereas its version adapted for human subjects is shown on the right with each slot filled with a bolt. See text for dimensions of the board and slots. Panel (B) shows the bimanual Brinkman board used for monkeys (on the left) and for humans (on the right). Similarly, in panel (C), the tube used for monkeys is shown on the left and the version adapted for humans on the right. See text for dimensions of the boards, slots, and tubes. In panel (D), the bimanual reach and grasp drawer set-up (used for monkeys only) is shown in a front view (left picture) and from top (right picture). In the top view, the slot in the drawer is clearly visible (with one white pellet inside), as well as the spring at the back of the drawer, imposing to hold the drawer open with one hand while grasping the pellet with the other hand.



board used for monkeys. In a single behavioral session, the human subjects had to execute the grasping of the 50 bolts as fast as possible, taking one bolt at a time, and putting it into a plastic box located in front of the board in a middle position. The human subjects were not allowed to throw the bolt into the box. These rules contributed normalizing the test. The subjects performed the task 20 times, using alternatively 10 times the right hand and 10 times the left hand (right, left, right, etc.). The experimenter determined with which hand the subject had to begin (see <http://www.unifr.ch/neuro/rouiller/research/PM/pm1.html> [video sequences 4–5]).

### Bimanual Brinkman board task

This task was adapted from the bimanual coordinated task of Mark and Sperry (1968). Our bimanual board is made of transparent acrylic glass (PMMA or Plexiglas<sup>®</sup>); Fig. 1B). The model for monkeys (Fig. 1B, left panel) measures 15.8 cm long, 13.1 cm large, and has a thickness of 2 cm. It comprises nine holes. Each hole has an upper diameter of 9.5 mm and a lower diameter of 7 mm and contains a sticky reward, like sultana or a little piece of apple. The board is fixed with an inclination of 20–30° from horizontal. The primate chair was placed in the front of the board and the two sliding doors were opened to allow access with both hands simultaneously. The monkeys had to retrieve the reward using both hands at the same time and following one or the other of two possible strategies (see below: analysis of data). One daily session included three to five repetitions of the whole board, with retrieval of each reward. Each hole represented an individual trial (see <http://www.unifr.ch/neuro/rouiller/research/PM/pm1.html> [video sequence 6]).

The model of the bimanual board adapted for human subjects (Fig. 1B, right panel) is a transparent acrylic glass board of 16 cm long, 13 cm wide, 2 cm thick, and comprising nine holes (diameter of 2.2 cm). The board is fixed with 30° of inclination from horizontal. Before the test started, each hole was filled with a pellet in modeling clay. Using both hands, the human subjects had to take only one pellet at a time and to put it into a plastic box placed in the front of the board. In one session, the subject had to empty the board 20 times. Each hole represented an individual trial (see <http://www.unifr.ch/neuro/rouiller/research/PM/pm1.html> [video sequence 7]).

### The tube task

This bimanual task was inspired by the tube task of Hopkins (1995), used to determine handedness in Chimpanzees and later in Old World monkeys (Zhao *et al.* 2012). Our tube, in transparent acrylic glass (PPMA

or Plexiglas<sup>®</sup>), was adapted to macaques with the following dimensions: the handle measures 4 cm long and 2 cm diameter, the tube itself is 9 cm long from the outside and 7 cm deep from the inside, with an external diameter of 6 cm and an internal diameter of 5 cm. At the bottom of the tube, there is a slot of 0.5 cm in diameter and 0.7 cm deep (Fig. 1C; left panel). The slot was filled with a sticky reward like sultana or little pieces of apple. The tube was attached to a rope by the handle and hung, in such a way that it was placed in front of the primate chair, aligned with the central bar between the sliding doors. The basis of the tube was positioned at the level as the basis of the sliding doors. The test was performed with the two sliding doors open and the animal had to hold the suspended tube with one hand while reaching the reward in the tube with the other hand and bring it to the mouth. A daily session comprised 10–20 trials (see <http://www.unifr.ch/neuro/rouiller/research/PM/pm1.html> [video sequence 8]).

The model of the tube adapted for human subjects is also made of acrylic glass tube (PPMA or Plexiglas<sup>®</sup>) with the following dimensions (Fig. 1C, right panel): the tube itself measures 14.7 cm long, 12.8 cm deep, with an external diameter of 12 cm and an internal diameter of 11 cm. The handle is 9.5 cm long and has a diameter of 3 cm. The slot positioned at the bottom of the tube is 2.2 cm in diameter and 0.9 cm deep. The reward was a candy (*Yupi strawberry kiss* or *Yupi MarshMallow*). A second tube was available for human subjects with smaller hands: the dimensions are the same, except the external diameter of 9 cm and the internal diameter of 8 cm. The tube was positioned vertically on the table, with the handle upwards. Starting with the hands placed on the table on each side of the tube, the human subjects had to collect the reward from the tube using both hands. They had the possibility to eat the reward or to give it to the experimenter. Then, the human subjects had to put the tube back on the table at its initial location. The task was performed 20 times to complete the session. One trial was achieved when the human subjects grabbed the tube with one hand while, simultaneously, they took the reward with the other hand (see <http://www.unifr.ch/neuro/rouiller/research/PM/pm1.html> [video sequence 9]).

### Reach and grasp drawer task

This bimanual task was used for the monkeys only and it is a simplified version of the set-up previously described (Kazennikov *et al.* 1994; Kermadi *et al.* 1998, 2000; Schmidlin *et al.* 2011). The primate chair was placed in front of the drawer with both sliding doors opened, so that the monkey used both hands. Because of a spring mechanism, once open, the drawer had to be maintained with one hand to avoid that it closed back, while the monkey

used the other hand to grasp the pellet, which was initially placed in a slot dig inside the drawer. The dimensions of the object are indicated on the Figure 1D. During one session, the animal executed about five to 15 trials. One trial was achieved when the monkey opened the drawer with one hand, kept it open, and grasped the pellet with the other hand (see <http://www.unifr.ch/neuro/rouiller/research/PM/pm1.html> [video sequence 10]).

### Handedness questionnaire

At the end of the manual dexterity tasks, the human subjects were asked to answer a handedness questionnaire, elaborated by MacManus (2009). It was chosen because it fills several pertinent criteria to assess handedness in human subjects (Oldfield 1971). The questions dealt with actions of daily life such as: with which hand do you write, do you hold a potato while you are peeling it, do you throw a ball, etc.

### Analysis of data

The data of the behavioral tasks were analyzed manually from the recorded video sequences. The software VirtualDubMpeg2<sup>®</sup> (Developer Avery Lee, free software, [www.virtualdub.org](http://www.virtualdub.org)) allowed visualizing the video sequences frame by frame, corresponding to a time resolution of 40 msec (acquisition at 25 frames per second). The data were processed first in Excel<sup>®</sup> worksheets, before they were transferred to Sigmaplot<sup>®</sup>/Sigmaplot<sup>®</sup> (Systat Software Inc., [www.sigmaplot.com](http://www.sigmaplot.com)) and SPSS<sup>®</sup> (SPSS Inc., Chicago, IL) allowing more elaborated graphic representation and statistical analysis.

The hand dominance was determined based on a single task, the modified Brinkman board task performed with one hand imposed at a time. Two types of data were analyzed for the monkeys (Schmidlin *et al.* 2011). (i) The score, defined as the number of pellets correctly retrieved during the first 30 sec; (ii) The contact time (CT), defined as the time interval between the first contact of a finger (most often the index finger) with the pellet and the moment when the fingers left the slot with the reward. The CT is a pertinent parameter in addition to the score, as the latter can sometimes be biased. Indeed, the animal may be disturbed by external noises, or may exhibit a lack of motivation or concentration. In such cases, the monkey may interrupt the test, leading to a distortion of the score. Moreover, the CT truly measures the actual manipulation of the pellets with the fingers. The CT was measured for the first five horizontal and the first five vertical slots in the 20 last daily sessions at plateau, whereas the score was calculated for every daily session. The onset of the plateau was defined, when the learning

curve tended to saturate (as estimated by visual inspection), as the first value in the nearly flat curve of the score that was not exceeded by one of the five following score values. For human subjects, the analysis of hand dominance was based mainly on the score in 30 sec, although the CT was also established for comparison in a sample of subjects.

The hand preference for monkeys was determined based on four tests: the modified Brinkman board task, when the animal was free to use both hands simultaneously, the reach and grasp drawer task, the tube task, and the bimanual Brinkman board task. For human subjects, two tests were considered, the tube task and the bimanual Brinkman board task, as well as the questionnaire indicating their self-assessed hand preference. For the tube task, the preferred hand was defined as the hand used to grasp the reward into the tube, playing the manipulative role, whereas the other hand, holding the tube, played the postural role. The preferred hand (left hand or right hand) was determined for each tube task trial performed by the subject (humans and monkeys), in order to calculate the handedness index (HI) (see below). For the bimanual board task, the subjects (humans and monkeys) used two different strategies to retrieve the reward. In the first one, the hand above the board pushed the reward while the other hand collected it below the board. In the second one, the hand positioned below the board pushed up the reward using one finger (usually the index finger) and the other hand grasped it above the board, performing the precision grip. In the first strategy (adopted in more than 98% of trials in five out of eight monkeys), the preferred hand is the one pushing the reward. Indeed its role is manipulative, whereas the role of the other hand is postural. For the second strategy, the preferred hand is the one retrieving the reward, as its action is more manipulative and more challenging (precision grip), as compared to the role of the other hand (one finger used). Additionally, the board has an inclination, making this movement still more difficult. This second strategy was used in about half of the trials in one monkey (Mk-MI) and it was predominant in two other monkeys (Mk-CA and Mk-AN; 68% and 98%, respectively). For the reach and grasp drawer task (in monkeys only), the preferred hand is the hand grasping the reward (manipulative role) while the other hand, the postural one, holds the drawer.

For these three tasks (bimanual Brinkman board task, reach and grasp drawer task, tube task), we computed the HI (Westergaard *et al.* 1997; Spinozzi *et al.* 1998; Hopkins *et al.* 2004; Schmitt *et al.* 2008), defined as follows: the number of trials the right hand (R) was used as preferred hand minus the number of times the left hand (L) was used as preferred hand, divided by the total number of trials:

$$HI = (R - L) / (R + L)$$

Consequently, a negative HI reflects a left bias whereas a positive HI reflects a right bias. The HI (lateralization) ranges between +1 (strongly right-handed) and -1 (strongly left-handed).

For the modified Brinkman board task, we measured the score in 30 sec when the animal was free to use both hands, and counted the number of pellets grasped with each hand. The hand with the highest score is considered as the preferred hand.

For the questionnaire, we calculated a handedness score by using the criteria of MacManus (2009):

*“Laterality scores (laterality indices):*

*Score all the items as -1 = Always left, -0.5 = Usually left, 0 = Either, +0.5 = Usually right and +1 = Always right. For items 4 (dish), 6 (jar), and 9 (potato) a strong right-hander would answer left. These three items should therefore be reverse scored by changing the sign on the values given previously (i.e., +1 = Always left, etc.). Having done this, then one can obtain the overall laterality score, an average of all 11 items.”*

The score was then transformed into percentage (-100% indicating strongly left-handed and +100%, strongly right-handed).

The statistical analysis was conducted as follows. For the tube task, the reach and grasp drawer task, and the bimanual Brinkman board task, we used a binomial test (SPSS<sup>®</sup>; see Fig. 7). For the scores of the modified Brinkman board task, we used either the paired *t*-test or the Wilcoxon signed-rank test (Sigmastat<sup>®</sup>). Finally, for the CT derived from the modified Brinkman board task, we used either the unpaired *t*-test or the Mann-Whitney *U* test (Sigmastat<sup>®</sup>).

In order to limit the duration of the behavioral session with human subjects to a reasonable extent, the modified Brinkman board task using both hands simultaneously, as well as the reach and grasp drawer task, were not performed with human subjects. These tests, aimed in the monkeys to determine their preferred hand, were considered redundant for human subjects with the handedness questionnaire.

## Results

### Hand dominance: unimanual modified Brinkman board task

#### Monkeys

For monkeys, the hand dominance was determined based on the total score in 30 sec (sum of vertical and horizontal slots in all behavioral sessions) and the CT (measured

for the first five horizontal and the first five vertical slots) in the 20 last recorded sessions of the modified Brinkman board task, at plateau. The performance of one hand was compared to the performance of the other hand, measured in the two consecutive unimanual tests carried out on the same day. The dominant hand is the hand exhibiting a higher score, respectively, a shorter CT, than the opposite hand. For this specific analysis of hand dominance, only the score at plateau was taken into consideration (see Fig. 2A). A typical example of the score data is illustrated for one monkey (Mk-AT: left and right hand for total, vertical and horizontal slots) in Figure 2A, with a vertical dashed line separating the plateau phase from the preceding learning phase.

The top panel of Figure 2B represents the distribution of the scores for the left and the right hands for each monkey at plateau, in the form of box and whiskers plots. In Mk-DI, immediately after the end of the learning phase, there was a transient period with a decrease in the number of grasped pellets (most likely due to a temporary drop of motivation), corresponding to a first plateau. Later, the level of score corresponding to the end of the learning phase reappeared, corresponding to a second plateau, which was considered for the data of the top panel in Figure 2B. Overall, three monkeys exhibited a significant difference of manual dexterity reflected by the score between the hands, namely Mk-AN, Mk-CA, and Mk-MA. The first one performed better with the left hand ( $P = 0.036$ ), whereas Mk-CA and Mk-MA were more dexterous with the right hand ( $P = 0.002$  and  $P < 0.001$ , respectively). Mk-AT, Mk-DI, Mk-LO, Mk-MI, and Mk-TH did not show any significant difference of manual dexterity between hands at plateau, as far as the total score is concerned.

The CT data are plotted in the two bottom panels of Figure 2B. As the combination of movements required to grasp pellets were different for the two slot orientations, the CT was plotted separately for the vertical slots (middle panel in Fig. 2B) and for the horizontal slots (bottom panel in Fig. 2B). Overall, and as expected, the CTs for the vertical slots tended to be shorter (less challenging task) than the CTs for the horizontal slots. It is important to recall that the shorter the CTs, the better the performance. For the vertical slots, the CTs were significantly shorter for the left hand in Mk-AN and Mk-DI ( $P = 0.002$  and  $P = 0.005$ , respectively), whereas they were significantly shorter for the right hand in Mk-CA and Mk-LO ( $P < 0.001$  for both). For the other monkeys (Mk-AT, Mk-MA, Mk-MI, and Mk-TH), there was no significant difference of CTs between the two hands for the vertical slots. Considering the horizontal slots, the CTs were significantly different between the two hands for seven out of the eight monkeys, as only Mk-AN

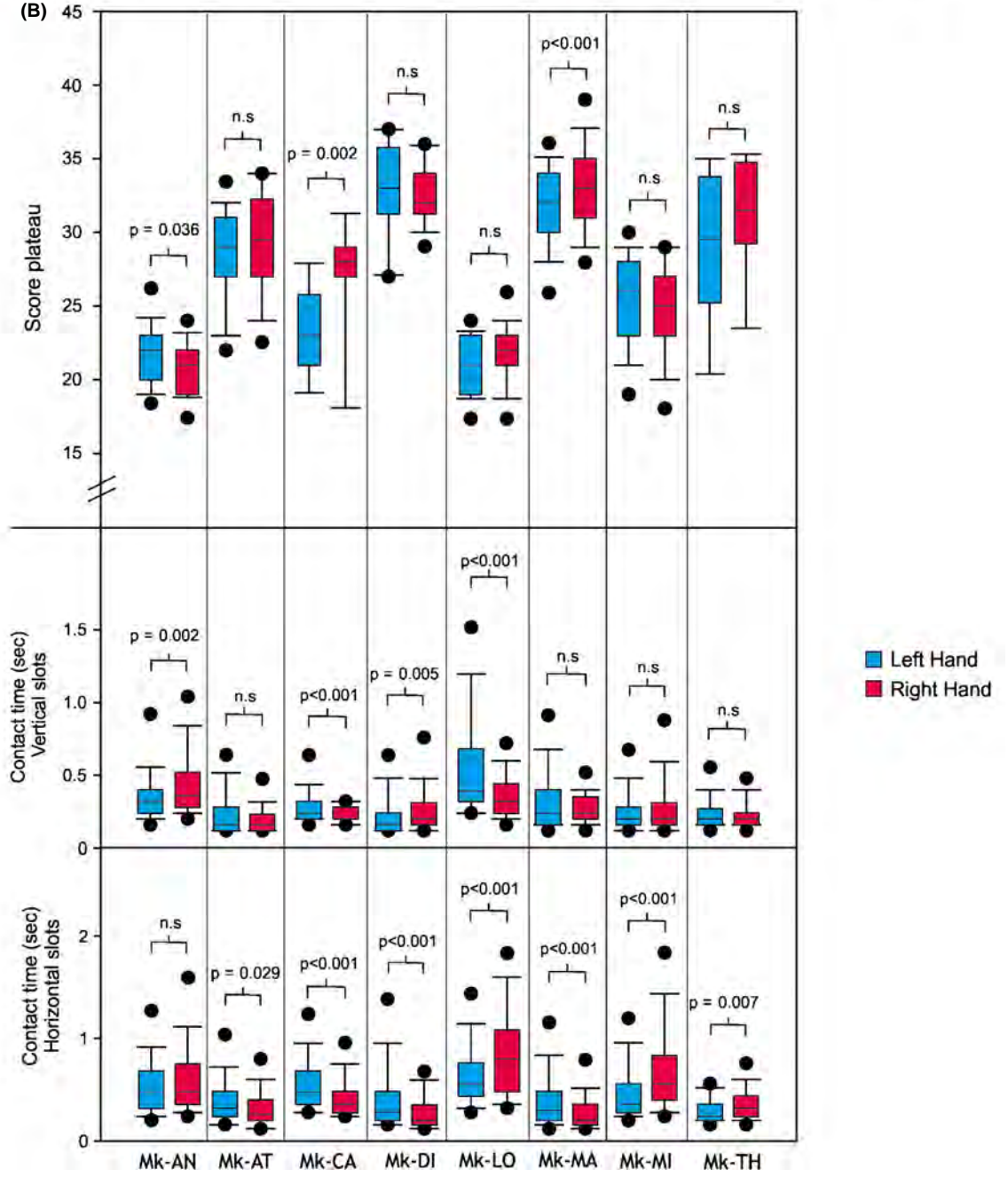
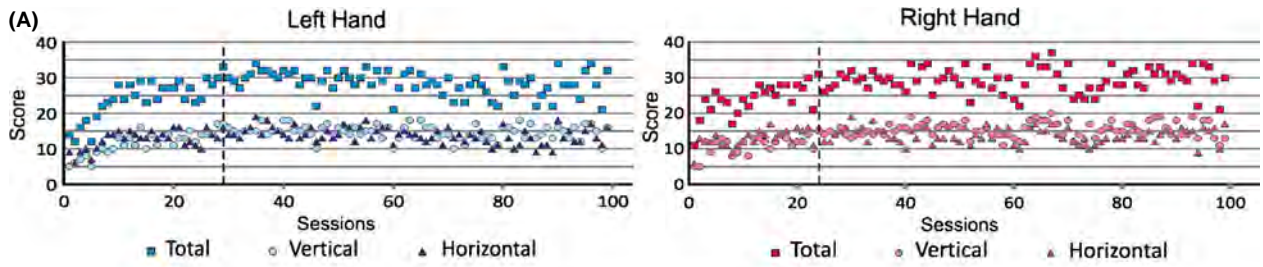




**Figure 2.** Hand dominance analysis for monkeys. An example of scores (Mk-AT) for the left and the right hand when the use of the hand was imposed in the modified Brinkman board task is shown in panel (A). Along the abscissa, the values refer to the consecutive daily session numbers, incremented by one for each individual session, irrespective of the actual date of the session. The regular interval between two consecutive sessions is thus not representative of the number of actual days separating the two sessions. In panel (B), three graphs in the form of box and whiskers plots represent for each monkey the distribution of the total scores (sum of horizontal and vertical slots) at the plateau (top graph), the distribution of contact times (CT, in seconds) for the vertical slots (middle graph) and for the horizontal slots (bottom graph), for the left hand (blue) and the right hand (red). These data concern the results when the use of one hand was imposed in the unimanual modified Brinkman board task. The statistical comparisons between the two hands in each daily session were performed using the paired *t*-test (normality test passed) or the nonparametric Wilcoxon rank signed test (normality test failed) for the score data (paired for the left hand and the right hand in a given daily session). In contrast, the CT data (five values per daily session for each slot orientation) are not paired and therefore the statistical comparisons between the two hands were performed using the unpaired *t*-test (normality test passed) or the nonparametric Mann–Whitney test (normality test failed) on the CT values pooled from 20 daily sessions.

exhibited comparable CTs for the left and the right hand. In four monkeys (Mk-AT, Mk-CA, Mk-DI, and Mk-MA), the CTs were shorter for the right hand, whereas the CTs were shorter for the left hand in three monkeys (Mk-LO, Mk-MI, and Mk-TH). Considering both the vertical and the horizontal slots, note that in two monkeys (Mk-DI and Mk-LO) exhibiting a significant difference of CTs between the two hands for both slot orientations, surprisingly the hand with the shortest CTs was not the same for the vertical and the horizontal slots.

### Human subjects

The hand dominance was determined for the human subjects by comparing the total score (sum of vertical and horizontal slots visited in 30 sec) between each hand in the unimanual modified Brinkman board task. Graphs derived from one self-assessed right-hander (AG) and one self-assessed left-hander (AH) are shown in Figure 3A, with the total score for each hand in the ten consecutive trials. Generally, there was a training effect along the sessions, as most subjects increased their performance (total score) after a few trials. In two human subjects, the learning effect was rapid (plateau reached after two trials) but of limited extent (small increase of score). In the other human subjects, the learning phase was longer, 4–6 trials in most cases. The gain in total score was for most subjects in the order of 10 additional bolts collected in 30 sec at plateau as compared to the score observed for the first trial, although overall the gain in total score ranged from about 5–15 additional bolts collected in 30 sec. Moreover, most subjects developed strategies (motor habits) to increase their performance: for instance, they began to grasp bolts from the vertical slots and then bolts from the horizontal ones, or they began each trial on one side and systematically scanned the board to the other extremity. Additionally, in this sample of 20 human subjects, the right-handers performed significantly better than the left-handers ( $P < 0.001$ ; Mann–Whitney test) and women exhibited higher total scores than men ( $P = 0.009$ ; Mann–Whitney test).

The hand dominance was determined by comparing the total scores between the left hand and the right hand in each subject (Fig. 3B). Generally, the total score ranged between 15 and 40. Out of the twenty subjects, only nine showed a significant hand dominance. In the left-handed subjects (ID initials in blue in Fig. 3B;  $n = 10$ ), five people exhibited a significant left-hand dominance: AB, AH, AP, MF, and VC ( $P = 0.038$ ,  $P = 0.002$ ,  $P < 0.001$ ,  $P = 0.045$ , and  $P < 0.001$ , respectively), whereas one self-declared left-hander surprisingly showed a significant right-hand dominance (SB with  $P = 0.015$ ). In the other four left-handers, there was no significant hand dominance. In the population of right-handed subjects (ID initials in red in Fig. 3B;  $n = 10$ ), three of them showed a right-hand dominance (AG, JG, and MS, with  $P = 0.025$ ,  $P = 0.004$ , and  $P = 0.005$ , respectively), whereas there was no significant hand dominance in the other seven self-declared right-handed subjects.

The CT was assessed in the human subjects as well, separately for the vertical and horizontal slots and illustrated in Figure 4 for four representative subjects. The subjects AP and MS were representative of lateralized humans, self-declared as left-hander and right-hander, respectively, and showed a dominance of the corresponding hand (left in AP and right in MS), with statistically shorter CTs as compared to the opposite hand. The CTs of two other subjects are displayed in Figure 4, one fast subject (AG) and one slow subject (MB), as exhibited in Figure 3B by their high and low scores, respectively. The fast subject (AG), declared as right-hander, also exhibited shorter CTs with the corresponding hand (the difference with the opposite hand was statistically significant only for the vertical slots). In contrast, the slow subject (MB), declared as left-hander, exhibited comparable CTs for both hands. As compared to monkeys (Fig. 2B), the human CT data (Fig. 4) reflect a somewhat shorter time interval needed to successfully grasp the object from the slots, especially for the horizontal slots. This species difference may be explained by the object properties, as the bolt with its angular contour and surface with a hole in it is easier to grasp than the round shape of the pellets presented to the monkeys.

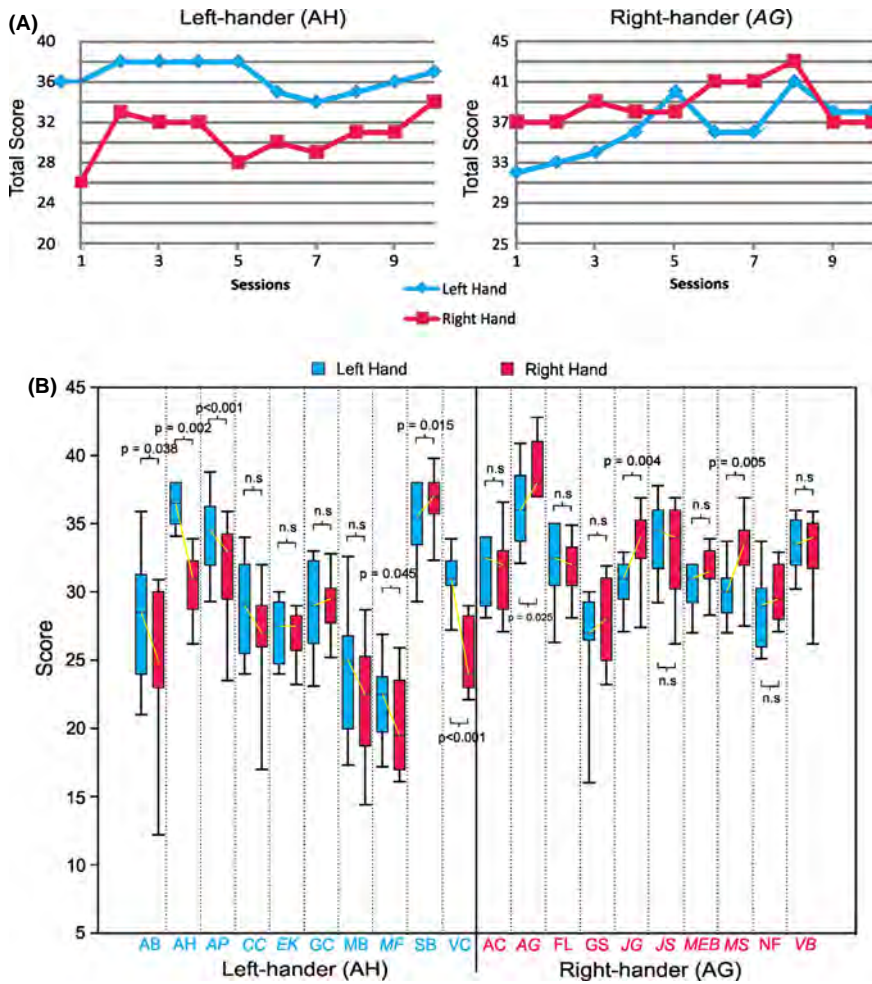


**Figure 3.** Hand dominance analysis for human subjects (women in italic), derived from the unimanual modified Brinkman board task. Examples of the total score (sum of the number of horizontal and vertical slots visited in 30 sec) for a left-handed subject (AH) and a right-handed subject (AG) are shown in panel (A). In panel (B), the box and whiskers plots represent the distribution of the total scores observed for the left hand (blue) and the right hand (red), for each human subject tested ( $n = 20$ , indicated by their ID initials). The ID initials of the subjects presented themselves as left-hander versus right-hander, respectively. The ID initials of males and females are shown with normal and italic type, respectively. The statistical comparisons of total score between the two hands in each of the 10 trials were performed using the paired *t*-test (normality test passed) or the nonparametric Wilcoxon rank signed test (normality test failed). In each subject, a yellow line connects the median values of the left and the right hands, in order to emphasize the intermanual comparison.

**Hand preference**

**Monkeys**

As reminder, the hand preference in monkeys was determined based on the results of the modified Brinkman board, when the use of the two hands was free, as well as on the results of three other specific tasks: the bimanual board, the tube, and the drawer tasks.

For the modified Brinkman board task (executed with both hands simultaneously), we made a distinction among the scores according to different phases, each characterized by distinct patterns of manual use. Indeed, the monkeys evolved in their manner to execute the task and in the choice of one hand to the detriment of the other along the daily sessions. There were mainly three different behavioral profiles exhibited by the animals (Fig. 5). In the first profile (for instance Mk-AN in Fig. 5A), the monkey used nearly always the same hand in phase I, whereas in phase II (to the right of the vertical dashed line), both hands were used more or less at the same frequency. In the second profile (for instance

Mk-LO in Fig. 5B), one of the hands was less used than the other hand along all daily sessions. However, two phases were distinguished, phase I corresponding to a minimal use of one hand followed, in phase II, by an increased contribution of the less used hand. The third profile (for instance Mk-MA, Fig. 5C) is the opposite to the first one: both hands were used more or less at the same frequency during phase I, whereas one hand was then less used than the other hand during phase II.

After determining the different phases corresponding to different profiles (manual patterns), we compared the score for the right hand with the one for the left hand, separately in the vertical (Fig. 6A) and in the horizontal slots (Fig. 6B), in each phase in each monkey. In the vertical slots in phase I, four monkeys exhibited a significant preference to use one hand over the other (left-hand preference in Mk-AN and Mk-TH; right-hand preference in Mk-DI and Mk-LO), whereas the other four monkeys did not show any significant hand preference (Mk-AT, Mk-CA, Mk-MA, and Mk-MI). In phase II, most of the scores for the vertical slots did not exhibit a significant

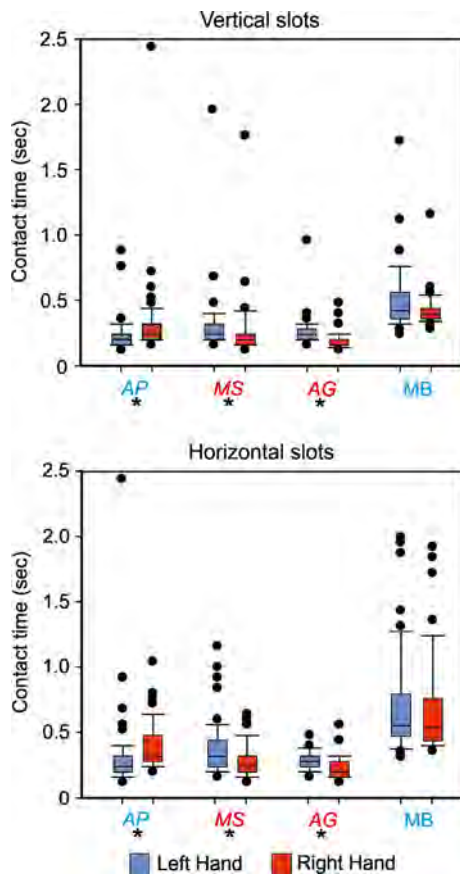


**Figure 4.** Hand dominance analysis for human subjects, derived from CTs obtained in the unimanual modified Brinkman board task, for four representative human subjects (see text), when the use of one hand was imposed. Both graphs, in the form of box and whiskers plots, represent the distribution of CTs in seconds, for the vertical slots (top graph) and for the horizontal slots (bottom graph), and separately for the left hand (blue) and the right hand (red). The CT data (five values per daily session for each slot orientation) are not paired and the statistical comparisons between the two hands were performed using the unpaired *t*-test (normality test passed) or the nonparametric Mann–Whitney test (normality test failed) on the CT values pooled from the 10 sessions. Same ID initial code as in Figure 3.

difference between both hands, except for Mk-LO and Mk-MA, with a significant preference for their right hand. In the horizontal slots (Fig. 6B), in phase I, all monkeys but Mk-MA showed a significant hand preference. Four monkeys (Mk-AN, Mk-AT, Mk-MI, and Mk-TH) used preferably their left hand, whereas three monkeys (Mk-CA, Mk-DI, and Mk-LO) used more often their right hand. In phase II, five out of eight monkeys showed a preference for one hand over the other, with a left-hand preference in Mk-AT and Mk-MI, whereas Mk-CA, Mk-LO, and Mk-MA exhibited a right-hand preference. Overall, there were clearly more significant hand

preferences observed for the horizontal slots than for the vertical slots (Fig. 6).

The HI, derived from the three other tasks performed by the monkeys (the bimanual board task (Fig. 1B), the tube task (Fig. 1C), and the drawer task (Fig. 1D)), were plotted on the same bar graph (Fig. 7A, rightmost part of the graph, separated from human subjects by a vertical black line). In most cases, these three tasks were lateralized (large positive or negative HI). Mk-TH was the only monkey to exhibit a coherent hand preference for all three tasks, with a systematically positive HI, corresponding to a significant right-hand preference ( $P < 0.05$ ; binomial test). In the other seven animals, there was an absence of systematic consistency across tasks.

Three monkeys (Mk-AN, Mk-CA, and Mk-DI) exhibited a preference for the right hand in the bimanual board and the tube tasks (positive HI) and a preference for the left hand in the drawer task (negative HI). These HI values were statistically significant (meaning lateralized; binomial test  $P < 0.05$ ), except in Mk-CA for the tube task (Fig. 7A).

Mk-LO and Mk-MI shared a comparable general pattern of HI distribution among the three tasks (Fig. 7A), namely a clearly positive HI ( $>0.5$ ) for the bimanual board and the drawer tasks, whereas the HI was strongly negative for the tube task (Fig. 7A). In these two animals, all HI values were statistically significant (lateralized;  $P < 0.05$ ).

The last three monkeys had each a unique general pattern of HI distribution among the three tasks. Mk-AT exhibited a significant preference for the right hand in the bimanual board task ( $P < 0.05$ ), whereas a significant left-hand preference was present for the tube and the drawer tasks ( $P < 0.05$ ). In Mk-MA, there was a significant left hand preference for the first two tasks ( $P < 0.05$ ), whereas for the drawer task the right hand was preferred ( $P < 0.05$ ).

## Human subjects

Two tasks, namely the tube and the bimanual Brinkman board tasks, as well as the handedness questionnaire were used to assess the hand preference in human subjects. The observed HI values obtained for the bimanual board and for the tube tasks were plotted on the same graph for all subjects (Fig. 7A, left and middle parts of the graph, separated from the rightmost part concerning monkeys by the solid vertical black line). Most human subjects exhibited a HI near to  $-1$  or  $1$ . The  $P$ -value for each test and for each subject was statistically significant ( $P < 0.05$ ; binomial test), except for the tube task in the subject FL ( $P > 0.05$ ). The results for both tasks (Fig. 7A) showed that most self-declared left-handers indeed used their left hand as the preferred hand (HI negative), and similarly most self-



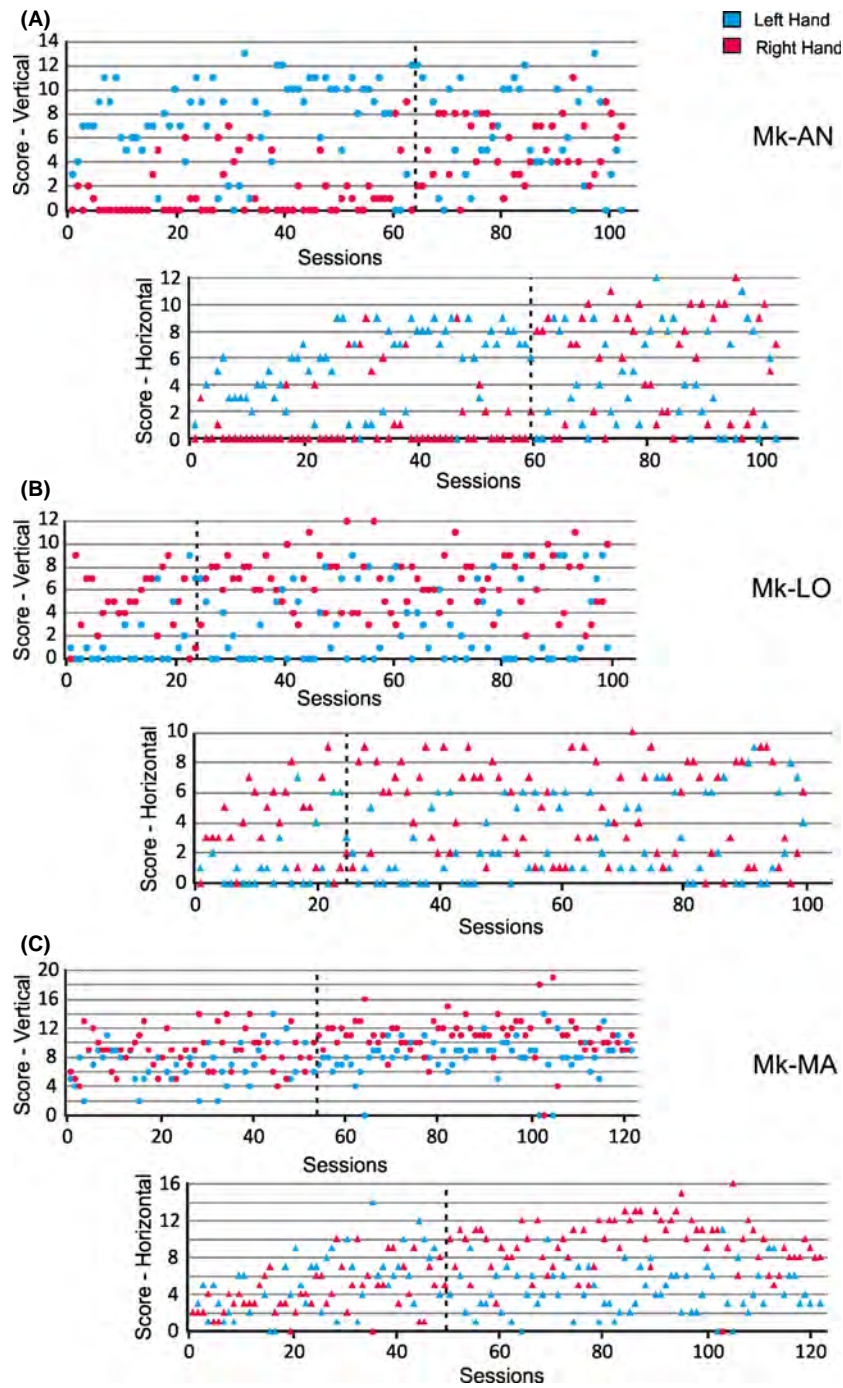


**Figure 5.** Hand preference in monkeys: distinction between different phases in the modified Brinkman board task, when the use of both hands was free. Different behaviors appear among monkeys. In panel (A), the scores for the vertical and horizontal slots for Mk-AN are shown. The vertical dotted line separates two phases: phase I in which the right hand (in red) was hardly ever used and phase II during which both hands were used more or less at the same frequency (see the corresponding statistical tests in Fig. 6). In panel (B), scores for vertical and horizontal slots for Mk-LO are shown. The vertical dotted line also separates two phases, but the distinction is here less marked. In phase I, the left hand was hardly ever used, whereas it was used more in phase II. However, the right hand seems to be more used in the two phases than the left one (see statistical tests in Fig. 6). In panel (C), scores for vertical and horizontal slots for Mk-MA are shown. The vertical dotted line separates two phases as well: phase I in which both hands were used more or less at the same frequency, and phase II, in which conversely the left hand was less used than the right hand (statistical tests in Fig. 6). As emphasis was put on the comparison between the two hands in each condition, the ordinate maximal values were variable among conditions.

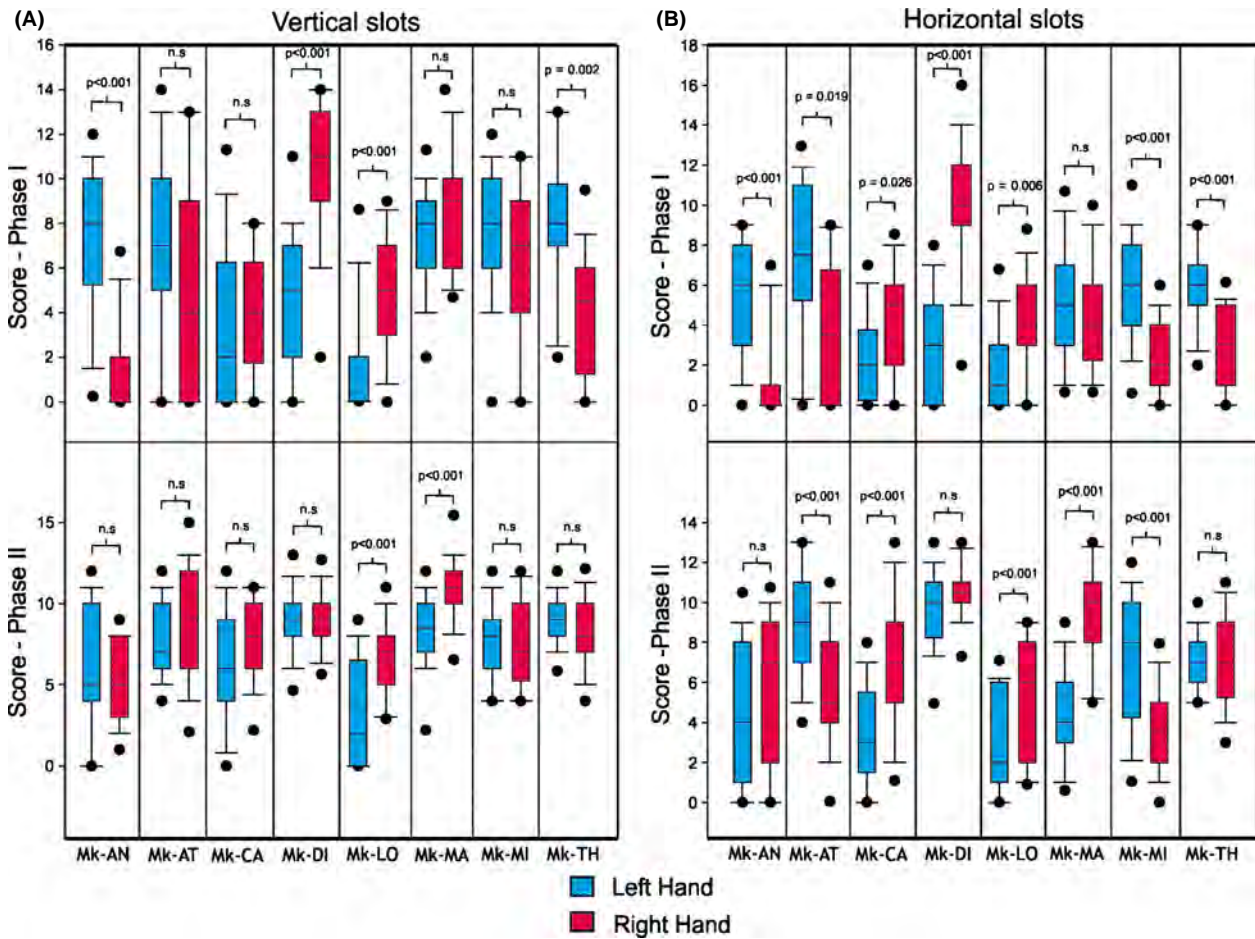


**Figure 6.** Hand preference statistical analysis for monkeys, applied to the modified Brinkman board task data, with free use of the two hands simultaneously, as illustrated in Figure 5, and represented by box and whiskers plots. Scores for vertical slots for phases I and II are shown for all monkeys in panel (A) and scores for the horizontal slots for phases I and II are displayed in panel (B).

declared right-handers indeed used their right hand as the preferred hand (HI positive). Only three left-handers exhibited a preference for the right hand in the tube task (subjects AP, CC, and MB). One of these three left-handed subjects (CC) furthermore showed a preference for the right hand in the bimanual board task. In the population of self-declared right-handers (Fig. 7A), four of them (subjects AC, GS, JG, and NF) showed a preference for their left hand in the tube task, whereas another right-handed subject (MS) exhibited a preference for the left hand in the bimanual board task. Statistical comparisons (*t*-test or Mann–Whitney) between the groups of right-handers versus left-handers for the tube task (blue bars in Fig. 7A) did not reveal any significant difference ( $P > 0.05$ ) for both the real HI values and the absolute HI values. On the other hand, for the bimanual board task (gray bars in Fig. 7A), there was a significant difference for the real HI values between the right-handers and the left-handers ( $P = 0.002$ ), but not for the absolute HI values ( $P = 0.33$ ), indicating

that the degree of lateralization is comparable in both groups.

The scores derived from the handedness questionnaire was calculated and transformed into percentages (Fig. 7B). The overall questionnaire scores for the self-announced right-handers (ID initials in red in Fig. 7B) were clearly positive, ranging between 53.85% and 100%. The questionnaire scores derived from the self-announced left-handers (ID initials in blue in Fig. 7B) were mostly negative, ranging between  $-30.77\%$  and  $-73.08\%$ . The exception was the subject AB, who surprisingly showed a positive questionnaire score (26.92%). The absolute values of laterality score were significantly larger in the right-handers than in the left-handers ( $P = 0.007$ ), confirming the well-established notion that right-handers are more lateralized.

An overview of all results is available in Table 1, separately for the monkeys (Part A) and for the human subjects (Part B). Generally, it can be concluded that comparable numbers of left- and right-handed occurrences appeared

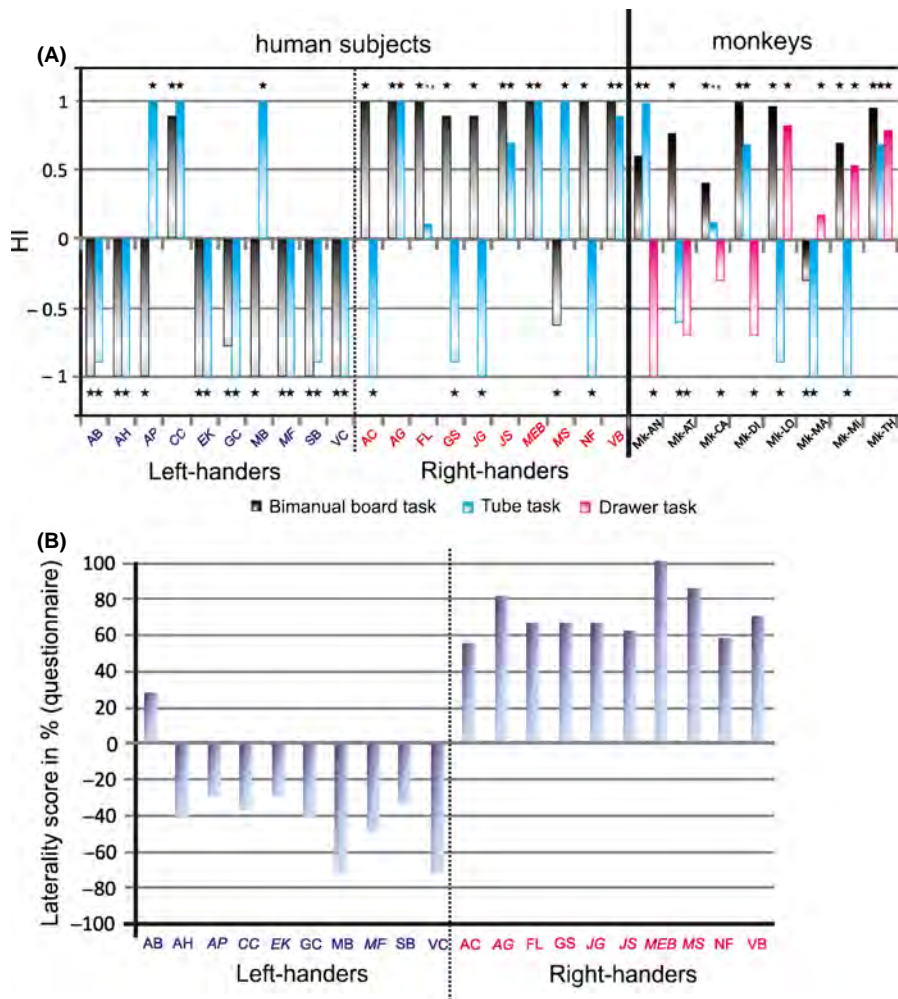


**Figure 7.** Hand preference analysis for monkeys and human subjects. In panel (A), the bar graph displays the handedness index (HI) for the bimanual Brinkman board and the tube tasks in human subjects and for the bimanual Brinkman board, the tube and the reach and grasp drawer tasks in monkeys. The solid vertical black line separates human subjects (left) from monkeys (right) and the vertical dotted line separates the human subjects who presented themselves as left-handers (left) from the subjects who presented themselves as right-handers (right). For each task and for each subject, the stars indicate a  $P \leq 0.05$  obtained in a binomial statistical test ( $ns =$  not significant,  $P > 0.05$ ), above or below each corresponding bar graph. In panel (B), the bar graph represents the overall laterality score from the handedness questionnaire in percentage for each human subject. The ID initials of the subjects are in blue versus red for the self-announced left-handers versus right-handers, respectively. See text for statistical analysis. For human subjects, same ID initial code as in Figure 3 (women in italic).

among monkeys, concerning both the hand dominance and the hand preference (Table 1, Part A). However, there was no general consistency in hand dominance or in hand preference in monkeys, neither between individuals nor within each individual. On the contrary, as far as human subjects are concerned, the hand preferences revealed by the two manual tests and the questionnaire were largely coherent with the self-assessment by the subject (Table 1, Part B), although the tube task revealed a few more discrepancies. There were less systematic occurrences of hand dominance (assessed with the unimanual modified Brinkman board task; Table 1, Part B) although, when present, it was consistent with the lateralization of the hand preference

(except in the subject SB). We also observed that hand dominance was somewhat more frequent in left-handers than in right-handers.

### Discussion

At least to the best of our knowledge, the present study introduced several new aspects of handedness assessment in primates, with emphasis on manual dexterity (use of precision grip). First of all, the data support the concept of separation of two hand attributes, namely the hand dominance and the hand preference. In monkeys, these two attributes were not systematically consistent, and in

**Table 1.** Overview of the results. The panel (A) shows a summary of all results derived from the eight monkeys. VS and HS mean vertical and horizontal slots, respectively. Pl refers to plateau. Pl.I/Pl.II mean phases I and II of the plateau. The letter L indicates a left-hand dominance/preference and the letter R, a right-hand dominance/preference, whereas ns means a statistically nonsignificant difference ( $P > 0.05$ ). The panel (B) shows an overview of all results in human subjects for the self-announced right-handers (ID initials in red) and left-handers (ID initials in blue). The letters L and R indicate a statistically significant left and right dominance/preference, respectively. ns means a statistically nonsignificant difference.

		Mk-AN	Mk-AT	Mk-CA	Mk-DI	Mk-LO	Mk-MA	Mk-MI	Mk-TH
Hand dominance	Total	ns	ns	R	R	R	L	L	ns
	Modified Brinkman board task	L	ns	R	ns	ns	R	ns	ns
	Score Pl	L	ns	R	R	R	R	ns	ns
	CT	L	ns	R	R	R	R	ns	ns
Hand preference	VS	ns	R	R	R	L	R	L	L
	Modified Brinkman board task	L	ns	ns	R	R	ns	ns	L
	Score Pl.I	ns	ns	ns	R	R	R	ns	ns
	Score Pl.II	ns	ns	ns	R	R	R	ns	ns
Bimanual board task	HS	L	L	R	R	R	ns	L	L
	Modified Brinkman board task	ns	L	R	ns	R	R	L	ns
	Score Pl.I	R	R	R	R	R	L	R	R
	Score Pl.II	R	R	R	R	R	L	R	R
Tube task	ns	L	ns	L	L	L	L	L	R
	R	R	R	R	R	R	R	R	R
Drawer task	L	L	L	L	L	R	R	R	R
	L	L	L	L	L	R	R	R	R

		Right-handers																					
		AB	AH	AP	CC	CC	EK	GC	MB	MF	SB	VC	AC	AG	FL	GS	JG	JS	MEB	MS	NF	VB	
Hand dominance	Modified Brinkman board task	L	L	L	ns	ns	ns	ns	ns	L	R	L	ns	ns	ns	ns	R	ns	ns	R	ns	ns	ns
	Bimanual board task	L	L	L	R	R	L	L	L	L	L	L	R	R	R	R	R	R	R	R	L	R	R
Hand preference	Tube task	L	L	L	R	R	L	L	L	L	L	L	L	R	ns	L	L	R	R	R	R	L	R
	Handedness questionnaire	R	L	L	L	L	L	L	L	L	L	L	R	R	R	R	R	R	R	R	R	R	R



human subjects the hand preference was not systematically accompanied by consistent hand dominance, at least for the modified Brinkman board task (Table 1). This may be different for more challenging manual dexterity tasks. Second, the present study is original in comparing nonhuman primates and human subjects with respect to their handedness, based on a set of comparable manual dexterity tasks performed by macaque monkeys and human subjects (see also Lacreuse and Frigaszy 1997; for a comparison between capuchin monkeys and humans). In particular, the modified Brinkman board task widely and classically used in monkeys (e.g., Brinkman and Kuypers 1973; Brinkman 1984; Liu and Rouiller 1999; Kaeser *et al.* 2010, 2011, 2013; Schmidlin *et al.* 2011) was tested in human subjects for the first time. Third, the manual performance in nonhuman primates was conducted here in well-defined conditions, such as reproducible posture and position of the animal with respect to the behavioral set-up, thanks to the use of the primate chair placed in the same position from one daily session to the next (in contrast to observations in the wild or in the detention cage). The primate chair offers also the possibility to test separately the left hand from the right hand, as needed to assess hand dominance for instance. Finally, in monkeys, the assessment of manual performance was not restricted to a single or very few time points, but it was monitored in daily sessions over several weeks or months.

Overall, the results confirmed our hypothesis that hand preference in *M. fascicularis* is variable across manual tasks and individuals (Table 1). Furthermore, the hand preference in monkeys did not systematically correspond to the hand dominance in the modified Brinkman board task (four out of eight monkeys: see Table 1). In contrast, human subjects are more lateralized and the correspondence between hand preference and hand dominance was systematic in the vast majority of cases (one exception out of 20 subjects: see Table 1).

As expected, our results related to hand preference show that left-handers are not a mirror image of right-handers, at least based on the questionnaire (Fig. 7B). Right-handers are clearly more lateralized, as laterality scores (absolute values) were significantly larger in right-handers than in left-handers. In monkeys, based on the three tasks they performed (Fig. 7A), only one animal exhibited a consistent lateralization (Mk-TH: right-hander), whereas in the others, the preferred hand was largely task dependent.

The part of the present study focused on human subjects, in spite of a relatively limited sample of subjects ( $n = 20$ , comprising 10 men and 10 women distributed in 10 right-handers and 10 left-handers based on their self-assessment) revealed some interesting differences.

First, the questionnaire data showed that left-handers are less lateralized than right-handers (Fig. 7B), as previously reported (see e.g., Kastner-Koller *et al.* 2007) and in line with our hypothesis (see Introduction and Methods). However, this lateralization difference between self-declared left- and right-handers reflected by the questionnaire was not found for the two bimanual tasks tested here: as shown in Table 1, there was a comparable number of hand preference deviations in each group (four right hand deviations in the left-handers and five left hand deviations in the right-handers). Second, in the context of hand dominance assessment based on the modified Brinkman board task, right-handers performed significantly better than left-handers, in the 10 trials conducted for each subject during the unique behavioral session. Whether this difference would be maintained along multiple sessions conducted at subsequent days remains an open question. Third, women performed significantly better than men in the modified Brinkman board task, as reflected by a higher total score. This result is in line with the previously reported notion that females perform better than males in tasks requiring high levels of manual dexterity (Kimura 2000). The gender difference was opposite in a computer-pointing task (Rohr 2006), with motor times shorter in men, favoring speed, than women, highlighting accuracy.

In the present study, fairly comparable results were obtained for human subjects and monkeys, as far as the hand dominance is concerned. Indeed, 62% of monkeys and 55% of human subjects did not show any statistically significant hand dominance, as assessed by the score derived from the modified Brinkman board task. Concerning the CTs, the results are more difficult to interpret in monkeys. The CTs were fully coherent with the score in one case only (Mk-CA), whereas for the other monkeys, there was no, or less, consistency (Table 1). As reminder, the CT is a parameter additional to the score, which eliminates possible biases in the score, due to inattention and/or lack of motivation of the monkey. In other words, it does not take into account the time interval between two slot manipulations. Moreover, we had taken into consideration only the last 20 sessions at plateau, to focus on the supposedly most stable daily behavioral sessions. It may, however, be interesting to consider the CT in more sessions in the plateau phase for a stricter comparison with the score for the very same sessions, although, in previous studies (e.g., Kaeser *et al.* 2010, 2011), the CTs were largely stable during the entire plateau phase. The discrepancy between score and CTs is likely to be due to other parameters, such as diverted attention in between the grasping of two consecutive pellets. It may also originate from the different motor habits reflected by the temporal sequence followed by the animal



to visit the slots (e.g., the monkey scans the board systematically from one side to the other or from the middle and then to the sides; see Kaeser et al. 2013). Moreover, at a given time point, the animal may change prehension strategy (e.g., collect two pellets at a time). As long as the new strategy is not fully mastered, the hand dominance may vary, although the CTs remain short. In human subjects, as for the score data, the CT data showed that the hand dominance is generally consistent with the hand preference.

The present study offers the opportunity to compare the hand dominance and the hand preference for both human subjects and nonhuman primates. As reminder, the human subjects exhibiting hand dominance showed, most of the time, the same laterality for hand preference. This was not the case for the monkeys, where the laterality of the hand dominance did not systematically correspond to the one of the hand preference (Table 1). The same conclusion was met in a study conducted on four female *M. fuscata* Japanese monkeys (Kinoshita 1998).

Concerning the hand preference, the results in human subjects are very consistent with their self-assessment. Indeed, for most subjects, the preferred hand revealed by the different tasks corresponded to the hand they used to write, except for the tube task, where the results were more disparate (Table 1). The tube task thus appears less appropriate than the bimanual Brinkman board task and the questionnaire to determine the hand preference in human subjects. This raises then the question whether this task is adequate to assess hand preference in monkeys. The results related to hand preference in monkeys were highly disparate. Only two animals showed similar results (Mk-DI and Mk-AN) and, for each monkey, there was no systematic hand preference among all the tasks performed. Considering the questionable suitability of the tube task in human subjects (see above), it was tried to eliminate the tube test from the monkey data: omitting the tube task data did not modify substantially the results, except for Mk-LO, which was a right-hander for each task except the tube one. Two conclusions maybe drawn from these results: either the tasks used here are not fully appropriate to determine the hand preference in monkeys, or the *M. fascicularis* monkeys do not show a stable and systematic hand preference for the present panel of tasks. In human subjects, the bimanual Brinkman board appears to be an adequate test, but is it also the case for the nonhuman primates? This question highlights the limits of our experiment. On the one hand, we compare for the first time handedness in human subjects and in nonhuman primates for the same tasks directly but, on the other hand, these manual tasks may not be equally relevant in both species. The complexity and the representation of the different tasks may well be different for

nonhuman primates and for human subjects. A difference is already present at the level of training. Clearly, human subjects reached more rapidly plateau values than monkeys, especially for the modified Brinkman board task. Human subjects are obviously more often engaged in bimanual coordination tasks in their everyday life than monkeys, a difference which may bias the comparison between the two groups performing the same manual tasks. At onset time of behavioral testing, the human subjects were already strongly lateralized, whereas this was most likely not the case in the nonhuman subjects. In the monkeys, the present data demonstrate that hand preference is more prominently revealed by a more challenging task (horizontal slots) than an easier task (vertical slots in the modified Brinkman board task, executed with both hands simultaneously; see Table 1). In the comparison between monkeys and humans, it has to be emphasized that reinforcement is not of the same nature (food in monkeys, a bolt in human) and therefore the motivational context is different. Furthermore, human subjects were asked to perform the task as rapidly as possible, whereas there was no such time constraint in monkeys. However, as the task represented the first access to food on that day, the monkeys were motivated and therefore they were fast too.

As compared to previous studies available in the literature, several aspects deserve further comments. As already mentioned above, few of the previous studies clearly distinguished hand dominance from hand preference, especially in nonhuman primates. Consequently, in previous studies conducted in monkeys with the aim to investigate the effect of different lesions of the central nervous system on the manual dexterity, it is often mentioned that a unilateral lesion was performed on the contralateral side with respect to the “dominant” hand. From the present study, such statement remains unclear as it is not obvious to distinguish whether the hand was more proficient (better motor performance reflecting hand dominance as defined here) or selected in priority (preferred hand) by the animal to perform a specific manual dexterity task. The difficulty is even increased when considering the data presented in Figure 5, demonstrating that the hand preference may vary with time along the daily behavioral sessions.

Focusing on hand preference (as defined in the present report), several studies showed similar results to ours, confirming an individual-level hand preference associated to different tasks (Old World Monkey in Westergaard et al. 2001a,b and Chapelain et al. 2006; Prosimians in Leliveld et al. 2008 and Hanbury et al. 2010). For Chapelain et al. (2006), this individual preference is an evidence of endogenous laterality, but to explain the differences between the animals, they propose an influence of differ-

ent factors dependent on the task specificity. Hopkins (2006) reached similar conclusions in great apes. Linked to this observation, several studies suggested dependence between handedness and task complexity (Lehman 1989; Fagot and Vauclair 1991; Hopkins 1995; Hopkins and Rabinowitz 1997; Spinozzi et al. 1998; Hopkins and Cantalupo 2005). Indeed, the more complex the task, the more prominent the hand preference. This is in line with the larger occurrences of hand preference observed here in the horizontal slots of the modified Brinkman board task, as compared to the less challenging vertical slots (Table 1). Overall, in our study, all tasks in which the monkeys were engaged may be considered as complex, so it explains why, for most of them, we found an individual manual laterality (hand preference; see Table 1). Moreover, previous studies emphasized the significance of the body position in relation to the task in order to determine the manual laterality (Hopkins and Cantalupo 2005; Meunier et al. 2011). In our study, the position of the animal was highly reproducible and this parameter thus did not influence our results.

Unlike to the first aforementioned studies, Hopkins et al. (2002), Westergaard et al. (1997), and Wesley et al. (2001) found a population-level handedness in macaques and chimpanzees, but the methods used to assess hand preference were a bit different. Indeed, Hopkins et al. (2002) and Westergaard et al. (1997) tested the hand preference using a lower number of tasks.

Concerning the different results obtained from human subjects and monkeys, several explanations appear pertinent. Sociability plays an important role for the handedness (Hopkins 2006). Indeed, pedagogical or cultural pressures can influence the hand preference in humans, which is not considered to be the case in nonhuman primates. The postural origin theory of handedness offers a possible explanation for the monkey data (MacNeilage et al. 1987). Indeed, several studies showed a right-hand preference for more terrestrial species, whereas a left-hand preference was found for more arboreal animals (Masataka 1989; Singer and Schwibbe 1999; Hopkins et al. 2011; Meguerditchian et al. 2012; Zhao et al. 2012). In our case, our animal model, the *M. fascicularis*, is considered to be both arboreal and terrestrial (Fooden 2006; South Asian Primate C.A.M.P. Report, 2003; [http://www.zooreach.org/downloads/ZOO\\_CAMP\\_PHVA\\_reports/2003%20Primate%20Report.pdf](http://www.zooreach.org/downloads/ZOO_CAMP_PHVA_reports/2003%20Primate%20Report.pdf)). Our results in *M. fascicularis* monkeys, showing a right- or left-hand preference depending on the tasks, is thus in line with the postural origin theory, in the sense that our animals did not show a clear right- or left-handedness, but an intermediate and variable position, consistent with the mixed arboreal and terrestrial status of *M. fascicularis*. These data are consistent with hand preference observations derived from

simple food reaching task, also in cynomolgus (*M. fascicularis*) monkeys (Lehman 1980b). In a longitudinal study (from birth to weaning) conducted on a large number of monkeys (*M. fascicularis*), and based also on a task using a slot board but emphasizing more the attribute of hand dominance than hand preference (Brinkman and Smithson 2007), it was found that the infant monkeys showed a “dominant” hand at individual level (but bimodal distribution at population level). Their hand “dominance” was the same as that of their mother and, moreover, their pattern of grip movement resembled their mothers’, suggesting imitation (Brinkman and Smithson 2007). In line with Hopkins (2004), the present data in *M. fascicularis* show that, as far as hand preference is concerned, they considerably diverge from human subjects (highly lateralized), whereas apes can be placed in between the two groups, with intermediate hand preference characteristics. This wide range of behavioral lateralization is consistent with its multifactorial origin (see e.g., Rogers 2009; Schaafsma et al. 2009; Uomini 2009; Forrester et al. 2013).

## Acknowledgments

The authors wish to thank the technical assistance of Josef Corpataux, Laurent Bossy and Jacques Maillard (animal house keeping), André Gaillard (mechanics), Bernard Aebischer (electronics), Laurent Monney (informatics). This study was supported by Swiss National Science Foundation, grants No. 31-61857.00, 310000-110005, 31003A-132465, and FZFS-0\_144990 (E. M. R.), 31-121646 (E. S.); the Novartis Foundation; the National Centre of Competence in Research (NCCR) on “Neural plasticity and repair” and the Christopher Reeves Foundation (Springfield, NJ). The experiments were conducted in the framework of the SPCCR (Swiss Primate Center for Competence in Research), financed by the State Secretariat for Education and Research.

## Conflict of Interest

None declared.

## References

- Brinkman, C. 1984. Supplementary motor area of the monkey's cerebral cortex: short- and long-term deficits after unilateral ablation and the effects of subsequent callosal section. *J. Neurosci.* 4:918–929.
- Brinkman, J., and H. G. J. M. Kuypers. 1973. Cerebral control of contralateral and ipsilateral arm, hand and finger movements in the split-brain rhesus monkey. *Brain* 96:653–674.
- Brinkman, C., and M. Smithson. 2007. Determinants of hand preference in monkeys (*M. fascicularis*): birth to weaning. *Aust. J. Psychol.* 59(Suppl. 1):21.

- Chapelain, A., P. Bec, and C. Blois-Heulin. 2006. Manual laterality in Campbell's Monkeys (*Cercopithecus c. campbelli*) in spontaneous and experimental actions. *Behav. Brain Res.* 173:237–245.
- Coren, S., and C. Porac. 1977. Fifty centuries of right-handedness: the historical record. *Science* 198:631–632.
- Dadda, M., C. Cantalupo, and W. D. Hopkins. 2006. Further evidence of an association between handedness and neuroanatomical asymmetries in the primary motor cortex of chimpanzees (*Pan troglodytes*). *Neuropsychologia* 44:2582–2586.
- Dassonville, P., X. H. Zhu, K. Uurbil, S. G. Kim, and J. Ashe. 1997. Functional activation in motor cortex reflects the direction and the degree of handedness. *Proc. Natl. Acad. Sci. USA* 94:14015–14018.
- Fagot, J., and J. Vauclair. 1988. Handedness and manual specialization in the baboon. *Neuropsychologia* 26:795–804.
- Fagot, J., and J. Vauclair. 1991. Manual laterality in nonhuman primates: a distinction between handedness and manual specialization. *Psychol. Bull.* 109:76–89.
- Fooden, J. 2006. Comparative review of fascicularis-group species of macaques (Primates: *Macaca*). *Fieldiana Zool.* 107:1–44.
- Forrester, G. S., C. Quaresmini, D. A. Leavens, D. Mareschal, and M. S. C. Thomas. 2013. Human handedness: an inherited evolutionary trait. *Behav. Brain Res.* 237:200–2006.
- Freund, P., E. Schmidlin, T. Wannier, J. Bloch, A. Mir, M. E. Schwab, et al. 2009. Anti-Nogo-A antibody treatment promotes recovery of manual dexterity after unilateral cervical lesion in adult primates—re-examination and extension of behavioral data. *Eur. J. Neurosci.* 29:983–996.
- Hanbury, D. B., K. D. Edens, D. A. Bunch, C. E. Legg, and S. L. Watson. 2010. Multiple measures of laterality in Garnett's bushbaby (*Otolemur garnettii*). *Am. J. Primatol.* 72:206–216.
- Hopkins, W. D. 1995. Hand preferences for a coordinated bimanual task in 110 chimpanzees (*Pan troglodytes*): cross-sectional analysis. *J. Comp. Psychol.* 109:291–297.
- Hopkins, W. D. 2004. Laterality in maternal cradling and infant positional biases: implications for the development and evolution of hand preferences in nonhuman primates. *Int. J. Primatol.* 25:1243–1265.
- Hopkins, W. D. 2006. Comparative and familial analysis of handedness in great apes. *Psychol. Bull.* 132:538–559.
- Hopkins, W. D., and C. Cantalupo. 2004. Handedness in chimpanzees (*Pan troglodytes*) is associated with asymmetries of the primary motor cortex but not with homologous language areas. *Behav. Neurosci.* 118:1176–1183.
- Hopkins, W. D., and C. Cantalupo. 2005. Individual and setting differences in the hand preferences of chimpanzees (*Pan troglodytes*): a critical analysis and some alternative explanations. *Laterality* 10:65–80.
- Hopkins, W. D., and D. L. Pilcher. 2001. Neuroanatomical localization of the motor hand area with magnetic resonance imaging: the left hemisphere is larger in great apes. *Behav. Neurosci.* 115:1159–1164.
- Hopkins, W. D., and D. M. Rabinowitz. 1997. Manual specialisation and tool use in captive chimpanzees (*Pan troglodytes*): the effect of unimanual and bimanual strategies on hand preference. *Laterality* 2:267–277.
- Hopkins, W. D., D. A. Washburn, and D. M. Rumbaugh. 1989. Note on hand use in the manipulation of joysticks by rhesus monkeys (*Macaca mulatta*) and chimpanzees (*Pan troglodytes*). *J. Comp. Psychol.* 103:91–94.
- Hopkins, W. D., D. A. Washburn, L. Berke, and M. Williams. 1992. Behavioral asymmetries of psychomotor performance in rhesus monkeys (*Macaca mulatta*): a dissociation between hand preference and skill. *J. Comp. Psychol.* 106:392–397.
- Hopkins, W. D., C. Cantalupo, M. J. Wesley, A. B. Hostetter, and D. L. Pilcher. 2002. Grip morphology and hand use in chimpanzees (*Pan troglodytes*): evidence of a left hemisphere specialization in motor skill. *J. Exp. Psychol. Gen.* 131:412–423.
- Hopkins, W. D., M. Hook, S. Braccini, and S. J. Schapiro. 2003. Population-level right handedness for a coordinated bimanual task in chimpanzees: replication and extension in a second colony of apes. *Int. J. Primatol.* 24:677–689.
- Hopkins, W. D., M. J. Wesley, M. K. Izard, M. Hook, and S. J. Schapiro. 2004. Chimpanzees (*Pan troglodytes*) are predominantly right-handed: replication in three populations of apes. *Behav. Neurosci.* 118:659–663.
- Hopkins, W. D., J. L. Russell, C. Cantalupo, H. Freeman, and S. J. Schapiro. 2005. Factors influencing the prevalence and handedness for throwing in captive chimpanzees (*Pan troglodytes*). *J. Comp. Psychol.* 119:363–370.
- Hopkins, W. D., J. P. Tagliatalata, J. L. Russell, T. M. Nir, and J. Schaeffer. 2010. Cortical representation of lateralized grasping in chimpanzees (*Pan troglodytes*): a combined MRI and PET study. *PLoS One* 5:e13383.
- Hopkins, W. D., K. A. Phillips, A. Bania, S. E. Calcutt, M. Gardner, J. Russell, et al. 2011. Hand preferences for coordinated bimanual actions in 777 great apes: implications for the evolution of handedness in hominins. *J. Hum. Evol.* 60:605–611.
- Kaerer, M., A. F. Wyss, S. Bashir, A. Hamadjida, Y. Liu, J. Bloch, et al. 2010. Effects of unilateral motor cortex lesion on ipsilesional hand's reach and grasp performance in monkeys: relationship with recovery in the contralesional hand. *J. Neurophysiol.* 103:1630–1645.
- Kaerer, M., J. F. Brunet, A. Wyss, A. Belhaj-Saif, Y. Liu, A. Hamadjida, et al. 2011. Autologous adult cortical cell transplantation enhances functional recovery following unilateral lesion of motor cortex in primates: a pilot study. *Neurosurgery* 68:1405–1416.
- Kaerer, M., T. Wannier, J. F. Brunet, A. Wyss, J. Bloch, and E. M. Rouiller. 2013. Representation of motor habit in a sequence of repetitive reach and grasp movements performed by macaque monkeys: evidence for a

- contribution of the dorsolateral prefrontal cortex. *Cortex* 49:1404–1419.
- Kastner-Koller, U., P. Deimann, and J. Bruckner. 2007. Assessing handedness in pre-schoolers: construction and initial validation of a hand preference test for 4–6 year olds. *Psychol. Sci.* 49:239–254.
- Kazennikov, O., U. Wicki, M. Corboz, B. Hyland, A. Palmeri, E. M. Rouiller, et al. 1994. Temporal structure of a bimanual goal-directed movement sequence in monkeys. *Eur. J. Neurosci.* 6:203–210.
- Kermadi, I., Y. Liu, A. Tempini, E. Calciati, and E. M. Rouiller. 1998. Neuronal activity in the primate supplementary motor area and the primary motor cortex in relation to spatio-temporal bimanual coordination. *Somatosens. Mot. Res.* 15:287–308.
- Kermadi, I., Y. Liu, and E. M. Rouiller. 2000. Do bimanual motor actions involve the dorsal premotor (PMd), cingulate (CMA) and posterior parietal (PPC) cortices? Comparison with primary and supplementary motor cortical areas. *Somatosens. Mot. Res.* 17:255–271.
- Kimura, D. 2000. *Sex and cognition*. MIT Press, Cambridge, MA.
- Kinoshita, M. 1998. Do monkeys choose the more skillful hand in manual problem-solving? *Percept. Mot. Skills* 87:83–89.
- Lacreuse, A., and D. M. Fragaszy. 1997. Manual exploratory procedures and asymmetries for a haptic search task: a comparison between capuchins (*Cebus apella*) and humans. *Laterality* 2:247–266.
- Lacreuse, A., L. A. Parr, H. M. Smith, and W. D. Hopkins. 1999. Hand preferences for a haptic task in chimpanzees (*Pan troglodytes*). *Int. J. Primatol.* 20:867–881.
- Lehman, R. A. 1978a. The handedness of rhesus monkeys: I. Distribution. *Neuropsychologia* 16:33–42.
- Lehman, R. A. 1978b. The handedness of rhesus monkeys: II. Concurrent reaching. *Cortex* 14:190–196.
- Lehman, R. A. 1980a. The handedness of rhesus monkeys: III. Consistency within and across activities. *Cortex* 16:197–204.
- Lehman, R. A. 1980b. Distribution and changes in strength of hand preferences of cynomolgus monkeys. *Brain Behav. Evol.* 17:209–217.
- Lehman, R. A. 1989. Hand preferences of rhesus monkeys on differing tasks. *Neuropsychologia* 27:1193–1196.
- Leliveld, L. M., M. Scheumann, and E. Zimmermann. 2008. Manual lateralization in early primates: a comparison of two mouse lemur species. *Am. J. Phys. Anthropol.* 137:156–163.
- Lemon, R. N. 1993. Cortical control of the primate hand. *Exp. Physiol.* 78:263–301.
- Lemon, R. N. 2008. Descending pathways in motor control. *Annu. Rev. Neurosci.* 31:195–218.
- Liu, Y., and E. M. Rouiller. 1999. Mechanisms of recovery of dexterity following unilateral lesion of the sensorimotor cortex in adult monkeys. *Exp. Brain Res.* 128:149–159.
- MacManus, I. C. 2009. Brief handedness questionnaire. Available at <http://www.ucl.ac.uk/medical-education/other-studies/laterality/laterality-questionnaires/BriefHandednessQuestionnaire2009.pdf> (accessed 22 July 2013).
- MacNeillage, P. F., M. G. Studert-Kennedy, and B. Lindblom. 1987. Primate handedness reconsidered. *Behav. Brain Sci.* 10:247–303.
- Mark, R. F., and R. W. Sperry. 1968. Bimanual coordination in monkeys. *Exp. Neurol.* 21:92–104.
- Masataka, N. 1989. Population-level asymmetry of hand preference in lemurs. *Behaviour* 110:244–247.
- Meguerditchian, A., J. Donnot, S. Molesti, R. Francioly, and J. Vauclair. 2012. Sex difference in squirrel monkey's handedness for unimanual and bimanual coordinated tasks. *Anim. Behav.* 83:635–643.
- Meunier, H., C. Blois-Heulin, and J. Vauclair. 2011. A new tool for measuring hand preference in non-human primates: adaptation of Bishop's Quantifying Hand Preference task for Olive baboons. *Behav. Brain Res.* 218:1–7.
- Murata, Y., N. Higo, T. Oishi, A. Yamashita, K. Matsuda, M. Hayashi, et al. 2008. Effects of motor training on the recovery of manual dexterity after primary motor cortex lesion in macaque monkeys. *J. Neurophysiol.* 99:773–786.
- Nudo, R. J., W. M. Jenkins, M. M. Merzenich, T. Prejean, and R. Grenda. 1992. Neurophysiological correlates of hand preference in primary motor cortex of adult squirrel monkeys. *J. Neurosci.* 12:2918–2947.
- Oldfield, R. C. 1971. The assessment and analysis of handedness: the Edinburgh inventory. *Neuropsychologia* 9:97–113.
- Papademetriou, E., C. F. Sheu, and G. F. Michel. 2005. A meta-analysis of primate hand preferences, particularly for reaching. *J. Comp. Psychol.* 119:33–48.
- Porter, R., and R. Lemon. 1993. *Corticospinal function and voluntary movement*. Clarendon Press, Oxford.
- Pouydebat, E., E. Reghem, P. Gorce, and V. Bels. 2010. Influence of the task on hand preference: individual differences among gorillas (*Gorilla gorilla gorilla*). *Folia Primatol. (Basel)* 81:273–281.
- Raymond, M., and D. Pontier. 2004. Is there geographical variation in human handedness? *Laterality* 9:35–51.
- Raymond, M., D. Pontier, A. B. Dufour, and A. P. Moller. 1996. Frequency-dependent maintenance of left handedness in humans. *Proc. Biol. Sci.* 263:1627–1633.
- Rogers, L. J. 2009. Hand and paw preferences in relation to the lateralized brain. *Philos. Trans. R. Soc. Lond. B Biol. Sci.* 364:943–954.
- Rohr, L. E. 2006. Gender-specific movement strategies using a computer-pointing task. *J. Mot. Behav.* 38:431–437.
- Rouiller, E. M., X. H. Yu, V. Moret, A. Tempini, M. Wiesendanger, and F. Liang. 1998. Dexterity in adult monkeys following early lesion of the motor cortical hand area: the role of cortex adjacent to the lesion. *Eur. J. Neurosci.* 10:729–740.

- Schaafsma, S. M., B. J. Riedstra, K. A. Pfannkuche, A. Bouma, and T. G. Groothuis. 2009. Epigenesis of behavioural lateralization in humans and other animals. *Philos. Trans. R. Soc. Lond. B Biol. Sci.* 364:915–927.
- Schmidlin, E., M. Kaeser, A. D. Gindrat, J. Savidan, P. Chatagny, S. Badoud, et al. 2011. Behavioral assessment of manual dexterity in non-human primates. *J. Vis. Exp.* 57:3258.
- Schmitt, V., S. Melchisedech, K. Hammerschmidt, and J. Fischer. 2008. Hand preferences in Barbary macaques (*Macaca sylvanus*). *Laterality* 13:143–157.
- Serrien, D. J., R. B. Ivry, and S. P. Swinnen. 2006. Dynamics of hemispheric specialization and integration in the context of motor control. *Nat. Rev. Neurosci.* 7:160–166.
- Sherwood, C. C., E. Wahl, J. M. Erwin, P. R. Hof, and W. D. Hopkins. 2007. Histological asymmetries of primary motor cortex predict handedness in chimpanzees (*Pan troglodytes*). *J. Comp. Neurol.* 503:525–537.
- Singer, S. S., and M. H. Schwibbe. 1999. Right or left, hand or mouth: general-specific preferences in marmosets and tamarins. *Behaviour* 136:119–145.
- Spinozzi, G., M. G. Castorina, and V. Truppa. 1998. Hand preferences in unimanual and coordinated-bimanual tasks by tufted capuchin monkeys (*Cebus apella*). *J. Comp. Psychol.* 112:183–191.
- Spinozzi, G., T. Lagana, and V. Truppa. 2007. Hand use by tufted capuchins (*Cebus apella*) to extract a small food item from a tube: digit movements, hand preference, and performance. *Am. J. Primatol.* 69:336–352.
- Triggs, W. J., R. Calvanio, M. Levine, R. K. Heaton, and K. M. Heilman. 2000. Predicting hand preference with performance on motor tasks. *Cortex* 36:679–689.
- Uomini, N. T. 2009. The prehistory of handedness: archaeological data and comparative ethology. *J. Hum. Evol.* 57:411–419.
- Vauclair, J., A. Meguerditchian, and W. D. Hopkins. 2005. Hand preferences for unimanual and coordinated bimanual tasks in baboons (*Papio anubis*). *Brain Res. Cogn. Brain Res.* 25:210–216.
- Ward, J. P., G. W. Milliken, D. L. Dodson, D. K. Stafford, and M. Wallace. 1990. Handedness as a function of sex and age in a large population of Lemur. *J. Comp. Psychol.* 104:167–173.
- Ward, J. P., G. W. Milliken, and D. K. Stafford. 1993. Patterns of lateralized behavior in prosimians. Pp. 43–74 in J. P. Ward and W. D. Hopkins, eds. *Primate laterality: current behavioral evidence of primate asymmetries*. Springer, New-York, NY.
- Wesley, M. J., S. Fernandez-Carriba, A. Hostetter, D. Pilcher, S. Poss, and W. D. Hopkins. 2001. Factor analysis of multiple measures of hand use in captive chimpanzees: an alternative approach to the assessment of handedness in non-human primates. *Int. J. Primatol.* 23:1155–1168.
- Westergaard, G. C., and I. D. Lussier. 1999. Left-handedness and longevity in primates. *Int. J. Neurosci.* 99:79–87.
- Westergaard, G. C., and S. J. Suomi. 1996. Hand preference for a bimanual task in tufted capuchins (*Cebus apella*) and rhesus macaques (*Macaca mulatta*). *J. Comp. Psychol.* 110:406–411.
- Westergaard, G. C., M. Champoux, and S. J. Suomi. 1997. Hand preference in infant rhesus macaques (*Macaca mulatta*). *Child Dev.* 68:387–393.
- Westergaard, G. C., I. D. Lussier, and J. D. Higley. 2001a. Familial influences on hand preference: genotypic variation between closely related primate species. *Dev. Neuropsychol.* 20:605–617.
- Westergaard, G. C., I. D. Lussier, and J. D. Higley. 2001b. Between-species variation in the development of hand preference among macaques. *Neuropsychologia* 39:1373–1378.
- Zhao, D., W. D. Hopkins, and B. Li. 2012. Handedness in nature: first evidence on manual laterality on bimanual coordinated tube task in wild primates. *Am. J. Phys. Anthropol.* 148:36–44.



## **6 – *Curriculum vitae***





# CURRICULUM VITAE



**SIMON BADOUD**

Rue François Guillimann 15

1700 Fribourg

SWITZERLAND

Nationality: Swiss

Date of birth: 22-04-1985

License to drive «B»

Phone: 0041797340733

simon.badoud@unifr.ch

Available from summer 2016

## EDUCATION AND TRAINING

**Sept. 2014 - present**

**Diploma of advance study (DAS) in “ Management of clinical trials GCP implementation and quality process. ”**

Diploma accredited by:

- Swissmedic
- Swiss Association of Pharmaceutical Professionals (SwAPP)
- Swiss Society of Clinical Pharmacology and Toxicology

**Oct. 2011 - present**

**PhD student:**

**University Hospital Geneva: Grp. Prof. P. Burkhard**

- Clinical neuroscience: Topic: Parkinson's Disease

**University of Fribourg: Grp. Prof. E.M. Rouiller**

- Neurophysiology: Topic: Motor system & Parkinson's Disease

**PhD student at Lemanic Neurosciences Doctoral School**

**Sept. 2009 - Jan. 2011**

**MSc. Developmental & cell biology , University of Fribourg (CH)**

**Language: English**

- Master thesis in neurophysiology (group Prof. E.M. Rouiller)

«Human Embryonic Stem Cells against Parkinson's Disease:  
A pilot study.»

**2006-2009**

**BSc. in Biology, University of Fribourg (CH)**

**Languages: bilingual German & French**

**Options:** Special biology (human anatomy & physiology)  
Neurosciences

**2001-2005**

**St-Michel High school, Fribourg, Switzerland**

- Federal maturity with mention (options: biology / chemistry, sport)

## EXPERIENCES

- **Internship at the University Hospital of Geneva / department of neurology (April 2011- October 2011)**  
Development of automatic differential diagnostic tools. Ref. Prof. Pierre Burkhard
  - **Teaching assistant in the department of medicine for practical lessons to Medical and Biomedical students. (University of Fribourg, since 2010)**
- 

## LANGUAGES

<b>French:</b>	mother tongue
<b>German:</b>	written, spoken and reading (professional competencies)
<b>English:</b>	written, spoken and reading (full professional competencies)

---

## INFORMATICS

<b>Statistics:</b>	GraphPad Prism, Matlab, "R"
<b>Imaging:</b>	OsiriX, FSL, SPM, Pmod
<b>Database:</b>	Access, Excel, Refmanager, Paper
<b>Microsoft Office:</b>	PowerPoint, Word, Excel
<b>Others:</b>	OpenProjet

---

## AWARDS

- **"Jean Falk-Vairant Award" for the best oral presentation in applied neurosciences 2015.**
  - **"Volker Henn Award" from the Swiss Society for Neuroscience (SSN) 2012.**
- 

## CERTIFICATES

- **Certificate of animal experimenter. (Module 1)**
- 

## MEMBERSHIP

- **Student member of the Swiss Society for Neuroscience.**
  - **Member of the science faculty conseil - University of Fribourg (CH) 2012-present**
  - **Vice-president of the Biology students association. (University of Fribourg CH) 2008-11**
-

## OTHERS

- **Head instructor in a martial arts training center in Bern (Võ Vietnam)**
- **Member of the national technical commission (Võ Vietnam)**
- **Hobbies: Sport, Photography, Travels, Music, Art, Design,.**

---

**More infos:**    **Linked****e:** **SIMON BADOUD**

## ***Publications' list***

1. **Badoud, S.**, Nicastro, N., Garibotto, V., Burkhard, P. R., & Haller, S. (2015). Distinct spatiotemporal patterns for disease duration and stage in Parkinson's disease. **European Journal of Nuclear Medicine and Molecular Imaging**, 1–9. <http://doi.org/10.1007/s00259-015-3176-5>
2. Chatagny, P\*., **Badoud, S\***., Kaeser, M., Gindrat, A. D., Savidan, J., Fregosi, M., et al. (2013). Distinction between hand dominance and hand preference in primates: a behavioral investigation of manual dexterity in nonhuman primates (macaques) and human subjects. **Brain and Behavior**, n/a–n/a. <http://doi.org/10.1002/brb3.160>
3. Fisch, L., Megevand, P., **Badoud, A.**, Seeck, M., & Burkhard, P. R. (2012). Pilomotor seizure When paroxysmal gooseflesh heralds brain tumor. **Neurology**, 78(15), 1189–1189. <http://doi.org/10.1212/WNL.0b013e31824f80f5>
4. Haller, S., **Badoud, S.**, Nguyen, D., Barnaure, I., Montandon, M.-L., Lovblad, K. O., & Burkhard, P. R. (2013). Differentiation between Parkinson disease and other forms of Parkinsonism using support vector machine analysis of susceptibility-weighted imaging (SWI): initial results. **European Radiology**, 23(1), 12–19. <http://doi.org/10.1007/s00330-012-2579-y>
5. Haller, S., **Badoud, S.**, Nguyen, D., Garibotto, V., Lovblad, K. O., & Burkhard, P. R. (2012). Individual Detection of Patients with Parkinson Disease using Support Vector Machine Analysis of Diffusion Tensor Imaging Data: Initial Results. **AJNR American Journal of Neuroradiology**. <http://doi.org/10.3174/ajnr.A3126>
6. Kaeser, M., Chatagny, P., Gindrat, A. D., Savidan, J., **Badoud, S.**, Fregosi, M., et al. (2014). Variability of manual dexterity performance in non-human primates (). **International Journal of Comparative Psychology**, 27(2).
7. Nicastro, N., Garibotto, V., Poncet, A., **Badoud, S.**, & Burkhard, P. R. (2015). Establishing On-Site Reference Values for 123I-FP-CIT SPECT (DaTSCAN®) Using a Cohort of Individuals with Non-Degenerative Conditions. **Molecular Imaging and Biology**, 1–11. <http://doi.org/10.1007/s11307-015-0889-6>
8. Schmidlin, E., Kaeser, M., Gindrat, A. D., Savidan, J., Chatagny, P., **Badoud, S.**, et al. (2011). Behavioral Assessment of Manual Dexterity in Non-Human Primates. **Journal of Visualized Experiments**, (57), e3258–e3258. <http://doi.org/10.3791/3258>